

Development of the filarial nematode *Cercopithifilaria johnstoni* as a Model System for Onchocerciasis

Kirsty McCann

BAnVetBioSc (Hons)

A thesis submitted in total fulfilment
of the requirements for the degree of

Doctor of Philosophy

College of Science, Health and Engineering

School of Life Sciences

Department of Physiology, Anatomy and Microbiology

La Trobe University

Victoria, Australia

August 2020

Table of Contents

Table of Contents	ii
List of Figures	xi
List of Tables	xv
List of Supplementary Material	xviii
List of Abbreviations	xxiii
List of Bioinformatics Programs	xxvii
Abstract	xxixx
Statement of authorship	xxxiii
Acknowledgements	xxxiii
Publications	xxxiii
Chapter One	1
General Introduction	1
1.1 Helminths	1
1.2 Filarial nematodes	4
1.3 Onchocerciasis	5
1.4 Established drugs used for the treatment of onchocerciasis	12
1.4.1 Ivermectin	12
1.4.2 Diethylcarbamazine.....	17
1.4.3 Doxycycline	17
1.4.4 Moxidectin	18
1.5 The Mazzotti reaction	21
1.6 Onchocerciasis treatment programs using ivermectin	22
1.7 Challenges to controlling onchocerciasis.....	23
1.7.1 Co-endemicity of onchocerciasis and loiasis.....	24
1.7.2 Ivermectin resistance	25
1.7.3 Political conflict and civil war	26

1.7.4 Geographical and population coverage.....	26
1.7.5 Non-compliance	27
1.8 Requirement for animal models to study onchocerciasis immunopathology and develop new drugs	28
1.9 Animal model requirements.....	29
1.10 Current animal models	30
1.10.1 <i>Onchocerca ochengi</i> model.....	30
1.10.2 Mouse model.....	31
1.10.3 Chimpanzee model	32
1.10.4 <i>Acanthocheilonema viteae</i> rodent model	33
1.10.5 <i>Loa loa</i> mouse model.....	33
1.10.6 <i>Litomosoides sigmodontis</i> rodent model	34
1.11 Key limitations to current models.....	38
1.12 <i>Cercopithifilaria johnstoni</i> (<i>Dipetalonema johnstoni</i>) as a model organism for onchocerciasis	39
1.12.1 <i>Cercopithifilaria johnstoni</i> life cycle	42
1.12.2 Pathology in the natural host, <i>Rattus fuscipes</i>	44
1.12.3 Vectors for <i>Cercopithifilaria johnstoni</i> animal model.....	44
1.12.4 Pathology in the laboratory host, <i>Rattus norvegicus</i>	48
1.13 Ticks: vectors of pathogens and parasites	49
1.13.1 Hard tick life cycles	50
1.13.2 Tick survival strategies.....	51
1.13.3 Challenges for using ixodid ticks to transmit <i>Cercopithifilaria johnstoni</i>	53
1.13.4 Characterising tick species for an animal model	55
1.14 Direct comparison of <i>Onchocerca volvulus</i> and <i>Cercopithifilaria johnstoni</i>	56
1.14.1 Parasite life cycles	56
1.14.2 Vectors.....	57

1.15 Genome assemblies and comparative genomics	58
1.15.1 Genomes: a resource for identifying drug or vaccine candidates or antigens recognised by sera	58
1.16 Onchocerciasis immunopathology and antigen based assays/targets	62
1.16.1 Ov-16 assay	63
1.16.2 Ov-39 protein	64
1.17 Limitation of <i>in silico</i> studies	65
1.18 Rationale for this body of work	67
1.19 Thesis aims	69

Chapter Two.....70

Comparison of evolutionary relationships between *Cercopithifilaria johnstoni* and filarial nematodes using the mitochondrial genome.....70

2.1 Introduction.....	70
2.1.1 Aims	73
2.2 Materials and Methods	74
2.2.1 Sequence accession numbers	74
2.2.2 Sample collection	74
2.2.3 DNA extraction, library preparation and sequencing	75
2.2.4 Genome assembly	75
2.2.5 Mitochondrial genome assembly	76
2.2.6 Genome annotation.....	76
2.2.7 Whole mitochondrial phylogeny	77
2.2.8 12S COI gene phylogeny of <i>Cercopithifilaria</i>	79
2.3 Results	82
2.3.1 Assembly of the mitochondrial genome	82
2.3.2 Mitochondrial genome phylogeny.....	88
2.3.3 Concatenated gene phylogeny.....	93
2.4 Discussion	96

2.4.1 Mitochondrial genome.....	96
2.4.2 Mitochondrial genome phylogeny.....	97
2.4.3 Exploring host species of filarial nematodes	99
2.4.4 Phylogeny of the genus <i>Cercopithifilaria</i>	104
2.5 Conclusion.....	108

Chapter Three109

Assembly of the *Cercopithifilaria johnstoni* nuclear genome and prediction of orthologous relationships with closely related filarial nematodes109

3.1 Introduction.....	109
3.1.1 Aims	113
3.2 Materials and Methods	114
3.2.1 Nuclear genome assembly.....	114
3.2.2 Masking repeats.....	114
3.2.3 Whole genome completeness.....	114
3.2.4 Comparison of <i>Cercopithifilaria johnstoni</i> scaffold content with <i>Onchocerca volvulus</i> and <i>Brugia malayi</i> genome content.....	115
3.2.5 Scaffold GC content and coverage analysis between <i>Cercopithifilaria johnstoni</i> and <i>Onchocerca volvulus</i>	116
3.2.6 Protein-coding gene prediction.....	116
3.2.7 Assessment of predicted protein-coding gene completeness	117
3.2.8 Prediction of shared orthologues using OrthoFinder2	118
3.2.9 Orthogroups and single-copy orthologue UpSet plots.....	119
3.3 Results	120
3.3.1 Genome assembly: <i>Cercopithifilaria johnstoni</i>	120
3.3.2 Whole genome completeness of <i>Cercopithifilaria johnstoni</i> compared to filarial nematodes	122
3.3.3 Analysis of genome repeats of filarial nematodes	125

3.3.4 Comparative genomics analyses: <i>Cercopithifilaria johnstoni</i> shares homology to <i>Onchocerca volvulus</i>	128
3.3.5 <i>Cercopithifilaria johnstoni</i> sequences are possibly X-linked.....	134
3.3.6 Genome annotation methods of the <i>Cercopithifilaria johnstoni</i> scaffolds	136
3.3.6.1 Different gene prediction methods change the BUSCO completeness results when using protein-coding genes.....	136
3.3.6.2 Different gene prediction methods result in different OrthoFinder2 predictions.....	138
3.3.7 OrthoFinder2 predicts orthologous relationships with closely related nematodes	144
3.3.8 Consistent filarial phylogenetic relationships.....	144
3.3.9 Orthogroup and single-copy orthologue relationships.....	146
3.4 Discussion	153
3.4.1 Genome assembly and completeness of <i>Cercopithifilaria johnstoni</i> scaffolds.....	153
3.4.2 Comparing genome similarity of filarial nematodes.....	154
3.4.3 Repeat regions and repeat masking in <i>Cercopithifilaria johnstoni</i> scaffolds.....	158
3.4.4 Comparison of the effects of three different gene annotation methods for gene prediction of <i>Cercopithifilaria johnstoni</i> scaffolds using BUSCO and OrthoFinder2.....	162
3.4.5 Predicting orthologous genes between <i>Cercopithifilaria johnstoni</i> and <i>Onchocerca volvulus</i>	165
3.5 Conclusions.....	168
Chapter Four	169
Evolution and sequence conservation of immunogenic orthologous proteins between <i>Cercopithifilaria johnstoni</i> and <i>Onchocerca volvulus</i> ...	169
4.1 Introduction.....	169

4.1.1 Aims	175
4.2 Materials and Methods	176
4.2.1 Curation of protein sequences representing immunologically relevant targets	176
4.2.2 Data extraction and sequence alignment	177
4.2.3 BLAST <i>Onchocerca volvulus</i> and <i>Cercopithifilaria johnstoni</i> protein sequences to predict putative functions	177
4.2.4 Exonerate analysis	178
4.2.5 Detection of diversifying or purifying selection	178
4.2.6 Epitope and motif search	179
4.2.7 BLAST <i>Cercopithifilaria johnstoni</i> proteins that matched to the epitope and three immunodominant <i>Onchocerca volvulus</i> motifs to identify putative functions	180
4.2.8 InterProScan analysis on <i>Cercopithifilaria johnstoni</i> proteins containing the <i>Onchocerca volvulus</i> immunodominant motifs and epitope	180
4.3 Results	181
4.3.1 <i>Onchocerca volvulus</i> immunogenic proteins and <i>Cercopithifilaria johnstoni</i> orthologues predicted putative functions	181
4.3.2 Evidence of evolutionary selection on <i>Cercopithifilaria johnstoni</i> and <i>Onchocerca volvulus</i> orthologues of proteins with a putative immunogenic function	192
4.3.3 Presence of immunodominant motifs and epitopes in <i>Cercopithifilaria johnstoni</i> protein-coding genes	194
4.4 Discussion	215
4.4.1 <i>Cercopithifilaria johnstoni</i> and <i>Onchocerca volvulus</i> share orthologues of known <i>Onchocerca volvulus</i> immunogenic proteins with putative functions associated with host immune response	215
4.4.2 Evolutionary selection identified in <i>Cercopithifilaria johnstoni</i> and <i>Onchocerca volvulus</i> orthologous compared to other closely related filarial nematodes	219

4.4.3 Immunogenic motifs and epitopes in filarial nematodes could be a potential avenue for drug targets providing evidence of immunoreactivity ..	222
4.5 Future outlook	225
4.6 Conclusions.....	229
Chapter Five.....	230
Cryptic species diversity in ticks that transmit disease in Australia	230
Preface	230
Abstract	232
1. Introduction.....	232
2. Materials and methods	233
2.1. Sample collection	233
2.2. Purifying tick DNA.....	233
2.3. PCR of mitochondrial and nuclear amplicons	233
2.4. Sequencing of amplicons.....	233
2.5. Sequencing analysis.....	233
2.6. Haplotype analysis.....	233
3. Results	234
3.1. Phylogenetic analysis	234
3.2. Haplotype analysis.....	235
4. Discussion	235
4.1. Genetic differentiation among Australian ixodid ticks	235
4.2 Differences in species diversity between sampling locations	236
5. Conclusions	237
Conflicts of interest.....	237
Declaration of interests	237
Acknowledgements	237
References	237

Chapter Six.....	239
Progress and prospects towards establishing the <i>Cercopithifilaria johnstoni</i> life cycle using <i>Rattus fuscipes</i> and ticks (<i>Ixodes spp</i>) as hosts in the laboratory	239
Preface	239
6.1 Introduction.....	240
6.2 Methods.....	243
6.2.1 Tick collection process at Kioloa and Mogo	243
6.2.1.1 Tick collection directly from the ground.....	243
6.2.1.2 Tick collection directly from rats.....	243
6.2.1.3 Precence of <i>Cercopithifilaria johnstoni</i>	244
6.2.2 Housing chambers for live ticks at La Trobe University.....	244
6.2.3 Tick attachment procedure in the laboratory (La Trobe University)....	245
6.2.4 Animal Ethics Approval and Wildlife Permits.....	247
6.3 Results	248
6.3.1 Samples collected	248
6.3.2 Tick attachments	248
6.4 Discussion	255
6.4.1 Collection of ticks for life cycle maintenance	255
6.4.1.1 Numbers of unfed questing ticks.....	255
6.4.1.2 Numbers of engorged ticks.....	257
6.4.2 Feasibility of maintaining ticks in the laboratory	257
6.4.3 Attachment of immature wild-caught ticks to infected bush rats.....	260
6.4.4 Determining the duration of an infection using captive, naturally infected wild-caught bush rats	261
6.4.5 Future directions for the <i>Cercopithifilaria johnstoni</i> -rodent animal model	262
6.4.5.1 Tick dissection and subcutaneous injection into rat.....	262

6.4.5.2 Possible future experiment using the paralysis tick, <i>Ixodes holocyclus</i> for vector of <i>Cercopithifilaria johnstoni</i> in a small animal model system.....	263
6.4.5.3 Future identification of <i>Cercopithifilaria johnstoni</i> presence in ticks and rodents using PCR.....	265
6.4.5.4 Tick morphological identification.....	265
6.5 Conclusions.....	266
Chapter Seven	268
General Discussion	268
7.1 Phylogenetic relationships of filarial nematodes.....	269
7.2 <i>In silico</i> analysis of the <i>Cercopithifilaria johnstoni</i> genome.....	273
7.3 Drivers of disease immunopathology: Evolutionary selection and immunogenic proteins	277
7.4 Developing a small animal model for onchocerciasis	281
7.5 Conclusions and future directions	288
Appendices	290
Appendix 1: Chapter Two Supplementary Material	290
Appendix 2: Chapter Three Supplementary Material.....	296
Appendix 3: Chapter Four Supplementary Material	317
Appendix 4: Chapter Five Supplementary Material	331
Appendix 5: Chapter Six Supplementary Material	337
References	342

List of Figures

Chapter One

- Figure 1.1:** Phylogeny of Nematoda based on the IQ-TREE maximum likelihood analysis (Smythe et al., 2019). Classification bar represents known taxonomic diversity of different taxa within Neamtoda. Habitat describes the lifestyle for each analysed species. Newly generated transcriptomes are marked with an asterisk (Smythe et al., 2019).3
- Figure 1.2:** Onchocercid clades from concatenated datasets of 12S rDNA, cox1, rbp1, hsp70, myoHC, 18S rDNA, and 28S rDNA sequences (Lefoulon et al., 2015).....6
- Figure 1.3:** *Onchocerca volvulus* life cycle adapted from Centers for Disease Control and Prevention (2015).....9
- Figure 1.4:** *Simulium damnosum* life cycle adapted from Service (2012).....11
- Figure 1.5:** Pre-treatment *Onchocerca volvulus* microfilarial load over time after a single, standard dose of ivermectin (150 µg/kg) (Basáñez et al., 2008).....16
- Figure 1.6:** a) Number of *Rattus fuscipes* trapped at Mogo State Forest every month over three years (1985, 1986, and 1987). b) Figure representing mean numbers of larval and nymphal *Ixodes* spp. (predominantly *Ixodes trichosuri*) harvested from bush rats (n above) naturally infected with *Cercopithifilaria johnstoni* at Mogo State Forest, April 1985 to July 1987 (Spratt and Haycock, 1988).....41
- Figure 1.7:** The life cycle of *Cercopithifilaria johnstoni*, transmitted by ixodid ticks to the Australian bush rats, *Rattus fuscipes*.....43
- Figure 1.8:** Evidence of *Cercopithifilaria johnstoni* in *Rattus fuscipes* and *Rattus norvegicus* (Spratt and Haycock, 1988).....45
- Figure 1.9:** *Cercopithifilaria johnstoni* in subcutaneous aponeuroses of dorsum of rats (Vuong et al., 1993).....46
- Figure 1.10:** *Cercopithifilaria johnstoni* in *Rattus fuscipes* above the red line and in *Rattus norvegicus* below the red line (modified from Vuong et al., 1993).....47

Figure 1.11: The general life cycle of <i>Ixodes</i> ticks, adapted from Wall and Shearer (1997).....	52
--	----

Chapter Two

Figure 2.1: Comparison of a) <i>Cercopithifilaria johnstoni</i> annotated mitochondrial genome and, b) <i>Onchocerca volvulus</i> annotated mitochondrial genome.....	84
--	----

Figure 2.2: Genome Ribbon alignment of the whole mitochondrial genomes <i>Onchocerca volvulus</i> as the reference sequence and a query of <i>Cercopithifilaria johnstoni</i> whole mitochondrial genome to illustrate conservation of mitochondrial genomes.....	85
--	----

Figure 2.3: Mauve alignment of the whole mitochondrial genomes of 20 filarial nematodes showing consistent and conserved gene order and content.....	86
---	----

Figure 2.4: Whole mitochondrial genome phylogeny of filarial nematodes using maximum likelihood/Bayesian inference.....	89
--	----

Figure 2.5: Three different subsampled datasets of the whole mitochondrial genome phylogeny of filarial nematodes using maximum likelihood/Bayesian inference.....	90
---	----

Figure 2.6: Concatenated 12S-COI phylogeny of filarial nematodes to position the <i>Cercopithifilaria</i> genus using maximum likelihood/Bayesian inference.....	94
---	----

Chapter Three

Figure 3.1: Comparative genomic analysis of <i>Brugia malayi</i> chromosomes against <i>Onchocerca volvulus</i> chromosomes showing two chromosome rearrangements.....	129
---	-----

Figure 3.2: Comparative genomic analysis of <i>Cercopithifilaria johnstoni</i> scaffolds synteny against two filarial nematodes: a) <i>Onchocerca volvulus</i> chromosomes. b) <i>Brugia malayi</i> chromosomes.....	131
---	-----

Figure 3.3: Genome ribbon representation of a) <i>Cercopithifilaria johnstoni</i> longest scaffold (NODE_1_length_588165) aligned to <i>Onchocerca volvulus</i> chromosome	
---	--

OM3 and b) <i>Cercopithifilaria johnstoni</i> longest scaffold (NODE_1_length_588165) aligned to <i>Brugia malayi</i> CHR1	133
--	-----

Figure 3.4: GC content vs coverage plot of the draft <i>Cercopithifilaria johnstoni</i> genome scaffolds with a <i>Onchocerca volvulus</i> chromosome projection overlayed onto the <i>Cercopithifilaria johnstoni</i> data based on nucleotide similarity.....	135
--	-----

Figure 3.5: Single-copy orthologue maximum likelihood phylogeny with bootstrap support for all the nematodes that were analysed in the OrthoFinder2 analysis.....	145
--	-----

Figure 3.6: UpSet plot representing the single-copy orthologue orthogroup relationships across the 12 filarial nematodes.....	148
--	-----

Figure 3.7: UpSet plot representing all the orthogroup relationships with one or more genes in each group across the 12 filarial nematodes.....	150
--	-----

Figure 3.8: UpSet plot representing the complete single-copy and multi-gene orthogroup relationships across <i>Cercopithifilaria johnstoni</i> and <i>Onchocerca volvulus</i>	152
--	-----

Chapter Five: Publication from IJP: Parasites and Wildlife

Fig. 1. Satellite maps of (a) Australia (b) Kioloa and (c) Mogo state forest sample collection sites with coordinates, latitude on the y axis and longitude on the x axis. (a) Yellow: NSW general location of sites (b) orange: Kioloa ANU campus, yellow: Kioloa dunes (c) blue: Mogo State Forest (Kahle and Wickham, 2013).....	234
--	-----

Fig. 2. Maximum likelihood estimate based on three markers of ticks collected at Kioloa and Mogo State Forest, NSW, Australia. Blue: Mogo State Forest (rats), yellow: Kioloa (flagging), red: identified voucher specimens.....	235
---	-----

Fig. 3. TCS haplotype network based on 3 markers sequenced from ticks collected from Kioloa and Mogo State Forest in NSW, Australia. Samples are coloured based on their collection site, Mogo State Forest (blue) or, Kioloa (yellow). Voucher specimens are coloured red.....	236
--	-----

Chapter Seven

Figure 7.1: Summary of the Omics data that is available for filarial parasites obtained from Grote et al. (2017).....276

Figure 7.2. General schematic of the membrane feeding apparatus (Bonnet and Liu, 2012).....286

List of Tables

Chapter One

Table 1.1: Summary of the current drugs approved for treating onchocerciasis in humans. The table describes the drug, drug class, the stage the drugs target (i.e., microfilaricidal or macrofilaricidal), problems or side effects and lastly whether the drug could be successfully used for treatment.....20

Table 1.2: Summary of animal models previously used to study onchocerciasis highlighting the advantages and disadvantages of each model system.....36

Chapter Two

Table 2.1: *Cercopithifilaria johnstoni* mitochondrial genome annotation using MITOS with a total genome length of 13,716 bp.....83

Table 2.2: Comparison (pairwise % identity) among nucleotides sequences of the filarial nematodes represented in the whole mitochondrial genome mauve alignment.....87

Table 2.3: Summary of the known location of microfilariae and adult worms in filarial nematodes.....101

Chapter Three

Table 3.1: Genome statistics of *Cercopithifilaria johnstoni* with all the filarial nematodes that have genome statistics available to compare variables such as assembly length, the longest sequence length (bp), N50 length, N90 length, GC%, number of Ns and the number of gaps within the assembly.....121

Table 3.2: Comparison of the genome completeness statistics of all filarial nematodes with CEGMA (248 sequences).....123

Table 3.3: Comparison of the genome completeness statistics of all filarial nematodes with BUSCO (982 groups).....124

Table 3.4: Comparison of the RepeatModeler repeat statistics of <i>Cercopithifilaria johnstoni</i> and closely related filarial nematodes.....	127
Table 3.5: Comparison of the BUSCO completeness across the <i>Cercopithifilaria johnstoni</i> proteomes of three different gene prediction methods, a) Augustus gene prediction, b) BRAKER gene prediction <i>ab initio</i> , and c) BRAKER gene prediction using <i>Acanthocheilonema viteae</i> training model.....	137
Table 3.6: Comparison of the OrthoFinder2 one-to-one orthologues using the <i>Cercopithifilaria johnstoni</i> proteomes of three different gene prediction methods, a) Augustus gene prediction.....	140
Table 3.6: Comparison of the OrthoFinder2 one-to-one orthologues using the <i>Cercopithifilaria johnstoni</i> proteomes of three different gene prediction methods, b) BRAKER gene prediction <i>ab initio</i> and c) BRAKER using <i>Acanthocheilonema viteae</i> for gene training.....	141
Table 3.7: Summary of the OrthoFinder2 analyses using the <i>Cercopithifilaria johnstoni</i> proteomes of three different gene prediction methods, a) Augustus gene prediction, b) <i>ab initio</i> BRAKER gene prediction and c) BRAKER <i>Acanthocheilonema viteae</i> training.....	142
Table 3.8: The average length of the <i>C. johnstoni</i> Augustus predicted protein-coding genes compared with the average protein length of the 12 filarial nematode proteomes.....	143

Chapter Four

Table 4.1: The 30 <i>Onchocerca volvulus</i> immunogenic proteins and corresponding <i>Cercopithifilaria johnstoni</i> orthologues are described revealing their top BLAST results to the NCBI database.....	185
Table 4.2: PAML dN/dS ratios for <i>Cercopithifilaria johnstoni</i> and <i>Onchocerca volvulus</i> compared to the phylogenetic tree for the 30 orthologous genes.....	193
Table 4.3: The <i>Cercopithifilaria johnstoni</i> proteins examined for the presence of the <i>Onchocerca volvulus</i> motif DGxDK from Lagatie et al. (2017).....	196

Table 4.4: The <i>Cercopithifilaria johnstoni</i> proteins examined for the presence of the <i>Onchocerca volvulus</i> motif PxxTQE from Lagatie et al. (2017).....	200
Table 4.5: The <i>Cercopithifilaria johnstoni</i> proteins examined for the presence of the <i>Onchocerca volvulus</i> motif QxSNxD from Lagatie et al. (2017).....	204
Table 4.6: Identification of three immunodominant motifs (PxxTQE, DGxDK, QxSNxD) in filarial nematodes (Lagatie et al., 2017).....	210
Table 4.7: The <i>Cercopithifilaria johnstoni</i> proteins examined for the presence of the <i>Onchocerca volvulus</i> epitope QQQQQQQQR from Lagatie et al. (2018)....	212
Table 4.8: Identifying the poly-glutamine stretch in the N-terminal region of <i>Onchocerca volvulus</i> protein (OVOC9988) 9-mer QQQQQQQQR in filarial nematodes.....	214

Chapter Six

Table 6.1: Rat weights and <i>Cercopithifilaria johnstoni</i> microfilariae counts at two different time points: March 2016 and April 2016.....	249
Table 6.2: Summary of the first tick attachment experiment for 2016.....	252
Table 6.3: Summary of the second tick attachment experiment for 2016.....	253
Table 6.4: Summary of the third tick attachment experiment for 2016.....	254

List of Supplementary Material

Supplementary Tables

Chapter Two

Supplementary Table 2.1: Recommended Partition Finder substitution models for the complete dataset (coding regions and intergenic regions) within the *Cercopithifilaria johnstoni* mitochondrial genome. All filarial nematodes, including outgroups, are used in this mitochondrial genome dataset.....290

Supplementary Table 2.2: Recommended Partition Finder substitution models for all filarial nematodes and outgroups using only the coding regions within the mitochondrial genome, excluding the intergenic regions.....291

Supplementary Table 2.3: Recommended Partition Finder substitution models for the complete dataset of coding regions and intergenic regions within the mitochondrial genome, excluding outgroups from the analysis.....292

Supplementary Table 2.4: Recommended Partition Finder substitution models for filarial nematodes of the coding regions within the mitochondrial genome, excluding the outgroups and the intergenic regions.....293

Supplementary Table 2.5: *Cercopithifilaria spp.* NCBI accession numbers for COI and 12S concatenated gene phylogeny.....294

Supplementary Table 2.6: Table adapted from McNulty et al. (2012), consisting of published mitochondrial genomes of the filarial nematodes with their accession numbers, genome length, AT-rich region length, and base content (%). The *Cercopithifilaria johnstoni* draft genome is added to compare genome content against other published mitochondrial genomes.295

Chapter Three

Supplementary Table 3.1: Missing BUSCO gene IDs from the genome completeness analysis for 12 filarial nematodes296

Supplementary Table 3.2: Complete RepeatModeler statistics including total repeats, number of base pairs (bp) and percentage (%).....315

Chapter Four

Supplementary Table 4.1: List of 17/49 <i>Onchocerca volvulus</i> immunogenic relevant proteins used to identify and extract from the OrthoFinder2 analysis any possible orthologues in <i>Cercopithifilaria johnstoni</i> for further analyses. Protein obtained from Norice-Tra et al. (2017).....	317
Supplementary Table 4.2: List of 33/49 <i>Onchocerca volvulus</i> serodiagnostic relevant proteins used to identify and extract from the OrthoFinder2 analysis any possible orthologues in <i>Cercopithifilaria johnstoni</i> for further analyses. Proteins obtained from McNulty et al. (2015).....	318
Supplementary Table 4.3: The blast results of the 30 <i>Cercopithifilaria johnstoni</i> orthologues of <i>Onchocerca volvulus</i> immunogenic proteins are described revealing their top BLAST results to the NCBI database, % identity, protein alignment length, e-value, bit score.....	319
Supplementary Table 4.4: The <i>Cercopithifilaria johnstoni</i> proteins examined for the presence of the <i>Onchocerca volvulus</i> motif DGxDK from Lagatie et al. (2017). The <i>Cercopithifilaria johnstoni</i> protein secondary BLAST hit and putative function is reported with % identity, e-value and bits (bit score).....	322
Supplementary Table 4.5: The <i>Cercopithifilaria johnstoni</i> proteins examined for the presence of the <i>Onchocerca volvulus</i> motif PxxTQE from Lagatie et al. (2017). The <i>Cercopithifilaria johnstoni</i> protein secondary BLAST hit and putative function is reported with % identity, e-value and bits (bit score).....	325
Supplementary Table 4.6: The <i>Cercopithifilaria johnstoni</i> proteins examined for the presence of the <i>Onchocerca volvulus</i> motif QxSNxD from Lagatie et al. (2017). The <i>Cercopithifilaria johnstoni</i> protein secondary BLAST hit and putative function is reported with % identity, e-value and bits (bit score).....	327
Supplementary Table 4.7: The <i>Cercopithifilaria johnstoni</i> proteins examined for the presence of the <i>Onchocerca volvulus</i> epitope QQQQQQQQR from Lagatie et al. (2018). The <i>Cercopithifilaria johnstoni</i> protein secondary BLAST hit and putative function is reported with % identity, e-value and bits (bit score).....	330

Chapter Six

Supplementary Table 6.1: Summary of tick collections from flagging field trips 2015.	339
Supplementary Table 6.2: Summary of tick collections from flagging field trips 2016.	340

Supplementary Figures

Chapter Five: Publication from IJP: Parasites and Wildlife

Fig. 4. Maximum likelihood estimate based on the amplicon 12S of ticks collected at Kioloa and Mogo State Forest, NSW, Australia. Blue = Mogo State Forest (rats), yellow = Kioloa (flagging), red = identified voucher specimens.....	331
Fig. 5. TCS haplotype network based on the amplicon 12S sequenced from ticks collected from Kioloa and Mogo State Forest in NSW, Australia. Samples are coloured coded based on their collection site, Mogo State Forest (blue) or, Kioloa (yellow). Voucher specimens are coloured red.....	332
Fig. 6. Maximum likelihood estimate based on the amplicon 16S of ticks collected at Kioloa and Mogo State Forest, NSW, Australia. Blue = Mogo State Forest (rats), yellow = Kioloa (flagging), red = identified voucher specimens.....	333
Fig. 7. TCS haplotype network based on the amplicon 16S sequenced from ticks collected from Kioloa and Mogo State Forest in NSW, Australia. Samples are coloured coded based on their collection site, Mogo State Forest (blue) or, Kioloa (yellow). Voucher specimens are coloured red.....	334
Fig. 8. Maximum likelihood estimate based on the amplicon ITS2 of ticks collected at Kioloa and Mogo State Forest, NSW, Australia. Blue = Mogo State Forest (rats), yellow = Kioloa (flagging), red = identified voucher specimens.....	335
Fig. 9. TCS haplotype network based on the amplicon ITS2 sequenced from ticks collected from Kioloa and Mogo State Forest in NSW, Australia. Samples are coloured coded based on their collection site, Mogo State Forest (blue) or, Kioloa (yellow). Voucher specimens are coloured red.....	336

Chapter Six

Supplementary Figure 6.1: (a) White fabric flag used for flagging in the field. (b) Tick collected from the flag and placed in falcon tube.....	337
Supplementary Figure 6.2: (a) Closed tube with small hole used for bush rat tick attachment. (b) Rat housing in tub with tray used throughout the tick attachment experiments.	338
Supplementary Figure 6.3: (a) Identification of adult female and adult male <i>Ixodes holocyclus</i> ticks. Lighter coloured middle legs differentiate the species from other ticks. The larger tick is the female. (b) Adult male and female <i>Ixodes holocyclus</i> ticks in scintillation tube before mating.	341

List of Abbreviations

<i>Ab initio</i>	Latin for “from the beginning”
AEC	Animal Ethics Committee
APOC	African Programme for Onchocerciasis Control
ATP	Adenosine triphosphate
AUS	Australia
BLAST	Basic Local Alignment Search Tool
bp	Base pair(s)
BUSCO	Benchmarking Universal Single-Copy Orthologues
CDC	Centre for Disease Control
CDS	Coding sequence
CEGMA	Core Eukaryotic Genes Mapping Approach
cm	Centimetre
<i>Dipetalonema johnstoni</i>	<i>Cercopithifilaria johnstoni</i>
/Cj	
CO ₂	Carbon dioxide
COI	Cytochrome c Oxidase subunit I
CYT	Cytochrome
DALYs	Disability-adjusted life years
DEC	Diethylcarbamazine
DRC	Democratic Republic of Congo
DNA	Deoxyribonucleic acid
dN	nonsynonymous
dS	synonymous
ELISA	Enzyme-linked immunosorbent assay
ESPEN	Expanded Special Project for Elimination of NTDs
G50	Number of genes in the orthogroup that 50% of genes are in orthogroups of that size or larger
GFF3	General Feature Format
GST	Glutathione S Transferase
h	hour(s)
HPC	High Performance Computing

hsp	heat shock protein family
IFN- γ	Interferon gamma
IgE	Immunoglobulin E
IgG	Immunoglobulin G
iL3	Infective larvae stage
IL-4/5	Interleukin
<i>in silico</i>	Pseudo-Latin for “in silicon”, i.e., performed on computer
ITS	Internal Transcribed Spacer
kg	kilogram
Kbp	kilo base pair(s)
Kmer	Sub-sequences of length k
L1	First larval stage
L2	Second larval stage
L3	Third larval stage
L4	Fourth larval stage
LF	Lymphatic filariasis
LINEs	Long Interspersed Nuclear Element(s)
LTR	Long Terminal Repeats
m	metre
MAFFT	Multiple Sequence Alignment program
Mb	Mega base
MDA	Mass Drug Administration
mf	Microfilaria/e
ml	Millilitre
mm	Millimetre
MSA	Multiple Sequence Alignment
mtDNA	Mitochondrial DNA
mtDNA	Mitochondrial Deoxyribonucleic acid
myoHC	myosin Heavy Chain
N50	Length for which the collection of all contigs of that length or longer contains at least 50% of the sum of the lengths of all contigs

N90	Length for which the collection of all contigs of that length or longer contains at least 90% of the sum of the lengths of all contigs
NCBI	National Center for Biotechnology Information
NAD/ND	Dehydrogenase subunit
ng	Nanogram
NGS	Next generation sequencing
NTD	Neglected Tropical Disease
NSW	New South Wales
O50	Smallest number of orthogroups that 50% of genes are in orthogroups of that size or larger.
OCP	Onchocerciasis Control Programme
<i>Ov</i>	<i>Onchocerca volvulus</i>
PAML	Phylogenetic Analysis by Maximum Likelihood
PIT	Passive integrated transponder
PCR	Polymerase chain reaction
PDB	Protein Data Bank
PE	Paired end
pM	Pico molar
PVC	Polyvinyl chloride
RAxML	Randomised Accelerated Maximum Likelihood
RBP	Retinol Binding Protein
rDNA	Ribosomal DNA
rpm	Revolutions per minute
RNA	Ribonucleic acid
rRNA	Ribosomal RNA
RNA-Seq	RNA sequencing data
s	Second(s)
Satellites	tandemly repeated sequences
<i>sensu lato</i>	Latin meaning “in broad sense”
SINEs	Short Interspersed Nuclear Element(s)
spp	species
TGF- β	Transforming Growth Factor beta
Th	CD4+ helper T cells
tRNA	Transfer Ribonucleic acid

μl	Micro litre
μM	Micro molar
US	United States
VIC	Victoria
W	Watt(s)
WHO	World Health Organisation

List of Bioinformatics Programs

Program	Function (publication or GitHub link)
Assembly stats v1.0.1	Statistics on genome assembly (https://github.com/sanger-pathogens/assembly-stats)
Augustus v3.0.2	Gene prediction (Stanke et al., 2008)
bedtools suite v2.26.0	Intersect, merge, count etc. files (Quinlan and Hall, 2010)
BLAST v2.6.0	Basic Local Alignment Search Tool NCBI
BRAKER v2.1.4	Gene prediction (Hoff et al., 2018)
BUSCO v4.0	Benchmarking Universal Single-Copy Orthologues (Simão et al., 2015)
Bwa v0.7.16a	Burrows-Wheeler Aligner (Li and Durbin, 2009)
CEGMA v2.4.010312	Core Eukaryotic Genes Mapping Approach (Parra et al., 2007)
Circos v0.67_5	Package for visualizing data and information (Krzywinski et al., 2009)
ClustalW v2.0.10	Multiple Sequence Alignment (Larkin et al., 2007)
Exonerate v2.2.0	A generic tool for pairwise sequence comparison (Slater and Birney, 2005)
FastQC	Quality control checks on raw sequence data (http://www.bioinformatics.babraham.ac.uk/projects/fastqc/)
Gblocks v0.91b	Selection of conserved blocks from multiple alignments (Talavera and Castresana, 2007)
Genome Ribbon	Visualising complex genome alignments and structural variation

(<https://github.com/MariaNattestad/Ribbon>)

InterProScan v5.24.63.0	A resource that provides functional analysis of protein sequences by classifying them into families and predicting the presence of domains and important sites (Jones et al., 2014)
Mesquite v3.04	A modular system for evolutionary analysis (Maddison and Maddison, 2008)
MITOS	Mitochondrial genome annotator (Bernt et al., 2013)
MrBayes v3.2.5	Bayesian inference and model choice (Ronquist et al., 2012)
OrthoFinder v2.2.7	Orthology prediction (Emms and Kelly, 2015, 2019)
PAML (GUI)	Phylogenetic Analysis by Maximum Likelihood (Xu and Yang, 2013; Yang, 2007)
PartitionFinder v1.1.1	Select best-fit partitioning schemes and models of molecular evolution for phylogenetic analyses (Lanfear et al., 2012)
progressiveMauve v20150213	Genome alignment (Darling et al., 2010)
PROmer v3.0.7	Rapid alignment of very large DNA and amino acid sequences (Kurtz et al., 2004)
RAxML v 8.0.19	Randomized Accelerated Maximum Likelihood (Stamatakis, 2006, 2014)
RepeatMasker 4.0.5	Screens DNA sequences for interspersed repeats and low complexity DNA sequences (Smit, 2015)
RepeatModeler v1.0.11	De novo transposable element (TE) family identification and modeling package (Saha et al., 2008)

SPAdes v3.10.1	Genome assembler (Nurk et al., 2013)
Trimmomatic v0.32	A flexible read trimming tool for Illumina NGS data (Bolger et al., 2014)
Velvet v1.2.10	Genome assembler (Zerbino, 2010)
Velvet-optimiser v2.2.5	Multi-threaded Perl script for automatically optimising Kmer for Velvet (Zerbino and Birney, 2008)

Abstract

Onchocerciasis is a neglected tropical disease in sub-Saharan Africa, caused by the parasitic filarial nematode *Onchocerca volvulus*. Host immune responses to the presence of dead or dying microfilariae in the skin and eyes drive the pathology associated with onchocerciasis, which is not well understood. An animal model that recapitulates the immunopathology could promote the improvement of current treatments for onchocerciasis, helping to develop new strategies to improve control of the parasite. Rodent infection with *Cercopithifilaria johnstoni*, a filarial nematode with skin and eye dwelling microfilariae, provokes similar skin and eye inflammatory pathology to *O. volvulus*-infected individuals, and therefore, has been proposed as an immunologically relevant model of the human disease. The aim of this thesis was to develop and characterise the genetic resources for *C. johnstoni* in the context of developing a resource to better understand onchocerciasis caused by *O. volvulus*. While some genetic resources are available for other closely-related filarial nematodes, none exist for *C. johnstoni*. First, a draft genome and mitochondrial genome were constructed for *C. johnstoni* and compared with *O. volvulus* and other filarial nematodes to confirm genetic similarity and to position *C. johnstoni* in the filarial nematode phylogeny. Second, the similarity in immunopathology between these two related parasites raises the question of whether similar antigens are responsible for the similarities in immune responses directed against the two species. To address this, an *in silico* approach to determine the suitability of *C. johnstoni* in a small animal model reveals orthologous genes between *C. johnstoni* and *O. volvulus* from known experimentally derived *O. volvulus* immunogenic proteins. Evidence of conserved protein structure and functions and evidence of diversifying and purifying selection on various orthologous genes could indicate the potential for these genes to be essential to the parasites or be involved in disease pathology. Finally, the vector species of *C. johnstoni*, the *Ixodes* ticks, were characterised which showed that ticks have cryptic species diversity complexes. This work is the first genome characterisation of *C. johnstoni* and genomic comparison with *O. volvulus* in the context of developing a model parasite to study onchocerciasis.

Statement of authorship

This thesis includes work by the author that has been published or accepted for publication as described in the text. Except where reference is made in the text of the thesis, this thesis contains no other material published elsewhere or extracted in whole or in part from a thesis accepted for the award of any other degree or diploma. This thesis has not been submitted for the award of any degree or diploma in any other tertiary institution.

No other person's work has been used without due acknowledgement in the main text of the thesis or as listed below:

Chapter Five: Collection and morphological characterisation of voucher *Ixodes* species used in the phylogenies were kindly provided by Dr David Spratt.

Kirsty McCann

Date:

14/08/2020

This work was supported by an Australian Government Research Training Program Scholarship and a La Trobe University Postgraduate Research Scholarship (LTUPRS).

All research procedures reported in the thesis were approved by the Animal Ethics Committee (AEC), La Trobe University animal ethics approval AEC 13–23 and New South Wales Scientific License 5 L 101280 and Victorian Scientific Permit 10007169.

Chapter Five consists of research published in the International Journal of Parasitology (IJP): Parasites and Wildlife:

McCann, K.M., Grant, W.N., Spratt, D.M., Hedtke, S.M. (2019). Cryptic species diversity in ticks that transmit disease in Australia. *International Journal for Parasitology: Parasites and Wildlife* 10, 125-131.

Acknowledgements

There are several people I would like to acknowledge that have played a significant role in supporting me throughout my PhD journey.

Firstly, my supervisor, Associate Professor Warwick Grant, thank you. It has been a memorable experience to be part of your nematode genetics lab. I am so grateful for being able to learn and grow as a researcher from you and be given perspectives on research that I would not have seen on my own. You have taught me a lot (especially writing structure), and I'll forever be grateful that you gave me this opportunity.

Thank you to Dr Shannon Hedtke for her support and pep talks but most importantly reassuring me that I do in fact know what I am doing even when I think I do not know anything. Thank you for your support, Shannon.

A very special thanks goes to Dr Stephen Doyle. I cannot possibly thank you enough for everything you have done for me. You have been a huge support and consistently reassure me when I'm panicking and feel like I have failed. I have learnt so much from you from bioinformatics, new programs to play with, to writing and communication skills. Your attention to detail and constructive criticism will forever be appreciated. Thank you for all your advice, I appreciate it so, so much!

I am eternally grateful for my friendship support team throughout my PhD. I am ever so thankful that I am lucky enough to have a group of friends all at different stages of our PhD's to vent over endless coffee dates and maintain some sort of normality throughout very stressful times. There is no way I would have got through the challenging times without the girl squad. More specifically, Suzannah, Ellen and Lauren— thank you ever so much for being the most amazing best friends. I have been ridiculously difficult for the last four years, and you haven't once left my side. Could not have asked for better support, you are amazing!

A general thank you is warranted to all my friends and family. I have been over-stressed, forgetful, broke, blunt and generally distant. I promise I will make up the lost time with all. Thank you for supporting me.

Lastly and most importantly, this is a perfect opportunity to put into words my sincerest gratitude for the support of my parents and partner Adrian throughout my PhD journey. I can't possibly say thank you enough to express how much I appreciate you putting up with me. I understand I'm a stress head and appreciate you supporting me in the ways you know how. I love you all!

Thank you all so much!

Publications

Journal Paper

McCann, K.M., Grant, W.N., Spratt, D.M., Hedtke, S.M. (2019). Cryptic species diversity in ticks that transmit disease in Australia. *International Journal for Parasitology: Parasites and Wildlife*, 10, 125-131

Conference abstracts

Poster, “Orthologues of the immunodominant antigens of *Onchocerca volvulus* in the rodent onchocerciasis model *Cercopithifilaria johnstoni*”, Parasitic Helminths: New Perspectives in Biology and Infection, Hydra, Greece, 1-6th Sept 2019.

5 min Presentation, “Orthologues of the immunodominant antigens of *Onchocerca volvulus* in the rodent onchocerciasis model *Cercopithifilaria johnstoni*”, Australian Parasitology Conference (ASP), 8-11th July 2019.

5 min Presentation, “Analysis of the *Cercopithifilaria johnstoni* mitochondrial genome and the genetic diversity compared with related filarial nematodes,” Australian Parasitology Conference (ASP), 24-27th Sept 2018.

Poster, “Analysis of the *Cercopithifilaria johnstoni* mitochondrial genome and the genetic diversity compared with related filarial nematodes,” Australian Parasitology Conference (ASP), 24-27th Sept 2018.

Presentation, “Development of the filarial nematode *Cercopithifilaria johnstoni* as a model system for onchocerciasis,” AgriBio Conference, 7-8th Nov 2018.

Presentation, “Cryptic species diversity in ticks that transmit disease,” TTP9-APRC1 Conference, 27-1st Sept 2017.

Presentation, “A small animal model bridging the gap between *in vitro* assay and human testing for drug development in onchocerciasis,” AgriBio Conference, 20-21st Oct 2016.

Poster, “Towards developing an animal model for testing anthelmintics on microfilarial nematodes,” Anthelmintics – Discovery to resistance II, 9-12th Feb 2016.

Chapter One

General Introduction

The focus of the following literature review is to provide foundation of knowledge on filarial nematodes and filarial disease and identify the gaps in the current body of literature. The thesis aims to address the question of developing a small animal model using a closely related filarial species that is amenable to research and further understand a complex, neglected disease.

1.1 Helminths

Helminths are incredibly diverse and are responsible for significant disease and mortality in numerous hosts (Grencis, 2015). Consequently, helminths have been a significant focus of human and veterinary research. They are a group of parasites that is highly successful at challenging the hosts' immune system. Helminth infections result in years of chronic inflammatory disorders causing consistent, ongoing, or delayed-onset pathology to their human or animal host (Budke et al., 2005; Bethony et al., 2006). For instance, parasitic nematodes such as *Haemonchus contortus*, a gastrointestinal parasite of ruminants, have had a significant and detrimental impact on the health and economic productivity in livestock worldwide (Qamar et al., 2011; Selemon, 2018). Currently, control of several helminths relies heavily on large-scale administration of anthelmintic drugs, including ivermectin from the macrocyclic lactone class (Omura and Crump, 2004; Geary and Moreno, 2012).

There are two major phyla of helminths. First are the nematodes that include soil-transmitted helminths and the filarial worms, and second are the platyhelminths that include flukes and tapeworms (Hotez et al., 2008). The focus of this thesis is within the Phylum Nematoda, which constitutes a diverse group of nematodes inhabiting a broad range of environments (Blaxter and Bird, 1997; Blaxter and Koutsovoulos, 2015). The classification of nematodes has changed frequently because of various phylogenetic approaches. The current view of nematodes is illustrated in Figure 1.1 (Smythe et al., 2019). Parasitism has evolved independently at least 15 times, based on molecular phylogenetic

analysis, to give rise to several groups of animal and plant parasites interspersed with their non-parasitic relatives (Blaxter and Koutsovoulos, 2015). Within Nematoda, parasitism has arisen independently in different groups of nematodes at different times throughout history, thus complicating the phylogenetic relationships. The current view of Phylum Nematoda consists of 15 classifications, all of which have both non-parasitic and parasitic species (Figure 1.1) (Smythe et al., 2019).

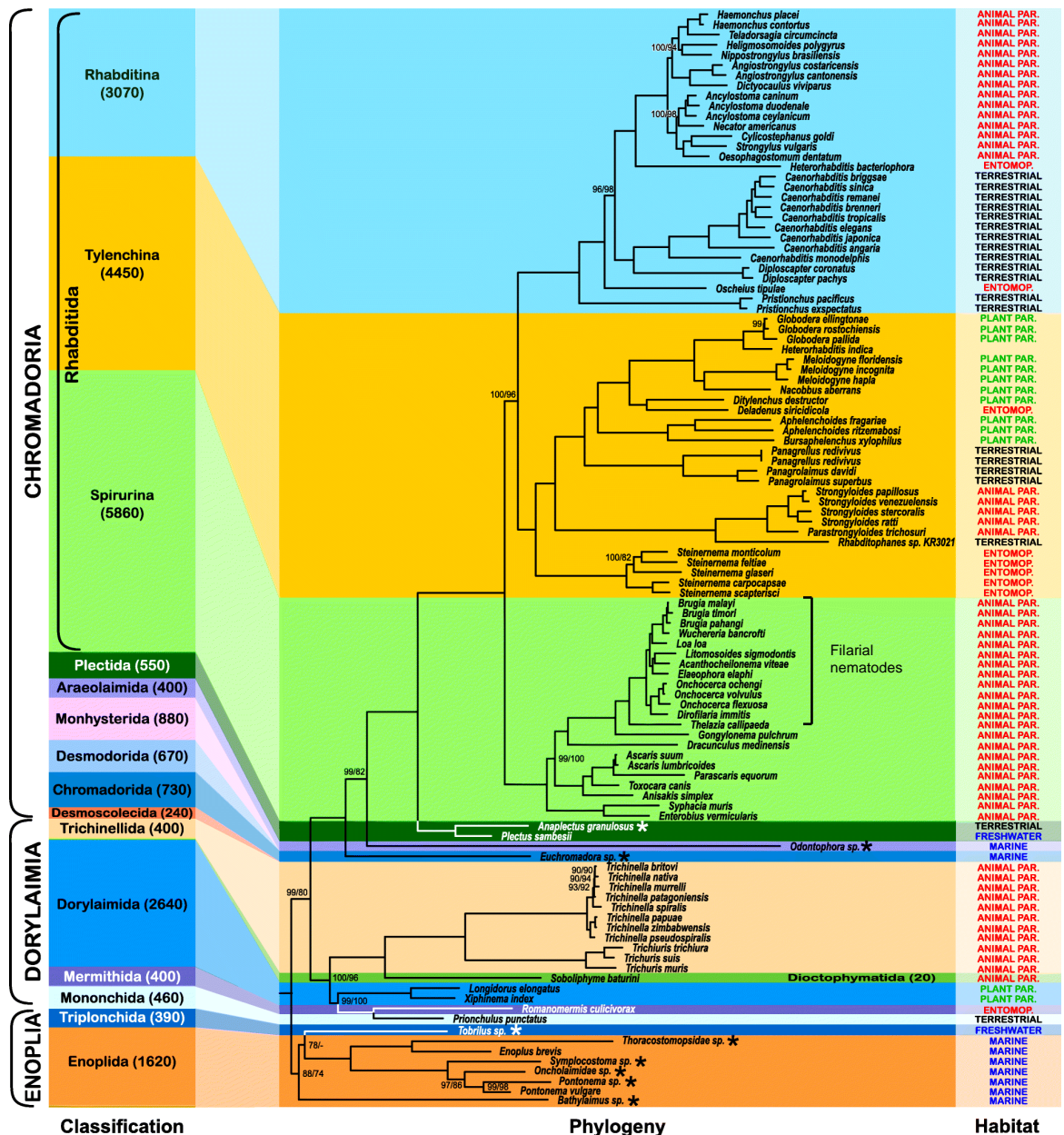


Figure 1.1: Phylogeny of Nematoda based on the IQ-TREE maximum likelihood analysis (Smythe et al., 2019). Classification bar represents known taxonomic diversity of different taxa within Neamtoda. Habitat describes the lifestyle for each analysed species. Newly generated transcriptomes are marked with an asterisk (Smythe et al., 2019). The figure has been amended to outline the filarial nematodes within the Spirurina classification.

1.2 Filarial nematodes

One of the 15 classifications within the Phylum Nematoda of particular focus for this thesis is Spirurina (Figure 1.1). Within this classification there are a group of filarial nematodes that are parasites of either vertebrates or invertebrates that commonly impact animal and human health (Stoltzfus et al., 2017). The remainder of this thesis will focus on filarial nematode relationships within Spirurina and filarial genomics. Filarial nematodes include *Acanthocheilonema viteae*, *Brugia malayi*, *Brugia pahangi*, *Brugia timori*, *Dirofilaria immitis*, *Dirofilaria repens*, *Dirofilaria hongkonensis*, *Loa loa*, *Litomosoides sigmodontis*, *Onchocerca flexuosa*, *Onchocerca gibsoni*, *Onchocerca cervipedes*, *Onchocerca lienalis*, *Onchocerca ochengi*, *Onchocerca volvulus* and *Wuchereria bancrofti*. Filarial nematodes have specialised biology which improves their ability to parasitise their hosts (Blaxter and Bird, 1997; Bain, 2002). They can increase their developmental speed and reproduce earlier in response to environmental factors. They have a range of intermediate hosts, including haematophagous arthropods, which are needed for life stage maturation and parasitic development (Blaxter and Bird, 1997). Intermediate hosts act as vectors for transmission of filarial parasites to their hosts (Bain, 2002).

Filarial diseases affect humans and animals worldwide at varying severities and are of significant concern in developing countries (Bandi et al., 1998; Blaxter et al., 2012). More than 150 million people throughout tropical or subtropical countries are infected with filarial parasites (Fischer et al., 2011; Grote et al., 2017), however, infected numbers are subjected to change year-by-year. Large human populations in developing countries are affected by a range of filarial diseases (Barry et al., 2016). The primary filarial nematodes responsible for infecting human hosts include *W. bancrofti*, *L. loa*, and *O. volvulus*, together infecting millions of people (Taylor et al., 2014). For example, more than 10 million people are affected with loiasis caused by *L. loa* infection (Klei and Rajan, 2002; Desjardins et al., 2013a; Whittaker et al., 2018), and greater than 120 million people are infected with lymphatic filariasis caused by *W. bancrofti* (Taylor et al., 2010; Grote et al., 2017).

The World Health Organisation (WHO) characterises these three major filarial diseases, loiasis, lymphatic filariasis and onchocerciasis as Neglected

Tropical Diseases (NTDs). Typically, neglected diseases are situated in the tropics in the poverty-stricken areas, rural areas and the most deprived communities of the world's population (Rodrigues and Ersching, 2015). NTDs have been neglected by research, as a result of minimal funding, corrupt governments, because the diseases are endemic in areas or countries that are difficult to access, or because the chronic nature of the NTDs have led to a lack of prioritisation (Klei and Rajan, 2002). Anthelmintic drugs are often used to treat filarial disease but have not been successful at eliminating the parasite. In some cases, they do not effectively kill the adult parasites, which increases treatment complexity, i.e., in onchocerciasis (Osei-Atweneboana et al., 2012; Doyle et al., 2017).

A particularly interesting group of filarial nematodes within the clade III Spirurida is the Onchocercidae genera that encompass *O. volvulus*, *L. loa* and *W. bancrofti*. Onchocercidae genera can be divided into three strongly supported clades ONC3 to ONC5 based on concatenated datasets including 12S rDNA, *cox1*, *rbp1*, *hsp70*, *myoHC*, 18S rDNA, and 28S rDNA (Figure 1.2) (Lefoulon et al., 2015). ONC3 consists of *Dirofilaria*, *Loxodontofilaria* and *Onchocerca*. ONC4 is composed of *Dipetalonema*, *Acanthocheilonema*, *Monanema*, *Cercopithifilaria* and *Litomosoides*. Lastly, ONC5 is composed of *Loa*, *Wuchereria* and *Mansonella* (Figure 1.2). These three clades (e.g., ONC3, ONC4, ONC5) have life cycles that involve an L3 infective stage (iL3) and transmission by arthropod vectors.

1.3 Onchocerciasis

Onchocerciasis, more commonly known as 'river blindness', is an ocular and dermatological disease, primarily affecting individuals in sub-Saharan West Africa and Central Africa (Taylor et al., 2010; Cheke and Garms, 2013). Dermatitis and blindness typically characterise the disease (Pearlman and Hall, 2000). The filarial parasitic nematode causing onchocerciasis is, *O. volvulus*, and is transmitted by the black fly, *Simulium damnosum* (Tang et al., 1996; Adler et al., 2010; Taylor et al., 2010; Cheke and Garms, 2013). The term river blindness originates from the location at which the *Simulium* vector breeds, i.e., near fast-flowing rivers and streams. Humans living adjacent to rivers of fast-flowing water

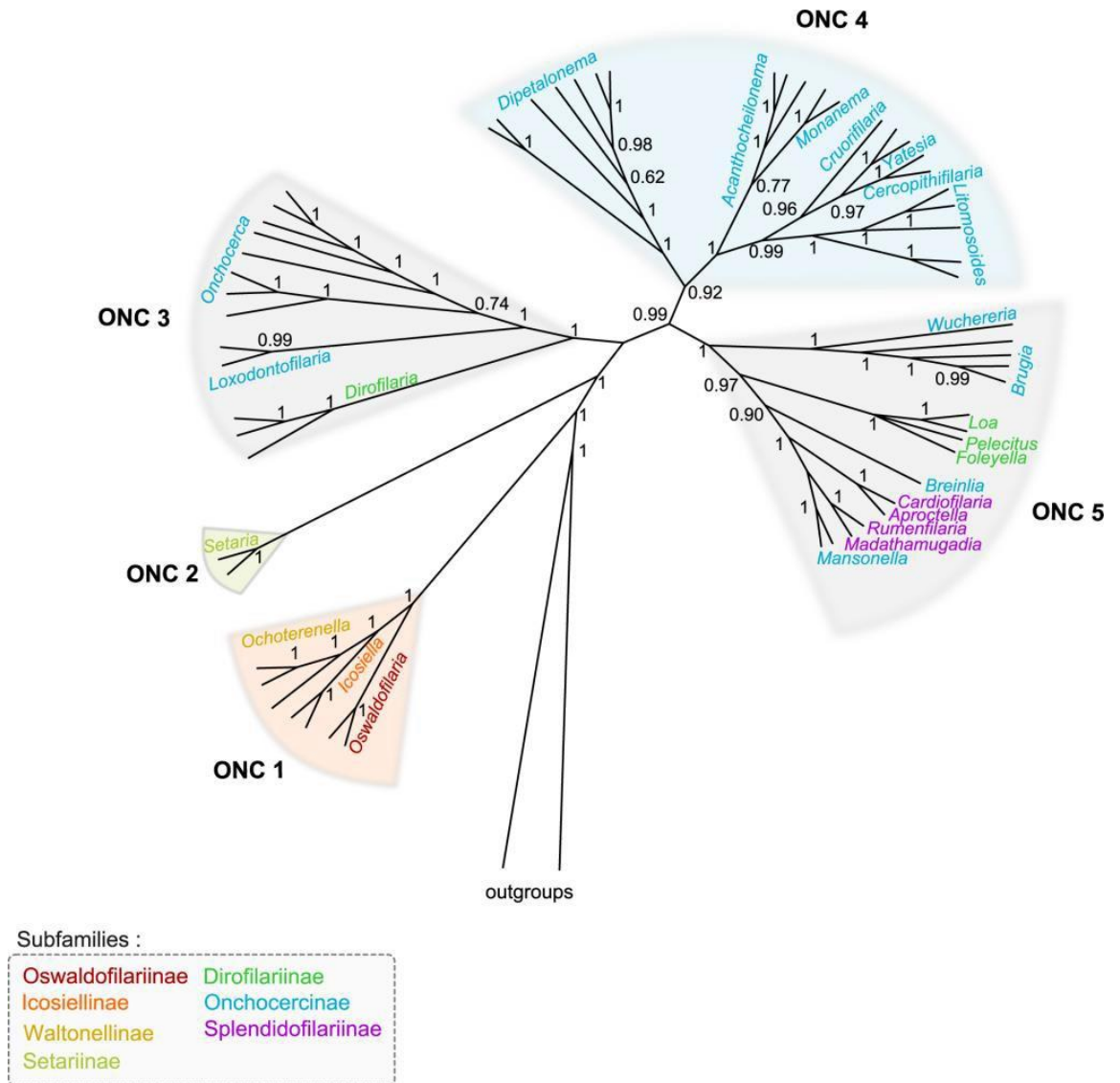


Figure 1.2: Onchocercid clades from concatenated datasets of 12S rDNA, cox1, rbp1, hsp70, myoHC, 18S rDNA, and 28S rDNA sequences (Lefoulon et al., 2015).

and in endemic areas have a higher disease burden than those living in non-endemic areas with fewer *Simulium* flies (Taylor et al., 2010).

Onchocerciasis is a human NTD posing significant public health and economic interest. Approximately 217.5 million people are present in areas known to be endemic for onchocerciasis and therefore at risk to contract the disease (World Health Organisation, 2019).

The economic and social impact of onchocerciasis has been estimated at 598,270 disability-adjusted life years (DALYs) (Wolstenholme et al., 2016). Surveillance of onchocerciasis in the 1970s in Africa demonstrated the socioeconomic implications were highly problematic. There were only a small proportion of abled people to work in these communities; thus, food shortages occurred, and overall economic losses led to entrenched poverty (Amazigo et al., 2006). The WHO has implemented programs intending to eliminate the disease, such as the Onchocerciasis Control Program (OCP) and the African Programme to Eliminate Onchocerciasis (APOC) (discussed in section 1.6).

The presence of *O. volvulus* does not directly cause symptoms of onchocerciasis, but instead, is caused by the hosts' immune responses to the death of the parasites (Ottesen, 1985). Symptoms include (1) mild itching from the microfilariae residing in the subcutaneous layers of tissue, (2) the appearance of leopard skin caused by the depigmentation of the skin as a result of prolonged localised immune responses, (3) thickening and deep scarring of the skin from the same chronic localised inflammation and, (4) visual impairment leading to blindness as a result of the immune responses to the presence of dead microfilariae in the cornea (Connor et al., 1970; Omura and Crump, 2004; Allen et al., 2008; Feasey et al., 2009; Cheke and Garms, 2013). The movement of microfilariae throughout the host is responsible for these disease symptoms (Debrah et al., 2015). The important aspect of onchocerciasis is how the microfilariae cause immunopathology by triggering the host immune response to the dying parasites. The immunopathology is not well understood and currently there are no animal models to safely study how the dying microfilariae trigger these symptoms and responses. The immunopathology of infection (to be discussed throughout this thesis) is the major feature of onchocerciasis and why it is important to develop an animal model with similar immunopathology.

The life cycle of *O. volvulus* begins when a female *Simulium* fly bites and feeds on the blood of a human (Figure 1.3). The blackfly ingests the microfilariae. The microfilariae then penetrate the midgut and migrates to the thoracic muscles where they develop into their first juvenile stage (L1). The L1's then mature into the second juvenile stage (L2) followed by maturity into the infective L3 larval stage (iL3). The iL3's migrates to the proboscis and are found in the saliva. Once the fly bites another human the iL3's move through the bite wound into the subcutaneous tissue where they mature into adult worms in nodules (Connor et al., 1970; Omura and Crump, 2004). The adult male and female worms produce unsheathed microfilariae (L1). The microfilariae migrate around the subcutaneous tissue causing skin lesions and depigmentation (Centers for Disease Control and Prevention, 2015). Should another *Simulium* fly come and bite an infected human and ingest the microfilariae, the life cycle will continue (Omura and Crump, 2004). The adult worms can live anywhere from 10 to 15 years, and microfilariae can live for nine to 18 months (Basáñez et al., 1994; Omura and Crump, 2004; Coffeng et al. 2013). Female worms can vary from 33 to 50 cm in length, males from 19 to 42 cm, while the microfilariae only reach 220 to 360 μm in length (Centers for Disease Control and Prevention, 2015).

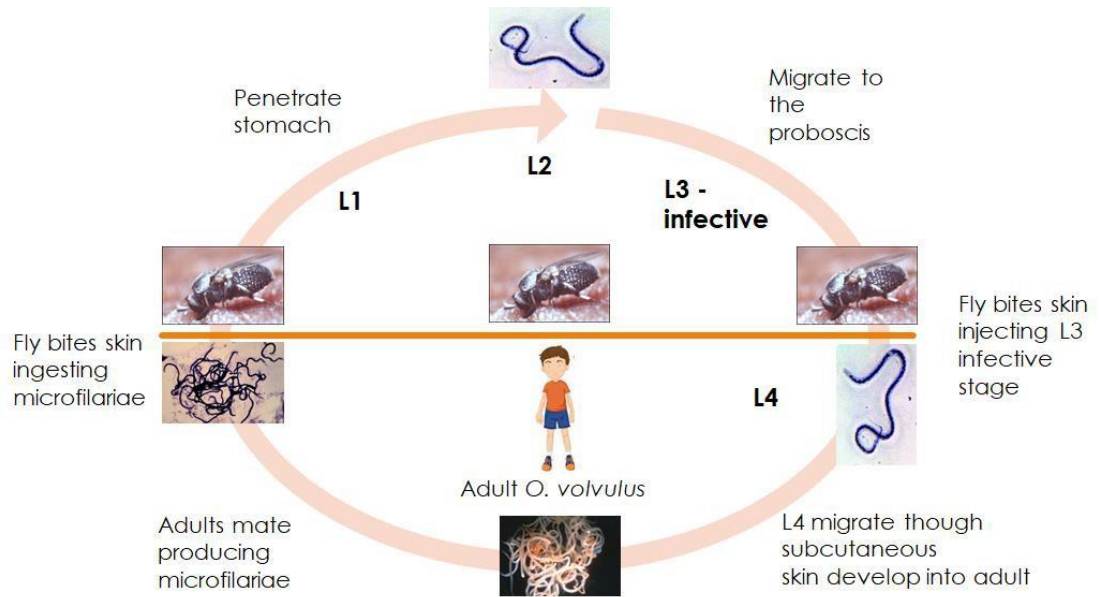


Figure 1.3: *Onchocerca volvulus* life cycle adapted from Centers for Disease Control and Prevention (2015).

The general life cycle of *S. damnosum* (Figure 1.4) begins when a female fly deposits approximately 200 to 800 eggs on vegetation located just below the water's surface (Butler and Hogsette, 1998). Larvae then emerge from the eggs and mature through six consecutive stages before reaching the pupal stage, where the cocoon shaped pupae are attached to vegetation (Figure 1.4). Adults then emerge from the pupal case and float to the water's surface after a period of two to three weeks (Butler and Hogsette, 1998). *Simulium* species are attracted to bite humans through olfactory senses and heat (Butler and Hogsette, 1998). Once a *Simulium* fly bites an infected human, they ingest *O. volvulus* (Taylor et al., 2010; Chandy et al., 2011; Cheke and Garms, 2013) allowing continuous transmission from person to person spreading the infection throughout communities (Connor et al., 1970). *Simulium* species also feed on animals and thus *Simulium* could be exposed to a variety of different parasites humans would not typically contain (Adler et al., 2010). Consistent with other filarial nematodes, *O. volvulus* requires an intermediate host stage such as *S. damnosum* to develop through the parasitic life stages.

The *O. volvulus* nematode contains a widespread bacterial endosymbiont, *Wolbachia* (Bandi et al., 1998; Brattig, 2004; Comandatore et al., 2015). *Wolbachia* is an obligate mutualistic endosymbiont that is transmitted transovarially (Tamarozzi et al., 2011; Pigeault et al., 2014). The *O. volvulus* parasite and *Wolbachia* have a symbiotic relationship indicating that *Wolbachia* may increase the fitness of the parasite, which is a challenge in itself to understand. The genus of *Wolbachia* is polyphyletic and has been a controversial and complex group for taxonomy (Bandi et al., 1998; Casiraghi et al., 2004; Comandatore et al., 2015). It has been suggested that *Wolbachia* molecules interact with the host's innate immune system and are responsible for inflammatory reactions seen in *O. volvulus*-infected individuals (Bandi et al., 1998; Tamarozzi et al., 2011). *Wolbachia* has become a focus for further drug developments as it is understood to play an essential part in filarial nematode reproduction (Bandi et al., 1998). There is a potential for *Wolbachia* to be the driving force behind the immune responses seen in onchocerciasis, but more analyses are required to confirm this hypothesis by identifying what is driving the immunopathology. *Wolbachia* has been identified in a range of filarial nematodes and arthropods and is currently being studied extensively to understand what role the endosymbiont plays in the individual host. The following thesis is not focused

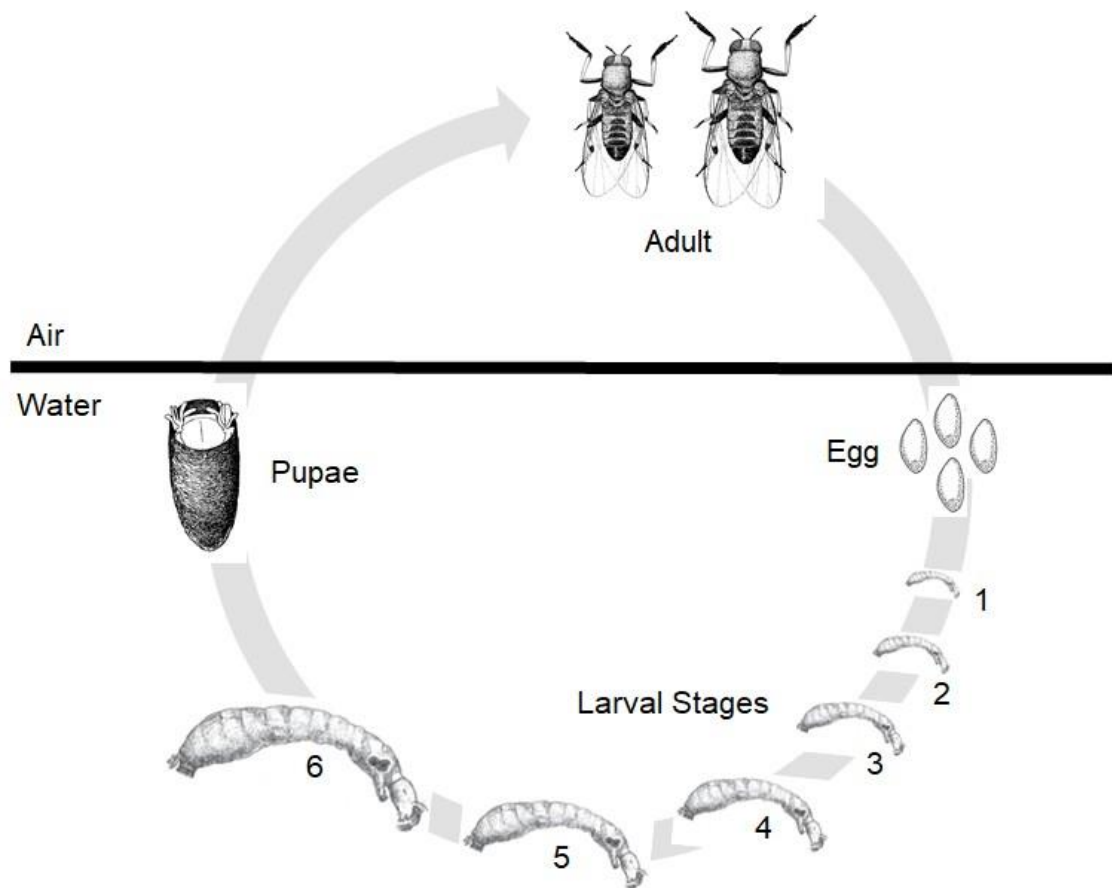


Figure 1.4: *Simulium damnosum* life cycle adapted from Service (2012).

on exploring *Wolbachia*, however, it is acknowledged to be an important component of onchocerciasis research which raises questions that alternate projects should aim to address.

The lack of understanding of the hosts' responses to the presence and death of microfilariae complicates all future treatment development and programmes. There are challenges associated with finding effective macrofilaricidal and microfilaricidal drugs to treat a sizeable, infected population. Understanding the human immune responses to the parasite is critical for not only diagnosis but a successful treatment regime (Ottesen, 1984; Grote et al., 2017; Tyagi et al., 2019b). *O. volvulus* is an obligate human parasite, and its life cycle is unable to be maintained alive outside a host species (Grote et al., 2017), making the study of this parasite in the laboratory more challenging. Thus, the development of appropriate treatment methods becomes a significant challenge. A system where we can observe the parasite in the laboratory would significantly increase our knowledge of *O. volvulus* as well as filarial nematodes in general (Grote et al., 2017).

1.4 Established drugs used for the treatment of onchocerciasis

There are several anthelmintic (e.g., diethylcarbamazine) and antibiotic (e.g. tetracycline) drugs trialled for the treatment of onchocerciasis. One successful group of anthelmintic drugs is the macrocyclic lactone filaricidal drugs (ivermectin and moxidectin). Macrocyclic lactones are a significant group of anthelmintics and are currently the most effective drugs of choice available with exceptional potency (Campbell, 1981; Wolstenholme and Rogers, 2005). These anthelmintics are currently the most important and commonly used control measures for parasite control across both livestock and human infections (Lespine et al., 2008). Every filaricide has advantages and disadvantages that need to be considered to determine whether the drug will be successful or unsuccessful in treating the disease.

1.4.1 Ivermectin

Ivermectin has been the predominant drug of choice for many years since its registration for human use in 1987 as Mectizan (Thylefors, 2008; Cupp et al.,

2011; Coffeng et al., 2013; Turner et al., 2013). Ivermectin was first used for treatment in some regions of Africa in 1988 and has since established the appropriate standards of cost, efficacy, and safety for Mass Drug Administration (MDA) treatment of onchocerciasis (Thylefors, 2008; Diawara et al., 2009). A dose of 150 µg/kg effectively kills microfilariae in the skin from four to six months after treatment (Table 1.1) (Awadzi et al., 1985). It can kill up to 99% of the microfilariae in a single treatment highlighting ivermectin's efficacy (World Health Organisation, 2010). Treatment is required for up to 15 years or possibly longer to remove the parasites from the body (Awadzi et al., 2004; Turner et al., 2013; Hess et al., 2014; Turner et al., 2014).

Ivermectin is a successful microfilaricidal drug but is not a successful macrofilaricidal drug as the adult parasites remain mostly unaffected (Diawara et al., 2009; Turner et al., 2013; Turner et al., 2014; Turner et al., 2015b). For a period after treatment, the adult worms are affected reproductively, but fertility returns (Eng and Prichard, 2005; Gyapong et al., 2005; Bourguinat et al., 2006). Nevertheless, elimination of onchocerciasis in areas of Africa using ivermectin treatment is feasible (Diawara et al., 2009). In some areas of Africa, onchocerciasis has been successfully eliminated using ivermectin treatment. The programmes that initiated drug treatment have since closed reducing targeted onchocerciasis treatment regimens throughout Africa thus onchocerciasis is still a concern throughout Africa.

Ivermectin treatment has usage limitations. It is not suitable for pregnant women, children under the age of five years old or individuals with central nervous system diseases or hypersensitivities (Fox, 2006). Ivermectin elicits slight adverse effects on patients when the microfilariae die in the skin (Keiser et al., 2002). Symptoms such as light-headedness, fever or worst-case postural hypotension (Gyapong et al., 2005). Despite these disadvantages, ivermectin has been a safe and excellent drug choice for onchocerciasis treatment.

Ivermectin's mechanism of action possibly involves the opening of glutamate-gated chloride ion channels of nematode neurons impairing their normal function (Wolstenholme and Rogers, 2005), however this has not been proven at the molecular level in *O. volvulus* or in filarial nematodes. The biological effect of ivermectin on *O. volvulus* is not clear and has not been explored. In *B. malayi*, ivermectin was found to inhibit protein release from the excretory-

secretory apparatus (Moreno et al., 2010). Ivermectin causes a rapid microfilarial clearance which could be due to the parasite not being able to secrete proteins that avoid exposure to the host's immune system (Moreno et al., 2010). In another *B. malayi* study, it was observed that there was a high level of expression of glutamate-gated chloride channels in the reproductive tissues (Li et al., 2014). The high expression of glutamate-gated chloride channels could explain the lack of microfilariae following ivermectin treatment (Li et al., 2014). Although these experiments have used *B. malayi*, it could be presumed that a similar response occurs within *O. volvulus* parasites treated with ivermectin.

Figure 1.5 summarises the effect of a single, standard dose of ivermectin on the *O. volvulus* microfilariae from several studies (Basáñez et al., 2008). The y-axis shows 'Percentage of pre-treatment GM microfilarial load' with the x-axis displaying time in months. The figure taken from Basáñez et al., (2008) explores results from 15 publications focussing on ivermectin treatment of *O. volvulus* with various sample sizes. The coloured dots represent different datasets from the list of 15 publications. Consistently, ivermectin treatment results in an initial, drastic reduction of microfilarial loads by approximately 98% in the first week of treatment (Figure 1.5). Microfilarial repopulation of the skin then begins to occur slowly from about three months remaining below 20% of their initial microfilarial load for around ten months after the single ivermectin dose. Without another treatment of ivermectin, the microfilarial load continues to increase 12 months after the individuals were treated (Figure 1.5) (Basáñez et al., 2008). Patients with onchocerciasis would require ivermectin treatment biannually or quarterly to eliminate any possibility of new parasite transmission (Collins et al., 1992; Cupp and Cupp, 2005). It has been suggested that by increasing the number of ivermectin treatments could increase the infertility effects on adult female *O. volvulus*, which then reduces the production of more microfilariae (Duke, 2004; Cupp and Cupp, 2005). After frequent treatments, it could be possible to break the transmission cycle for *O. volvulus* within 10 to 14 years (Taylor et al., 2014). Breaking the transmission cycle would require regular MDA and continuous monitoring of individuals' disease burdens. Aiming to break the transmission cycle appears to be an efficient method of controlling onchocerciasis that does not rely on understanding the complex immunopathology associated with disease symptoms. It also means that treatment does not need to be macrofilaricidal but instead targeting the crucial life stages involved in disease transmission to

interrupt the cycle. The process will take years to successfully interrupt transmission and reduce disease burdens leading toward elimination. Alternative plans will need to be devised to achieve elimination. Elimination is to reduce transmission of the parasite below a designated level where the parasite persists with low level transmission in the community but is low enough that infection rates will not increase. The success of ivermectin treatment is dictated by the epidemiological context, i.e., solely using ivermectin in areas of hyper-endemicity will not successfully remove *O. volvulus* (Stolk et al., 2015). The infection levels and transmission rate in these areas are too high for ivermectin alone, to be successful (Stolk et al., 2015). Mathematical modelling has shown that a macrofilaricidal drug will have a significant impact on treating disease in these areas. Using a macrofilaricidal drug with a stronger microfilaricidal drug than ivermectin, also shows a significant treatment impact (Basáñez et al., 2016). Thus the question of how to discover new drugs, either macrofilaricidal or more sensitive microfilaricidal targets, remains. An animal model will allow further discovery of successful drugs that follow this mathematically modelling and can target these hyper-endemic regions.

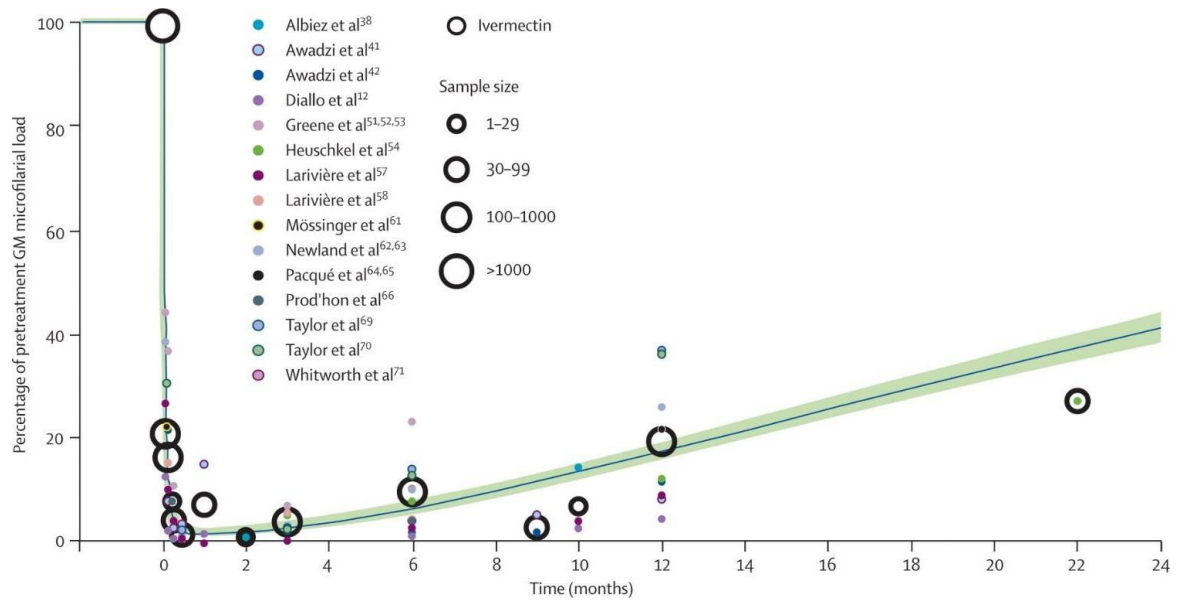


Figure 1.5: *Onchocerca volvulus* microfilarial load over time after a single, standard dose of ivermectin (150 µg/kg) (Basáñez et al., 2008).

Other possible drugs have been explored to determine whether they also meet the appropriate cost, efficacy, and safety standards for MDA treatment of onchocerciasis.

1.4.2 Diethylcarbamazine

Diethylcarbamazine (DEC) has been used since 1940 and is an effective drug for rapidly eradicating microfilariae from the host (Table 1.1). Diethylcarbamazine cannot kill adult worms, thus is a microfilaricidal drug (Ottesen, 1984; Stingl et al., 1984). It is absorbed rapidly after oral administration, but the mechanism of action against the filariae is unknown (Gyapong et al., 2005). Diethylcarbamazine is an affordable drug proven to be effective at killing the microfilariae and has been used extensively to treat lymphatic filariasis patients (Ottesen, 1984; Stingl et al., 1984). However, diethylcarbamazine is an unsafe alternative because although it meets the critical standards of cost and efficacy, it does not meet the safety requirements for MDA treatment of onchocerciasis.

Symptoms of diethylcarbamazine administration without *O. volvulus* microfilariae in the body consist of drowsiness, headache, nausea, and vomiting (Dreyer et al., 1994). Symptoms of diethylcarbamazine for those who have an *O. volvulus* microfilariae burden consist of dizziness, headache, fever, muscle pain and blood in the urine (Dreyer et al., 1994). Increased inflammation has been observed in those patients who had additional ocular lesions (Stingl et al., 1984). In some cases, these adverse side-effects have caused death if the patient had a high microfilarial burden (Stingl et al., 1984). Accordingly, diethylcarbamazine should be used with caution and not be used regularly for treatments of onchocerciasis because of the severe adverse effects of the Mazzotti reaction (discussed further in section 1.5) (Stingl et al., 1984). Diethylcarbamazine will, therefore, never be used as a solution to treat onchocerciasis but could be useful for other diseases or purposes.

1.4.3 Doxycycline

A macrofilaricidal or chemotherapeutic method with long-term sterilising effects would be an ideal outcome for the treatment of onchocerciasis (Table 1.1)

(Debrah et al., 2015). Doxycycline has been proven to target the adult *O. volvulus* worms and is considered a successful macrofilaricidal drug that has also been able to deplete *Wolbachia*, the bacterial endosymbiont of *O. volvulus* (Taylor et al., 2014; Walker et al., 2015). Various community-based trials have concluded that doxycycline would be a successful drug for MDA and is ideal to use for treatment in *L. loa* co-infected areas (Tamarozzi et al., 2012; Debrah et al., 2015). Doxycycline is known to target the bacterial endosymbiont, *Wolbachia*, which has been proven by using the chemotherapy treatment on patients infected with *L. loa*. The chemotherapy treatment does not negatively affect loiasis patients because *Wolbachia* is absent from *L. loa* nematodes (Wanji et al., 2009; Turner et al., 2010; Debrah et al., 2015). Overall parasite burdens have been drastically reduced in many doxycycline trials (Hoerauf et al., 2003; Hoerauf et al., 2008; Tamarozzi et al., 2012; Debrah et al., 2015; Specht et al., 2018; Taylor et al., 2019).

Further research is required to obtain MDA approval of doxycycline for endemic African regions with onchocerciasis. Doxycycline is not safe for pregnant women or children under the age of nine (Hoerauf, 2008; Tamarozzi et al., 2012). There needs to be further research conducted on how to include these groups in treatment. The earlier drug trials have also not identified the drug uptake into *O. volvulus* nodules in humans. The drug must be able to access the parasites deep in the subcutaneous skin within these nodules. Although this has been successful in rodent models, trials are needed in humans to understand the process (Taylor et al., 2019). Finally, there is not a clear correlation between drug dose and the duration at which the dose is to be provided to the infected individuals, a relationship that needs to be ascertained before confirming the success of doxycycline treatment for onchocerciasis (Taylor et al., 2019). Doxycycline is potentially a safe alternative to ivermectin except for children and pregnant women; however, it has practicality issues due to the long duration of treatment that could result in compliance issues and therapeutic coverage (Wanji et al., 2009).

1.4.4 Moxidectin

Moxidectin is a promising microfilarial drug for the control and elimination of onchocerciasis (Table 1.1) (Turner et al., 2015a). The skin microfilarial loads

are reduced at a faster rate than what has been observed with ivermectin and appear to be reduced for longer, successfully halting transmission between yearly treatments (Awadzi et al., 2014; Turner et al., 2015a). As moxidectin can kill more microfilariae than ivermectin in one dosage, it could have the same problem with co-infected *L. loa* patients producing adverse reactions associated with the sudden death of parasites (Turner et al., 2015a). It had also been recorded that moxidectin, similar to ivermectin, also results in mild adverse reactions in onchocerciasis patients such as pruritus, rash and increased pulse rate (Awadzi et al., 2014). Moxidectin appears to be an excellent alternative drug to use for onchocerciasis because drug trials have revealed moxidectin is likely to be more effective than ivermectin and can suppress reproduction longer than ivermectin. The current limitation of moxidectin is that the drug is a microfilaricidal drug, although further drug testing could reveal its success with targeting the adult worms. The use of moxidectin with a successful macrofilaricidal drug would greatly improve the treatment of onchocerciasis.

Table 1.1: Summary of the current drugs approved for treating onchocerciasis in humans. The table describes the drug, drug class, the stage the drugs target (i.e., microfilaricidal or macrofilaricidal), problems or side effects and lastly whether the drug could be successfully used for treatment.

Drug	Class	Target	Problems/Side effects	Success
Ivermectin	Anthelmintics – macrocyclic lactone (avermectins)	Microfilaricidal	<ul style="list-style-type: none"> - Cannot give to pregnant women and children under the age of 5 - Slow – 10 to 15 years to remove the parasites - Not macrofilaricidal 	Successful
Diethylcarbamazine	Anthelmintics	Microfilaricidal	<ul style="list-style-type: none"> - Not macrofilaricidal - Elicits the Mazzotti reaction - Death 	Unsuccessful
Doxycycline	Tetracycline antibiotics	Macrofilaricidal	<ul style="list-style-type: none"> - Cannot give to pregnant women and children under the age of 9 - Long treatment duration 	Successful
Moxidectin	Anthelmintics – macrocyclic lactone (milbemycin)	Microfilaricidal	<ul style="list-style-type: none"> - Not a known macrofilaricide - Kills high volume of microfilariae at once – be careful of host immune reactions 	Successful

1.5 The Mazzotti reaction

The most important component concerning the treatment of onchocerciasis was first observed in 1948 and identified as the 'Mazzotti reaction' (Mazzotti, 1948). The Mazzotti reaction is characterised by symptoms of fever, tachycardia, hypotension and inflammation of lymph nodes as observed in humans after treatment for onchocerciasis. Inflammation in the patients' eyes was observed in individuals with ocular infections (Francis et al., 1985; Keiser et al., 2002). Previously, it was unconfirmed whether the Mazzotti reactions were a result of the diethylcarbamazine dosage or a host immune response to the death of parasites (Ottesen, 1985; Dreyer et al., 1994). It had been hypothesised that the reactions correlated with infection intensity (Francis et al., 1985). Research confirmed that the host immunological responses trigger adverse reactions which are caused by the sudden and extensive release of parasite associated molecules from dead microfilariae by diethylcarbamazine (Dreyer et al., 1994; Bandi et al., 2001; Gyapong et al., 2005; Fox, 2006).

The Mazzotti reaction is the main reason and context for this PhD. The immunopathology associated with dying microfilariae makes it difficult to determine successful drugs to treat onchocerciasis. While there are many good microfilaricidal drugs, they are used with risk in patients with a higher microfilarial burden. The higher the infection burden, the more likely the infected individual will experience severe side effects from the rapid death of a high parasite burden. Diethylcarbamazine elicits a severe Mazzotti reaction in onchocerciasis infected patients, although the other drugs can also elicit mild symptoms. The Mazzotti reaction presents multiple risks and complications for future drug development. As the reaction correlates with infection intensity, it will be pivotal to assess the rate of parasite death with other drugs to ensure the rapid death of parasites does not elicit this response. The observation of the Mazzotti reaction in treated infected patients raises the need for an appropriate animal model to test new drugs and treatments before commencing human trials thereby minimising the risk of these undesirable side effects. An animal model is very appealing because it allows safe drug testing enabling a drug to be developed that does not trigger the immunopathology associated from the rapid death of the microfilariae. Future control of onchocerciasis would be more successful if more was known about the complex immunopathology associated with treating *O. volvulus*-infected patients.

1.6 Onchocerciasis treatment programs using ivermectin

In 1974, the WHO developed the Onchocerciasis Control Programme (OCP) in West Africa to target onchocerciasis infected individuals (Boatin, 2008; Colebunders et al., 2016). The programme's goal was to eliminate onchocerciasis within the targeted regions of Africa. Mass insecticide spraying was conducted to control the vectors (Boatin, 2008), which consisted of helicopters conducting weekly spraying over the *Simulium* breeding sites (Remme, 2004). Larvicide treatment with vector control was considered expensive and costly for long term control of onchocerciasis (Diawara et al., 2009; Noma et al., 2014). The OCP closed in 2002.

The African Programme for Onchocerciasis Control (APOC) launched in 1995 to eliminate onchocerciasis as a public health problem throughout Africa. At this stage, Africa accounted for over 80% of the global disease burden (Gebrezgabiher et al., 2019). The primary focus of APOC was to identify areas of endemicity of onchocerciasis with high transmission areas, and flag these areas for MDA treatment (Hopkins, 2017). APOC targeted the flagged areas with the annual treatment of ivermectin. APOC recommended 65% ivermectin therapeutic coverage to treat onchocerciasis, but for elimination to be achieved more than 80% therapeutic coverage across the 100% geographical range would be required (Colebunders et al., 2016). These treatment efforts covered over 190,000 communities in hard-to-reach areas, effectively controlling onchocerciasis (Coffeng et al., 2013; Turner et al., 2014). Between 1995 and 2010, APOC's expenditure was US\$370 million (Coffeng et al., 2013). Due to the successful treatment outcomes, WHO considered this to be cost-effective and overall an excellent programme.

APOC was replaced with the Expanded Special Project for Elimination of NTDs (ESPEN). One of the main targets of ESPEN was onchocerciasis elimination in Africa (Hopkins, 2017; Colebunders et al., 2018a). Focus on controlling the disease shifted towards aiming for elimination. The definition of onchocerciasis elimination is "the reduction of infection and transmission to the extent that interventions can be stopped, but post-intervention surveillance is still necessary" (World Health Organisation, 2010). To reach this goal of onchocerciasis elimination, WHO identified three phases of guidelines in which need to be followed and completed to achieve elimination:

- Phase one is MDA intervention using ivermectin. Phase one consists of 80% therapeutic coverage for 12-15 years a point at which parasite transmission ceases. Vector control throughout Africa will aim to support the MDA efforts in hope to stop transmission of parasites from the vectors (World Health Organisation, 2016).
- Phase two involves post-treatment surveillance for any new emerging infections that last three to five years. Phase two uses the O-150 PCR test to confirm whether there is an interruption of *O. volvulus* transmission in black flies. The aim was to have less than one infected black fly within 2000 flies, at this point Ov-16 serology test confirmed whether there had been an interruption of parasite transmission in children (further discussion on Ov-16 in section 1.16.1). If there has also been an interruption of *O. volvulus* transmission in areas of Africa and vector elimination is successful, this is the stage where phase three begins (World Health Organisation, 2016).
- Phase three involved post-elimination surveillance in detecting any reintroductions of onchocerciasis that may occur within Africa. Phase three will be the phase that confirms if there has been a successful and permanent interruption or better yet, the elimination of onchocerciasis in regions of Africa (World Health Organisation, 2016).

Elimination could be achievable for onchocerciasis if guidelines and treatment plans are followed rigorously. Onchocerciasis has been close to elimination in endemic areas of Africa and should be possible to eliminate the disease from areas of Africa where endemicity is low (Diawara et al., 2009; Tekle et al., 2012; World Health Organisation, 2016).

1.7 Challenges to controlling onchocerciasis

There are some significant challenges associated with controlling onchocerciasis, consequently complicating the elimination of onchocerciasis throughout Africa. Some of which include co-endemicity of onchocerciasis and loiasis, ivermectin resistance, political conflict and civil war, geographical and population coverage and financial challenges. Complete control of onchocerciasis would require overcoming these challenges, and while that has been possible for

some aspects, there is still a long road ahead before onchocerciasis will be eliminated from Africa.

1.7.1 Co-endemicity of onchocerciasis and loiasis

A considerable concern for the treatment of onchocerciasis is the co-existence of *O. volvulus* and *L. loa* in the same endemic areas of Africa. Loiasis is a filarial disease caused by a related filarial nematode *L. loa* (Zoure et al., 2011; Desjardins et al., 2013a). There is a high prevalence of loiasis in the West and East of Africa. *L. loa* causes chronic infections characterised by angioedema and ocular manifestations (Desjardins et al., 2013a; Gebrezgabiher et al., 2019).

Onchocerciasis patients co-infected with loiasis with considerably high *L. loa* microfilaraemia are at significant risk of an adverse neurological reaction as well as potential fatality when treated for either disease (Gardon et al., 1997; Boussinesq, 2006; Taylor et al., 2014; Debrah et al., 2015). These reactions have led to a lack of treatment in co-endemic areas because the standard ivermectin treatment was not suitable for MDA (Gardon et al., 1997; Colebunders et al., 2018b; Gebrezgabiher et al., 2019).

There have been efforts to overcome the significant risk of adverse reactions because of the treatment of co-endemic individuals. One possible solution is to use a combination of drugs within these areas of co-endemicity (Turner et al., 2010). A six-week course of doxycycline has proven to reduce the microfilarial load of *L. loa* and *O. volvulus*. In individuals with low to moderate microfilarial intensities, this method is often very successful and can be implemented to aid in treating both onchocerciasis and loiasis (Turner et al., 2010). It has not been established whether individuals with a high *L. loa* intensity will still be at risk of significant adverse reactions when treated with drug combinations. An independent solution has been to use a diagnostic tool, LoaScope, to quantify *L. loa* in peripheral blood to confirm those individuals that are high risk for adverse effects (Kamgno et al., 2017). The process enabled community-wide ivermectin distribution in areas that previously could not be treated as a result of being co-endemic with *L. loa* (Kamgno et al., 2017).

1.7.2 Ivermectin resistance

Reliance on any single drug for disease treatment increases the risk of emerging resistance (Turner et al., 2013). Ivermectin has been used for onchocerciasis control for decades, continuing to be a highly effective microfilaricidal drug when used biannually (Cupp and Cupp, 2005; Frempong et al., 2016). Despite the success of ivermectin as a microfilaricidal drug, evidence of resistance is emerging with reports of inadequate parasite response to the treatment. Adult females are remaining unaffected after treatment of ivermectin instead of showing reproductive sterility which is confirming the fears of resistance (Osei-Atweneboana et al., 2011; Taylor et al., 2014). These observations indicate the potential emergence of ivermectin resistance.

The term 'sub-optimal responders' is used to describe a spectrum of resistant *O. volvulus* parasites. The spectrum consists of moderate responders to treatment, poor responders and very poor responders to treatment. Conversely, "good responders" are parasites that will respond to treatment. Typically, sub-optimal responders are prevalent in parasite populations that are starting to develop resistant *O. volvulus* parasites (Osei-Atweneboana et al., 2011; Osei-Atweneboana et al., 2012; Frempong et al., 2016; Doyle et al., 2017). The evolution of drug-resistant parasites is not surprising considering ivermectin has been the predominant drug used for human treatment for decades (Awadzi et al., 2004; Osei-Atweneboana et al., 2007). Osei-Atweneboana et al. (2007) determined that there are resistant adult parasite populations that are not responding to ivermectin as they initially responded on the first administration of treatment. If adult parasites can repopulate the skin with microfilariae after each treatment, then the parasite transmission will continue. The recrudescence of the disease could occur with ivermectin-resistance parasites (Osei-Atweneboana et al., 2007). A genome-wide analysis of *O. volvulus* revealed that sub-optimal responses to ivermectin are determined by selective sweeps of pre-existing quantitative trait loci (Doyle et al., 2017). The sub-optimal response phenomenon could negatively impact the overall aim of onchocerciasis elimination. Ivermectin will remain the primary drug of choice to eliminate onchocerciasis in Africa unless new drugs are developed to compete with ivermectin usage. There is a requirement for alternative drugs such as macrofilaricidal drugs to be developed and trialled. The aim would be to either permanently sterilise adult female worms

or kill the adult worms stopping the production of microfilariae and therefore the immunopathology (Grote et al., 2017).

1.7.3 Political conflict and civil war

Numerous countries throughout Africa have been afflicted by various political conflicts and civil war impeding the administration of treatment to onchocerciasis infected individuals. For example, the Democratic Republic of Congo (DRC) between 1996 and 1997 was devastated by political unrest and then had two wars between 1998 and 2003 (Makenga et al., 2015). There was no possibility of reaching the DRC for the treatment of onchocerciasis under these circumstances. All political conflicts and wars have drastic consequences on treatments available for the communities affected. These communities thus need to be treated when conflicts subside or cease. Communities within DRC have been treated since 2003 successfully with ivermectin post political unrest or war conflicts, although more control efforts are required to eliminate the disease from the DRC (Makenga et al., 2015).

Conflict interrupts treatment programs and weakens overall political support, leading to the potential of new cases every year (Hopkins, 2017). The socio-political and conflict challenges throughout Africa have been previously reported as significant reasons for impeding control of onchocerciasis (Amazigo, 2008; Makenga et al., 2015). The consistent political instability, however, will be a continuing constraint for onchocerciasis elimination and future successful MDA programmes throughout Africa (Mackenzie et al., 2012). Communities in countries such as the DRC, Cote d'Ivoire, Sierra Leone and Sudan have been challenging to treat and are likely to remain challenging regions to target onchocerciasis in the future (Mackenzie et al., 2012; Gebrezgabiher et al., 2019).

1.7.4 Geographical and population coverage

Controlling onchocerciasis has required the geographic distribution of onchocerciasis and endemic communities to be defined. Any area of Africa that had a prevalence of onchocerciasis infection greater than 20% is considered high risk and therefore requires continuous ivermectin treatment (Hopkins, 2017; Gebrezgabiher et al., 2019). The concern now lies in areas that did not have

greater than 20% infections and were not the targets for ivermectin treatment within previous treatment programmes. These areas may be responsible for the consistent transmission of disease or re-transmission of disease (Gebrezgabiher et al., 2019).

Human population and vector migration have also significantly complicated the treatment of onchocerciasis throughout Africa (Gustavsen et al., 2016). Programs aimed at the elimination of onchocerciasis can often oversee borders of countries with shared transmission zones (Gustavsen et al., 2016). Infected people migrating back and forth from country to country can pose challenges for treatment as they can spread the infection to disease-free areas. Alternatively, uninfected individuals travelling to endemic regions can, therefore, contract the disease (Gebrezgabiher et al., 2019). The *Simulium* black fly vectors can seasonally migrate from one country to another and would be able to continue transmission in areas that were thought to have eliminated onchocerciasis. The black flies could be a factor that reintroduces onchocerciasis into disease-free zones (Koala et al., 2017). These uncontrolled migration events complicate the control and treatment of onchocerciasis (Gebrezgabiher et al., 2019).

1.7.5 Non-compliance

Compliance is a critical issue that directly impacts the success of the elimination of onchocerciasis in Africa. Individuals throughout Africa need to be willing to consume the provided medication for onchocerciasis treatment. Evidence that members in communities refused to take the drugs in the MDA programmes raises concern on how to administer effective treatment methods to obtain elimination (Bockarie et al., 2013). Many individuals wanted to avoid any possible side effects of ivermectin treatment. Some were of the belief that the companies administering the treatment were not doing their job correctly. Lastly, some of those individuals that have had treatment previously did not want to continue further treatment (Bockarie et al., 2013; Gebrezgabiher et al., 2019). Reports highlight that over 10% of the African population are individuals of non-compliance, which could be enough of a reservoir for re-infection of the disease (Wanji et al., 2015).

1.8 Requirement for animal models to study onchocerciasis immunopathology and develop new drugs

Previous treatment of onchocerciasis has been successful at targeting the microfilariae and reducing nematode burdens throughout African communities despite having not reached elimination. Importantly, it is not the parasite itself which causes severe reactions or death but rather the immunopathological response from the host as a result of the dead *O. volvulus* microfilariae that leads to adverse responses of drug treatments (Ottesen, 1985). The immune response needs to be understood to identify an appropriate treatment method for onchocerciasis.

There are several critical limitations associated with effectively treating onchocerciasis that is made more challenging without the availability of an animal model. There is now the requirement to develop new novel drugs for effective treatment or alternative treatment methods to continue the elimination trajectory (Kaplan and Vidyashankar, 2012; Tyagi et al., 2019b).

The following delineates caveats in onchocerciasis research in which an animal model may assist in resolving:

- a) The driving force behind the immunopathology associated with the death of the *O. volvulus* microfilariae is still poorly understood.
- b) There are no appropriate drugs without problematic side effects suitable for targeting the adult worms and thus macrofilaricidal.
- c) Lastly, and most importantly, there are no immunocompetent small animal models available to study the complicated host immune responses to novel drug treatments and thus the death of the microfilariae that are responsible for characteristic symptoms (Bennuru et al., 2017).

There could be particular *O. volvulus* antigens when presented to the host's immune system that are responsible for causing the immunopathology. However, several of these studies are conducted *in silico* because, to explore this concept, a suitable animal model is required and that is currently unavailable (McNulty et al., 2015; Cotton et al., 2016; Bennuru et al., 2017; Norice-Tra et al., 2017; Bennuru et al., 2018; Bennuru et al., 2019). The development of an animal model that is capable of recapitulating the immune responses of onchocerciasis would

allow researchers to conduct comparative studies to further understand this immunopathology and develop new drugs to eliminate the disease.

There have been various attempts at finding an appropriate animal model. However, none of the models (described in section 1.10) recapitulate the immunopathology observed in onchocerciasis patients and thus are unable to understand onchocerciasis further and improve current treatment.

1.9 Animal model requirements

The requirements for a successful animal model are as follows:

1. Convenient laboratory host,
2. Preferably natural host,
3. The life cycle can be maintained, and,
4. Recapitulate the most important disease features.

There are many essential facets of developing animal models. One of the most important is to choose the species of laboratory animal that is best suited for a particular purpose. Ideally, a convenient laboratory host would be a small host, easily maintained in the laboratory and relatively inexpensive. Depending on the purpose of the animal model, the chosen host should enable exploration of the immunology associated with onchocerciasis disease symptoms. This includes the death of the microfilariae which complicates treatment of individuals and is currently not understood. Another use for the small animal model is for drug development. There are currently no macrofilaricidal drugs available for treating patients with onchocerciasis. Therefore, an animal model that can explore other potential drugs for treatment while avoiding adverse reactions caused by the death of the microfilariae would be invaluable. A host or model system that has known information about drug metabolism would fast track the development of macrofilaricidal drugs.

The second requirement would be to use a natural host if possible. A natural host is one where the parasite is found commonly and is suitable for the parasite to complete its developmental stages. However, an unnatural host is one that the parasite does not usually parasitise (hosts discussed in 1.12.1).

Thirdly, the life cycle needs to be maintained. Life cycle maintenance requires not only the nematode life cycle to be maintained in a host and the corresponding vector, but also requires the vector life cycle to be maintained in laboratory conditions. The life cycle is arguably one of the most important steps because if the life cycles cannot be maintained, then it is not a recapitulated life cycle of onchocerciasis disease. Maintenance of the vector and parasite life cycles in the laboratory means that laboratory experiments are not limited to immunoreactivity experiments or parasite drug development and control but also could be expanded to vector control and host responsiveness. Every aspect of the disease life cycle can be explored thoroughly to determine the best and most appropriate method to control onchocerciasis.

Finally, the most important disease features of onchocerciasis, i.e., microfilariae in the eye, blindness and skin lesions, need to be recapitulated in the animal model system. If the characteristic features of the disease are not recapitulated, then the disease in the small animal model is not comparable to the human disease and treatments, and thus, strategies for disease control are limited.

1.10 Current animal models

There have been several attempts to find an appropriate animal model to improve the understanding of an *O. volvulus* infection and to explore drug effectiveness, reactions and therefore, success targeting the parasite.

1.10.1 *Onchocerca ochengi* model

The sister filarial species *O. ochengi* has been explored in its natural host, cattle (Trees et al., 1992; Trees, 1992). Cattle are permissive to the infection of *O. ochengi* (Table 1.2). The adults reside in nodules similarly to *O. volvulus* in humans, and the microfilariae migrate through the skin (Trees et al., 1992; Trees et al., 2000). Infected cattle do not display pathology consistent with the pathology observed in *O. volvulus*-infected humans. There are no ocular lesions or dermatitis in cattle associated with the presence of *O. ochengi* (Trees et al., 1992; Trees et al., 2000).

The *O. ochengi* cattle model has many benefits for understanding onchocerciasis but equally has as many disadvantages. One of the benefits includes drug testing. The model has been used to test numerous drugs, including ivermectin and moxidectin. Both drugs have demonstrated successful clearing of the microfilariae from the host. Another study identified oxytetracycline as a potential macrofilaricidal with long term treatment of the parasites (Trees et al., 2000). Another benefit of the cattle model is the use of natural infection in endemic areas. The model can explore host-parasite relationships and determine the effectiveness of the vaccines. Once the animals are vaccinated and continue to live in endemic areas, vaccine success is challenged and this would enable a clear assessment as to whether the vaccine is working as efficiently as is required (Trees et al., 2000).

Conversely, the *O. ochengi* cattle model is not suitable to focus on the disease. It has not been possible to replicate the Mazzotti reaction, even when using diethylcarbamazine, which is known to have adverse effects with and without parasite infection in humans (Dreyer et al., 1994; Trees et al., 2000). The *O. ochengi* cattle model is intensive and expensive to run and conduct experiments. Lastly, and most importantly, the immunopathology associated with onchocerciasis is not replicated within the model. The cattle do not show any signs of dermatitis, ocular lesions or lesions in the skin (Trees et al., 2000). Consequently, it is not possible to accurately assess the hosts' immune response to the death of the parasites. The pathology observed in *O. volvulus*-infected individuals, i.e., skin and eye lesions, blindness, is a result of the host immune system responding to the dying parasites. Without any observable pathology in cattle, the host immune responses are not comparable to thoroughly understand onchocerciasis. The *O. ochengi* cattle model is not suitable for understanding immunopathology or developing new macrofilaricidal drugs to treat currently infected humans.

1.10.2 Mouse model

A study conducted by Chakravarti et al. (1993) developed a murine model for sclerosing keratitis (Table 1.2). They successfully injected antigens from *O. volvulus* intrastromally into mice resulting in inflammatory responses, tissue scarring and cellular patterns histopathologically similar to those seen in

onchocerciasis patients. The murine model was successful at eliciting a similar response as seen in humans but could not recapitulate the main characteristic disease feature, i.e., blindness. Without microfilariae in the cornea, this model does not present an accurate recapitulation of onchocerciasis symptoms. An additional disadvantage of using mice is that they are not permissive to infection and thus is not ideal for drug development.

1.10.3 Chimpanzee model

A study conducted by Eberhard et al. (1995) used chimpanzees as a model for onchocerciasis because they are more closely related to humans than any alternative host (Table 1.2). Accordingly, they are more likely to give an accurate representation of immune responses that are observed in humans. Studies have shown that chimpanzees are permissive for infection of *O. volvulus* (Duke et al., 1980; Prince et al., 1992; Eberhard et al., 1995). They were inoculated with the L3 infective stage (iL3) of *O. volvulus* and became infected for downstream experiments. The chimpanzees exhibited similar symptoms to those observed in *O. volvulus*-infected humans including nodules where the adult male and female worms resided (Duke, 1980; Morris et al., 2013). In some studies, there was evidence that the chimpanzees also developed microfiladermia indicating a similarity in symptoms with the human disease.

Unfortunately, not all chimpanzees developed microfiladermia which indicated that there are differences in infection susceptibility between individual chimpanzees (Prince et al., 1992; Eberhard et al., 1995). None of the chimpanzees experienced eye lesions which is the major characteristic symptom in human onchocerciasis (Duke, 1980; Morris et al., 2013).

Johnson et al. (1991) elucidated that chimpanzees develop immune responses to defend themselves against the microfilariae, therefore killing them. This explains why some chimpanzees develop microfiladermia and other do not. It was therefore concluded that despite chimpanzees being a close relative of humans, the ability of the chimpanzee's immune system to kill the microfilariae early in infection, means this model system would not be appropriate to study onchocerciasis further. In addition, using chimpanzees as a model to study

disease is unethical, thus the chimpanzee model will never be considered for further experiments.

1.10.4 *Acanthocheilonema viteae* rodent model

A. viteae is a filarial nematode of mainly rodent species with natural hosts such as gerbils and jirds (Table 1.2) (Johnson et al., 1974; Morris et al., 2013). Animal models with *A. viteae* have been used to explore the protective immunity to *O. volvulus* (Abraham et al., 2002). The most common experimental hosts include the jird, *Meriones unguiculatus* (Eisenbeiss et al., 1991; Lucius and Textor, 1995) or *Meriones libycus* (Harnett et al., 1989) with soft ticks *Ornithodoros moubata* (Morris et al., 2013). Typically, the adult *A. viteae* parasites reside in the subcutaneous skin and the microfilariae are present in the blood (Haque et al., 1978; Morris et al., 2013). Jirds are permissive to infection and develop microfilaremia for over 18 months which makes this model successful for vaccine studies (Beaver et al., 1974). There is no obvious pathology in the natural host, jirds, other than the potential for extremely high microfilaremia levels with several mating parasite pairs resulting in potential death of the host (Beaver et al., 1974). There have been no reports of microfilariae migrating to the cornea in jirds and therefore is not recapitulating the same disease features of onchocerciasis.

Infection trialled in hamsters has resulted in transient microfilaremia with symptoms such as hepatitis, glomerulonephritis and cellular infiltrates of the lung (Simpson and Neilson, 1976). Infection with *A. viteae* in hamsters results in weak associated immunity against the L3 larvae, which will not be an appropriate model to study possible treatments for onchocerciasis.

Importantly, *A. viteae* animal models do not recapitulate the same immunopathology that is seen in *O. volvulus*-infected humans and therefore is only suitable to be used for small studies associated with vaccines if the *A. viteae*, jird model is used in the future.

1.10.5 *Loa loa* mouse model

The development of a successful *L. loa* mouse model for loiasis in co-infected patients with onchocerciasis was developed which can be used in

developing therapeutic or diagnostic drugs against the disease (Pionnier et al., 2019). The *L. loa* iL3 parasites were extracted from wild-caught *Chrysops silacea* (tabanid flies) to be later subcutaneously implanted into mice (Table 1.2). Mice were treated orally with ivermectin or with flubendazole and injected with ivermectin. They were then CO₂ euthanised to obtain results identifying up-regulation of inflammatory markers associated with Th-2 immune responses post-ivermectin treatment (Pionnier et al., 2019). The *L. loa* model is suitable to be used as a control model to counter-screen candidate onchocerciasis treatments ensuring there are no ivermectin-associated adverse effects that are problematic for MDA treatment throughout the population (Pionnier et al., 2019).

1.10.6 *Litomosoides sigmodontis* rodent model

L. sigmodontis is a filarial nematode of rodents. The natural host of *L. sigmodontis* is the cotton rat, *Sigmodon hispidus* (Table 1.2) (Morris et al., 2013). This animal model has been extensively used to investigate immune systems and pathways observed by the human filarial infections (Hübner et al., 2009; Frohberger et al., 2019). As *L. sigmodontis* contains the bacterial endosymbiont, *Wolbachia*, several of these studies have focused actively on *Wolbachia* depletion (Specht et al., 2018; Hübner et al., 2019b; Taylor et al., 2019). Macrofilaricidal drugs are being considered and slowly developed, which potentially could be used in *O. volvulus*-infected individuals successfully eliminating the adult worms (Hübner et al., 2019a).

There have been three rodent hosts used to explore infection of *L. sigmodontis* including albino rats, the cotton rat and jirds. The pathology in the each of hosts resulting from *L. sigmodontis* infection is similar. In albino rats, the microfilariae are present in the blood with the adults, residing in the pleural cavities. Pathology includes pathological changes in the lungs and decreased function of the liver and spleen (Mukhopadhyay and Ghosh, 1988). The microfilariae and adults are also present in the blood and pleural cavities in the natural host, cotton rats. Cotton rats display lymphadenopathy, papillary nodules, oedema, alveolar thickening and myocarditis pathology (Wharton, 1947). Lastly, the same pathology observed in cotton rats is displayed in jirds with increased severity (Wharton, 1947). Very high microfilariae infections will result in the death of the jirds in approximately three days.

These three *L. sigmodontis* animal models have been successful for different reasons. Albino rats, cotton rats and jirds are all permissive for infection and have all resulted in moderate to high microfilarial burdens. Albino rats could be excellent models to study filarial latency as a latent infection mediated by a different mechanism from other models was observed. It could be that protection against microfilaremia is a result of local immune responses rather than antibodies (Bagai and Subrahmanyam, 1968). There have been substantial levels of protection after vaccination demonstrated in the hosts, especially in jirds, and have observable effects of immunomodulation on parasite survival which may be vital in understanding helminth infections.

Unfortunately, these animal models are not appropriate models of human disease. In cotton rats, with high infection levels, the dying microfilaraemia congregates in the lungs, which could lead to more severe symptoms if a vaccination to kill the worms were used. In all hosts, the *L. sigmodontis* microfilaraemia do not migrate to the cornea. Thus, the eye pathology characteristic of onchocerciasis is not recapitulated in the *L. sigmodontis* models. The same symptoms in *O. volvulus*-infected individuals, including skin lesions, nodules, inflammatory and blindness, are also not recapitulated in the *L. sigmodontis* models. Therefore, these models would not be successful in understanding the disease immunopathology of onchocerciasis, although they may be useful to develop a novel drug.

Table 1.2: Summary of animal models previously used to study onchocerciasis highlighting the advantages and disadvantages of each model system.

Model	Advantages	Disadvantages
<i>O. ochengi</i> model	<ul style="list-style-type: none"> - <i>O. ochengi</i> is a sister species to <i>O. volvulus</i> this genetically closely related. - Adult <i>O. volvulus</i> reside in nodules - Suitable for drug testing - Exploring host-parasite relationships 	<ul style="list-style-type: none"> - The cattle model is intensive and expensive. - No skin pathology. - No ocular pathology. - Cannot study the host's immune response to the death of the parasites.
Mouse model	<ul style="list-style-type: none"> - Demonstrates sclerosing keratitis - Inflammatory responses and tissue scarring - Successfully can inject <i>O. volvulus</i> antigens intrastromally - Appropriately sized model for experiments 	<ul style="list-style-type: none"> - There were no microfilariae in the eye therefore could not recapitulate blindness - Not permissive to infection - Not ideal for drug development
Chimpanzee model	<ul style="list-style-type: none"> - They are a close relative of humans - Permissive to infection - Pathology similar to onchocerciasis - Adults reside in nodules - Some chimpanzees developed microfiladermia 	<ul style="list-style-type: none"> - Large animal and not ethical for experiments - Not all chimpanzees developed microfiladermia - No evidence of eye lesions - Chimpanzees could develop host immune responses to kill the microfilariae
<i>A. viteae</i> model (hamsters)	<ul style="list-style-type: none"> - Small model system - Explore protective immunity to <i>O. volvulus</i> - Evidence of parasites in the subcutaneous skin 	<ul style="list-style-type: none"> - Microfilariae present in the blood - Weak associated immunity against the L3 larvae - Do not show comparable pathology to onchocerciasis patients

<i>A. viteae</i> model (jirds)	<ul style="list-style-type: none"> - Small model system - Permissive to infection - Develop microfilaremia for over 18 months 	<ul style="list-style-type: none"> - No obvious pathology similar to onchocerciasis - Extremely high microfilaremia levels putting host at risk of dying
<i>L. loa</i> model	<ul style="list-style-type: none"> - Small model system - Can explore co-infections of <i>L. loa</i> and <i>O. volvulus</i> - Appropriate as a control model to counter-screen candidate onchocerciasis treatment 	<ul style="list-style-type: none"> - Not suitable for developing microfilaricidal or macrofilaricidal drugs
<i>L. sigmodontis</i> model (albino rats)	<ul style="list-style-type: none"> - Small model system - Microfilariae are present in the blood with the adults, residing in the pleural cavities - Permissive to infection 	<ul style="list-style-type: none"> - Pathological changes in the lungs and decreased function of the liver and spleen - No evidence of microfilaria in the cornea - Skin lesions, nodules, inflammatory and blindness, are not recapitulated
<i>L. sigmodontis</i> model (cotton rat)	<ul style="list-style-type: none"> - Small model system - Microfilariae and adults are also present in the blood and pleural cavities - Permissive to infection 	<ul style="list-style-type: none"> - Lymphadenopathy, papillary nodules, oedema, alveolar thickening and myocarditis pathology - Dying microfilaria congregates in the lungs - No evidence of microfilaria in the cornea - Skin lesions, nodules, inflammatory and blindness, are not recapitulated
<i>L. sigmodontis</i> model (jirds)	<ul style="list-style-type: none"> - Small model system - Microfilariae and adults are also present in the blood and pleural cavities 	<ul style="list-style-type: none"> - Lymphadenopathy, papillary nodules, oedema, alveolar thickening and myocarditis pathology with very high intensity and severity - No evidence of microfilaria in the cornea - Skin lesions, nodules, inflammatory and blindness, are not recapitulated

1.11 Key limitations to current models

None of the animal models was successful at recapitulating all the important features observed in *O. volvulus*-infected individuals. It is currently not possible to answer different hypotheses using the same animal model. For example, an animal model that is used to test drug efficacy will be suitable for observing the success of a new drug by eradicating the parasite. However, it may not be suitable for assessing the disease features, i.e., blindness and skin lesions, because the animal model does not display these features observed in humans and therefore the model cannot confirm whether the drug will treat these symptoms or elicit adverse reactions.

Animal models have proven to be a vital component of disease research enabling the current controls of onchocerciasis and other filarial diseases whose parasites are unable to survive outside of a host (Grote et al., 2017). Although the discussed animal models have significantly improved our knowledge of treating onchocerciasis and understanding the filarial disease, it is disadvantageous to use the current small animal models for understanding the disease pathology because none of the models truly recapitulate the immunopathology seen in *O. volvulus*-infected patients. If reactions, including the Mazzotti reaction, cannot be replicated, then accurate drug responses are challenging to achieve. Research using these models has been beneficial in improving our understanding of alternative methods of treatment of onchocerciasis and potential development of vaccines. However, it would be more beneficial to have a small animal model, similar to the ones previously developed, that could accurately recapitulate the immunopathology in *Onchocerca*-infected patients and present similar antigens to the host immune systems that could be involved in disease pathology. Equally, the lessons learnt in the existing animal models could be adapted to an immunopathology-focused model to gain a comprehensive understanding of onchocerciasis.

Several of these previously discussed animal models have explored vaccine candidates. It cannot be ruled out that an additional animal model that shares immunopathological parallels could be suitable for developing vaccines. However, vaccine development is outside of the scope for this PhD and is not an important consideration for the work that has been done to establish this animal

model for onchocerciasis. Vaccine development could be an interesting extension of this PhD but is not relevant for the remaining experiments.

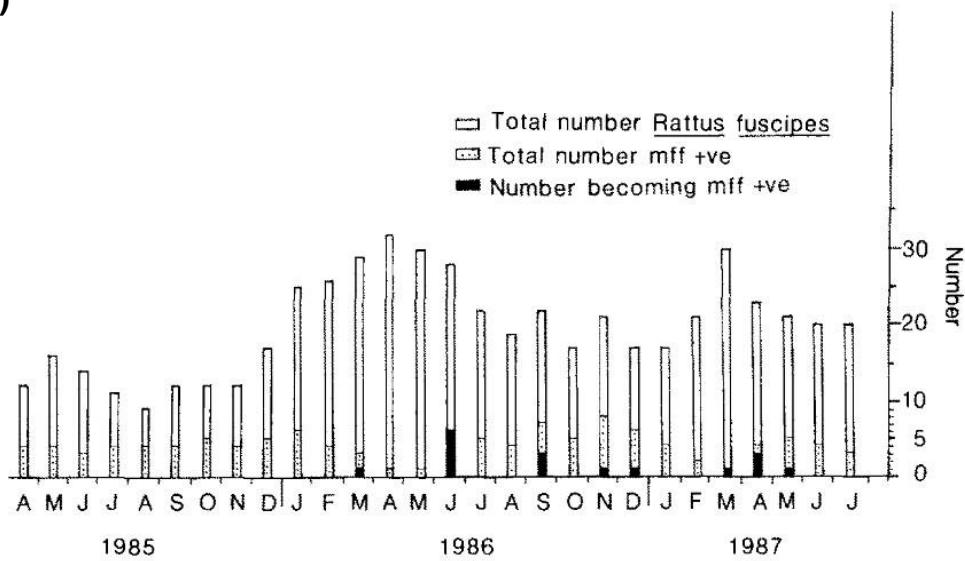
1.12 *Cercopithifilaria johnstoni* (*Dipetalonema johnstoni*) as a model organism for onchocerciasis

Dipetalonema johnstoni was first described in the 1950s in *Isodon obesulus* (Southern brown bandicoot) in Australia (Mackerras, 1954). In the 1960s, *D. johnstoni* was further identified in other Australian hosts and more specifically characterised morphologically compared to other related filarial species identified in Australian marsupials (Mackerras, 1962). A study conducted by Spratt and Varughese (1975) intended to improve the taxonomy of Filarioidea by morphologically differentiating between all the filarial nematodes that had been identified in Australian hosts. Several of these earlier descriptions and illustrations were of varying quality and potentially is the reason why the taxonomy of this group is so controversial. Spratt and Varughese (1975) illustrated morphological differences of *D. johnstoni* compared to other *Dipetalonema* species; hence *D. johnstoni* was later renamed as *Cercopithifilaria johnstoni* because morphologically is more similar to the genus *Cercopithifilaria* (Mackerras, 1954, 1962; Spratt and Varughese, 1975). In all host species, *C. johnstoni* appeared to be one of the only nematodes, especially in marsupials, to be present throughout the subcutaneous skin (Spratt and Varughese, 1975). Upon histologic examination of the rodents skin infected with *C. johnstoni* microfilariae revealed similar characteristics comparable to lesions present in human onchocerciasis (Vuong et al., 1985). Thus the idea came to be that *C. johnstoni* may be appropriate to study onchocerciasis. Spratt and Haycock (1988) then used *Ixodes trichosuri* to transmit *C. johnstoni* to a laboratory rat, *Rattus norvegicus*, determining the life cycle of the parasite and then exploring whether *C. johnstoni* demonstrated similar pathology compared with other Onchocercidae members. Their investigations have led to confirming that *C. johnstoni* has the potential to be used in an informative and inexpensive small animal model to study onchocerciasis.

A field study conducted from April 1985 to July 1987 that captured *Rattus fuscipes* (Australian bush rat) from Mogo State Forest observed relatively consistent infection of *C. johnstoni* in *R. fuscipes* (Figure 1.6a). It is presumed

that the prepatent period from *C. johnstoni* transmission is 90 days from their experimental studies (Figure 1.6a) (Spratt and Haycock, 1988; Vuong et al., 1993). At the same time of observing *C. johnstoni* microfilariae, the number of larvae and nymphs were recorded from the captured rodents (Figure 1.6b). It was these observations that provided the evidence that ixodid ticks could be transmitting *C. johnstoni* to the various Australian hosts.

a)



b)

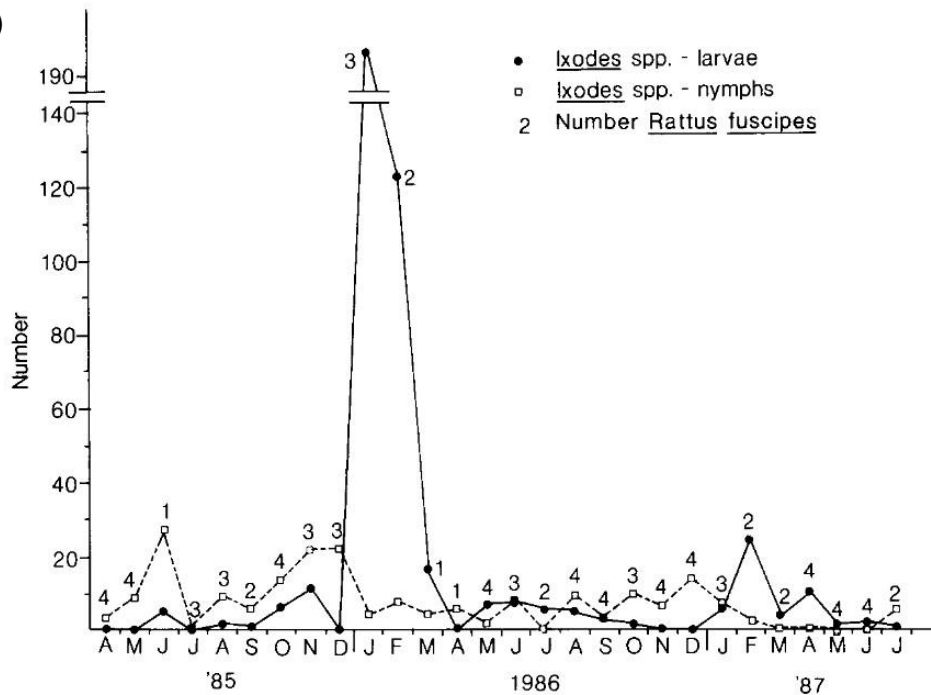


Figure 1.6: a) Number of *Rattus fuscipes* trapped at Mogo State Forest every month over three years (1985, 1986, and 1987). Dotted section of bar graph indicates number of rats with *Cercopithifilaria johnstoni* microfilariae in the skin. Black section of bars represents rodents with no microfilariae that changed to positive. b) Figure representing mean numbers of larval and nymphal *Ixodes* spp. (predominantly *Ixodes trichosuri*) harvested from bush rats (n above) naturally infected with *Cercopithifilaria johnstoni* at Mogo State Forest, April 1985 to July 1987 (Spratt and Haycock, 1988).

1.12.1 *Cercopithifilaria johnstoni* life cycle

The life cycle of *C. johnstoni* is similar to the life cycle stages of *O. volvulus*, due to being transmitted between definitive hosts by an intermediate vector species (Figure 1.7). Ticks are responsible for the transmission of *C. johnstoni* to a range of hosts (Spratt and Varughese, 1975; Spratt and Haycock, 1988). The tick will bite and feed on the small rodent injecting the infective (iL3) stage of *C. johnstoni* into the subcutaneous skin of the rodent. The infective *C. johnstoni* worm will develop into the fourth stage larvae (L4) and then into adults who also reside in the subcutaneous skin. The adults will produce microfilariae (L1) which will move around in the skin and elicit pathological symptoms. Another tick will bite and feed on the rodent and ingest the microfilariae for *C. johnstoni* to develop into the L2 and iL3 stages for the cycle to continue (Figure 1.7) (Spratt and Varughese, 1975; Spratt and Haycock, 1988).

There are several host species that *C. johnstoni* has been identified to parasitise, however it is not known whether all of these species are natural hosts. The described species consist of *R. fuscipes* (Australian bush rat), *I. obesulus* (Southern brown bandicoot), *Perameles nasuta* (long-nosed bandicoot), *Isodon macrourus* (Northern brown bandicoot), *Rattus lutreolus* (Australian swamp rat), *Sarcophilus harrisii* (Tasmanian devil), *Uromys caudimaculatus* (giant white-tailed rat), *Petauroides volans* (greater glider) and *Ornithorhynchus anatinus* (platypus) (Spratt and Varughese, 1975).

Continuing the discussion of a convenient laboratory host for a small animal model in section 1.9, a likely natural host of *C. johnstoni* is *R. fuscipes*, which would be a more appealing host species for developing an animal model over the more commonly used hosts in animal models, rabbits or gerbils. A natural host guarantees *C. johnstoni* can survive and maintain its life cycle within this host and also simplifies the model system. The natural host of *C. johnstoni* has not been confirmed, but it is assumed to be species within the genus *Rattus* including *R. fuscipes*. If it is confirmed that the parasites identified in each of the recorded hosts were correctly identified as *C. johnstoni*, then there is the possibility that *R. norvegicus* is also a natural host of *C. johnstoni*, despite not being recorded in the wild. Nevertheless, if *R. norvegicus* is not a natural host of *C. johnstoni*, *R. norvegicus* could still be used as an appropriate small animal for the *C. johnstoni* animal model. As *R. norvegicus* is used as a laboratory rodent

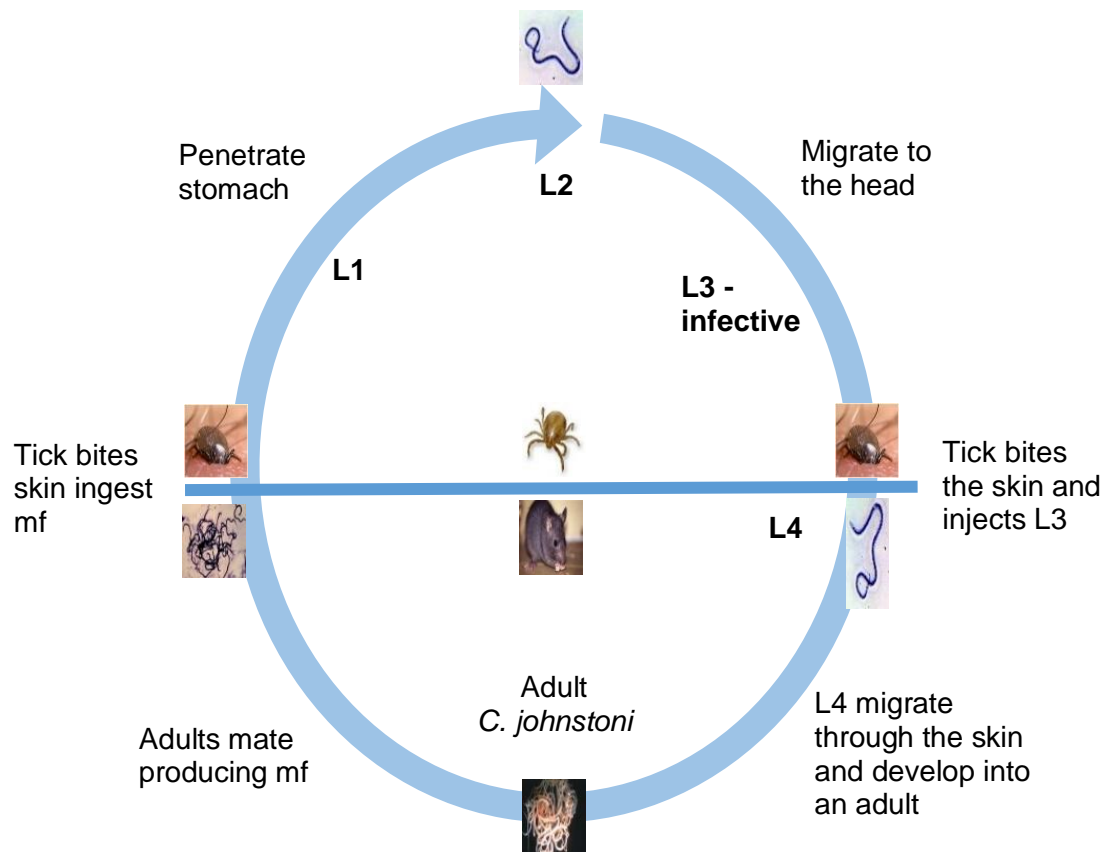


Figure 1.7: The life cycle of *Cercopithifilaria johnstoni*, transmitted by ixodid ticks to the Australian bush rat, *Rattus fuscipes*.

for many studies, there are abundant resources available to understand host immunology. The experiments using *R. norvegicus* demonstrate identical biology compared with *R. fuscipes* when infected with *C. johnstoni* (Spratt and Haycock, 1988; Vuong et al., 1993).

1.12.2 Pathology in the natural host, *Rattus fuscipes*

The natural host of *C. johnstoni* is presumed to be *R. fuscipes* and has been shown to exhibit similar pathology to the immunopathology displayed in humans caused by *O. volvulus*. Initial observations of *C. johnstoni* in *R. fuscipes* suggest that the rats are consistently positive for infection with *C. johnstoni* throughout the year, which was determined using skin snips (Figure 1.6a).

Spratt and Haycock (1988) then examined the captured rodents more closely in laboratory experiments and had shown the microfilariae migrating through the extravascular connective tissue of the skin in *R. fuscipes* (Figure 1.8b, 1.8c). They also observed eosinophils and mastocytes surrounding the site of microfilariae in the skin (Figure 1.8d). Inflammatory granulomas were identified, indicating parasite presence, and adult nematodes were surrounded by acute and sub-acute inflammatory lesions (Figure 1.9a, 1.9b) (Vuong et al., 1993). Inflammatory, fibrotic tissue was observed surrounding a dying female *C. johnstoni* worm (Figure 1.9c). Further observation led to seeing acute, sub-acute inflammatory lesions and then chronic lesions and fibrosis in the pinna of *R. fuscipes* (Figure 1.9e). Microfilariae were also observed in the eyelids, cornea and limbus and frequently spread to the peripheries in *R. fuscipes* (Figure 1.10b, 1.10c) (Vuong et al., 1993).

1.12.3 Vectors for *Cercopithifilaria johnstoni* animal model

The vector assumed to be competent at transmitting *C. johnstoni* was *I. trichosuri* from the hard tick family (Spratt and Haycock, 1988). Similar to many tick species, *I. trichosuri* requires full engorgement before developing into an adult (Spratt and Haycock, 1988). Studies conducted by Spratt and Haycock (1988) revealed that transmission of *C. johnstoni* to *R. fuscipes* occurred in December, January, February, March, June and August (Figure 1.6a) which

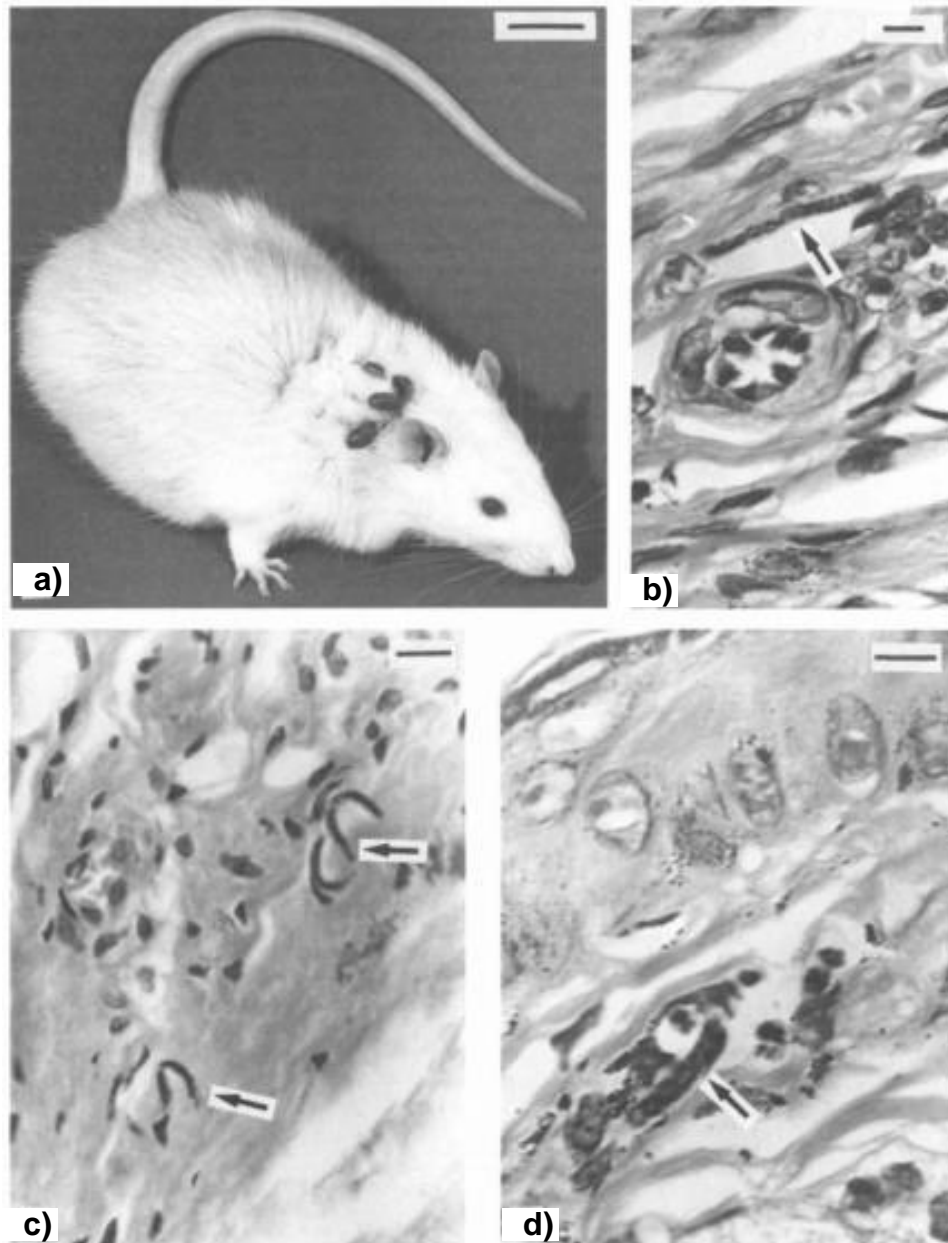


Figure 1.8: Evidence of *Cercopithifilaria johnstoni* in *Rattus fuscipes* and *Rattus norvegicus* (Spratt and Haycock, 1988). a) Attachment of adult female *Ixodes trichosuri* infected with *Cercopithifilaria johnstoni* to the neck of *Rattus norvegicus*, b) microfilariae (arrow) in lymphatic capillary in aural skin of *Rattus fuscipes*, c) microfilariae (arrows) in extravascular connective tissue of aural skin of *Rattus fuscipes*, d) microfilaria (arrow) surrounded by eosinophils and mastocytes in aural skin of *Rattus fuscipes*.

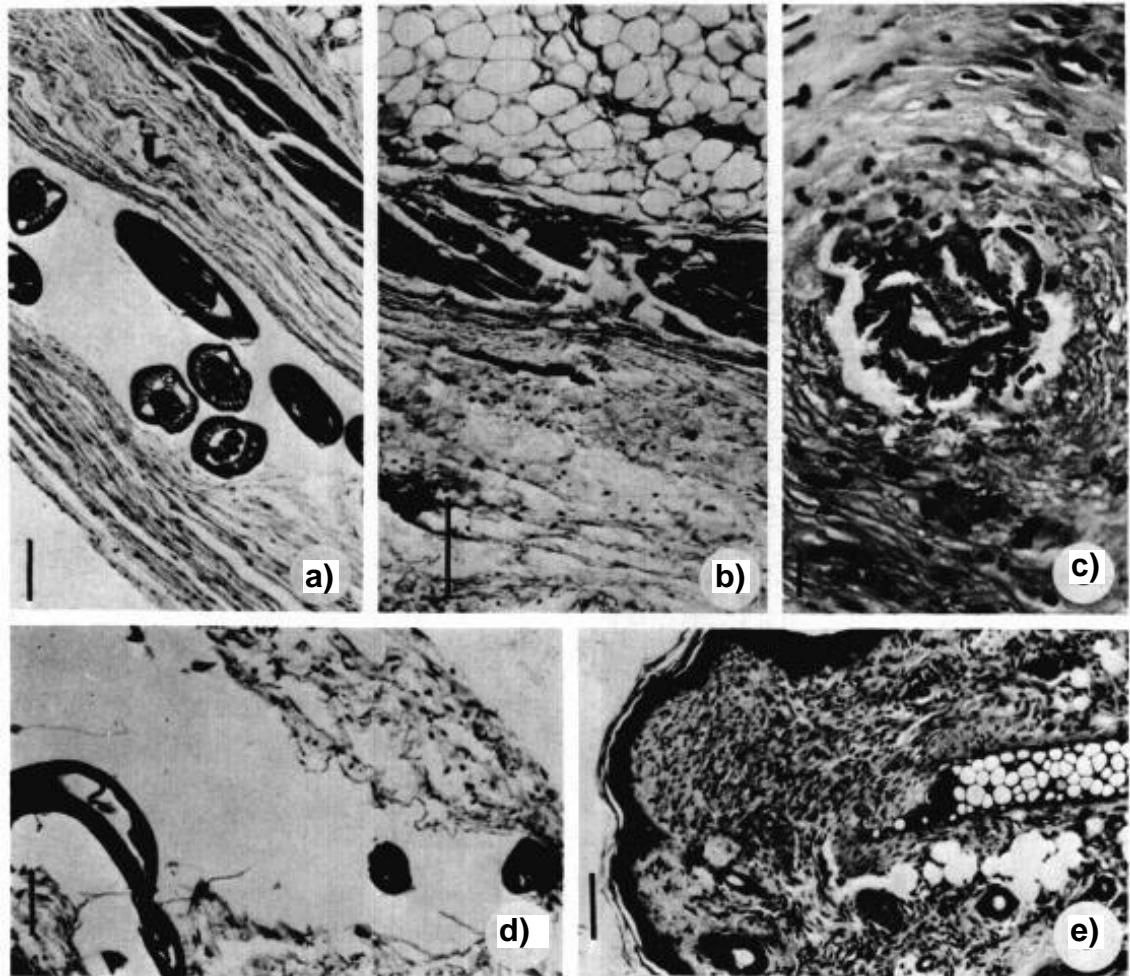


Figure 1.9: *Cercopithifilaria johnstoni* in subcutaneous aponeuroses of dorsum of rats (Vuong et al., 1993). a) Male in cavity in *Rattus fuscipes*, b) sub-acute inflammatory lesions in *Rattus fuscipes*, c) dying female surrounded by inflammatory and fibrotic tissue in *Rattus fuscipes*, d) in *Rattus norvegicus* a *Cercopithifilaria johnstoni* male surrounded by acute and sub-acute inflammatory reactions, e) acute and sub-acute inflammatory reactions in *Rattus fuscipes* with chronic lesions and fibrosis in the pinna.

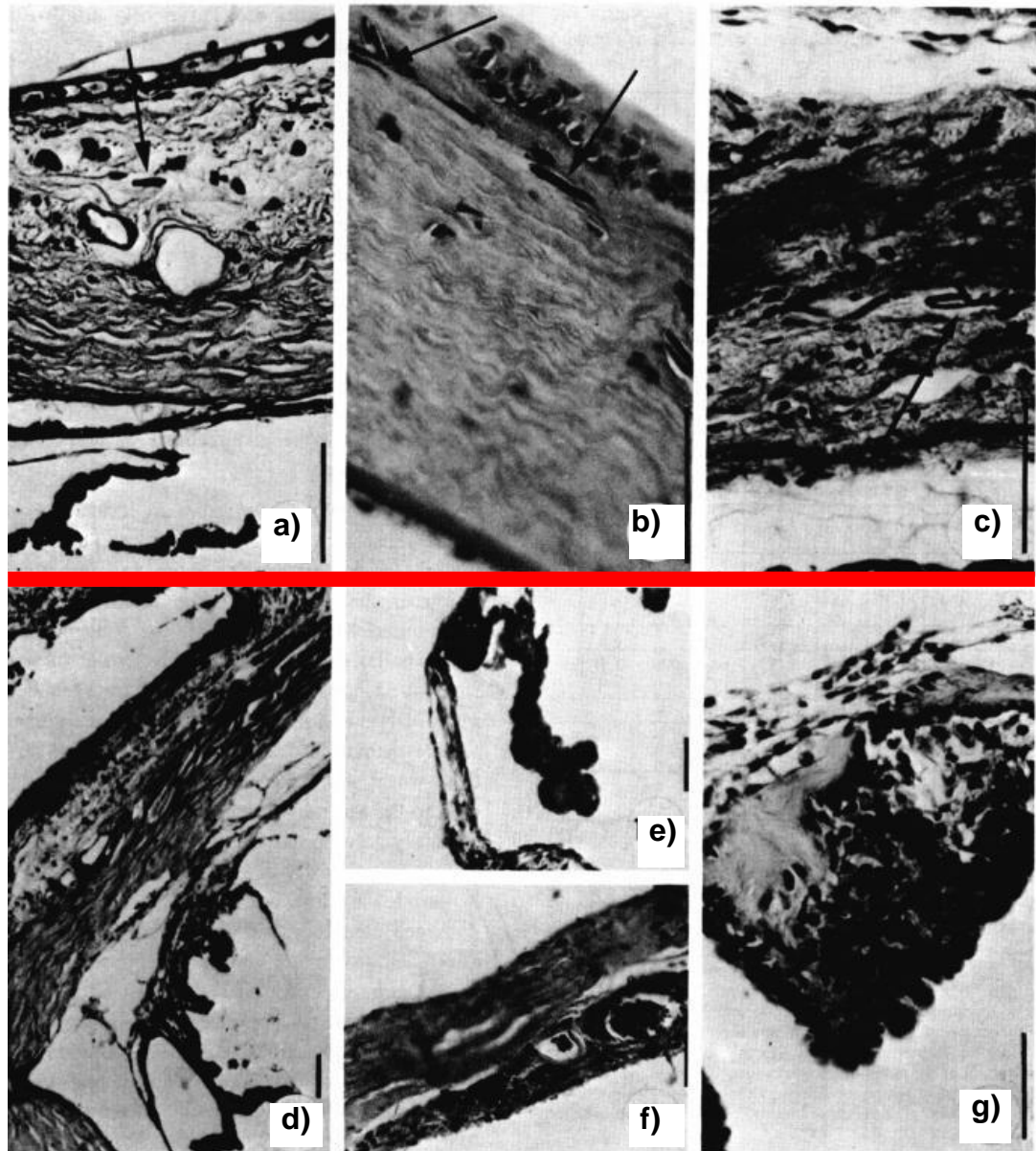


Figure 1.10: *Cercopithifilaria johnstoni* in *Rattus fuscipes* above the red line and in *Rattus norvegicus* below the red line (modified from Vuong et al., 1993). a) Microfilaria inflammatory reaction, b) cornea microfilaria without inflammatory reactions, c) microfilariae in eyelid with inflammation, d) sub-acute lesions in the corneal limbus, e) absence of melanin pigment, inflammatory lesions of iris and (f) choroid, g) nodular fibrosis of iris.

corresponded very closely to the high peaks of larval and nymphal numbers of ticks (Figure 1.6b). The predominant species of tick observed throughout these observations was *I. trichosuri* hence appears to be a likely vector of parasite transmission.

Currently, it is not known whether *I. trichosuri* is the most competent species for transmission or if other *Ixodes* species would be more suitable (Spratt and Haycock, 1988; Vuong et al., 1993). For example, *Ixodes ricinus* is not suitable for *Cercopithifilaria bairdii* development, whereas *Rhipicephalus sanguineus* is a competent vector for *C. bairdii* and parasite development (Ramos et al., 2014). As there is evidence of more competent vectors than others for parasite development, the question is raised whether *I. trichosuri* would be the only competent vector for *C. johnstoni* and how could this affect transmission in the small animal model.

1.12.4 Pathology in the laboratory host, *Rattus norvegicus*

The observations of *C. johnstoni* microfilariae in the skin and eye of *R. fuscipes* led to the extraction of the iL3 stage of *C. johnstoni* from tick dissections to inoculate the nematode into *R. norvegicus* subcutaneously. The ticks carrying *C. johnstoni* were also permitted to feed directly on *R. norvegicus*, allowing the iL3 stage of *C. johnstoni* to infect the laboratory rat (Figure 1.8a) (Spratt and Haycock, 1988). The results from both techniques were consistent, confirming that *C. johnstoni* could infect *R. norvegicus*. The dermal microfilariae live in the lymphatic vessels where they can move to the perivascular connective tissue inducing inflammatory responses. The adults were located in the subcutaneous tissue of the skin (Spratt and Haycock, 1988; Vuong et al., 1993; Uni et al., 2013) and when they died caused an inflammatory response with lesions on the skin and eye (Figure 1.9d, 1.9e) (Vuong et al., 1993). Finally, ocular lesions were observed in *R. norvegicus* (Figure 1.10e, 1.10f, 1.10g) (Vuong et al., 1993).

The similar physiological symptoms that are seen in onchocerciasis patients are also apparent in *R. norvegicus* and *R. fuscipes*. The pathology is caused by the microfilariae (L1's) (Spratt and Haycock, 1988) moving through the skin with more severe symptoms caused by the death of the microfilariae or adult

worms (Vuong et al., 1993). Ocular lesions are a characteristic of onchocerciasis in humans. Observing ocular lesions in *R. norvegicus* was a significant discovery, indicating *R. norvegicus* could be the successful small animal model able to recapitulate essential disease characteristics.

C. johnstoni could be maintained in the laboratory in naturally infected hosts such as *R. fuscipes* or experimentally infected *R. norvegicus* (Vuong et al., 1993). *C. johnstoni* is parasitic and cannot be cultured outside of a host similar to other parasitic nematodes (Grote et al., 2017). If a complete animal model life cycle were to be developed, a significant hurdle is the maintenance of vector species. Ticks are a complex species that are difficult to maintain in the laboratory and complicated to distinguish between closely related species within a genus.

1.13 Ticks: vectors of pathogens and parasites

Ticks are vectors for transmitting a wide variety of pathogens and parasites to livestock and humans (McCoy et al., 2013). Ticks greatly surpass other arthropods with the volume of pathogens they carry, thus reinforcing the importance of tick research (Brossard and Wikel, 2004; Bonnet and Liu, 2012). Ticks are known worldwide to transmit rickettsial diseases to humans (Grattan-Smith et al., 1997; Storer et al., 2003) and transmit diseases from animals to humans (Caporale et al., 1995; Brossard and Wikel, 2004). They are obligate hematophagous ectoparasites divided into two categories, hard and soft ticks (Anderson, 2001; Bonnet and Liu, 2012). Hard and soft ticks have been a significant focus of research with high medical importance and interest (Klompen et al., 1996; Storer et al., 2003; Anderson et al., 2004; Bonnet and Liu, 2012; Zhang and Zhang, 2014). For this thesis, hard ticks will remain the predominant focus as they encompass the ticks responsible for *C. johnstoni* transmission.

Ixodidae is a family consisting of hard ticks (Anderson, 2001). Ixodidae consists of approximately 900 species (Barker and Walker, 2014). There are 250 species in the Prostriata group and 464 species in the Metastriata in which the genus *Ixodes* is situated (Anderson et al., 2004; Barker and Murrell, 2004). *Ixodes* are arguably the most crucial group of ticks to study due to the parasites they transmit to innumerable hosts (Lv et al., 2014a). For example, *Ixodes*

scapularis is potentially one of the most studied species of tick in the Northern Hemisphere due to its ability to transmit Lyme disease to humans (LoGiudice et al., 2003; Kocan et al., 2015; Gulia-Nuss et al., 2016).

1.13.1 Hard tick life cycles

The typical *Ixodes* life cycle (Figure 1.11) has four stages, egg, larva, nymph, and adult (Anderson, 2001; Barker and Walker, 2014). They feed as larvae, moult to nymphs, feed on another host, and then moult to adults. The adult females must feed a third time after mating before they can lay eggs (Bonnet and Liu, 2012). Males feed twice with moults following each feeding and do not feed as adults (Barker and Walker, 2014). Females can lay 2,500-3,000 eggs with an egg survival rate of 0.08% (Doubé, 1979; Grattan-Smith et al., 1997; Masina and Broady, 1999). Only mated females can rapidly engorge due to an uncharacterised physiological control mechanism (Sojka et al., 2016) and can ingest 100 times their body weight (Sauer et al., 1995). Generally, tick feeding is a slow process with the complete time frame varying depending on the species (Grandjean and Aeschlimann, 1972; Sojka et al., 2013). Nearly all species of *Ixodes* have a two or three-host life stage, which in turn results in a quickly spreading disease. One and two-host ticks moult while on the host, three-host ticks drop off the host to moult (Jongejan and Uilenberg, 2004). Their small size and broad host range allow ease of transportation to numerous locations (Lv et al., 2014b).

Different species of ixodid ticks undergo either a one-host, two-host, or three-host life cycle (Barker and Walker, 2014; Guglielmone et al., 2014). In a one-host life cycle, the tick remains on the same host for larval, nymphal, and adult stages, only dropping off the host when it is an engorged female to lay eggs (Barker and Walker, 2014). The cattle tick, *Rhipicephalus microplus*, is an example of a tick undergoing a one-host life cycle (Barker and Walker, 2014). The two-host life cycle spans over two years where the larval stage attaches to the first host, feeds, and moults to the nymphal stage on that first host. The nymph drops off the host moulting into an adult, which then feeds on the second host until the engorged female drops off to lay her eggs (Barker and Walker, 2014). The genus *Hyalomma* are usually two-host tick species (Guglielmone et al., 2014). Finally, the three-host life cycle, as generally described above,

involves the larval, nymphal, and adult stages feeding on a host and then dropping off after each life stage to moult into the next life stage. Adults can mate on and off the host depending on the species, but most *Ixodes* species mate off the host on the vegetation (Needham and Teel, 1991; Barker and Walker, 2014).

1.13.2 Tick survival strategies

Blood feeding is an essential physiological process for survival and growth and evolved more than 20 times independently in Arthropoda (Mans and Neitz, 2004; Sojka et al., 2013). Ticks are the most ancient terrestrial arachnids evolving blood-feeding capabilities (Mans and Neitz, 2004; Bellgard et al., 2012). The host's blood is a source of energy and nutrients, which is called hematophagy (Sojka et al., 2016). The tick midgut is responsible for digestion of a blood meal (Grattan-Smith et al., 1997). The most important organs in their body are the salivary glands, an evolutionary adaptation for specialised feeding (Grattan-Smith et al., 1997). These salivary glands are essential to the biological success of ticks and are involved in pathogen transmission (Sauer et al., 1995).

The questing behaviour of ticks is consistent across *Ixodes*. Generally, ixodid ticks are attracted by physical and chemical stimuli such as carbon dioxide, heat and odours (Wall and Shearer, 1997; Bonnet and Liu, 2012). When recognised, ticks crawl to the top of a blade of grass when sensing the presence of a potential host. Optimal hosts vary depending on the age and species of tick. Larvae and nymphs are more likely to feed on smaller mammals, i.e., rodents, while adult females are more likely to feed on larger mammals, i.e., kangaroos (Bonnet and Liu, 2012).

Depending on the species of tick, the complete life cycle can be longstanding taking one to three years to develop from eggs to adults (Grattan-Smith et al., 1997). There are also some considerable differences in tick survival strategies that depend on the species and life cycle. In the Northern Hemisphere, the life cycle is often longer because of the harsh winters requiring ticks to include a period of cold-induced diapause which is observed in species including *I. scapularis*, the vector responsible for Lyme disease (Kocan et al., 2015; Beati

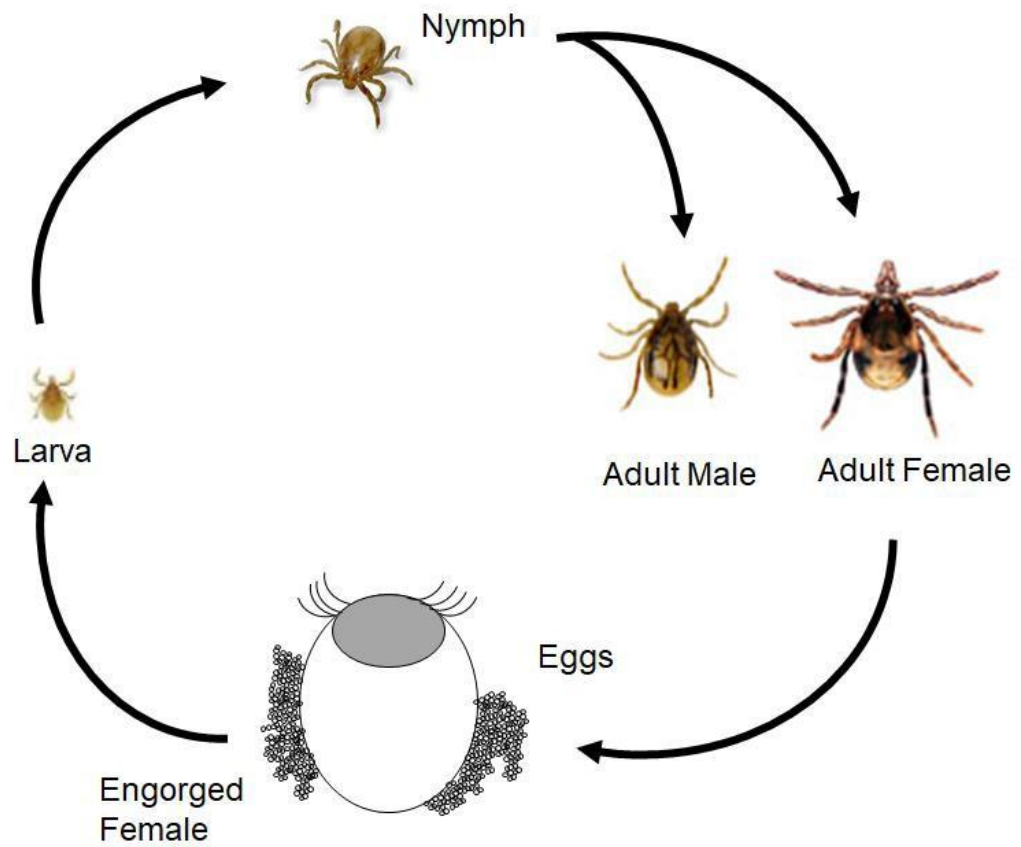


Figure 1.11: The general life cycle of *Ixodes* ticks, adapted from Wall and Shearer (1997).

and Klompen, 2019). The tick attaches to a host varies depending on its species and life stage. In the Southern Hemisphere, Australian ixodid ticks become more active once the humidity level increases to a satisfactory level, primarily a relative humidity of 85% (Oorebeek and Kleindorfer, 2008). Ticks rely on high humidity as desiccation is the leading cause of death, and they will typically only quest when humidity is high (Oorebeek and Kleindorfer, 2008).

Generally, larvae attach for three to four days, nymphs attach for four to seven days, (Grattan-Smith et al., 1997) and adult females attach approximately eight to 24 days. Ixodid ticks spend 94-97% of their life off the host waiting for a potential host (Klompen et al., 1996). Few *Ixodes* species require mating to occur on the host. For example, *I. scapularis* mates on the host and successfully has been able to live its life cycle in laboratory conditions (Kocan et al., 2015).

Interestingly, ticks survive longer than any other arthropod without food or water (Needham and Teel, 1991). Characteristically, it is the off-host period which is an essential stage for *Ixodes* because it is entirely a survival strategy. Not all ticks will survive the periods between attachments to the host. Aforementioned, ticks in Australia rely heavily on high humidity, rainfall and low temperatures for survival (Needham and Teel, 1991; Oorebeek and Kleindorfer, 2008). Temperature significantly affects the rate of growth for ticks (Chilton, 1992) and consequently, the prevalence of ticks fluctuates depending on the season.

1.13.3 Challenges for using ixodid ticks to transmit *Cercopithifilaria johnstoni*

In the context of developing an animal model of *C. johnstoni* with *Ixodes* as the vector for parasite transmission, the number of pathogens and toxins ticks carry can be a problem. Some species do not transmit viral or bacterial agents alone, but their bites result in paralysis or hyper-susceptibility (Grattan-Smith et al., 1997). In Australia, priority for extensive research is the paralysis ticks, *Ixodes holocyclus* and *Ixodes cornuatus*. It is difficult to distinguish between these two paralysis species despite having a different geographical range (Jackson et al., 2000). *I. holocyclus* alone is a very economically important tick and is endemic to Australia (Jackson et al., 2000; Song et al., 2011) generally living on the East coast of Australia (Spratt and Haycock, 1988; Stone et al., 1989; Grattan-Smith et

al., 1997). *I. cornuatus* predominately inhabits Tasmania and Southern Australia (Jackson et al., 2000).

Host preferences for *I. holocyclus* have not been well defined (Jackson et al., 2007). *I. holocyclus* is known to cause fatalities in small mammals but it is currently unknown whether the paralysis tick prefers small or large hosts (Kaire, 1966; Grattan-Smith et al., 1997; Storer et al., 2003). A study conducted by Binnington and Stone (1981) demonstrated that mice die after the paralysis ticks fed on them for more than 96 hours. The neurotoxin comes from the salivary glands in *I. holocyclus* (Grattan-Smith et al., 1997; Storer et al., 2003). The symptoms associated with the toxin injected by *I. holocyclus* are loss of appetite, incoordination of hind limbs, decrease of body temperature and then a fatal coma (Dodd, 1921; Stone et al., 1989; Masina and Broady, 1999). These symptoms occur approximately three to five days after attachment, allowing time for the tick to feed and fully engorge (Kaire, 1966; Binnington and Stone, 1981; Grattan-Smith et al., 1997). In humans, an intense allergic reaction such as a rash can occur when bitten by multiple *I. holocyclus* larvae (Grattan-Smith et al., 1997). Children that are bitten by a paralysis tick are more likely to exhibit symptoms from the toxin consisting of, drowsiness, tiredness, slurred speech, and paralysis in legs, inability to drink and if left untreated, death (Grattan-Smith et al., 1997). However, animals indigenous to the country appear to be immune to the paralysis tick (Dodd, 1921; Doube, 1979) and small mammals appear to be resistant to the immature stages of paralysis ticks. In contrast, some small birds and even cases of bandicoots are shown to be affected and die from paralysis (Doube, 1979).

The paralysis ticks are common in areas where Spratt and Haycock (1988) found *C. johnstoni*-infected rodents. For the successful development of a small animal model with *C. johnstoni*, it is necessary to develop an appropriate laboratory colony or source of the most efficient tick species to transmit *C. johnstoni* to its host. Due to the paralysing nature of the paralysis ticks, it would be preferable to avoid transmission of *C. johnstoni* with *I. holocyclus* to avoid the potential toxin effects on immunocompromised small mammals. The *I. holocyclus* toxin will affect small rodents, especially species such as *R. norvegicus* and would obscure the observation of disease symptoms due to the paralysis symptoms deeming the animal model unsuccessful. It is therefore essential to identify the appropriate tick species for transmission of *C. johnstoni*.

1.13.4 Characterising tick species for an animal model

Identification of tick species is an essential aspect of developing the animal model. Ticks have a small body size of one to three millimetres when they are not engorged and vary depending on the life stage of the tick. As they are small in general, it is difficult to morphologically differentiate between species without dissection (Guglielmone et al., 2014). Studies have developed morphological characteristics which enable the identification of some adult tick species (Roberts, 1970; Barker and Walker, 2014). Morphological identification of Metastriate ticks is possible at the adult stage with these characteristics, but the younger life stages are much more challenging (Anderson et al., 2004). Species-level morphological identification of ixodid ticks is difficult at the larval and nymph life stages due to a lack of easily identified, taxonomically informative morphological characteristics (Anderson et al., 2004; Lv et al., 2014a).

Morphological characterisation has subdivided the genus *Ixodes* into 15 sub-genera but the monophyly of many of the sub-genera are challenged (Clifford et al., 1973; Nava et al., 2009). Commonly, many molecular studies have been challenging the original morphological classification of ixodid ticks (Nava et al., 2009). Other studies suggest *Ixodes* is polyphyletic and Australian species are positioned separately within the phylogeny (Klompen and Oliver, 1993; Klompen et al., 2007). Typically, the morphological and molecular characterisation of ticks has been conducted independently and are usually a topic of debate for what are the correct phylogenetic relationships. The incongruence between molecular and morphological characterisation is partly a result of minimal sequence data of identified ticks. Currently, there are approximately seven of 243 *Ixodes* species that have complete mitochondrial genomes (Burnard and Shao, 2019).

I. holocyclus has one sequence available and now *Ixodes tasmani* has a genome available. Phylogenetic relationship predictions are drastically improved by using complete mitochondrial genome sequences and further improved using complete nuclear genomes as this includes more information on genetic variation and results in highly supported phylogenetic trees. As a result of minimal whole mitochondrial genomes for ticks, taxonomic relationships are typically predicted using mitochondrial or nuclear genes (Norris et al., 1999) or those species without appropriate genetic information are excluded from analyses. Many

intraspecies relationships throughout *Ixodes* are unresolved (Shaw et al., 2002; Song et al., 2011; Burnard and Shao, 2019)

The incongruence between morphological and molecular species identification is also a result of two *Ixodes* ticks morphologically appearing identical but having different genetic sequences (Andrews et al., 1992). It is these complications that make tick phylogenetics a problematic component of research and will be a significant hurdle in the development of an animal model using ticks to transmit *C. johnstoni* to rodents. Accurate discrimination and identification of tick species could be the basis of controlling tick-borne diseases (Lv et al., 2014b) and also enable them to be used confidently as vectors of parasitic models such as the *C. johnstoni* animal model.

1.14 Direct comparison of *Onchocerca volvulus* and *Cercopithifilaria johnstoni*

1.14.1 Parasite life cycles

The life cycles of *C. johnstoni* and *O. volvulus* are similar (Figure 1.3, 1.7). Transmission of *C. johnstoni* and *O. volvulus* rely on the vectors, ticks and black flies, respectively, to develop and mature into the infective L3 stage. The iL3 stage of *O. volvulus* penetrates the human host (Figure 1.3) equivalent to the iL3 stage of *C. johnstoni* (Figure 1.7). The iL3 matures into the L4 stage and then into adults. The adults produce microfilariae in which migrate throughout the subcutaneous tissue (Figure 1.3, 1.7). A *Simulium* fly will bite a human and ingest an *O. volvulus* microfilaria (Figure 1.3) and an ixodid tick will bite a rodent ingesting the *C. johnstoni* microfilariae (Figure 1.7) for the parasites to mature to the L2 and iL3 stages within the vectors. The vectors will bite their respective hosts, and the life cycle continues.

The main difference between *C. johnstoni* and *O. volvulus* within their respective hosts is that *Onchocerca* adults reside in nodules in the human's bodies. In contrast, *Cercopithifilaria* adults reside in the subcutaneous tissues. There is no evidence to suggest the difference in the presence of nodules in *O. volvulus*-infected humans and absence of nodules in the *C. johnstoni*-infected rodents is pivotal in understanding onchocerciasis. There is a possibility that the adult worms in nodules within the human host could be more protected and thus

macrofilaricidal drug development would need to ensure the adult worms could still be targeted through the nodule. Although this is only speculation and considering *C. johnstoni* recapitulates every other symptom *O. volvulus* cause, *C. johnstoni* is still the most convincing candidate to pursue further for animal model development. The clear similarity of *C. johnstoni* and *O. volvulus* parasitic life cycles makes *C. johnstoni* an appealing parasite to explore (Spratt and Haycock, 1988). The life cycle can be replicated to mimic the life cycle of *O. volvulus*, but more importantly, *C. johnstoni* recapitulates the characteristic immunopathology and disease features of *O. volvulus*.

1.14.2 Vectors

An added complication to the development of an animal model for onchocerciasis is the vector species responsible for transmitting the parasite. As well as maintaining the parasite life cycle in an appropriate and convenient host, the vector life cycle also needs to be maintained. The *C. johnstoni* animal model requires ixodid ticks to transmit the parasite to small mammals. *Simulium* and *Ixodes* are complicated groups of intermediate vectors containing cryptic species.

Vector species are a primary component of studying disease as they are responsible for transmitting parasites to various hosts (Jongejan and Uilenberg, 2004; Guglielmone et al., 2014). Simuliidae is comprehensively studied as they are blood-feeding insects that play a considerable role in onchocerciasis, significantly impacting the medical, economic and veterinary industries (Connor et al., 1970). However, it has been complicated to differentiate between sibling species known as the *S. damnosum* Complex (Connor et al., 1970). The *S. damnosum* Complex was named in the 1950s because studies indicated *S. damnosum sensu lato* consisted of numerous complex sibling species (Le Berre et al., 1979; Walsh et al., 1979; Krueger and Hennings, 2006) with increased divergence (Rivera and Currie, 2009). The most widely distributed member of the complex is *S. damnosum* (Ibeh et al., 2006), hence *S. damnosum sensu lato*. There are approximately 65 morphologically distinct species and sibling species in the *S. damnosum* Complex (Rivera and Currie, 2009).

Similarly, ixodid ticks also form a cryptic species complex. There has been a prolonged controversy between morphological characterisation and molecular

characterisation of tick species (Nava et al., 2009; Barker and Walker, 2014). Several ixodid ticks are morphologically identical but molecularly appear to be a different species, thus complicating taxonomy (Barker and Walker, 2014).

1.15 Genome assemblies and comparative genomics

The improvement of next-generation sequencing technology combined with advances in computational biology and bioinformatics has drastically improved and accelerated the process of understanding parasite biology and disease (Stoltzfus et al., 2017; Bennuru et al., 2018; Tyagi et al., 2019b). Helminth genomes range between approximately 10,000 and 20,000 protein-coding genes per genome, specifically filarial nematodes ranging between approximately 8,000 and 15,000 protein-coding genes (Bennuru et al., 2018). Approximately half of these predicted genes are functionally unknown. They are most likely going to be parasite-specific, making them difficult to identify and explore (Palevich et al., 2018). Many of these protein-coding genes are characterised as hypothetical proteins.

Comparative genomics can offer a short-cut for animal model development for several diseases by identifying antigens or proteins that could be useful in targeting the parasites. Bioinformatics is a tool that can assist in exploring genomic data to identify putative antigens, identifying their structures and potential functions, which could be useful in future control and treatment of diseases. Consequently, the analysis of genome assemblies *in silico* is a fundamental component of onchocerciasis research because of the absence of an immunocompetent animal model to test identified targets for novel treatments.

1.15.1 Genomes: a resource for identifying drug or vaccine candidates or antigens recognised by sera

High-quality reference genomes provide a platform to investigate the underlying biological processes by describing the transcriptomics, proteomics, metabolomics and other specialised 'omic' technologies (Bennuru et al., 2016; Bennuru et al., 2018; Tyagi et al., 2019a). Bioinformatics tools can then aid easy and rapid identification of drug, vaccine or serodiagnostic candidates that could be used in the context of disease treatment (Bennuru et al., 2016). An omics-

driven knowledge-based identification of drug targets is a powerful approach to identify targets essential for organisms' survival (Coghlan et al., 2019; Tyagi et al., 2019a). Specifically, for filarial nematodes, omics approaches are essential for understanding the evolution of the Phylum Nematoda (Mitreva et al., 2011). Transcriptomic and proteomic data have been used as a resource for exploring and understanding biological pathways that are critical for the development of the parasite. Previous studies in *O. volvulus* have concentrated on biological pathways required in the vector and human hosts, host-parasite interactions and for identifying novel targets for various interventions (Bennuru et al., 2016). These new multi-omics approaches may be the best way to evaluate the most appropriate drug targets. There have been two protein groups identified that could be appropriate for drug development including conserved nematode-specific proteins and proteins sharing homology but are sufficiently diverged from those in the host (Tyagi et al., 2019b). Conserved nematode-proteins are very important to understand the biology of parasites and also parasitism but can also be rather difficult to study because there are many functional unknowns about these proteins. The conserved nematode-protein group could be an excellent target for developing novel drug targets.

Draft genomes of *B. malayi*, *W. bancrofti*, *O. volvulus* and *L. loa* have been valuable resources for nematode genomics (Ghedini et al., 2007; Desjardins et al., 2013a; Cotton et al., 2016). Genomes provide genomic information that was not previously available. Once the genomic information is assembled into genes, it can be further used to identify proteins that are possibly antigenic, based on a set of criteria. The proteome from draft genomes can then be connected with immunological data that identifies the host's immune response to antigens. Finally, it is possible to construct a list of antigens that elicit an immune response that may be useful in understanding the immunopathology of a disease. The *L. loa* genome enabled comparative proteomic analyses of urine and sera from infected patients to identify novel antigens that can be used to detect infected individuals (Tallon et al., 2014). Without the genome to be used as a resource, identifying appropriate antigens that can distinguish between infected and uninfected individuals would be more complicated (Bennuru et al., 2018).

Bioinformatics has emerged as an excellent tool for analysing datasets in various fields, thus promoting *in silico* approaches to research (Sharma et al.,

2013). The filarial genomes have been used *in silico* to identify novel targets that could be examined and studied to understand diseases such as onchocerciasis and lymphatic filariasis. These targets could then be used to design anti-filarial drugs or macrofilaricidal drugs used to treat diseases (Sharma et al., 2013). The multiple MDA treatment programmes that have targeted onchocerciasis with ivermectin have instigated the need to identify more effective treatment options such as a macrofilaricidal drug (Bennuru et al., 2018).

Comparative genomics of filarial parasites provides a dataset of potential targets that could be used to understand or treat disease. Comparing various genomes and their inferred pathways identifies evolutionarily conserved features or features that are divergent between organisms which can be beneficial in understanding novel organisms or those that already cause disease (Bennuru et al., 2018; Bennuru et al., 2019). Through comparative genomic studies, several genes, proteins or critical pathways have been identified and can be further exploited to develop improved diagnostic and therapeutic tools. Identifying genes and proteins in novel organisms such as *C. johnstoni* would be essential to understand the parasite in more detail. Moreover, the identification of proteins could lead to understanding how *C. johnstoni* can elicit similar immunopathology in a different host species comparative to *O. volvulus*. *In silico* studies are an excellent first approach to understand initial genomic information about a parasite before devoting resources and funding to physical experiments.

There are several publications using similar *in silico* methods to identify immunogenic *O. volvulus* proteins that could be used to (a) explain the host immune responses to the death of the parasites, or (b) develop possible drug or vaccine targets for onchocerciasis treatment. Two publications have used moderate to high throughput approaches to refine the list of identified *O. volvulus* proteins to a small list of highly immunogenic proteins. The first approach by Norice-Tra et al. (2017), focused on a multilocus immunophenotyping serological method of testing peptides to characterise various *O. volvulus* populations from *O. volvulus*-infected patients (Norice-Tra et al., 2017). They derived pairs of 15-mer peptides from the sera of patients from 16 known immunogenic *O. volvulus* proteins and discovered significant immunoreactivity (Norice-Tra et al., 2017). The second approach focused on multi-omics (genomics, transcriptomics, proteomics and immunomics), to find immunodiagnostic antigens for

serodiagnosis of onchocerciasis (McNulty et al., 2015). A group of 241 immunoreactive proteins were identified initially and then further refined through a rigorous bioinformatics pipeline to a list of 33 *O. volvulus*-specific candidate antigens that were seen to be consistently expressed throughout the life stages. Several of the 33 antigens are potential serodiagnostic candidates and are consistently identified in other studies suggesting the list of *O. volvulus* candidates are important. The multi-omics study has been one of the more carefully structured studies conducted on identifying immunodiagnostic antigens because they have developed stringent criteria for identifying *O. volvulus*-specific antigens.

Different research groups have taken a different approach to explore the *O. volvulus* proteome. Instead of focusing on whole proteins, the targets are immunogenic peptides within each protein identified using peptide microarrays (Lagatie et al., 2017; Lagatie et al., 2018). These studies screened serum samples of *Onchocerca* microfilaridermic patients to identify peptide targets that could be used for the development of immunodiagnostic tests (Lagatie et al., 2017). The microarray experiments resulted in 1,110 immunoreactive peptides with 249 of these being immunodominant and three highly overrepresented with motifs of PxxTQE, DGxDK, QxSNxD (Lagatie et al., 2017). IgG1, IgG3, IgE and IgM are all dominating the immune response against each of the motifs. Identified peptides could be used to develop immunodiagnostic applications based on the peptide serology from *O. volvulus*-infected patients (Lagatie et al., 2017). The advantages of working with peptides over whole proteins are that synthetic peptides do not rely on biological material thus making them an appealing approach for developing tests such as the Ov-16 test (Lagatie et al., 2017). Full proteins are more reliant on complex biological material often complicating experiments. Minimal samples of the biological material required would then impact experiments and slow the diagnostic test development.

A follow-up study investigated whether chosen vaccine candidates contain peptide fragments that are recognised by antibodies in *O. volvulus*-infected individuals (Lagatie et al., 2018). It was discovered that the poly-glutamine stretch in the N-terminal region of RAL-2 (OVOC9988) is a 9-mer peptide and a possible serological marker that should be explored further (Lagatie et al., 2018). Multiple vaccine candidates successfully contained immunodominant linear epitopes, but

the 9-mer peptide was highlighted as a more interesting peptide to explore because it was found explicitly in *O. volvulus* and not in other filarial nematodes (Lagatie et al., 2018).

Collectively these studies provide a comprehensive list of *O. volvulus* proteins that show immunogenic properties which could lead to a more thorough understanding of onchocerciasis. Onchocerciasis has very complex immunopathology which is poorly understood. If an organism were to be used to study *O. volvulus* in an animal model such as *C. johnstoni*, it would be important to identify possible orthologues of known immunogenic *O. volvulus* proteins or peptides throughout the proteome. If *C. johnstoni* contains similar immunogenic proteins, then it would be possible to explore alternate drug candidates or host immune responses in the *C. johnstoni*-rodent animal model that are comparable to the *O. volvulus* human infection.

1.16 Onchocerciasis immunopathology and antigen based assays/targets

One area of onchocerciasis research that has not been well defined is understanding the immunopathology. It is clear on the pathology that is caused by an *O. volvulus* infection, however the antigens that could play a role in the host's immune response are unknown and understudied. It is known that there are antigens that have been shown, through immunoblotting, proteomic and immune assay experiments, to elicit strong antibody responses and therefore shown to drive an immunogenic response. Unfortunately, this is the only level of understanding about onchocerciasis immunopathology relating to antigenic determinants. Thus draft genomes are very useful in this context because the genomes can be used to compare across closely related species to look for orthologues of proteins that appear immunogenic, i.e., McNulty et al., (2015), Norice-Tra et al., (2017), and Bennuru et al., (2018, 2019). It is this research that can lead to appropriate immunology experiments to identify the antigens eliciting an immune response. An animal model that shares similar immunopathology with *O. volvulus*-infected individuals will enable these investigations and improve the understanding of antigenic recognition and immunopathology.

Other fields of research have focussed on the development of assays to identify onchocerciasis infection or surveillance of disease transmission

throughout and after treatment programmes, including APOC. There is an abundant body of literature targeting different antigens to explore different measures of assessing infection, but only two will be briefly described here. Ov-16 is used to identify *O. volvulus* infection and infection surveillance while OV-39 has been explored to determine the cause of the immunopathology associated with *O. volvulus*. The two targets have provided further evidence to understand the symptoms associated with the disease.

1.16.1 Ov-16 assay

The Ov-16 assay has been successful in identifying onchocerciasis infection. It uses the recombinant antigen Ov-16 to measure immunoglobulin G4 (IgG4) antibody prevalence in patients (Lipner et al., 2006; Higazi et al., 2013). The Ov-16 design was to be used for field diagnosis and to eventually assess whether there has been a successful interruption of *O. volvulus* transmission throughout affected communities (Higazi et al., 2013; Vlamincx et al., 2015; Unnasch et al., 2018). The most successful aspect of the Ov-16 ELISA is that the antigen is present in all life stages of *O. volvulus* and thus can identify infection at any stage (Unnasch et al., 2018). It has been excellent for monitoring young children that are born in areas that are towards the end of elimination programmes. The test assists identification of whether the programmes have worked and whether the children have any antibodies indicating whether transmission has been interrupted (Lipner et al., 2006). Despite Ov-16 ELISA being successful, not all patients with onchocerciasis will develop antibodies against Ov-16, and therefore there is an error associated with the test (Lipner et al., 2006; Unnasch et al., 2018). There is a lack of research on this test in various endemic settings. The Ov-16 test may not be the most successful approach for epidemiological surveillance, and thus alternative methods would need to be developed (Lagatie et al., 2017). The need for new techniques for surveillance of onchocerciasis and the need for new treatments as a result of potential resistance occurring in endemic communities had facilitated the vast amount of studies pursuing diagnostic targets to eliminate or at a minimum monitor the current treatment of onchocerciasis in Africa.

1.16.2 Ov-39 protein

Immunologic cross-reactivity between host and parasite antigens has been explored in *O. volvulus* research which may be playing an important role in immunological disease. It was found that the *O. volvulus* antigen Ov-39 is cross-reactive with the human retinal antigen hr44 that induces ocular inflammation in rats after immunisation. It was confirmed in naïve rats, the CD4+ cell lines specific to Ov-39 induce ocular inflammation (McKechnie et al., 2002). Ov-39 and hr44 are not homologous antigens; however, reactivity using monoclonal antibodies and T-cell lines have demonstrated antibody and T-cell cross-reactivity. The cross-reactivity of the *O. volvulus* antigen Ov-39 with the human hr44 is of particular interest because ocular inflammation and pathology is the principal characteristic of onchocerciasis (McKechnie et al., 2002). The identification of these types of antigens may improve the understanding of onchocerciasis immunopathology and improve diagnostic tools to target the antigens driving the pathology.

1.17 Limitation of *in silico* studies

Despite the abundant source of omics data available to study parasite-host relationships of parasitic nematodes, there is still so much that is unknown and needs to be explored to understand these relationships. There are several limitations of *in silico* projects that are important to acknowledge in the current thesis. There are three major steps involved in *in silico* studies: genome assembly, discovery of genes and improving gene prediction. The genome can be assembled using short-read, long-read or a combination of sequencing data. However, using only short-read data means it is highly unlikely the genome can be assembled to large scaffolds or into chromosomes. Using only long-read data to assemble the genome could lead to misassembled regions due to the sequencing chemistry. Whereas using a combination of short and long-read data allows the short reads to be mapped onto the long reads and assembled into chromosomes as several of the best genomes have been assembled. Nevertheless, as long as the assembled genome contains the majority of the genome, regardless of how fragmented, it can still be very informative to use in comparative analyses.

One major limitation of *in silico* studies is the discovery of unknown genes using bioinformatics. Once a genome is assembled it is important to annotate the genome identifying gene regions. A current hurdle in gene discovery is that it is only possible to use previously discovered genes to predict the new genes in another species (Stoltzfus et al., 2017). Typically, unknown genes are labelled as uncharacterised or hypothetical genes. Unless the genes share homology to known and characterised gene, it is unlikely to be identified thus missing potentially valuable information about the parasites' biology (Grote et al., 2017; Stoltzfus et al., 2017). One method to identify genes of a new parasite it to use a closely related species to train the gene prediction. The limitation with these methods is that the gene prediction is only going to be as successful as the gene information provided to the bioinformatics tool, i.e., fragmented, missing genes will result in the prediction of fragmented or missing genes in the novel species.

Discovering genes using bioinformatics is and essential step in annotating the genome. It is then important to validate these genes to improve the gene prediction. Validating the gene prediction requires abundant fresh parasite material to obtain RNA-Seq data. The RNA-Seq data can then be assembled to

validate the bioinformatics gene predictions thus confirming a gene set for a particular parasite.

Parasitic nematodes have unique biology in which is highly likely to be regulated by the species-specific or novel genes that are so difficult to characterise (Stoltzfus et al., 2017). In an ideal situation, the species-specific, potentially novel genes are the genes to focus data analyses efforts to learn more about the novel biology of filarial parasites. Unfortunately, this is not always possible. The following thesis encompasses these similar limitations. The putative *C. johnstoni* protein-coding genes are used to explore orthology with known *O. volvulus* proteins and little focus directly on "novel" *C. johnstoni* proteins. Conducting such analyses would require complete genome, proteome and transcriptome assemblies to be more confident in gene and functional annotations. Further, *C. johnstoni* projects should focus on the complete *C. johnstoni* proteome to determine how similar or different the protein-coding genes are to further understand filarial disease control.

1.18 Rationale for this body of work

There is a high-quality genome assembly of *O. volvulus* that has been used for many genomic studies to further understand the filarial parasite in the context of disease (Cotton et al., 2016). The *O. volvulus* genome is one of the best-curated genomes available for a non-model organism consisting of RNA-Sequencing (RNA-Seq) transcriptomic data, proteomic data and genomic data to inform and guide gene predictions and protein-coding regions accurately (Cotton et al., 2016). The genome has been assembled to chromosomal level, including the sex chromosome. The abundance of genomic information for *O. volvulus* allows for future analyses in identifying potential drug targets and candidates for experimental validation to eliminate onchocerciasis. The improvement of the *O. volvulus* genome has drastically fast-tracked onchocerciasis research and has allowed for many comparative studies providing a much better understanding of the disease. The absence of an animal model to provide the various *O. volvulus* life stages, imposes major impediment to immunological studies (Lucius et al., 1988).

C. johnstoni could be a filarial nematode to use in a small animal model to study onchocerciasis. The parasite has demonstrated similar immunopathology in rats that *O. volvulus* causes in humans. Most importantly, original research has identified ocular lesions caused by microfilariae that other small animal models, i.e., *A. viteae* in jirds and *L. sigmodontis* in hamsters, have not been able to recapitulate (Spratt and Haycock, 1988; Vuong et al., 1993). It is unclear, however, whether the similar immunopathology is a result of specific parasite antigenic proteins, parasite presence, host immune system or another driving force of disease features.

Currently, there are no genomic resources available for *C. johnstoni*. Typically, the absence of genetic information for parasites is a consequence of complex life cycles and not having relevant animal models to study disease *in vivo* (Tyagi et al., 2019b). Ideally, obtaining comparable genomic data would enable the comparison of *C. johnstoni* and *O. volvulus*. It could then be determined whether *C. johnstoni* is genetically and immunologically similar enough to *O. volvulus* to justify the use of *C. johnstoni* in a small animal model to troubleshoot novel disease treatments for onchocerciasis.

There is no suitable animal or immunologically relevant model to study onchocerciasis. Without a suitable model, drug development is more complicated and are not able to test potential treatments that may be more suitable for disease elimination. There are no successful macrofilaricidal drugs that can be used to target the adult worms of *O. volvulus*. The absence of a suitable animal model makes basic biology even more challenging to understand.

The use of genomics will aid in understanding *C. johnstoni* and enable direct comparison with *O. volvulus* and other filarial nematodes to identify potential orthologous targets that may be involved in onchocerciasis immunopathology. Comparative genomics thus provides an avenue for model development.

1.19 Thesis aims

The overall aim of this PhD is to determine the suitability of *C. johnstoni* as a model organism used in a small animal model for onchocerciasis, and is explored through the following sub-aims:

1. To place *C. johnstoni* phylogenetically by determining its relationship with other filarial nematodes.
 - a. To assemble the mitochondrial genome, compare with other filarial species and position within the filarial nematode clade (Chapter Two).
 - b. To assemble the nuclear genome, compare genome completeness, content and synteny with other filarial nematodes (Chapter Three).
2. To catalogue characterised immunogenic proteins in the *O. volvulus* genome and determine if they are conserved in *C. johnstoni*.
 - a. To identify one-to-one orthologues, comparing protein structure and putative function to see if there is an immunological similarity between *O. volvulus* and *C. johnstoni* (Chapter Four).
 - b. To explore any diversifying or purifying selection acting on orthologous putative immunogenic genes (Chapter Four).
3. Characterise the vector species of *C. johnstoni* and establish a life cycle in the laboratory.
 - a. To examine the species diversity of ixodid ticks collected on vegetation at two field sites in NSW to identify a suitable vector for *C. johnstoni* transmission in a laboratory model (Chapter Five).
 - b. To conduct tick attachment experiments and observe how the ticks will feed and transmit the parasite to the rodent host (Chapter Six).

The thesis will aim to demonstrate the ability to use closely related filarial nematodes to understand *O. volvulus*, the filarial nematode responsible for onchocerciasis. Comparative genomics will be used to identify key features or antigens that may be involved in onchocerciasis disease immunopathology. The following thesis will explore a possible animal model that could significantly improve the current knowledge of onchocerciasis facilitating the development of more appropriate drugs for treating the disease.

Chapter Two

Comparison of evolutionary relationships between *Cercopithifilaria johnstoni* and filarial nematodes using the mitochondrial genome

2.1 Introduction

The mitochondrion is an organelle present in the majority of eukaryotes and contains its own closed circular DNA genome. This mitochondrial genome is typically inherited maternally in animals (Awise et al., 1987). The mitochondrial DNA (mtDNA) of many animals, including nematodes, evolves at a much faster rate than single-copy nuclear DNA (Brown et al., 1979; Awise et al., 1987), a trait that may be advantageous when differentiating between closely related taxa (Brown et al., 1979; Vawter and Brown, 1986). There is a core mitochondrial genome that consists primarily of the genes encoding components of the electron transfer chain. Several organism's mitochondrial genomes encode 13 protein genes which include ATP8 a subunit of the electron transfer chain (Feagin, 2000). All filarioid mitochondrial genomes encode two ribosomal RNA genes, 22 transfer RNA genes, and 12 protein-coding genes (Ramesh et al., 2012). *Trichinella spiralis* is an exception and has retained the ATP8 gene (Hu and Gasser, 2006). There are a lot of genes that are also present or absent in different taxa but these group of 12-13 genes are generally throughout to be conserved amongst all taxa.

Typically, CO1 (cytochrome c oxidase subunit 1) or 12S sequencing of mitochondrial DNA has been used to characterise nematodes and then position them in the phylogenetic tree (Casiraghi et al., 2004; Bain et al., 2008; Ferri et al., 2009). Gene sequencing has many advantages, especially for novel species, because it requires less genetic material. It is fast and efficient and can quickly differentiate between species. Single locus sequencing also allows comparison of species for which whole genomes are not available. The disadvantage for sequencing only the CO1 or 12S mitochondrial genes is that there is missing information that could be valuable for interpreting evolutionary relationships of species (Duchêne et al., 2011). The understanding of parasites has been improved through the development and construction of mitochondrial genomes as

by using complete mitochondrial genome data; it is possible to get a more reliable estimate of phylogeny. Sequencing the genomes of more species allows for more accurate phylogenetic analyses, leading to more detailed comparative studies of evolutionary history. There are still gaps in our knowledge of genomics for the Phylum Nematoda and thus it is important to continue to sequence, assemble and study the genomes of filarial nematodes. Two major gaps are taxonomic sampling and phylogenetic analyses based on a small number of markers. Aforementioned, sequencing the genomes of more species will correct the historical taxonomic sampling bias that focused primarily on a few groups of parasites and a small number of closely related free-living species. The 1000 genomes project consortium has made considerable progress in sequencing the genomes of 959 new species that sample the phylum Nematoda more broadly (Kumar et al., 2012). Initiatives such as these will vastly improve phylogenetic analyses with an abundance of molecular information. The second problematic gap in genomics is the use of a small number of markers. Phylogenetic analyses using a couple of mitochondrial markers are likely to be significantly less informative than whole mitochondrial or nuclear genomes. An important reason not to rely on mitochondrial genes alone is that the mitochondrion behaves as a single linkage group i.e., effectively a single gene, due to the uniparental inheritance and absence of recombination. Thus, although it accumulates mutations faster than the nuclear genome it is often less variable than the nuclear genome, where variation is generated by more processes than just mutation. It is important to have a combination of genetic markers to infer phylogenetic relationships. Not every species has a whole genome sequenced, thus there are still several species that do not have informative nuclear genetic sequence, hence this a considerable gap in research.

Mitochondrial genomes are resources for studying phylogenetic relationships and the evolutionary history of parasites. It is assumed in nematodes that mitochondrial genomes are maternally inherited and may not be subjected to genetic recombination resulting in conserved gene arrangement even across deep evolutionary history (Wolstenholme, 1992; Keddie et al., 1998). Nucleotide substitutions occur at much higher rates in the animal mitochondrial genome than in the nuclear genome and have highly variable non-coding regions that are presumably evolving neutrally (Avise et al., 1987; Wolstenholme, 1992; Keddie et al., 1998; Li et al., 2018). These differences in the mitochondria

between nematode species enable determination of evolutionary relationships (Osawa et al., 1992; Wolstenholme, 1992; Le et al., 2000) and thus the complex life histories and transmission of filarial nematodes could be better understood by using comparative genomics. Mitochondrial genomes have been sequenced and assembled for *B. malayi* (filarial nematode of humans causing lymphatic filariasis, the only filarial nematode able to be maintained in jirds, a non-human, permissive host; (Ghedini et al., 2007)), *O. volvulus* (which causes onchocerciasis in humans; (Keddie et al., 1998)), *O. ochengi* (which infects cattle; (Jaleta et al., 2018)), *O. flexuosa* (which infects deer; (McNulty et al., 2012)), *D. immitis* (transmitted by mosquitos and causes heartworm disease in canines; (Hu et al., 2003)), *L. loa* (causes loiasis in humans; (McNulty et al., 2012)), *A. viteae* (a model organism in jirds to study human filariasis (McNulty et al., 2012)) and *W. bancrofti* (causes lymphatic filariasis in humans; (McNulty et al., 2012)).

The highly conserved nature of filarial mitochondrial genomes can provide valuable phylogenetic comparative information between species (Hu and Gasser, 2006; Duchêne et al., 2011; Li et al., 2018). As there are no genetic resources available for *C. johnstoni* and no information regarding the relationships of *C. johnstoni* with other nematodes, the assembly of a genome is imperative to position *C. johnstoni* in the phylogeny and identify close evolutionary relationships. The mitochondrial genome of *C. johnstoni* will be the first genomic resource generated to position *C. johnstoni* with the other close nematode relatives.

2.1.1 Aims

In this chapter, *C. johnstoni* is phylogenetically positioned to determine evolutionary relationships with other filarial nematodes. To achieve this, I aimed to:

- 1) Assemble the mitochondrial genome from sequencing data of one adult female worm to compare gene order and content.
- 2) To compare *C. johnstoni* with other filarial species and position within the filarial nematode clade.
- 3) To use available gene data to position *C. johnstoni* phylogenetically with other *Cercopithifilaria* species.
- 4) To determine whether the location of the microfilariae in the host, i.e., subcutaneous skin, is a phylogenetic characteristic possibly resulting in disease pathology.

2.2 Materials and Methods

2.2.1 Sequence accession numbers

The NCBI accession numbers of the species used in the whole mitochondrial genomes analysis were: *A. viteae* (HQ186249.1), *B. malayi* (NC_004298.1), *B. pahangi* (AP017680.1), *B. timori* (AP017686.1), *Chandlerella quiscali* (NC_014486.1), *D. immitis* (AJ537512.1), *D. repens* (KX265047.1), *D. hongkonensis* (NC_031365.1), *L. sigmodontis* (AP017689.1), *L. loa* (HQ186250.1), *O. flexuosa* (HQ214004.1), *O. volvulus* (NC_001861.1), *O. ochengi* (KX181290.2), and *W. bancrofti* (HQ184469.1), and outgroups *Thelazia callipaeda* (KY908320.1), *Setaria digitata* (GU138699.1), *Spirocerca lupi* (KC305876.1), *Gongylonema pulchrum* (AP017685.1) and *Heliconema longissimum* (NC_016127.1).

The NCBI accession numbers of the *Cercopithifilaria* species analysed in the COI-12S phylogeny were: *Cercopithifilaria rugosicauda* (COI - KC610813; 12S - KC610808), *Cercopithifilaria binae* (COI - KF270686; 12S - KX156956), *Cercopithifilaria grassi* (COI - JQ837810; 12S - JQ837812), *Cercopithifilaria roussilhoni* (COI - AM749264; 12S - AM779798), *Cercopithifilaria japonica* (COI - AB771722; 12S - AM779794), *Cercopithifilaria tumidivervicata* (COI - AB178853; 12S - AM779790), *Cercopithifilaria minuta* (COI - AB178847; 12S - AM779786), *Cercopithifilaria bulboidea* (COI - AB178839; 12S - AM779780), *Cercopithifilaria longa* (COI - AB178845; 12S - AM779784) and *C. johnstoni*.

2.2.2 Sample collection

Bush rats were collected from Mogo State Forest (-35.7689484, 150.1027441; New South Wales, Australia) using baited Elliot traps set under logs and in covered areas (permits: AEC 13-23, NSW – Scientific Licence 5L 101280, VIC – Scientific Permit 10007169). Collected rats were housed with food, water, and shelter before being screened for the presence of dermal microfilariae by taking a small ear biopsy that was subsequently placed in 0.9% physiological saline to observe microfilariae migration out of the tissue.

2.2.3 DNA extraction, library preparation and sequencing

A single adult female worm (approximately 7 cm in length) was cut into approximately 1 cm length pieces using a sterile scalpel blade before being placed in a lysis solution (lysis buffer and proteinase K solution) for 18 h. Genomic DNA from the worm lysate was extracted using an ISOLATE II Genomic DNA Kit (Bioline, Australia) following the manufacturer's instructions, except for the following modification: the sample was eluted from the extraction column in 50 µl of extraction buffer, which was passed back through the extraction column a second time to concentrate the DNA before further analysis.

Genomic DNA (2X 500 ng in 50 µl) was sheared prior to library preparation using a Covaris S220 Focused-ultrasonicator with the following settings optimised for generating fragments approximately 400-600 bp: Peak incidence power = 175 W; Duty factor = 5%; cycles per burst = 200; treatment time = 55 s.

A DNA library was prepared from 500 ng starting DNA using a NEBNext Ultra Library Prep Kit for Illumina following the manufacturer's instructions. The resulting library was run on a 2% agarose gel, from which a gel cut was made to extract the 500-700 bp fragment fraction, which was subsequently purified using a Promega Gel and PCR clean-up kit (Promega, Australia).

The library was diluted to 15 pM and spiked with 1% PhiX control DNA (Illumina) before being sequenced on an Illumina MiSeq using Illumina V3 2x301 bp PE sequencing chemistry. In total, 24,374,948 reads (91.16% of total) passed filter and were used for further analysis.

2.2.4 Genome assembly

Raw sequencing reads were first visualised for quality and inherent bias using FastQC (<http://www.bioinformatics.babraham.ac.uk/projects/fastqc/>) and were adapter and quality trimmed using Trimmomatic version 0.32 (Bolger et al., 2014) (CROP:150 SLIDINGWINDOW:10:20 MINLEN:100). Post trimming, 22,065,411 PE reads were retained for assembly.

2.2.5 Mitochondrial genome assembly

The trimmed reads were mapped using bwa version 0.7.16a (Li and Durbin, 2009) to a multi-fasta file of the mitochondrial genomes of *O. volvulus*, *A. viteae*, *B. malayi*, *D. immitis*, *L. sigmodontis*, *L. loa*, *O. ochengi*, and *W. bancrofti*. All reads that mapped to any related filarial nematode were then used for assembly. A relaxed stringency was used to ensure all possible reads were obtained for genome assembly. A *de novo* assembly was then conducted using Velvet version 1.2.10 (Zerbino, 2010) using default parameters. Velvet-optimiser version 2.2.5 (Zerbino and Birney, 2008) identified a kmer of 99 was optimal for the Velvet assembly.

Velvet was not able to join all the resulting contigs together but instead provided seven separate overlapping contigs. There were two methods used to improve the assembly of the mitochondrial genome. Firstly, iterative mapping was performed to appropriately join the seven contigs from the Velvet assembly. The process consisted of mapping the raw *C. johnstoni* reads onto the seven contigs to add overlapping sequence to the end of each contig. The process was conducted repeatedly to grow the contig sequences until there was sequence overlap between the contigs. If two independently assembled contigs overlap following iterative read mapping, i.e., share sequences at their ends, then these contigs were joined at the overlapping region. The combination of iterative mapping and end joining where contigs overlap eventually produced a single circular assembly of a candidate mitochondrial genome. The second method consisted of a homology directed scaffolding approach where the iteratively mapped *C. johnstoni* sequence was mapped to the multi-fasta file of filarial nematode mitochondrial genomes to confirm gene order. Lastly, the *C. johnstoni* raw reads were then aligned for the final time to the final reference of the *C. johnstoni* mitochondrial genome to ensure assembly contiguity. These analyses produced a 13,716 bp mitochondrial genome.

2.2.6 Genome annotation

The mtDNA genome sequence was initially annotated using MITOS (Bernt et al., 2013) using the invertebrate translation table. The *C. johnstoni* annotation was improved manually by comparing the GFF3 annotation files from *L. loa*, *D. immitis*, *A. viteae*, *B. malayi*, *O. ochengi*, *O. volvulus*, *W. bancrofti* and

observing the multi-sequence alignment as a guide to see concordance using Mesquite version 3.04 (Maddison and Maddison, 2008) to observe the alignment.

2.2.7 Whole mitochondrial phylogeny

Whole mitochondrial genomes of *A. viteae*, *B. malayi*, *B. pahangi*, *B. timori*, *Chandlerella quiscali*, *D. immitis*, *D. repens*, *D. hongkonensis*, *L. sigmodontis*, *L. loa*, *O. flexuosa*, *O. volvulus*, *O. ochengi*, and *W. bancrofti*, and outgroups *Thelazia callipaeda*, *Setaria digitata*, *Spirocerca lupi*, and *Gongylonema pulchrum* were aligned to the assembled *C. johnstoni* genome. *Heliconema longissimum* was also included in the whole genome alignments but due to poor alignment was removed from the whole mitochondrial genome phylogenies.

The first analysis included visualisation of the aligned genomes, which was conducted by using the nucleotide sequences from each nematode aligned in Mesquite version 3.04 (Maddison and Maddison, 2008) and visualised in progressiveMauve version 20150213 (Darling et al., 2010). The progressiveMauve analysis was produced using the following command: “./progressiveMauve –collinear –output”. Secondly, the mitochondrial genomes were realigned using ClustalW version 2.0.10 (Larkin et al., 2007), and phylogenies were estimated using maximum likelihood as implemented in the program RAxML for high-performance computing version 8.0.19 (Stamatakis, 2006, 2014). The best model for each partition was assessed using PartitionFinder version 1.1.1 (Lanfear et al., 2012) on the complete aligned genome. The Maximum Likelihood and Bayesian analyses were conducted under three substitution models as defined by PartitionFinder so that each codon position could be explicitly analysed. Ten character sets were run with 20 million generations under the GTRIGAMMA model (Supplementary Table 2.1), one was run with 20 million generations under the HKYGAMMA model (Supplementary Table 2.1) and five with 20 million generations under the GTRGAMMA model (Supplementary Table 2.1). The Maximum Likelihood analysis was run using the best of 20 replicates under the above models of sequence evolution and 1,000 long bootstrap replicates to estimate support for bipartitions. Posterior probabilities for nodes were estimated with MrBayes version 3.2.5 (Ronquist et al., 2012), using two runs with four chains each and sampling every 1,000

generations. Convergence between the two runs and stationarity were assessed using Tracer version 1.6 (Rambaut et al., 2014).

To confirm that the phylogenetic relationships inferred were not susceptible to long-branch attraction (e.g., is when rapidly evolving lineages appear to be closely related, regardless of their true evolutionary relationships), the data were subsampled in three different ways. Long-branch attraction typically occurs due to the assumptions that all lineages evolve at the same rate which is not always true (Felsenstein, 1987). Long branches contain several substitutions and are typically distantly related lineages compared to the shorter branches in the tree. When lineages evolve rapidly and over a short period of evolutionary time, there is a higher probability two lineages evolve the same nucleotides at the same site independently of one another. The higher chance is a result of only having four nucleotides and 20 amino acids for rapidly evolving sites to change to, thus it is common for many of these changes to identify erroneous similarities to one another and assume they have evolved once in the common ancestor (Felsenstein, 1987; Bergsten, 2005). It is more likely that two lineages with many substitutions evolved independently of one another. The erroneous similarities therefore result in overriding the true phylogenetic signal producing strongly supported but incorrect phylogenies (Felsenstein, 1987; Bergsten, 2005). Maximum likelihood and Bayesian methods are known to improve the phylogeny because these methods are less prone to long-branch attraction hence were used in this study (Bergsten, 2005). The only changes in the analysis parameters for these subsamples were the models estimated by PartitionFinder. All other parameters remained the same. For all the Bayesian analyses, a conservative burn-in fraction of 25% was used.

The first subsample consisted of only the coding regions of the mitochondrial genomes and retained the outgroups in the analysis. The Bayesian analysis was conducted under two substitution models as defined by PartitionFinder. Six character sets were conducted with 20 million generations under the GTRGAMMA model (Supplementary Table 2.2), and four were conducted with 20 million generations under the GTRGAMMA model (Supplementary Table 2.2).

The second subsample analysed the coding regions and intergenic regions of the mitochondrial genomes but excluded outgroups from the analysis.

The Bayesian analysis was conducted under three substitution models as defined by PartitionFinder. Nine character sets were run with 20 million generations under the GTRIGAMMA model (Supplementary Table 2.3), two was run with 20 million generations under the HKYGAMMA model (Supplementary Table 2.3) and five with 20 million generations under the GTRGAMMA model (Supplementary Table 2.3).

The last subsample consisted of only the coding regions of the mitochondrial genomes and also excluded outgroups from the analysis. The Bayesian analysis was conducted under three substitution models as defined by PartitionFinder. Six character sets were conducted with 20 million generations under the GTRIGAMMA model (Supplementary Table 2.4), two were conducted with 20 million generations under the HKYGAMMA model (Supplementary Table 2.4), and two were conducted with 20 million generations under the GTRGAMMA model (Supplementary Table 2.4).

The resulting trees were visualised in R version 3.5.3 (R Core Team, 2017) using the following packages: ggplot2 version 3.2.0 (Kahle and Wickham, 2013), ggimage version 0.2.1, ggtree version 1.12.7 (Yu et al., 2017), pegas version 0.11 (Paradis et al., 2017), phytools version 0.6-60 (Revell, 2012), and phylopic images (<http://phylopic.org/>) for the silhouettes. Silhouettes are colour coded by the host animal: human (green), cat (orange-pink), bird (blue), rodent (brown), cow (grey), bandicoot (light pink), platypus (light grey), possum (red), Tasmanian devil (aqua), deer (purple), dog (orange), and ram (cyan).

Support values were represented on the branches indicating bootstrap support followed by Bayesian posterior probabilities (98/100).

2.2.8 12S COI gene phylogeny of *Cercopithifilaria*

Phylogenetic comparison of *Cercopithifilaria* species was performed using concatenated 12S and COI sequences. The *Cercopithifilaria* species analysed were *Cercopithifilaria rugosicauda*, *Cercopithifilaria bainae*, *Cercopithifilaria grassi*, *Cercopithifilaria roussilhoni*, *Cercopithifilaria japonica*, *Cercopithifilaria tumidivervicata*, *Cercopithifilaria minuta*, *Cercopithifilaria bulboidea*, *Cercopithifilaria longa* and *C. johnstoni*. Three *Cercopithifilaria* species were

excluded from the analysis because they were missing 12S sequences: *Cercopithifilaria shohoi*, *Cercopithifilaria multicauda* and *Cercopithifilaria crassa*.

The filarial nematode 12S and COI sequences were extracted from the whole mitochondrial genome phylogeny. The following nematodes were used as outgroups for the *Cercopithifilaria* phylogeny, *A. viteae*, *B. malayi*, *B. pahangi*, *B. timori*, *C. quiscali*, *D. immitis*, *D. repens*, *D. hongkongensis*, *L. sigmodontis*, *L. loa*, *O. flexuosa*, *O. volvulus*, *O. ochengi*, *W. bancrofti*, *T. callipaeda*, *S. digitata*, *S. lupi*, and *G. pulchrum*.

The nucleotide sequences of 12S and COI were first concatenated to combine sequence data to result in one sequence per species. The concatenated sequences were then aligned using ClustalW version 2.0.10 (Larkin et al., 2007) within Mesquite version 3.04 (Maddison and Maddison, 2008). Gblocks version 0.91b (Talavera and Castresana, 2007) was used to remove ambiguously aligned blocks and thus remove misaligned regions between the 12S and COI genes. Phylogenies were estimated using maximum likelihood as implemented in the program RAxML for high-performance computing version 8.0.19 (Stamatakis, 2006, 2014) using the best of 20 replicates under the GTRCAT model of sequence evolution and 1,000 long bootstrap replicates to estimate support for bipartitions. The best model was assessed again using PartitionFinder version 1.1.1 (Lanfear et al., 2012), and posterior probabilities for nodes were estimated with MrBayes version 3.2.5 (Ronquist et al., 2012), using two runs with four chains each and sampling every 1,000 generations. Convergence between the two runs and stationarity were assessed using Tracer version 1.6 (Rambaut et al., 2014). The Bayesian analysis for the concatenated 12S-COI tree was conducted under one substitution model as defined by PartitionFinder. Both gene 12S and gene COI were conducted with 20 million generations under the GTRIGAMMA model.

Support values were represented on the branches indicating bootstrap support followed by Bayesian posterior probabilities (98/100).

The resulting tree was visualised in R version 3.5.3 (R Core Team, 2017) using the following packages: ggplot2 version 3.2.0 (Kahle and Wickham, 2013), ggimage version 0.2.1, ggtree version 1.12.7 (Yu et al., 2017), pegas version 0.11 (Paradis et al., 2017), phytools version 0.6-60 (Revell, 2012), and phylopic

images (<http://phylopic.org/>) for the silhouettes. Silhouettes are colour coded by the host animal and are the same colours used for the whole mitochondrial genome phylogeny. Additional silhouettes added for the *Cercopithecifilaria* genus are coloured: bear (black) and Japanese serrow (lime green).

2.3 Results

2.3.1 Assembly of the mitochondrial genome

The assembly of the complete sequence of the mitochondrial genome of *C. johnstoni* has a total length of 13,716 bp. The length of the complete *C. johnstoni* genome is slightly shorter than *O. volvulus*, *A. viteae*, and *O. ochengi* (Supplementary Table 2.5). The MITOS annotation of the mitochondrial genome can be found in Table 2.1. The *C. johnstoni* mitochondrial genome contains 12 protein-coding genes (ATP6, COX1, COX2, COX3, CYTB, ND1, ND2, ND3, ND4, ND4L, ND5, and ND6) and 23 transfer RNA genes, small subunit ribosomal RNA genes and large subunit ribosomal RNA genes (Table 2.1).

A comparison of the *C. johnstoni* mitochondrial genome to the published mitochondrial genome of *O. volvulus* (13,747 bp; Accession NC_001861.1) identifies the degree of similarity of genome content and gene order (Figure 2.1). The *C. johnstoni* mitochondrial genome is predominately AT-rich at 76% with a GC content of 24%, which is consistent with *O. volvulus* (73.3% AT, 26.7% GC) and with other filarial nematodes (Supplementary Table 2.5). Similarly, the gene content and order of *C. johnstoni* are conserved compared with *O. volvulus* (Figure 2.1). The mitochondrial genome of *C. johnstoni* is highly conserved with *O. volvulus* consisting of five blocks of similarity between either species (Figure 2.2). The regions that do not show strong conservation indicate a divergence between *O. volvulus* and the *C. johnstoni* mitochondrial genome sequence.

The pairwise nucleotide percentage (%) identities have been recorded corresponding to the Mauve alignment (Figure 2.3) of all the filarial nematode mitochondrial genomes (Table 2.2). Nucleotide similarity of *C. johnstoni* with all filarial nematodes ranges between 68% and 79% and is least similar to *T. callipaeda* with 68.9% similarity, which is one of the outgroup species and therefore more divergent and an expected result (Table 2.2). The highest nucleotide similarity of *C. johnstoni* is with *L. loa* at 78.9%. The highest nucleotide similarity between filarial nematodes is between *O. volvulus* and *O. ochengi* at 96%. The *C. johnstoni* and *O. volvulus* mtDNA genomes share nucleotide similarity of 77.8% (Table 2.2).

While the coding regions of the mitochondrial genome alignment are aligned well accounting for the moderate to high nucleotide pairwise percentage

Table 2.1: *Cercopithifilaria johnstoni* mitochondrial genome annotation using MITOS with a total genome length of 13,716 bp.

Gene	Type	Start	End	Start codon	Length (bp)	Length (aa)
trnE	tRNA	2	59		58	
trnS1	tRNA	67	118		52	
ND2	CDS	119	880	ATG	762	254
trnT	tRNA	972	1027		56	
ND4	CDS	1028	2308	TTG	1281	427
COX1	CDS	2310	3902	ATT	1593	531
trnW	tRNA	3906	3958		53	
ND6	CDS	3999	4427	ATT	429	143
trnR	tRNA	4450	4503		54	
CYTB	CDS	4569	5615	ATG	1047	349
trnL	tRNA	5656	5710		55	
COX3	CDS	5711	6487	ATT	777	259
trnA	tRNA	6908	6964		57	
trnL	tRNA	6967	7019		53	
trnN	tRNA	7029	7091		63	
trnM	tRNA	7090	7145		56	
trnK	tRNA	7146	7202		57	
ND4L	CDS	7212	7442	ATT	231	77
rrnS	rRNA	7444	8116		673	
trnY	tRNA	8117	8171		55	
ND1	CDS	8178	9026	TTG	849	283
trnF	tRNA	9032	9085		54	
ATP6	CDS	9106	9687	TTG	582	194
trnI	tRNA	9693	9748		56	
trnG	tRNA	9720	9777		58	
COX2	CDS	9857	10471	ATT	615	205
trnH	tRNA	10482	10536		55	
rrnL	rRNA	10934	11442		509	
ND3	CDS	11443	11820	TTA	378	126
trnC	tRNA	11828	11884		57	
trnS2	tRNA	11885	11938		54	
trnP	tRNA	11940	11997		58	
trnD	tRNA	12002	12059		58	
trnV	tRNA	12060	12115		56	
ND5	CDS	12124	13716	GTT	1593	531

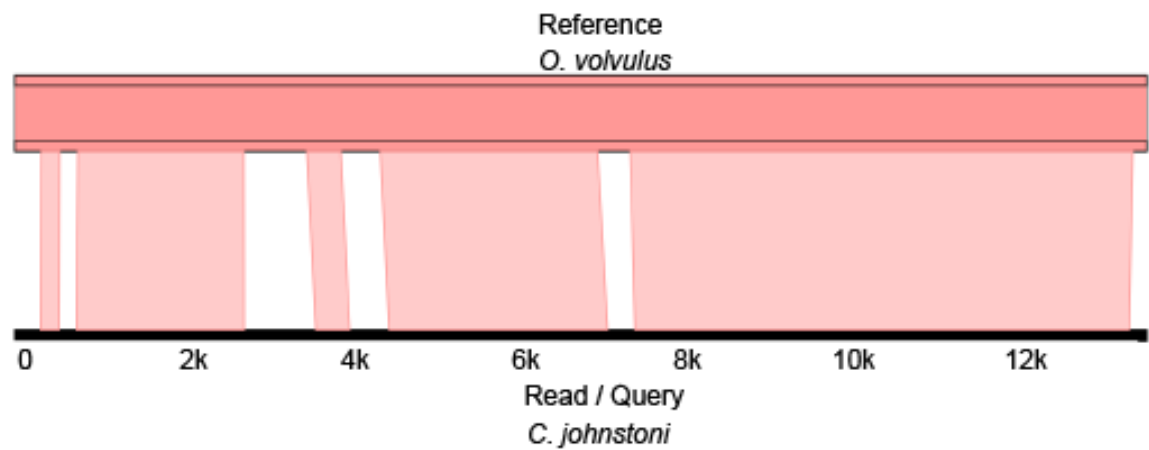


Figure 2.2: Genome Ribbon alignment of the whole mitochondrial genomes *Onchocerca volvulus* as the reference sequence and a query of *Cercopithifilaria johnstoni* whole mitochondrial genome to illustrate conservation of mitochondrial genomes.

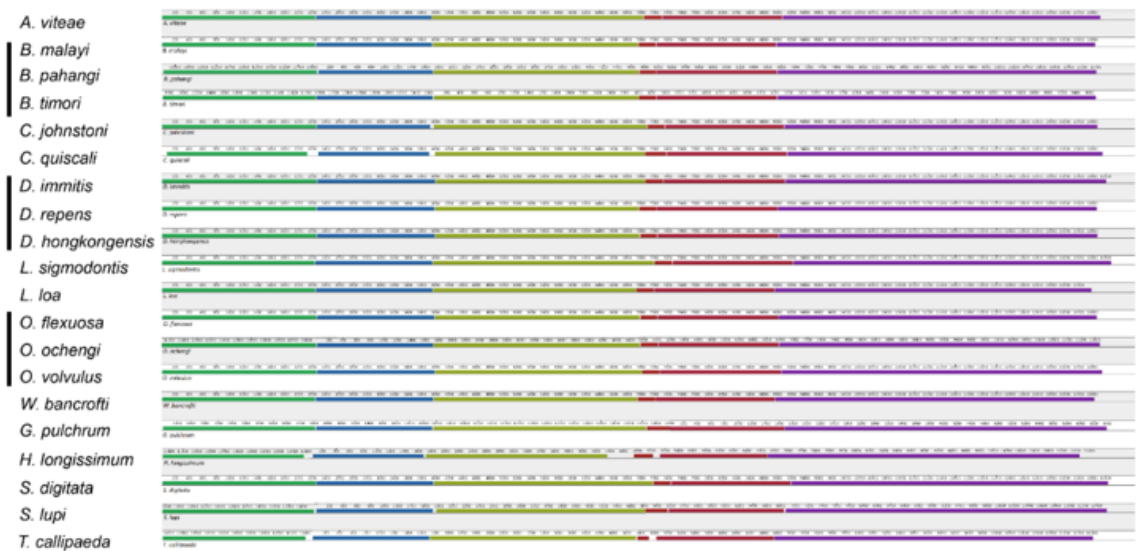


Figure 2.3: Mauve alignment of the whole mitochondrial genomes of 20 filarial nematodes (*Acanthocheilonema viteae*, *Brugia malayi*, *Brugia pahangi*, *Brugia timori*, *Cercopithifilaria johnstoni*, *Chandlerella quiscali*, *Dirofilaria immitis*, *Dirofilaria repens*, *Dirofilaria hongkongensis*, *Litomosoides sigmodontis*, *Loa loa*, *Onchocerca flexuosa*, *Onchocerca ochengi*, *Onchocerca volvulus*, *Wuchereria bancrofti*, *Gongylonema pulchrum*, *Heliconema longissimum*, *Setaria digitata*, *Spirocerca lupi* and *Thelazia callipaeda*) showing consistent and conserved gene order and content. Vertical black lines represent same genera. The mauve alignment is a visual representation identifying sequence that is similar to other sequences. The coloured blocks represent regions of similarity, i.e., there are considerable nucleotide similarities between each species within the same colour group.

Table 2.2: Comparison (pairwise % identity) among nucleotides sequences of the filarial nematodes represented in the whole mitochondrial genome mauve alignment. *Av* (*Acanthocheilonea viteae*), *Bm* (*Brugia malayi*), *Bp* (*Brugia pahangi*), *Bt* (*Brugia timori*), *Cj* (*Cercopithifilaria johnstoni*), *Cqui* (*Chandlerella quiscalii*), *Di* (*Dirofilaria immitis*), *Dr* (*Dirofilaria repens*), *Dh* (*Dirofilaria hongkongensis*), *Ls* (*Litomosoides sigmodontis*), *LI* (*Loa loa*). *Of* (*Onchocerca flexuosa*), *Oo* (*Onchocerca ochengi*), *Ov* (*Onchocerca volvulus*), *Wb* (*Wuchereria bancrofti*), *Gp* (*Gongylonema pulchrum*), *Sd* (*Setaria digitata*), *Sl* (*Spirocerca lupi*) and *Tc* (*Thelazia callipaeda*).

Species	<i>Av</i>	<i>Bm</i>	<i>Bp</i>	<i>Bt</i>	<i>Cj</i>	<i>Cqui</i>	<i>Di</i>	<i>Dr</i>	<i>Dh</i>	<i>Ls</i>	<i>LI</i>	<i>Of</i>	<i>Oo</i>	<i>Ov</i>	<i>Wb</i>	<i>Gp</i>	<i>Sd</i>	<i>Sl</i>	<i>Tc</i>
<i>Av</i>	-	80.4	79.5	79.9	78.3	76	79.5	80.6	80.4	76.8	81.2	81.5	81.3	81.2	80.1	71.9	78.9	72.2	70.6
<i>Bm</i>		-	89.9	91.2	77.7	76.2	80.1	81.6	81.4	76.1	82.6	82.3	81.6	81.4	87.3	72.5	78.8	82.3	70.9
<i>Bp</i>			-	89.5	77.6	75.5	79.7	81.1	81	75.5	81.9	81.5	80.8	80.6	86.5	72.2	78.3	71.8	70.4
<i>Bt</i>				-	78	76.3	80.1	81.6	81.5	76.2	82.9	82	81.2	81.2	87.7	72.9	78.8	72.7	71.3
<i>Cj</i>					-	74.8	77.1	78.7	78.8	74.8	78.9	78.2	77.9	77.8	78.1	70.6	76.1	70.3	68.9
<i>Cqui</i>						-	75.8	77.4	77.2	73.1	77.6	76.8	76.5	76.4	76.3	69.9	76	69.6	69
<i>Di</i>							-	85.9	85.5	77.3	81.7	82.9	82.6	82.5	80.4	72.9	80.2	73.2	71.4
<i>Dr</i>								-	93.6	78.2	83.3	84.7	84.5	84.4	82.2	74.5	81.6	74	72.4
<i>Dh</i>									-	78.1	83.1	84.2	83.8	83.5	82.2	74.1	81.3	73.7	72.2
<i>Ls</i>										-	77.6	77.3	77.1	77.1	76.6	69.9	75.7	70.1	68.8
<i>LI</i>											-	84.3	83.4	83.2	83.5	73.7	80.7	73.4	72
<i>Of</i>												-	88.2	87.9	82.7	73.6	80.8	73.6	72
<i>Oo</i>													-	96	82.3	73.2	80.9	73.7	71.6
<i>Ov</i>														-	82	73.2	80.8	73.7	71.5
<i>Wb</i>															-	72.8	79.3	73.1	71.4
<i>Gp</i>																-	73.7	74	70
<i>Sd</i>																	-	74	72
<i>Sl</i>																		-	69.9
<i>Tc</i>																			-

identities, the non-coding (intergenic) regions are not well aligned and are quite divergent. The comparison between *O. volvulus* and *C. johnstoni* genomes highlights regions of potential divergence showing gaps where the alignment is not as successful (Figure 2.2).

2.3.2 Mitochondrial genome phylogeny

The phylogeny constructed using whole mitochondrial genomes (Figure 2.4) is supported strongly by Bayesian posterior probabilities and bootstrap proportions. The phylogeny positions *C. johnstoni* in a strongly supported clade shared with *L. sigmodontis* and *A. viteae*, with a bootstrap value and Bayesian posterior probability of 100. Within this clade, *C. johnstoni* could be more closely related to *A. viteae* or *L. sigmodontis* (bootstrap/Bayesian posterior probability support of only 50/62).

Subsamples of the dataset using three separate analyses were analysed to be confident that the nematode relationships in this analysis were concordant and not susceptible to long-branch attraction. The coding-only regions, including outgroups dataset (Figure 2.5a), has identical filarial nematode relationships and remains the same as the complete dataset (Figure 2.4). Bayesian posterior probabilities and bootstrap proportions remain the same as Figure 2.4.

When subsampling coding regions and intergenic regions, excluding outgroups (Figure 2.5b), the relationships of the filarial nematodes remain the same as the previous two datasets (Figure 2.4, 2.5a), the Bayesian posterior probabilities and bootstrap proportions remain the same across most of the clades. The only discrepancy between phylogenies is the Bayesian posterior probability between *C. johnstoni* and *A. viteae* relationship decreasing to 47 rather than 50, which is not significant.

The final subsample consists of coding-only regions and excluded outgroups (Figure 2.5c). The phylogenetic relationships are again consistent with the other three analyses (Figure 2.4, 2.5a, 2.5b) with slight variation in Bayesian posterior probabilities and bootstrap proportions. The exercise has identified the

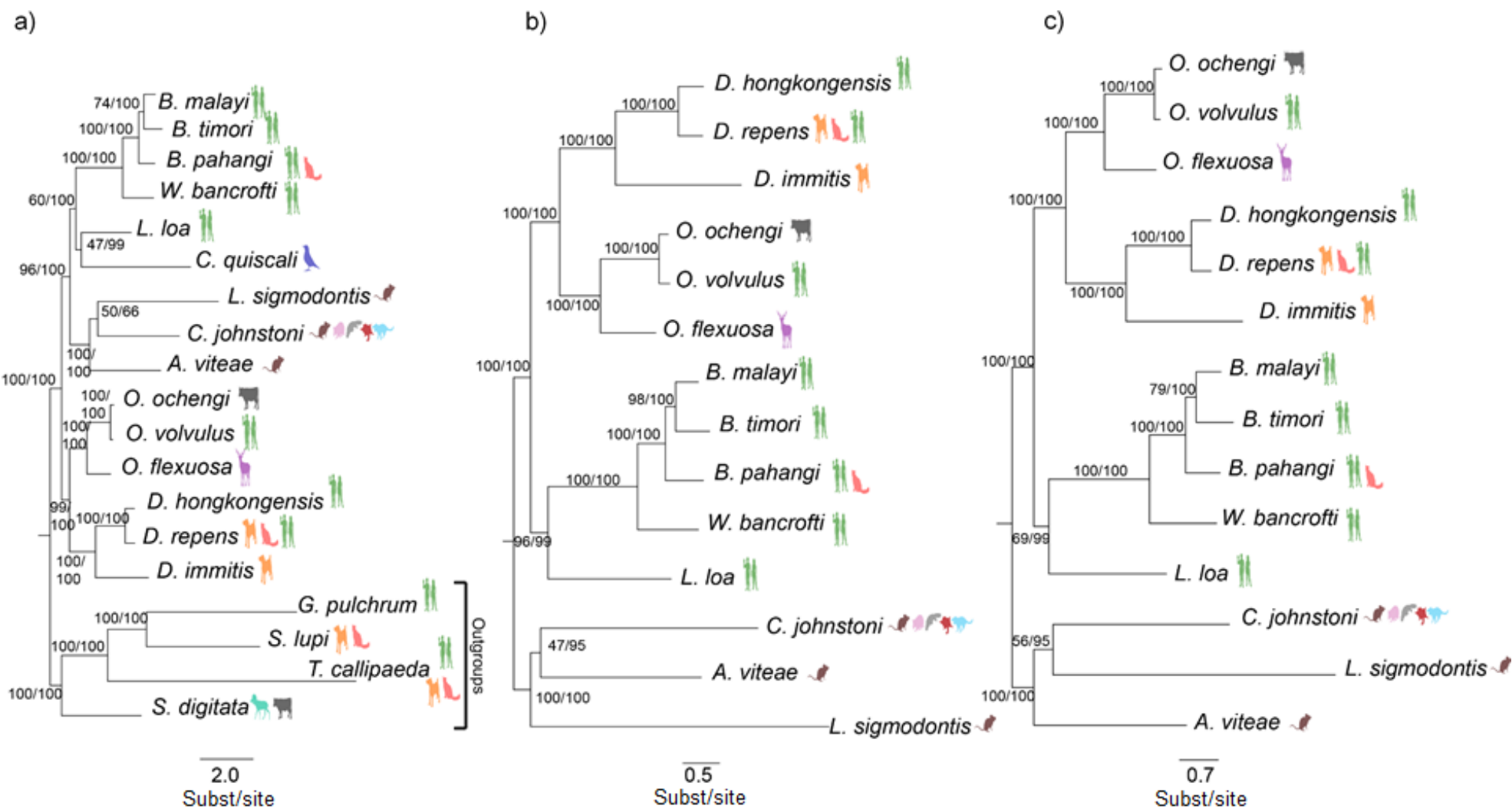


Figure 2.5: Maximum likelihood trees of the three different subsampled datasets of the whole mitochondrial genome phylogeny of filarial nematodes using maximum likelihood/Bayesian inference. Host species for each filarial nematode is represented as colour-coded silhouettes adjacent to the species names. (a) Only coding regions of the mitochondrial genome with outgroups. (b) Coding and intergenic regions of the mitochondrial genome, excluding outgroups. (c) Only coding regions of the mitochondrial genome excluding outgroups. Scale substitutions per site.

best combination of sequence sets for the phylogeny based on the data available. Optimisation of datasets can maximise the phylogenetic signal in datasets consistent with the filarial nematode whole mitochondrial genome dataset.

The four different datasets used in the mitochondrial genome analysis are congruent with one another and support the relationships of these nematodes as presented in previous literature (McNulty et al., 2012; Lefoulon et al., 2015). As all the subsampled phylogenies illustrate the same phylogenetic relationships with very close Bayesian probabilities and bootstrap proportions, Figure 2.4 will be referred to for the remainder of this chapter as it contains the whole mitochondrial genome of the filarial nematodes.

Coloured silhouettes of the host species known to be infected by each parasitic filarial nematode were mapped onto the phylogeny (Figure 2.4). The parasites that are known to cause pathological symptoms in their hosts are illustrated by the asterisk (*). The host species were mapped onto the phylogeny to identify whether the filarial nematodes of a phylogenetic clade were infecting the same host species, i.e., all species of *Dirofilaria* infecting humans. Unsurprisingly, there was not a clear relationship between parasitic nematode and infected host consistent with the literature identifying a lack of relationship between parasite and host phylogenies (Hasegawa, 1999; Fenn et al., 2006; Larose and Schwander, 2016). The phylogeny instead implies this lack of congruence between parasite relationships and the evolutionary relationships of their hosts is driven largely by host switching of the parasites between phylogenetically unrelated hosts (Paterson and Gray, 1997; Page, 2003). It would seem likely that host switching is prevalent amongst filarial parasites because in general their intermediate hosts are haematophagous arthropods with low host specificity (Fenn et al., 2006). It has been reported that *C. johnstoni* is present in rodents, bandicoots, platypus, gliders, and Tasmanian devils (Spratt and Varughese, 1975; Spratt and Haycock, 1988; Viggers and Spratt, 1995), although remains unknown whether these are all-natural hosts or reservoir hosts and whether there has been any host switching events. Several of the other filarial species only infect one or two hosts.

Without further analyses, there is no conclusion that can be formulated from the mapped host species on the phylogenetic tree. Nematodes causing pathology in their hosts are dispersed throughout the phylogeny and are not

grouped in a clade or sharing similar phylogenetic relationships and thus may not be a phylogenetic character.

2.3.3 Concatenated gene phylogeny

The concatenated 12S-COI gene phylogeny has an overall low bootstrap/Bayesian posterior probability support across the phylogeny (Figure 2.6). The filarial species form a monophyletic *Cercopithifilaria* clade which is poorly to moderately supported that contains all *Cercopithifilaria*, including *C. johnstoni* (Figure 2.6). Within the *Cercopithifilaria* clade, *C. johnstoni* is more distantly related than the others and has overall clade support of 17/64, which is very low. Nevertheless, the refined alignment removing regions that do not align with Gblocks has shown the *Cercopithifilaria* genus to be monophyletic and closely related compared to the other filarial nematodes throughout this study. Prior to the Gblocks analysis the alignment consisted of 874 positions (bp). After the Gblocks analysis the alignment was reduced to 681 positions (bp) in eight selected blocks. A total of 77% of the alignment aligned and 23% was removed after the Gblocks analysis.

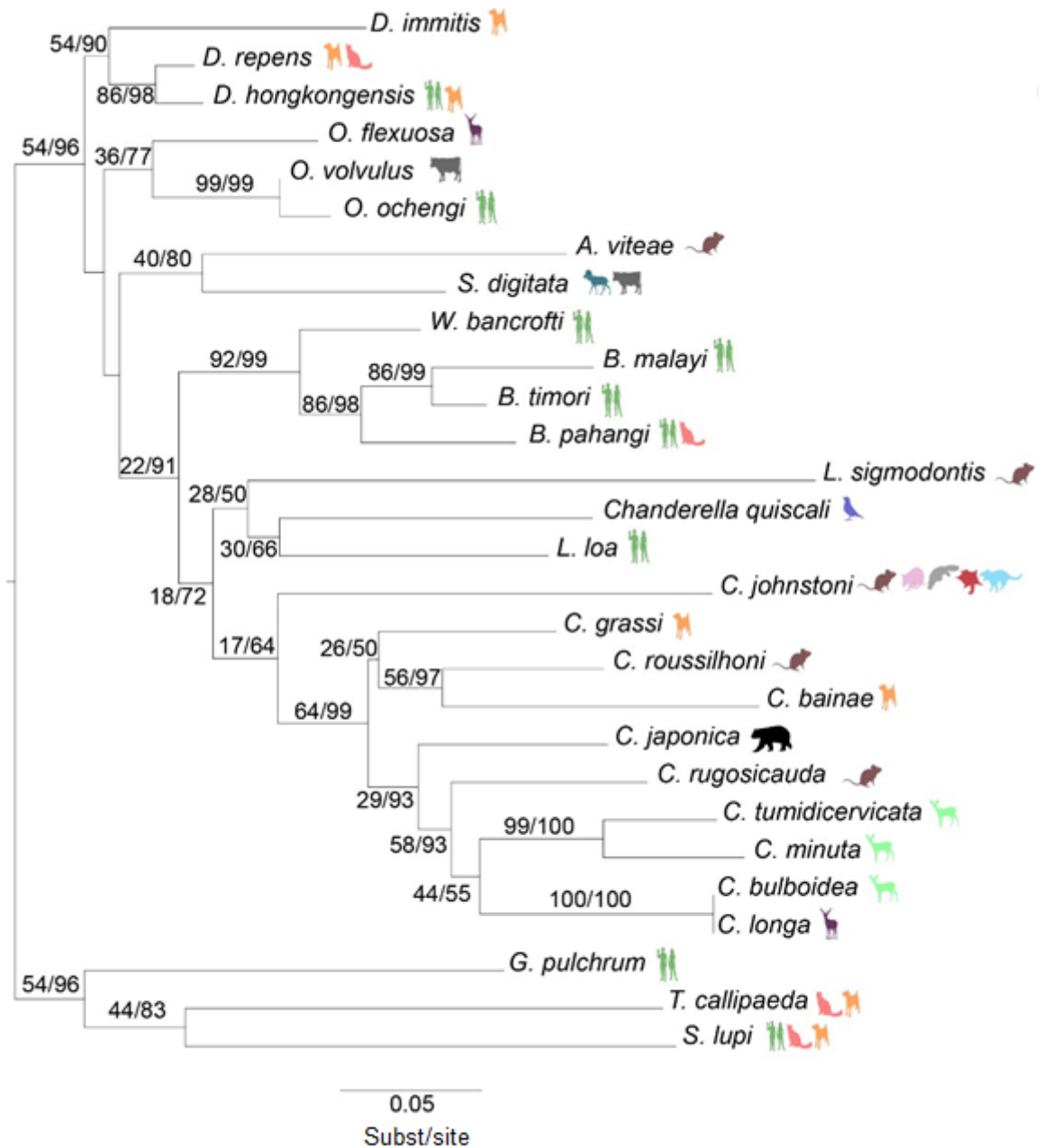


Figure 2.6: Maximum likelihood tree of the concatenated 12S-COI data of filarial nematodes to position the *Cercopithifilaria* genus using maximum likelihood/Bayesian inference. Host species for each filarial nematode is represented as colour coded silhouettes. Scale 0.05 substitutions per site.

There is very low to moderate support throughout the majority of sub-clades with a few exceptions. *W. bancrofti*, *B. timori*, *B. malayi*, and *B. pahangi* are strongly supported in their clade with bootstrap support of 95 and posterior probability of 99 (95/99) (Figure 2.6), consistent with the whole genome phylogeny (Figure 2.4). The genus *Onchocerca* and *Dirofilaria* are both monophyletic and are sister taxa with moderate support (79/99, 94/99), but consistent with other analyses (Figure 2.4). Within the *Cercopithifilaria* clade, a strongly supported relationship is present between *C. longa* and *C. bulboidea* and between *C. minuta* and *C. tumidicervicata* with 100/100 and 99/100 respectively.

Overall, the concatenated 12S-COI gene tree is consistent with previous research and with the whole genome phylogenies estimated here. The phylogeny constructed with 12S-COI sequences generally less well supported than those constructed using whole mitochondrial genomes.

The host silhouettes of the *Cercopithifilaria* species also does not reveal anything interesting about phylogenetic relationships and position within the 12S-COI gene tree. The filarial parasites do not appear to group together in a clade based on the host they parasitise, i.e., rodent, or human clades. Further data is required to confirm these relationships as the tree is poorly supported, however it appears there is a possible geographical correlation amongst the *Cercopithifilaria* genus. The European and African *Cercopithifilaria* species are monophyletic with one another, the Asian species are monophyletic to one another and *C. johnstoni* is positioned on its own separate from the other groups.

2.4 Discussion

The analyses of mitochondrial genomes have been a valuable resource for comparative genomics and population genetics in parasitic nematodes (Ramesh et al., 2012; Small et al., 2016). Filarial nematode mitochondrial genomes are much shorter in length compared to their nuclear genomes and are between 13-14 kbp (Blaxter et al., 1998; Yatawara et al., 2010; McNulty et al., 2012). The small genome size makes them a great first genomic resource for the initial phylogenetic placement of an understudied species. *C. johnstoni* may be an appropriate organism to be used in a small animal model to study onchocerciasis, but nothing is known about the genomics of *C. johnstoni*. It, therefore, was an essential first step to construct the mitochondrial genome and position *C. johnstoni* in the nematode phylogeny determining potential evolutionary relationships with *O. volvulus* and other filarial nematodes understanding more about *C. johnstoni* genomics (Figure 2.1).

2.4.1 Mitochondrial genome

Filarial nematode mitochondrial DNA encodes ribosomal RNAs, transfer RNAs and proteins that are only used by the mitochondrion (Ramesh et al., 2012; Li et al., 2018). Consistently across all published filarial nematodes, the mitochondrial genome contains 12 protein-coding genes (Yatawara et al., 2010) and two ribosomal genes (Unnasch and Williams, 2000). Protein coding and ribosomal genes consist of NADH dehydrogenase 1, 2, 3, 4L, 5 and 6, cytochrome c oxidase subunit I, II and III, cytochrome b, mitochondrially encoded ATP synthase membrane subunit 6, ribosomal ribonucleic acid S, and ribosomal ribonucleic acid L (Unnasch and Williams, 2000; Yatawara et al., 2010).

The mitochondrial genome of *C. johnstoni* was assembled from whole-genome sequence data and is consistent with other filarial nematodes in length, gene content, and AT-richness (Figure 2.1, 2.3). Several studies have confirmed the conserved gene order and content of the mitochondrial genome within the filarial nematodes, and now *C. johnstoni* is another filarial species that share the conserved genome structure (Osawa et al., 1992; Wolstenholme, 1992; Le et al., 2000). The mitochondrial genomes of *C. johnstoni* and *O. volvulus* are almost identical in genome content and order (Figure 2.1). The AT and GC content vary

slightly between the two species but mostly remains consistent (Figure 2.1a, 2.1b).

The *C. johnstoni* assembly was aligned to other published filarial nematode mitochondrial genomes (Figure 2.3) using progressiveMauve version 20150213 (Darling et al., 2010) to explore if there were any differences in genome content and organisation; however, the analyses revealed that it was conserved. Mauve's algorithm aligns the genomes using anchors and what Mauve does differently to other aligners is to allow rearrangements of the genome if these are present using a modified global alignment algorithm (Darling et al., 2010). Mauve uses coloured collinear blocks to identify regions of sequence similarity in the output illustration of genome alignment (Darling et al., 2010). Each colour represents that region of sequence similarity, for example, the green region of the genomes share similarity but cannot be directly connected to the blue region most likely as a result of intergenic regions or less similarity of genome content (Figure 2.3). Comparing *O. volvulus* and *C. johnstoni* directly to observed genome similarity, resulted in conservation of five sequence blocks (Figure 2.2) which is partially consistent to the mauve alignment that consists of five different blocks of colour (Figure 2.3). The GenomeRibbon similarity indicates four regions between the five sequence blocks of similarity that are intergenic regions in which do not align successfully (Shabalina and Spiridonov, 2004; Deng et al., 2006).

The Mauve alignment successfully aligned the mitochondrial genomes of the closely related filarial species showing genome conservation, however, to determine how closely related the species were in the alignment, a pairwise nucleotide analysis was used (Table 2.2). The pairwise nucleotide identities were moderate to high, indicating that there were regions such as the intergenic regions of the alignment that did not align well between the filarial nematodes most likely a result of rapid divergence. Thus the pairwise nucleotide identities are not very high (Shabalina and Spiridonov, 2004; Deng et al., 2006).

2.4.2 Mitochondrial genome phylogeny

Four different datasets were analysed to determine the whole mitochondrial genome phylogeny and to ensure that the phylogenetic

relationships were not susceptible to long-branch attraction (Figure 2.5). These were (1) whole mitochondrial genomes (Figure 2.4), (2) coding-only regions with filarial outgroups (Figure 2.5a), (3) intergenic regions and coding regions excluding outgroups (Figure 2.5b), and lastly, (4) coding-only regions excluding outgroups (Figure 2.5c). These analyses were conducted to ensure that the phylogenetic relationships represented are an accurate representation of the data. Intergenic regions are known to be highly variable non-coding DNA that is usually not highly conserved between species as they appear to be involved in controlling RNA and DNA synthesis (Shabalina and Spiridonov, 2004; Deng et al., 2006). Commonly, intergenic regions are excluded from phylogenies as they do not align well when comparing different species. Analysing these four separate datasets excluding and including intergenic regions has confirmed that for this particular filarial nematode dataset, the intergenic regions do not change or negatively affect the phylogenetic relationships of the species. The four analyses conclude the same phylogenetic relationships and therefore, Figure 2.4, which is the result of analysing the complete mitochondrial genome data, is referred to in all subsequent discussions.

Bayesian posterior probabilities and bootstrap proportions strongly support most of the filarial relationships presented (Figure 2.4). The mitochondrial genome phylogeny positioned *C. johnstoni* in a clade with *A. viteae* and *L. sigmodontis* with robust support (Figure 2.4); however, there is low support for relationships within this clade. The inclusion of more complete, whole mitochondrial genome datasets from other filarial nematodes and other *Acanthocheilonema*, *Cercopithifilaria* and *Litomosoides* species would improve the support in the clade of *A. viteae*, *C. johnstoni* and *L. sigmodontis*. It could potentially highlight a more accurate representation of phylogenetic relationships (Sanderson et al., 2010). Despite not having strong support within the clade, the relationships of the three species are consistent with the literature (Mitreva et al., 2005; McNulty et al., 2012; Lefoulon et al., 2015). The inclusion of more complete mitochondrial genome datasets would expand the phylogeny and could potentially reveal more strongly supported relationships. Another possibility is that the relationship remains unchanged as a result of more data (Zwickl and Hillis, 2002; Hedtke et al., 2006). Alternatively, the sequencing of more genes, i.e., nuclear genome, from each of these species in the analysis could also improve supported relationships (Sanderson et al., 2003; Rokas and Carroll, 2005).

2.4.3 Exploring host species of filarial nematodes

Understanding nematode-host relationships have been very challenging because of the lack of information available. The current section aims to explore possible avenues for future research that would be beneficial to understand filarial nematode relationships in more detail.

The mitochondrial genome phylogeny illustrates the host species for every filarial parasite used throughout the analyses (Figure 2.4). Visually mapping the host silhouettes onto the phylogeny does not reveal any clear associations between the infected host species and parasite phylogenetic relationships. For example, *Dirofilaria* species do not solely infect dogs within the clade. Some species of *Dirofilaria* infect humans or cats. Secondly, the genus of *Cercopithifilaria* infects a range of different host species that does not show a clear relationship between parasite species and infected host species (Figure 2.4). An avenue that has not been explored is whether the location of microfilariae in the host's body is a phylogenetically informative character. It could be further hypothesised that filarial nematodes whose microfilariae occupy the same biological compartment, i.e., reside in the skin, are more likely to be related than those that occupy different biological compartments. To explore this idea, the location of microfilariae in the hosts body have been summarised in Table 2.3. In Onchocercidae the microfilariae are found either in circulating blood or in the skin. The phylogeny contains a highly supported clade made up of clade of *Onchocerca* species and one of *Dirofilaria* species consistent with previous literature (Mitrevva et al., 2005; McNulty et al., 2012; Lefoulon et al., 2015; Coghlan et al., 2019). *Onchocerca volvulus* are skin dwelling parasites (Cotton et al., 2016) and *D. immitis* adults are found in the cardiac arteries while the microfilariae are found in the blood (Table 2.3) (Mircean et al., 2017). *D. repens* adults are found in the subcutaneous tissue similarly to *C. johnstoni*, while the microfilariae are found in the blood similarly to *D. immitis* (Table 2.3) (Mircean et al., 2017). Previous research has indicated *C. johnstoni* is also a skin dwelling parasite (Spratt and Haycock, 1988; Vuong et al., 1993), *A. viteae* has been reported to be present in the skin (Eisenbeiss et al., 1991) and *L. sigmodontis* is present in peripheral blood (Table 2.3) (Hübner et al., 2009). Thus the location of the microfilariae or adult worms in each species is not a phylogenetically informative character and could potentially be an evolutionarily labile trait that has changed multiple times in the clade. One would expect to observe all the filarial

nematodes that reside in the skin grouping in a separate clade compared to the parasites in the blood if microfilariae location was a phylogenetically informative character. Therefore, the phylogeny cannot explain the evolution behind the different location of microfilariae between species. Microfilariae location in the host's body does not appear to be a phylogenetic characteristic.

Table 2.3: Summary of the known location of microfilariae and adult worms in filarial nematodes.

Parasite	Location of microfilariae	Location of adults	Hosts
<i>C. johnstoni</i>	Skin	Subcutaneous tissue	Rodents Bandicoots Possums Tasmanian devils Platypus
<i>O. volvulus</i>	Skin	Nodules	Humans
<i>D. immitis</i>	Blood	Cardiac arteries	Dogs
<i>D. repens</i>	Blood	Subcutaneous tissue	Dogs Cats
<i>A. viteae</i>	Skin	Subcutaneous tissue	Rodents
<i>L. sigmodontis</i>	Skin	Pleural/peritoneal cavities	Rodents

A second question to explore while observing the relationships in the phylogeny is whether the parasites causing host pathology can be predicted using filarial relationships. The position of the filarial nematodes within the clade III phylogeny also does not represent whether the parasite can cause pathological symptoms within its host. The asterisk highlights those filarial species known to elicit pathology (Figure 2.4) and is scattered throughout the phylogeny; thus, the phylogenetic position of the nematode does not indicate pathology. Again, if the phylogenetic relationships could indicate pathology, then all the species observed to cause host pathology would be positioned within closely related clades. The pathology associated with *D. immitis* is related to the adults blocking coronary arteries and it is neither immunological nor is it related to the microfilariae migration or death (Hu et al., 2003; Capelli et al., 2018). This is significantly different from the pathology associated with *C. johnstoni* and *O. volvulus*. The pathology observed in hosts infected with *C. johnstoni* or *O. volvulus* is immunological and is a result of the dead microfilariae with no issues or influence from the adult worms. The driving force behind shared immunopathological characteristics of *C. johnstoni* and *O. volvulus* may be a result of the location of where the microfilariae are found in their hosts. In other *Cercopithifilaria* species, the microfilariae are known to cause edematous changes or intestinal dermatitis in dogs and are also found in the subcutaneous skin (Otranto et al., 2012; Otranto et al., 2013; Ramos et al., 2014), supporting this hypothesis that possibly the microfilariae in the subcutaneous skin is the driving force behind immunopathology. Alternatively, it could be a result of how the hosts' immune system is affected by the death of the microfilariae and not have anything to do with their evolutionary relationship, a hypothesis that requires further investigation.

The phylogeny can also be used to examine the evolution of filarial nematodes and to ask questions about their different host species. Host species of filarial nematodes are represented as silhouettes on the phylogenetic tree (Figure 2.4). The *Onchocerca* clade consists of filarial nematodes predominately of ungulates and includes other species that do not have genomes available and thus are not represented in Figure 2.4 (such as *O. gibsoni*, *O. cervipedes* and *O. lienalis* (Anderson, 2001)). *O. volvulus* appears to have gone through a host switching event and begun parasitising humans rather than cattle (Unnasch and Williams, 2000; Krueger et al., 2007) despite *O. volvulus* and *O. ochengi* are

vectored by the same blackfly (Doyle et al., 2016). *O. ochengi* does not have any veterinary significance causing disease or economic loss (Allen et al., 2008; Makepeace and Tanya, 2016) unlike the immunopathology elicited by *O. volvulus*.

C. johnstoni has been identified in several different host species, completely atypical of nematodes. This is an intriguing aspect of *C. johnstoni* biology that is not currently understood raising the question of whether *C. johnstoni* is more permissive for host switching, to be present in so many host species. Other *Cercopithifilaria* species in the Northern Hemisphere, such as *C. bairdii* and *C. grassii*, infect dogs, while *C. rugosicauda* and *C. longa* infect deer (Figure 2.6) (Uni et al., 2002; Otranto et al., 2013; Ramos et al., 2013). *C. johnstoni* is a geographically distinct parasite from the other *Cercopithifilaria* species. Native rodents arrived in Australia relatively recently in evolutionary terms whereas marsupials and monotremes evolved within Australia. If *C. johnstoni* was previously established in small ground-dwelling marsupials such as bandicoots in Australia, then an evolutionarily recent switch into placental mammal bush rats could be a possibility. It is also likely that *C. johnstoni* infection in rats is an evolutionarily recent host-switching event that possibly increased pathological symptoms.

Several species of ticks attach to all of these small mammals transmitting a range of different parasites (Bonnet and Liu, 2012; McCoy et al., 2013). It could be possible that by having multi-host ticks that feed for several days on each host might be a predisposing factor. Considering *O. volvulus* and *O. ochengi* share *Simulium* vectors that triggered the *Onchocerca* host switch, this hypothesis should be explored further. The primary importance for the parasite would be the ability for the parasite to survive within the new host species after the switch. It is unknown what species are natural reservoirs of *C. johnstoni*. The exact number of recorded hosts exhibiting severe immunopathology, as reported in Vuong et al. (1993) is also not well documented. There is the potential that the pathology of *C. johnstoni* is, because of a recent host switch, similar to that hypothesised in *O. volvulus* as host switching is known to trigger disease emergence (Laetsch et al., 2012; Susoy and Herrmann, 2014; Suh et al., 2016). Despite the number of recorded host species infected with *C. johnstoni*, there have not been detailed morphological descriptions of each parasite, nor have there been any genetic

analyses conducted on each species. Therefore there is a potential for the presence of cryptic species, which would be morphologically similar but would not be interbreeding. One approach to identify cryptic species would be to sequence the DNA of each parasite found in the recorded hosts and use phylogenetics to determine whether they are genetically distinct enough to be species or whether they are very similar and can be considered all *C. johnstoni*. *Ixodes* transmit *C. johnstoni* to various small mammals such as gliders, Tasmanian devils, bandicoots and rodents (Spratt and Varughese, 1975; Spratt and Haycock, 1988; Vuong et al., 1993; Viggers and Spratt, 1995). It appears that *C. johnstoni* is now the only *Cercopithifilaria* species with an assembled mitochondrial genome. Assembled whole mitochondrial and nuclear genomes of the other *Cercopithifilaria* species could be a necessary first step into understanding the relationships of the *Cercopithifilaria* genus.

2.4.4 Phylogeny of the genus *Cercopithifilaria*

C. johnstoni has been placed in the overall filarial phylogeny using analysis of whole mitochondrial genomes. The question now arises about *C. johnstoni*'s relationship with other *Cercopithifilaria* species, and whether the genus of *Cercopithifilaria* is truly monophyletic.

There are approximately 11 *Cercopithifilaria* species known to date, and nine of which have been included in the gene tree analysis to position *C. johnstoni* that had both 12S and COI genes available. These genes were chosen for analysis, as they were the only data accessible. The genes were concatenated to improve the resolution of the phylogeny. Any *Cercopithifilaria* species that did not have data for both genes were excluded (Sanderson et al., 2003; Sanderson et al., 2010). There is a chance that this exclusion of some species could affect the phylogenetic relationship support in each clade as has been reported in other organisms and analyses (Sanderson et al., 2003; Sanderson et al., 2010; Som, 2014). It was required to use Gblocks to eliminate poorly aligned positions and divergent regions of the DNA sequences to see a clear representation of the filarial relationships (Talavera and Castresana, 2007). Gblocks successfully removed un-alignable regions to improve the overall alignment used for the analyses. There is confidence in the final phylogenetic

analysis as there was sufficient number of sites in the alignment for COI and 12S genes to give a reasonably accurate phylogenetic tree.

The 12S and COI genes for all filarial species did not produce a well-resolved phylogeny (Figure 2.6). The relationships of the filarial nematodes are consistent with the whole mitochondrial genome (Figure 2.4), and published literature (McNulty et al., 2012; Lefoulon et al., 2016), however, the support for the majority of filarial relationships is low. A feature of the 12S-COI phylogeny is that *Cercopithifilaria* is a monophyletic genus as *C. johnstoni* is positioned with the other *Cercopithifilaria* species. Nevertheless, these relationships have poor support, and *C. johnstoni* appears to have a longer branch length indicating *C. johnstoni* could be more distantly related than the other *Cercopithifilaria* species (Figure 2.6). It could be explained by the overall poor support of the tree and could be improved with the inclusion of more genomic information for each species, i.e., whole genome. The 12S and COI sequences cannot correctly position all the outgroup relationships, i.e., *S. digitata*. The outgroups for these analyses were chosen because they are outside of the Onchocercidae, *S. digitata*, *G. pulchrum*, *T. callipaeda* and *S. lupi*. However, in this analysis, *S. digitata* is positioned with *A. viteae* with poor support of 40/80 instead of the outgroup species (Figure 2.6). The *Dirofilaria* and *Onchocerca* clades have been consistently closely related, although within the 12S-COI tree has very poor support. The *Brugia-Wuchereria* clade is the only clade with very high support illustrating similar confidence as seen in the whole mitochondrial phylogeny (Figure 2.6).

The *Cercopithifilaria* genus clade is poorly supported (bootstrap and Bayesian posterior probability of 17/64) (Figure 2.6). Some relationships such as *C. minuta* and *C. tumidercervicata* are strongly supported together consistent with the literature (Otranto et al., 2013), whereas *C. grassi* and *C. japonica* should be grouped within the same sub-clade but are not and also have weak support (Otranto et al., 2013). In the 12S-COI phylogeny, *C. grassi* is in the same clade with *C. roussilhoni* and *C. bainaie* contrary to previous literature when *C. bainaie* is positioned in a different clade within the overall *Cercopithifilaria* phylogeny (Otranto et al., 2013). A possible explanation for the slight variation in filarial relationships and overall poor phylogeny support between the whole mitochondrial tree and the 12S-COI tree is that the gene tree has fewer genes

represented and therefore has less informative sites to construct a phylogeny resulting in reduced resolution and overall lower confidence in the predicted relationships (Wiens, 1998). The 12S and COI genes must not be variant enough to position all these nematodes accurately. Datasets that are concatenated with several genes are more likely to result in stronger relationships and improved support (Sanderson et al., 2003; Sanderson et al., 2010), hence why the mitochondrial genome is so strongly supported (Figure 2.4).

The relationships between the remaining nematodes in the 12S-COI tree are consistent with the literature and other analyses. Lefoulon et al. (2015) also used partitioned concatenated datasets of 12S and COI, but also used sequences from the nuclear genome: *rbp1*, *hsp70*, *myoHC*, and 18S and 28S sequences. Their analysis could position *C. baina* and *C. rugosicauda* within in the same overall clade as *A. viteae* and *L. sigmodontis* as monophyletic because this published phylogeny was based on additional information to resolve and generate more robustly supported relationships. There are no nuclear genes that are available for every *Cercopithifilaria* species using in the 12S-COI phylogeny, thus it is not possible to concatenate the genes to improve the alignment.

The support for the 12S-COI tree was very low. The data was further explored to determine whether removing the outgroups would improve support and resolution of the *Cercopithifilaria* clade. Reducing the outgroups or removing the outgroups did not affect the topology of the tree, nor did it improve the support for the relationships significantly. Thus the conclusion remains that 12S-COI phylogeny did not have enough informative sites to result in strongly supported phylogenetic relationships.

As the whole mitochondrial genome phylogeny is strongly consistent with published literature, it can be concluded that the 12S-COI phylogeny lacks sufficient information to make conclusive statements about phylogenetic relationships, including whether the current definition of the genus *Cercopithifilaria* is truly monophyletic. More sequence data could change where *C. johnstoni* is positioned concerning the genus clade or could result in a more highly supported monophyletic *Cercopithifilaria* clade. The apparent divergence of *C. johnstoni* from the other *Cercopithifilaria* species could be explained by geography. *C. baina*, *C. rugosicauda* and *C. grassi* all originated in Europe (Otranto et al., 2012), *C. roussilhoni* originated in Africa (Bain et al., 1986) and

C. japonica, *C. longa*, *C. bulboidea*, *C. tumidicervicata* originated in Japan (Uni et al., 2002). *C. johnstoni* is the first *Cercopithifilaria* species in Australia and therefore this analysis may represent these vast geographic differences. The addition of genes to the COI-12S phylogeny will improve the *Cercopithifilaria* clade relationships. It is likely by adding more genomic data that the species originating from the same location will group together with high nodal support. The addition of other *C. johnstoni* sequences from other reported hosts would enhance the credibility of the *Cercopithifilaria* phylogeny and illustrate clearly where the Australian species are positioned compared to the European, African and Asian species.

2.5 Conclusion

In this chapter, the mitochondrial genome of *C. johnstoni*, a parasitic filarial nematode of Australian bush rats, has been successfully constructed and annotated which has not been sequenced before. The *C. johnstoni* mitochondrial genome has consistent gene content and order compared to *O. volvulus* and other published filarial nematode mitochondrial genomes. The whole mitochondrial genome and 12S-COI gene tree with added *Cercopithifilaria* species is consistent with previously published filarial nematode phylogenies. An abundance of genomic information drastically improves the predicted phylogenetic relationships as seen when comparing the 12S-COI gene tree and the whole mitochondrial genome phylogeny. The relationship between *C. johnstoni* and other *Cercopithifilaria* species will have to be confirmed with the addition of more genomic information.

Comparing the *C. johnstoni* mitochondrial genome with published filarial nematode genomes has been the first step in understanding the evolutionary relationships of this parasite and confirms the overall position with filarial nematodes. *C. johnstoni* does not have a very close relationship with *O. volvulus*, but as a result, this raises questions about why *C. johnstoni* elicits such a similar immunopathology that is observed in *O. volvulus*-infected humans.

Chapter Three

Assembly of the *Cercopithifilaria johnstoni* nuclear genome and prediction of orthologous relationships with closely related filarial nematodes

3.1 Introduction

A key criterion to developing the *C. johnstoni*-rodent animal model of onchocerciasis is the ability to recapitulate the most important disease characteristics so that the molecular mechanisms driving these features can be understood (features discussed in detail in the general introduction (Chapter One)). *O. volvulus* and *C. johnstoni* are obligate filarial parasites that cannot be maintained outside of their hosts. It is therefore difficult to culture and study these parasites to identify features that are driving the immunopathology without an animal model. However, one approach to begin to address this question is to compare the genome composition using comparative genome approaches to identify relevant genes that may be involved in infection, immune response, or drug response that can be compared with *O. volvulus*.

Until recently, comparative studies of filarial parasites have been hampered by the relative scarcity of genome sequences (Mitreva et al., 2011). However, since the introduction of high-throughput sequencing technologies in the early 2000s, more nematodes are being sequenced, and the genome assemblies are of high quality (Stoltzfus et al., 2017; Coghlan et al., 2019; Tyagi et al., 2019b). Currently, there are 134 genomes available on WormBase Parasite from the Phylum Nematoda with variations of genome completeness, quality and size. These genomes can all be used for a range of computational studies. Nematode genomes can vary in size from *Parastrongyloides trichosuri* at ~42 Mb (Hunt et al., 2016), *O. volvulus* ~96 Mb (Cotton et al., 2016), *B. malayi* ~90 Mb (Ghedini et al., 2004), *Caenorhabditis elegans* ~100 Mb (Stein et al., 2003), to a larger nematode genome such as *H. contortus* ~283 Mb (Doyle et al., 2020). There are now many filarial species that have been sequenced for comparative

genomic studies and are part of the 134 Nematoda genomes available on WormBase Parasite. The available filarial genomes include *D. immitis* (Godel et al., 2012), *B. malayi* (Ghedini et al., 2007), *B. pahangi* and *B. timori* (Coghlan et al., 2019), *O. volvulus* (Cotton et al., 2016), *O. ochengi* (Coghlan et al., 2019), *L. loa* (Desjardins et al., 2013b; Tallon et al., 2014) and *W. bancrofti* (Small et al., 2016). These filarial parasites have life cycles that are difficult to maintain or replicate in the laboratory, and therefore comparative genomics can be useful to understand parasite biology and explore host-parasite relationships (Tallon et al., 2014; Grote et al., 2017).

The *O. volvulus* genome was the first high-quality filarial nematode genome with nearly complete chromosome assembly, including the sex chromosome (97 Mb nuclear (Cotton et al., 2016), 13,747 bp mitochondrial (Keddie et al., 1998; Unnasch and Williams, 2000)). The *O. volvulus* genome comprises three autosomes and a pair of sex chromosomes. The assembly consists of four large scaffolds totalling 94% of the genome. Sequence data from female and male worms were used to assemble the chromosomes and identified that OM2 is the X chromosome (Cotton et al., 2016). There have been 12,143 protein-coding genes predicted guided by RNA-Seq data from eight stages of the *O. volvulus* life cycle. Approximately 91% of these genes had orthologues in other nematode species, and approximately 9% identified as species-specific (Cotton et al., 2016). Importantly, the construction of the *O. volvulus* genome now enables functional analyses of the predicted genes finding that 44% of the protein-coding genes had no predicted function (Cotton et al., 2016). Parasites are known to have unique biology, and therefore this finding is consistent that many of these genes have not been defined thus far with a known function (Stoltzfus et al., 2017). The high-quality *O. volvulus* genome has enabled exploration and discovery of many gene duplication events such as the G-protein-coupled receptor (GPCR) expansion and has facilitated metabolic reconstruction at genome-scale to identify and understand the metabolic pathways essential in parasitism (Bennuru et al., 2017; Shey et al., 2018). The construction of the genome for *O. volvulus* has now provided a resource to explore parasitism and host-parasite relationships *in silico* to work towards identifying potential targets for experimental testing and validation for diagnosis or treatment of onchocerciasis (Cotton et al., 2016; Grote et al., 2017; Lustigman et al., 2017).

Whole genomes have been an excellent resource for a range of biological and theoretical hypothesis throughout nematode research. There are now several resources available to develop and annotate nematode genomes from the vast majority of nematodes that have already been sequenced (Blaxter and Koutsovoulos, 2015; Coghlan et al., 2019). WormBase ParaSite is the primary resource for nematode and flatworm genomics (Howe et al., 2017). WormBase ParaSite aims to provide both integration and presentation of the sequenced helminth genomes and transcriptomes for researchers to become engaged with parasite worm genomics (Howe et al., 2017). The data available include genome sequence, annotation, protein sequence, and gene orthology (Howe et al., 2017).

Comparative genomics is not possible without a genome assembly. Genome assembly refers to the process of joining nucleotide sequences in the correct order for a particular organism (Foxman, 2012; Choudhuri, 2014). Typically, *de novo* or comparative assembly approaches are used to assemble a genome (Foxman, 2012; Choudhuri, 2014). Comparative assembly uses the sequence of a closely related organism as a guide for genome assembly and annotation or a previous draft genome assembly of the same species. The sequences are then mapped onto the reference genome for improving the genome assembly (Pop et al., 2004). *De novo* assembly is required when it is the first assembly of that species and is not similar to organisms previously sequenced. The process involves assembling the genome as complete as possible and then annotate with the available data (Baker, 2012). The general steps of a genome assembly include sequencing, sequence quality checks, trimming adapters and poor quality reads, assemble sequences taking into consideration the variety of different thresholds that can be set that determine whether a given run of sequence or entire read will be included, and then using parameters to determine how the assembly proceeds. The last step of the genome assembly is annotation. There are several criteria that are important when assessing the quality of a genome such as read length, N50, number of gaps, ability to fill these gaps, longest sequence, number of contigs and scaffolds, the number of mis-assemblies, and BUSCO and CEGMA statistics. Thus, the quality of genomes varies between species because it is highly dependent upon the sequencing data available (Baker, 2012). For example, draft genomes generally have improved quality statistics with a combination of short and long read DNA sequencing data compared to draft genomes with only short read DNA

sequencing or poor sequencing data. Long read sequences greatly improve the genome assembly, although short-read DNA sequencing can still provide valuable information for comparative analyses. One last criterion of genome quality is gene prediction. Furthermore, gene prediction is of higher quality when RNA-Seq data are available to verify the gene predictions. The abundance of genome assemblies have now enabled closely and distantly related species to be compared to explore genome repeat regions (Whitton et al., 2004), gene discovery (Mitreva et al., 2005; Nutman et al., 2016), parasitism, possible drug targets for disease (Foster et al., 2005; Godel et al., 2012; Bennuru et al., 2017; Bennuru et al., 2018), phylogenetic relationships (Mitreva et al., 2005; McNulty et al., 2012; Coghlan et al., 2019), the discovery of bacterial endosymbionts (Bandi et al., 1998; Casiraghi et al., 2001; Bennuru et al., 2011) and more. Thus, genome assembly is one of the most important steps in exploring a new or understudied species.

In Chapter Two, there was a description of the first genomic characterisation of *C. johnstoni* using mitochondrial DNA; however, there are currently no nuclear genome resources available for *C. johnstoni* to compare with other filarial nematodes. A genome assembly and annotation for *C. johnstoni* will provide a valuable resource for understanding the relationships between *C. johnstoni* and *O. volvulus*, including other closely related filarial nematodes. The availability of the *C. johnstoni* genome would facilitate *in silico* comparisons between *C. johnstoni* and *O. volvulus*, which would guide laboratory experiments should the analyses support *C. johnstoni* as an appropriate organism for a small animal model to study onchocerciasis. Specifically, a genome could be the beginning in comparing protein-coding genes, identifying orthologues between closely related species providing potential protein targets that may be responsible for driving the immunopathology of the disease. The *in silico* analyses could identify a new pathway in discovering novel gene targets for diagnostic assays or treatments for onchocerciasis. A *C. johnstoni* genome would be the first step to provide a fundamental genetic resource that can be used to compare against *O. volvulus* and predict orthologous genes that may have a role in the disease immune responses.

3.1.1 Aims

In Chapter Three, the draft genome of *C. johnstoni* was compared with closely related filarial nematodes to study genome statistics, phylogenetic relationships and genomic content. The *C. johnstoni* genome content is explored by studying the following aims:

- 1) Assemble and annotate the nuclear genome of *C. johnstoni*.
- 2) Estimate and compare genome completeness with other published related filarial nematodes to determine the quality of *C. johnstoni* genome assembly.
- 3) Compare the genome content and genetic similarity with *O. volvulus*.
- 4) Identify orthologous protein-coding genes between the *C. johnstoni*, *O. volvulus* and other filarial nematode proteomes.

3.2 Materials and Methods

Chapter Three utilises the same Next-Generation Sequencing data as for the mitochondrial genome assembly described in Chapter Two: Materials and Methods, “Sample collection” and “DNA extraction library preparation and sequencing” for details on sequencing and quality control methods.

3.2.1 Nuclear genome assembly

De novo genome assembly was conducted using all quality trimmed reads using SPAdes version 3.10.1 (Nurk et al., 2013). Default parameters were used. Comparative genome assembly statistics were generated for *C. johnstoni* and for the other filarial nematodes to be used for comparison with assembly stats version 1.0.1 (<https://github.com/sanger-pathogens/assembly-stats>). The mitochondrial genome assembled in Chapter Two was used to identify and remove assembled scaffolds from the mitochondrial genome.

3.2.2 Masking repeats

Repeats were masked by RepeatModeler version 1.0.11 (Saha et al., 2008) and RepeatMasker version 4.0.5 (Smit, 2015) on the *C. johnstoni* genome scaffolds file from SPAdes using default parameters. The same analysis was conducted on the other filarial nematodes used for comparison throughout this thesis: *A. viteae*, *B. malayi*, *B. pahangi*, *B. timori*, *D. immitis*, *L. sigmodontis*, *L. loa*, *O. flexuosa*, *O. ochengi*, *O. volvulus* and *W. bancrofti*. Genome versions for the nematodes used in the RepeatModeler analysis were *A. viteae* (PRJEB1697.WBPS13), *B. malayi* (PRJNA10729.WBPS13), *B. pahangi* (PRJEB497.WBPS13), *B. timori* (PRJEB4663.WBPS13), *D. immitis* (PRJEB1797.WBPS13), *L. sigmodontis* (PRJEB3075.WBPS13), *L. loa* (PRJNA246086.WBPS13), *O. flexuosa* (PRJEB512.WBPS13), *O. ochengi* (PRJEB1204.WBPS13), *O. volvulus* (PRJEB513.WBPS14) and *W. bancrofti* (PRJEB536.WBPS13).

3.2.3 Whole genome completeness

Genome completeness was estimated using CEGMA (Core Eukaryotic Genes Mapping Approach) version 2.4.010312 (Parra et al., 2007) and BUSCO

(Benchmarking Universal Single-Copy Orthologues) version 4 (Simão et al., 2015). CEGMA was conducted with genome default parameters. BUSCO analyses were conducted with default parameters and lineage set to *nematode_odb9* and mode set to “genome” using “*Caenorhabditis*” as a training species for gene identification.

CEGMA and BUSCO similarly attempt to estimate what proportion of a core set of conserved genes can be found in an assembly as a proxy for genome completeness when experimental data is not available. CEGMA uses Markov models to improve estimates of gene structures and searches for orthologues of core proteins to determine exon-intron structures (Parra et al., 2007). Its average accuracy has been estimated at around 98% at the nucleotide level and 90% at the internal exon-level when compared to 6 model genomes (Parra et al., 2007). BUSCO uses hidden Markov models and calculates complete, duplicated, fragmented, and missing metrics within one of the six phylogenetic sets available to describe the genome (Simão et al., 2015). BUSCO can run much faster than CEGMA and has a higher resolution of genome content (Simão et al., 2015). BUSCO is an updated program for the prediction of genes present in the genome. BUSCO and CEGMA were collectively used to compare results.

3.2.4 Comparison of *Cercopithifilaria johnstoni* scaffold content with *Onchocerca volvulus* and *Brugia malayi* genome content

Genome alignment of *C. johnstoni* RepeatMasked scaffolds and *O. volvulus* chromosomes was conducted using the PROmer package version 3.07 of MUMmer (Kurtz et al., 2004). A separate PROmer analysis was conducted using *C. johnstoni* RepeatMasked scaffolds and *B. malayi*. Synteny between the genomes was visualised in two separate plots using Circos version 0.67_5 (Krzywinski et al., 2009).

Circos plots illustrate networks representing different analyses of large datasets and have entirely changed the way comparative genomics has been presented (Krzywinski et al., 2009). Circos plots do not analyse or produce datasets. A “story” is depicted by layering important information onto the Circos plot (Krzywinski et al., 2009); however, too much data can cause the plot to look crowded, messy or unclear (Krzywinski et al., 2009). Since the *C. johnstoni*

assembly consists of assembled large scaffolds and many small contigs, comparing *C. johnstoni*'s genome to more than one species at a time using a Circos plot creates an uninterpretable visual representation. Thus, the species comparisons to *O. volvulus* and *B. malayi* were separated.

Genome Ribbon (Nattestad et al., 2016) was used to explore the conservation of the whole nuclear genome between *C. johnstoni* and *O. volvulus*. The longest scaffold from *C. johnstoni* genome assembly was extracted from the PROmer analysis and input into Genome Ribbon where it illustrated where on the *O. volvulus* chromosomes the *C. johnstoni* scaffold aligns.

3.2.5 Scaffold GC content and coverage analysis between *Cercopithifilaria johnstoni* and *Onchocerca volvulus*

The coverage (read depth) and GC content of the *C. johnstoni* genome sequencing data were calculated. Trimmed reads of *C. johnstoni* were mapped to the *de novo* *C. johnstoni* genome scaffolds using bwa version 0.7.16a (Li and Durbin, 2009). Coverage was calculated using bedtools version 2.26.0 (Quinlan and Hall, 2010) using default parameters across 10kb windows. The GC content was calculated using bedtools nuc (Quinlan and Hall, 2010). The outputs from coverage and GC content analyses were then combined to construct a scatterplot diagram comparing GC content and coverage using the R package ggplot2 version 3.2.1 (Wickham, 2016; Wickham et al., 2016). The dataset was filtered to illustrate only the contigs with a sequence length greater than 10,000.

The PROmer analysis between *C. johnstoni* and *O. volvulus* were used to assign the *C. johnstoni* reads to *O. volvulus* chromosomes. The GC content vs coverage scatterplot was then coloured based on the homology between the *C. johnstoni* reads and *O. volvulus* chromosomes. The *C. johnstoni* reads that shared homology to OM1, OM2 (X chromosome), OM3, OM4 and OM5 were therefore coloured to represent these relationships.

3.2.6 Protein-coding gene prediction

Gene prediction of the *C. johnstoni* scaffolds was compared and conducted using three separate methods to confirm the most appropriate gene prediction. Initially, the scaffolds were input into the Augustus pipeline version

3.0.2 (Stanke et al., 2008) using default parameters and trained using the *C. elegans* dataset. These *C. johnstoni* scaffold repeats were unmasked. Second, the gene prediction of *C. johnstoni* scaffolds was conducted using BRAKER version 2.1.4 (Hoff, 2018) with *ab initio* default parameters. These *C. johnstoni* scaffold repeats were unmasked. The final gene prediction of the masked repeats *C. johnstoni* scaffolds was conducted using BRAKER version 2.1.4 (Hoff, 2018). The protein-coding gene set from a closely related species, *A. viteae* (Chapter Two), was used in the BRAKER pipeline to improve gene prediction accuracy. GenomeThreader version 1.7.1 was used in the BRAKER pipeline for producing complete gene structures by aligning the proteins to the genome (Hoff et al., 2019). Augustus-master training (Stanke et al., 2008) was used in the BRAKER pipeline based on spliced alignment information from the closely related species protein input file.

3.2.7 Assessment of predicted protein-coding gene completeness

The completeness of the protein-coding gene lists after gene prediction was assessed to determine the suitability of the proteins for the purpose of searching for orthologues of the proteins that consistently elicit strong serum antibody responses in people infected with *O. volvulus* (Chapter Four).

Genome completeness was estimated using BUSCO (Benchmarking Universal Single-Copy Orthologues) version 4 (Simão et al., 2015). The BUSCO analysis was conducted using default parameters and lineage set to nematode_odb9. The mode was set to “protein” which is a mode used for annotated gene sets. The protein parameter uses HMMER a program designed to search for homologous sequences in biological sequence databases.

There are four main categories used to interpret BUSCO results: Complete and single-copy, Complete and duplicated, Fragmented and Missing BUSCOs. There is also a category, ‘Complete’ which combines the single-copy and duplicated results. Complete refers to a full-length orthologue being identified based on the expected length of the BUSCO alignment. Fragmented refers to partial lengths of orthologues being identified which is less than the expected length of the BUSCO alignment. Missing refers to BUSCO being unable to

identify any significant alignments and thus missing from the list (Simão et al., 2015).

3.2.8 Prediction of shared orthologues using OrthoFinder2

The prediction of orthologous genes was conducted using OrthoFinder version 2.2.7 (Emms and Kelly, 2015, 2019). Protein sequence from *A. viteae*, *B. malayi*, *B. pahangi*, *B. timori*, *D. immitis*, *L. sigmodontis*, *L. loa*, *O. flexuosa*, *O. ochengi*, *O. volvulus* and, *W. bancrofti*, were used for the OrthoFinder2 analysis. The predicted *C. johnstoni* proteins from the Augustus, *ab initio* BRAKER and BRAKER with *A. viteae* training analyses were separately utilised in three OrthoFinder2 analyses for comparison of the datasets.

The Augustus predicted protein-coding list was chosen for downstream analyses as it was the best gene prediction method according to BUSCO and CEGMA. Aforementioned, the Augustus predicted proteins was utilised in the OrthoFinder2 analysis. The orthogroups were identified using OrthoFinder2 using default parameters. The sequences were extracted from the analyses using `-M msa, -os` parameters.

A phylogenetic tree was then created from the 1,447 single copy orthologues predicted by OrthoFinder from the protein sequences predicted by Augustus. The phylogenetic tree illustrated the overall phylogenetic relationships of the included nematodes. The alignments of these orthogroups were for each species were concatenated using the `catfasta2phylml.pl` script (<https://github.com/nylander/catfasta2phylml>). Alignments were visualised in Mesquite version 3.04 (Maddison and Maddison, 2008) and the sequences were trimmed manually. A maximum likelihood phylogeny was estimated using RAxML using the best 20 replicates under the PROTGAMMALGF model of sequence evolution, and 1000 bootstrap replicates to estimate support for bipartitions.

The OrthoFinder2 algorithm produces orthogroups that contain orthologous genes for which the root of the tree is the gene derived common ancestor (Emms and Kelly, 2019). Within these orthogroups there can be four different orthologue relationships occurring between the species:

- 1) Genes can have a one-to-one orthologous relationship where there is only one gene per species.

- 2) Genes can be many-to-many whereby there have been multiple gene duplication events in both species after speciation, and therefore there are numerous orthologues for each species.
- 3) Genes can be many-to-one with multiple orthologous genes from the derived state to one gene in the ancestral state.
- 4) Lastly, genes can be one-to-many indicating that one gene from the derived state is orthologous to many genes of the ancestral state (Emms and Kelly, 2019).

3.2.9 Orthogroups and single-copy orthologue UpSet plots

The Orthogroups.GeneCount.csv file generated from the OrthoFinder2 analysis was used to generate the UpSet plots to represent orthologous relationships between the 12 filarial species. There were two analyses involved in representing the orthologue data. First, the one-to-one orthologues were extracted from Orthogroups.GeneCount.csv. Only data where the number of genes is 0 or 1, i.e., absent or in single-copy, were extracted to generate the single-copy orthologous UpSet plot. The second dataset focused more on the orthogroups shared between filarial nematodes. Any orthogroup that had a gene number of 1 or greater than 1 was extracted for that analysis.

The figures were generated using UpSetR version 1.4.0 (Conway et al., 2017) specifying `nsets = 12` representing the 12 filarial species and `nintersects = 70`. The `nintersects` parameter needed to be restricted because showing all the intersects between the 12 filarial nematodes would have resulted in an uninterpretable figure.

3.3 Results

3.3.1 Genome assembly: *Cercopithifilaria johnstoni*

The genome assembly statistics for all the filarial nematodes are represented in Table 3.1. The SPAdes genome assembly of *C. johnstoni* results in large scaffolds and many small contigs. The complete genome assembly combining the scaffolds and contigs consists of a total length of 79,062,707 bp and an N50 of 88,758 bp. The longest sequence of an assembled scaffold has 588,165 bp. There are 57,700 Ns and 299 gaps throughout the scaffold assembly of *C. johnstoni* (Table 3.1).

The *C. johnstoni* genome assembly has been evaluated by comparing assembly length, longest sequence, N50, N90, GC content, number of Ns and number of gaps. The *C. johnstoni* genome is smaller than the *O. volvulus* genome assembly length of 96,427,137 bp and an N50 of 25,485,961 bp. The longest sequence in the *C. johnstoni* assembly is much smaller than the *O. volvulus* of 28,345,163 bp (Table 3.1). GC content is consistent across all the filarial nematode whole genomes. The largest N50 value across the nematodes are from the two complete chromosomal assembled genomes of *B. malayi* and *O. volvulus* (Table 3.1). The draft *C. johnstoni* assembly has a moderately high N50 length while the draft genomes assemblies of *A. viteae*, *B. pahangi*, *B. timori*, *L. sigmodontis*, *O. ochengi*, *O. flexuosa* and *W. bancrofti* have much lower N50s ranging from 2,943 bp to 65,666 bp (Table 3.1).

There is no evidence of a complete *Wolbachia* genome present within the *C. johnstoni* scaffolds. As there was no large segments or indication of a *Wolbachia* genome from mapping readings to the scaffolds, *Wolbachia* exploration in *C. johnstoni* was not taken further. *Wolbachia* is also not a focus of this thesis, but could be explored in more detail for future analyses.

Table 3.1: Genome statistics of *Cercopithifilaria johnstoni* with all the filarial nematodes that have genome statistics available to compare variables such as assembly length, the longest sequence length (bp), N50 length, N90 length, GC%, number of Ns and the number of gaps within the assembly.

Species	Assembly length	Longest sequence	N50 length	N90 length	GC %	Ns	Gaps
<i>C. johnstoni</i>	79,062,707	588,165	88,758	15,919	29.6	57,700	299
<i>A. viteae</i>	77,350,906	172,453	25,808	5,125	29.9	175,459	3,735
<i>B. malayi</i>	88,235,797	24,943,668	14,214,749	13,467,244	28.5	277,365	8
<i>B. pahangi</i>	90,545,113	1,059,003	65,666	1,776	28	1,264,446	1,926
<i>B. timori</i>	64,930,714	45,194	4,919	1,041	30.2	751,488	16,893
<i>D. immitis</i>	88,309,529	1,085,577	71,281	1,636	28	3,430,609	13,431
<i>L. loa</i>	96,405,338	1,570,872	180,288	13,467	30.8	0	0
<i>L. sigmodontis</i>	64,813,410	402,953	45,863	10,481	34.1	999,760	13,720
<i>O. volvulus</i>	96,427,137	28,345,163	25,485,961	2,816,604	29.2	3,074,367	581
<i>O. ochengi</i>	91,660,559	230,458	16,199	1,633	29.8	382,758	9,025
<i>O. flexuosa</i>	86,175,476	55,543	2,943	749	29.4	1,532,536	8,443
<i>W. bancrofti</i>	76,991,470	144,416	9,917	2,372	28.8	69,948	3,280

3.3.2 Whole genome completeness of *Cercopithifilaria johnstoni* compared to filarial nematodes

CEGMA and BUSCO are used to assess the completeness of the *C. johnstoni* genome assembly. Each program assesses the presence of complete or fragmented highly conserved genes (a total of 248 for CEGMA & 982 for BUSCO Nematoda datasets) that are expected to be present within a complete nematode genome assembly. The *C. johnstoni* assembly contains 93.50% complete (232/248 sequences; 1.16 average orthologous sequences) and 97.45% partial (242/248 sequences; 1.24 average orthologous sequences) CEGMA genes. In total, 242 out of 248 CEGMA genes are predicted in the *C. johnstoni* genome, which is equivalent to the *O. volvulus*, *B. malayi*, and *L. loa* published genome assemblies (Table 3.2). The remaining six CEGMA genes missing from the assembly corresponding to KOG IDs KOG0622, KOG0933, KOG1468, KOG2303, KOG2531, and KOG2770 are also missing from the other filarial nematode genomes, suggesting that these six genes may be missing from at least these filarial species used in the CEGMA analysis.

The *C. johnstoni* and *O. volvulus* genomes have the highest CEGMA prediction of 242 genes out of 248, *O. volvulus* with only five additional complete genes predicted (Table 3.2). CEGMA predicts 240 genes out of a possible 248 and predicts complete genes ranging between 230 and 235 for *A. viteae*, *B. malayi*, *D. immitis*, *L. loa* and *L. sigmodontis* (Table 3.2). The genomes that have the least number of predicted genes are *B. timori* and *O. flexuosa* (Table 3.2). The remaining nematodes *B. pahangi*, *O. ochengi* and *W. bancrofti* all have relatively good CEGMA gene predictions but are missing some genes (Table 3.2).

Approximately 94.09% (924 of 982) of the BUSCO genes are identified in the *C. johnstoni* genome assembly, comprised of 917 (93.40%) complete, seven (0.70%) complete and duplicated, 43 (4.40%) fragmented & 15 (1.50%) missing genes (Table 3.3). Although 15 of the BUSCO sequences are missing from the assembly, it is similar to BUSCO scores from several filarial genomes (Table 3.3). The missing genes are not the same across the 12 filarial nematodes, however several of the missing genes are missing in at least one other species. A list of the missing genes for each filarial species can be found in Supplementary Table 3.1.

Table 3.2: Comparison of the genome completeness statistics of all filarial nematodes with CEGMA (248 sequences).

Species	Complete (total)	Complete (%)	Complete (average orthologous sequences per CEG)	Partial (total)	Partial (%)	Partial (average orthologous sequence per CEG)
<i>C. johnstoni</i>	232	93.55	1.16	242	97.45	1.24
<i>A. viteae</i>	230	92.74	1.42	240	96.77	1.60
<i>B. malayi</i>	233	93.95	1.18	240	96.77	1.26
<i>B. pahangi</i>	225	90.73	1.24	236	95.16	1.39
<i>B. timori</i>	149	60.08	1.97	195	78.63	2.18
<i>D. immitis</i>	235	94.76	1.14	240	96.77	1.29
<i>L. loa</i>	235	94.76	1.14	240	96.77	1.23
<i>L. sigmodontis</i>	232	93.55	1.30	240	93.77	1.41
<i>O. volvulus</i>	237	95.56	1.08	242	97.58	1.18
<i>O. ochengi</i>	212	85.48	1.42	233	93.95	1.62
<i>O. flexuosa</i>	132	53.23	1.95	194	78.23	2.18
<i>W. bancrofti</i>	180	72.58	1.68	207	83.47	1.86

Table 3.3: Comparison of the genome completeness statistics of all filarial nematodes with BUSCO (982 groups). C (%) – Complete (%), CS (%) – Complete and single copy (%), D (%) – Complete and duplicated (%), F (%) – Fragmented (%), M (%) – Missing (%).

Species	C (total)	C (%)	CS (total)	CS (%)	D (total)	D (%)	F (total)	F (%)	M (total)	M (%)
<i>C. johnstoni</i>	942	95.9	917	93.4	7	0.7	43	4.4	15	1.5
<i>A. viteae</i>	889	90.5	872	88.8	17	1.7	69	7.0	24	2.5
<i>B. malayi</i>	951	96.8	940	95.7	11	1.1	18	1.8	13	1.4
<i>B. pahangi</i>	881	89.7	874	89.0	7	0.7	65	6.6	36	3.7
<i>B. timori</i>	523	53.3	519	52.9	4	0.4	207	21.1	252	25.6
<i>D. immitis</i>	902	91.8	881	89.7	21	2.1	44	4.5	36	3.7
<i>L. loa</i>	958	97.5	945	96.2	13	1.3	20	2.0	4	0.5
<i>L. sigmodontis</i>	900	91.6	881	89.7	19	1.9	54	5.5	28	2.9
<i>O. volvulus</i>	958	97.6	955	97.3	3	0.3	17	1.7	7	0.7
<i>O. ochengi</i>	841	85.6	836	85.1	5	0.5	93	9.5	48	4.9
<i>O. flexuosa</i>	465	47.3	463	47.1	2	0.2	213	21.7	304	31.0
<i>W. bancrofti</i>	736	74.9	732	74.2	4	0.4	113	11.5	133	13.6

BUSCO has identified that *B. timori* and *O. flexuosa* genomes have the highest number of missing genes consistent with the CEGMA analysis. Three-hundred and five genes are missing from *O. flexuosa* and 253 genes missing from *B. timori*. The gene prediction for the *O. volvulus* genome is the highest quality of 97.60% with 1.70% fragmented and 0.70% missing. The *L. loa* genome follows with 97.50% complete predicted genes, 2.00% fragmented and 0.50% missing. Then *B. malayi* with 96.80% complete predicted genes, 1.80% fragmented and 1.40% missing. Lastly, *C. johnstoni* has 94.10% complete predicted genes, 4.40% fragmented with 1.50% missing (Table 3.3). The *C. johnstoni* scaffolds have comparable genome completeness statistics to the highly curated filarial nematode genomes, i.e., *O. volvulus* and *B. malayi* genome assemblies.

3.3.3 Analysis of genome repeats of filarial nematodes

RepeatModeler and RepeatMasker identify the number of repeats within the assembled *C. johnstoni* scaffolds. RepeatModeler has identified the categories of repeats estimated in the *C. johnstoni* genome. The total interspersed repeats consist of long interspersed nuclear elements (LINEs), short interspersed nuclear elements (SINEs), DNA transposons (DNA), long terminal repeats (LTR), and unclassified. Other repeats of small RNA, satellites, simple repeats and low complexity repeats are also determined by RepeatModeler (Table 3.4, Supplementary Table 3.2).

The *C. johnstoni* scaffolds consist of a total of 2.41% interspersed repeats and 3.82% of satellites, simple and low complexity repeats. These repeats make up the total repeats masked (bases masked) of 4,925,102 bp (6.23%) within the *C. johnstoni* scaffolds (Table 3.4, Supplementary Table 3.2). The bases masked has increased from 56,933 bp Ns to 4,925,102 bp Ns after RepeatMasker.

The *A. viteae* genome compared to the *C. johnstoni* scaffolds consists of less interspersed repeats of 1.22% and less simple and low complexity repeats with 2.74%. These repeats make up the total repeats masked of 3,054,604 bp (3.96%) within the *A. viteae* genome which has ~2.00% less masked repeats compared to *C. johnstoni* (Table 3.4, Supplementary Table 3.2).

The *L. sigmodontis* genome consists of a total of 0.44% interspersed repeats and of 2.38% simple and low complexity repeats which is again lower than the masked repeats in the *C. johnstoni* scaffolds. These repeats make up the total of repeats masked of 1,826,171 bp (2.82%) within the *L. sigmodontis* genome significantly less than the 6.23% for the *C. johnstoni* scaffold assembly (Table 3.4, Supplementary Table 3.2).

The *O. volvulus* genome consists of an increased number of interspersed repeats with 6.57% than the *C. johnstoni* scaffolds, and slightly fewer satellites, simple and low complexity repeats with 3.69% and the addition of small RNA repeats. These repeats make up the total of the repeats masked of 9,890,502 bp (10.26%) within the *O. volvulus* genome significantly higher than *C. johnstoni* (Table 3.4, Supplementary Table 3.2).

Consistent with the *O. volvulus* genome, the *O. ochengi* genome consists of a total of 6.75% interspersed repeats and of 3.54% of small RNA, satellites, simple and low complexity repeats which is greater than the repeats for the *C. johnstoni* scaffolds. These repeats make up the total of repeats masked of 9,358,768 bp (10.21%) within the *O. ochengi* genome, which is higher than the masked repeats in the *C. johnstoni* scaffolds (Table 3.4). A summary of all the filarial nematode repeat masked percentages can be found in Table 3.4 and the complete data including number of base pairs in Supplementary Table 3.2.

The *C. johnstoni*, *A. viteae* and *L. sigmodontis* genomes have not identified any small RNA repeats. There are no satellites reported in the *A. viteae* and *L. sigmodontis* genomes and only 0.01% identified in the *C. johnstoni* genome. In contrast, the *O. volvulus* and *O. ochengi* genome have small RNA, satellites, simple and low complexity repeats making up a higher percentage of repeats than the other filarial genomes.

The highest number of masked repeats across these nematodes is within the *L. loa* genome at 13,119,135 bp (13.61%), followed by *B. malayi* with 10,494,094 bp (11.80%) (Table 3.4).

Table 3.4: Comparison of the RepeatModeler repeat statistics of *Cercopithifilaria johnstoni* and closely related filarial nematodes. Total percentages (%) of interspersed repeats consisting of LINEs (long interspersed nuclear elements), SINEs (short interspersed nuclear elements), DNA (DNA Transposons), LTR (long terminal repeat) and unclassified repeats. Small RNA, satellites, simple repeats and low complexity repeats are also represented in the table. The percentage of masked repeat bases in each filarial genome are represented as “bases masked”.

Species	bases masked	SINEs	LINEs	LTR	DNA	Unclassified	Total interspersed repeats	Small RNA	Satellites	Simple repeats	Low complexity
<i>C. johnstoni</i>	6.23	0.00	0.15	0.00	0.07	2.20	2.41	0.00	0.01	3.11	0.70
<i>A. viteae</i>	3.96	0.00	0.01	0.44	0.18	0.59	1.22	0.00	0.00	2.08	0.66
<i>B. malayi</i>	11.80	0.00	0.43	1.26	0.26	4.12	6.07	0.12	0.26	4.28	1.20
<i>B. pahangi</i>	7.88	0.03	0.37	0.46	0.28	1.04	2.18	0.03	0.01	4.37	1.33
<i>B. timori</i>	5.02	0.00	0.26	0.44	0.16	0.59	1.44	0.01	0.06	2.77	0.75
<i>D. immitis</i>	6.10	0.02	0.19	0.58	0.10	1.33	2.22	0.08	0.06	2.94	0.83
<i>L. loa</i>	13.61	0.04	0.92	2.56	0.93	3.84	8.29	0.15	0.28	4.14	0.81
<i>L. sigmodontis</i>	2.82	0.00	0.03	0.16	0.09	0.17	0.44	0.00	0.00	1.91	0.47
<i>O. flexuosa</i>	8.06	0.00	0.06	1.47	0.06	3.87	5.47	0.04	0.02	2.02	0.53
<i>O. ochengi</i>	10.21	0.06	0.99	1.12	0.30	4.26	6.75	0.11	0.20	2.51	0.72
<i>O. volvulus</i>	10.26	0.00	0.10	1.29	0.17	5.02	6.57	0.08	0.09	2.73	0.79
<i>W. bancrofti</i>	6.96	0.06	0.08	0.86	0.19	0.48	1.68	0.00	0.08	4.12	1.09

3.3.4 Comparative genomics analyses: *Cercopithifilaria johnstoni* shares homology to *Onchocerca volvulus*

Before analysing the synteny between *C. johnstoni* and *O. volvulus* or *B. malayi*, a Circos plot was created to compare the chromosome conservation, gene content and order between *O. volvulus* and *B. malayi* to then determine how these chromosomes relate when compared to *C. johnstoni*. The *O. volvulus* and *B. malayi* genomes are assembled into chromosomes while the *C. johnstoni* genome assembly is fragmented. The Circos plots highlight the different conservation of gene content and order between the three species. When discussing synteny between *O. volvulus* and *B. malayi* (Figure 3.1), it is possible to discuss synteny at a macrosyntenic level as there are tens of thousands of genes that share conservation between each species. The following analysis of synteny between *C. johnstoni*, *O. volvulus* and *B. malayi* (Figure 3.2) are looking at how many scaffolds share conservation with genes in the highly assembled filarial genomes. However, the Circos plot is unable to resolve clear microsyntenic relationships and thus required the GenomeRibbon analysis to take a closer look at one scaffold of *C. johnstoni* compared to the *O. volvulus* and *B. malayi* chromosomes (Figure 3.3). The Circos plot represents sequence similarity above 80% and a minimum sequence length of 1,000 bp for *C. johnstoni* scaffolds hence macrosyteny cannot be considered in this analysis.

The *O. volvulus* genome has a 3A+XY chromosome karyotype, three autosomes with X and Y chromosomes, compared to *B. malayi* with a 4A+XY karyotype, four autosomes with X and Y chromosomes (Foster et al., 2020). The Circos plot represents each *B. malayi* chromosome (yellow bars) aligning the chromosomes of the *O. volvulus* reference genome (Figure 3.1). A chromosome rearrangement can be observed when comparing the X chromosomes. OM2 the X chromosome of *O. volvulus* is split across half of the CHRX and CHR4 of *B. malayi* (Figure 3.1). Most importantly, the Circos plots illustrate significant blocks of colour representing chromosomes that share gene content conservation, i.e., OM4 is strongly conserved with CHR2 (Figure 3.1). The Y chromosomes are not labelled or present on the Circos plot because they are poorly defined.

The synteny analysis between *C. johnstoni* and *O. volvulus* chromosomes reveals large segments of *C. johnstoni*'s fragmented assembly linking with the three autosomes and one X chromosome in the *O. volvulus* genome (Figure

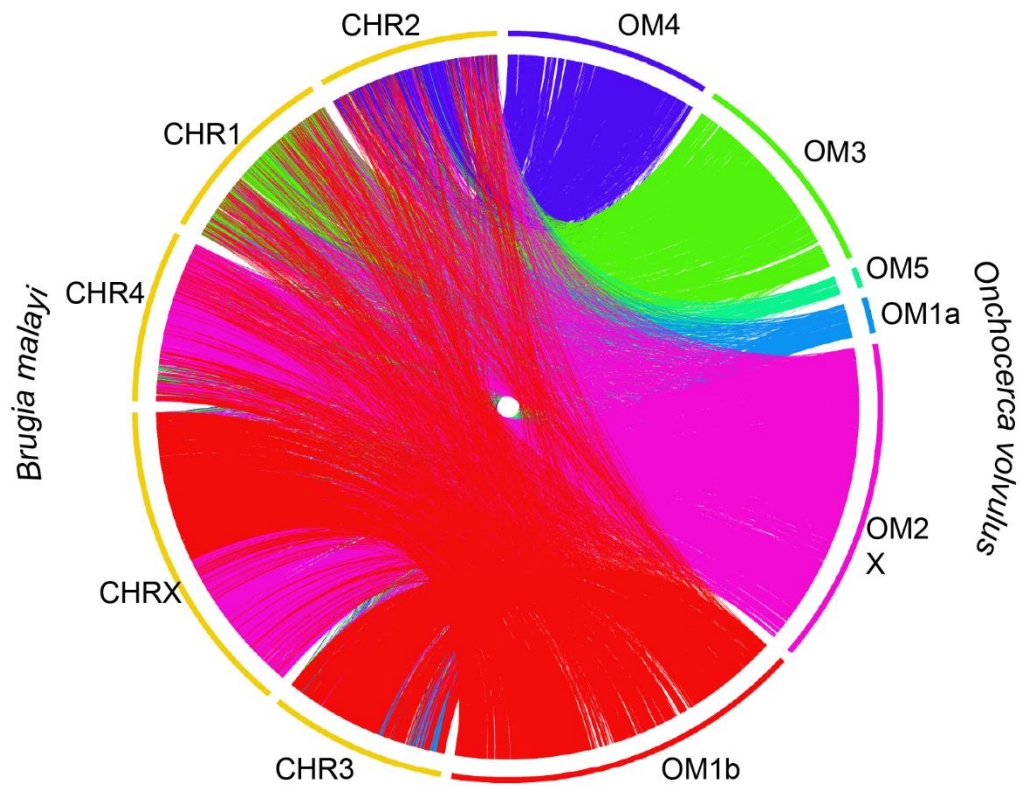


Figure 3.1: Comparative genomic analysis of *Brugia malayi* chromosomes against *Onchocerca volvulus* chromosomes in a Circos plot showing PROmer sequence similarity. Coloured lines and blocks represent the PROmer link hits with similarity to the *Onchocerca volvulus* chromosomes. *Onchocerca volvulus* X chromosome is OM2 X and *Brugia malayi* X chromosome is CHRX. *Onchocerca volvulus* OM1a/OM1b are two scaffolds derived from the largest autosome. The Y chromosomes for *Onchocerca volvulus* and *Brugia malayi* are not represented as they are poorly defined.

3.2a). The synteny analysis between *C. johnstoni* and *B. malayi* similarly reveals there are large segments of *C. johnstoni*'s fragmented assembly linking to the *B. malayi* chromosomes (Figure 3.2b). The links represent PROmer hits of similarity between the two genomes and are coloured according to *O. volvulus* chromosome location. The relationship between *C. johnstoni* and *O. volvulus* genomes likely represent groups of scaffolds belonging to the same chromosome in *C. johnstoni*; however, this requires further confirmation because it is likely that *C. johnstoni* will have an extra chromosome relative to *O. volvulus* and instead have the same number of chromosomes as *A. viteae* (karyotype 5A+X0). There is evidence that karyotype is an evolutionarily labile character (Post, 2005). The karyotype for *C. johnstoni* had not been assessed and cannot be predicted from consideration of other filaria thus will require further analyses to confirm how many chromosomes *C. johnstoni* will contain. The synteny analysis is a representation of the entire *O. volvulus* and *B. malayi* genomes corresponding to the complete predicted yet fragmented assembly of *C. johnstoni* scaffolds. There are conserved orthologous segments throughout the plot between *B. malayi* and *O. volvulus*. However, it was challenging to see within these plots how conserved the genome regions are compared to one another. Thus, it is not possible to infer microsynteny or macrosynteny from the current Circos plot. The Circos plot is unable to resolve relationships between a fragmented assembly and a chromosome assembly and therefore it is necessary to look at a section of the genome, i.e., largest assembled scaffold, using GenomeRibbon to explore microsyntenic relationships (Figure 3.3).

The longest scaffold (588,165 bp) of *C. johnstoni* is extracted from the PROmer analysis and input into GenomeRibbon to observe whether there are regions of the genome taking shape with an ordered genome content, to explore the synteny and orthology between *C. johnstoni* and *O. volvulus*. GenomeRibbon then allows observation of the genome similarity more closely rather than the Circos large scale comparative plot.

The longest complete scaffold of *C. johnstoni* aligns with the *O. volvulus* autosome OM3 but does not share complete homology and conservation with *O. volvulus* (Figure 3.3a). The figure illustrates multiple links of similarity between OM3 and the *C. johnstoni* scaffold but appears that the start of OM3 aligns with *C. johnstoni*'s second half of the scaffold. As this pattern shows the scaffold

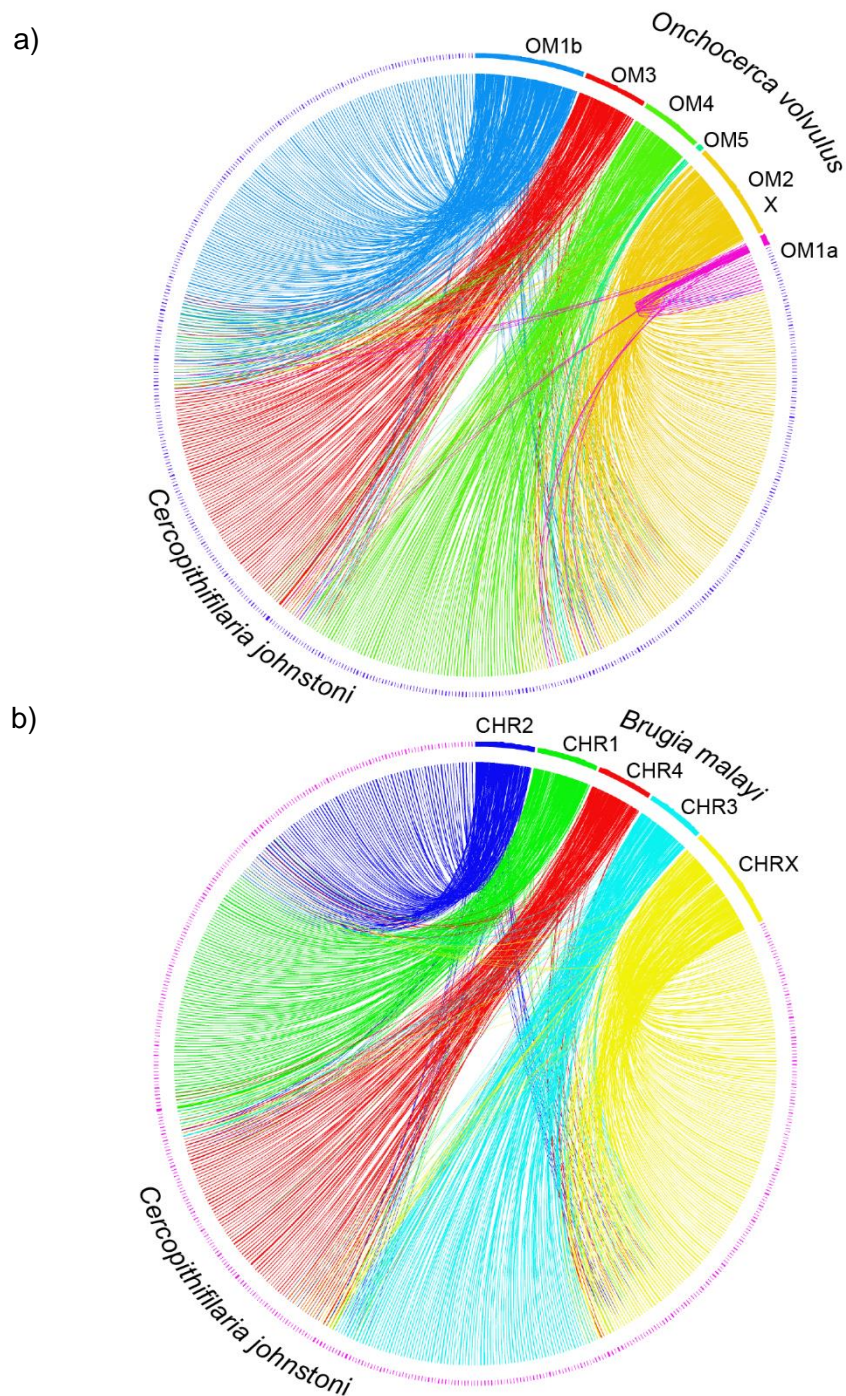


Figure 3.2: Comparative genomic analysis of *Cercopithifilaria johnstoni* scaffolds syntenicity against two filarial nematodes: a) *O. volvulus* chromosomes. Coloured lines represent the PROmer link hits with similarity to *Onchocerca volvulus* chromosomes. Cotton et al. (2016) identified OM2 as X chromosome. b) *Brugia malayi* chromosomes. Coloured lines represent the PROmer link hits with similarity to *Brugia malayi* chromosomes. The Y chromosomes are not represented as they are poorly defined.

mapping to two distinct locations it is likely a chromosomal translocation (Figure 3.3a). The complete length of the *C. johnstoni* longest scaffold links to the *O. volvulus* autosome OM3. However, the complete length of the *C. johnstoni* longest scaffold does not align to the *B. malayi* CHR1. Instead, there are gaps throughout the *C. johnstoni* sequence that are not present in the *B. malayi* CHR1 (Figure 3.3b). There are sections of the *C. johnstoni* scaffold that do not link to the *B. malayi* chromosome. The regions that do align are highly fragmented and not aligned in solid sections (Figure 3.3b). The sequence conservation between *C. johnstoni* and *B. malayi* can be best described by the hourglass shape, indicating that the sequence is inverted in *C. johnstoni*.

B. malayi, and *C. johnstoni* share 64.9% of the PROmer links above 70% sequence similarity, while *O. volvulus* and *C. johnstoni* share 61.4% of the PROmer links above 70% sequence similarity.

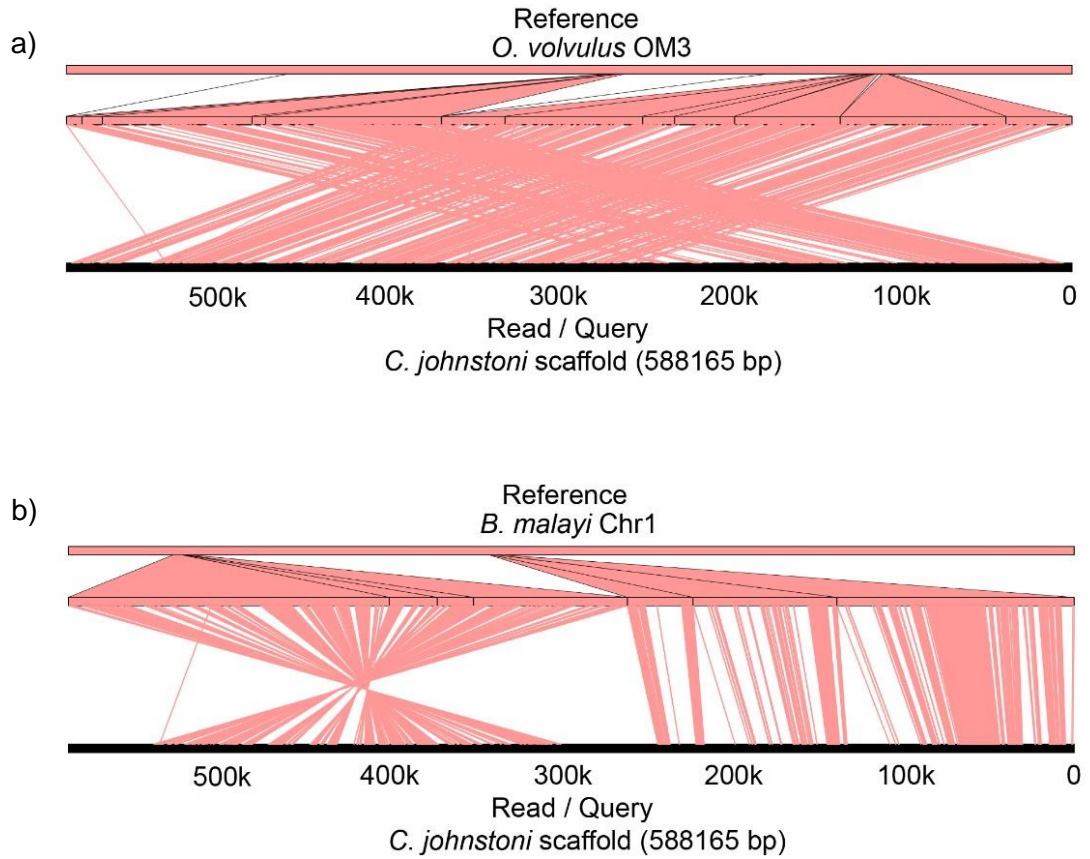


Figure 3.3: Genome ribbon representation of a) *Cercopithifilaria johnstoni* longest scaffold (NODE_1_length_588165) aligned to *Onchocerca volvulus* chromosome OM3 and b) *Cercopithifilaria johnstoni* longest scaffold (NODE_1_length_588165) aligned to *Brugia malayi* CHR1. The top line indicates the reference chromosome. The red indicates the region of *Cercopithifilaria johnstoni* scaffold that is aligned. Each line positions which part of the scaffold is aligning to which region of the chromosome. The bottom line indicates the *Cercopithifilaria johnstoni* scaffold query sequence.

3.3.5 *Cercopithifilaria johnstoni* sequences are possibly X-linked

The *C. johnstoni* X chromosome-linked sequences can be further identified based on GC and coverage differences and are consistent with *O. volvulus* X-linked chromosomes (Figure 3.4). A GC content and coverage scatterplot has been generated to illustrate the similarity in X-linked chromosomes between *C. johnstoni* and *O. volvulus* (Figure 3.4). The *C. johnstoni* scaffolds that match to *O. volvulus* scaffolds and chromosomes identified by PROmer are projected onto this figure representing *C. johnstoni* GC and coverage values based on similarity to the *C. johnstoni* sequence. The scatterplot is coloured based on *O. volvulus* chromosomes that share homology with the *C. johnstoni* scaffolds. There are two main groups of sequences represented in the scatterplot. There is one large group and one smaller group of sequences that differ in GC content and coverage following a linear relationship of low GC content with low read depth coverage to high GC content and high read depth coverage (Figure 3.4). When the *C. johnstoni* sequences are coloured by *O. volvulus* chromosome ID, the smaller group that differ in GC content and coverage are almost exclusively OM2 X, which suggests these *C. johnstoni* sequences might also be X-linked.

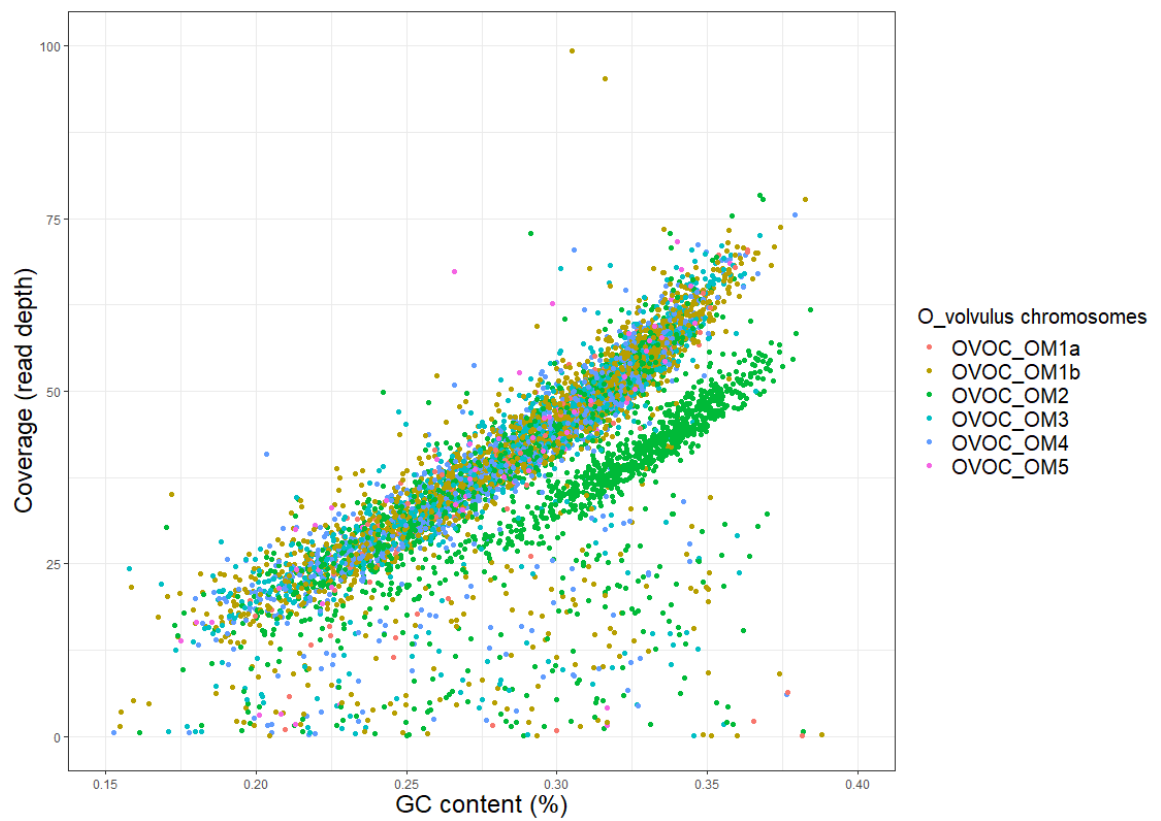


Figure 3.4: GC content vs coverage plot of the draft *Cercopithifilaria johnstoni* genome scaffolds with an *Onchocerca volvulus* chromosome projection overlaid onto the *Cercopithifilaria johnstoni* data based on nucleotide similarity. OM2 is the X chromosome for *Onchocerca volvulus*.

3.3.6 Genome annotation methods of the *Cercopithifilaria johnstoni* scaffolds

Three different gene prediction methods are compared to assess the most suitable gene prediction of the *C. johnstoni* scaffolds for this study, i) Augustus gene prediction, ii) *ab initio* BRAKER gene prediction and iii) BRAKER gene prediction using *A. viteae* for gene training.

Augustus predicts 10,458 genes from the *C. johnstoni* scaffolds sequence, BRAKER *ab initio* predicts 8,978 genes and BRAKER using *A. viteae* for gene training predicts 8,234 genes.

3.3.6.1 Different gene prediction methods change the BUSCO completeness results when using protein-coding genes

The three gene prediction datasets are assessed using BUSCO to determine the completeness of the predicted protein-coding genes (Table 3.5). Comparing the BUSCO datasets can highlight whether a gene prediction method has predicted more, or fewer genes based on the conserved orthologues. In this case, BUSCO uses the protein input parameter rather than the whole genome parameter because the datasets only include protein-coding genes. The database used for BUSCO was Nematode_obd9. The Augustus gene prediction method results in the highest number of complete BUSCOs with 893 (90.9%) out of a possible 982 BUSCO groups. The *ab initio* BRAKER gene prediction method follows with 878 (89.4%) complete BUSCO groups and the BRAKER gene prediction using *A. viteae* for gene training results in 753 (76.7%) BUSCO complete groups (Table 3.5). Thus, the Augustus gene prediction method trained using the default *C. elegans* dataset is the best gene prediction method according to these genome completeness results determined by the highest number of genes predicted.

Table 3.5: Comparison of the BUSCO completeness across the *Cercopithifilaria johnstoni* proteomes of three different gene prediction methods, a) Augustus gene prediction, b) BRAKER gene prediction *ab initio*, and c) BRAKER gene prediction using *Acanthocheilonema viteae* training model.

		Complete BUSCOs (C)	Complete and single-copy BUSCOs (S)	Complete and duplicated BUSCOs (D)	Fragmented BUSCOs (F)	Missing BUSCOs (M)
AUGUSTUS	TOTAL	893	885	8	65	24
	(%)	90.9	90.1	0.8	6.6	2.5
BRAKER AB INITIO	TOTAL	878	868	10	73	31
	(%)	89.4	88.4	1.0	7.4	3.2
BRAKER AV TRAINING	TOTAL	753	742	11	142	87
	(%)	76.7	75.6	1.1	14.5	8.8

3.3.6.2 Different gene prediction methods result in different OrthoFinder2 predictions

The gene prediction of *C. johnstoni* has been conducted using three individual methods resulting in a slightly different number of predicted genes. To be confident that the correct gene prediction method is used, OrthoFinder2 uses the three different protein files for comparison. These are (1) Augustus gene prediction protein list, (2) BRAKER *ab initio* gene prediction list and (3) BRAKER using *A. viteae* for gene training (Table 3.6). The OrthoFinder2 analyses predict 7,052 one-to-one orthologues between *C. johnstoni* and *O. volvulus*, using the protein list predicted from solely the Augustus analysis (Table 3.6a). OrthoFinder2 predicts 6,137 one-to-one orthologues between *C. johnstoni* and *O. volvulus*, using the protein list predicted from the *ab initio* BRAKER analysis (Figure 3.6b). Lastly, OrthoFinder2 predicts 5,803 one-to-one orthologues between *C. johnstoni* and *O. volvulus*, using the BRAKER analysis using a closely related nematode, *A. viteae*, for gene training (Figure 3.6c).

When comparing the overall OrthoFinder2 statistics, the Augustus gene prediction uses 155,539 genes, 140,340 genes within orthogroups, 42 species-specific orthogroups and 1,447 single copy orthogroups (Table 3.7a). The *ab initio* BRAKER gene prediction uses 154,059 genes in the OrthoFinder2 analysis with 139,065 genes within orthogroups, 38 species-specific orthogroups and 1,319 single copy orthogroups (Table 3.7b). The final gene prediction method using *A. viteae* for gene training in BRAKER uses 153,317 genes, 138,765 within orthogroups, 42 species-specific orthogroups and 1,233 single-copy orthogroups (Table 3.7c). The Augustus gene prediction method results in the highest number of genes than the *ab initio* method and lastly, the *A. viteae* gene training method results in the lowest number of genes.

The Augustus gene prediction method has performed the best in both the BUSCO analyses and the OrthoFinder analyses. Augustus predicted the highest number of complete genes according to BUSCO (Table 3.5) and predicted the highest number of one-to-one orthologues according to OrthoFinder (Table 3.6), thus the Augustus protein-coding list is chosen for downstream analyses. The purpose of comparing the different gene prediction methods was to identify the most suitable protein list for orthologue discovery of proteins that consistently elicit strong serum antibody responses in people infected with *O. volvulus*.

Furthermore, the Augustus gene prediction method resulted in the best protein list for identifying orthologues between *C. johnstoni* and *O. volvulus*.

The Augustus annotation of the *C. johnstoni* protein-coding genes has 10,458 predicted protein-coding genes, which is less than the other closely related nematodes, although may increase once the genome is further improved. It does appear that *C. johnstoni* has a smaller genome than many filarial nematodes but again, requires improvement of the genome to confirm this conclusion. The *O. volvulus* genome has 12,225 genes, and *B. malayi* has 14,013 genes. The *A. viteae* and *L. sigmodontis* genomes are generally smaller than the other nematodes and *C. johnstoni* with 10,397 and 10,246 genes respectively.

The average length of the Augustus predicted *C. johnstoni* protein-coding genes is 434.42 bp compared to the average length of 412.676 bp for the *O. volvulus* protein-coding genes (Table 3.8). The average length for *A. viteae* proteins is 441.207 while the average length of *L. sigmodontis* proteins is 440.036 bp (Table 3.8). The average length of the predicted *C. johnstoni* proteins are consistent with previously predicted filarial nematode proteins. The two filarial nematode genomes with the shortest average protein length are *B. timori* and *O. flexuosa* with 232.425 bp and 243.903 bp respectively (Table 3.8).

Table 3.6: Comparison of the OrthoFinder2 one-to-one orthologues using the *Cercopithifilaria johnstoni* proteomes of three different gene prediction methods, a) Augustus gene prediction, b) BRAKER gene prediction *ab initio* and c) BRAKER using *Acanthocheilonema viteae* for gene training.

Av (*Acanthocheilonema viteae*), *Bm* (*Brugia malayi*), *Bp* (*Brugia pahangi*), *Bt* (*Brugia timori*), *Cj* (*Cercopithifilaria johnstoni*), *Di* (*Dirofilaria immitis*), *LI* (*Loa loa*), *Ls* (*Litomosoides sigmodontis*), *Of* (*Onchocerca flexuosa*), *Oo*, (*Onchocerca ochengi*), *Ov* (*Onchocerca volvulus*), *Wb* (*Wuchereria bancrofti*).

a)

	<i>Av</i>	<i>Bm</i>	<i>Bp</i>	<i>Bt</i>	<i>Cj</i>	<i>Di</i>	<i>LI</i>	<i>Ls</i>	<i>Of</i>	<i>Oo</i>	<i>Ov</i>	<i>Wb</i>
<i>Av</i>	0	5557	6798	6130	7052	6830	6980	6752	6092	6889	6859	6767
<i>Bm</i>	5557	0	6763	6087	5714	5878	5764	5843	5068	5790	6163	6155
<i>Bp</i>	6798	6763	0	7732	6843	7020	6804	6889	6637	7324	7154	8048
<i>Bt</i>	6130	6087	7732	0	6011	6312	6207	5815	7100	6821	6295	8036
<i>Cj</i>	7052	5714	6843	6011	0	6848	7144	7063	5886	6944	7052	6726
<i>Di</i>	6830	5878	7020	6312	6848	0	6942	7030	6537	7377	7423	6952
<i>Ls</i>	6980	5764	6804	6207	7144	6942	0	6963	6072	6969	7021	6736
<i>LI</i>	6752	5843	6889	5815	7063	7030	6963	0	5622	6896	7336	6660
<i>Of</i>	6092	5068	6637	7100	5886	6537	6072	5622	0	7823	6848	6886
<i>Oo</i>	6889	5790	7324	6821	6944	7377	6969	6896	7823	0	8660	7297
<i>Ov</i>	6859	6163	7154	6295	7052	7423	7021	7336	6848	8660	0	6900
<i>Wb</i>	6767	6155	8048	8036	6726	6952	6736	6660	6886	7297	6900	0

b)

	<i>Av</i>	<i>Bm</i>	<i>Bp</i>	<i>Bt</i>	<i>Cj</i>	<i>Di</i>	<i>LI</i>	<i>Ls</i>	<i>Of</i>	<i>Oo</i>	<i>Ov</i>	<i>Wb</i>
<i>Av</i>	0	5463	6641	6092	6318	6812	6995	6737	6204	6955	6816	6710
<i>Bm</i>	5463	0	6772	6147	4926	5768	5687	5883	4945	5662	5972	6185
<i>Bp</i>	6641	6772	0	7779	5803	6873	6672	6928	6529	7185	6975	8145
<i>Bt</i>	6092	6147	7779	0	5202	6255	6141	6113	7066	6765	6183	8126
<i>Cj</i>	6318	4926	5803	5202	0	6030	6272	6122	5245	6026	6137	5760
<i>Di</i>	6812	5768	6873	6255	6030	0	6955	7008	6660	7506	7471	6843
<i>Ls</i>	6995	5687	6672	6141	6272	6955	0	6907	6147	6931	6952	6600
<i>LI</i>	6737	5883	6928	6113	6122	7008	6907	0	5948	6966	7116	6806
<i>Of</i>	6204	4945	6529	7066	5245	6660	6147	5948	0	7886	6921	6775
<i>Oo</i>	6955	5662	7185	6765	6026	7506	6931	6966	7886	0	8709	7237
<i>Ov</i>	6816	5972	6975	6183	6137	7471	6952	7116	6921	8709	0	6768
<i>Wb</i>	6710	6185	8145	8126	5760	6843	6600	6806	6775	7237	6768	0

c)

	<i>Av</i>	<i>Bm</i>	<i>Bp</i>	<i>Bt</i>	<i>Cj</i>	<i>Di</i>	<i>LI</i>	<i>Ls</i>	<i>Of</i>	<i>Oo</i>	<i>Ov</i>	<i>Wb</i>
<i>Av</i>	0	5550	6866	6262	6134	6770	6762	6976	6096	6796	6687	6870
<i>Bm</i>	5550	0	6802	6198	4613	5907	5886	5728	5107	5790	6016	6214
<i>Bp</i>	6866	6802	0	7820	5692	7016	7032	6850	6760	7320	6981	8195
<i>Bt</i>	6262	6198	7820	0	5296	6205	6255	6337	7138	6673	6027	8179
<i>Cj</i>	6134	4613	5692	5296	0	5825	6038	6114	5353	5914	5803	5720
<i>Di</i>	6770	5907	7016	6205	5825	0	7024	6915	6471	7379	7429	6941
<i>Ls</i>	6762	5886	7032	6255	6038	7024	0	6910	5948	6915	6982	6922
<i>LI</i>	6976	5728	6850	6337	6114	6915	6910	0	6038	6875	6893	6799
<i>Of</i>	6096	5107	6760	7138	5353	6471	5948	6038	0	7789	6758	6958
<i>Oo</i>	6796	5790	7320	6673	5914	7379	6915	6875	7789	0	8653	7296
<i>Ov</i>	6687	6016	6981	6027	5803	7429	6982	6893	6758	8653	0	6740
<i>Wb</i>	6870	6214	8195	8179	5720	6941	6922	6799	6958	7296	6740	0

Table 3.7: The proteomes of all 12 filarial nematodes (listed in the previous table, Table 3.6) have been included in the OrthoFinder2 analyses to compare the three different gene prediction methods using to predict *Cercopithifilaria johnstoni* protein-coding genes, a) Augustus gene prediction, b) *ab initio* BRAKER gene prediction and c) BRAKER *Acanthocheilonema viteae* training.

	a) AUGUSTUS	b) <i>ab initio</i> BRAKER	c) BRAKER AV TRAINING
Number of genes	155,539	154,059	153,317
Number of genes in orthogroups	140,340	139,065	138,765
Number of unassigned genes	15,199	14,994	14,552
Percentage of genes in orthogroups	90.2	90.3	90.5
Percentage of unassigned genes	9.8	9.7	9.5
Number of orthogroups	13,043	12,931	12,887
Number of species-specific orthogroups	42	38	42
Number of genes in species-specific orthogroups	284	214	219
Percentage of genes in species-specific orthogroups	0.2	0.1	0.1
Mean orthogroup size	10.8	10.8	10.8
Median orthogroup size	12	12	12
G50 (assigned genes)	13	13	13
G50 (all genes)	13	13	13
O50 (assigned genes)	3,747	3,690	3,697
O50 (all genes)	4,332	4,267	4,257
Number of orthogroups with all species present	5,372	5,045	4,996
Number of single-copy orthogroups	1,447	1,319	1,233

Table 3.8: The average length of the *C. johnstoni* Augustus predicted protein-coding genes compared with the average protein length of the 12 filarial nematode proteomes.

Nematodes	Average protein length (bp)
<i>C. johnstoni</i>	434.42
<i>A. viteae</i>	441.207
<i>B. malayi</i>	478.708
<i>B. pahangi</i>	343.235
<i>B. timori</i>	243.903
<i>D. immitis</i>	378.059
<i>L. loa</i>	409.402
<i>L. sigmodontis</i>	440.036
<i>O. flexuosa</i>	232.425
<i>O. ochengi</i>	359.469
<i>O. volvulus</i>	412.676
<i>W. bancrofti</i>	331.107

3.3.7 OrthoFinder2 predicts orthologous relationships with closely related nematodes

The OrthoFinder2 analysis depicts a total of 153,317 genes across the 12 species in the analysis (Table 3.7c). Out of these 153,317, only 14,552 are unassigned to any of the 12,887 orthogroups (Table 3.7c). The number of orthogroups with all 12 nematodes present consist of 4,996 (Table 3.7c) and 1,233 orthogroups contain only single-copy genes (Table 3.7c).

A total of 6,465 *C. johnstoni* orthologues are identified between *O. volvulus* and *C. johnstoni* that includes one-to-one, one-to-many, many-to-one and many-to-many orthologous relationships. Table 3.6c highlights the number of nematode genes that share one-to-one orthologues between each species. Across the entire genome, *C. johnstoni* shares 5,803 one-to-one orthologues with *O. volvulus* (Table 3.6c). The highest number of one-to-one orthologues with *C. johnstoni* is with *A. viteae* with a total of 6,134 orthologues (Table 3.6c), closely followed by *L. sigmodontis* with 6,114 orthologues. The least number of orthologues is 4,613 between *C. johnstoni* and *B. malayi* (Table 3.6c).

3.3.8 Consistent filarial phylogenetic relationships

The 1,447 single-copy protein-coding genes (Figure 3.5) are consistent with the filarial nematode mitochondrial genome (Chapter Two) but provides greater resolution than the mitochondrial trees. The phylogeny illustrates *C. johnstoni* is in a clade with *A. viteae* and *L. sigmodontis* (Figure 3.5). The *Onchocerca* clade, consistent with published literature (Blaxter and Koutsovoulos, 2015; Cotton et al., 2016; Coghlan et al., 2019), is monophyletic with *D. immitis* (Figure 3.5). The three *Brugia* species, *W. bancrofti*, and *L. loa* form the third clade, again consistent with previous results (Chapters Two, Three). The single-copy orthologue phylogeny has strong bootstrap support, supporting the filarial nematode relationships (Figure 3.5).

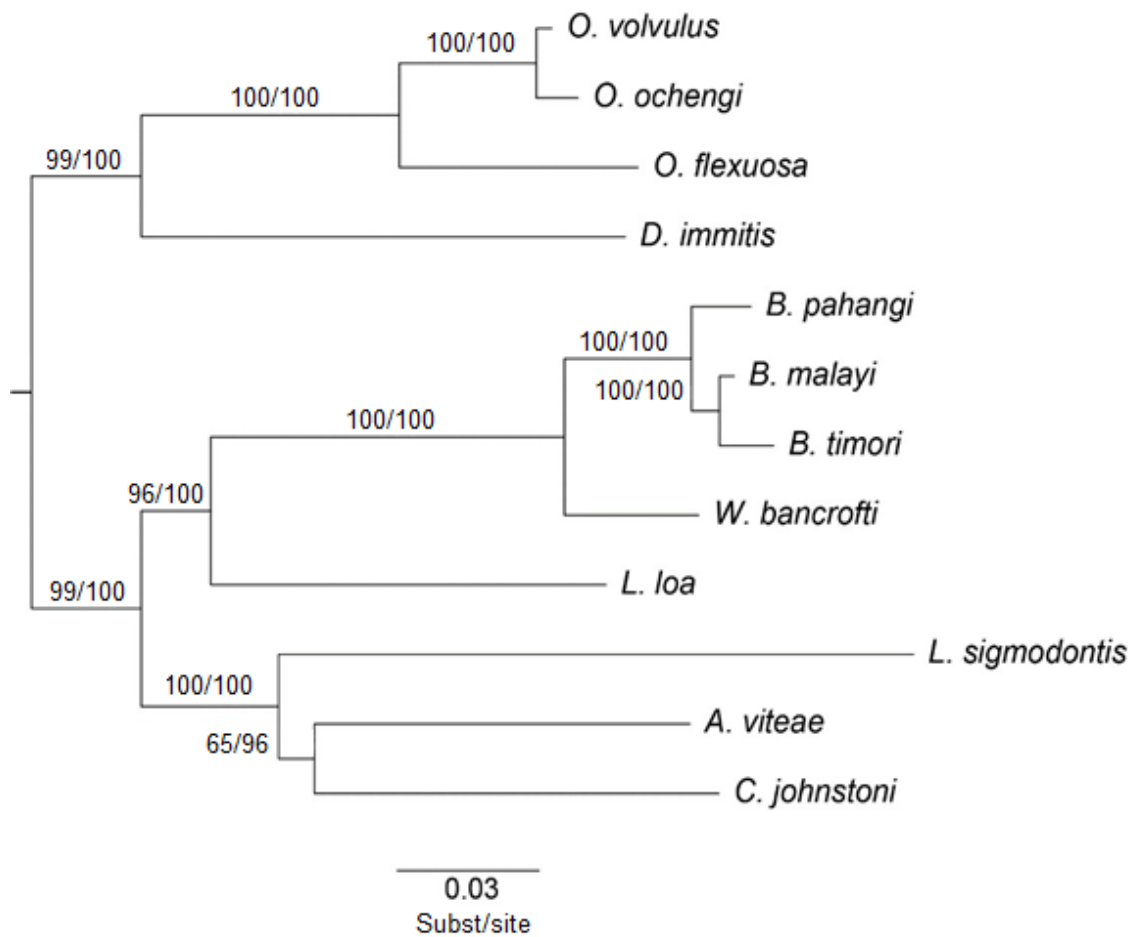


Figure 3.5: Single-copy orthologue maximum likelihood phylogeny with Bayesian and bootstrap support for all the nematodes that were analysed in the OrthoFinder2 analysis. Scale 0.3 substitutions per site.

3.3.9 Orthogroup and single-copy orthologue relationships

One thousand four hundred forty-seven orthogroups contain single-copy genes for all 12 filarial nematodes in the analysis (Figure 3.6). Three hundred forty-one orthogroups are containing single-copy orthologues for only *O. volvulus* and *O. ochengi* but not for any of the remaining filarial nematodes (Figure 3.6). There are 14 orthogroups shared between *C. johnstoni* and *L. loa* with single-copy orthologues excluding other nematodes, and 28 orthogroups shared between *C. johnstoni* and *O. flexuosa* (Figure 3.6).

The UpSet plot represents 70 possible relationships of the hundreds of other possible relationships. The figure would become uninterpretable if all relationships were illustrated and thus only the highest frequency (intersection size) relationships are illustrated. The plot illustrates from 11 shared orthogroups to 1,447 shared orthogroups. There are relatively few one-to-one orthogroups that are present in all species except *C. johnstoni*. There is no relationship illustrated in the plot between *C. johnstoni* and *O. volvulus* because they share only two orthogroups with single-copy orthologues excluding all the other nematodes. Four orthogroups contain only single-copy genes between *A. viteae* and *C. johnstoni*. Two orthogroups are shared between *C. johnstoni* and *L. sigmodontis* and also between *C. johnstoni* and *D. immitis*. Finally, only one orthogroup containing single-copy genes is shared between *C. johnstoni* and *O. ochengi* and between *C. johnstoni* and *W. bancrofti*.

The second UpSet plot illustrates 5,372 orthogroups where all the filarial nematodes contain at least one gene assigned to that orthogroup (Figure 3.7). Similar to the single-copy UpSet plot, the majority of orthogroups are present across all 12 nematodes with only 148 orthogroups where all the filarial nematodes excluding *C. johnstoni* contain at least one gene assigned to that orthogroup (Figure 3.7). There are 352 orthogroups with at least one gene in the orthogroup shared only between *O. volvulus* and *O. ochengi* (Figure 3.7). Similar to the single-copy UpSet plot, not all the relationships can be illustrated. Only an intersection size of 20 and above are illustrated in the UpSet plot. There are consistently two orthogroups shared between *C. johnstoni* and *O. volvulus* that contain at least one gene that excludes all other filarial nematodes. Five orthogroups are containing at least one genes shared between only *A. viteae* and *C. johnstoni*.

An important relationship to illustrate is between *C. johnstoni* and *O. volvulus*. A total of 7,557 orthogroups are shared between *C. johnstoni* and *O. volvulus* containing all one-to-one, one-to-many, many-to-one and many-to-many orthologous relationships (Figure 3.8). The final UpSet plot illustrates a total of 1,778 orthogroups that *O. volvulus* does not share with *C. johnstoni*. There are 682 orthogroups that *C. johnstoni* does not share with *O. volvulus*. Thus the majority of the orthogroups in *O. volvulus* and *C. johnstoni* sets are shared between one another (Figure 3.8).

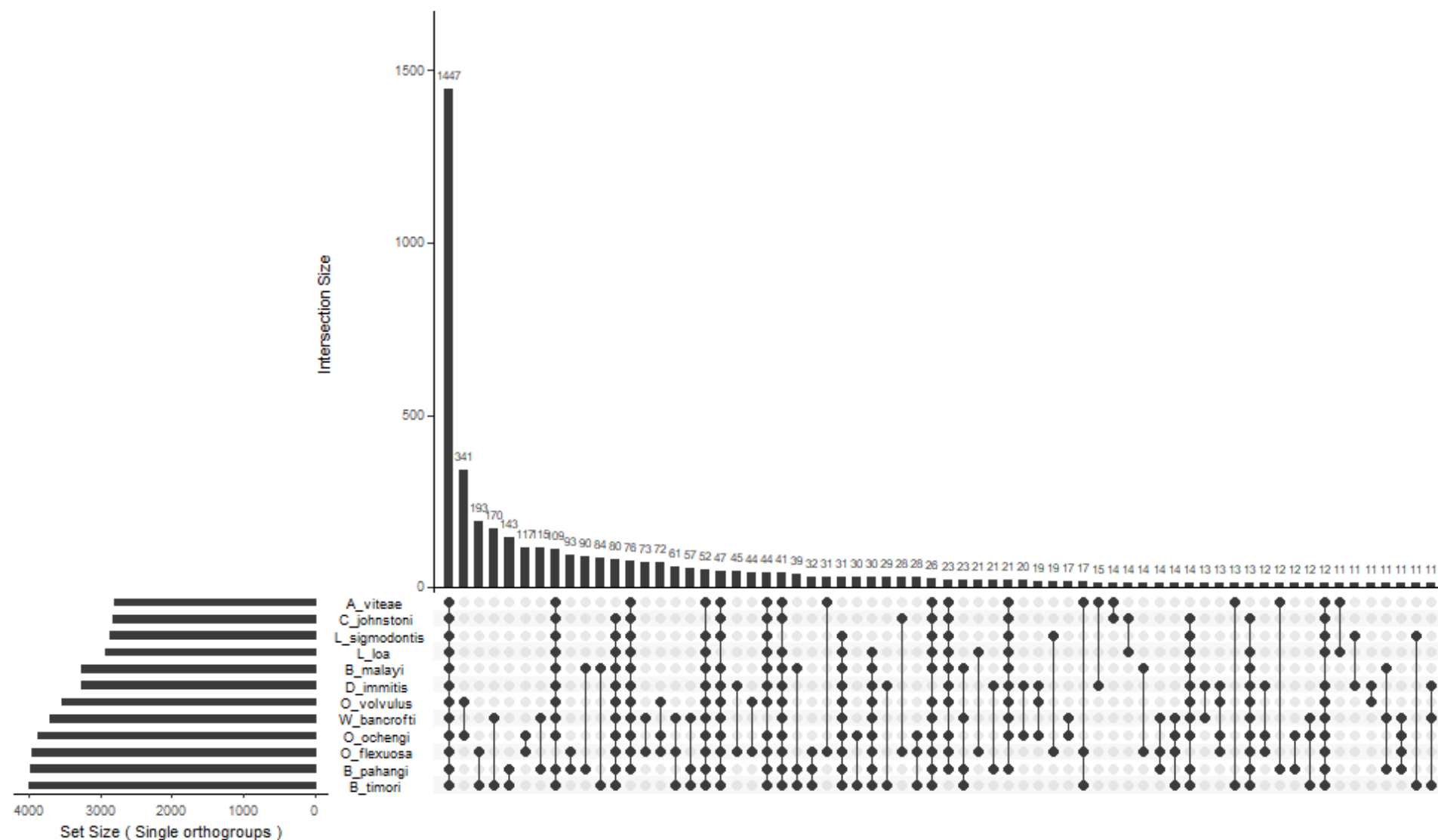


Figure 3.6: UpSet plot representing the single-copy orthologue orthogroup relationships across the 12 filarial nematodes. Bars represent the total number of orthogroups for that relationship, thus intersection size. Black dots represent the species that has a single-copy gene in those orthogroups. The lines joining the dots represent the relationships of those orthogroups. The set size bar represents the number of orthogroups is represented in the figure for each species. Only intersections over 11 are depicted.

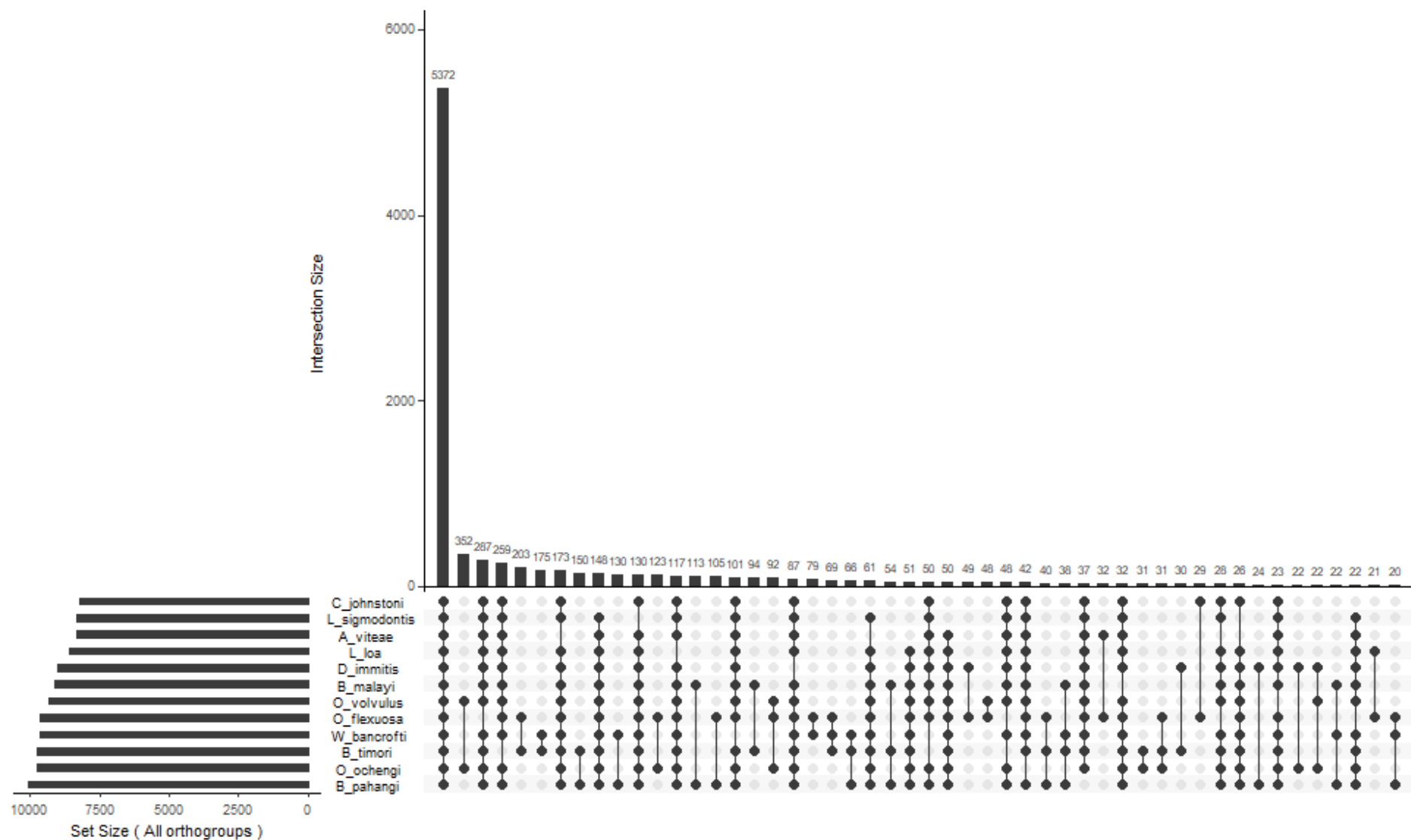


Figure 3.7: UpSet plot representing all the orthogroup relationships with one or more genes in each group across the 12 filarial nematodes. Bars represent the total number of orthogroups for that relationship, thus intersection size. Black dots represent the species that have at least one gene in those orthogroups. The lines joining the dots represent the relationships of those orthogroups. The set size bar represents the number of orthogroups is represented in the figure for each species. Only intersections over 20 are depicted.

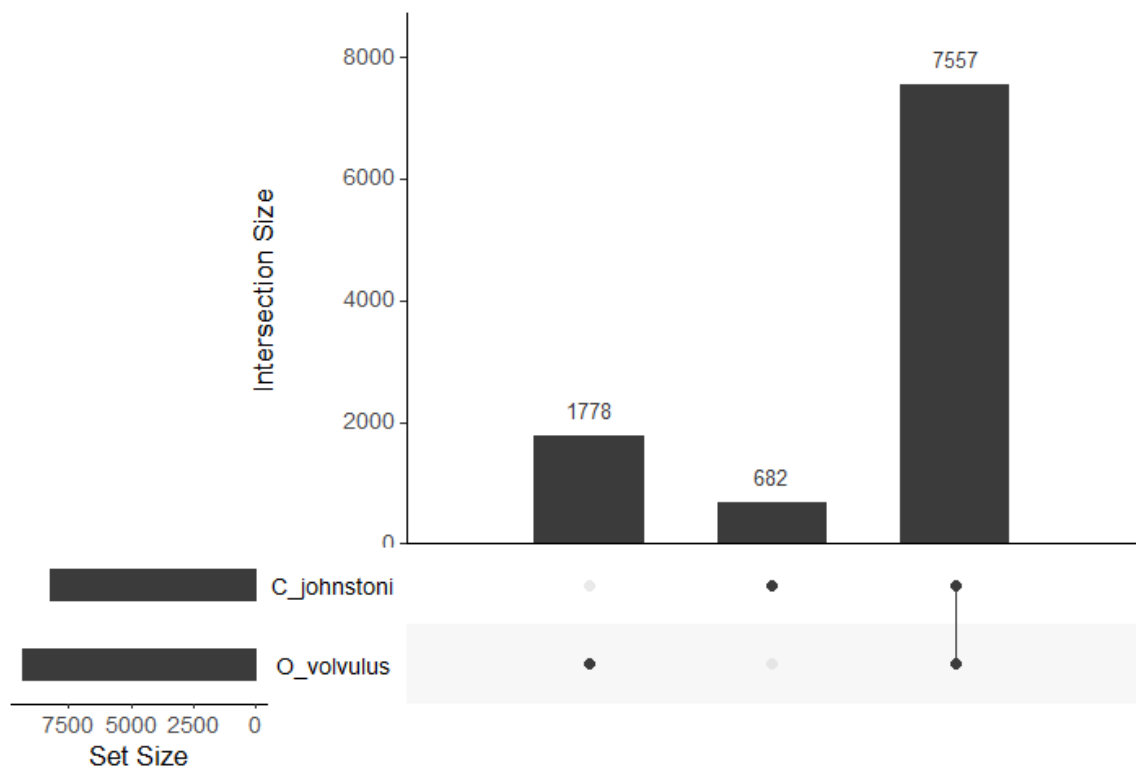


Figure 3.8: UpSet plot representing the complete single-copy and multi-gene orthogroup relationships across *Cercopithifilaria johnstoni* and *Onchocerca volvulus*. Bars represent the total number of orthogroups for that relationship, thus intersection size. Black dots represent the species that share orthogroups. The lines joining the dots represent the relationships of those orthogroups. The set size bar represents the number of orthogroups is represented in the figure for each species.

3.4 Discussion

3.4.1 Genome assembly and completeness of *Cercopithifilaria johnstoni* scaffolds

The *C. johnstoni* genome has been assembled into scaffolds using short-read sequencing data from one adult female worm and compared with published filarial nematodes. The assembly of the *C. johnstoni* genome has a total length of 79,062,707 bp, which is the eighth largest genome assembly length compared with the other 11 nematodes analysed (Table 3.1). The largest assembly lengths are from *O. volvulus*, *L. loa* and *O. ochengi*. The GC content of the *C. johnstoni* genome is very consistent with the closely related filarial nematode genomes previously assembled (Table 3.1). Among the 12 genomes compared in this chapter, *C. johnstoni* was ranked the fourth highest genome assembly based on the N50 statistics (Table 3.1). The lowest three N50 scores are assigned to *W. bancrofti*, *B. timori* and *O. flexuosa*. They also have the shortest sequence length in the assembly. The best three genomes out of the 12 genomes analysed are *L. loa*, *B. malayi* and *O. volvulus* in ascending order. *B. malayi* and *O. volvulus* are assembled in chromosomes. These genomes have been extensively and manually curated with multiple sequence technologies and an abundance of parasite material. Thus, they have large, joined sequences, i.e., N50 above 150,000 bp or in the context of *O. volvulus* an N50 above 25,000,000 bp, of excellent quality. None of the other filarial nematodes have been assembled to such high quality; hence the *C. johnstoni* genome assembly is of good quality being the fourth highest filarial genome available (Table 3.1). N50 is not the only determinant to assess genome quality. The *C. johnstoni* genome performed well compared to other nematodes in the N90 statistics. The *C. johnstoni* genome was again the fourth highest filarial genome. The BUSCO and CEGMA analyses also revealed that the *C. johnstoni* genome performed well compared the other filarial nematodes. BUSCO and CEGMA analyses are excellent criteria to assess the quality of the genome. The purpose of assembling the *C. johnstoni* genome was to determine the suitability of the assembly for the purpose of gene prediction and search for orthologues of the proteins that consistently elicit strong serum antibody responses in people infected with *O. volvulus* (Chapter Four). Thus identifying using BUSCO whether all the genes are present in the genome is one of the most important criteria to assess the quality of the *C. johnstoni* genome. The genome completeness analyses confirm that the assembly of the

C. johnstoni scaffolds contains over 90% of the expected genome based on conserved orthologues (Tables 3.2, 3.3). Consistently, the *C. johnstoni* scaffolds are the fourth most complete genome assemblies among the 12 other filarial nematodes including *A. viteae*, *O. volvulus*, *B. malayi*, *B. pahangi*, *B. timori*, *D. immitis*, *L. sigmodontis*, *L. loa*, *O. ochengi*, *O. flexuosa* and *W. bancrofti* consistent with the N50 score. The top three BUSCO results are *B. malayi*, *L. loa* and *O. volvulus*, in ascending order. The *C. johnstoni* assembly has a higher proportion of identified conserved genes using either CEGMA or BUSCO than the WormBase Parasite published versions of *A. viteae*, *B. pahangi*, *B. timori*, *O. flexuosa*, *O. ochengi*, and *W. bancrofti*. The success rate of *C. johnstoni* genome completeness prediction is noteworthy because the *C. johnstoni* scaffolds are assembled using only short-read Illumina MiSeq sequences.

A strongly positive feature of this project is that the *C. johnstoni* genome has been assembled from a single female worm. As the primary aim was to characterise the *C. johnstoni* genome, using one adult worm makes genome assembly easier compared to genome assemblies of pooled data. Having genomic data from one worm makes it possible to differentiate variants of a single gene and assembly variant reads into a single contig instead of reads that are divergent because they are derived from paralogous members of a gene family thus assembled into separate contigs.

3.4.2 Comparing genome similarity of filarial nematodes

A Circos plot represents the syntenic regions i.e., conservation of gene order between *O. volvulus* and *B. malayi*. The comparison between *O. volvulus* and *B. malayi* illustrates the chromosomal conservation that is observed between these filarial species setting the context before comparing a highly fragmented *C. johnstoni* genome assembly with these species (Figure 3.1). The synteny conservation between *C. johnstoni* and two other filarial nematodes with chromosome-level assemblies, *O. volvulus* and *B. malayi*, are represented by another two Circos plots (Figure 3.2). The plots show solid conservation of chromosome gene content and order between *B. malayi*, and *O. volvulus* (Figure 3.1). Both filarial nematodes have X and Y chromosomes different from other filarial nematodes that do not have a Y chromosome (Post, 2005). However, the

Y chromosomes are not illustrated in the Circos plots because they are poorly defined.

In both comparative figures, the *O. volvulus* and *B. malayi* chromosomes are well represented by scaffolds in the fragmented *C. johnstoni* assembly (Figure 3.2). The segment conservation could indicate that these scaffold regions of the *C. johnstoni* genome are part of a single chromosome, although long-read sequencing data would be required to join the current *C. johnstoni* scaffolds into chromosomes accurately. The Circos plots reveal many lines indicating microsynteny between *C. johnstoni* and the filarial nematodes, even though there are not solid blocks of colour within these plots (Figure 3.2). Thus, there is an abundance of microsynteny observed with no evidence of macrosynteny. The Circos plot is also unable to illustrate what kind of microsynteny is present because the *C. johnstoni* scaffolds are highly fragmented and compared against complete chromosomes. Macrosynteny in this analysis refers to conservation of gene order over a minimum sequence length of 30,000 bp with a sequence identity above 80%. As a result, it was concluded that the Circos plots are not able to infer microsyntenic or macrosyntenic relationships between a fragmented *C. johnstoni* genome and chromosome assembled filarial genomes. Furthermore, GenomeRibbon using the longest *C. johnstoni* scaffold was explored to reveal the microsyntenic relationships present (Figure 3.3). The N50 of *C. johnstoni*, although being the fourth-highest N50 compared to all the filarial nematodes, is still much lower than the N50 for *O. volvulus* and *B. malayi* (Table 3.1) which could limit the usefulness of these Circos plots. The figure also indicates there is a requirement for long-read data to align the scaffolds for the genome assembly more accurately (Figure 3.3). There is synteny between the *C. johnstoni* genome and other filarial nematodes, however the *C. johnstoni* genome is very fragmented, either as a result of the genome short-read assembly or species divergence. It is important to discuss that the microsyntenic relationships observed in Figure 3.2a and Figure 3.2b illustrate regions of sequence conservation. Synteny in this context describes sequences with a minimum hit length of 1,000 bp within the *C. johnstoni* scaffolds that align with regions of the *O. volvulus* and *B. malayi* chromosomes. It is so not possible to observe macrosyntenic relationships with the current *C. johnstoni* genome assembly.

The similarity using the longest *C. johnstoni* scaffold reveals that the *C. johnstoni* genome shares genomic similarity with a chromosome from both *B. malayi* and *O. volvulus* but does not share perfect homology, i.e., large similarity blocks (macrosynteny) representing genomic similarity (Figure 3.3). Therefore, there are sections of the *C. johnstoni* scaffold that differ in genomic content compared with *O. volvulus* and *B. malayi*. It is expected that *C. johnstoni* is more divergent than *O. volvulus* and *B. malayi* as phylogenetically *C. johnstoni* is more distantly related to these two species (Figure 3.5).

The Circos plot was unable to illustrate clear macrosyntenic or microsyntenic relationships because the *C. johnstoni* genome is highly fragmented. Each line represented a minimum sequence identity of 80% and a minimum hit length of 1,000. Future analyses to improve the current Circos plot between *C. johnstoni* and *O. volvulus* could explore various parameters such as increasing the minimum hit length to 10,000. The Circos plot would then only be able to display similarity hits of 10,000 or more which could improve the visualisation of gene structure within the plot. The Circos plot will still not be the most appropriate figure to display macrosyntenic relationships even if the stringency is increased because the *C. johnstoni* genome is highly fragmented. An alternative approach to infer synteny would be to identify the location of all the *C. johnstoni* single copy genes and use these for an accurate representation. Single-copy genes are advantageous because there is no addition of paralogous relationships to weaken synteny. A future direction would be to explore these single-copy sites to take a deeper look into inferring synteny between *C. johnstoni* and related nematodes.

Synteny and sequence similarity is not the only two methods that can be explored to determine genome similarity with *O. volvulus*. A GC-coverage analysis can visualise whether there is any similarity between filarial chromosomes based on the GC content of the genome. From the *C. johnstoni* data available, the genome cannot be assembled into chromosomes, but it may be possible to observe which *C. johnstoni* scaffolds may be linked in a chromosome assembly based on their GC and coverage relationships. The GC content and coverage plot illustrate a linear relationship between *C. johnstoni* GC content and *C. johnstoni* scaffold read coverage. The *C. johnstoni* data in the GC/coverage plot has been coloured by similarity to the *O. volvulus*

chromosomes. The bottom group predominately shares similarity with the *O. volvulus* chromosome OM2, which is the X chromosome (Figure 3.4). Thus the *C. johnstoni* scaffolds and contigs within this bottom group of sequences are likely sex-linked as it appears the sex chromosome has a distinct GC content compared to the other chromosomes and sequences (Figure 3.4). These *C. johnstoni* scaffolds that have grouped are likely to be part of the same X chromosome. The GC content and coverage plot have clearly illustrated that it is possible to discriminate the X chromosome based on *C. johnstoni* GC content and sequence homology with *O. volvulus*, which is a remarkable result. With the inclusion of more data, it would be possible to assemble the *C. johnstoni* genome into chromosomes and determine whether these scaffolds overlapping with OM2 are assembled into a sex chromosome for *C. johnstoni*.

Filarial nematodes have either XO or XY sex determination. Filarial nematodes *A. viteae*, *L. sigmodontis*, and *L. loa*, similar to *C. elegans*, have a chromosome complement of 5A+XO, (Post, 2005; McLaren, 2009) while *D. immitis* is 4A+XO (Taylor, 1960). Both the *O. volvulus* and *O. gibsoni* have XY sex determination, with chromosome complement of 3A+XY (Post, 2005; Choi et al., 2016; Cotton et al., 2016; Foster et al., 2020), while *O. ochengi*, *B. pahangi*, *B. malayi*, and *W. bancrofti* are 4A+XY. It is difficult to predict what sex determination system or chromosome complement *C. johnstoni* would likely have compared to the other closely related nematodes with the current data available. As *C. johnstoni* is so closely related phylogenetically to *A. viteae* and *L. sigmodontis*, it could be assumed that *C. johnstoni* would follow an XO system. Although, *C. johnstoni* does exhibit significant conservation with both the *B. malayi* and *O. volvulus* X chromosome in the synteny analysis (Figures 3.2, 3.3, 3.4). However, from the current dataset, it is impossible to tell whether *C. johnstoni* has a Y chromosome, similar to *O. volvulus* and *B. malayi*, or whether the Y chromosome is absent. Karyotypes are evolutionarily labile in filarial nematodes; for example, while *O. volvulus* is phylogenetically more closely related to *O. ochengi*, it shares the same karyotype as *O. gibsoni* because of two independent fusion events (Post, 2005). Karyotyping would be helpful to resolve the chromosome complement and sex determination of *C. johnstoni* identifying whether *C. johnstoni* follows the XO system as a result of phylogenetic relationships with *A. viteae* or whether *C. johnstoni* also has a Y chromosome and therefore follows the XY system. As the *A. viteae* genome is not assembled

into chromosomes, further assembly is required to compare the chromosomal structure between *C. johnstoni* and *A. viteae*.

The introduction of long-read sequencing technology such as PacBio could be used in combination with the Illumina sequencing data to increase confidence in chromosome-level assembly and improve the *C. johnstoni* genome as has been mentioned throughout this discussion (English et al., 2012; Koren and Phillippy, 2015; Tyson et al., 2018). With both karyotype information and sequencing, the chromosomes could be assembled. However, for this research project, chromosomal assembly is not required, and the genome completeness estimates indicate the *C. johnstoni* genome has been successfully assembled for the desired comparative analyses to follow within this thesis. It would be an excellent project to follow this study to assemble the *C. johnstoni* genome is to a high-quality genome assembly equivalent to *O. volvulus* and *B. malayi* genome assemblies.

3.4.3 Repeat regions and repeat masking in *Cercopithifilaria johnstoni* scaffolds

There are two general types of repeats: local repeats (tandem, inverted, or simple sequence repeats) and dispersed repeats throughout the genome (Lovett, 2001; Shapiro and Von Sternberg, 2005). Genome scaffolds are analysed using RepeatMasker to screen the sequence for any interspersed repeats or low complexity DNA sequence, which can affect downstream analyses (Table 3.4) (Smit, 2015). RepeatMasker is designed to search for these repeats and provide annotation and output with a modified sequence masking the repeats with Ns (Tarailo-Graovac and Chen, 2009; Smit, 2015). The number of Ns present before RepeatMasking was 56,933 bp (Table 3.1) in the *C. johnstoni* scaffolds and after increased to 4,925,102 bp after repeat masking (Table 3.4). The number of Ns was introduced after RepeatMasking which is typical of draft genomes. The number of Ns is consistent with the 6.23% of bases masked.

It is common when sequencing a short-read Illumina library for there to be an increased number of Ns. Short-read sequences use algorithms such as the *de Bruijn* graphs which overlap consensus sequences (Dominguez et al., 2018). It is unlikely that a short-read library will be assembled into large scaffolds or

chromosomes. Generally, short reads are assembled into contigs of various sizes which could be further assembled into scaffolds. As a result of producing many contigs, there are gaps present between contigs. Thus, Ns are introduced into the assembly filling the gaps between the assembled contigs (Dominguez et al., 2018). The addition of long-read sequences allows the short reads to be mapped onto the long reads to close the gaps between the sequence (English et al., 2012; Salmela et al., 2014). The combination of short and long-read data removes ambiguity and mis-assemblies which is common in short-read Illumina sequencing and fills in the gaps between the contigs and scaffolds developing super-scaffolds (Salmela et al., 2014).

A significant feature of repeats throughout genomes is the evolution of SINEs, LINEs and LTRs. Retrotransposons are widely distributed repeat elements in genomes that have been known to play a role in genome structure and function (Ganko et al., 2001; Szitenberg et al., 2016). Identifying LTR retrotransposons and comparing with different species provide the opportunity to study the evolutionary history of organisms such as filarial nematodes (Ganko et al., 2001). It is not possible to study and compare the evolutionary history of *C. johnstoni* LTR retrotransposons because the genome is highly fragmented and is likely to not have all the repeat regions correctly identified from short-read sequences. However, a future research direction for *C. johnstoni* would be to identify confidently the LTRs, SINEs and LINEs and compare with other filarial nematodes to identify the phylogenetic relationships of the LTR, SINE, LINE families (Szitenberg et al., 2016) to learn more about *C. johnstoni* evolutionary history.

The genome sizes of filarial nematodes vary (Table 3.1) in large part because of differences in proportions of repetitive DNA (Leroy et al., 2003; Coghlan, 2005). For example, the repeat regions across the closely related filarial nematodes used within this study were compared with genome size. Repeat contents range from 2.82% (*L. sigmodontis*) to 13.61% (*L. loa*) (Table 3.4) which corresponds to genome size assembly length with the smallest genome of *L. sigmodontis* (64,813,410 bp) and the second-largest genome of *L. loa* (96,405,338 bp) (Table 3.1). The *O. volvulus* genome is the largest assembled filarial genome (96,427,137 bp) and has the third-highest repeat content of 10.26% (Table 3.4). Repeats are typical of eukaryote genomes, generally

distributed randomly throughout the genome, but are more commonly found in intergenic regions (The *C. elegans* Sequencing Consortium, 1998). Genome size variation is thus primarily due to the non-coding elements.

There is a correlation between the qualities of the genome assembly with the repeat content concluding estimates of repeat content may be higher in better-assembled genomes. As discussed previously, quality refers to a range of features including the sequence length, N50, number of gaps and mis-assemblies, and size of assembled contigs and scaffolds. The best assembled filarial genome is *O. volvulus* with an N50 of 25,485,961, followed by *B. malayi* (14,214,749), and *L. loa* (180,288) (Table 3.1). The genomes with the highest repeat content are *L. loa* (13.61%), followed by *B. malayi* (11.8%) and *O. volvulus* (10.26%) (Table 3.4). These three nematodes are studied extensively and have rather excellent genome assemblies which may account for the high repeat content as a result of more genomic information. *O. volvulus*, *L. loa* and *B. malayi* all have short and long read data that have allowed for accurate annotation of the repeats throughout the genomes.

The *C. johnstoni* genome has 6.23% repeat content consistent with the *D. immitis* and *B. pahangi* genomes that range from 6.1% to 7.88% masked repeats (Table 3.4). These *C. johnstoni* repeats were introduced into the assembly after the RepeatMasker analysis. There is more likely to be missing repeat information in more fragmented genomes, i.e., *C. johnstoni* genome than there is in the *O. volvulus* genome that has been assembled into chromosomes using abundant parasite material and sequence technologies.

It is possible to estimate the repeat content based on the contiguity of the genome assembly. In the case of the *C. johnstoni* assembly, the genome was assembled using a short-read Illumina library sequenced from one adult female filarial nematode. It is likely that the regions between the assembled contigs and scaffolds do not have enough genomic information to assemble accurately without mis-assembly. Repeat regions also influence the genome assembly because if the reads are not long enough to provide unique sequences flanking the repeats, then the assembly tools may not be able to accurately distinguish between the repeats (Dominguez et al., 2018), leading to mis-assembly or incorrect repeat estimation. It is also well known that tandem repeat regions are difficult to assemble, therefore, it is likely tandem repeat regions will be missing

from the *C. johnstoni* genome. In the current *C. johnstoni* genome assembly, these tandem repeat regions have not been well assembled. The *C. johnstoni* genome is highly fragmented as a result of using only short-read sequences and thus the assembly tools may have been unable to distinguish between the repeats (Dominguez et al., 2018). Improving the current *C. johnstoni* repeat annotation will require long reads to enable complete repeats to be identified. The *O. volvulus* genome is a great example of short tandem repeats known as the O-150 repeat region (Lagatie et al., 2016). Due to the combination of short-read and long-read sequencing of *O. volvulus* parasites, the O-150 region has been improved and now the genomic sequence collapses into a small number of loci that represents diversity of the family, although the complete O-150 regions is still difficult to completely assemble. The O-150 region has been an interesting target to explore genetic diversity of the various *O. volvulus* parasites from different locations and to identify infections (Toe et al., 1998; Higazi et al., 2001; Lagatie et al., 2016). Repeat content within parasitic genomes is important to identify to further understand parasite diversity. Future analyses of *C. johnstoni* should include long reads to accurately identified tandem repeat regions that may be useful for *C. johnstoni* identification, i.e., identify *C. johnstoni* infection in rodents.

The *C. johnstoni* genome has been assembled to good quality according to the N50 statistics, the size of assembled contigs and scaffolds, assembly length and repeat content. Considering the *C. johnstoni* draft genome has been assembled using short-read Illumina reads from one adult female worm, the genome has been assembled to a very good standard. However, there are areas where the *C. johnstoni* genome could use improvement such as the number of gaps, number of Ns and repeats, and lastly, longest scaffold size. As the *C. johnstoni* genome was only assembled using short-read data, it is not possible to improve the assembly quality of these features. Hence, long reads will increase the N50, reduce the number of gaps and mis-assemblies, increase the longest scaffold and predict repeat regions with confidence.

3.4.4 Comparison of the effects of three different gene annotation methods for gene prediction of *Cercopithifilaria johnstoni* scaffolds using BUSCO and OrthoFinder2

The increase in genome sequencing for a range of organisms has resulted in the improvement of bioinformatics programs that predict and annotate genes (Li et al., 2003; Gabaldón et al., 2009; Nichio et al., 2017; Glover et al., 2019). Many of the gene prediction programs rely on high-quality data to be provided for analyses. Typically researchers cannot obtain these datasets, and therefore the prediction programs are unable to provide the most accurate predictions as the information required is absent (Nichio et al., 2017). The genome annotation of *C. johnstoni* is assessed using three different annotation algorithms to determine the best and most accurate method to predict the novel genes of *C. johnstoni*. Augustus is the first gene prediction method used without the addition of other genomic information. BRAKER was developed to combine prediction programs to improve annotation accuracy (Hoff et al., 2019). BRAKER is a pipeline that has been generated to predict protein-coding genes in eukaryotic genomes such as *C. johnstoni* (Hoff et al., 2019). The pipeline uses GeneMark-ES/ET and AUGUSTUS to predict genes and uses statistical models with many different parameters to ensure the gene prediction is species-specific (Hoff et al., 2019). Thus, BRAKER is used for the following two comparative methods as it gives the option to predict protein-coding genes using the *ab initio* parameter, using RNA-Seq data, or using proteomes from other species as hints for protein prediction (Hoff et al., 2019). For these analyses, the *ab initio* and closely related species proteome parameters are used to compare against Augustus, as there is no RNA-Seq data for *C. johnstoni*.

BUSCO uses the output of protein-coding genes from the three gene prediction methods to determine which methods provide the most accurate and complete gene prediction (Table 3.5). Interestingly, Augustus produced the highest number of predicted genes according to BUSCO (Table 3.5) and the highest number of predicted one-to-one orthologues (Tables 3.6, 3.7). It is likely that the Augustus prediction method predicted more genes than the two BRAKER methods because it used *C. elegans* for gene training (a distantly related nematode). The BRAKER with *A. viteae* training prediction method produced the least number of protein-coding genes and had the highest number of incomplete genes according to BUSCO (Table 3.5). There are several reasons that could

explain the differences in number of genes predicted and number of partial genes predicted. Firstly, the *A. viteae* proteome (10,397 genes) is much smaller than the *C. elegans* proteome (~19,800 genes) and thus there is less information training the *C. johnstoni* annotation. Secondly, *C. elegans* is a divergent nematode from the filarial nematodes and therefore it is likely that there are gene deletions that have occurred as the filarial nematodes have evolved which could explain why there are a reduced number of genes. Thirdly, the *A. viteae* genome is highly fragmented and is not assembled to the high quality of the *O. volvulus* genome into chromosomes. The fragmented nature of the *A. viteae* genome has likely impacted the prediction of complete genes in the *C. johnstoni* scaffolds. The *A. viteae* protein-coding sequence set is likely to contain some poor-quality sequences or incomplete genes which means the number of robustly mapped protein-coding sequences is limited. The total number of *A. viteae* orthologues that can be used by BRAKER may, therefore, be less than 100% thus the proportion of predicted genes for *C. johnstoni* is less than possibly would be expected. *A. viteae* was chosen for gene prediction over other nematodes such as *O. volvulus* because *A. viteae* is more closely related to *C. johnstoni* and therefore should improve genome annotation (Yandell and Ence 2012; Hoff et al., 2019). Even though *A. viteae* may appear the most appropriate genome to use for gene training because it is a closely related species to *C. johnstoni* (Figure 3.5), there could be missing information from the *A. viteae* genome that results in missing gene predictions for *C. johnstoni*.

The *ab initio* BRAKER and *A. viteae* trained BRAKER methods were explored because Augustus typically is not used alone for gene prediction because it is deemed less reliable than gene prediction pipelines such as BRAKER (Hoff et al., 2019) or MAKER (Holt and Yandell, 2011). Several genome publications predicting genes for novel genomes rely on more than one gene prediction method, i.e., BRAKER using geneMark (Ter-Hovhannisyanyan et al., 2008) and Augustus (Stanke et al., 2008), or MAKER (Holt and Yandell, 2011) using geneMark, Augustus and SNAP (Korf, 2004). The reliance on multiple gene prediction programs in these pipelines has been shown to improve the quality of the genes predicted for further downstream analyses (Korf, 2004; Hoff et al., 2019). Including more genomic information for the gene predictions programs to use will normally improve the accuracy of the gene prediction (Hoff et al., 2019). *Ab initio* prediction methods are complicated without the inclusion of proteome or

RNA-Seq data to train the dataset and thus would not be a reliable method to choose (Dominguez et al., 2018; Salzberg 2019). Moreover, additional information improves the completeness of genes and mis-assemblies. It was therefore presumed that using a phylogenetically closely related filarial nematode such as *A. viteae* (Figure 2.4, 3.5) to predict protein-coding genes for *C. johnstoni* should, in principle, robustly and accurately predict *C. johnstoni* genes (Yandell and Ence 2012; Hoff et al., 2019). However, in this analysis, the *A. viteae* BRAKER gene prediction performed poorly, and Augustus predicted the highest number of genes and orthologues using BUSCO and OrthoFinder respectively (Figure 3.5, 3.6, 3.7). The results from BUSCO and OrthoFinder2 directly correspond to the number of genes predicted by the three prediction methods.

The gene prediction method that was chosen for further downstream analyses was the Augustus gene prediction as it performed the best gene predictions based on BUSCO and OrthoFinder2 analyses (Table 3.5, 3.6, 3.7). The average length of the Augustus predicted *C. johnstoni* proteins is consistent with the other filarial nematodes (Table 3.8). The average length of *C. johnstoni* proteins are longer than *O. volvulus* and shorter than *A. viteae* (Table 3.8). The average protein length is consistent with highly studied nematodes such as *B. malayi* and *L. loa* thus it can be presumed Augustus successfully predicted complete and near-complete protein-coding genes for *C. johnstoni*.

The *C. johnstoni* genome has been assembled using only genomic DNA from one adult female worm and contains over 90% of the genome content according to BUSCO. There is no doubt after conducting this comparative study between gene prediction methods that there is the requirement for more *C. johnstoni* data, i.e., RNA-Seq data, protein data and long-read sequence technology data (PacBio), to improve the genome assembly (English et al., 2012; Salmela et al., 2014; Dominguez et al., 2018; Salzberg 2019). With the improvement of the genome assembly, the same gene prediction method could provide a higher prediction accuracy and an increased number of predicted genes because there is an increase of *C. johnstoni* genomic information to provide abundant gene predictions. The most important step required to improve the confidence of the *C. johnstoni* gene prediction in future assemblies is to include long reads to assemble larger contigs/scaffolds and RNA-Seq data to confirm the gene predictions (Salzberg 2019).

3.4.5 Predicting orthologous genes between *Cercopithifilaria johnstoni* and *Onchocerca volvulus*

Now that the appropriate genomic resources are available for *C. johnstoni*, it is possible to identify and compare orthologous proteins and explore the similarity of the *C. johnstoni* genome and related filarial nematodes. Appropriate genetic resources are useful to determine the suitability of *C. johnstoni* as an organism in a small animal model to study onchocerciasis by understanding the biology of obligate parasites. In the previous chapter, the mitochondrial genome of *C. johnstoni* is described, and the phylogenetic relationships with filarial nematodes are defined (Chapter Two). The current chapter describes the *C. johnstoni* nuclear genome and predicts protein-coding genes to use in further analyses, including the search for orthologous relationships.

New computing resources enable *in silico* computational identification of orthologues between *C. johnstoni* and *O. volvulus*. Chapter Three uses OrthoFinder2 to predict orthologues between *C. johnstoni* predicted protein-coding genes and the proteomes of closely related filarial nematodes. Accurate resolution of species orthologue and paralogue relationships is an essential aspect of comparative genomics and evolutionary studies (Gabaldón et al., 2009; Trachana et al., 2011; Glover et al., 2019). Understanding how genes are derived from closely and distantly related species could provide information on the function and gene annotation for new species (Kuzniar et al., 2008; Linard et al., 2011; Glover et al., 2019).

The 7,557 orthologues shared between *C. johnstoni* and *O. volvulus* consist of one-to-one, one-to-many and many-to-many relationships (Figure 3.8) (Emms and Kelly, 2019). The one-to-one orthologues are true orthologues as they share only one gene from each species, whereas many-to-many relationships are paralogous sharing multiple genes from each species within the gene family as a result of gene expansions. Of the 7,557 *C. johnstoni* orthologues, 7,052 orthologues share a one-to-one relationship with *O. volvulus*, which is just under half of the *O. volvulus* genes available for orthology prediction (Table 3.6c). Out of a total 20,459 genes between *O. volvulus* and *C. johnstoni*, 68.93% of total genes are one-to-one orthologues. Two species have the highest orthologous gene predictions, *A. viteae* and *L. sigmodontis* (Table 3.6c). Once more, this result is not surprising as *A. viteae* and *L. sigmodontis* have repeatedly

shown similar phylogenetic relationships with a range of different datasets. It could be presumed that *A. viteae*, *L. sigmodontis* and *C. johnstoni* are all sharing numerous genes and gene families and thus share many orthologous relationships. The per cent orthology between *C. johnstoni* and *A. viteae* is 75.70% out of a combined 18,631 genes which is unsurprising as *A. viteae* was used for the gene training to predict *C. johnstoni* genes.

To place the orthologue prediction in more context, *O. volvulus* and *O. ochengi* share 8,653 one-to-one orthologues (Table 3.6c). The *O. volvulus* genome has 12,225 genes, and *O. ochengi* has 12,816 genes, although only 8,653 genes share a one-to-one relationship. They share a very close phylogenetic relationship, commonly referred to as “sister species” consistently is positioned in the same clade (Blaxter and Koutsovoulos, 2015; Coghlan et al., 2019). With such a close relationship of species sharing the same genus, it would be expected they would share countless orthologous relationships. Understandably 8,653 is only the number of one-to-one relationships, not including gene family expansions and other paralogous relationships. Hence the 8,653 one-to-one genes or 69.11% of a total 25,041 possible genes from *O. volvulus* and *O. ochengi* can be concluded as a reasonably high orthologous result.

One thousand two hundred thirty-three orthogroups are containing single-copy orthologous genes shared among the 12 filarial nematode protein-coding genes (Figure 3.6). The few one-to-one orthogroups and other multi-gene orthogroups, i.e., one-to-many, many-to-one, many-to-many, that are present in all species except *C. johnstoni* (Figure 3.6) suggest that most of the widely shared one-to-one orthologues amongst the 12 species are also shared in *C. johnstoni*, approximately greater than 80% (Figure 3.6). The same can be observed for the multi-gene orthogroups in Figure 3.7. There are only 148 multi-gene orthogroups that exclude *C. johnstoni* (Figure 3.7) which suggests and confirms that *C. johnstoni* shares the majority of orthogroups with other filarial nematodes. Across both analyses, there is consistently only two orthogroups that contain unique orthologous relationships between *C. johnstoni* and *O. volvulus*, excluding other filarial nematodes which is a very significant relationship to explore in the context of this PhD.

When all the orthologous relationships are included in the analysis, i.e., one-to-one, one-to-many, many-to-one, many-to-many, there are 7,557 orthogroups shared between *C. johnstoni* and *O. volvulus* (Figure 3.8). These 7,557 orthogroups include the 7,052 one-to-one orthologues shared between *C. johnstoni* and *O. volvulus* (Table 3.6c). There is now a defined set of shared orthologues between *O. volvulus* and *C. johnstoni* from which can be explored in more detail to understand the filarial relationships and also to explore the possibility of *C. johnstoni* being used in an animal model to study onchocerciasis. The following chapter will use this data to identify whether *C. johnstoni* could have orthologues of *O. volvulus* proteins that are strongly immunogenic in humans.

All the available proteomes of closely related filarial nematodes species are included in orthologue identification and species-tree estimation of OrthoFinder2. The single-copy orthologue tree, based on 1,447 orthogroups of one-to-one relationships (Figure 3.5), of all 12 nematodes show strongly supported phylogenetic relationships consistent with published literature (Blaxter and Koutsovoulos, 2015; Lefoulon et al., 2015; Cotton et al., 2016; Shey et al., 2018; Coghlan et al., 2019), mitochondrial genomes (Chapter Two), and nuclear genome alignments. *B. malayi*, and *W. bancrofti* are positioned in the same clade consistent with previous phylogenies (Blaxter and Koutsovoulos, 2015; Lefoulon et al., 2015). The relationship between *C. johnstoni* and *O. volvulus* also appears consistent with the mitochondrial genome phylogeny (Chapter Two). The phylogeny illustrates that *C. johnstoni* is more closely related to the *Brugia-Wuchereria* clade than to the *Onchocerca* clade and thus *O. volvulus* (Figure 3.5).

The position of *C. johnstoni* among the filarial nematode clade has now been established using mitochondrial genes, nuclear genome genes, and single-copy genes and is consistently positioning *C. johnstoni* with *A. viteae* and *L. sigmodontis* (Figure 3.5). The use of more genomic information has resulted in more strongly supported and confident predictions of the phylogenetic relationships within the clade III filarial nematodes.

3.5 Conclusions

The nuclear genome of *C. johnstoni* was assembled into scaffolds using MiSeq short-read sequencing data from one female adult worm. The assembly length and genome statistics are consistent with most of the other sequenced filarial nematodes and are better than several of the assembled filarial nematode genomes. The assembly of *C. johnstoni* nuclear data results in 95% of the entire genome present according to CEGMA and BUSCO analyses, representing a better genome assembly than most of the other filarial nematodes currently available. Synteny comparisons show *C. johnstoni* scaffolds are similar to both *O. volvulus* and *B. malayi* chromosomes. Additional sequencing of *C. johnstoni* life stages and using long-read sequencing technology could improve the genome assembly to chromosome level to be directly comparable with *O. volvulus*. The filarial nematodes share 1,447 single-copy orthologous genes and produce a single-copy phylogenetic tree supporting previously published phylogenies (Chapter Two) (Blaxter and Koutsovolos, 2015; Lefoulon et al., 2015).

For the first time, the genome sequence of *C. johnstoni* is assembled into large scaffolds and smaller contigs annotated and compared with *O. volvulus* and other filarial nematodes. A comparative analysis of the relationship between *A. viteae*, *B. malayi*, *B. pahangi*, *B. timori*, *C. johnstoni*, *D. immitis*, *L. loa*, *L. sigmodontis*, *O. flexuosa*, *O. ochengi*, *O. volvulus*, and *W. bancrofti* across mitochondrial and nuclear genomes has shown consistent phylogenetic relationships and several shared orthologous genes. The following chapter will utilise the orthologous data identified here to specifically compare orthologous genes relevant to immunopathology between *C. johnstoni* and *O. volvulus*, to explore whether similarities in proteins could be driving the observed similarities in disease immunopathology.

Chapter Four

Evolution and sequence conservation of immunogenic orthologous proteins between *Cercopithifilaria johnstoni* and *Onchocerca volvulus*

4.1 Introduction

Onchocerciasis has complex immunopathology (Kawabata et al., 1984; Petralanda and Piessens, 1994), characterised by disfiguring skin lesions, mild itching, chronic inflammation of the skin and blindness caused by the presence of dead *O. volvulus* microfilariae in the skin and cornea (Connor et al., 1970; Brady et al., 2006; Allen et al., 2008; Control and Prevention, 2013). *C. johnstoni* elicits similar immunopathology in rats which have been observed from locating dermal microfilariae living in the lymphatic vessels and moving to the perivascular connective tissue inducing inflammatory responses (Spratt and Haycock, 1988; Vuong et al., 1993). These responses were identified by observing eosinophils and mastocytes surrounding the site of dead microfilariae in the rodent skin, similar to *O. volvulus* microfilariae in humans (Spratt and Haycock, 1988; Vuong et al., 1993). Inflammatory, fibrotic tissue was observed surrounding a dead *C. johnstoni* female worm as well as chronic lesions and fibrosis in the rats' ears (Spratt and Haycock, 1988; Vuong et al., 1993). *C. johnstoni* microfilariae were observed in the eyelids, cornea and corneal limbus and frequently spread to the peripheries in *R. fuscipes* and *R. norvegicus*. Finally, ocular lesions were observed in both host species (Spratt and Haycock, 1988; Vuong et al., 1993). Thus, *C. johnstoni* and *O. volvulus* microfilariae behave similarly in their respective hosts and elicit very similar immunopathology. The *C. johnstoni* adult worms can be located in the subcutaneous tissue of the skin where they are surrounded by acute and sub-acute inflammatory lesions (Spratt and Haycock, 1988; Vuong et al., 1993). However, the location of adult worms is dissimilar in *O. volvulus*-infected humans where the adult worms reside in nodules (Connor et al., 1970; Omura and Crump, 2004). The characteristic feature of onchocerciasis is

blindness resulting from the microfilariae in the eyes thus the observation of lesions in the cornea in rodents was an exciting discovery (Brady et al., 2006; Control and Prevention, 2013). Identifying how *C. johnstoni* and *O. volvulus* elicit these similar symptoms would be a necessary step in understanding onchocerciasis and immunopathology.

The immunopathology associated with *O. volvulus* has been explored for decades aiming to understand the immunological responses in humans (McKechnie et al., 1993; Abraham et al., 2002; McKechnie et al., 2002; Abraham et al., 2004; Shey et al., 2018). The investigation into understanding these immunological responses is still ongoing and has not yet been solved. CD4+ helper T cells (Th) play a critical role in coordinating cellular and antibody responses to antigens. Th1 and Th2 cells are characterised by their contrasting cytokine profiles, primarily IFN- γ (Th1) or IL-4 and IL-5 (Th2) (Romagnani, 1997; Kerepesi et al., 2005). T regulatory-1 cells can suppress Th1 or Th2 responses by secreting IL-10 or TGF- β (Groux, 2003) and have been cloned from the nodules of patients with chronic onchocerciasis (Satoguina et al., 2002). Other studies have focused on putatively immune individuals; individuals that appear to produce antigen-specific Th1 type responses that may provide immunity to *O. volvulus* (Elson et al., 1995; Soboslay et al., 1997). Further studies discovered that immunity is associated with the development of a Th2 response to larval and adult antigens with partial production of a Th1 response and thus likely to be a mixed Th1/Th2 response (Turaga et al., 2000; Cooper et al., 2001). Finally, mice studies have revealed that a Toll-like receptor 4 (TLR4) is required for Th2-dependent responses in mice and that there is a TLR4-dependent larval killing mechanism that is poorly understood and requires further research to thoroughly explain the immune mechanisms at play (Kerepesi et al., 2005). These studies highlight the uncertainty around protective immunity in humans to *O. volvulus*.

One major hypothesis that is being explored throughout onchocerciasis research is that *Wolbachia* the bacterial endosymbiont in *O. volvulus* is driving the immunopathology observed in humans (Bandi et al., 1998; Tamarozzi et al., 2011). It appears that *Wolbachia* plays an essential part in nematode reproduction and thus could be an excellent target to halt the production of microfilariae (Bandi et al., 1998). Doxycycline has been recorded to target and deplete *Wolbachia* within the *O. volvulus* adults and successfully reducing

parasite burden (Taylor et al., 2014; Walker et al., 2015). Thus it has been presumed that if the *Wolbachia* can be depleted, then it will be possible to control *O. volvulus* infection. Interestingly, *Wolbachia* appears to be absent from the *C. johnstoni* genome. Several small contigs share homology to regions of the *Wolbachia* genome indicating that there are remnants of *Wolbachia* but do not appear to have an intact genome as seen in *O. volvulus*. Thus is likely not to have a parasite-endosymbiont symbiotic relationship. There have been several studies that have discovered *Wolbachia* sequences within filarial genomes which resemble nuwts (nuclear *Wolbachia* transfers) (McNulty et al., 2010). Two hypotheses that explore 1) the presence of nuwts in the absence of an intact *Wolbachia* genome due to ancestral absence (Bain et al., 2008; Ferri et al., 2011; Lefoulon et al., 2012), and 2) *Wolbachia* have been lost throughout evolution (Casiraghi et al., 2004; McNulty et al., 2010; Koutsovolos et al., 2014) have been proposed. *Wolbachia* is absent and only contains nuwts in the closely related *A. viteae* genome and in *O. flexuosa* (McNulty et al., 2010; McNulty et al., 2012) although is present in the *L. sigmodontis* genome (Specht et al., 2018; Hübner et al., 2019b). These studies confirm that not all filarial nematodes contain a *Wolbachia* genome and it is possible for *Wolbachia* to have been lost. The exact mechanism driving the immunopathology of onchocerciasis is not known; however, there is evidence to show that both *Wolbachia* and individual molecules may play a role in the immunopathology. Understanding what is driving the similar immunopathology that is independent of *Wolbachia* would have implications for understanding onchocerciasis. An immunologically relevant model could assist in understanding the mechanisms involved in the immunopathology. As *Wolbachia* is absent in *C. johnstoni*, molecules known to be immunoreactive in *O. volvulus* are being explored in *C. johnstoni* throughout Chapter Four to determine if there is any similarity between the species.

There has been an abundant number of possible candidate antigens identified that could be used for detecting *O. volvulus* infections (Lustigman et al., 2002; McNulty et al., 2015; Bennuru et al., 2016; Norice-Tra et al., 2017; Bennuru et al., 2019). Thus far, several of the *O. volvulus* proteins that have shown immunogenic expression in their hosts, are hypothetical proteins with uncharacterised functions. However, numerous *O. volvulus* proteins have been predicted to be involved in signal transduction processes of adult female worms, moulting or metamorphosis and parasite development (Bennuru et al., 2016;

Bennuru et al., 2019). A couple of examples of the types of proteins studied consist of G-protein coupled receptors (GPCR) that are commonly conserved in closely related filarial nematodes. Fructose 1,6 bisphosphate aldolase (Ov-fba-1) has been another target identified from immunologic screening to be expressed by larval stages of *O. volvulus* and could potentially be a valuable candidate for treating *O. volvulus* infection (McCarthy et al., 2002).

A typical problem highlighted in various *O. volvulus* studies that are exploring potential antigens or proteins for targeting treatment of onchocerciasis, is that there is no experimental animal model suitable for maintaining the *O. volvulus* life cycle in the laboratory (Grote et al., 2017). Proteins are commonly studied in mice models which do not accurately recapitulate onchocerciasis disease features. Mice models may be useful for exploring drug mechanisms but are not relevant to explore the characteristic disease immunopathology. Identifying the most promising protein targets to develop further treatments for eliminating onchocerciasis, is often limited to using an *in silico*-based approach, and filtering targets based on defined criteria because there is not a suitable animal model available.

There are two examples of moderate to high-throughput studies to identify immunogenic proteins that are of particular interest. The first approach by Norice-Tra et al. (2017), focused on peptide profiling using multi-locus immunophenotyping based on a serologically based method derived in *Toxoplasma gondii* from Kong et al. (2003). The serological based immunophenotyping approach was used to investigate *O. volvulus* population diversity from *O. volvulus*-infected patient sera (Norice-Tra et al., 2017). Nonsynonymous single-nucleotide polymorphisms (SNPs) were identified in 16 major immunogenic *O. volvulus* proteins: Ov-CHI-1/Ov-CHI-2, Ov16, Ov-FAR-1, Ov-CPI-1, Ov-B20, Ov-ASP-1, Ov-TMY-1, OvSOD1, OvGST1, Ov-CAL-1, M3/M4, Ov-RAL-1, Ov-RAL-2, Ov-ALT-1, Ov-FBA-1, and Ov-B8. The immunoreactivity of *O. volvulus*-infected patient sera was assessed against these SNP containing peptides. Four proteins were rich in SNPs, including Ov-CHI-1/Ov-CHI-2, Ov-ASP-1, and Ov-ALT-1. Eight SNP-containing peptides showed significant immunoreactivity, including OVOC1192, OVOC9988, OVOC9225, OVOC7453, OVOC11517, OVOC3177, OVOC7911 and OVOC12628 (Norice-Tra et al., 2017). The results from this study demonstrated the success of using

patterns of host immunoreactivity to *O. volvulus* antigenic peptides to characterise population biology of *O. volvulus* that was previously inaccessible due to a lack of parasite material (Norice-Tra et al., 2017). As *O. volvulus*-infected sera exhibited high immunoreactivity against these proteins, the proteins may be not only useful for exploring *O. volvulus* population biology but also elucidate features associated to onchocerciasis (Norice-Tra et al., 2017). An immunophenotyping approach is a non-invasive approach that has the potential to inform vaccine development or monitor the success of MDA treatment throughout communities. As these proteins are known to show high immunoreactivity in sera of *O. volvulus*-infected humans, it would be valuable to determine if these proteins had orthologues in *C. johnstoni* that could be further explored in a rodent animal model.

The second approach focused on multi-omics (genomics, transcriptomics, proteomics and immunomics), to find immunodiagnostic antigens for serodiagnosis of onchocerciasis using mass spectrometry proteomic identification (McNulty et al., 2015). Adult worms were extracted from nodules of *O. volvulus*-infected individuals. A group of 241 immunoreactive proteins were identified. McNulty et al., (2015) were aiming to find a list of *O. volvulus*-specific proteins that were consistently expressed serodiagnostic antigens thus the 181 proteins that shared greater than 70% amino acid identity and greater than 70% total protein length with other species were excluded. This left 60 protein candidates, 51 of which were expressed in 8 female worms from the RNA-Seq data and 33 were shown to have consistently high expression among all the worms. Thus, the 33 proteins were the final list of proteins because they were *O. volvulus*-specific candidate antigens that were seen to be consistently expressed. Two commonly researched proteins *Ov*-16 and *Ov*-33 failed their priority pipeline because they did not meet their criteria, sharing too much identity with other nematodes. The multi-omics study has been one of the more carefully structured studies conducted on identifying immunodiagnostic antigens because they have developed stringent criteria for identifying *O. volvulus*-specific antigens that are not going to lead to cross-reactivity problems with other filarial nematodes. The 33 serodiagnostic candidates can now be validated further studying candidate antigens' reactivity with antibodies in serum samples from *O. volvulus*-infected patients. It would be valuable to identify whether *C. johnstoni* has any shared orthologues to any of these 33 *O. volvulus*-specific candidates that may lead to

identifying whether *C. johnstoni* would be suitable to study onchocerciasis or whether these candidates are not species-specific enough to use for onchocerciasis treatment.

A separate approach identified immunodominant motifs and a 9-mer peptide in *O. volvulus* with the intention of developing serodiagnostics candidates from the immunodominant motifs (Lagatie et al., 2017, 2018). Three highly immunodominant motifs were PxxTQE, DGxDK and QxSNxD (Lagatie et al., 2017). The poly-glutamine stretch in the N-terminal region of *O. volvulus* protein, Ov-RAL-2 identified as a 9-mer peptide (QQQQQQQQR) could be used as a serological marker for *O. volvulus*. The poly-glutamine stretch appears absent from all other closely related helminths and is a highly immunoreactive peptide making it an attractive target to explore further for identifying onchocerciasis using serodiagnostic (Lagatie et al., 2018).

One possible *in silico* approach to compare *C. johnstoni* and *O. volvulus* eliciting similar immunopathology in two very different hosts, i.e., rats and humans respectively, is to identify orthologues of known immunogenic proteins. The identification of orthologues would be the first step in understanding the similar immunopathology observed. Importantly, an immunogenic protein is one that provokes an immune response while the downstream consequence of that response is generally unknown in most hosts. In principle, there could be no effect, presence of immunopathology or a protective response, i.e., prevents infection or causes expulsion of an existing infection. The similarity in immunopathology between *O. volvulus* and *C. johnstoni* could be a result of shared orthologues that contain antigens that are presented in the same immunological context, i.e., skin and eye in rodents and humans from *C. johnstoni* and *O. volvulus* respectively; the hosts are likely to produce similar immune responses. Therefore, part of the immune response observed in *C. johnstoni*-infected rats could be driven by *C. johnstoni* orthologues of *O. volvulus* antigens. I would, therefore, predict if the *O. volvulus* proteins that are immunogenic in humans are structurally conserved in *C. johnstoni*, then there will be a similar response in rats infected with *C. johnstoni*.

4.1.1 Aims

The aim is to obtain a list of *C. johnstoni* proteins that appear to be involved in the immune response of the host that may aid to explain the similar immunopathology observed in *C. johnstoni*-infected rodents and *O. volvulus*-infected humans in downstream experiments. To do so, I will:

- 1) Identify *C. johnstoni* one-to-one orthologues of 49 *O. volvulus* candidate proteins that have been identified in onchocerciasis research as immunologically relevant.
- 2) Explore the orthologues sequence similarity and putative protein functions using BLAST to compare *C. johnstoni* and *O. volvulus*.
- 3) To determine whether the *C. johnstoni* and *O. volvulus* orthologues are under diversifying, purifying or neutral selection.
- 4) Identify immunodominant motifs of significance and a serological 9-mer peptide marker for *O. volvulus* within the *C. johnstoni* scaffolds and explore putative functions using BLAST of those *C. johnstoni* genes that contain the motifs or peptide.

4.2 Materials and Methods

Chapter Four utilises the same genome assembly and orthologue analyses conducted in Chapter Three: Materials and Methods, “Nuclear genome assembly” and “Prediction of orthologues”.

4.2.1 Curation of protein sequences representing immunologically relevant targets

Immunogenic relevant target proteins of *O. volvulus* were selected from Norice-Tra et al. (2017) and McNulty et al. (2015). The Norice-Tra et al. (2017) study took a serological based immunophenotyping approach using serum from Ov-infected patients to explore 17 previously identified Ov-specific immunogenic proteins reviewed in Lustigman et al. (2002). Lustigman et al. (2002) had reviewed the previous and current literature at the time of potentially immunogenic proteins that could be used as vaccine candidates. All of these proteins were chosen to compare with the *C. johnstoni* predicted protein list.

Serodiagnostic candidates of *O. volvulus* were selected from McNulty et al. (2015). This study aimed to use a multi-omics approach to identify novel immunodiagnostic Ov-antigens that could be used for future serodiagnostic tests and assist elimination programs. The identification of *O. volvulus* proteins was conducted by mass spectrometry from extracted *O. volvulus* worms from nodules. An experimental pipeline allowed an initial identification of 241 immunogenic proteins to be filtered to 60 *O. volvulus* specific proteins, 51 consistent expressions in adult female worms, 41 high expressions and 33 of those with low variability (McNulty et al., 2015). The 33 highly expressed with low variability serodiagnostic candidates of *O. volvulus* were chosen to compare against *C. johnstoni* predicted proteins.

There were only two proteins (OVOC9988 and OVOC7453) that overlapped in the Norice-Tra et al. (2017) and McNulty et al. (2015) publications. One protein in particular that has been highlighted in *O. volvulus* literature was not included in either study, OVOC1952 but due to the importance of the protein in onchocerciasis research, it was also investigated. OVOC1952 has been referred to as Ov-28CRP (an antigenic protein recognised by host sera in an immunological study) and as Ov-GM2AP (a functional annotation based on

conservation of structural domains). For the remainder of this chapter, this protein will be referred to as the WormBase Parasite protein ID, OVOC1952.

The final protein list consisted of 16 from Norice-Tra et al. (2017) (duplicate sequences removed), 32 from McNulty et al. (2015) (duplicate sequences removed) and OVOC1952 equalling to 49 protein sequences (Supplementary Table 4.1 and 4.2). The data associated with the 49 protein sequences was extracted from the OrthoFinder2 results described in Chapter Three.

4.2.2 Data extraction and sequence alignment

The 49 targeted proteins from Norice-Tra et al. (2017) and McNulty et al. (2015) were placed in a multi-fasta file that was then used to identify the relevant OrthoFinder2 results which were extracted and exported into a file with only the target *O. volvulus* immunogenic protein orthogroups (Supplementary Table 4.1 and 4.2).

The sequences for each orthogroup were aligned separately (align sequences of orthogroup to other sequences in the same orthogroup) using ClustalW version 2.0.10 (Larkin et al., 2007). Alignments were trimmed manually using Mesquite version 3.04 (Maddison and Maddison, 2008). Only regions of the alignment that overlapped were used for the analyses and thus a comparable study.

4.2.3 BLAST *Onchocerca volvulus* and *Cercopithifilaria johnstoni* protein sequences to predict putative functions

The *C. johnstoni* proteins orthologous to the 30 *O. volvulus* immunogenic proteins were combined in a multi-fasta file for a BLAST analysis. The *C. johnstoni* and *O. volvulus* proteins were used as the query in a BLASTP analysis as implemented in NCBI BLAST version 2.6.0 and searched against the NR database, with the results reported in tabular format and an e-value threshold of 1e-05. The top match of the *C. johnstoni* and *O. volvulus* gene were then reported in a table for comparison.

4.2.4 Exonerate analysis

The *O. volvulus* genes that had missing *C. johnstoni* orthologues were searched for against the *C. johnstoni* scaffolds using exonerate version 2.2.0 using default parameters (Slater and Birney, 2005). The complete *C. johnstoni* masked scaffolds was input as the query file, and the list of missing *O. volvulus* proteins was input as the target to determine whether the *O. volvulus* genes could be present within the *C. johnstoni* scaffolds but had not been predicted as *C. johnstoni* protein-coding genes.

4.2.5 Detection of diversifying or purifying selection

The shared orthogroups between *C. johnstoni* and *O. volvulus* immunogenic proteins were used in the PAML analysis. The filarial nematodes within each orthogroup consist of the same 12 filarial nematodes studied throughout this thesis, *C. johnstoni*, *O. volvulus*, *A. viteae*, *B. malayi*, *B. pahangi*, *B. timori*, *D. immitis*, *L. loa*, *L. sigmodontis*, *O. ochengi*, *O. flexuosa*, and *W. bancrofti*. Orthogroup protein alignments of the filarial nematodes present in each orthogroup and their corresponding phylogenies were extracted from the OrthoFinder2 analysis and analysed using PAML to identify selection among the protein-coding genes (Phylogenetic Analysis by Maximum Likelihood) (Yang, 1997, 2000). The protein sequence alignments were back-translated into codon alignments in Mesquite version 3.04 (Maddison and Maddison, 2008) and aligned to the genomic sequences to avoid degeneracy. Once confirmed they were realigned using ClustalW version 2.0.10 (Larkin et al., 2007). The codon alignments were individually inputted into the GUI version of CodeML in the PAML package (Xu and Yang, 2013; Yang, 2007) each using the following parameters: seqtype = 1:codons and typical codon model = branch model. Default parameters were used for the two-branch type model. To determine selection on the *O. volvulus* and *C. johnstoni* branches compared to the other filarial nematodes within each orthogroup using PAML, every orthogroup tree file was manually amended to include a '1' before the tree matrix, and a '#1' is placed after the *O. volvulus* and *C. johnstoni* branch. The same manual editing process was conducted on all of the 30 orthogroups containing an orthologous relationship between *C. johnstoni* and *O. volvulus*.

PAML estimates synonymous and nonsynonymous substitution rates and detects positive selection using the codon substitution model of Goldman and Yang (1994). Strength of selection on protein-coding genes can be measured by the nonsynonymous to synonymous rate ratio, $\omega = dN/dS$, with $\omega < 1$, $\omega = 1$ and $\omega > 1$ indicating purifying, neutral and diversifying selection, respectively (Anisimova et al., 2001; Gharib and Robinson-Rechavi, 2013). The ω ratio is commonly calculated as the average over sites (Anisimova et al., 2001). However, codon-based models that account for the variation of ω among sites may be more sensitive in detecting persistent diversifying selection (Yang, 2000; Anisimova et al., 2001; Yang and Dos Reis, 2010). To estimate ω among genes from closely related species such as these filarial nematode orthogroups, maximum likelihood models of codon substitutions are used to determine whether there are higher nonsynonymous (dN) or synonymous (dS) at particular codon sites or branch sites (Anisimova et al., 2001; Yang, 2007; Yang and Dos Reis, 2010; Gharib and Robinson-Rechavi, 2013). Diversifying positive selection on the protein-coding genes is the selection for change in the amino acids that is faster than expected under a neutral model. Thus, a higher nonsynonymous substitution rate ($\omega > 1$) is evidence of adaptive molecular evolution in that gene (Anisimova et al., 2001; Yang, 2007; Yang and Dos Reis, 2010).

4.2.6 Epitope and motif search

The three immunogenic motifs, PxxTQE, DGxDK and QxSNxD (Lagatie et al., 2017) were text searched using the following command “grep –color=auto <MOTIF> cercopithifilaria_johnstoni_protein.fasta” within all the predicted genes of the *C. johnstoni* genome where <MOTIF> was “P..TQE”, “DG.DK”, “Q.SN.D”. These same motifs were also searched using the same command in the proteomes of *A. viteae*, *B. timori*, *B. pahangi*, *D. immitis*, *L. loa*, *L. sigmodontis*, *O. flexuosa* and *O. ochengi*.

The 9-mer peptide, QQQQQQQQR, from RAL-2 (OVOC9988) (Lagatie et al., 2018) was searched for in all the predicted proteins of *C. johnstoni*. The same epitope was text searched using the following command “grep –color=auto “QQQQQQQQR” cercopithifilaria_johnstoni_protein.fasta” within the proteomes of *A. viteae*, *B. timori*, *B. pahangi*, *D. immitis*, *L. loa*, *L. sigmodontis*, *O. flexuosa* and *O. ochengi* that were downloaded from WormBase Parasite.

4.2.7 BLAST *Cercopithifilaria johnstoni* proteins that matched to the epitope and three immunodominant *Onchocerca volvulus* motifs to identify putative functions

The *C. johnstoni* proteins containing the motifs or epitope were combined in a multi-fasta file for a BLAST analysis. The *C. johnstoni* proteins were used as the query in a BLASTP analysis as implemented in NCBI BLAST version 2.6.0 and searched against the NR database, with the results reported in tabular format and an e-value threshold of 1e-05. The top match of the *C. johnstoni* genes was then reported in a table for comparison. The second top BLAST match was reported in tabular format to identify possible putative functions to explore the type of proteins in these lists further.

4.2.8 InterProScan analysis on *Cercopithifilaria johnstoni* proteins containing the *Onchocerca volvulus* immunodominant motifs and epitope

The *C. johnstoni* genes containing either an immunodominant motif or 9mer epitope were input into an InterProScan analysis to identify the GO (Gene Ontology) terms associated with identifying putative gene function. The protein sequences were combined in a multi-fasta file and run using InterProScan version 5.24.63.0 (Jones et al., 2014) specifying –goterms –formats GFF3 and –applications Pfam.

4.3 Results

The predicted protein-coding genes of *C. johnstoni* and proteomes of closely related filarial nematodes were analysed using OrthoFinder2 to identify potential orthologues in Chapter Three. A total of 7,557 orthogroups were identified that shared orthologous relationships between *C. johnstoni* and *O. volvulus*, i.e., one-to-one, one-to-many, many-to-one, and many-to-many. A total of 7,025 one-to-one orthologues between *C. johnstoni* and *O. volvulus* were identified throughout their genomes (Chapter Three Figure 3.8). A combined list of *O. volvulus* proteins with previously characterised immunogenic profiles was used to search for putative immunogenic proteins in *C. johnstoni*, and filter the 7,557 orthologous orthogroups identified (McNulty et al., 2015; Norice-Tra et al., 2017). The immunogenic list of 49 *O. volvulus* proteins was used to filter the OrthoFinder2 results for further comparative analyses. OrthoFinder2 identified 30 of the 49 genes sharing orthologous proteins in *C. johnstoni*. Exonerate was run to see whether the remaining 19 *O. volvulus* immunogenic proteins that no one-to-one *C. johnstoni* orthologue could be identified were present in any of the other *C. johnstoni* protein-coding genes. The exonerate analysis reveals all 19 proteins share amino acid homology; however, have very short sequence hits. The 19 *O. volvulus* genes are OVOC1192, OVOC1213, OVOC4612, OVOC5718, OVOC6327, OVOC7430, OVOC7453, OVOC9325, OVOC9475, OVOC9748, OVOC10638, OVOC11218, OVOC11487, OVOC11951, OVOC12448, OVOC12569, OVOC12628, OVOC12769, and OVOC12871 (Supplementary Table 4.1 and 4.2). It is likely that the gene annotation program did not predict all of the *C. johnstoni* genes correctly and thus OrthoFinder2 could not predict all the orthologues and paralogues thus the above missing genes could only be identified by searching the *C. johnstoni* scaffolds rather than the protein-coding genes.

4.3.1 *Onchocerca volvulus* immunogenic proteins and *Cercopithifilaria johnstoni* orthologues predicted putative functions

The *C. johnstoni* and *O. volvulus* orthologous proteins were explored by performing BLAST to determine putative function according to hits in the NCBI database. Several of the known *O. volvulus* immunogenic proteins have been previously researched and thus have various annotations on WormBase Parasite

and the NCBI database. Thirteen of the 30 *C. johnstoni* proteins match to the same or highly similar *O. volvulus* BLAST result with good e-values and bit scores (Table 4.1, Supplementary Table 4.3). These 13 genes include OVOC2486, OVOC3203, OVOC7314, OVOC7381, OVOC7786, OVOC7911, OVOC8600, OVOC8754, OVOC9575, OVOC9592, OVOC9752, OVOC9990, and OVOC10103. Previous *O. volvulus* studies have confirmed 15 of the 30 proteins are excretory/secretory proteins or are found in the hypodermis of the host and thus can be inferred that the *C. johnstoni* orthologues are similarly either excretory/secretory proteins or located in the hypodermis. The remaining 15 proteins are located within the cells either in the nucleus, endoplasmic reticulum, cytoskeleton, transmembrane or are generally intracellular proteins that are yet to be characterised (Table 4.1).

A summary of where or when the genes are expressed in *O. volvulus* can be useful to infer when they may be expressed in *C. johnstoni*. Several of the 30 *O. volvulus* immunogenic proteins appear to be expressed in all the life stages of the parasite. Others are specific to either the adult stage or the infective larval stage (iL3) (Table 4.1). As an immune response is observed when the *O. volvulus* microfilariae die in the host skin, it could be presumed that the antigen must be present in the microfilariae for such a response to occur. The location of where these genes are expressed could be useful for identifying the antigens driving the observed immunopathology in *O. volvulus*-infected patients. As many of these proteins are excretory/secretory proteins, it is plausible to assume they are available to be recognised by the hosts' immune response more commonly than those hidden in the cell.

Several of the proteins top BLAST matches are to another closely related nematode as expected but not to a known structure or function that has been previously characterised for these studied *O. volvulus* proteins. For example, OVOC1952 top result is to a *W. bancrofti* hypothetical protein, and WormBase Parasite identifies OVOC1952 as an orthologue of C34E7.4 (*C. elegans*) while in previous publications has also been identified as a putative ganglioside GM2 activator protein (Ov-GM2AP) (Table 4.1) (Njume et al., 2019). Another example is OVOC5823 top BLAST result matching to a LisH motif of *W. bancrofti*, but WormBase Parasite identified this as an orthologue of *C. elegans* unc-60 (Table 4.1). Nematode proteins that are recognised by the host's immune system are

largely understudied, thus there is likely to be variations of protein characterisation. There are still *O. volvulus* genes that have not been characterised, and thus functions that are not recorded on NCBI and WormBase Parasite consequently making interpretation of these proteins difficult.

OVOC10995 is the only protein whose *C. johnstoni* orthologue (Cjn_gene9844) does not have a BLAST result (Table 4.1). Cjn_gene9844 has an amino acid length of 114 bp, which is a short sequence and appears that BLAST is unable to match to the NR database with reliable e-value and bit scores (Supplementary Table 4.3). Other *C. johnstoni* query sequences are approximately this length but conversely shared enough similarity and matched to a BLAST result (Supplementary Table 4.3). As several of the other *C. johnstoni* proteins appear to have a similar putative function to the *O. volvulus* immunogenic proteins, it could be reasonable to infer Cjn_gene9844 would have a similar function as OVOC10995, succinate semi aldehyde dehydrogenase (Table 4.1, Supplementary Table 4.3).

Commonly the *C. johnstoni* top BLAST result matches to very closely related nematodes which are very promising for these gene candidates and the quality of the predicted proteins (Table 4.1, Supplementary Table 4.3). Norice-Tra et al. (2017) and McNulty et al. (2015) identified the host's immune system recognises this set of *O. volvulus* proteins. The BLAST results are consistently matching to proteins that appear to be recognised in some way by the host's immune system (Table 4.1, Supplementary Table 4.3). Some of these proteins include calponin OV9M, ganglioside GM2 activator (Ov-GM2AP), ShK domains, adenylyl cyclase-associated protein (CAP), glutathione S-transferase (GST), reticulon-like proteins, fructose-bisphosphate aldolase, calreticulin, Sh2 domain, TTR-52, superoxide dismutase, and Ov33 immunodominant antigen (Table 4.1, Supplementary Table 4.3).

The percentage (%) similarity of amino acid sequence between *C. johnstoni* and *O. volvulus* is represented in Table 4.1, revealing substantial differences across the 30 orthologues. OVOC860, OVOC5823, OVOC9984, OVOC9225, OVOC8985, OVOC8754 have amino acid similarities above 80%, while OVOC1897, OVOC1952, OVOC2486, OVOC9990, OVOC10995, OVOC11847 and OVOC12769 have amino acid similarities below 50% (Table 4.1).

All the genes share a one-to-one orthologous relationship except for OVOC1952 and OVOC7314 who share a many-to-one and one-to-many orthologous relationship, respectively with their *C. johnstoni* orthologues.

Table 4.1: The 30 *Onchocerca volvulus* immunogenic proteins and corresponding *Cercopithifilaria johnstoni* orthologues are described revealing their top BLAST results to the NCBI database, % identity, protein alignment length, e-value, bit score, location of expression in the cell (derived from *Onchocerca volvulus* experimentation), is the protein secreted and the % amino acid alignment similarity. Lastly, the orthology relationships between *Cercopithifilaria johnstoni* and *Onchocerca volvulus* are described.

Query (C. johnstoni)	Query (O. volvulus)	subject (blast NCBI)	description (NCBI)	OVOC putative function (WBP)	% identity	alignment length	e-value	bit score	Location in cell, surface, secreted?	When expressed	Orthology (1-to-1, 1-to-many etc.)
Cjn_gene4340	OVOC860	P37801.2	Calponin homolog OV9M	Calponin homolog OV9M	99.72	357	0	741	longitudinal muscles below the hypodermis	all life stages	1-to-1
Cjn_gene7687	OVOC1897	CRZ21860.1	BMA-EAT-20 [B. malayi]	EAT-20	46.687	649	2.04E-158	488	hypodermis	adult, L3	1-to-1
Cjn_gene5098	OVOC1952	EJW86002.1	hypothetical protein WUBG_03087 [W. bancrofti]	A0A2K6VRV9 - uncharacterised protein (C. elegans orthologue C34E7.4)	72.973	259	1.33E-140	403	excretory/secretory	all life stages	many-to-1

Cjn_gene7514	OVOC2486	EJD74931.1	hypothetical protein LOAG_17826 [L. loa]	A0A2K6VUT6 - uncharacterised protein OR ShK domain	58.497	306	9.64E-94	295	intracellular	all life stages	1-to-1
Cjn_gene6823	OVOC3177	EFO26240.2	hypothetical protein LOAG_02238 [L. loa]	A0A044SS43 - PHD-type (ZINC finger) domain-containing protein	79.15	1271	0	1868	nucleus, secretory vesicles	L3	1-to-1
Cjn_gene380	OVOC3203	XP_001891888.1	CAP protein [B. malayi]	Adenylyl cyclase-associated protein	71.494	1091	0	1509	excretory/secretory	all life stages	1-to-1
Cjn_gene6492	OVOC5419	EJW87928.1	3-hydroxyacyl-CoA dehydrogenase [W. bancrofti]	A0A044TS06 - uncharacterised protein (C. elegans orthologue ard-1)	94.841	252	1.05E-176	494	hypodermis	all life stages	1-to-1
Cjn_gene5271	OVOC5823	EJW78284.1	hypothetical protein WUBG_10805 (CTLH/CRA C-terminal to LisH motif domain) [W. bancrofti]	A0A044TYD3 - uncharacterised protein (C. elegans orthologue unc-60)	94.894	235	2.53E-153	434	intracellular	all life stages	1-to-1

Cjn_gene5847	OVOC7314	AAG44695.1	glutathione S-transferase Ia [<i>O. volvulus</i>]	Glutathione S-transferase	100	250	0	514	outer surface of hypodermis	all life stages	1-to-many
Cjn_gene413	OVOC7381	VDK80440.1	unnamed protein product [<i>O. ochengi</i>]	Reticulon-like protein	82.308	130	3.25E-66	213	Endoplasmic reticulum	all life stages	1-to-1
Cjn_gene8088	OVOC7786	AAD38403.1	fructose 1,6 bisphosphate aldolase [<i>O. volvulus</i>]	Fructose-bisphosphate aldolase	100	363	0	756	body wall muscle/reproductive tract adult females	L3	1-to-1
Cjn_gene8269	OVOC7911	P11012.2	Calreticulin (RAL1 antigen)	A0A044UWC0 - uncharacterised protein (<i>C. elegans</i> orthologue crt-1 - calreticulin)	99.408	338	0	681	Endoplasmic reticulum lumen	larval	1-to-1
Cjn_gene2996	OVOC8600	XP_003143117.1	SH2 domain-containing protein [<i>L. loa</i>]	SH2 domain-containing protein	70.43	186	9.32E-86	261	cytoskeleton		1-to-1
Cjn_gene_11	OVOC8754	Q25619.1	Fatty-acid and retinol-binding protein 1 (Ov20)	Fatty-acid and retinol-binding protein 1	100	173	5.40E-121	347	membrane		1-to-1

Cjn_gene5764	OVOC8985	CDQ04841.1	BMA-CYN-16 [<i>B. malayi</i>]	PPlase cyclophilin-type domain-containing protein (<i>C. elegans</i> orthologues tpi-1)	85.281	462	0	719	cytoplasm	all life stages	1-to-1
Cjn_gene3138	OVOC9225	CRZ22798.1	Bm5820, partial [<i>B. malayi</i>]	A0A044V9G2 - uncharacterised protein	90.82	512	0	931	cuticle, hypodermis, excretory/secretory	adult	1-to-1
Cjn_gene5845	OVOC9575	AAB69625.2	activation-associated secreted protein-1 [<i>O. volvulus</i>]	Activation-associated secreted protein-1	96.216	185	7.11E-131	374	Granules of GE, excretory/secretory	L3 stage	1-to-1
Cjn_gene8368	OVOC9592	EJD73678.1	hypothetical protein LOAG_18910 (TTR-52) [<i>L. loa</i>]	A0A044VD77 - uncharacterised protein (TTR-52)	71.014	138	9.20E-57	182	extracellular domain, excretory/secretory	L3, mf	1-to-1
Cjn_gene1728	OVOC9752	AAC77922.1	peroxidoxin-2 [<i>O. ochengi</i>]	A0A044VFS3 - uncharacterised protein (<i>C. elegans</i> orthologue prdx-2)	95.652	184	2.61E-128	367	excretory/secretory	all life stages	1-to-1

Cjn_gene5663	OVOC9984	CAA31690.1	immunodominant antigen, partial [<i>O. volvulus</i>]	Immunodominant antigen Ov33-3	100	132	3.22E-92	275	extracellular region or secreted	L3	1-to-1
Cjn_gene3696	OVOC9988	ACB70199.1	rainforest immunodominant hypodermal antigen [<i>O. ochengi</i>]	OV-17 antigen	99.39	164	4.19E-114	328	hypodermal layer (excretory/secretory)	all life stages	1-to-1
Cjn_gene3697	OVOC9990	AAB53809.1	RAL-2 homolog, partial [<i>A. viteae</i>]	DUF148 domain-containing protein	50.806	124	1.18E-36	130	hypodermal, excretory/secretory	adult, L3	1-to-1
Cjn_gene3855	OVOC10067	EYC07471.1	hypothetical protein Y032_0070g452 [<i>Ancylostoma ceylanicum</i>]	A0A044QKJ7 - uncharacterised protein (c. elegans orthologue unc-52)	49.981	2593	0	2380	extracellular region or secreted, basement membrane	all life stages	1-to-1
Cjn_gene2748	OVOC10103	KHN78795.1	Neprilysin-2 [<i>T. canis</i>]	A0A044QL85 - uncharacterised protein (<i>C. elegans</i> orthologue nep-11)	72.48	625	0	985	transmembrane	all life stages	1-to-1

Cjn_gene9844	OVOC1099 5	XP_00189856 3.1	hypothetical protein Bm1_35580 [<i>B. malayi</i>]	A0A2K6VGV2 - uncharacterised protein OR ALDH5A1 - succinate- semialdehyde dehydrogenase	37.615	109	2.41E- 06	52	pharyngeal muscle cell	adult, L3	1-to-1
Cjn_gene6611	OVOC1151 7	P24706.1	Superoxide dismutase [Cu-Zn]	Superoxide dismutase [Cu- Zn]	100	151	9.05E- 105	304	cytoplasm		1-to-1
Cjn_gene235	OVOC1184 7	CRZ23009.1	Bm8924 (Chondroitin proteoglycan 4) [<i>B. malayi</i>]	A0A044RF89 - uncharacterised protein OR RNA-binding protein Nova	45.626	423	1.80E- 92	293	neurons	all life stages	1-to-1
Cjn_gene4402	OVOC1240 0	EJW76014.1	hypothetical protein WUBG_1307 6, partial [<i>W. bancrofti</i>]	A0A044RNX4 - uncharacterised protein (<i>C. elegans</i> orthologue C08E8.2 - adipocyte plasma membrane associated protein)	67.273	110	1.14E- 47	158	endoplasmic reticulum	adult, L3	1-to-1

Cjn_gene1041 1	OVOC1244 9	CDQ06623.1	Bm8327 [<i>B. malayi</i>]	A0A044RPP5 - uncharacterised protein	64.865	74	1.98E- 31	119	transmembrane	adult female	1-to-1
Cjn_gene5503	OVOC1276 9	AAD27587.1	SLAP-1 protein [<i>O. volvulus</i>]	Larval 18 kDa protein; Ov64; SLAP-1 protein	93.443	122	9.20E- 75	226	granules of GE, cuticle	L3	1-to-1

4.3.2 Evidence of evolutionary selection on *Cercopithifilaria johnstoni* and *Onchocerca volvulus* orthologues of proteins with a putative immunogenic function

PAML is used to assess the measure of strength and mode of selection acting on the protein-coding genes. dN/dS is a measure of the ratio of nonsynonymous to synonymous nucleotide substitutions in an alignment of coding nucleotide sequences, and that dN/dS ratios greater than one indicate diversifying selection. In contrast, dN/dS ratios less than one indicate purifying selection. dN/dS ratios approximately equal to one suggest they are evolving neutrally. The aim is to identify protein-coding sequences that show diversifying or purifying selection in both *C. johnstoni* and *O. volvulus* genes compared to the other filarial species within each orthogroup including *A. viteae*, *B. malayi*, *B. pahangi*, *B. timori*, *D. immitis*, *L. loa*, *L. sigmodontis*, *O. flexuosa*, *O. ochengi* and *W. bancrofti*.

Among the 30 proteins, diversifying selection ($dN/dS > 1$) is detected in 16 of the 30 orthologues, with two orthologues demonstrating strong diversifying selection ($dN/dS > 2$), OVOC860 and OVOC10103 (Table 4.2). Purifying selection ($dN/dS < 1$) is detected in the remaining 13 orthologues, with evidence for strong purifying selection ($dN/dS < 0.6$) in five orthologous proteins, OVOC12769, OVOC7381, OVOC8600, OVOC9984 and OVOC9988 (Table 4.2).

Table 4.2: PAML dN/dS ratios for *Cercopithifilaria johnstoni* and *Onchocerca volvulus* compared to the phylogenetic tree for the 30 orthologous genes. The number of nonsynonymous sites (N) and synonymous sites (S).

<i>O. volvulus</i> ID	<i>C. johnstoni</i> ID	N	dN	S	dS	dN/dS
OVOC860	Cjn_gene4340	822.4	2.280	284.6	0.873	2.612
OVOC10103	Cjn_gene2748	1495.3	2.020	520.7	0.907	2.228
OVOC8985	Cjn_gene5764	1028.4	1.550	381.6	0.816	1.899
OVOC7786	Cjn_gene8088	968.5	1.730	339.5	0.983	1.760
OVOC12400	Cjn_gene4402	234.3	2.035	95.7	1.351	1.506
OVOC9592	Cjn_gene8368	332.1	1.739	117.9	1.175	1.480
OVOC11517	Cjn_gene6611	351.8	1.607	122.2	1.179	1.417
OVOC1952	Cjn_gene5098	500.8	2.039	177.0	1.494	1.365
OVOC1897	Cjn_gene7687	1454.8	1.819	537.2	1.363	1.334
OVOC11847	Cjn_gene235	1074.7	1.834	377.3	1.402	1.308
OVOC5419	Cjn_gene6492	574.1	1.491	196.9	1.148	1.299
OVOC7911	Cjn_gene8269	818.2	1.712	297.8	1.404	1.219
OVOC2486	Cjn_gene7514	1447.5	2.050	496.5	1.764	1.162
OVOC8754	Cjn_gene_11	384.6	1.141	134.4	1.004	1.136
OVOC9990	Cjn_gene3697	483.0	2.450	162.0	2.288	1.071
OVOC10995	Cjn_gene9844	264.9	2.210	89.1	2.157	1.025
OVOC3203	Cjn_gene380	2452.9	1.342	886.1	1.323	1.014
OVOC3177	Cjn_gene6823	2992.9	1.518	1075.1	1.541	0.985
OVOC10067	Cjn_gene3855	6042	1.572	2112	1.610	0.976
OVOC7314	Cjn_gene5847	489.3	1.819	170.7	1.919	0.948
OVOC9575	Cjn_gene5845	411.5	2.160	146.5	2.501	0.864
OVOC9752	Cjn_gene1728	509.1	1.245	171.9	1.453	0.857
OVOC12449	Cjn_gene10411	167.3	1.473	57.7	1.755	0.839
OVOC5823	Cjn_gene5271	533.1	0.874	180.9	1.042	0.839
OVOC9225	Cjn_gene3138	1215.1	1.548	419.9	1.928	0.803
OVOC9988	Cjn_gene3696	371.6	1.987	126.4	3.277	0.606
OVOC8600	Cjn_gene2996	721.2	1.989	241.8	3.491	0.570
OVOC7381	Cjn_gene413	271.1	1.080	100.9	2.006	0.538
OVOC9984	Cjn_gene5663	290.6	0.747	105.4	1.451	0.515
OVOC12769	Cjn_gene5503	302.3	1.621	99.7	4.849	0.334

4.3.3 Presence of immunodominant motifs and epitopes in *Cercopithifilaria johnstoni* protein-coding genes

The *C. johnstoni* proteome is examined for the presence of three immunodominant motifs (PxxTQE, DGxDK, QxSNxD) that have been identified across the *O. volvulus* proteome. These *O. volvulus* proteins containing the motifs could lead to novel candidates for diagnostic development (Lagatie et al., 2017). The three motifs have now been identified in *C. johnstoni*. They are present in various *C. johnstoni* protein-coding genes, DGxDK in 27 genes (Table 4.3), PxxTQE in 14 genes (Table 4.4) and QxSNxD are present in 34 genes throughout the predicted *C. johnstoni* protein-coding genes (Table 4.5).

The *C. johnstoni* genes that contain the immunodominant motifs are analysed using BLAST to determine possible putative function. Several of the top BLAST results match to NCBI proteins of very closely related filarial nematodes mostly *A. viteae* and *L. sigmodontis* (Table 4.3, 4.4, 4.5). As these nematodes do not have high-quality genome assemblies and gene annotations, many genes are uncharacterised and appear as unnamed proteins without derived functions. The second top BLAST result is then reported to determine the kind of protein the *C. johnstoni* gene could be that contains these immunodominant motifs (Supplementary Table 4.4, 4.5, 4.6). Cjn_gene1838 and Cjn_gene9587 did not share homology to any result on NCBI (Table 4.3). Cjn_gene7018 did not share homology to a result on NCBI (Table 3.4). Lastly, Cjn_gene10102 did not share homology to a NCBI result (Table 3.5).

None of the proteins identified with the presence of one of the three immunodominant motifs appears to have any functions in the regulation of the host's immune response. Several *C. johnstoni* genes appear to be involved in biological function and structural function of the proteins but not specifically functions known to control or be important towards the effects on the host immune system (Table 4.3, 4.4, 4.5). Several of the *C. johnstoni* genes containing an *O. volvulus* immunodominant motif GO terms included DNA or RNA binding, myosin complex, protein binding, metabolic processes and signalling pathways (Table 4.3, 4.4, 4.5).

Twenty-four genes with the presence of the DGxDK motif did not match to a GO term result or an InterPro result from the InterProScan analysis (Table 4.3). Nine genes with the presence of the PxxTQE motif did not match to a GO term

result or an InterPro result (Table 4.4). Finally, 29 genes with the presence of the QxSNxD motif did not match to a GO term result or an InterPro result (Table 4.5).

The search continued into the filarial nematode proteomes that have not been previously explored in the original publications. PxxTQE is present in 12 *A. viteae* genes, nine *B. pahangi* genes, nine *B. timori* genes, 23 *D. immitis* genes, 28 *L. loa* genes, 21 *L. sigmodontis* genes, 16 *O. ochengi* genes and nine *O. flexuosa* genes. DGxDK is present in 28 *A. viteae* genes, 34 *B. pahangi* genes, 24 *B. timori* genes, 36 *D. immitis* genes, 41 *L. loa* genes, 36 *L. sigmodontis* genes, 27 *O. ochengi* genes and 20 *O. flexuosa* genes. Lastly, QxSNxD is present in 43 *A. viteae* genes, 44 *B. pahangi* genes, 30 *B. timori* genes, 35 *D. immitis* genes, 30 *L. loa* genes, 28 *L. sigmodontis* genes, 37 *O. ochengi* genes and 31 *O. flexuosa* genes (Table 4.6).

Table 4.3: The *Cercopithifilaria johnstoni* proteins examined for the presence of the *Onchocerca volvulus* motif DGxDK from Lagatie et al. (2017). The *Cercopithifilaria johnstoni* protein top BLAST hit and putative function is reported with % identity, e-value and bits (bit score). The secondary BLAST hit is also reported as several of the BLAST hits are similar to uncharacterised proteins.

<i>C. johnstoni</i> protein	Ov Motif (DGxDK)	Top Blast Hit	Description (NCBI)	% identity	e-value	bits	GO term or InterPro	Description
Cjn_gene113	DGIDK	VDO29516.1	unnamed protein product [<i>Brugia timori</i>]	95	2.06E-62	209	IPR027791 IPR029044	Galactosyltransferase, C-terminal Nucleotide-diphospho-sugar
Cjn_gene298	DGDDK	XP_003135790.1	hypothetical protein LOAG_00202 [<i>Loa loa</i>]	66	5.4E-29	119		
Cjn_gene723	DGGDK	VBB27786.1	unnamed protein product [<i>Acanthocheilonema viteae</i>]	71.569	6.37E-35	137		
Cjn_gene896	DGWDK	VBB29410.1	unnamed protein product [<i>Acanthocheilonema viteae</i>]	77.5	7.95E-22	95.9		
Cjn_gene1838	DGSDK	No significant result found						
Cjn_gene2051	DGSDK	VBB28280.1	unnamed protein product [<i>Acanthocheilonema viteae</i>]	66.316	2.87E-38	141	IPR002486 GO:0042302	Nematode cuticle collagen, N-terminal Structural constituent of cuticle

Cjn_gene2143	DGSDK	VDO26168.1	unnamed protein product [<i>Onchocerca flexuosa</i>]	80.412	3.17E-49	161		
Cjn_gene2749	DGFDK	VDO83353.1	unnamed protein product [<i>Onchocerca flexuosa</i>]	75.789	6.67E-44	148		
Cjn_gene3213	DGKDK	CDP97362.1	BMA-MLT-8, isoform c [<i>Brugia malayi</i>]	96.774	8.17E-36	126		
Cjn_gene3906	DGTDK	VBB29280.1	unnamed protein product [<i>Acanthocheilonema viteae</i>]	87.368	3.47E-47	169	IPR011059 GO:0016810	Metal-dependent hydrolase, composite domain superfamily Hydrolase activity, acting on carbon- nitrogen (but not peptide) bonds
Cjn_gene3910	DGRDK	OZC10549.1	MOZ/SAS family protein [<i>Onchocerca flexuosa</i>]	95	2.39E-57	201		
Cjn_gene3959	DGLDK	VDK82394.1	unnamed protein product [<i>Litomosoides sigmodontis</i>]	76.667	2.19E-21	94.7		
Cjn_gene4253	DGEDK	VDK68607.1	unnamed protein product [<i>Litomosoides sigmodontis</i>]	88	5.47E-50	176		
Cjn_gene5140	DGSDK	VDO51626.1	unnamed protein product [<i>Onchocerca flexuosa</i>]	62	0.000000108	58.5		
Cjn_gene5421	DGGDK	VBB27562.1	unnamed protein product [<i>Acanthocheilonema viteae</i>]	76.25	2.31E-32	122		
Cjn_gene5897	DGVDK	VBB26915.1	unnamed protein product [<i>Acanthocheilonema viteae</i>]	81	3.9E-47	171		

Cjn_gene5916	DGTDK	VBB30828.1	unnamed protein product [<i>Acanthocheilonema viteae</i>]	59	4.17E-24	105		
Cjn_gene6634	DGLDK	XP_001902097.1	hypothetical protein Bm1_53145 [<i>Brugia malayi</i>]	79	5E-49	161		
Cjn_gene6658	DGSDK	EJW87161.1	DNA topoisomerase 2 [<i>Wuchereria bancrofti</i>]	99	4.13E-60	208	IPR002205 IPR013760 GO:0003918 GO:0005524 GO:0003677	DNA topoisomerase, type IIA, subunit A/C-terminal DNA topoisomerase, type IIA-like domain superfamily DNA topoisomerase type II (double strand cut, ATP-hydrolyzing) activity ATP binding DNA binding
Cjn_gene6700	DGSDK	OZC08743.1	hypothetical protein X798_04291 [<i>Onchocerca flexuosa</i>]	79	1.15E-49	179		
Cjn_gene7127	DGQDK	VBB28779.1	unnamed protein product [<i>Acanthocheilonema viteae</i>]	69.307	3.47E-30	123		
Cjn_gene7304	DGNDK	VBB30664.1	unnamed protein product [<i>Acanthocheilonema viteae</i>]	74	1.08E-39	150		
Cjn_gene7413	DGDDK	VDK78052.1	unnamed protein product [<i>Litomosoides sigmodontis</i>]	84	1.96E-28	117		

Cjn_gene7553	DGIDK	EJW73100.1	hypothetical protein WUBG_15993 [<i>Wuchereria bancrofti</i>]	95	1.71E-62	196	IPR001609 IPR027417 IPR036961 GO:0003774 GO:0005524	Myosin head, motor domain P-loop containing nucleoside triphosphate hydrolase Kinesin motor domain superfamily motor activity ATP binding
Cjn_gene7626	DGLDK	VDO41167.1	unnamed protein product [<i>Brugia timori</i>]	89	4.52E-59	187		
Cjn_gene8139	DGWDK	VBB34511.1	unnamed protein product [<i>Acanthocheilonema viteae</i>]	96	9.46E-61	202	SSF57603	Fnl-like domain
Cjn_gene8417	DGNDK	XP_001896085.1	hypothetical protein Bm1_23140 [<i>Brugia malayi</i>]	82.353	1.21E-49	171		
Cjn_gene9043	DGEDK	VBB29800.1	unnamed protein product [<i>Acanthocheilonema viteae</i>]	74.747	2.54E-40	149	IPR016181	Acyl-CoA N-acyltransferase
Cjn_gene9091	DGFDK	VBB29500.1	unnamed protein product [<i>Acanthocheilonema viteae</i>]	91.803	2.11E-32	122		
Cjn_gene9587	DGGDK	no significant result found						
Cjn_gene9909	DGGDK	EJW83096.1	hypothetical protein WUBG_05992 [<i>Wuchereria bancrofti</i>]	56.897	0.001	46.6		

Table 4.4: The *Cercopithifilaria johnstoni* proteins examined for the presence of the *Onchocerca volvulus* motif PxxTQE from Lagatie et al. (2017). The *Cercopithifilaria johnstoni* protein top BLAST hit and putative function is reported with % identity, e-value and bits (bit score). The secondary BLAST hit is also reported as several of the BLAST hits are similar to uncharacterised proteins.

<i>C. johnstoni</i> protein	Ov Motif (PxxTQE)	Top Blast Hit	Description (NCBI)	% identity	e-value	bits	GO term or InterPro	Description
Cjn_gene1496	PPETQE	VIO92450.1	F-box domain containing protein [<i>Brugia malayi</i>]	98	1.56E-64	207	IPR039719	F-box only protein 28
Cjn_gene2474	PQTTQE	VDN89017.1	unnamed protein product [<i>Brugia pahangi</i>]	65.517	7.54E-16	82		
Cjn_gene2824	PIDTQE	VDK87984.1	unnamed protein product [<i>Onchocerca ochengi</i>]	91	2.18E-59	189	IPR039796 IPR002744 IPR034904 GO:0106035	MIP18 family MIP18 family-like Fe-S cluster assembly domain superfamily Protein maturation by [4Fe-4S] cluster transfer
Cjn_gene3131	PIITQE	EJW79843.1	hypothetical protein WUBG_09247 [<i>Wuchereria bancrofti</i>]	85	1.25E-55	188	IPR003961 IPR036116 IPR013783 GO:0005515	Fibronectin type III Fibronectin type III superfamily Immunoglobulin-like fold Protein binding

Cjn_gene5166	PAVTQE	VBB34862.1	unnamed protein product [<i>Acanthocheilonema viteae</i>]	85	2.83E-56	182	IPR015212 IPR036305 GO:0005085 GO:0005737	Regulator of G protein signalling-like domain RGS domain superfamily Guanyl-nucleotide exchange factor activity Cytoplasm
Cjn_gene6484	PDETQE	EJW75397.1	hypothetical protein WUBG_13695 [<i>Wuchereria bancrofti</i>]	83.333	6.84E-11	60.1		
Cjn_gene6592	PTSTQE	EJW87958.1	hypothetical protein WUBG_01133 [<i>Wuchereria bancrofti</i>]	95	2.69E-60	192	IPR027640 IPR001752 IPR027417 GO:0007018 GO:0005524	Kinesin-like protein Kinesin motor domain P-loop containing nucleoside triphosphate hydrolase Microtubule-based movement ATP binding
Cjn_gene6623	PQVTQE	VDO47880.1	unnamed protein product [<i>Brugia timori</i>]	97	1.35E-63	206	IPR006140 IPR036291 GO:0055114 GO:0051287	D-isomer specific 2-hydroxyacid dehydrogenase, NAD-binding domain NAD(P)-binding domain superfamily Oxidation-reduction process NAD binding
Cjn_gene6756	PQYTQE	VIO94858.1	Uncharacterized protein BM_BM6058 [<i>Brugia malayi</i>]	80.769	3.57E-42	154		
Cjn_gene6854	PYTTQE	VBB30928.1	unnamed protein product [<i>Acanthocheilonema viteae</i>]	62.264	1.86E-12	67.8		

Cjn_gene6926	PKITQE	VIO96872.1	conserved hypothetical protein [<i>Brugia malayi</i>]	94.898	1.64E-61	200		
Cjn_gene7018	PSVTQE	No significant result						
Cjn_gene7205	PKHTQE	VBB26933.1	unnamed protein product [<i>Acanthocheilonema viteae</i>]	73	2.32E-35	138		
Cjn_gene8203	PSSTQE	VDK78150.1	unnamed protein product [<i>Litomosoides sigmodontis</i>]	75	1.14E-39	150		
Cjn_gene8783	PIVTQE	XP_020304849.1	hypothetical protein LOAG_18712 [<i>Loa loa</i>]	76.19	1.26E-37	143		
Cjn_gene8792	PEMTQE	VBB30575.1	unnamed protein product [<i>Acanthocheilonema viteae</i>]	81	3.19E-53	174	IPR010326 GO:0006887 GO:0000145	Exocyst complex component EXPC3/Sec6 Exocytosis exocyst
Cjn_gene9173	PDSTQE	VBB34141.1	unnamed protein product [<i>Acanthocheilonema viteae</i>]	93	1.9E-63	202	IPR003094 GO:0006003 GO:0005524 GO:0003824	Fructose-2,6-bisphosphatase Fructose 2,6-bisphosphate metabolic process ATP binding Catalytic activity
Cjn_gene9345	PESTQE	EJW76844.1	dynactin subunit 5 [<i>Wuchereria bancrofti</i>]	95.181	2.82E-50	166	IPR011004 IPR001451	Trimeric LpxA-like superfamily Hexapeptide repeat

Cjn_gene9881	PVRTQE	VDK84305.1	unnamed protein product [<i>Litomosoides sigmodontis</i>]	37.255	5.06E-23	101	IPR000668 IPR008765 GO:0006508 GO:0008234	Peptidase C1A, papain C-terminal Papain-like cysteine peptidase superfamily Proteolysis Cysteine-type peptidase activity
--------------	--------	------------	--	--------	----------	-----	--	--

Table 4.5: The *Cercopithifilaria johnstoni* proteins examined for the presence of the *Onchocerca volvulus* motif QxSNxD from Lagatie et al. (2017). The *Cercopithifilaria johnstoni* protein top BLAST hit and putative function is reported with % identity, e-value and bits (bit score). The secondary BLAST hit is also reported as several of the BLAST hits are similar to uncharacterised proteins.

<i>C. johnstoni</i> protein	Ov Motif (QxSNxD)	Top Blast Hit	Description (NCBI)	% identity	e-value	bits	GO term or InterPro	Description
Cjn_gene236	QLSNLD	VDM15452.1	unnamed protein product [<i>Wuchereria bancrofti</i>]	90	1.88E-59	192	IPR036595 GO:0005576	Alpha-macroglobulin, receptor-binding domain superfamily Extracellular region
Cjn_gene566	QVSNID	VBB34262.1	unnamed protein product [<i>Acanthocheilonema viteae</i>]	88.889	6.54E-56	189	IPR023578	Ras guanine nucleotide exchange factor domain superfamily
Cjn_gene740	QTSNID	VDO08428.1	unnamed protein product [<i>Brugia timori</i>]	91.919	3.8E-61	194		
Cjn_gene1272	QTSNFD	VBB32416.1	unnamed protein product [<i>Acanthocheilonema viteae</i>]	88.889	3.16E-29	114		
Cjn_gene1872	QQSNRD	VDM12400.1	unnamed protein product [<i>Wuchereria bancrofti</i>]	91.837	4.31E-55	185		
Cjn_gene2060	QVSNYD	VBB31776.1	unnamed protein product [<i>Acanthocheilonema viteae</i>]	75	4.79E-42	154		
Cjn_gene2092	QCSNLD	CTP81868.1	BMA-CLIP-1 [<i>Brugia malayi</i>]	81.905	1.45E-46	162		
Cjn_gene2177	QSSNSD	VDK88972.1	unnamed protein product [<i>Litomosoides sigmodontis</i>]	52.885	7.98E-19	90.9		

Cjn_gene2237	QSSNID	VBB27890.1	unnamed protein product [<i>Acanthocheilonema viteae</i>]	96.703	1.25E-53	181		
Cjn_gene2285	QLSNID	XP_020305302.1	hypothetical protein LOAG_18297 [<i>Loa loa</i>]	55.882	1.27E-21	99		
Cjn_gene2338	QDSNED	VBB25552.1	unnamed protein product [<i>Acanthocheilonema viteae</i>]	73.016	3.86E-14	75.9		
Cjn_gene2504	QRSNDD	VDM14604.1	unnamed protein product [<i>Wuchereria bancrofti</i>]	79.798	1.08E-42	147		
Cjn_gene2830	QRSNLD	VDO80627.1	unnamed protein product [<i>Onchocerca flexuosa</i>]	84.043	1.14E-49	164		
Cjn_gene3336	QNSNND	VIO94179.1	Uncharacterized protein BM_BM2531 [<i>Brugia malayi</i>]	87.755	6.78E-47	171		
Cjn_gene3426	QHSNED	VBB25233.1	unnamed protein product [<i>Acanthocheilonema viteae</i>]	84	5.45E-51	179	IPR002018 IPR029058	Carboxylesterase, type B Alpha/Beta hydrolase fold
Cjn_gene3912	QQSNDD	VDM94223.1	unnamed protein product [<i>Onchocerca ochengi</i>]	83	6.37E-56	179		
Cjn_gene4366	QSNWD	VDM92573.1	unnamed protein product [<i>Litomosoides sigmodontis</i>]	83.784	1.98E-51	183		
Cjn_gene4382	QSSNKD	XP_020303021.1	hypothetical protein LOAG_04731 [<i>Loa loa</i>]	93	4.7E-55	194		
Cjn_gene4529	QISNID	XP_001900642.1	von Willebrand factor type A domain containing protein [<i>Brugia malayi</i>]	89	1.85E-58	193	IPR002035 IPR036465	Von Willebrand factor, type A Von Willebrand factor A-like domain superfamily

Cjn_gene4783	QMSNED	OZC09104.1	hypothetical protein X798_03851 [<i>Onchocerca flexuosa</i>]	98	7.16E-62	213	IPR011603 IPR005475 IPR029061 GO:0003099 GO:0055114 GO:0030976	2-oxoglutarate dehydrogenase E1 component Transketolase-like pyrimidine-binding domain Thiamin diphosphate-binding fold Tricarboxylic acid cycle Oxidation-reduction process Thiamine pyrophosphate binding
Cjn_gene4935	QISNED	VDO22403.1	unnamed protein product [<i>Brugia timori</i>]	87	5.97E-48	160	IPR014851	BCS1, N-terminal
Cjn_gene5157	QKSNKD	VDM23186.1	unnamed protein product [<i>Wuchereria bancrofti</i>]	89	3.28E-57	190	IPR001619 IPR027482 IPR036045 GO:0016192	Sec1-like protein Sec1-like, domain 2 Sec1-like superfamily Vesicle-mediated transport
Cjn_gene5767	QASNSD	CDP93228.1	Bm9216 [<i>Brugia malayi</i>]	64.835	2.72E-31	119		
Cjn_gene5823	QPSNTD	EJW77691.1	hypothetical protein WUBG_11401 [<i>Wuchereria bancrofti</i>]	77.027	1.03E-28	109		
Cjn_gene6256	QLSNVD	VBB27931.1	unnamed protein product [<i>Acanthocheilonema viteae</i>]	78	2.66E-47	167	IRP036971 GO:0007165	3'-5'-cyclic nucleotide phosphodiesterase, catalytic domain superfamily Signal transduction

Cjn_gene6471	QNSNQD	VBB28331.1	unnamed protein product [<i>Acanthocheilonema viteae</i>]	82.178	9.25E-40	145		
Cjn_gene6608	QYSNND	VBB31882.1	unnamed protein product [<i>Acanthocheilonema viteae</i>]	79	3.64E-47	166		
Cjn_gene6761	QLSNED	VBB31958.1	unnamed protein product [<i>Acanthocheilonema viteae</i>]	89.744	3.63E-14	74.7		
Cjn_gene7385	QFSNDD	VBB28338.1	unnamed protein product [<i>Acanthocheilonema viteae</i>]	95	1.28E-60	206	IPR001930 IPR034015 IPR027268 GO:0006508 GO:0008237 GO:0008270	Peptidase M1, alanine aminopeptidase/leukotriene A4 hydrolase Aminopeptidase, leukotriene A4 hydrolase-like Peptidase M4/1, CTD superfamily Proteolysis Metallopeptidase activity Zinc ion binding
Cjn_gene7401	QDSNVD	VBB31503.1	unnamed protein product [<i>Acanthocheilonema viteae</i>]	95	6.22E-56	183	IPR042237 IPR002833 IPR023476 GO:0004045	Putative peptidyl-tRNA hydrolase PTRHD1 Peptidyl-tRNA hydrolase, PTH2 Peptidyl-tRNA hydrolase II domain superfamily Aminoacyl-tRNA hydrolase activity
Cjn_gene7670	QISNQD	VBB29893.1	unnamed protein product [<i>Acanthocheilonema viteae</i>]	43	6.49E-11	68.6		

Cjn_gene7777	QISNSD	VDK74113.1	unnamed protein product [<i>Onchocerca ochengi</i>]	78	2.52E-48	169		
Cjn_gene7945	QLSNDD	VDM07855.1	unnamed protein product [<i>Wuchereria bancrofti</i>]	48.507	1.61E-27	115		
Cjn_gene8122	QRSNND	VDK68243.1	unnamed protein product [<i>Onchocerca ochengi</i>]	82.828	7.33E-51	172	IPR000571 GO:0046872	Zinc finger, CCCH-type Metal ion binding
Cjn_gene8203	QISNTD	VDM12534.1	unnamed protein product [<i>Wuchereria bancrofti</i>]	82.243	1.79E-47	167		
Cjn_gene8213	QISNND	VDK65350.1	unnamed protein product [<i>Onchocerca ochengi</i>]	92	4.73E-55	188	IPR027059 IPR028565 IPR036168 GO:0006890 GO:0030126	Coatomer delta subunit Mu homology domain AP-2 complex subunit mu, C-terminal superfamily Retrograde vesicle-mediated transport, Golgi to endoplasmic reticulum COPI vesicle coat
Cjn_gene8516	QTSNID	EJW80653.1	phosphate transporter [<i>Wuchereria bancrofti</i>]	89.899	5.18E-59	190	IPR001204 GO:0006817 GO:0005315 GO:0016020	Phosphate transporter Phosphate ion transport Inorganic phosphate transmembrane transporter activity membrane
Cjn_gene8580	QQSNHD	VBB33965.1	unnamed protein product [<i>Acanthocheilonema viteae</i>]	78	5.28E-41	151		

Cjn_gene8849	QRSND	VBB31387.1	unnamed protein product [<i>Acanthocheilonema viteae</i>]	73.276	6.99E-46	168		
Cjn_gene8879	QSSNYD	VBB28303.1	unnamed protein product [<i>Acanthocheilonema viteae</i>]	76.699	2.71E-31	123		
Cjn_gene8897	QESNDD	VDM94342.1	unnamed protein product [<i>Onchocerca ochengi</i>]	81	1.86E-46	162		
Cjn_gene9527	QNSNKD	VBB34526.1	unnamed protein product [<i>Acanthocheilonema viteae</i>]	90	4.02E-41	146		
Cjn_gene10102	QKSNDD	No significant results					IPR000380 GO:0006265 GO:0003677 GO:0003916	DNA topoisomerase, type IA DNA topological change DNA binding DNA topoisomerase activity

Table 4.6: Number of genes containing immunodominant motifs (PxxTQE, DGxDK, QxSNxD) in filarial nematodes (Lagatie et al., 2017).

	PxxTQE	DGxDK	QxSNxD
<i>A. viteae</i>	12	28	43
<i>B. pahangi</i>	9	34	44
<i>B. timori</i>	9	24	30
<i>D. immitis</i>	23	26	35
<i>L. loa</i>	28	41	30
<i>L. sigmodontis</i>	21	36	28
<i>O. flexuosa</i>	9	20	31
<i>O. ochengi</i>	16	27	37

Thus, the presence of the 9-mer peptide is explored within the *C. johnstoni* genome and other filarial species not previously explored. The 9-mer peptide is present in 12 *C. johnstoni* predicted genes in the genome (Table 4.7). The *C. johnstoni* genes g6148.t1 and g6887.t1 have two instances of the 9-mer peptide present in the gene.

The *C. johnstoni* genes were analysed using BLAST to reveal the top and secondary BLAST result to infer putative functions for this group of genes containing the 9-mer peptide. All of the top BLAST results (Table 4.7) and secondary BLAST results (Supplementary Table 4.7) match to NCBI proteins of very closely related filarial nematodes mostly *A. viteae* and *L. sigmodontis*, but *W. bancrofti* and *L. loa* are also very common results. Similarly, to the motif BLAST results, the majority of the genes share homology to unnamed protein products because these set of nematode genes are not characterised with putative or known functions.

The *C. johnstoni* genes containing the poly-glutamine stretch 9-mer peptide do not have distinct immunogenic properties associated with the host's immune response. Only one of the *C. johnstoni* proteins matched to an InterPro result, Cjn_gene5989 (Table 4.7). The remaining *C. johnstoni* proteins containing the 9mer did not have a GO term or InterPro results (Table 4.7).

The search for the 9-mer, QQQQQQQQR peptide in the other filarial nematodes results in *A. viteae* containing the 9-mer in nine genes, three *B. timori* genes, 15 *B. pahangi* genes, nine *D. immitis* genes, 29 *L. loa* genes, 10 *L. sigmodontis* genes, seven *O. ochengi* genes, and is present in two *O. flexuosa* genes (Table 4.8).

The three *O. volvulus* motifs and the poly-glutamine stretch 9-mer peptide are not present in any of the 30 *C. johnstoni* genes that OrthoFinder2 predicted as an orthologue of the *O. volvulus* immunogenic proteins.

Table 4.7: The *Cercopithifilaria johnstoni* proteins examined for the presence of the *Onchocerca volvulus* epitope QQQQQQQQR from Lagatie et al. (2018). The *Cercopithifilaria johnstoni* protein top BLAST hit and putative function is reported with % identity, e-value and bits (bit score). The secondary BLAST hit is also reported as several of the BLAST hits are similar to uncharacterised proteins.

<i>C. johnstoni</i> protein	Top Blast Hit	Description (NCBI)	% identity	e-value	bits	GO term or InterPro	Description
Cjn_gene194	VBB34096.1	unnamed protein product [<i>Acanthocheilonema viteae</i>]	61.818	1.27E-11	70.1		
Cjn_gene2327	VBB32108.1	unnamed protein product [<i>Acanthocheilonema viteae</i>]	60.825	1.17E-20	96.3		
Cjn_gene2766	VDK87033.1	unnamed protein product [<i>Onchocerca ochengi</i>]	63.265	1.3E-19	90.9		
Cjn_gene2772	VBB32708.1	unnamed protein product [<i>Acanthocheilonema viteae</i>]	61	4.87E-20	94.4		
Cjn_gene5035	VDK79452.1	unnamed protein product [<i>Litomosoides sigmodontis</i>]	60	0.00000447	52		
Cjn_gene5350	CDP96346.1	Bm9981, isoform b [<i>Brugia malayi</i>]	70.33	8.01E-34	133		
Cjn_gene5989	VBB35186.1	unnamed protein product [<i>Acanthocheilonema viteae</i>]	94.915	4.83E-34	124	IPR000859 IPR035914	CUB domain

							Spermahesin, CUB domain superfamily
Cjn_gene6920	VDM92520.1	unnamed protein product [<i>Onchocerca ochengi</i>]	73	5.44E-13	74.3		
Cjn_gene7343	EJW80037.1	hypothetical protein WUBG_09053 [<i>Wuchereria bancrofti</i>]	54.082	2.69E-21	95.5		
Cjn_gene7486	No significant result					No significant result	
Cjn_gene8464	EJW82009.1	hypothetical protein WUBG_07080 [<i>Wuchereria bancrofti</i>]	78.481	3.21E-33	125		
Cjn_gene8597	No significant result					No significant result	

Table 4.8: Identifying the poly-glutamine stretch in the N-terminal region of *Onchocerca volvulus* protein (OVOC9988) 9-mer QQQQQQQQR in filarial nematodes.

Species	9-mer
<i>A. viteae</i>	9
<i>B. pahangi</i>	15
<i>B. timori</i>	3
<i>D. immitis</i>	9
<i>L. loa</i>	29
<i>L. sigmodontis</i>	10
<i>O. flexuosa</i>	2
<i>O. ochengi</i>	7

4.4 Discussion

The filarial nematode *C. johnstoni* can cause immunopathology in rats similar to that in which *O. volvulus* elicits in human onchocerciasis (Vuong et al., 1993). It could be hypothesised that if there are antigens present that have identical or near-identical structures presented in the same immunological context, i.e., skin and eye in rodents and humans from *C. johnstoni* and *O. volvulus* respectively, then the hosts are likely to produce similar immune responses. Therefore, part of the immune response observed in *C. johnstoni*-infected rats could be driven by *C. johnstoni* orthologues of *O. volvulus* antigens.

The chapter aimed to identify *C. johnstoni* orthologous proteins of *O. volvulus* immunogenic antigens. The long-term goal is to reduce the long list of known *O. volvulus* immunogenic proteins to a concentrated short-list of candidates. The concentrated list could then be explored in the *C. johnstoni* animal model to aid onchocerciasis research in understanding the immunopathology at play in *O. volvulus*-infected individuals. As *C. johnstoni* has not been studied previously, bioinformatics analyses are heavily reliant on previously identified *O. volvulus* proteins. The proteins from Norice-Tra et al. (2017) and McNulty et al. (2015) were chosen to be the focus of Chapter Four as these proteins have been very commonly explored in previous literature and have been the focus of multiple reviews, thus were an excellent starting point to identify whether there are any *C. johnstoni* orthologues.

4.4.1 *Cercopithifilaria johnstoni* and *Onchocerca volvulus* share orthologues of known *Onchocerca volvulus* immunogenic proteins with putative functions associated with host immune response

There were 30 of the 49 chosen *O. volvulus* immunogenic proteins from Norice-Tra et al. (2017) and McNulty et al. (2015) that shared an orthologous relationship with *C. johnstoni* (Table 4.1, Supplementary Table 4.3) leaving 19 proteins unaccounted for in the *C. johnstoni* protein-coding list. Exonerate was used to explore these 19 proteins and identify whether they are absent from the *C. johnstoni* genome or do not share enough sequence similarity to be considered an orthologue of *O. volvulus* genes. The 19 *O. volvulus* immunogenic proteins do not have one-to-one orthologues with *C. johnstoni* but were identified using exonerate. It appears that these 19 *O. volvulus* genes share some

sequence homology with *C. johnstoni* but appear to have more divergent sequences that cannot be identified as orthologues by OrthoFinder2 for further analysis. These genes would not have passed the rigorous criteria set by the OrthoFinder2 algorithm and simply do share orthologues for these particular genes (Emms and Kelly, 2019).

C. johnstoni and *O. volvulus* are more divergent species than *O. volvulus* and sister species *O. ochengi*. Thus, it is plausible to assume that there are multiple genes throughout the *C. johnstoni* genome that are divergent as a result of differences in gene content between the two species. There are likely to be other immunogenic proteins in *C. johnstoni* that have not been identified throughout this study that do not share orthologues in *O. volvulus* purely because they are different species. Alternatively, these 19 genes could be misassembled or misaligned in the *C. johnstoni* genome. Three gene prediction methods were used in Chapter Three to determine the most appropriate gene prediction method for the *C. johnstoni* genome. The Augustus protein prediction method was chosen because it performed the best according to BUSCO and OrthoFinder2 analyses predicting the highest number of genes (Chapter Three). A significant conclusion from Chapter Three was more *C. johnstoni* data; specifically, RNA-Seq data is required to confirm the predicted protein-coding genes, which was beyond the scope of this project. It will be necessary to revisit the 19 poorly aligned *O. volvulus* immunogenic genes when it is possible to include RNA-Seq data and determine whether the proteins are divergent from *C. johnstoni* or whether they were misaligned and misassembled as a result of the gene prediction method used. The addition of RNA-Seq data and improvement in the prediction of protein-coding genes could improve the overall prediction of the 19 genes that appear to be divergent from *C. johnstoni*. Further exploration of these genes is required.

The proteins matching to putative functions involved in the host immune response are of particular interest for this study because they could be initial targets to experimentally explore whether the similarity in antigens between *C. johnstoni* and *O. volvulus* is driving the similar immunopathology. Without further research, it is not possible to identify which of the candidates are more important targets over the others and thus the 30 candidates (Table 4.1) are a good starting point to explore in the physical *C. johnstoni* animal model. There

are a few criteria that could be considered to refine the list of 30 genes. Firstly, the *C. johnstoni* proteins that have high sequence similarity compared to the *O. volvulus* proteins that could be involved in the host's immune responses could be an ideal starting list to use in experiments to observe protein expression levels in the *C. johnstoni*-rodent animal model. The *C. johnstoni* proteins with confident one-to-one orthology to *O. volvulus* immunogenic proteins that displayed high percentage identity and low e-value probabilities that occurred by chance. These alignments sharing similarity to the query sequence could be suitable candidates to explore first before trialling other protein candidates experimentally. It would be worth isolating and purifying the *C. johnstoni* proteins to characterise their function determining whether they are true orthologues of the *O. volvulus* proteins or have the same putative function as bioinformatically identified throughout this thesis. Finally, comparing immunoreactivity profiles of the *O. volvulus* and *C. johnstoni* orthologues would be highly beneficial to identify whether these proteins react similarly.

Several of the immunogenic proteins have been studied in onchocerciasis, for example, OVOC7314 is characterised as a glutathione S-transferase structure which has been proposed to act as an immune modulator mostly because it is an extracellular enzyme on the outer surface of the hypodermis (Perbandt et al., 2008). OVOC7314 is known to have highly antigenic sites and Prostaglandin D Synthases (PGDS) activity which could indicate that parasite-derived eicosanoids influence host inflammatory and immune cells (Hirai et al., 2001). Another example is OVOC7911 matching to a RAL-1 antigen, calreticulin. Calreticulin is known to be part of the MHC 1 peptide loading complex more specifically in the transient multi-subunit membrane complex in the endoplasmic reticulum that is essential for establishing a hierarchical immune response (Blees et al., 2017). OVOC7786 is a fructose-1, 6-bisphosphate aldolase and has been demonstrated as a target for initiating protective immunity to onchocerciasis (McCarthy et al., 2002). It has also been explored as a good target for controlling infections caused by pathogens or parasites (Prasad et al., 2013). Peroxifoxin-2 is a protein structure that provides antioxidant protection and acts as a signalling molecule or chaperone and has been studied to some extent in *O. volvulus* (OVOC9752). OVOC11847 or Ov-39 has been identified as an antigenically cross-reactive protein with the human retinal antigen hr44 and has been found to induce ocular inflammation in naive rats, which leads to the hypothesis that autoimmune

reactivity could play a role in ocular lesion development in onchocerciasis (McKechie et al., 1993; McKechie et al., 2002). Lastly, OVOC2486 match to a ShK domain which is a selective inhibitor of voltage-gated potassium channels (Chhabra et al., 2014). As potassium channels have been widely regarded as a therapeutic target for immunomodulation in autoimmune diseases, the inhibiting nature of ShK-like immunomodulatory peptide could explain the protective effects of parasitic worms in autoimmune diseases (Chhabra et al., 2014; Chang et al., 2018). The *C. johnstoni* orthologues of these *O. volvulus* proteins encodes very similar protein structures from NCBI (Supplementary Table 4.3) and thus could be expressed in the rodent model in a similar way to how these studied *O. volvulus* proteins have been expressed. These *O. volvulus* targets could be involved in the unique immunopathology observed in *O. volvulus*-infected individuals. If the *C. johnstoni* orthologues of these *O. volvulus* immunogenic proteins prove to be immunogenic in the future rodent model experiments, then this evidence could lead to explain what is driving the immunopathology and thus disease. Alternatively, future experiments reveal the host immune system responds differently to these *C. johnstoni* orthologues compared to the proteins of *O. volvulus* and thus concludes the proteins themselves are not driving the similar immunopathology observed in rats and humans.

Despite the list of proteins explored throughout Chapter Four that were known *O. volvulus* immunogenic proteins, there were still a few matches are to DUFs (Domain of Unknown Function) and proteins more commonly involved in protein structure or binding, i.e., adenylyl cyclase-associated proteins (CAP), calponin and 3-hydroxy acyl-CoA dehydrogenase. DUFs are known to be common throughout filarial nematode genomes because of the vast number of uncharacterised genes. Without an abundance of genomic and proteomic data, it is often difficult to characterise all identified genes within filarial genomes. It would be worth exploring the DUFs and structural proteins in future laboratory experiments to characterise and confirm their functions and roles the proteins play within the parasite or in host-parasite relationships. An interesting question to explore could be to determine whether these structural proteins and DUFs are essential to the survival or fitness of *O. volvulus* and then whether the orthologues in *C. johnstoni* are also essential to *C. johnstoni*.

The bioinformatics approach has now provided a list of known *O. volvulus* immunogenic targets and their corresponding *C. johnstoni* orthologues with putative functions.

4.4.2 Evolutionary selection identified in *Cercopithifilaria johnstoni* and *Onchocerca volvulus* orthologous compared to other closely related filarial nematodes

Identifying selection pressures on genes of *C. johnstoni*, *O. volvulus*, and other filarial nematodes could identify evolutionary responses to the hosts' immune systems. A preliminary analysis has been conducted to identify whether the 30 orthologues between *C. johnstoni* and *O. volvulus* immunogenic proteins are under selective pressure. Proteins that are involved with the immunogenic response of onchocerciasis should be accessible to the hosts' immune system. The immunogenic proteins in *O. volvulus* elicit strong antibody responses in infected people. There could be immunogenic traits that are benefiting *C. johnstoni* and *O. volvulus* that are not observed in other nematodes but are examined here. If a host immune response can damage the parasite, i.e., is protective to the host, then it will exert a selection pressure to which the parasite may then respond. One response, the immunological "arms race" is that the pathogen or parasite varies the antigenic character of the protein that is targeted (Kosiol and Anisimova, 2019).

Orthogroups OVOC860 and OVOC10103 appear to have strong diversifying selection observed in both *C. johnstoni* and *O. volvulus* genes compared to the remaining filarial nematodes (Table 4.2). A site will only be considered under positive (diversifying) selection if the nonsynonymous rate, averaged over all of the lineages in the phylogeny, is higher than the synonymous rate (Yang, 2000). OVOC860 is known as Ov9M a calponin homolog and CJg3607.t1 shared homology to *B. malayi* UNC87 isoform b which is also part of the calponin family (Table 4.1). As calponin is likely to be involved in muscle contraction, it could be inferred that these proteins are more important structurally than they are involved in the host immune response. Both OVOC10103 and CJg2309.t1 are part of the Neprilysin metallopeptidase family (Table 4.1). Neprilysin is known to be an amyloid- β degrading enzyme in *C. elegans* (Hafez et al., 2011). The neprilysin function in *O. volvulus* and now *C. johnstoni* has not

been explored in detail to determine its effect on the host response. Indubitably, further analyses and confirmation of the current preliminary results are required to be confident about the genes undergoing diversifying selection.

Numerous orthogroups appear to have close to neutral or weak diversifying selection which is to be expected for the vast number of genes. Interestingly, the genes used throughout this study are known to be *O. volvulus* immunogenic proteins, thus exhibiting strong immune responses, yet many of the similar genes do not show strong diversifying or purifying selection. Neutral selection of these genes indicates that any variation is most likely due to random genetic drift of mutant alleles that are selectively neutral, i.e., do not affect the phenotype of the nematode and are not acted on by natural selection (Kimura and Crow, 1969; Yang, 2000). If this were true, then it could imply the putative immunogenic proteins occur as a result of random genetic drift and are not selected for throughout evolution (Kimura and Crow, 1969).

Purifying negative selection reduces the nonsynonymous substitution rate of protein-coding genes by selecting against change in amino acids (Siltberg and Liberles, 2002), which is common in many genes of nematodes for most of their evolutionary history. Orthogroups OVOC7381, OVOC8600, OVOC9984, OVOC9988 and OVOC12769 showed strong purifying selection on the *C. johnstoni* and *O. volvulus* genes (Table 4.2). The purifying selection indicates probable importance of these genes in both species and that the presence or absence of these genes' functions is likely to affect a worm's ability to survive to reproductive age; hence why many of the genes are under purifying selection. Several of these genes, with strong purifying selection, share homology to proteins which have previously shown to be immunogenic. For example, OVOC9984 and CJg4068.t1 match to Ov33 and Av33 immunodominant antigens, OVOC9988 and CJg3087.t1 match to Ov17 immunodominant antigen and DUF148, a possible *B. malayi* antigen, respectively which is an expected result as the *O. volvulus* proteins are known to be immunogenic. OVOC12769 is a SLAP1 (Src-like adapter) protein that negatively regulates T-cell receptor signalling and CJg6767.t1 shared homology to Av18 chromadorea abundant larval transcript protein (Table 4.1, Supplementary Table 4.3). The exceptions are OVOC7391 and CJg342.t1 that match to the reticulon protein family and OVOC8600 and CJg2910.t1 sharing homology to SH2 domain which are both

structurally conserved protein domains (Table 4.1, Supplementary Table 4.3). The proteins with putative structural functions may be equally as important to the parasites as the proteins with immunogenic functions.

These preliminary analyses have highlighted some key areas to explore further to understand how vital these putative immunogenic proteins are likely to be and what affect these proteins have that are undergoing diversifying or purifying selection. As this is the first, preliminary analysis using predicted *C. johnstoni* protein-coding genes; they should be cautiously interpreted because it is not known if they are robust predictions without more data to improve the accuracy of the *C. johnstoni* genome and thus gene prediction. The purpose of looking at diversifying and purifying selection was to explore if any of the *O. volvulus* and *C. johnstoni* orthologues were under selection compared to the other filarial nematodes within the orthogroups.

The protein-coding genes used in the selection analysis have been predicted from a first draft of the *C. johnstoni* genome assembled from genome data of one adult female worm. The genome will still require additional transcriptomic and proteomic information to improve gene prediction accuracy and thus improve the evolutionary selection analyses. Additional analyses could improve the confidence of detection of selection on these genes once the *C. johnstoni* genome annotation has been improved. The first analysis worth conducting with a larger *C. johnstoni* dataset could include running positive and neutral models of evolution on these putative immunogenic orthologues and determine statistical significance. The neutral theory of evolution states that most genetic variation observed in natural populations is due to the accumulation of neutral mutations that do not affect the phenotype or fitness of the organism (Brooker 2012). Once one adopts the hypothesis that sequence variation is neutral as the null hypothesis then it is possible to test whether the observed variation conforms to this expectation. If the selection is larger or smaller than the neutral expectation, then this will confidently predict diversifying or purifying selection, respectively. Conducting the analysis on a larger dataset than the 30 orthologues will provide more information on the selection acting upon these genes. It could reveal diversifying or purifying selection is more common on genes characterised as immunogenic over uncharacterised genes, or it could identify other proteins that have not been previously studied that are under very

strong diversifying or purifying selection that could be informative to understand disease immunopathology.

A genome-wide scan of diversifying and purifying selection could identify which regions of the filarial nematode genomes, specifically in *O. volvulus* and *C. johnstoni*, where new mutations are beneficial (Kosiol and Anisimova, 2019). Equally, it would identify regions of the genome that are not selectively conserved and thus rapidly evolving. The analysis could give a more accurate and detailed prediction of the selection in particular regions of the genome.

4.4.3 Immunogenic motifs and epitopes in filarial nematodes could be a potential avenue for drug targets providing evidence of immunoreactivity

Another avenue to identify immunologically relevant proteins is to identify the immunodominant motifs characterised in *O. volvulus* and identify these in *C. johnstoni* proteins. It may not be specific proteins that are involved in the disease immunopathology but rather particular motifs that elicit the host responses. The Lagatie et al. (2017, 2018) publications aimed to identify possible serodiagnostic candidates from motifs that were immunodominant. Thus a first step to identify whether *C. johnstoni* is a suitable model organism to study onchocerciasis is to determine whether *C. johnstoni* proteins contain any of the known *O. volvulus* immunodominant motifs. All three motifs, PxxTQE, DGxDK and QxSNxD, are present throughout the *C. johnstoni* proteome in various genes (Table 4.3, 4.4, 4.5). Knowing that *C. johnstoni* contains the same motifs, experiments can be conducted to determine whether these motifs are also immunodominant as was observed in the *O. volvulus* experiments (Lagatie et al. 2017).

The unknown *C. johnstoni* genes that contain the immunodominant motifs were analysed using BLAST and InterProScan to determine whether there was homology to immunogenic functions. Unfortunately, none of the *C. johnstoni* genes containing the immunodominant motif or 9-mer epitope has BLAST results, GO terms, or InterPro results matching to known filarial proteins involved in immune responses (Table 4.3, 4.4, 4.5, 4.7). Thus, the only way to know whether these genes are good candidates to explore immune responses is to determine

whether they are immunogenic, and if they are, proceed to further experiments in the possible *C. johnstoni* animal model.

The immunodominant motifs that were identified in other organisms in the peptide microarray experiments including *B. malayi*, *W. bancrofti*, *L. loa*, *Homo sapiens*, *Wolbachia*, *Plasmodium falciparum*, *Ascaris lumbricoides*, *Trichuris trichura*, *Ancylostoma duodenale*, *Necator americanus* and *Toxocara canis* (Lagatie et al., 2017) are expanded by including the filarial species used throughout this thesis. The three motifs PxxTQE, DGxDK and QxSNxD, are present in multiple genes of *A. viteae*, *B. timori*, *B. pahangi*, *D. immitis*, *L. loa*, *L. sigmodontis*, *O. ochengi* and *O. flexuosa* (Table 4.6). It is not surprising that the motifs are present in several filarial nematodes as they could be conserved throughout the species. It is currently unknown whether these motifs are immunodominant in all species of filarial nematodes or just in *O. volvulus* and thus would be an excellent question to answer using experimental evidence.

A follow-up study investigated whether chosen vaccine candidates contain peptide fragments that are recognised by antibodies in Ov-infected individuals and if recognised, whether these immunodominant epitopes could be attractive serodiagnostic candidates (Lagatie et al., 2018). The conclusions led to identifying that the poly-glutamine stretch 9-mer peptide from RAL-2 (OVOC9988) is a serological marker that should be explored further (Lagatie et al., 2018). Multiple vaccine candidates successfully contained immunodominant linear epitopes, but the 9-mer peptide was highlighted as a more interesting peptide to explore (Lagatie et al., 2018). The list of *C. johnstoni* protein-coding genes was searched to identify the presence of the 9-mer throughout its proteome. The 9-mer, QQQQQQQQR, is present multiple times throughout the *C. johnstoni* proteome and in a couple of cases is found twice in the same gene (Table 4.7). Interestingly, the OVOC9988 protein contains the 9-mer (QQQQQQQQR), but the *C. johnstoni* orthologue of OVOC9988 does not.

The results from the BLAST and InterProScan analyses reveal the *C. johnstoni* genes containing the 9-mer epitope are predominately protein binding genes or DNA binding genes (Table 4.7). It is not clear from these analyses and the predicted putative functions that any of the *C. johnstoni* genes are directly involved in immune responses. However, future analyses into the *C. johnstoni* proteins to identify their function could reveal immunogenic

properties that are currently not observed, which could highlight the importance of exploring these genes for onchocerciasis research. The 9-mer is also found several times in all the other filarial nematodes, suggesting that it may be something conserved throughout filarial nematodes (Table 4.8).

The peptide and motifs have been targeted for research as they could be useful for onchocerciasis surveillance or treatment (Lagatie et al., 2017; Lagatie et al., 2018). Now that it is confirmed that *C. johnstoni* also contains the same motifs and 9-mer peptide, further exploration within the *C. johnstoni* animal model could assist in identifying the appropriate use for these targets. The first step would be to determine whether these genes play any role in the immune response. The motifs and epitopes can then be a target for developing either serodiagnostic tests or vaccines in the *C. johnstoni* small animal model studying onchocerciasis. As both Lagatie et al. (2017) and Lagatie et al. (2018) publications are targeting immunodominant epitopes, there is still a long road ahead to determine the exact use for these immunodominant epitopes. Identifying how immunodominant they could be in *O. volvulus*-infected individuals could be the first step in understanding their purpose in onchocerciasis research (Lagatie et al., 2018).

4.5 Future outlook

In this chapter, I hypothesised that the similarities in immunopathology between *O. volvulus* and *C. johnstoni* are due to shared orthologues containing antigens that the host responds to in a similar immunological context, i.e., skin and eye in rodents and humans from *C. johnstoni* and *O. volvulus* respectively. Thus the hosts are likely to produce similar immune responses. Therefore, part of the immune response observed in *C. johnstoni*-infected rats could be driven by *C. johnstoni* orthologues of *O. volvulus* antigens. However, there is an alternate hypothesis that can be explored in future projects that could explain the similarity in immunopathology. The alternate hypothesis states that the host immune response is species-specific, and therefore protein conservation does not drive the immunological response. This hypothesis is contextual and means that although the same immunopathology can be presented in the different species, i.e., humans and rodents, they are a response to different antigenic proteins. The immune system of a rat is different from the human immune system, and it is, therefore, plausible to assume that responses to different antigens could generate a similar immunopathology caused by rats and humans. As *Wolbachia* is present in *O. volvulus* and not in *C. johnstoni*, it is worth exploring what other mechanisms may be at play that is driving similar immunopathology. Future research into *C. johnstoni* should continue exploring molecules and antigens that could play a role in immunopathology because it may lead to identifying that the molecules in *O. volvulus* are more important to focus on rather than the *Wolbachia* hypothesis.

Currently, it is not clear what is driving the immunopathology in *Onchocerca*-infected individuals. The two parasites share orthologues throughout their proteomes, but this study does not answer alone whether protein conservation or species immune systems drive the immunopathology. Thus, it will be essential to follow up on the work conducted throughout this thesis with experimental evidence to acquire more information about the immunopathology. Chapter Four has identified conserved orthologues in *C. johnstoni* of proteins shown to be immunoreactive in *O. volvulus*. It is not yet known whether this list of identified orthologues are also immunoreactive in the *C. johnstoni*-rodent model and thus to test this the following experiments would be required. These orthologues will be tested by measuring antibody responses in rats against each of these 30 targets. Then, the same validated antigens that stimulate similar

serum antibody responses will be used in the physical small rodent model (to be discussed in Chapter Six) to investigate whether these antigens or antibodies produced in response to the antigens are playing any role in the disease immunopathology. The final phase involves correlating the ability to stimulate antibodies with a role in immunopathology which has not currently been conducted for onchocerciasis. It may be more straightforward using a rodent animal model which in turn will further explain the complicated immunopathology observed in *O. volvulus*-infected patients.

It will be essential to obtain *C. johnstoni* samples from the rats to explore these hypotheses. Collecting the microfilariae, adult worms and then sera samples from infected and uninfected rodents will allow comparable studies with the *O. volvulus* research. Two general experiment pipelines should be considered to study *C. johnstoni* further. First, is to use the sera taken from infected and uninfected rats with *C. johnstoni* DNA and generate synthetic peptides from the list of known *C. johnstoni* orthologues of *O. volvulus* immunoreactive proteins. An ELISA would then be used to test the immunoreactivity against the *C. johnstoni* peptides. The data obtained from this experiment would then be directly comparable to the Norice-Tra et al. (2017) as it would be possible to compare the OD values for *C. johnstoni* and *O. volvulus* immunoreactive orthologues and determine whether they are responding similarly or differently. Ideally, it would be expected to see similar immunoreactivity between orthologous proteins if they are responsible for similar immunopathology. The second experiment that would be highly advantageous to conduct improving *C. johnstoni* research is High-performance Liquid Chromatography with High-resolution Tandem Mass Spectrometry. For this experiment, the transcriptomic data and proteomic data from *C. johnstoni* worms would be generated to compare with the *O. volvulus* data directly. The *C. johnstoni* worm lysates from infected and uninfected rats would be used in a total IgG ELISA and immunoprecipitation experiment to identify immunogenic *C. johnstoni* proteins. These targets are then run on High-performance Liquid Chromatography with High-resolution Tandem Mass Spectrometry and then the targets will be filtered based on quality. The experiment will then obtain a list of immunogenic *C. johnstoni* proteins which can be directly compared to the immunogenic list of *O. volvulus* proteins. The *C. johnstoni* orthologues of immunogenic *O. volvulus* proteins should be within the generated immunogenic *C. johnstoni* list and possibly more candidates that

could not have been identified *in silico*. The study will lead to specific *C. johnstoni* proteins that do not share orthologues with any other filarial nematode which would be worth exploring to understand more about *C. johnstoni*. Finally, this analysis will enable a clear comparison of *O. volvulus* and *C. johnstoni* immunogenic expression profiles and determine how similar the orthologues proteins are or how differently they behave in the different hosts. Consequently, these experiments will be able to determine whether the similar immunopathology observed in rats and humans caused by *C. johnstoni* and *O. volvulus* respectively are driven because of similar proteins being presented to the host or because the immune response is species-specific.

As onchocerciasis is a filarial disease in humans, research into the parasite biology and various treatments are often complicated to study within the human host. Hence why the development of an animal model is so appealing because it would then be possible to explore several different avenues of research concerning onchocerciasis that have not been explored previously. If an animal model were available it could be used to explore the host-parasite relationship within the host, immune evasion by the parasite, alternate drug targets, the possibility of vaccine targets, it would enable new drug screening opportunities and lastly, enable exploration into the exact drivers of immunopathology that are currently not understood. These concepts are typically challenging to study in humans and thus have not been prosperous areas of research.

An interesting concept to explore is the host-parasite relationship within the host. Previous literature focused on the estimation of adult worms within nodules and estimation of microfilarial loads using skin snips in the human host (Duke, 1993). As much of this research is using estimates, an animal model system that would allow accurate recording of adult worms and microfilariae would add to this body of research and create a more accurate depiction of the relationships occurring within the host.

Vaccine development has encountered significant experimental limitations as a result of *O. volvulus*-infected humans and no model organisms. Vaccine experiments have been conducted in a range of possible animal models. A missing link has been the immune responses of these hosts are unlikely to reflect those of significance in a naturally evolved host-parasite relationship (Abraham et

al., 2002). Several studies have highlighted the potential of researching the host-parasite relationship to investigate mechanisms of parasite modulation of host response and protective immunity (Greene et al., 1985; Ward et al., 1988; Lüder et al., 1993). Typically, onchocerciasis research has focussed on drug targets, and vaccine development, specifically OVOC9988 but have been limited by the unsuitable animal models available for testing (summarised in Chapter One). If the *C. johnstoni* animal model were successful, targets such as OVOC9988 and the *C. johnstoni* orthologue could be more accurately tested for possible vaccine development.

There have been other proteins explored in onchocerciasis research that were not a focus of Norice-Tra et al. (2017) and McNulty et al. (2015) or the focus of Chapter Four. These studies had similar goals of identifying antigenic targets that could be involved in an assay for detection, vaccine or treatment of onchocerciasis. Thirty-one proteins from the Bennuru et al. (2016) and Bennuru et al. (2019) and Ov58PCR (OVOC5284) (Shey et al., 2018) have not been explored throughout this thesis. Future bioinformatics projects could explore these lists of proteins that also appear to be interesting targets and identify orthologues in *C. johnstoni*. A project that combined this bioinformatics exploration with immunoreactivity experiments in the *C. johnstoni*-rodent model would be more beneficial to determine which protein orthologues exhibit similar immunoreactivity profiles compared with the studied *O. volvulus* proteins.

Finally, further exploration would be required in *O. volvulus* and now in *C. johnstoni* to determine the usability of the identified immunodominant motifs and epitope for the potential development of serodiagnostic resources in the *C. johnstoni*-rodent model. There may be a possibility that the identification of the immunodominant motifs identified in *O. volvulus* in uncharacterised *C. johnstoni* proteins would identify other putative immunogenic molecules. The *C. johnstoni*-rodent animal model would be required to test the identified *C. johnstoni* genes containing the motif. In the previous studies, sera were collected from infected humans in various locations to explore immunoreactivity (Lagatie et al., 2017). The successful infection of an animal model would allow the animal sera to be tested to determine the reactivity of the associated motifs. The study could provide valuable targets that could be used to assist in treating onchocerciasis but is beyond the scope of this thesis.

4.6 Conclusions

Chapter Four has inferred 30 orthologues across filarial nematodes of important *O. volvulus* immunogenic and serodiagnostic proteins that have putative immunogenic functions. Amongst these orthologues, two genes are undergoing diversifying selection and five genes that are undergoing purifying selection. The orthologues investigated are from a list of known *O. volvulus* immunogenic proteins for which *C. johnstoni* orthologues exist, and thus as expected, these orthologues share similar putative functions.

The completion of this *in silico* exploration has identified *C. johnstoni* proteins that are orthologous of *O. volvulus* immunogenic proteins. The immunogenicity of the *C. johnstoni* orthologues can now be tested in the physical animal model to determine if structural conservation is predictive of immunogenicity.

Chapter Five

Cryptic species diversity in ticks that transmit disease in Australia

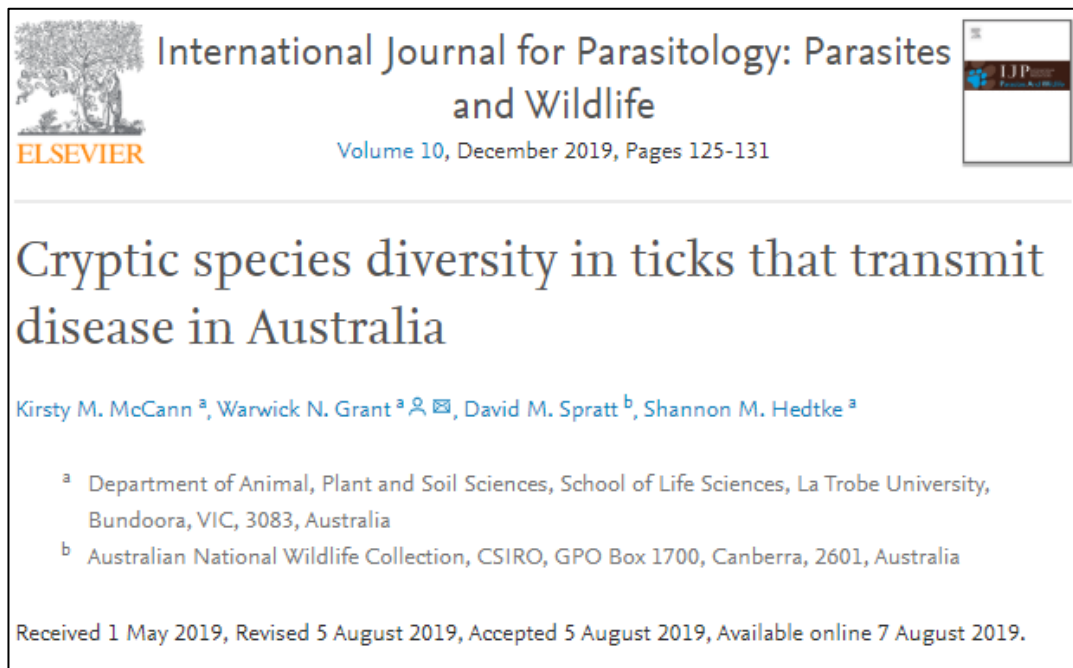
Preface

An essential component of developing a small animal model for onchocerciasis is to identify the most competent vector for *C. johnstoni* transmission to a small animal model system. A significant hurdle that arose during the troubleshooting of the laboratory animal model was the identification of the tick species that were collected either off bush rats or from flagging the environment (Chapter Six). The following chapter focuses on the complex biology of ticks and tick phylogenetics and where standard molecular characterisation techniques may not be suitable for identifying closely related species (Chapter Five). Vectors transmit the parasite and thus are an important part of the model system. There is a need for accurate identification of tick species as there are some species, i.e., *I. holocyclus*, which would likely kill the small animal in the model system by injecting a toxin making it possibly an unsuitable vector species for *C. johnstoni* transmission.

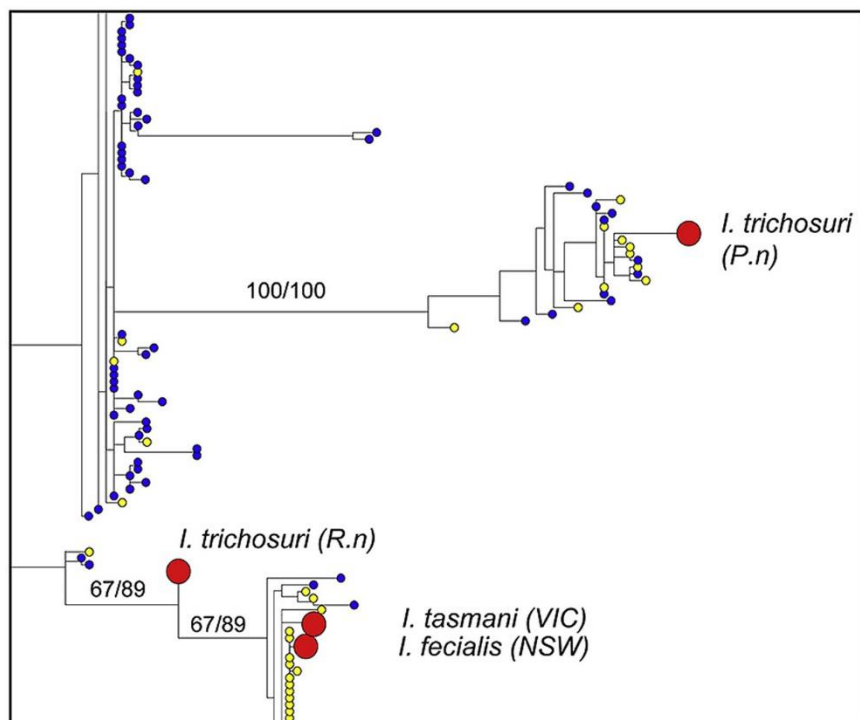
There are several ixodid ticks that are morphologically similar (Barker et al., 2014); thus, phylogenies using morphological characterisation is often not taxonomically informative. Molecular characterisation typically provides a greater level of taxonomic resolution. Markers that have been commonly used to discriminate between *Ixodes* species consist of mitochondrial genes 16S, 12S, COI (Cruickshank, 2002; Lv et al., 2014a; Lv et al., 2014b) and nuclear genes ITS1, ITS2, 18S rDNA, 5.8S rDNA and 28S rDNA (Cruickshank, 2002). The following study uses some of the most common and successful markers previously reported, 16S, 12S and COI, to explore the ticks collected from Kioloa and Mogo State Forest. The following chapter aimed to use molecular techniques to speciate the ticks, understand tick diversity in the field, and learn what species of tick are likely to be transmitting *C. johnstoni* to small hosts as a result of their prevalence in the environment and on bush rats (Chapter Five).

Published article

McCann, K.M., Grant, W.N., Spratt, D.M., Hedtke, S.M. (2019). Cryptic species diversity in ticks that transmit disease in Australia. *International Journal for Parasitology: Parasites and Wildlife*, 10, 125-131, <https://doi.org/10.1016/j.ijppaw.2019.08.002>



Graphical abstract





Cryptic species diversity in ticks that transmit disease in Australia

Kirsty M. McCann^a, Warwick N. Grant^{a,*}, David M. Spratt^b, Shannon M. Hedtke^a^a Department of Animal, Plant and Soil Sciences, School of Life Sciences, La Trobe University, Bundoora, VIC, 3083, Australia^b Australian National Wildlife Collection, CSIRO, GPO Box 1700, Canberra, 2601, Australia

ARTICLE INFO

Keywords:
Ixodidae
Ticks
Cryptic species
Phylogenetics
Species diversity

ABSTRACT

Ticks are important vectors of a broad range of pathogens in Australia. Many tick species are morphologically similar and are therefore difficult to identify using morphology alone, particularly when collected in the larval and nymphal life stages. We report here the application of molecular methods to examine the species diversity of ixodid ticks at two sites in southern New South Wales, Australia. Our taxon sampling included six morphologically characterised adult stage voucher specimens of *Ixodes trichosuri*, *Ixodes tasmani*, *Ixodes feicilis* and *Ixodes holocyclus* (the paralysis tick) and ~250 field collected specimens that were in the larva or nymph stage and thus not morphologically identifiable. One nuclear and two mitochondrial amplicons were sequenced using a combination of Sanger and Illumina MiSeq sequencing. Phylogenetic relationships were estimated using both maximum likelihood and Bayesian methods. Two clades with strong bootstrap and Bayesian support were observed across trees estimated from each of three markers and from an analysis of the concatenated sequences. One voucher specimen of *I. trichosuri* was located in one of these clades, while the other *I. trichosuri* voucher specimen was in a second clade with the remaining three identified species, suggesting these morphologically similar ticks may represent different cryptic species. Unidentified specimens were found across both clades, and molecular divergence of many of these is equal to or greater than that observed between identified species, suggesting additional unidentified species may exist. Further studies are required to understand the taxonomic status of ticks in Australia, and how this species diversity impacts disease risk for livestock, domestic animals, wildlife and humans.

1. Introduction

Ticks are obligate hematophagous ecto-parasites responsible for transmitting a diverse range of micro- and macro- parasites to animals and humans (Klomp et al., 1996; Bonnet and Liu, 2012; McCoy et al., 2013; Lv et al., 2014b; Zhang and Zhang, 2014). Hard ticks are of particular medical and veterinary importance, as their broad host range makes them excellent vectors for disease transmission (Barker and Walker, 2014). For example, in Australia, *Ixodes* ticks attach to a very diverse range of vertebrate hosts that include native species, livestock and companion animals, and humans (Spratt and Haycock, 1988; Atwell et al., 2001; Jongejans and Uilenberg, 2004; Murdoch and Spratt, 2006; Barker and Walker, 2014) and have been shown to harbour an equally diverse range of known and potential pathogens identified through metagenomics (Barker and Murrell, 2004; Carpi et al., 2011; Gofton et al., 2015; Greay et al., 2018). Given that there is a range of potential pathogens that ticks can transmit, a thorough understanding of their species diversity and phylogenetic relationships may be beneficial in assessing disease and transmission risks.

The typical *Ixodes* life cycle has four stages: egg, larva, nymph and adult (Anderson et al., 2004). They feed on blood as larvae, moult to nymphs, feed, and then moult to adults. Adult females must feed a third time after mating before they can lay eggs (Black et al., 1997; Bonnet and Liu, 2012). Thus, ixodid ticks are three-host ticks, with moulting occurring off the host, so that all three stages (larva, nymph and adult) are found on vegetation as they quest for hosts.

This multi-host life cycle facilitates pathogen transmission and zoonotic pathogen detection. During feeding, ticks may ingest a broad range of blood- and tissue-dwelling pathogens from their hosts, which they can then transmit to subsequent hosts during feeding (Caporale et al., 1995; Commins and Platts-Mills, 2013). For example, ixodid ticks are known to carry rickettsial pathogens, including *Borrelia burgdorferi*, the causative organism of Lyme disease (Kilpatrick et al., 2017; Walter et al., 2017), protozoan parasites such as those causing babesiosis in cattle and humans (Spielman et al., 1985; de la Fuente and Kocan, 2006; Graves and Stenos, 2009; Izzard et al., 2009), and many viruses, such as those that cause yellow fever (Telford et al., 1997; de la Fuente et al., 2008; Gould and Solomon, 2008; Vilcins et al., 2008, 2009).

* Corresponding author.

E-mail address: W.Grant@latrobe.edu.au (W.N. Grant).<https://doi.org/10.1016/j.ijppaw.2019.08.002>

Received 1 May 2019; Received in revised form 5 August 2019; Accepted 5 August 2019

2213-2244/ © 2019 The Authors. Published by Elsevier Ltd on behalf of Australian Society for Parasitology. This is an open access article under the CC BY-NC-ND license (<http://creativecommons.org/licenses/by-nc-nd/4.0/>).

In Australia, a “Lyme-like” disease of uncertain etiology has arisen (Mayne et al., 2014; Chalada et al., 2016). Ticks in the *I. ricinus* complex responsible for transmitting Lyme disease are not found in Australia (Schmid, 1985), but several tick-borne rickettsioses (Graves and Stenos, 2009; Izzard et al., 2009; Vilcins et al., 2009), including Q fever (Spelman, 1982), scrub typhus (Wang et al., 2009), and Flinders Island spotted fever (Stenos et al., 1998; Parola and Raoult, 2001) are all transmitted by native ixodid ticks. Although vector competence varies among tick species and is correlated with disease risk, there have been few studies examining tick species diversity and competence in Australian wild spaces. A first step in such a study is to develop a robust, preferably molecular, phylogeny of Australian ixodid ticks that could be used to identify species simultaneously with molecular screening for pathogen presence.

Previous research has focused on ticks collected from companion animals at veterinary clinics (Atwell et al., 2001; Day, 2011; Greay et al., 2016), bacterial studies (Murrell et al., 2003; Vilcins et al., 2009; Andreotti et al., 2011), and paralysis ticks (Stone et al., 1983; Grattan-Smith et al., 1997; Jackson et al., 2002, 2007; Eppleston et al., 2013). However, to appropriately quantify transmission potential and disease risk, we must first understand biogeographic variation in tick species diversity in environments where animals and humans might be exposed to ticks.

The strategy we have employed was to sample at two locations: one at a pasture/bushland margin where large numbers of Eastern grey kangaroos (*Macropus giganteus*, an Australian ecological equivalent of white-tailed deer in the north-eastern USA) are at high density and human contact with ticks is likely, and at a nearby regenerating native bush site where Eastern grey kangaroos are markedly less numerous, there is generally greater wildlife diversity, and human-tick encounters are less likely. At the bush/pasture margin site ticks were collected from vegetation, and at the regenerating bushland site we collected (mostly larval) ticks from Australian bush rats (*Rattus fuscipes*). Tick molecular diversity was analysed using DNA sequences for three markers: mitochondrial ribosomal RNA 12S and 16S genes and the nuclear internal transcribed spacer 2 (Cruickshank, 2002; Song et al., 2011; de Mandal et al., 2014; Lv et al., 2014a, 2014b; Lv et al., 2014a).

2. Materials and methods

2.1. Sample collection

Un-engorged ticks were collected by flagging on pasture and in clearings at or close to the bush/pasture margins at two locations on the Australian National University Coastal Campus, Kioloa, NSW (Fig. 1) in February, April, and June in 2015, and in October and November in 2016. To flag, an approximately 1 × 1.5 m piece of white fabric was dragged along the ground: ticks caught up on the fabric were picked off with tweezers and placed into tubes that contained a mix of plaster of Paris and charcoal (Konnai et al., 2008). In 2015, we collected a total of 633 larvae, 34 nymphs, and 3 adults: ~120 larvae, 13 nymphs and 1 adult at the dunes and 513 larvae, 21 nymphs and 1 adult on the ANU campus. In 2016, we collected ~300 larvae, ~250 nymphs, and ~80 adults from the ANU campus.

Engorged ticks were collected from Australian bush rats, *R. fuscipes*, that had been captured at the site reported by Spratt and Haycock (1988) in the Mogo State Forest, approximately 40 km south of Kioloa. This is an area of regenerating dry eucalypt forest that had been subjected to periodic commercial forestry of native vegetation and fire. Rats were captured in small Elliott traps and held in an approved animal facility at the ANU Coastal Campus for up to 3 days in wire-bottomed cages. Engorged ticks were collected each morning from collection containers beneath the cages, and stored live in glass vials containing dry, clean, fine sand. Trapping of bush rats, and the subsequent holding of captured rats for 3 days post-trapping to allow collection of engorged ticks, were performed with the appropriate

regulatory permits (La Trobe University approval AEC 13–23, New South Wales – Scientific Licence 5 L 101280, Victorian – Scientific Permit 10007169). We collected ~343 engorged larvae, ~68 engorged nymphs, and no adults from native bush rats at Mogo State Forest.

Six (6) specimens preserved in 70% ethanol were identified morphologically and used as vouchers for this study: *I. tasmani* ex *Vombatus ursinus* (from Lucyvale, Victoria), *I. feicalis* ex *Dasyurus maculatus* (from Spirabo Nat Pk., NSW), *I. tasmani* ex *V. ursinus* (from Jerangle, NSW), *I. trichosuri* ex *R. norvegicus* (Lab-reared, experimental), and *I. trichosuri* ex *Perameles nasuta* (Lab reared, experimental). An adult *I. holocyclus* was identified after collection by flagging from Kioloa. The *R. norvegicus* host was laboratory bred and used as an experimental animal in parasite life cycle studies (Spratt and Haycock, 1988). The *P. nasuta* host had been removed from the Mogo study site, maintained in the laboratory, and used as an experimental animal in the same parasite life cycle studies.

2.2. Purifying tick DNA

DNA was extracted using a Bioline ISOLATE II Genomic DNA kit following the manufacturer's instructions (Bioline (Aust) Pty Ltd, Alexandria NSW, Australia, 2015). Tweezers or a scalpel blade were used to remove a back leg from live ticks and placed immediately into extraction buffer. Alternatively, whole bodies of dead, small ticks or whole carapaces from moulted ticks were used. In total, DNA was extracted from 128 larvae and 1 nymph from Kioloa, and 83 larvae and 11 nymphs from Mogo State Forest.

2.3. PCR of mitochondrial and nuclear amplicons

The 16S gene was amplified using the primer pair mt_16S_NGS-F (5'-TCG TGG GCA GCG TCA GAT GTG TAT AAGA -3') and mt_16S_NGS-R (5'-GTC TCG TGG GCT CGG AGA TGT GTA TAA G -3'). The 12S gene was amplified using the primer pair mt_12S_NGS-F (5'-TCG TCG GCA GCG TCA GAT GTG TAT AAGA -3') and mt_12S_NGS-R (5'-GTC TCG TGG GCT CGG AGA TGT GTA TAA G -3'). Lastly the ITS2 gene was amplified using the primer pair Nc ITS2_NGS-F (5'-TCG TCG GCA GCG TCA GAT GTG TAT AAG AGA CAG GGG TCG GAT CAT ATA TCA -3') and Nc ITS2_NGS-R (5'-GTC TCG TGG GCT CGG AGA TGT GTA TAA GAG ACA GCA ACT TCC TCG GCA ACA -3'). PCR conditions were initial denaturation at 98 °C for 1 min, followed by 38 cycles of denaturation at 98 °C for 15 s, annealing at 61.6 °C (16S) or 63.4 °C (ITS2) or 59.8 °C (12S) for 15 s, and extension at 72 °C 15 s, with a final extension reaction at 72 °C for 5 min.

2.4. Sequencing of amplicons

Amplicons were prepared and sequenced on an Illumina MiSeq. An in-house amplicon barcoding and sequencing protocol was followed (prepared by Dr Stephen Doyle, see Appendix for protocol and for barcoding primers used). The DNA concentration of the final pooled library was adjusted to 2500 pM following Qubit fluorometric quantitation. Two MiSeq runs were carried out: a pilot experiment using a v2 500 cycle kit (2x250 bp paired-end), and a second experiment of v3 600 cycle kit (2x300 bp paired end), following the manufacturer instructions (Illumina MiSeq reagent kit V3 preparation guide, 2013). The final sequencing mix included 10% PhiX DNA. Sanger sequencing was also used to confirm sequences of some samples. Amplicons for Sanger sequencing were cleaned using Ampure XP beads (Beckman-Coulter) and sequenced at Macrogen Inc., Korea.

2.5. Sequencing analysis

MiSeq data were imported into CLC Genomics Workbench version 7.5. Adapters and primer sequences were trimmed from both Sanger and MiSeq samples using a quality score of > 20. Reads were then

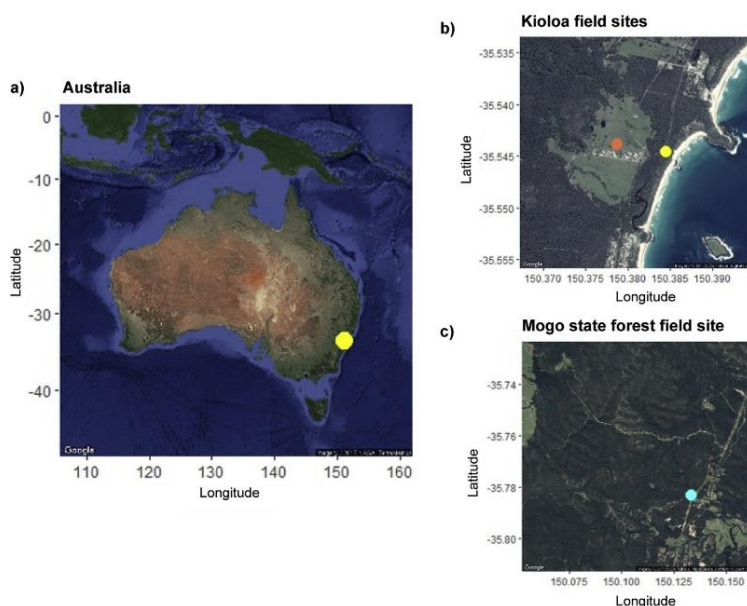


Fig. 1. Satellite maps of (a) Australia (b) Kioloa and (c) Mogo state forest sample collection sites with coordinates, latitude on the y axis and longitude on the x axis. (a) yellow: NSW general location of sites (b) orange: Kioloa ANU campus, yellow: Kioloa dunes (c) blue: Mogo State Forest (Kahle and Wickham, 2013). (For interpretation of the references to colour in this figure legend, the reader is referred to the Web version of this article.)

mapped to the whole mitochondrial genome of *I. holocyclus* (NC_005293) and three ITS2 *I. holocyclus* reference sequences (GenBank accession numbers: AF208344 (Wesson et al., 1993; McLain et al., 1995), AB025591, AB025595 (Fukunaga et al., 2000)).

Prior to running the phylogenetic analysis, 12 samples were removed as they did not map to *Ixodes* spp. (e.g., suspected bacterial contaminants) or were of poor sequencing quality.

The alignments of consensus sequences for each individual tick were exported and refined in ClustalW2 (Larkin et al., 2007). Sequences from closely-related outgroups were downloaded from NCBI's GenBank database and added to the 16S alignment: *Haemaphysalis humerosa* (JX573138), *Haemaphysalis parva* (JX573136), *Rhipicephalus appendiculatus* (KC503257) and *Amblyomma triguttatum* (AB113317). The alignment was checked and further refined by eye using Mesquite v3.04 (Maddison and Maddison, 2008).

Phylogenies were estimated using maximum likelihood as implemented in the program RAxML for high-performance computing version 8.0.19 (Stamatakis, 2006, 2014) using the best of 20 replicates under the GTRCAT model of sequence evolution and 1000 long bootstrap replicates to estimate support for bipartitions. The best model for each partition was assessed using PartitionFinder version 1.1.1 (Lanfear et al., 2012), and posterior probabilities for nodes were estimated with MrBayes 3.2.5 (Ronquist et al., 2012), using 2 runs with 4 chains each and sampling every 1000 generations. Convergence between the 2 runs and stationarity were assessed using Tracer version 1.6 (Rambaut et al., 2014). The m16S Bayesian analysis was conducted with 13 million generations under GTR + I + G substitution model. The 12S Bayesian analysis was conducted with 18 million generations under the HKY + I + G substitution model. The ITS2 Bayesian analysis was conducted with 10 million generations under the K80 + G substitution model. The concatenated Bayesian analysis was conducted with 8 million generations under the above 3 substitution models, unlinked so each gene could be treated differently. We used a conservative burn-in fraction of 25%.

The phylogenetic trees were imported into R version 3.4.1 (R Core Team, 2017) and edited for publication using pegas package version 0.10 (Paradis et al., 2017), in conjunction with Geiger version 2.0.6 (Harmon et al., 2015) and Phytools version 0.6–44 (Revell, 2012).

2.6. Haplotype analysis

The aligned nexus files were imported into the program PopArt (Population analysis with reticulate trees) version 1.7 (Leigh and Bryant, 2015) to produce haplotype networks. PopArt does not accept missing data (Leigh and Bryant, 2015), so only individuals sequenced for all three markers were used in the final concatenated haplotype analysis (200 individuals).

Haplotype networks were produced using two algorithms: TCS network analysis (Clement et al., 2002) and median-joining network analysis (Bandelt et al., 1999). Both analyses illustrated the same topology; we present here the TCS network analyses (Clement et al., 2002).

3. Results

3.1. Phylogenetic analysis

All three trees – 12S, 16S, and ITS2 – showed a single, well-supported bipartition resulting in two clades. It was only possible to root one tree, 16S, because there were no suitable outgroup sequences that could be confidently aligned for more rapidly evolving 12S and ITS-2.

Consistent across all three markers and the concatenated analysis, *I. trichosuri* (P.n) was positioned in a separate clade from the other five voucher specimens (Fig. 2; Supplementary Figs. 4, 6, 8). The other five voucher specimens of *I. holocyclus* (Kioloa), *I. trichosuri* (R.n), *I. tasmani* (NSW), *I. tasmani* (VIC) and *I. fecialis* (NSW) were positioned together in the same clade across all markers with minimal differentiation between each species despite their obvious morphological characteristic differences (Fig. 2). As the genetic similarities in sequences among voucher specimens were unexpected, we confirmed each sequence by re-extracting DNA, amplifying, and sequencing each amplicon using Sanger sequencing.

Preliminary phylogenetic analysis of the ITS-2 marker revealed that samples 00618, 00596, 0597 and 00612 had very long branch lengths, which can reduce phylogenetic accuracy; these were removed and maximum likelihood analyses re-run (Heath et al., 2008).

When the amplicons were concatenated, the resolution of the

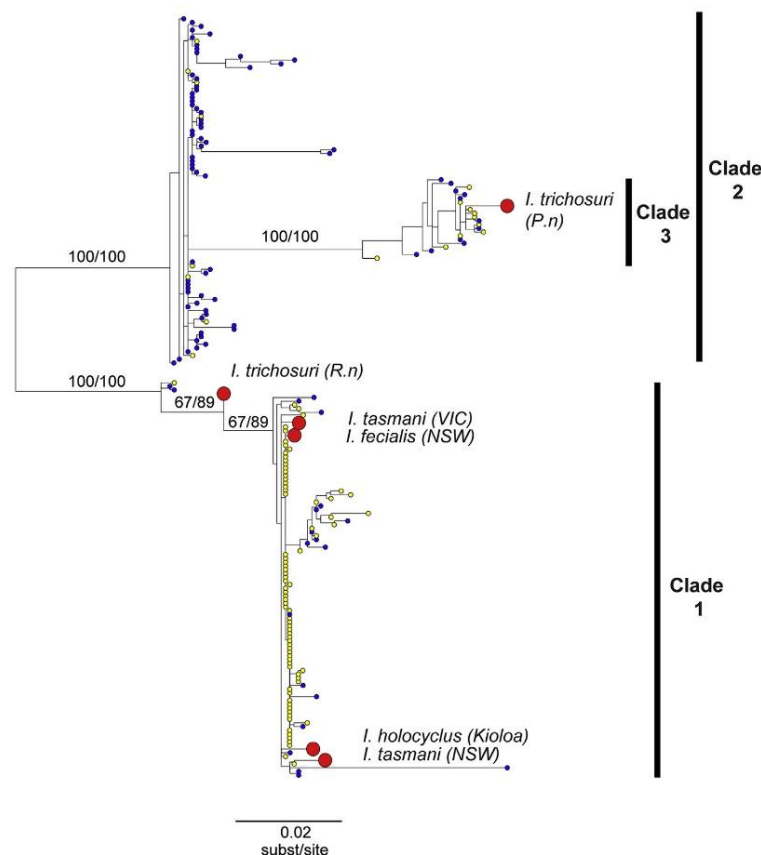


Fig. 2. Maximum likelihood estimate based on three markers of ticks collected at Kioloa and Mogo State Forest, NSW, Australia. Blue: Mogo State Forest (rats), yellow: Kioloa (flagging), red: identified voucher specimens. (For interpretation of the references to colour in this figure legend, the reader is referred to the Web version of this article.)

phylogenetic tree improved. The topology of this tree is consistent (Supplementary Figs. 4, 6, 8); therefore, only the concatenated tree is presented (Fig. 2). *I. trichosuri* (P.n) was situated in a separate clade from the other five voucher specimens with strong bootstrap (100%) and Bayesian support (100%).

3.2. Haplotype analysis

The haplotype network analysis was conducted individually on three amplicons 12S, 16S and ITS-2 (Supplementary Figs. 5, 7, 9). The three individual haplotype networks were congruent with each other (Fig. 3) and with the results of the phylogenetic analysis. *Ixodes trichosuri* (P.n) was strongly differentiated and situated in a separate haplotype group (III) from the other five voucher specimens (II).

More Kioloa samples were present in clade I/haplotype group I with *I. holocyclus* (Kioloa), *I. tasmani* (VIC), *I. tasmani* (NSW), *I. trichosuri* (R.n), and *I. feicalis* (NSW) (Figs. 2 and 3). Haplotype group II contained no voucher specimens and was dominated by Mogo samples (Fig. 3); these represent individuals in clade II, but not clade III, in the phylogenetic tree (Fig. 2). In clade III/haplotype group III, *I. trichosuri* (P.n) was found with approximately half of the unidentified specimens from Mogo and half from Kioloa (Figs. 2 and 3).

4. Discussion

We collected ixodid ticks from vegetation and Australian bush rats in order to examine the phylogenetic diversity at two field sites in southern New South Wales, with the assumption that sequence diversity could be informative about species diversity. We found that *I. trichosuri* (P.n) is genetically distinguishable from *I. holocyclus* (Kioloa) and remaining unknown *Ixodes* spp., although several other morphologically defined *Ixodes* spp. were not well resolved by these amplicons. This suggests rapid evolution of morphological characteristics in *Ixodes*, leading to morphological differentiation in the absence of molecular divergence for some species.

4.1. Genetic differentiation among Australian ixodid ticks

We identified the species of six adult voucher specimens using morphological characteristics, including the presence or absence of the palpal spur, separation or fusion of palps 2 and 3, mouthpart type, presence or absence of a sternal plate, coxa with or without a spur, presence or absence of cornua, and the colouring of the legs (Jackson et al., 1998, 2002). These voucher specimens fell into two clades: one with a large number of unidentified larvae and *I. trichosuri* (P.n) from bandicoots, while the other specimens, *I. feicalis* (NSW), *I. tasmani* (NSW), *I. tasmani* (VIC) and lab-reared *I. trichosuri* (R.n) aligned in the

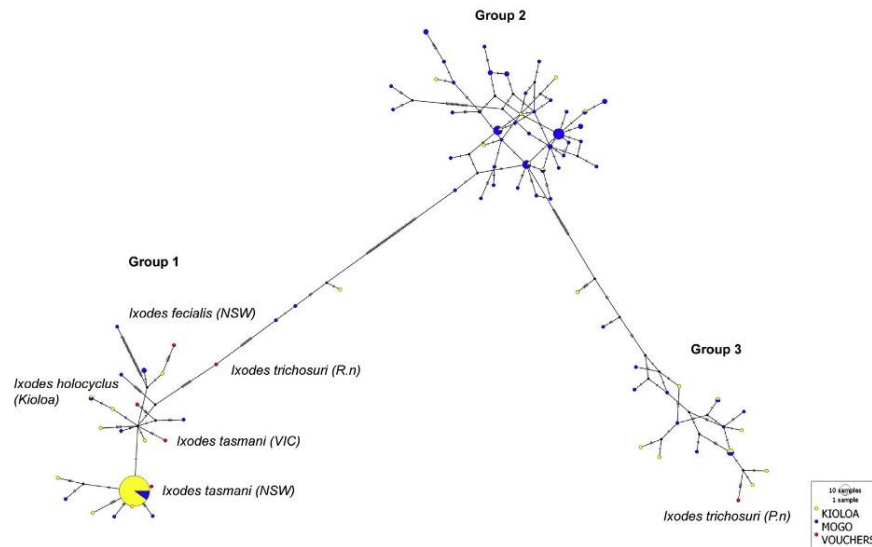


Fig. 3. TCS haplotype network based on 3 markers sequenced from ticks collected from Kioloa and Mogo State Forest in NSW, Australia. Samples are coloured based on their collection site, Mogo State Forest (blue) or Kioloa (yellow). Voucher specimens are coloured red. (For interpretation of the references to colour in this figure legend, the reader is referred to the Web version of this article.)

same clade with the paralysis tick, *I. holocyclus* (Fig. 2). The short branch lengths among voucher specimens in this second clade compared to ticks sampled as a whole was unexpected, considering the species were all morphologically distinguishable. Furthermore, the phylogenetic and haplotype analyses illustrate the potential for cryptic diversity within the genus (Fig. 3). The two specimens were morphologically identified as *I. trichosuri* are not monophyletic, and were found in distinctly separate clades, suggesting that these specimens may be cryptic species. Morphological distinctions are not yet visible in the nymphs collected for this study, but molecular divergence was greater than among morphologically identified species, suggesting that species diversity might be considerable. In the absence of additional data on interbreeding, we would conclude at a minimum that there is poor concordance between morphological and molecular diversity.

4.2. Differences in species diversity between sampling locations

We collected nymphs in two field sites, Kioloa and Mogo State Forest in NSW, Australia. In both phylogenetic and haplotype analyses, clade I/haplotype group I contained five of the voucher specimens and predominantly undetermined species from Kioloa, haplotype group II (which contained specimens in clade II but not clade III) contained no voucher specimens and predominantly undetermined specimens from Mogo, while clade III (nested within clade II)/ haplotype group II contained the voucher *I. trichosuri* ex *P. nasuta* and is evenly divided between undetermined specimens from Kioloa and Mogo (Figs. 2 and 3). There are several possibilities that might explain the observed differentiation in species diversity between these two locations:

(1) Geographic variation. The Kioloa and Mogo State Forest sites are only approximately 55 km apart, yet their vegetation is markedly different: open, regenerating eucalypt forest at Mogo compared with native, unimproved pasture at Kioloa. Ticks in Australia rely heavily on high humidity for their survival strategy, preferring a relative humidity of 85%, rainfall, and low temperatures (Needham and Teel, 1991; Oorebeek and Kleindorfer, 2008). Differences in vegetation may impact microenvironment humidity, and if tick

species vary in off-host environmental preferences, this may in turn affect the species diversity between the two locations.

(2) Host availability. Differences in habitat and vegetation also markedly affect the hosts present at each site (Allan et al., 2003; LoGiudice et al., 2003; Oorebeek and Kleindorfer, 2008; Kilpatrick et al., 2017). Although ixodid ticks broadly will attach to many mammals, including Australian bush rats (Spratt and Haycock, 1988), kangaroos, bandicoots (Barker and Walker, 2014), domestic animals (Atwell et al., 2001), possums, livestock, and humans (Jongejan and Uilenberg, 2004; Murdoch and Spratt, 2006), there are differences in host preferences. For example, approximately 30 years ago, bandicoots were the predominate host for all life stages of *I. holocyclus* ticks in southeast coastal Qld (Doube, 1979). However, population densities of three bandicoot species, *Isodon macrourus*, *Isodon obesulus* and *P. nasuta* have since declined. Eastern grey kangaroos are now a preferred host for *I. holocyclus* (Storer et al., 2003; Jackson et al., 2007; Kolonin, 2007; Dawood et al., 2013), and the current kangaroo density at the Kioloa field site is considerably higher than at Mogo State Forest, where the bush rat density is higher. Consistent with this host preference, *I. holocyclus* and closely related ticks may be more common at the kangaroo-dominated Kioloa than they are at Mogo. This tentative explanation is tempered by the fact that ticks from Kioloa were collected exclusively by flagging, whereas ticks from Mogo were all collected from bush rats. The apparent difference in tick diversity between the two sites may, therefore, represent strong host preference of ticks at Mogo for bush rats.

(3) Life stage. The life stage – larva, nymph or adult—could also be important in determining host choice (Bonnet and Liu, 2012). Larval and nymphal ticks, which have smaller mouth parts than adults, may not be able to penetrate the skin of a kangaroo, whereas an adult may be too big to feed on a bush rat. In a study creating an artificial tick feeding assay, the membrane thickness needed to be altered depending on the life stage of the tick (Krull et al., 2017). Larvae are also small in size, and small mammals such as bush rats that have bodies close to the ground may reduce the effort required for questing larvae (Oorebeek and Kleindorfer, 2008). Adults

however, feed much longer and require a large blood meal. Unengorged adults could be questing further up the vegetation toward large mammals and are able to do so when they are fully developed (Bonnet and Liu, 2012). Thus, the observed variation may not be driven by differing tick species at the two sites, but rather differences in timing of developmental stages.

- (4) Time of year. Species diversity differences between locations could reflect differences in the time of year the ticks were collected. Ticks were collected only at Kioloa in February, April, and June 2015 and at both Kioloa and Mogo in October and November 2016. In Australia, the summers are hot and the winters are relatively cold, but, more importantly, rainfall and humidity is inconsistent all year round. Spratt and Haycock (1988) observed a mild fluctuation but relatively steady tick prevalence across every month of the year on Australian bush rats. Some months there was a reduction of ticks observed on this host, but overall, ticks were active at Mogo State Forest all year round. The same is not true for other hosts; Oorebeek and Kleindorfer (2008) did not find any ticks on the Australian birds in their study from December to March, but attached ticks were observed for the remaining months of the year. Various studies have indicated a variation in responses to the climate, ecology, time of year and hosts present from different tick species (Needham and Teel, 1991; Randolph, 1998; Perret et al., 2004; Oorebeek and Kleindorfer, 2008).

5. Conclusions

Our results indicated that (1) four morphologically identified species were genetically closely related despite having distinct morphological features, based on selected primer sets, while one (*I. trichosuri*) was distinctly different, (2) we observed remarkable genetic diversity among the tick samples collected in a very small geographic area, and that (3) this genetic diversity was not clearly correlated with known species boundaries. Only *I. trichosuri* (P.n) collected from a bandicoot was easily distinguishable genetically from other identified ticks, and specimens identified as *I. trichosuri* were not monophyletic. We conclude that there has been rapid evolution of morphological characteristics in species of *Ixodes*, leading to morphological differentiation in the absence of molecular divergence for some species, and possible convergence in morphological characteristics, or retention of ancestral traits, in those that are genetically distinct.

The species diversity throughout the *Ixodes* genus likely influences parasite and pathogen transmission to a range of hosts, including humans (McCoy et al., 2013). As the overlap between wilderness and human habitats increases, the zoonotic disease risks from these multi-host vectors may also increase. Determining the potential for ticks to transmit pathogens of medical and veterinary importance is hampered by challenges in species identification of the ticks concerned (Lv et al., 2014a, 2014b). Molecular methods characterising tick species diversity across different environments may be required to effectively meet these challenges.

Conflicts of interest

The authors declare they have no conflict of interest regarding the work described in this manuscript.

Declaration of interests

None.

Acknowledgements

We would like to thank Dr. Stephen Doyle for his contributions in assisting with MiSeq preparation and sequencing of tick samples and the Grant Lab for their assistance and guidance. Many thanks to Andrew

Robinson, ICT Research support officer, for the continuous support and updates of the LIMS-HPC resource used for our bioinformatic analyses.

Appendix A. Supplementary data

Supplementary data to this article can be found online at <https://doi.org/10.1016/j.ijppaw.2019.08.002>.

References

- Allan, B.F., Keesing, F., Ostfeld, R.S., 2003. Effect of forest fragmentation on Lyme disease risk. *Conserv. Biol.* 17, 267–272.
- Anderson, J.M., Ammerman, N.C., Norris, D.E., 2004. Molecular differentiation of metastriate tick immatures. *Vector Borne Zoonotic Dis.* 4, 334–342.
- Andreotti, R., de León, A.A.P., Dowd, S.E., Guerrero, F.D., Bendeke, K.G., Scoles, G.A., 2011. Assessment of bacterial diversity in the cattle tick *Rhipicephalus (Boophilus) microplus* through tag-encoded pyrosequencing. *BMC Microbiol.* 11, 6.
- Atwell, R., Campbell, F., Evans, E., 2001. Prospective survey of tick paralysis in dogs. *Aust. Vet. J.* 79, 412–418.
- Bandelt, H.J., Forster, P., Röhl, A., 1999. Median-joining networks for inferring intraspecific phylogenies. *Mol. Biol. Evol.* 16, 37–48.
- Barker, S.C., Murrell, A., 2004. Systematics and evolution of ticks with a list of valid genus and species names. *Parasitology* 129, S15–S36.
- Barker, S.C., Walker, A.R., 2014. Ticks of Australia. The species that infest domestic animals and humans. *Zootaxa* 3816, 1–144.
- Black, W., Klompen, J.S.H., Keirans, J.E., 1997. Phylogenetic relationships among tick subfamilies (Ixodidae: ixodidae: Argasidae) Based on the 18S nuclear rDNA gene. *Mol. Phylogenetics Evol.* 7, 129–144.
- Bonnet, S., Liu, X.Y., 2012. Laboratory artificial infection of hard ticks: a tool for the analysis of tick-borne pathogen transmission. *Acarologia* 52, 453–464.
- Caporale, D.A., Rich, S.M., Spelman, A., Telford, S.R., Kocher, T.D., 1995. Discriminating between Ixodes ticks by means of mitochondrial DNA sequences. *Mol. Phylogenetics Evol.* 4, 361–365.
- Carpi, G., Cagnacci, F., Wittekindt, N.E., Zhao, F., Qi, J., Tomsho, L.P., Drautz, D.I., Rizzoli, A., Schuster, S.C., 2011. Metagenomic profile of the bacterial communities associated with *Ixodes ricinus* ticks. *PLoS One* 6, e25604.
- Chalada, M.J., Stenos, J., Bradbury, R.S., 2016. Is there a Lyme-like disease in Australia? Summary of the findings to date. *One Health* 2, 42–54.
- Clement, M., Snell, Q., Walker, P., Posada, D., Crandall, K., 2002. TCS: Estimating Gene Genealogies. *Ipdis. IEEE*, pp. 0184.
- Commins, S.P., Platts-Mills, T.A., 2013. Tick bites and red meat allergy. *Curr. Opin. Allergy Clin. Immunol.* 13, 354.
- Cruickshank, R.H., 2002. Molecular markers for the phylogenetics of mites and ticks. *Syst. Appl. Acarol.* 7, 3–14.
- Dawood, K.E., Morgan, J.A., Busfield, F., Srivastava, M., Fletcher, T.I., Sambono, J., Jackson, L.A., Venus, B., Philbey, A.W., Lew-Tabor, A.E., 2013. Observation of a novel *Babesia* spp. in eastern grey kangaroos (*Macropus giganteus*) in Australia. *Int. J. Parasitol.* 2, 54–61.
- Day, M.J., 2011. One health: the importance of companion animal vector-borne diseases. *Parasites Vectors* 4, 49.
- de la Fuente, J., Estrada-Pena, A., Venzal, J.M., Kocan, K.M., Sonenshine, D.E., 2008. Overview: ticks as vectors of pathogens that cause disease in humans and animals. *Front. Biosci.* 13, 6938–6946.
- de la Fuente, J., Kocan, K., 2006. Strategies for development of vaccines for control of ixodid tick species. *Parasite Immunol.* 28, 275–283.
- de Mandal, S., Chhakchhuak, L., Gurusubramanian, G., Kumar, N.S., 2014. Mitochondrial Markers for Identification and Phylogenetic Studies in Insects—A Review. vol. 2 DNA Barcodes.
- Doube, B.M., 1979. Seasonal patterns of abundance and host relationships of the Australian paralysis tick, *Ixodes holocyclus* Neumann (Acarina: ixodidae), in south-eastern Queensland. *Aust. J. Ecol.* 4, 345–360.
- Eppleston, K., Kelman, M., Ward, M., 2013. Distribution, seasonality and risk factors for tick paralysis in Australian dogs and cats. *Vet. Parasitol.* 196, 460–468.
- Fukunaga, M., Yabuki, M., Hamase, A., Oliver Jr., J.H., Nakao, M., 2000. Molecular phylogenetic analysis of ixodid ticks based on the ribosomal DNA spacer, internal transcribed spacer 2, sequences. *J. Parasitol.* 86, 38–43.
- Goffon, A.W., Oskam, C.L., Lo, N., Beninati, T., Wei, H., McCarl, V., Murray, D.C., Paparini, A., Greay, T.L., Holmes, A.J., 2015. Inhibition of the endosymbiont *Candidatus Midichloria mitochondrii* during 16S rRNA gene profiling reveals potential pathogens in *Ixodes* ticks from Australia. *Parasites Vectors* 8, 345.
- Gould, E., Solomon, T., 2008. Pathogenic flaviviruses. *Lancet* 371, 500–509.
- Grattan-Smith, P.J., Morris, J.G., Johnston, H.M., Yiannikas, C., Malik, R., Russell, R., Ouvrier, R.A., 1997. Clinical and neurophysiological features of tick paralysis. *Brain* 120, 1975–1987.
- Graves, S., Stenos, J., 2009. Rickettsioses in Australia. *Ann. N. Y. Acad. Sci.* 1166, 151–155.
- Greay, T.L., Goffon, A.W., Paparini, A., Ryan, U.M., Oskam, C.L., Irwin, P.J., 2018. Recent insights into the tick microbiome gained through next-generation sequencing. *Parasites Vectors* 11, 12.
- Greay, T.L., Oskam, C.L., Goffon, A.W., Rees, R.L., Ryan, U.M., Irwin, P.J., 2016. A survey of ticks (Acar: ixodidae) of companion animals in Australia. *Parasites Vectors* 9, 207.
- Harmon, L., Weir, J., Brock, C., Gior, R., Challenger, W., Hunt, G., FitzJohn, R., Pennell, M., Slater, G., Brown, J., 2015. Package ‘gelgel’. R Package Version 2.

- Heath, T.A., Hedtke, S.M., Hillis, D.M., 2008. Taxon sampling and the accuracy of phylogenetic analyses. *J. Syst. Evol.* 46, 239–257.
- Izzard, L., Graves, S., Cox, E., Fenwick, S., Unsworth, N., Stenos, J., 2009. Novel Rickettsia in ticks, tasmania, Australia. *Emerg. Infect. Dis.* 15, 1654.
- Jackson, J., Beveridge, I., Chilton, N.B., Andrews, R.H., 2007. Distributions of the paralysis ticks *Ixodes cornuatus* and *Ixodes holocyclus* in south-eastern Australia. *Aust. Vet. J.* 85, 420–424.
- Jackson, J., Beveridge, I., Chilton, N.B., Andrews, R.H., Dixon, B., 2002. Morphological comparison of the adult and larval stages of the Australian ticks *Ixodes holocyclus* Neumann, 1899 and *I. cornuatus* Roberts, 1960 (Acari: Ixodidae). *Syst. Appl. Acarol.* 7, 91–108.
- Jackson, J., Chilton, N.B., Beveridge, I., Morris, M., Andrews, R.H., 1998. An electrophoretic comparison of the Australian paralysis tick, *Ixodes holocyclus* Neumann, 1899, with *I. cornuatus* Roberts, 1960 (Acari: Ixodidae). *Aust. J. Zool.* 46, 109–117.
- Jongejans, F., Uilenberg, G., 2004. The global importance of ticks. *Parasitology* 129, S3–S14.
- Kahle, D., Wickham, H., 2013. ggmap: spatial Visualization with ggplot2. *R Journal* 5, 144–161.
- Kilpatrick, A.M., Dobson, A.D.M., Levi, T., Salkeld, D.J., Swei, A., Ginsberg, H.S., Kjemtrup, A., Padgett, K.A., Jensen, P.M., Fish, D., Ogden, N.H., Diuk-Wasser, M.A., 2017. Lyme disease ecology in a changing world: consensus, uncertainty and critical gaps for improving control. *Philos. Trans. R. Soc. Lond. B Biol. Sci.* 372, 20160117.
- Klompen, J., Black IV, W., Keirans, J., Oliver Jr., J., 1996. Evolution of ticks. *Annu. Rev. Entomol.* 41, 141–161.
- Koloinin, G., 2007. Mammals as hosts of Ixodid ticks (Acarina, Ixodidae). *Entomol. Rev.* 87, 401–412.
- Konnai, S., Saito, Y., Nishikado, H., Yamada, S., Imamura, S., Mori, A., Ito, T., Onuma, M., Ohashi, K., 2008. Establishment of a laboratory colony of taiga tick *Ixodes persulcatus* for tick-borne pathogen transmission studies. *Jpn. J. Vet. Res.* 55, 85–92.
- Krull, C., Böhme, B., Clausen, P.-H., Nijhof, A.M., 2017. Optimization of an artificial tick feeding assay for *Dermacentor reticulatus*. *Parasites Vectors* 10, 60.
- Lanfear, R., Calcott, B., Ho, S.Y.W., Guindon, S., 2012. PartitionFinder: combined selection of partitioning schemes and substitution models for phylogenetic analyses. *Mol. Biol. Evol.* 29, 1695–1701.
- Larkin, M., Blackshields, G., Brown, N., Chenna, R., McGettigan, P., McWilliam, H., Valentin, F., Wallace, I., Wilm, A., Lopez, R., 2007. Clustal W and clustal X version 2.0. *Bioinformatics* 23, 2947.
- Leigh, J.W., Bryant, D., 2015. popart: full-feature software for haplotype network construction. *Methods Ecol. Evol.* 6, 1110–1116.
- LoGiudice, K., Ostfeld, R.S., Schmidt, K.A., Keeling, F., 2003. The ecology of infectious disease: effects of host diversity and community composition on Lyme disease risk. *Proc. Natl. Acad. Sci.* 100, 567–571.
- Lv, J., Wu, S., Zhang, Y., Chen, Y., Feng, C., Yuan, X., Jia, G., Deng, J., Wang, C., Wang, Q., Mei, L., Lin, X., 2014a. Assessment of four DNA fragments (COI, 16S rDNA, ITS2, 12S rDNA) for species identification of the Ixodida (Acari: Ixodida). *Parasites Vectors* 7, 93–93.
- Lv, J., Wu, S., Zhang, Y., Zhang, T., Feng, C., Jia, G., Lin, X., 2014b. Development of a DNA barcoding system for the Ixodida (Acari: Ixodida). *Mitochondrial DNA* 25, 142–149.
- Maddison, W., Maddison, D., 2008. Mesquite: a Modular System for Evolutionary Analysis. Version 2.5, build j55.
- Mayne, P., Song, S., Shao, R., Burke, J., Wang, Y., Roberts, T., 2014. Evidence for *Ixodes holocyclus* (Acarina: Ixodidae) as a vector for human Lyme borreliosis infection in Australia. *J. Insect Sci.* 14.
- McCoy, K.D., Léger, E., Dietrich, M., 2013. Host specialization in ticks and transmission of tick-borne diseases: a review. *Front. Cell. Infect. Microbiol.* 3, 57.
- McLain, D.K., Wesson, D.M., Oliver, J.H., Collins, F.H., 1995. Variation in ribosomal DNA internal transcribed spacers 1 among eastern populations of *Ixodes scapularis* (Acari: Ixodidae). *J. Med. Entomol.* 32, 353–360.
- Murdoch, F.A., Spratt, D.M., 2006. Ecology of the common marsupial tick (*Ixodes tasmani* Neumann) (Acarina: Ixodidae), in eastern Australia. *Aust. J. Zool.* 53, 383–388.
- Murrell, A., Dobson, S.J., Yang, X., Lacey, E., Barker, S.C., 2003. A survey of bacterial diversity in ticks, lice and fleas from Australia. *Parasitol. Res.* 89, 326–334.
- Needham, G.R., Teel, P.D., 1991. Off-host physiological ecology of Ixodid ticks. *Annu. Rev. Entomol.* 36, 659–681.
- Oorebeek, M., Kleindorfer, S., 2008. Climate or host availability: what determines the seasonal abundance of ticks? *Parasitol. Res.* 103, 871.
- Paradis, E., Jombart, T., Schliep, K., Potts, A., Winter, D., Paradis, M.E., 2017. Package ‘pegas’.
- Parola, P., Raoult, D., 2001. Ticks and tickborne bacterial diseases in humans: an emerging infectious threat. *Clin. Infect. Dis.* 32, 897–928.
- Perret, J.-L., Rals, O., Gern, L., 2004. Influence of climate on the proportion of *Ixodes ricinus* nymphs and adults questing in a tick population. *J. Med. Entomol.* 41, 361–365.
- R Core Team, 2017. R: A Language and Environment for Statistical Computing.
- Rambaut, A., Suchard, M., Xie, D., Drummond, A., 2014. Tracer V1.6. Available from: <http://beast.bio.ed.ac.uk/Tracer>.
- Randolph, S.E., 1998. Ticks are not insects: consequences of contrasting vector biology for transmission potential. *Parasitol. Today* 14, 186–192.
- Revell, L.J., 2012. phytools: an R package for phylogenetic comparative biology (and other things). *Methods Ecol. Evol.* 3, 217–223.
- Ronquist, F., Teslenko, M., Van Der Mark, P., Ayres, D.L., Darling, A., Höhna, S., Larget, B., Liu, L., Suchard, M.A., Huelsenbeck, J.P., 2012. MrBayes 3.2: efficient Bayesian phylogenetic inference and model choice across a large model space. *Syst. Biol.* 61, 539–542.
- Schmid, G.P., 1985. The global distribution of Lyme disease. *Rev. Infect. Dis.* 7, 41–50.
- Song, S., Shao, R., Atwell, R., Barker, S., Vankan, D., 2011. Phylogenetic and phylogeographic relationships in *Ixodes holocyclus* and *Ixodes cornuatus* (Acari: Ixodidae) inferred from COX1 and ITS2 sequences. *Int. J. Parasitol.* 41, 871–880.
- Spelman, D., 1982. Q fever: a study of 111 consecutive cases. *Med. J. Aust.* 1, 547–553.
- Spelman, A., Wilson, M., Levine, J., Piesman, J., 1985. Ecology of *Ixodes dammini*-borne human babesiosis and Lyme disease. *Annu. Rev. Entomol.* 30, 439–460.
- Spratt, D.M., Haycock, P., 1988. Aspects of the life history of *Cercaphiphilaria johnstoni* (nematoda: filarioidae). *Int. J. Parasitol.* 18, 1087–1092.
- Stamatakis, A., 2006. RAXML-VI-HPC: maximum likelihood-based phylogenetic analyses with thousands of taxa and mixed models. *Bioinformatics* 22, 2688–2690.
- Stamatakis, A., 2014. RAXML version 8: a tool for phylogenetic analysis and post-analysis of large phylogenies. *Bioinformatics* 30, 1312–1313.
- Stenos, J., Roux, V., Walker, D., Raoult, D., 1998. *Rickettsia honst* sp. nov., the aetiological agent of Flinders Island spotted fever in Australia. *Int. J. Syst. Evol. Microbiol.* 48, 1399–1404.
- Stone, B., Commings, M., Kemp, D., 1983. Artificial feeding of the Australian paralysis tick, *Ixodes holocyclus* and collection of paralysing toxin. *Int. J. Parasitol.* 13, 447–454.
- Storer, E., Sheridan, A.T., Warren, L., Wayte, J., 2003. Ticks in Australia. *Australas. J. Dermatol.* 44, 83–89.
- Telford, S., Armstrong, P.M., Katavolos, P., Foppa, I., Garcia, A., Wilson, M.L., Spielman, A., 1997. A new tick-borne encephalitis-like virus infecting New England deer ticks. *Ixodes dammini*. *Emerg. Infect. Dis.* 3, 165.
- Vilcins, I.-M.E., Old, J.M., Deane, E., 2009. Molecular detection of *Rickettsia*, *Coxiella* and *Rickettsiella* DNA in three native Australian tick species. *Exp. Appl. Acarol.* 49, 229–242.
- Vilcins, I.-M.E., Old, J.M., Deane, E.M., 2008. Detection of a spotted fever group rickettsia in the tick *Ixodes tasmani* collected from koalas in Port Macquarie, Australia. *J. Med. Entomol.* 45, 745–750.
- Walter, K.S., Carpi, G., Caccone, A., Diuk-Wasser, M.A., 2017. Genomic insights into the ancient spread of Lyme disease across North America. *Nat. Ecol. Evol.* 1, 1569.
- Wang, J.-M., Hudson, B.J., Watts, M.R., Karagiannis, T., Fisher, N.J., Anderson, C., Roffey, P., 2009. Diagnosis of Queensland tick typhus and African tick bite fever by PCR of lesion swabs. *Emerg. Infect. Dis.* 15, 963–965.
- Wesson, D.M., Denson Kelly, M., Oliver, J.H., Piesman, J., Collins, F.H., 1993. Investigation of the validity of species status of *Ixodes dammini* (Acari: Ixodidae) using rDNA. *Proc. Natl. Acad. Sci. U.S.A.* 90, 10221–10225.
- Zhang, R.L., Zhang, B., 2014. Prospects of using DNA barcoding for species identification and evaluation of the accuracy of sequence databases for ticks (Acari: Ixodida). *Ticks Tick Borne Dis* 5, 352–358.

Chapter Six

Progress and prospects towards establishing the *Cercopithifilaria johnstoni* life cycle using *Rattus fuscipes* and ticks (*Ixodes spp*) as hosts in the laboratory

Preface

Thus far, genomic resources have been assembled for *C. johnstoni* to resolve the phylogenetic relationship and genomic synteny with *O. volvulus*, the parasitic filarial nematode responsible for onchocerciasis (Chapter Two, Three). In chapters Two, Three and Four, these genomic resources of *C. johnstoni* has been used to compare with related filarial nematodes, specifically with *O. volvulus* in determining the suitability of using *C. johnstoni* in a small animal model system. Previously, Spratt and Haycock (1988) observed immunopathology, provoked by *C. johnstoni* in rats that is comparable to the human disease, onchocerciasis. Thus *C. johnstoni* is worth studying in the context of an animal model for onchocerciasis. The first phase of developing a physical animal model was to identify the tick species that are likely to transmit *C. johnstoni* to the rat host (Chapter Five). Chapter Five began to explore the diversity of ixodid ticks collected on *C. johnstoni*-infected rats and ticks collected on vegetation. Ticks appear to be morphologically similar but genetically distinct, identifying a potential cryptic species diversity. Thus, the standard molecular amplicons, i.e., COI, 12S and 16S, are essential for discriminating between species in the genus. In general, further improvement of ixodid tick taxonomy is required to improve the confidence of phylogeny. A comprehensive study assaying ticks for *C. johnstoni* presence is necessary to affirm the most competent *C. johnstoni* vector which has not been identified throughout this project. The following chapter explores a small project beginning to address the tick attachment to rodent processes. Finally, recommendations for future animal model development are proposed to emphasise the suitability of the *C. johnstoni* animal model for onchocerciasis.

6.1 Introduction

The fundamental problem in studying filarial diseases is the challenge of studying obligate parasites such as *O. volvulus* because as with all parasitic nematodes, they cannot be maintained outside their hosts (Grote et al., 2017). Both *O. volvulus* and *C. johnstoni* are parasites in which require a host to survive, which in turn enables further study into their effects on their respective hosts. Therefore, the development of additional methods to study their biology is required, such as a laboratory-based animal model or more specifically using *C. johnstoni* in a rodent model. To successfully develop the *C. johnstoni*-rodent model it is critical to establish a parasite life cycle, and this involves also establishing an intermediate host life cycle, as well as infection of the definitive host, the rat.

A laboratory model for onchocerciasis should have the following key features, as discussed in detail in the general introduction (Chapter One):

- 1) a convenient animal host able to be easily maintained in the laboratory
- 2) the laboratory host should be the natural host,
- 3) maintenance of the intermediate host/vector life cycle in the laboratory, and most importantly,
- 4) recapitulation of critical disease features, i.e., microfilarial-induced immunopathology in the skin and eye.

Chapter Six focuses predominately on feature (2) and (3) to explore the feasibility of developing the *C. johnstoni*-rodent animal model. The chapter leads to specific recommendations about what is required for the model to be feasible discussing the most important future directions learnt from these preliminary experiments.

The life cycle of *C. johnstoni* begins with the tick biting and feeding on the small rodent injecting the infective (iL3) stage of *C. johnstoni* into the subcutaneous skin of the rodent. The infective *C. johnstoni* worm will develop into the fourth stage larvae (L4) and into adults who also reside in the subcutaneous skin. The adults will produce microfilariae (L1) which elicit the pathological symptoms. Another tick will bite and feed on the rodent ingesting the microfilariae for *C. johnstoni* to develop into the L2 and iL3 stages and the cycle will continue (Figure 1.7) (Spratt and Varughese, 1975; Spratt and Haycock, 1988). Currently,

it is unknown how long it takes for the microfilariae to mature into their infective L3 stage within the tick intermediate host.

The *Ixodes* life cycle (Figure 1.11) has four stages—egg, larva, nymph and adult—taking approximately 12 months to complete (Anderson et al., 2004; Bonnet and Liu, 2012). The length of time required for a single generation is a challenge for animal model development. An additional complicating factor is that ticks require a relative humidity of 85% and a temperature of approximately 25°C to be highly active (Spratt and Haycock, 1988; Ghosh and Azhahianambi, 2007; Troughton and Levin, 2007). However, the high humidity increases the risk of mould and therefore requires constant maintenance of tick housing. Finally, ticks must feed on a suitable host in order to develop into the next life stage, and it is, therefore, essential for a blood meal to be provided in the laboratory, either with live animals or artificial feeding methods (Konnai et al., 2008; Krull et al., 2017).

Maintaining the ticks' life cycle in the laboratory is fundamental for understanding the ticks' developmental cycle and for providing tick numbers for future research. The genus *Ixodes* has many species that are medically important causing harm to both animals and humans and thus are a significant group to study (Clifford et al., 1973; Parola et al., 2013). A source of laboratory-reared ticks will facilitate advancements to understand the tick biology, exploring its role as a vector and studying the pathogens or toxins transmitted to several hosts (Donnelly and Peirce, 1975; Konnai et al., 2008; Kocan et al., 2015). The access to laboratory-reared ticks also provides vectors for parasite transmission to replicate the life cycle in animal models. There are many valuable purposes for successfully maintaining the life cycle of ticks in the laboratory.

Several laboratories have proven tick-rearing to be successful and useful for their intended purposes. For example, Kocan et al. (2015) successfully maintained *I. scapularis*, a tick transmitting *Borrelia burgdorferi*, the causative agent of Lyme disease in the laboratory for future research into vaccines. Konnai et al. (2008) successfully established a laboratory colony of *Ixodes persulcatus* to explore tick biology and pathogen transmission. Lastly, Donnelly and Peirce (1975) have successfully reared *Ixodes ricinus* for several years to explore the transmission of *Babesia divergens*. These few examples highlight that it is worthwhile and possible to rear *Ixodes* ticks for a range of different purposes. A critical observation of these studies is that different laboratory-reared tick species

have different optimal life cycle requirements. A rearing method used for Northern hemisphere ixodid ticks may not be appropriate for Southern hemisphere ticks and consequently require specific optimisation based on the ixodid tick used for the laboratory colony.

Nevertheless, there can be significant hurdles in maintaining a vector life cycle in the laboratory which will be discussed in detail throughout this chapter. One major limitation of maintaining ticks in laboratory is the time required for ticks to moult into their next life stage after a blood meal. These ticks are required to be maintained and kept alive for the duration of moulting before they can be reattached to a host. Furthermore, a method is described by Spratt and Haycock, (1988), that was developed to have more control of a *C. johnstoni* infection by dissecting the ticks to obtain iL3 life stage and subcutaneously injecting the parasite into the host. There is the potential for this method to provide a more efficient method to guarantee *C. johnstoni* infection. Identifying a suitable method to guarantee infection in a host would reduce the limitations already associated with maintaining ticks in the laboratory.

The following chapter is a series of incomplete preliminary experiments to test the feasibility of (a) maintaining the tick life cycle in the laboratory, (b) attaching immature wild-caught ticks to infected bush rats to generate infective ticks after a single moult rather than attempting to maintain the complete vector life cycle, and (c) determining the duration of an infection using captive, naturally infected wild-caught bush rats.

6.2 Methods

There is evidence of *C. johnstoni* infection in bush rats at Mogo State Forest and therefore was a suitable field site to collect samples for future model development. The experiments took place in two locations, Kioloa ANU campus (NSW) and La Trobe University (VIC). Typically, field trips were conducted over a week, and thus any ticks or rats collected would need to be housed at the ANU field campus laboratory. At the end of each field trip, tick material was transported back to La Trobe University using the tubes described in section 6.2.1.1 in order to continue troubleshooting tick attachments on the rodents we had obtained that were now being housed at La Trobe University.

6.2.1 Tick collection process at Kioloa and Mogo

6.2.1.1 Tick collection directly from the ground

Un-engorged (i.e., unfed and questing) ticks were collected on pasture and in clearings at or close to the bush/pasture margins at two locations on the Australian National University Coastal Campus, Kioloa, New South Wales, Australia, by flagging in February, April and June 2015, and in October and November 2016 (map of locations presented in Chapter Five, Fig. 1). The process of flagging consisted of dragging an approximately 1 x 1.5 m piece of white fabric along the ground (Supplementary Figure 6.1a). The dark-coloured ticks caught up on the fabric were visually contrasting and were picked off with tweezers and placed into temporary tubes. Falcon tubes (15 ml) were placed at a 45-degree angle and filled with a mixture of plaster of Paris (50 g), Milli-Q water (30 ml) and activated charcoal (2 g) being a modification of the plaster and water ratios from Konnai et al. (2008). The lids had pierced holes for air ventilation that were not large enough for a tick to escape (Supplementary Figure 6.1b).

6.2.1.2 Tick collection directly from rats

Native Australian bush rats, *R. fuscipes*, were captured at two sites in the Mogo State Forest, New South Wales using small Elliot traps baited with a paste of approximately equal proportions of rolled oats and peanut butter. The traps were spaced at roughly 10 m intervals in trap lines approximately 200 m in length, with four parallel lines approximately 10 m apart (i.e., a grid of approximately 200 x 40 m with 80 traps). Permits for trapping were AEC 13-23, NSW – Scientific

Licence 5L 101280 and VIC – Scientific Permit 10007169. The traps were open overnight, then cleared within three to four hours of sunrise. The rats were transported in the traps to the laboratory at the Australian National University Coastal Campus, Kioloa where they were transferred to a calico bag, scanned for the presence of a passive integrated transponder (PIT) and weighed. Those rats without a PIT when scanned were fitted with a tag inserted subcutaneously between the shoulder blades. Rats were housed individually in a wire bottom cage with food and water *ad libitum*. Each cage contained a short length of PVC pipe in which the rats could hide. A catchment tray under each cage allowed the recovery of engorged ticks that had dropped from the rats overnight (Spratt and Haycock, 1988).

The following day, any engorged ticks that had dropped off the rats into the collection trays were recovered, counted, assessed for developmental stage (larva, nymph, adult) and placed into new tubes containing charcoal, plaster of Paris mixture. The rats were released to the site of capture after three nights of housing.

6.2.1.3 Presence of *Cercopithifilaria johnstoni*

Rats were tested for infection with *C. johnstoni* by placing a skin biopsy snip taken bilaterally from the margin of each ear using a 2 mm diameter skin biopsy punch in 0.9% physiological saline and left to sit for one hour to facilitate the migration of microfilariae out of the snip (Spratt and Haycock, 1988; Vuong et al., 1993). The ear snip was then teased with tweezers to allow the microfilariae to escape the subcutaneous layer of skin and was poured into a petri dish to observe under a microscope. Only alive, twitching microfilariae were counted because dead microfilariae are challenging to identify if at all possible.

6.2.2 Housing chambers for live ticks at La Trobe University

To house ticks in the laboratory, two different sized vials were used to house different numbers of ticks. Glass scintillation vials of 20 ml with a diameter of 27 mm or glass scintillation vials of 7 ml with a diameter of 17 mm were prepared. The scintillation vials were placed at a 45-degree angle and filled with a mixture of plaster, as previously mentioned (section 6.2.1.1). The activated

charcoal was added to avoid the tubes acquiring mould. The lids of the scintillation tubes had a hole cut out that was then covered with stainless steel mesh (0.154 mm x 0.10 mm) to prevent ticks from escaping but still allow constant airflow. Plastic containers (particularly polypropylene) were not used due to the increase tick mortality that results.

All tick containers were initially stored in an incubator at 25°C and 80% relative humidity as per Spratt and Haycock (1988) and others (Burgdorfer, 1984; Ghosh and Azhahianambi, 2007; Troughton and Levin, 2007). The incubator in use stopped functioning approximately halfway through the collection, at which point all tick containers were transferred to a constant environment room at 20°C and 65% relative humidity.

In the laboratory, every bush rat was regularly weighed by transferring them from their enclosures to a clear Perspex tube which had previously been weighed, as part of the regular program to monitor their health. The tube was then placed on the scales and recorded the weight in grams. The clear Perspex tube additionally allowed viewing of each rat to check for any visible signs of physical illness or distress.

The bush rats that were microfilariae positive by skin biopsy at the time of capture were transported to LTU and were housed for a total of three years from capture to the end of experiments for subsequent tick attachment experiments.

6.2.3 Tick attachment procedure in the laboratory (La Trobe University)

A critical part of using an animal model to study a disease such as onchocerciasis is to be able to recapitulate the characteristic disease features. The recapitulation of these features requires transmission of the parasite to the hosts in laboratory conditions hence the *C. johnstoni*-rodent animal model. Tick attachment is a crucial component of this animal model because the ticks are responsible for allowing *C. johnstoni* to mature into the iL3 stage and are equally responsible for transmitting the iL3 stage to the rat for infection. It is vital to get the tick attachment process right to ensure the success of the *C. johnstoni* animal model.

It was important for the tick attachment procedure to obtain the larvae and nymph life stages of the ticks. The larvae and nymphs can ingest the microfilariae

from the bush rats whereas the adult females only feed on rats for a blood meal after mating to engorge and produce eggs (Figure 1.11). Thus, adults were not attached to the bush rats during the attachment procedures.

Two independent procedures were tested for tick attachment to the maintained wild-caught captive rats. The first method involved anaesthesia with halothane performed under veterinary supervision using a rat-adapted delivery system that was used to sedate the bush rats performed under AEC 13–23. A small metal ring was glued to the back of the bush rats where ticks were placed, confining the tick to attach in that area and this was then covered so the ticks could not escape.

A second method was developed that removed the risk of anaesthesia and potential discomfort from the glued metal ring and reduced rat handling. Rats were placed in a small PVC tube with caps at either end of the tube and a 3-5 mm hole in the side of the tube (Supplementary Figure 6.2a). The rats naturally move into the tube when it is placed in the rat enclosure as it is a dark space, and thus they were easily confined. The ticks were placed on the back of the rats' necks through the small hole in the tube, allowing natural attachment. Rats were confined in this tube for 40 minutes to allow the ticks time to attach.

Rats with attached ticks, from both methods, were placed in wire-floor cages with food and water for five to seven days until the ticks dropped off (Supplementary Figure 6.2b). On the bottom tray, a thick layer of Vaseline was smeared around the edge to capture any ticks that tried to escape. The Vaseline was observed daily to ensure there were no apparent gaps for ticks to crawl through and escape.

The total number of ticks placed on each rat was determined by (1) the number of ticks that were collected from the flagging field trips, (2) the number of ticks that survived transportation and storage and (3) whether rats were infected with *C. johnstoni* or were naïve rodents.

The rats used for tick attachment experiments were either wild-caught captive bush rats and had patent infections by skin biopsy or were accidental naïve captive-bred juvenile bush rats, which were not a result of a deliberate breeding program. The final method chosen for the tick attachment results was the second method where the rats were placed in a PVC tube.

6.2.4 Animal Ethics Approval and Wildlife Permits

The trapping of the bush rats and the subsequent holding of captured rats for three days post-trapping to allow the collection of engorged ticks were all tasks performed with the appropriate regulatory permits. The maintenance and anaesthesia of captured bush rats for subsequent tick attachment experiments were also performed with appropriate AEC permit approval.

- La Trobe University animal ethics approval AEC 13–23
- New South Wales – Scientific License 5 L 101280
- Victorian – Scientific Permit 10007169.

6.3 Results

6.3.1 Samples collected

Large numbers of unfed, questing ticks were collected from two sites, Mogo State Forest and Kioloa ANU campus in NSW, Australia in 2015 (Supplementary Table 6.1) and 2016 (Supplementary Table 6.2). Across both field sites, larvae were the most collected life stage, and adults were rarely collected either from rats or from flagging on pasture. Thousands of larvae, ~700 nymphs and ~150 adults were collected in total (Supplementary Table 6.1, 6.2).

Engorged ticks were only collected from rats caught at Mogo State Forest in February and April of 2015 (Supplementary Table 6.1). Most of the engorged ticks collected were at the larval stage. A total of 343 engorged larvae were collected, and a total of 68 engorged nymphs were collected (Supplementary Table 6.1). No engorged adults were acquired from the captured bush rats.

The collected ticks were maintained in the laboratory to allow engorged ticks to moult for re-attachment to pass on *C. johnstoni* iL3s. The exact number of ticks that survived through their first moulting stage was not recorded, but approximately half of the ticks moulted. Nymphs had better success, in general, at surviving to re-attachment than larvae.

6.3.2 Tick attachments

A summary of the wild-caught infected bush rats and the naïve captive-bred bush rat is recorded in Table 6.1. The rats were identified by either male (M) or female (F) and a corresponding number identifier (Table 6.1). All the rats were weighed at two different time points, March and August in 2016. Ear snips were taken from the wild-caught rats to observe their patent infections (Table 6.1). The bush rats ranged from low (<10 microfilariae) to high (>200 microfilariae) patent infections. A wild-caught male bush rat (M13) had the highest microfilarial burden out of all the wild-caught bush rats (Table 6.1). Most of the bush rats maintained their *C. johnstoni* infection over the six months except for wild-caught bush rat M2, which had a low patent infection in March and had no microfilariae observed from a skin biopsy in August (Table 6.1).

Table 6.1: Rat weights and *Cercopithifilaria johnstoni* microfilariae counts at two different time points: March 2016 and April 2016. The table contains information on tub number of where each rat was housed, the rat numbers, animal house codes for each bush rats, recorded weights, whether the rats were ear snipped and the microfilarial burden.

Bush rat #	Wild caught/captive bred	Tub #	Sample date: March 2016			Re-sample date: August 2016		
			Weight (kg)	Ear Snip (Y/N)	Mf burden (total from bilateral 2mm diameter ear punch biopsy)	Weight (kg)	Ear Snip (Y/N)	Mf burden (total from bilateral 2mm diameter ear punch biopsy)
M13	Wild-caught	1	0.253	Y	High >200	0.381	Y	Medium >80
F14	Wild-caught	2	0.177	Y	Low <10	0.249	Y	Low <10
M20	Captive-bred	3	0.28	N	-	0.419	N	-
M21	Captive-bred	4	0.152	N	-	0.348	N	-
F8	Wild-caught	5	0.279	Y	Low <10	0.281	Y	Low <10
M4	Wild-caught	6	0.112	Y	Medium >80	0.227	Y	Medium >80
F16	Captive-bred	8	0.201	N	-	0.346	N	-
F17	Captive-bred	8	0.218	N	-	0.333	N	-
F18	Captive-bred	8	Not weighed	N	-	0.32	N	-
F19	Captive-bred	8	0.203	N	-	0.329	N	-
M2	Wild-caught	9	0.152	Y	Low <10	0.278	Y	None
M10	Wild-caught	11	0.277	Y	Low <10	0.391	Y	Low <10
M18	Wild-caught	12	0.324	N	-	0.357	N	-

In 2016, three independent experiments of tick attachments to bush rats occurred (Tables 6.2, 6.3, 6.4). In the first attachment experiment (Table 6.2), 30 tick larvae and 16 tick nymphs that were collected from flagging in Kioloa were equally divided between four rats. Importantly the tick attachment process could not be observed directly through the Perspex tube method. A total of four engorged nymphs and one engorged larva dropped off the host (Table 6.2). Three nymphs dropped off one female rat F8 (LIT5265– wild-caught) on days four, five and six after attachment. One nymph dropped off the other female rat F14 (LIT6301 – wild-caught) six days after attachment. One slightly engorged larva had dropped from a male rat number M20 (LIT7116 – captive-bred) on the third day of the experiment; however, the larva was dead. Another engorged larva dropped from the same male host M20 (LIT7116 – captive-bred) on the fourth day after attachment (Table 6.2).

The second attachment experiment used two rats with 30 nymphs divided between them (Table 6.3). The ticks used in this attachment experiment consisted of a combination of nymphs collected from flagging Kioloa and Mogo State Forest. Only one engorged nymph was collected from one single rat F14 (LIT6301 – wild-caught) five days after attachment. The remaining ticks were not accounted for and presumed to have been consumed by the bush rat or were able to crawl undetected through the Vaseline escaping the enclosures.

The third attachment experiment used two rats and 30 nymphs equally divided between each rat (Table 6.4). Again, these ticks were a combination of the flagged nymphs collected from Kioloa and Mogo Stage Forest. Attachment three was the most successful attachment experiment, resulting in a total collection of six engorged nymphs. Four engorged nymphs dropped off the male host M18 (LIT6515 – captive-bred) four days after attachment, and one dropped five days after attachment. One engorged nymph dropped off the female host F14 (LIT6301 – wild-caught) four days after attachment (Table 6.4).

Overall, the attachment rates of the ticks to the bush rats was low. Many of the ticks were unaccounted for throughout the attachment processes. At least three ticks would not attach, and over 20 ticks disappeared during the experiment. The experiments confirmed that ticks could be attached to bush rats for engorgement in the laboratory; however, the attachment rates drastically need

to improve for the successful development of an animal model to improve the chance of infection.

Table 6.2: Summary of the first tick attachment experiment for 2016. Four Australian bush rats with a *Cercopithifilaria johnstoni* infection were used with 15 larvae on the two male rats and eight nymphs each on the female rats. Observations record whether there were any changes in the movement of ticks and when the ticks dropped off their hosts. The 'Returned' observation referred to when the rats were returned to their enclosures.

	Attachment Date/no. ticks attached	Observations								
Bush rat	14.4.2016	15.4.2016	16.4.2016	17.4.2016	18.4.2016	19.4.2016	20.4.2016	21.4.2016	22.4.2016	TOTAL
Tub #4 male M21 LIT7116(2)	15 Larvae	No Activity	No Activity	No Activity	No Activity	No Activity	Returned			0
Tub #3 male M20 LIT7116(2)	15 Larvae	No Activity	No Activity	1 larva found dead in Vaseline tried to escape	1 engorged Larva dropped	No Activity	Returned			1 larva
Tub #5 female F8 LIT5265 3765455	8 Nymphs	No Activity	No Activity	No Activity	1 engorged Nymph dropped	1 engorged Nymph dropped	1 engorged Nymph dropped	No Activity	Returned	3 nymphs
Tub #2 female F14 LIT6301 3769088	8 Nymphs	No Activity	No Activity	No Activity	No Activity	No Activity	1 engorged Nymph dropped	No Activity	Returned	1 nymph

Table 6.3: Summary of the second tick attachment experiment for 2016. Two Australian bush rats with a *Cercopithifilaria johnstoni* infection were used with 15 nymphs on the two female rats. Observations record whether there were any changes in the movement of ticks and when the ticks dropped off their hosts. 'Returned' refers to when the rats were returned to their enclosures.

	Attachment Date/no. ticks attached	Observations							
Bush rat	19.5.2016	20.5.2016	21.5.2016	22.5.2016	23.5.2016	24.5.2016	25.5.2016	26.5.2016	TOTAL
Tub #5 female F8 LIT5265 3765455	15 Nymphs	No Activity Unattached ticks dropped off	No Activity	No Activity	No Activity	No Activity	No Activity	Returned	0
Tub #2 female F14 LIT6301 3769088	15 Nymphs	No Activity	No Activity	No Activity	No Activity	1 engorged Nymph dropped	No Activity	Returned	1 nymph

Table 6.4: Summary of the third tick attachment experiment for 2016. Two Australian bush rats with a *Cercopithifilaria johnstoni* infection were used with 15 nymphs on the two rats. Observations record whether there were any changes in the movement of ticks and when the ticks dropped off their hosts. 'Returned' refers to when the rats were returned to their enclosures.

	Attachment Date/no. ticks attached	Observations								
Bush rat	1.12.2016	2.12.2016	3.12.2016	4.12.2016	5.12.2016	6.12.2016	7.12.2016	8.12.2016	9.12.2016	TOTAL
Tub #12 male M18 LIT6515	15 Nymphs	No Activity	No Activity	No Activity	4 engorged Nymphs dropped	1 engorged Nymph dropped	No Activity	No Activity	Returned	5 nymphs
Tub #2 female F14 LIT6301 3769088	15 Nymphs	No Activity	No Activity	No Activity	1 engorged Nymph dropped	No Activity	No Activity	No Activity	Returned	1 nymph

6.4 Discussion

Obligate parasites, i.e., *O. volvulus* and *C. johnstoni* cannot be maintained outside of their hosts (Grote et al., 2017) impeding research into the biology of *O. volvulus* and understanding what is driving the immunopathology observed in *O. volvulus*-infected humans. The aim was to explore a possible animal model system using the related filarial nematode *C. johnstoni* in rodents as *C. johnstoni* has proven to elicit similar immunopathology comparable to that observed in *O. volvulus*-infected patients (Spratt and Haycock 1988). A successful animal model requires either an established parasite life cycle and vector host life cycle, or a suitable method to obtain infective larvae to infect a host. Chapter Six consisted of a series of incomplete preliminary experiments to test the feasibility of (a) maintaining the tick life cycle in the laboratory, (b) attaching immature wild-caught ticks to infected bush rats to generate infective ticks after a single moult rather than attempting to maintain the complete vector life cycle, and (c) determining the duration of an infection using captive, naturally infected wild-caught bush rats.

There were two groups of ticks independently collected for attachment procedures in the animal house and used to explore the possibility of maintaining the tick life cycle in the laboratory discussed below, (section 6.4.1.1) numbers of unfed questing ticks collected by flagging and (section 6.4.1.2) numbers of engorged ticks collected from captured *C. johnstoni*-infected bush rats. An important term used throughout the discussion is "questing ticks". The term questing refers to a behaviour exhibited by hard ticks, Ixodida, as a method of increasing the possibility to interact with a suitable host. The behaviour involves climbing up blades of grass or vegetation waiting with their front legs outstretching making themselves available for attachment on anything or anyone that brushes past them (Murdoch and Spratt, 2006; Tomkins et al., 2014).

6.4.1 Collection of ticks for life cycle maintenance

6.4.1.1 Numbers of unfed questing ticks

Flagging the vegetation at Kioloa and Mogo State Forest proved to be a successful method for collecting questing ticks for future rat attachments. Hundreds of ticks were collected from the environment at multiple life stages, with the ticks being predominately larvae and nymphs (Supplementary Table 6.1, 6.2).

The flagging sites consisted of tall and grazed grass, small bushes and short grass around the base of trees. Observationally, confined areas with bushes and trees had an increased number of ticks, perhaps because small mammals are more commonly present in these covered areas and thus an ideal place for ticks to be questing for an appropriate host.

While the flagging of ticks was successful, it is often time consuming to collect many ticks. Alternate methods of collecting ticks from the environment have now been considered for future collection of ticks. Tick traps have been known to be successful at trapping questing ticks. For example, one commonly used trap is the CO₂-baited trap (Falco and Fish, 1991, 1992; van Duijvendijk et al., 2017). As *Ixodes* are attracted by physical and chemical stimuli released by hosts, such as carbon dioxide, heat and odours (Wall and Shearer, 1997; Bonnet and Liu, 2012; van Duijvendijk et al., 2017), ticks are attracted to the CO₂ gas emitted by dry ice and then get caught in a Styrofoam reservoir by a simple method involving tape (Falco and Fish, 1991, 1992). Alternatively, a pheromone trap has been developed as described in Anish et al. (2017). The trap is simple to construct, consisting of an acrylic sheet with double-sided sticky tape. Filter paper discs soaked with 5 µl of pheromone nanogold solution were used to attract questing ticks (Anish et al., 2017). The simplicity of these methods makes the chemical stimuli traps appealing to trial in future tick collection field trips.

The advantage of using baited tick traps rather than flagging is that it enhances the collection of questing ticks and reduces risk to the researcher by minimising physical exposure to probable tick bites. For example, to flag vegetation for questing ticks, the researcher must walk through the same vegetation, thus being a risk for the questing ticks to attach to their clothing and then skin. However, baited tick traps do not require the researcher to have as much contact with the environment where the ticks are possibly questing and therefore lessens the risk.

Nevertheless, these approaches would require additional verification to guarantee that ticks stuck to tape could be removed without injury so they could be later attached to rats for *C. johnstoni* transmission. These trap methods also require more equipment and thus are not as simple to conduct compared to flagging. As the current flagging method was successful for the intended purposes and is reliable to collect appropriate numbers of ticks, flagging should

still be a simple and effective method to be considered for obtaining ticks for the small animal model.

6.4.1.2 Numbers of engorged ticks

Wild bush rats that were caught from Mogo State Forest had several ticks attached. While many rats had less than fifty engorged ticks drop off within the three-night housing period, several bush rats had greater than a hundred engorged ticks drop off over the same period. The rats were released after three nights, and therefore there may have been additional ticks that had not yet dropped. Larvae generally take three days to drop after initial attachment, but nymphs can range from four to seven days after initial attachment to drop off their host (Grattan-Smith et al., 1997). The life stages of ticks attached to the bush rats at the time of collection would have been entirely dependent on when the ticks attached to their host and whether there had been enough time for them to feed, engorge and drop.

The numbers of ticks collected were discussed from the two groups, unfed questing ticks and engorged ticks. The survival of the two groups collected for attachment in the laboratory was then independently explored, discussed below, (section 6.4.2) feasibility of maintaining ticks in the laboratory.

6.4.2 Feasibility of maintaining ticks in the laboratory

The unfed questing ticks collected from the environment at Kioloa and Mogo State Forest were collected to troubleshoot the tick attachment process. The ticks collected at Kioloa were unlikely to be infective with *C. johnstoni* iL3s because there have been no reports of *C. johnstoni* infection in bush rats detected throughout the Kioloa area, and thus any ticks collected there are unlikely to carry *C. johnstoni*. *C. johnstoni* has not been previously reported anywhere in Kioloa. However, it was not possible to determine if the nymphs had previously fed on a naturally infective bush rat because there is currently no assay developed for live ticks. The larvae collected were uninfected as they would not have previously fed on a host.

The advantage to collecting unfed questing ticks over the engorged ticks is that the unfed questing ticks can be collected and attached to infected rats to ingest and obtain an initial *C. johnstoni* microfilariae burden that they did not previously contain. As questing ticks were only used for troubleshooting the attachment process, initially they did not require the long-term maintenance through moulting and their life stages. From the moment the engorged ticks drop from wild-caught naturally infected bush rats, the ticks need to be maintained through their moulting before they can be used as a source of *C. johnstoni*-infective larvae. Unfed ticks can be attached to naturally infected bush rats immediately as they have been acquired from the environment questing for a host to feed. Once the unfed questing ticks are attached to a host and feed, the newly engorged ticks were then maintained through moulting and thus treated like the engorged ticks acquired from the wild-caught naturally infected bush rats.

The engorged ticks were obtained from naturally infected bush rats and thus are more likely to have a *C. johnstoni* infection with parasites that are maturing to the iL3 infective stage than the ticks collected on vegetation. These ticks would require maintenance through their moulting stage for future attachment to an uninfected laboratory rat host. A significant difficulty with the development of an animal model lies with the intensive maintenance for ticks to survive through moulting stages. The ticks throughout these experiments proved to be highly sensitive to changes in relative humidity and temperature which is supported by several tick species relying heavily on 85-100% relative humidity for their survival (Burgdorfer, 1984; Ghosh and Azhahianambi, 2007; Troughton and Levin, 2007), and drastic variations in temperature significantly affect tick growth rate (Chilton, 1992).

A significant challenge for the development and maintenance of a tick colony is that the life cycle is relatively long, taking up to a year from larvae to adults. *I. scapularis* in the Northern hemisphere has a two-year life cycle as a result of a period of diapause during the winter as the harsh freezing temperature of winter results in desiccation (Kocan et al., 2015). A critical goal in the United States has been to study and understand how to control *I. scapularis* on account of the increasing medical importance *I. scapularis* has in transmitting Lyme disease to humans (Burgdorfer et al., 1982; Spielman et al., 1985; Piesman, 2002; Gulia-Nuss et al., 2016). The use of a tick colony will enable a vast number of studies to

focus on understanding *I. scapularis* biology, pathogen transmission and development of a vaccine for Lyme disease (Piesman, 2002; Kocan et al., 2015). A laboratory in the US has successfully reduced the total rearing time of *I. scapularis* to 7.5 months instead of two years (Kocan et al., 2015). The reduction of the life cycle timeframe for *I. scapularis* could indicate that with optimal conditions, the life cycles of all *Ixodes* species, even in Australia, could be reduced when optimised in the laboratory. If a tick species such as *I. trichosuri* or *I. holocyclus* could be reared in the laboratory and life decreased from one year, then the maintenance of a tick colony may provide a valuable resource to pursue.

There are a range of experiments and techniques that could be trialled for future experiments if it is required that ticks be maintained in the laboratory. Some laboratories have successfully developed tick colonies (Troughton and Levin, 2007; Konnai et al., 2008), using artificial feeding methods such as skin membranes mimicking a host, as these are more easily controlled. An advantage of using artificial feeding methods with membranes is the reduction in the requirement for animal numbers and maintaining the hosts in the laboratory, reducing overall costs. However, they are very tedious to set-up, clean and maintain (Soares et al., 2005; Bonnet et al., 2006; Krull et al., 2017).

As an alternative to artificial feeding methods, rabbits are a more common host for tick colonies (Burgdorfer, 1984; Ghosh and Azhahianambi, 2007) and similarly guinea pigs (Jones et al., 1988). These could be an option to maintain the colony before tick attachment to *R. norvegicus* for *C. johnstoni* transmission. The use of rabbits or guinea pigs significantly increases the expense of the animal model. Ideally, it is important to find a balance between affordability and a successful model to attach ticks and study disease.

However, due to the results from these preliminary experiments collecting and maintaining the ticks in the laboratory maintenance of the tick life cycle was discontinued. There are several caveats in maintaining the life cycle and it is not necessary for studying the host immune responses of parasite infection. Thus, maintaining the tick life cycle is not feasible in the context of developing an animal model for onchocerciasis research. A more important feature of the animal model is obtaining the infective stage of *C. johnstoni*. Appropriate attachment methods would need to be devised to allow *C. johnstoni* to be transmitted from the bush rats.

6.4.3 Attachment of immature wild-caught ticks to infected bush rats

Tick attachment is an essential step to determine whether the *C. johnstoni*-rodent animal model is feasible. Two methods were explored to determine a suitable method of attaching ticks. The first method required anaesthesia of the bush rats and uncomfortable rings glued to the back of the bush rats' neck, thus would not be a feasible long-term method of attaching ticks for an animal model. The second method proved to be ethically acceptable, provided minimal discomfort to the bush rats and allowed a more natural tick attachment process to occur. However, the efficiency of tick attachment was very low (Tables 6.2, 6.3, 6.4). Developing a highly efficient and successful tick attachment method is challenging to develop.

Findings from the Kocan et al., (2015) *I. scapularis* experiments revealed the ticks attached better to hosts when the laboratory rearing cycle coincided with their cycle in nature. However, the exact attachment efficiency of *I. scapularis* is unknown. Throughout the experiments, Kocan et al., (2015) infested their hosts with a high number of ticks because of the high mortality rate for the ticks. The efficiency of tick attachment to Australian bush rats using the ethically acceptable attachment method has also not been resolved. The preliminary experiments conducted proved we would require a large number of ticks and large number of rats to ensure a good attachment rate and useful number of infected rats. For example, if the ticks attached to the bush rats, 10 infected rats per three months would be acceptable to maintain *C. johnstoni* parasites providing the ticks attached and transmitted the parasite. Based on the results from the preliminary tick attachment experiments, 20-30 larvae would be required per rat or 10-20 nymphs per rat to get a couple of ticks feeding on the bush rat. Thus requiring approximately 250 larvae or 150 nymphs every three months to successfully obtain infective rats. However, these numbers would only be acceptable providing that the ticks already had ingested *C. johnstoni* and allowed *C. johnstoni* to develop into iL3. If the ticks needed to be fed on an infected rat to infest *C. johnstoni*, engorge and then moult into the proceeding life stage, the numbers of ticks would need to be increased by at least three-fold. Improving the current Australian tick attachment rate may require following similar studies such as Kocan et al., (2015) by including light and dark photoperiods that could aid in replicating a more accurate, natural environment for the ticks to moult and feed.

While it would be desirable to have captive-bred ticks and produce a tick colony for constant supply of ticks for attachment to bush rats, it is not essential. These experiments have identified technical challenges that would need to be overcome that was beyond the scope of this PhD project. Developing a tick life cycle is very time consuming and sensitive to a range of factors thus the initial experimental approach of maintaining the entire life cycle in the laboratory was not successful and not further pursued in this project. The most important requirement for the *C. johnstoni*-rodent animal model is to obtain infective larvae. There are a range of different experiments that can be conducted to obtain the infective larvae that do not rely on the maintenance of a tick colony or even re-attachment of a tick to a bush rat eliminating the challenges observed throughout these experiments, discussed in section 6.4.5.

6.4.4 Determining the duration of an infection using captive, naturally infected wild-caught bush rats

Naturally infected wild-caught bush rats from Mogo State Forest were transferred to the La Trobe University animal house and progressively monitored by conducting ear biopsies every three to six months to observe *C. johnstoni* infection (Table 6.1). The bush rats successfully maintained a *C. johnstoni* infection over the three years since they were captured from Mogo State Forest. The consistent infection over three years implies that a *C. johnstoni* infection could be lifelong in bush rats which is an important conclusion if the *C. johnstoni*-rodent animal model was to be pursued. A lifelong *C. johnstoni* infection in bush rats allows for a range of various experiments to observe infection over time identifying symptoms and studying the host immune responses to infection and treatment. Retaining *C. johnstoni* infection also mimics the long infection period of *O. volvulus* where an individual can be infected with the adult *O. volvulus* worms for 15 years (Basáñez et al., 1994; Omura and Crump, 2004; Coffeng et al., 2013). The *C. johnstoni* infection lasts for the majority the hosts lifespan of less than 3 years and appears to have a longer infection than several of the current animal models using *A. viteae* or *L. sigmodontis* (Beaver et al., 1974; Hubner et al., 2009).

The three year duration of *C. johnstoni* infection in Australian bush rats is an important finding for future development of the *C. johnstoni*-rodent model that will be useful for future experiments.

6.4.5 Future directions for the *Cercopithifilaria johnstoni*-rodent animal model

6.4.5.1 Tick dissection and subcutaneous injection into rat

An alternate method for improving *C. johnstoni* transmission was conducted in the experiments of Spratt and Haycock (1988). The *I. trichosuri* ticks were dissected to recover the infective larvae *C. johnstoni* stage iL3 and then injected the iL3s subcutaneously into *R. norvegicus* to obtain experimentally infected rats (Spratt and Haycock, 1988; Vuong et al., 1993). An obstacle for the injection method is knowing the time required for *C. johnstoni* microfilariae to reach maturity to iL3s. Currently, it is not reported nor known how long it takes for *C. johnstoni* to mature to the iL3 stage within an ixodid tick. It has been assumed that the development of *C. johnstoni* from microfilariae to iL3 occurs when the tick has dropped off the host during the tick moulting stage (Spratt and Haycock, 1988). There is an increased possibility that maturity to iL3 occurs sooner than the duration of tick moulting. Therefore, this method will reduce the need to maintain the tick life cycle in the laboratory for future experiments (Spratt and Haycock, 1988). A simple experiment that can be conducted in the future to determine the optimal time for dissection would be to obtain engorged ticks that fed on *C. johnstoni*-infected rodents and dissect the salivary glands and midguts of the ticks to extract *C. johnstoni*. Each group of ticks will be at varying time points, i.e., five days after dropping off the host, ten days, 20 days and so on. The results from this experiment should reveal the optimal point at which *C. johnstoni* is an iL3 and ready for dissection to be then injected into a new host for infection.

Spratt and Haycock (1988) presumed that there is a 90-day pre-patent period of *C. johnstoni* transmission; however, they had not identified the exact time point that *C. johnstoni* matures into the iL3 and can be dissected. Ideally, it would not take as long for *C. johnstoni* microfilariae to mature to the iL3 stage compared to the time it takes for the ticks to moult to their next life stage, thus drastically reducing the time required for tick life cycle maintenance and therefore removing many of the procedures requiring troubleshooting. In previous

experiments, *C. johnstoni* was dissected from the moulted ticks and therefore indicating that the ticks are still required to mature through their moulting phase before *C. johnstoni* could be used to infect rats (Spratt and Haycock, 1988). The same method could be trialled in future experiments or troubleshooting could be done to identify at what stage of the tick's engorgement, *C. johnstoni* mature into the iL3.

6.4.5.2 Possible future experiment using the paralysis tick, *Ixodes holocyclus* for vector of *Cercopithifilaria johnstoni* in a small animal model system

I. holocyclus, the paralysis tick, is a widespread species on the East coast of Australia that causes paralysis in small mammals (discussed in detail in Chapter One; (Jackson et al., 1998; Jackson et al., 2000; Jackson et al., 2002; Graves et al., 2016). The nymph or adult stages of *I. holocyclus* must not be fed on laboratory rats because the toxin will paralyse them. The sensitivity of laboratory rats to the larval stages of *I. holocyclus* has not been quantified. Accurate identification of ticks before the attachment to a host or the use of artificial membranes for feeding ticks during development would collectively reduce the risk to small laboratory animals.

That said whether *I. holocyclus* nymph and adult stages cause deleterious effects to bush rats has not yet been investigated. There is a marked difference in species present on rats at Mogo State Forest compared with species present on vegetation at Kioloa (Chapter Five), with very few *I. holocyclus* found on bush rats in Mogo compared to a large number of all *I. holocyclus* life stages found on the vegetation at Kioloa. There was evidence of *I. holocyclus* adults and larvae from flagging around the same locations at Mogo State Forest, where the bush rats were collected (Chapter Five). The lack of *I. holocyclus* implies that the bush rats could be relatively insensitive to *I. holocyclus* tick toxins representing some immunity rather than a fatality. Bush rats may not be appealing hosts for *I. holocyclus* ticks to feed. As *I. holocyclus* causes severe reactions in small mammals and children, it would be a useful project to quantify whether bush rats do have immunity to the toxin or whether there is just varying number of tick species in these different areas.

As all vectors competent to transmit *C. johnstoni* have not been identified, it may be possible that *I. holocyclus* can equally transmit *C. johnstoni* to hosts. From various field trips, *I. holocyclus* appears the most accessible species from flagging the vegetation on the East coast of Australia. They are also the most easily identifiable species compared to other ticks in *Ixodes*. Thus, it may be possible to devise experiments using field-collected *I. holocyclus* ticks without harming the bush rats or laboratory rats. Such experiments would be designed to explore parasite transmission competency and host immune system responses. We know more about the biology of *I. holocyclus* than other ixodid species because the paralysis tick is responsible for paralysing small mammals and children and thus has been a focus of research (Kaire, 1966; Stone et al., 1983; Stone et al., 1989; Song et al., 2011; Graves et al., 2016). It may be worth pursuing *I. holocyclus* to use for transmission of *C. johnstoni* to bush rats because of how much is already known about this vector species. The experiment would not be appropriate to use on laboratory rats that are naïve to the toxin. Ideally, if it is possible to improve the identification process of ixodid ticks and use *I. trichosuri* or other species that do not inject a toxin would be the preferred option moving forward. The following system could be implemented for any *Ixodes* tick that is identified and proves to be the most successful at transmitting *C. johnstoni* to a host. For explanation purposes, *I. holocyclus* will be used to elucidate the system.

A membrane feeding system developed to maintain the life cycle of *I. holocyclus* (or other competent *Ixodes*) in the lab would make it possible to feed larvae on *C. johnstoni*-infected laboratory rats, then dissect the tick's post-engorgement to obtain *C. johnstoni* iL3s. The iL3s would then be injected subcutaneously into naïve laboratory rats, a method which was discussed in section 6.4.5.1.

Feeding membranes would be maintained with 85% relative humidity and constant temperature of 25°C to facilitate growing and feeding of the ticks. Based on the various tick flagging field trips conducted for this work, large numbers of *I. holocyclus* are not only easy to locate in Kioloa, but adults are easy to identify due to their lighter coloured second and third leg (Supplementary Figure 6.3a). The male and female *I. holocyclus* adult ticks were straightforwardly identified and observed them mating in their tick tubes in the laboratory, resulting in

thousands of eggs (Supplementary Figure 6.3). Thus, occasional supplementation of the tick colony via flagging high *I. holocyclus* prevalent areas would be possible. Feeding membranes would be used for unfed adult females until they lay their eggs, excluding the time required to produce larval ticks and *C. johnstoni* iL3s. Membranes would be a more efficient method to maximise *C. johnstoni* transmission.

6.4.5.3 Future identification of *Cercopithifilaria johnstoni* presence in ticks and rodents using PCR

There are likely several tick species that ingest and transmit *C. johnstoni* in the wild (see Chapter Five for analysis of cryptic diversity). Currently, not all those tick species are compatible for developing a laboratory life cycle, as some tick species will be lethal to the rat hosts, i.e., *I. holocyclus* (possible option discussion in 6.4.5.2). The most competent vector species for *C. johnstoni* transmission is currently unknown and thus is an important future direction if tick attachment is a requirement for the *C. johnstoni*-rodent model.

A robust assay that could detect the presence or absence of *C. johnstoni* in engorged ticks while simultaneously identifying the species of the tick would be beneficial to this research. It is the most important next stage of the *C. johnstoni* animal model to develop a PCR for *C. johnstoni* detection in engorged ticks. The results of such a test would identify the most common species of tick present on the rats and identify the presence of *C. johnstoni* in the ticks thus exploring *C. johnstoni* genetic diversity.

6.4.5.4 Tick morphological identification

Currently, morphological identification is slow and requires significant taxonomic knowledge (Chapter Five). Alternatively, to developing a PCR to simultaneously identify *C. johnstoni* presence and tick species, another option would be to collect ticks and identify them using both morphological characteristics and DNA barcoding to then dissect each tick thus identifying those with parasites such as, *C. johnstoni*.

A sensitive molecular assay would vastly improve the process of identifying the most appropriate vector to transmit *C. johnstoni*, as this could be high throughput, allowing rapid screening of abundant ticks. An example of a molecular assay could involve the collection of tick faeces during the post-engorgement period to detect filarial DNA from the microfilariae that did not mature to the iL3 stage, similar to work done in mosquitoes for lymphatic filariasis (Pilotte et al., 2016).

6.5 Conclusions

Chapter Six has explored three important features of developing a successful *C. johnstoni*-rodent animal model (a) maintaining the tick life cycle in the laboratory, (b) attaching immature wild-caught ticks to infected bush rats to generate infective ticks after a single moult rather than attempting to maintain the complete vector life cycle, and (c) determining the duration of an infection using captive, naturally infected wild-caught bush rats.

It is very challenging to maintain the tick life cycle in the laboratory and there were several technical challenges that need to be overcome before maintenance of the life cycle will be feasible which was beyond the scope of this PhD project. Captive-bred ticks may appear desirable but have been deemed unnecessary as the major goal for the success of the *C. johnstoni*-rodent model is to obtain infective larvae. There are alternate methods to obtain infective larvae that do not require an intensive approach such as maintaining the tick life cycle. Methods such as the tick dissection and iL3 subcutaneous injection into rodents should be considered for future development of the *C. johnstoni*-rodent model system.

The ethically acceptable alternative tick attachment method to bush rats proved to be challenging to develop. The method had limitations and the attachment rate was not efficient. Further troubleshooting of this method is required to allow the ticks to obtain a blood meal to engorge.

Lastly, wild-caught bush rats maintained a *C. johnstoni* infection for three years post-capture indicating that the infection is lifelong in bush rats. A very important finding from this series of incomplete experiments. Future work into

developing the *C. johnstoni*-rodent model can ensure that once the rodents have a *C. johnstoni* infection, they are likely to maintain these infections for a long time.

There is further research required before we have a successful laboratory model for studying onchocerciasis immunopathology. However, the experimental work presented here suggests that future *C. johnstoni* animal model trials may be feasible given a stable funding source that would allow for enough equipment, space, and staffing.

Chapter Seven

General Discussion

The overall objective was to explore the possibility and suitability of *C. johnstoni*, a filarial nematode of rats, to be used in a small animal model to study onchocerciasis, a disease caused by the filarial nematode *O. volvulus*. Spratt and Haycock (1988) identified *C. johnstoni* in Australian bush rats and other small mammals, demonstrating that it can elicit similar immunopathology in bush rats and laboratory rats that transpires in *Onchocerca*-infected individuals. The ability of *C. johnstoni* to recapitulate the characteristic disease symptoms, i.e., lesions and microfilariae and lesions in the cornea, are the critical features of this proposed animal model system. The recapitulation of corneal lesions infers *C. johnstoni* is a parasite of interest to use in an animal model investigating onchocerciasis (Vuong et al., 1993).

The first logical step was to establish genomic resources by assembling the mitochondrial (Chapter Two) and nuclear (Chapter Three) genomes and position *C. johnstoni* in phylogenetic context with other closely related filarial nematode species (Chapter Two, Three). Then, the assembled draft genome was used to explore genomic similarity and synteny (Chapter Three) and as a resource for orthologue discovery (Chapter Four). Potential antigenic proteins that may be important in disease immunopathology experimentally derived from *O. volvulus* was investigated (Chapter Four). Several studies have explored antigens that appear to be involved in the immune responses of *O. volvulus*-infected humans (Lustigman et al., 2002; McNulty et al., 2015; Bennuru et al., 2016; Bennuru et al., 2017; Norice-Tra et al., 2017; Bennuru et al., 2019). The *C. johnstoni* orthologues of strongly immunogenic *O. volvulus* proteins are now a logical foundation to begin the investigation of the parallels between *C. johnstoni* and rat, and *O. volvulus* and human, immunology. *C. johnstoni* appears to be a comparable nematode that could be a successful candidate to study onchocerciasis. Thus, the following step is to identify the logistics of establishing a small animal model. The next step is to define the tick species that is the primary vector of *C. johnstoni*. The data presented in Chapter Five, which show that the diversity of ticks present in the study sites is higher than current

taxonomy suggests that identification of the species that transmit *C. johnstoni* may be more complex than initially thought. The study revealed a group of cryptic species (Chapter Five) that has highlighted a knowledge gap in the development of a *C. johnstoni*-rodent animal model. It will be vital to ascertain the most efficient vector responsible for the transmission of *C. johnstoni* to the rats to replicate parasite transmission. Finally, the prospects of establishing the *C. johnstoni* transmission cycle in the laboratory were considered identifying how the animal model system would function and what would be required to study the immunopathology successfully (Chapter Six).

7.1 Phylogenetic relationships of filarial nematodes

An initial aim was to position *C. johnstoni* in the clade III filarial nematode phylogeny to determine the phylogenetic relationship with *O. volvulus* and other closely related nematodes. The mitochondrial and the nuclear *C. johnstoni* genomes revealed the same phylogenetic relationships with the other closely related filarial nematodes (Chapter Two, Three) and was consistent with previous publications (McNulty et al., 2012; Blaxter and Koutsovoulos, 2015; Lefoulon et al., 2015). It was apparent with the inclusion of additional genomic data, i.e., adding whole-genome nuclear data, improved the maximum likelihood bootstrap support and Bayesian posterior probabilities. Consistently, the phylogenies positioned *C. johnstoni* with *A. viteae*, and *L. sigmodontis* in a highly supported clade, thus indicating close relationships with one another compared with the other nematodes (Chapter Two, Three).

Despite excellent resolution and support within the mitochondrial and nuclear phylogenies, there are still uncertainties concerning the phylogenetic relationships of the *Cercopithifilaria* clade using 12S and COI amplicons. A secondary aim was to identify whether *C. johnstoni* was closely related to other *Cercopithifilaria* species. There were only 12S and COI gene data available for the species in the *Cercopithifilaria* genus restricting the phylogenetic analysis. There have not been whole genomes assembled for *Cercopithifilaria* species other than *C. johnstoni*. The *Cercopithifilaria* clade was very poorly supported using 12S and COI genes (Chapter Two). Within the clade, there were a few highly supported relationships but mostly poor support across all other species and low support for the outgroups in this tree, such as *A. viteae*, *L. sigmodontis*

and other related filarial nematodes. The uncertain low support for the *Cercopithifilaria* clade and variation in filarial relationships raises concerns about the credibility of the 12S-COI phylogeny. For example, the 12S-COI phylogeny positioned *A. viteae* and *S. digitata* together with poor support. Conversely in the whole mitochondrial phylogeny, *A. viteae* and *L. sigmodontis* were positioned together with high support while *S. digitata* was positioned as an outgroup outside of Onchocercidae thus distantly related.

There is the possibility that with the addition of more genomic information, there could be variation in the current 12S-COI filarial relationships, including the relationships within the *Cercopithifilaria* clade. The phylogeny positions *C. johnstoni* more distantly related to the other *Cercopithifilaria* species within the same clade, i.e., long-branch length, which could be expected as *C. johnstoni* is geographically more divergent than the others (Chapter Two). As evolutionary relationships of *C. johnstoni* to other *Cercopithifilaria* species was not a focus of Chapter Two, future analyses should focus on these evolutionary relationships of *Cercopithifilaria* species to verify how closely related *C. johnstoni* is to *Cercopithifilaria* species in the Northern Hemisphere. The separation between Northern and Southern Hemisphere *Cercopithifilaria* populations could suggest that *C. johnstoni* has undergone host switches at some point in their evolutionary history.

A host switch is defined by a parasite jumping from one host species to another (Webster et al., 2016). To identify the potential of *C. johnstoni* host switching throughout its history could be explored through a study of genetic variation between various populations of *C. johnstoni* within a host and between hosts. Previous parasite surveys in Australian mammals have identified *C. johnstoni* infection in bandicoots, Tasmanian devils, gliders, and different species of rodents (Mackerras, 1962; Spratt and Varughese, 1975). A desirable investigation would involve determining whether the *C. johnstoni* species described in the recorded hosts demonstrate genetic variation or are categorised as the same species. It could be expected to see an Australian clade of cryptic *Cercopithifilaria* species from different Australian hosts that are separate from the *Cercopithifilaria* species identified in Europe and Asia. A study of genetic variation between *Cercopithifilaria* isolated from different hosts would be invaluable to understand this species in a broader context to determine if they are likely to be

members of the same species or separate cryptic species. Providing the species are all *C. johnstoni*, we could explore the possibility of specific sub-populations associated with different hosts, alternatively whether there is a single panmictic population with transmission occurring freely amongst all hosts.

Host switching is of interest as a result of the other filarial species evolutionary history. The *Onchocerca* clade's origin dates back to the Miocene radiation resulting in new hosts such as cervids and bovids (Bain, 2002). Since this event, *Onchocerca* species have undergone many sympatric speciations through host switching (Bain, 2002; Krueger et al., 2007; Sréter and Széll, 2008). Other host switches consist of *Onchocerca dewittei* to boar, *Onchocerca ramachandrini* in the warthog, *Onchocerca fasciata* in camel, and onchocercosis has been reported in dogs (Sréter and Széll, 2008). Host switching events influence parasite evolution by leading to reproductive isolation between those parasites from the old host and those in the new host (Mackenstedt et al., 2015; Webster et al., 2016). In parasitic nematodes, it is prevalent and has been known to trigger the emergence of disease with increased severity in pathology and symptoms (Laetsch et al., 2012; Susoy and Herrmann, 2014; Suh et al., 2016; Webster et al., 2016). The ability of filarial nematodes to host switch into divergent host species, i.e., bovine to human, raises many questions to be explored. It may be possible to identify the driving force behind the host switches of parasitic nematodes, leading to the understanding of evolutionary benefits of switching to a new host. Currently, with the information known about *C. johnstoni*, all that can be concluded is that *C. johnstoni* infects several host species, which is very atypical of helminths. Ultimately, this raises the question of whether *C. johnstoni* is more permissive for host switching or whether *C. johnstoni* is not just one species and requires further morphological characterisation supported with genetic characterisation. Providing *C. johnstoni* is a recent host switch, this could explain the increased severity in the immunopathology in rodents comparable to that observed in *O. volvulus*-infected humans.

Host silhouette figures were placed on the phylogenies in Chapter Two to explore whether there were any relationships between the filarial nematodes and their host species. There were no conclusive results concerning the hosts species relationships of nematodes. However, it could be interesting to investigate the location of where the microfilariae are established in the host's body to

understand evolutionary history. The location of the microfilariae could be an evolutionarily labile trait that has changed multiple times throughout evolutionary history within the filariae. In Onchocercidae, the microfilariae are found in circulating blood or the skin while the adults are located within nodules (Cotton et al., 2016). *L. loa* adults are subcutaneous parasites and migrate through the eyes, hence the “eye worm” while the microfilariae are in the circulation (Desjardins et al., 2013). *D. immitis* adults are found in the cardiac arteries, while the microfilariae are found in the blood (Hu et al., 2003). However adult *D. repens* reside in the subcutaneous skin and the microfilariae reside in the circulation, commonly infecting dogs and humans (Capelli et al., 2018). The microfilariae of *A. viteae* have been reported in the skin (Eisenbeiss et al., 1991), and *L. sigmodontis* microfilariae are present in peripheral blood (Hübner et al., 2009). *C. johnstoni* is known to be a skin dwelling parasite where the microfilariae and adult worms are present in the subcutaneous skin of their host (Spratt and Haycock, 1988; Vuong et al., 1993). It appears that the adult worms residing in subcutaneous skin are common in filarial nematodes; however, the location of the microfilariae for *C. johnstoni* is unusual compared to the well-known filarial nematodes. The microfilariae of other *Cercopithifilaria* species from the Northern Hemisphere have also been reported in the subcutaneous skin in dogs causing epidermal and sub-epidermal edematous changes or perivascular intestinal dermatitis (Otranto et al., 2012; Otranto et al., 2013; Ramos et al., 2014). The location of microfilariae in the skin of their hosts could perhaps be a characteristic of all *Cercopithifilaria* species. It would be interesting to explore the different filarial nematodes microfilariae location in the host to determine whether this could have any impact on parasite pathogenicity or the immune response of the host. The understanding of microfilarial location could lead to another avenue to target for treatment or control of filarial diseases.

In conclusion, a genetic variation study identifying potential variation in *C. johnstoni*, confirming host switching events and then exploring whether the location of microfilariae could be an evolutionarily labile trait, could together begin to answer the question about how *C. johnstoni* can elicit similar immunopathology in rodents that *O. volvulus* can elicit in humans. All that is understood about *C. johnstoni* is a few publications from 1970 to 2000 (Spratt and Varughese, 1975; Spratt and Haycock, 1988; Vuong et al., 1993) and now the contents of this thesis. Further exploration into the evolutionary context of *C. johnstoni* could

eventually shed light into the similar manifestation of immunopathology between *C. johnstoni* and *O. volvulus*.

7.2 *In silico* analysis of the *Cercopithifilaria johnstoni* genome

C. johnstoni did not have a genome assembly, transcriptomic or proteomic data. Hence no genetic resources were available for genetic comparison with *O. volvulus* in which has extensive genomic resources available (Cotton et al., 2016). Consequently, the genome of *C. johnstoni* was assembled so it could be used to explore and compare the filarial parasites *in silico* determining the overall genome similarity and relationships (Chapter Two, Three). One adult female *C. johnstoni* worm was sequenced with short-read sequence technology which enabled the assembly of a mitochondrial and nuclear genome. According to BUSCO and CEGMA analyses, *C. johnstoni* contains 95% of nematode genome content based on conserved orthologues and thus could be used for downstream analyses as a large proportion of the genome content is present. The genome consists of large scaffolds and small contigs but is unable to be assembled to the chromosomal level. Compared to the other 11 filarial nematodes, *C. johnstoni* is the fourth-best genome assembly according to BUSCO and CEGMA statistics, indicating a reasonably high genome assembly quality. However, with only short-read genomic sequence data, there will be vital information missing from the *C. johnstoni* genome compared to the higher quality genome assemblies of *O. volvulus* and *B. malayi*.

The aim of this PhD was to characterise the *C. johnstoni* genome in comparison with other filaria, with a focus on immunogenic proteins. However, characterisation of genetic variation within the species was outside the scope of the project. As the aim was to characterise the genome, the highlight of this project is that the *C. johnstoni* genome has been assembled from a single female worm. Ideally, the sequencing would be of a single worm to minimise heterozygosity and aid assembly using short reads because there will be fewer variable sites. The project allowed for genome comparison with *O. volvulus* and other filarial nematodes as the first genomic research for *C. johnstoni*. A possible extension of this project could be to explore *C. johnstoni* population genetics and genetic variation within the species. Such a project would involve further sequencing of other *C. johnstoni* parasites to explore possible genetic

differences. Currently, population genetic data has only been generated for *O. volvulus* and is missing from the remaining filarial nematode literature. Thus, this PhD was designed to focus on exploring *C. johnstoni*'s genome because there were abundance genomic resources available for comparison. Future research could aim to produce population genetic data for the other filarial nematodes to investigate genetic variation within each species aiming to further understand the filarial nematode clade.














Improvement of the *C. johnstoni* genome assembly would improve the overall confidence in all downstream analyses. Highly annotated and robust genome assemblies provide extensive information on the parasites that are used in comparative genomics (Stoltzfus et al., 2017; Coghlan et al., 2019; Tyagi et al., 2019b). Draft genomes can be limited in their application. The *C. johnstoni* genome requires the addition of RNA-Seq data and proteomic data to improve the direct comparison with *O. volvulus*. As a result of only having genomic data from one adult female worm, it is acknowledged that the data presented within the thesis is a predicted *in silico* approach requiring experimental confirmation. Nevertheless, this work has framed the overall context and provided a convincing case that *C. johnstoni* is an appropriate organism to study onchocerciasis immunology in the rodent model.

There is genomic and proteomic information for every life stage of *O. volvulus* (Figure 7.1) (Cotton et al., 2016; Grote et al., 2017). It would be beneficial to obtain transcriptomic data of *C. johnstoni* larval stages (L1, L2, iL3), and the adult male and female stage to then directly compare the different stages with *O. volvulus* to continue *C. johnstoni* research. Extracting any DNA and RNA for all *C. johnstoni* life stages was unfeasible within the scope of this PhD thesis as a result of limited parasite material. However, it would be one of the next steps into exploring *C. johnstoni* further and using *C. johnstoni* to study onchocerciasis immunopathology. It is clear from the summarised table of omics data available for filarial parasites from Grote et al. (2017) (Figure 7.1) that there is more work to be done to obtain transcriptome data on all stages of the filarial nematodes such as *W. bancrofti* and *O. ochengi* and also assemble the proteomic data for various life stages of the filarial nematodes.

Striking observations from the synteny analysis of *C. johnstoni* and *O. volvulus* revealed that there is abundant microsynteny conservation

throughout the scaffolds of *C. johnstoni* and chromosomes of *O. volvulus* and no evidence of macrosynteny (Chapter Three). It appeared that the longest scaffold of *C. johnstoni* was predominately aligning to OM3 illustrating microsyntentic relationships indicating sequence conservation and possible gene order arrangement. The longest scaffold of *C. johnstoni* illustrates partial sequence homology with *B. malayi* and *O. volvulus* but implies there is gene divergence as *C. johnstoni* is more distantly related phylogenetically. Further exploration in *C. johnstoni*'s chromosomal arrangement could reveal whether *C. johnstoni* has four autosomes, and an X and Y chromosome (4A+XY) similar to *B. malayi*, three autosomes and an X and Y chromosome (3A+XY) similar to *O. volvulus* or follows the arrangement of its closely related nematode *A. viteae* with four autosomes and X0 chromosomes (4A+X0) (Post, 2005). The 4A+X0 system may be more likely to be *C. johnstoni*'s chromosomal arrangement. The following steps for the *C. johnstoni* draft genome will be to assemble the genome with long-read data. Then, a hybrid assembly will be required to correct the errors associated with long-read assemblies (Chen et al., 2020). The hybrid assembly will use a combination of short-read Illumina data and long-read data, either PacBio or MinION providing a confident assembly of larger scaffolds that can be assembled into chromosomes (English et al., 2012; Salmela et al., 2014; Chen et al., 2020).

The development of genetic resources for *C. johnstoni* has enabled close comparison between *C. johnstoni* and other filarial nematodes previously studied. The assembly of the mitochondrial and nuclear genome allowed *C. johnstoni* to be positioned in the nematode clade (clade III) with strong support (Chapter Two, Three). The genome of *C. johnstoni* has enabled direct comparison with *O. volvulus* to show genetic conservation and led to identifying thousands of shared orthologues across the filarial nematode orthologue investigation (Chapter Three). The orthologue investigation led to the prediction of 30 one-to-one orthologues from a list of known *O. volvulus* immunogenic targets. A total of 7,557 orthogroups were identified between the whole *O. volvulus* and *C. johnstoni* proteomes including the 30 orthologues from the immunogenic protein list. The completion of Chapters Two, Three and Four concluded *C. johnstoni* is a closely related nematode of the other filarial nematodes with orthologues of known *O. volvulus* immunogenic proteins that could be essential in

Organism	Host	Date	Data Available			Wolbachia Data Available		
			 Genome	 Transcriptome	 Proteome	 Genome	 Transcriptome	 Proteome
<i>L. loa</i>		2013 ¹	✓	Mf ¹		NA		
<i>W. bancrofti</i>		2013 ¹	✓					
<i>O. volvulus</i>		2016 ²	✓	L2, L3, L3D1, L3D2, L3D3, L4 AF, AM, Mf ⁶	L3, L3D1, L3D2, L3D3, L4, AF, AM, Emb ⁶	✓		
<i>B. malayi</i>		2007 ³	✓	L3 ⁷ , L4 ^{7,8} , F30 ⁸ , F42 ⁸ , AF ^{7,8} , M30 ⁸ , M42 ⁸ , AM ^{7,8} , Mf ⁷	L3, AF, AM, Mf ¹¹	✓	L4, F30, F42, AF, M30, M42, AM ⁸	L3, AF, AM, Mf ¹¹
<i>B. pahangi</i>		2015 ⁴	✓	Mf ⁹				
<i>D. immitis</i>		2012 ⁵	✓	L3, L4, AF, AM, Mf ¹⁰	AF, AM ¹²	✓	L3, L4, AF, AM, Mf ¹⁰	
<i>O. ochengi</i>		2016 ²	✓		L3, AF, AM, Mf ¹³	✓	AF, AM ¹⁴	AF ¹⁴

¹Desjardins, C.A., et al., Genomics of *Loa loa*, a Wolbachia-free filarial parasite of humans. *Nat Genet*, 2013. 45(5): p. 495-500.

²Cotton, J.A., et al., The genome of *Onchocerca volvulus*, agent of river blindness. *Nat Microbiol*, 2016. 2: p. 16216. ³Ghedini, E., et al., Draft genome of the filarial nematode parasite *Brugia malayi*. *Science*, 2007. 317(5845): p. 1756-60. ⁴Lau, Y.L., et al., Draft genome of *Brugia pahangi*: high similarity between *B. pahangi* and *B. malayi*. *Parasit Vectors*, 2015. 8: p. 451. ⁵Godel, C., et al., The genome of the heartworm, *Dirofilaria immitis*, reveals drug and vaccine targets. *FASEB J*, 2012. 26(11): p. 4650-61. ⁶Bennuru, S., et al., Stage-Specific Transcriptome and Proteome Analyses of the Filarial Parasite *Onchocerca volvulus* and Its Wolbachia Endosymbiont. *MBio*, 2016. 7(6). ⁷Choi, Y. J., et al. (2011). A deep sequencing approach to comparatively analyze the transcriptome of lifecycle stages of the filarial worm, *Brugia malayi*. *PLoS Negl Trop Dis* 5(12): e1409. ⁸Grote A., et al., "Uncovering putative mechanisms of filarial endosymbiosis using stage-specific Dual RNAseq in *Brugia malayi* and Wolbachia." Accepted at PLoS NTD. ⁹Kariuki, M. M., et al. (2010). "Differential transcript expression between the microfilariae of the filarial nematodes, *Brugia malayi* and *B. pahangi*." *BMC Genomics* 11: 225. ¹⁰Luck, A. N., et al. (2014). "Concurrent transcriptional profiling of *Dirofilaria immitis* and its Wolbachia endosymbiont throughout the nematode life cycle reveals coordinated gene expression." *BMC Genomics* 15: 1041. ¹¹Bennuru, S., et al. (2011). "Stage-specific proteomic expression patterns of the human filarial parasite *Brugia malayi* and its endosymbiont Wolbachia." *Proc Natl Acad Sci U S A* 108(23): 9649-9654. ¹²Luck, A. N., et al. (2015). "Tissue-specific transcriptomics and proteomics of a filarial nematode and its Wolbachia endosymbiont." *BMC Genomics* 16: 920. ¹³Armstrong, S. D., et al. (2016). "Stage-specific Proteomes from *Onchocerca ochengi*, Sister Species of the Human River Blindness Parasite, Uncover Adaptations to a Nodular Lifestyle." *Mol Cell Proteomics* 15(8): 2554-2575. ¹⁴Darby, A. C., et al. (2012). "Analysis of gene expression from the Wolbachia genome of a filarial nematode supports both metabolic and defensive roles within the symbiosis." *Genome Res* 22(12): 2467-2477.

Figure 7.1: Summary of the Omics data that is available for filarial parasites obtained from Grote et al. (2017).

the immunopathology evoked by *C. johnstoni* and *O. volvulus* in rodents and humans, respectively.

7.3 Drivers of disease immunopathology: Evolutionary selection and immunogenic proteins

The orthologous relationships investigated in Chapter Four between *C. johnstoni* and *O. volvulus* may be predictive of broader orthology across all or most filaria. Prospective analyses should aim to confirm these orthologous relationships between *C. johnstoni* and *O. volvulus* and subsequently the other filarial nematodes within the clade. A preliminary evolutionary selection analysis established some of the *C. johnstoni* and *O. volvulus* orthologues are undergoing diversifying and purifying selection. The preliminary selection analysis identifies a new avenue for comparative research between *C. johnstoni* and *O. volvulus*, which can be extended to comparing *C. johnstoni* and *O. ochengi* or *C. johnstoni* and *B. malayi* depending on the pressing questions. A worthwhile exercise could be to identify whether the orthologues of these genes show evidence of similar selection in species in which microfilariae are not in the skin or are transmitted by other vectors providing additional information to verify whether the immunogenic orthologues play a role in the immunopathology.

Possible future directions of the preliminary diversifying and purifying selection analyses conducted in Chapter Four could involve identifying selection on all predicted genes across the *C. johnstoni* genome. The whole-genome study could then ascertain whether novel genes are undergoing strong diversifying or purifying selection are immunogenic targets or are genes that could play a role in immune responses to the presence of microfilariae to explain the similarity in immunopathology between rodents and humans infected with *C. johnstoni* and *O. volvulus*, respectively. Conducting these analyses across all of the genes predicted for *C. johnstoni* could identify a list of new, noteworthy *C. johnstoni* immunogenic targets that could then be investigated in *O. volvulus* to identify orthologues. The orthologues of the newly identified *C. johnstoni* immunogenic targets could provide novel *O. volvulus* candidates that could be new targets for drugs to expedite treatment of the disease, thus onchocerciasis elimination.

Another avenue that could be explored is the identification of gene expansion events within *C. johnstoni*. Several studies have identified selection that has driven the evolution of parasitism (Baskaran et al., 2017; Coghlan et al., 2019). Understanding the evolution of parasitism can lead to an explanation into how some species of a genus parasitise their hosts and others do not (Hunt et al., 2016; Coghlan et al., 2019). The investigation into gene family expansion events could identify particular genes families that are also expanded in other parasites, i.e., *O. volvulus*, that are involved in the evolution of parasitism (Coghlan et al., 2019).

Following the completion of this thesis, the utmost important question that remains unanswered is identifying what is driving the similar immunopathology in rodents and humans caused by *C. johnstoni* and *O. volvulus*, respectively. Thus far, it has not been discovered how two different parasites may be causing similar symptoms and immunopathology in two divergent hosts. There are two possible hypotheses to contemplate that could elucidate the apparent similarity in immunopathology, an idea which has been explored throughout Chapter Four. (1) The conserved orthologues between *O. volvulus* and *C. johnstoni* could indicate the similarity in the skin, and eye pathology between rats and humans infected with *C. johnstoni* or *O. volvulus* respectively is in part driven by the conserved proteins. (2) The host immune response is species-specific, and therefore protein conservation does not drive the immunological response. The same immunopathology can be present in different species, i.e., humans and rodents, but they have different antigenic protein properties. Rat's immune systems are very different to human immune systems and therefore would be plausible to assume they respond differently to the way the human's immune system responds.

Assuming that the first hypothesis is the explanation for what is driving the similar immunopathology between rats and humans infected with *C. johnstoni* or *O. volvulus* respectively, then the *O. volvulus* immunogenic proteins could be in part, the drivers of immunopathology. Ultimately, this research is focusing on the presentation of structurally conserved antigens in the same physiological context in two different host-parasite interactions. As discussed in Chapter Four, the first phase in answering the hypothesis is to test whether there is any gene conservation between *C. johnstoni* and *O. volvulus in silico*. With a suitable draft

genome, this first phase has now been achieved, and a list of 30 putative *C. johnstoni* orthologues of *O. volvulus* immunogenic proteins was discovered (Chapter Four). The list of putative orthologues can now be used as a foundation to determine whether they display immunoreactivity when presented to the rodent immune system consistent with what is currently observed when they are presented to the human immune system. *In silico* analyses alone are not satisfactory to confirm whether the rodent immune system will respond similarly to these same set of antigens that the human immune system responds. Therefore, immunology experiments within the host are necessary; hence the driver of disease immunopathology has not been determined thus far. Ultimately understanding the similarity in disease immunopathology will confirm *C. johnstoni*'s suitability as a model for onchocerciasis but will also shed light on alternative methods to treat the human disease.

A significant complication of the conditional hypotheses is the limitation of the available information on the antigens that initiate immunopathology in *O. volvulus*-infected humans. However, the antigens that drive humoral antibody responses are known, and thus antibody responses measured in human serum should reflect the antigens that initiate the immunopathology. It is advantageous to determine whether rat and human immune systems recognise the same antigens, and consequently, *C. johnstoni* immunoreactivity may be predictive of *O. volvulus* immunoreactivity. Therefore, testing the hypothesis of rat and human conservation of antibody response to the conserved antigenic structure is the future aim of the *C. johnstoni* animal model. It would be possible to explore this concept by observing infected rat sera to identify what the host recognises. Rat sera infected with *C. johnstoni* has currently not been explored and therefore would provide some support for the idea that investigating skin and eye immunomechanisms in *C. johnstoni*-infected rats may be informative for *O. volvulus*-infection in humans.

The second phase is thus to follow up on this idea and measure antibody responses in rats against these structures identified in phase one. The complete life cycle animal model would not be required, but *C. johnstoni*-infection in rats would be needed to directly compare whether the *C. johnstoni* antigens stimulate similar serum antibody responses that are known for these antigens in *O. volvulus*. It would be possible to take the 30 orthologous proteins of known

O. volvulus immunogenic proteins and determine the immunoreactivity of the proteins in *C. johnstoni*-infected rodents. A potential experiment that could inquire about whether the *C. johnstoni* orthologues or antigens elicit similar and strong antibody responses in the rodent model as is observed in *O. volvulus* orthologues expressed from human sera would be beneficial. Aforementioned, the only indicators of immunoreactivity available are antigens recognised by serum antibodies thus this phase determines whether rat and human immune systems identify the same antigens providing the appropriate information to determine whether the rat immunological responses to microfilaricidal drugs may be predictive of likely human responses, i.e., drug safety and suitability.

Alternatively, with fresh *C. johnstoni* samples at different life stages, the transcriptomes can be assembled for gene expression analyses similarly to McNulty et al. (2015). These newly assembled transcriptomes can be used for evidence-based gene prediction training to provide confident prediction of *C. johnstoni* genes. Worms dissected from the rat could be used in the process of immunoaffinity purifications and immunoprecipitation of total IgG. Then analyse the fraction using Western blot and those with the highest reactivity undergo peptide purification for high-performance liquid chromatography and high-resolution mass spectrometry to directly compare to those proteins explored in *O. volvulus* worms (McNulty et al., 2015). The process could then confirm whether the orthologues predicted in Chapter Four are also expressed in rodents after conducting the same experiments as conducted for *O. volvulus*. The list of possible *O. volvulus* serodiagnostic antigens could then be directly compared with that of *C. johnstoni* concluding whether, the orthologous proteins identified *in silico* are potential candidates for future experimentation. Some proteins may be more useful combined with other proteins for diagnosis of a disease or disease treatment which could be determined by exploring onchocerciasis through the *C. johnstoni* model if there is an appropriate overlapping list of target antigens. Ultimately, these experiments rely heavily on new *C. johnstoni* samples. Providing that the future immunology experiments reveal that *C. johnstoni* elicits similar immunopathology that *O. volvulus* elicits in humans as a result of the similar orthologous protein structures and antigenic profiles, then this would be an excellent small animal model to formulate alternate treatment methods for onchocerciasis. These alternative treatment methods could then be used in

combination with a MDA programme using a macrofilaricidal drug treatment in African communities.

The third and final phase is to use the established *C. johnstoni* animal model to investigate whether these validated antigens from phase two and even antibodies that are produced in response to the antigens, could play a role in immunopathology. At this stage, specific disease pathology, i.e., skin pathology, can also be explored and observed with various antigenic structures to determine whether any may be driving the response. Currently, antigens that drive the physical pathology are not known in *O. volvulus*. Thus need to be determined to further explore the specific pathological symptoms in the *C. johnstoni*-rodent model and identify whether *C. johnstoni* would have any orthologues to those antigens that are responsible for the specific immunopathology. Onchocerciasis research is typically complicated because *O. volvulus* cannot be maintained outside of the host in a laboratory (Grote et al., 2017) and disease immunopathology is different for different individuals. An animal model, for instance, the proposed *C. johnstoni*-rodent model, has the likelihood of exploring the ability of structures to stimulate antibodies with a role in immunopathology more easily than attempting to explore this concept in humans.

Currently, there are no small animal models that can recapitulate the important disease characteristics, i.e., cornea lesions of onchocerciasis. Elimination of the disease is dependent on the interruption of *O. volvulus* transmission, usually using ivermectin, a microfilaricidal drug (World Health Organisation, 2016). There is a possibility due to the similarities observed *in silico* that *C. johnstoni* is a suitable parasite to study onchocerciasis. The *C. johnstoni*-rodent model could be used to develop macrofilaricidal drugs which will vastly and rapidly improve disease treatment. A small animal model also has the capacity of accelerating onchocerciasis research and potential macrofilaricidal treatments. Nevertheless, there is further validation required before *C. johnstoni* can be considered the most suitable comparative model for onchocerciasis.

7.4 Developing a small animal model for onchocerciasis

A set of criteria was established and discussed in detail in Chapter One that is important for developing a successful animal model. These comprise, (1) a

convenient laboratory host, (2) preferably natural host, (3) the life cycle can be maintained and, (4) recapitulate the most important disease features. The first two criteria have been previously identified in various publications (Spratt and Haycock, 1988; Vuong et al., 1993) and explored in Chapter Six. Spratt and Haycock (1988) morphologically characterised *C. johnstoni* in *R. fuscipes* and were also able to infect *R. norvegicus* using the iL3 stage of the parasite. Chapter Six explored the idea of developing the physical animal model and confirmed that *R. fuscipes* was infected with *C. johnstoni* through various ear snips and microfilarial count data.

It has been confirmed that *R. fuscipes* and *R. norvegicus* can both be infected with *C. johnstoni* through subcutaneous injection (Spratt and Haycock, 1988; Vuong et al., 1993). The focus on this thesis was not to develop the complete animal model as this was well beyond the scope of a three-to-four-year PhD. However, the focus was to explore various aspects of the *C. johnstoni* biology and troubleshoot these aspects, providing a rationale for accelerating the development of the *C. johnstoni* small animal model. Two particular methods could be used to develop the *C. johnstoni* animal model, each with various advantages and disadvantages. First, the complete vector and parasite life cycles could be maintained in the laboratory to replicate the entire cycle of infection from the uptake of iL3, bite of the host injecting iL3 parasite to the host and finally the recapitulation of the disease immunopathology. Alternatively, instead of maintaining the vector and parasite life cycles in the laboratory, the parasite iL3 stage could be dissected out of the vector once reaching maturity, which reduces the delay for the vector to moult and placed into the host to replicate the parasite life cycle.

The first requirement for the success of the *C. johnstoni* animal model is to determine the most competent tick vector that transmits *C. johnstoni*. Previous literature has indicated the *I. trichosuri* is a competent vector for *C. johnstoni* transmission (Spratt and Haycock, 1988; Vuong et al., 1993). However, there is no published evidence or further investigation into how successful the vector is at transmitting *C. johnstoni*. Chapter Five, therefore, explored the potential of using the standard 16S, 12S and COI molecular markers to initially identify the species by removing one back leg of the tick and extracting its DNA as these markers had been identified as useful tick species identification (Lv et al., 2014a; Lv et al.,

2014b). The back leg was chosen to avoid impacting on the ticks' ability to attach to a host and thus be able to develop an assay that could identify *C. johnstoni* presence or absence. The analysis of the ticks collected in Mogo State Forest and Kioloa, NSW revealed a lot of cryptic species diversity within the genus *Ixodes* (Chapter Five). Consequently, markers chosen are not sufficient to differentiate between tick species.

There are two important steps involved in identifying the most competent tick species to transmit *C. johnstoni*, (1) identify a quick and easy molecular method to identify the tick species collected. The disadvantage of this method is that at least one leg would need to be taken to extract DNA, and there is the potential that the removal of the leg is enough to reduce tick attachment success. There is no evidence suggesting that removal of a back leg would impede attachment and thus this is something that should be experimentally tested. (2) The ticks attached to bush rats would need to be screened to determine the volume of *C. johnstoni* microfilariae in each species. There may be multiple ixodid ticks that can transmit *C. johnstoni*, but some may have a lower prevalence than others. Ideally, the tick that takes up the maximum number of microfilariae would be more appropriate for transmission. These ticks would then need to be attached to naïve rodents to monitor how successful the transmission process of *C. johnstoni* is to a host. Future research is, thus, required to determine the most competent vector of *C. johnstoni*.

Maintaining the life cycle of ixodid ticks was discussed in Chapter Six. The primary focus is to determine an appropriate tick attachment method because then the appropriate vector could be fed on the host using this method to maintain its life cycle. Initially, the attachment method consisted of using anaesthesia with halothane using a rat-adapted delivery system under veterinary supervision. A small ring was attached to the rat, where the ticks were enclosed for attachment. It was decided that a new method would be trialled that did not require excessive rat handling, and that avoided the use of anaesthesia. The method (described in Chapter Six) enabled the ticks to attach wherever they preferred, rather than being restricted within the ring. It was less stressful for the rodents because no handling or anaesthesia was required, and they were enclosed in a dark tube, thereby feeling safe and secured.

A tick colony, with the most competent vector, could reduce the time associated with travel and fieldwork. It would also increase the ticks accessible for tick attachments. The tick colony could provide numbers of different life stages of ticks rather than only being subjected to larval stages or nymph stages from flagging particular times of the year. A tick colony will improve tick attachments and will enable more frequent attachments to increase *C. johnstoni* microfilarial burdens and thus increase infection. However, the establishment and maintenance of the tick colony pose many challenges. Briefly recapping the general ixodid life cycle discussed in Chapter One, the life cycle comprises four stages egg, larva, nymph, and adult (Anderson, 2001; Barker and Walker, 2014). Generally, tick feeding is a slow process with the full-time frame varying depending on the species between one to three years (Grandjean and Aeschlimann, 1972; Sojka et al., 2013). Larvae attach for three to four days, nymphs attach for four to seven days (Grattan-Smith et al., 1997), and adult females attach approximately eight to 24 days consistent with what was observed during the tick attachments experiments in Chapter Six. The general timeframe of the ticks' life cycle is a huge challenge for developing the animal model and is a substantial hurdle to overcome.

A Centralised Tick Rearing Facility at Oklahoma State University has successfully devised methods for large-scale production of *I. scapularis*, the primary vector of Lyme disease (Kocan et al., 2015). They have perfected and reduced *I. scapularis* life cycle from two years to a rearing time of 7.5 months in the laboratory, although still highlights the time-consuming nature of tick colonies. The success of the reducing *I. scapularis* life cycle to 7.5 months provides confidence that it would be possible to reduce the *I. trichosuri* life cycle to a similar timeframe. Australian ticks do not have the same diapause or hibernating stage that ticks in harsh winter environments add to their life cycle duration. However, with an efficient laboratory process, it could be possible to reduce the life cycle duration for animal model purposes.

Another important aspect and a significant time-consuming challenge of developing a thriving tick colony is tick feeding. Blood feeding is an essential physiological process for survival and growth of ticks (Mans and Neitz, 2004; Sojka et al., 2013). The host's blood is a source of energy and nutrients and therefore is an essential requirement to maintain a tick life cycle in the laboratory

(Sojka et al., 2016). Ticks require a blood meal to continue through the multiple life stages, and various laboratories have relied on different blood sources to sustain their ticks. Rabbits are often used for tick attachments as their ears are a perfect source for various tick species to feed (Bonnet and Liu, 2012). Rabbits are often rather expensive and, therefore, may not be the most optimal feeding source (Bonnet and Liu, 2012).

There have been various laboratories targeting artificial feeding methods within tick colonies. These methods reduce the number of animals required for maintaining the tick colony and, therefore, may be more useful. Overall, *in vitro* feeding techniques for mass rearing arthropods are more convenient, have higher productivity, and reduce expenditure over *in vivo* methods. Capillary feeding has been a standard method of tick feeding (Soares et al., 2005; Bonnet and Liu, 2012; Gonsioroski et al., 2012). Capillary feeding is promising as there is control over the amount of blood ingested by the ticks and more control over the overall feeding (Bonnet and Liu, 2012). The limitations with capillary feeding are that it is very labour intensive and technically challenging, but if successfully developed may only require a few individual females for feeding, mating, and thus the production of larvae (Bonnet and Liu, 2012).

More recently and possibly more promising, an artificial feeding assay method for tick feeding has been generated using silicon membranes to mimic the skin of a host (Waladde et al., 1991; Montes et al., 2002; Krull et al., 2017). One particular method used borosilicate glass tubes with silicon membranes. The membranes were thinner for larvae and nymphs and were thicker for adults mimicking the type of hosts they would be feeding on in nature. Bovine blood was used in the glass tubes for the ticks to feed on from the tick chamber (Figure 7.2) (Bonnet and Liu, 2012). The ticks can move freely around the tick chamber and choose when to attach and feed on the blood through the silicon membrane (Figure 7.2). Such a method could be trialled in future experiments to maintain ticks carrying *C. johnstoni*.

All of the challenges discussed concerning the maintenance of the tick life cycle for the small animal model to study onchocerciasis are laborious. In developing a tick colony successfully, there is a range of factors that require to be accomplished before it is possible. Tick feeding will be costly, maintaining the tick habitats will be time-consuming and potentially costly, and overall, the process

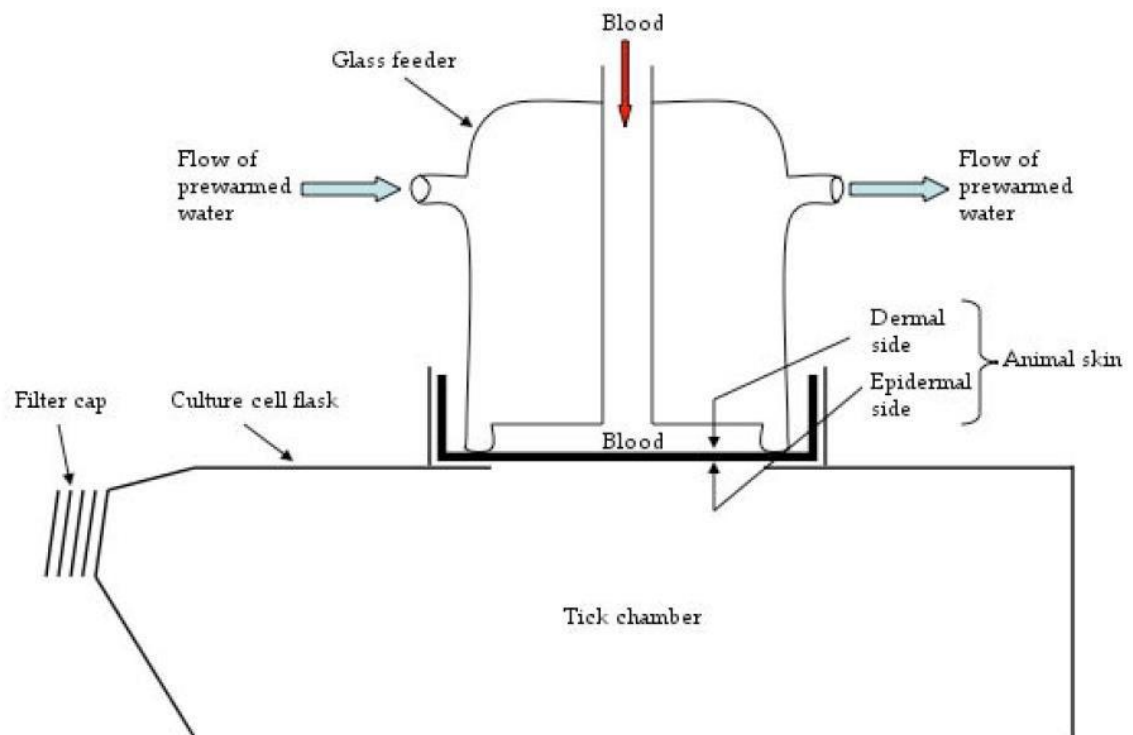


Figure 7.2. General schematic of the membrane feeding apparatus (Bonnet and Liu, 2012).

could be considered inconvenient. It is, therefore, necessary to consider an alternative method that would still result in the recapitulation of the *C. johnstoni* infection, but without the added complication of maintaining the ticks in the laboratory. A tick colony may not be the most suitable nor appropriate method to develop an animal model to study onchocerciasis.

Determining when the microfilariae mature into iL3s in their vectors, thus ready for transmission is an alternative method for the development of the animal model. Currently, the time of maturation for *C. johnstoni* L1 to iL3 is unknown. The time required for *C. johnstoni* microfilariae to develop to infective, mature iL3 may be significantly shorter than the several weeks required for the tick to moult and be ready to feed again. If this is confirmed, then the high mortality of fed ticks during the long period between feeding and moulting would be shortened considerably and, additionally, the losses incurred when ticks fail to attach to the host are also avoided because larvae are injected directly to the host immediately following dissection from the tick. Consequently, if the time required for the ingested microfilariae to mature were known, unfed (questing) ticks collected from the environment could be placed on an infected rodent to feed. The tick would then be dissected once *C. johnstoni* has matured to the iL3 stage to recover the iL3 stage for infection of naïve rodents by injecting the iL3 stage subcutaneously, consistent with the procedures conducted in Spratt and Haycock (1988). The proposed method has the potential to be more routinely successful, as discussed in Chapter Six. The dissection process would thus eliminate the need for maintaining a tick colony in the laboratory and therefore reduce the overall maintenance of the animal model.

Despite how time-consuming collecting ticks from field trips can be, it may be the more appropriate method. The dissection method takes away many other unknowns that are not directly important for onchocerciasis research, i.e., maintenance of tick life cycles. The subcutaneous injection would mean complete control of the animal model, knowing exactly how many iL3s are transmitted to a naïve rodent. It would require expertise on dissection of the ticks and injection of the iL3 and then consistent maintenance of the infected rodents in the laboratory rather than on a tick colony. There is the potential for this method to be more valuable in the long term and mean there is more time to focus on what is driving the immunopathology of the disease. The dissection method to obtain iL3s should

be considered in future studies developing the *C. johnstoni*-rodent model to study onchocerciasis.

7.5 Conclusions and future directions

In conclusion, *C. johnstoni*, a filarial nematode of Australian bush rats, has been sequenced and the genome assembled to provide appropriate genetic resources for *C. johnstoni* to facilitate genetic comparison with other related filarial nematodes. The phylogenetic relationships have been established that *C. johnstoni* appears closely related to *A. viteae* and *L. sigmodontis*. Orthology analyses concluded that *C. johnstoni* and *O. volvulus* share putative orthologues of protein-coding genes throughout their genomes. Known immunogenic proteins identified from *Onchocerca*-infected human sera were used to determine whether any of the orthologues of *C. johnstoni* could have similar potential immunogenic properties to the *O. volvulus* proteins. Thirty orthologues of strongly immunogenic *O. volvulus* proteins were found between *C. johnstoni* and *O. volvulus*. A number of these orthologues could be proteins that should be explored in future immunoreactivity experiments to determine whether they are part of the disease immunopathology.

Finally, just as differentiating between members of species complexes for *Simulium* blackflies have proven difficult, so too is the differentiation between what appears to be a species complex of Australian ixodid ticks. Additional work is required to identify and categorise tick species to fully understand the relationships of these species to develop a tick colony for the development of a small animal model for onchocerciasis. A small animal model comprised of *C. johnstoni*, ixodid vectors and rodents has been proposed as a potential animal model to study onchocerciasis. The analyses conducted throughout the thesis highlight the similarity between *C. johnstoni* and *O. volvulus* genetically, and the protein similarity of putative immunogenic targets for onchocerciasis. In future, immunoreactivity experiments can be conducted to provide further evidence within the small animal model system to identify precisely why *O. volvulus* and *C. johnstoni* can elicit similar immunopathology in different hosts. If these experiments lead to the findings that similar protein structures presented to the host are driving the immunopathological disease features, then the *C. johnstoni*

small animal model will be vital to understand parasite biology in diseases such as onchocerciasis.

The work described throughout this thesis provides an entry point to a different avenue of onchocerciasis research. For example, *C. johnstoni* proteins have a very similar structure and function to *O. volvulus* proteins. These proteins could have something to do with what is driving immunopathology-related disease symptoms. Prospective work targeting *C. johnstoni* could lead to understanding the host immune response to the death of the microfilariae in the host. Ultimately, if the causation of the disease immunopathology could be identified, then treatment methods could be designed specifically to target the immunopathology leading towards elimination of onchocerciasis throughout Africa.

Appendices

Appendix 1: Chapter Two Supplementary Material

Supplementary Table 2.1: Recommended Partition Finder substitution models for the complete dataset (coding regions and intergenic regions) within the *Cercopithifilaria johnstoni* mitochondrial genome. All filarial nematodes, including outgroups, are used in this mitochondrial genome dataset.

Character set	Substitution Model	Region of mtDNA
1	GTRGAMMA	ATP6_pos1, Intergenic1
2	GTRIGAMMA	Intergenic5, ND3_pos1, ND6_pos1
3	GTRGAMMA	ND3_pos2, ND6_pos2
4	GTRGAMMA	COX2_pos3, COX3_pos3, ND6_pos3
5	GTRGAMMA	Intergenic2, Intergenic9
6	GTRIGAMMA	COX3_pos1, CYTB_pos1, ND1_pos1, ND4_pos1, ND5_pos1
7	GTRIGAMMA	COX3_pos2, CYTB_pos2, ND1_pos2, ND4_pos2, ND5_pos2
8	GTRGAMMA	ATP6_pos3, COX1_pos3, CYTB_pos3
9	GTRGAMMA	Intergenic3
10	GTRIGAMMA	Intergeneic11, Intergeneic4
11	GTRIGAMMA	ND1_pos3, ND3_pos3, ND4_pos3, ND5_pos3
12	GTRIGAMMA	COX1_pos1, COX2_pos1, COX2_pos2
13	GTRIGAMMA	COX1_pos2
14	GTRIGAMMA	Intergenic6, Intergenic7, Intergenic8
15	GTRIGAMMA	ATP6_pos2, ND5_pos2
16	GTRIGAMMA	Intergenic10

Supplementary Table 2.2: Recommended Partition Finder substitution models for all filarial nematodes and outgroups using only the coding regions within the mitochondrial genome, excluding the intergenic regions.

Character set	Substitution Model	Region of mtDNA
1	GTRIGAMMA	ND3_pos1, ND6_pos1
2	GTRGAMMA	ND3_pos2, ND6_pos2
3	GTRGAMMA	COX2_pos3, COX3_pos3, ND6_pos3
4	GTRIGAMMA	ATP6_pos1, COX3_pos1, CTYB_pos1, ND1_pos1, ND4_pos1, ND5_pos1
5	GTRIGAMMA	COX2_pos2, COX3_pos2, CTYB_pos2, ND1_pos2, ND4_pos2
6	GTRGAMMA	COX1_pos3, CTYB_pos3
7	GTRGAMMA	ATP6_pos3, ND1_pos3, ND3_pos3, ND4_pos3, ND5_pos3
8	GTRIGAMMA	COX1_pos1, COX2_pos1
9	GTRIGAMMA	COX1_pos2
10	GTRIGAMMA	ATP6_pos2, ND5_pos2

Supplementary Table 2.3: Recommended Partition Finder substitution models for the complete dataset of coding regions and intergenic regions within the mitochondrial genome, excluding outgroups from the analysis.

Character set	Substitution Model	Region of mtDNA
1	GTRIGAMMA	ATP6_pos1, Intergenic1, ND1_pos1
2	HKYGAMMA	ND3_pos1, ND6_pos1
3	GTRGAMMA	ND3_pos2, ND6_pos2
4	GTRIGAMMA	ATP6_pos3, COX1_pos3, COX3_pos3, CYTB_pos3, ND6_pos3
5	GTRGAMMA	Intergenic2, Intergenic5
6	GTRIGAMMA	COX3_pos1, CYTB_pos1, Intergenic10
7	GTRIGAMMA	COX2_pos2, COX3_pos2, CYTB_pos2, ND1_pos2, ND4_pos2
8	GTRIGAMMA	Intergenic3, Intergenic6, Intergenic7, Intergenic8, Intergenic9
9	GTRIGAMMA	Intergenic4
10	GTRGAMMA	ND4_pos1, ND5_pos1
11	GTRGAMMA	ND1_pos3, ND3_pos3, ND4_pos3, ND5_pos3
12	GTRIGAMMA	COX1_pos1, COX2_pos1
13	GTRIGAMMA	COX1_pos2
14	GTRIGAMMA	ATP6_pos2, ND5_pos2
15	HKYGAMMA	COX2_pos3
16	GTRGAMMA	Intergenic11

Supplementary Table 2.4: Recommended Partition Finder substitution models for filarial nematodes of the coding regions within the mitochondrial genome, excluding the outgroups and the intergenic regions.

Character set	Substitution Model	Region of mtDNA
1	HKYGAMMA	ND3_pos1, ND6_pos1
2	GTRGAMMA	ND3_pos2, ND6_pos2
3	GTRIGAMMA	ATP6_pos3, COX1_pos3, COX3_pos3, CTYB_pos3, ND6_pos3
4	GTRIGAMMA	ATP6_pos1, COX3_pos1, CTYB_pos1, ND1_pos1
5	GTRIGAMMA	ATP6_pos2, COX2_pos2, COX3_pos2, CTYB_pos2, ND1_pos2, ND4_pos2, ND5_pos2
6	GTRGAMMA	ND4_pos1, ND5_pos1
7	GTRIGAMMA	ND1_pos3, ND3_pos3, ND4_pos3, ND5_pos3
8	GTRIGAMMA	COX1_pos1, COX2_pos1
9	GTRIGAMMA	COX1_pos2
10	HKYGAMMA	COX2_pos3

Supplementary Table 2.5: *Cercopithifilaria* spp. NCBI accession numbers for COI and 12S concatenated gene phylogeny.

Species	COI	12S
<i>Cercopithifilaria rugosicauda</i>	KC610813	KC610808
<i>Cercopithifilaria bainaie</i>	KF270686	KX156956
<i>Cercopithifilaria grassii</i>	JQ837810	JQ837812
<i>Cercopithifilaria roussilhonii</i>	AM749264	AM779798
<i>Cercopithifilaria japonica</i>	AB771722	AM779794
<i>Cercopithifilaria tumidivervicata</i>	AB178853	AM779790
<i>Cercopithifilaria minuta</i>	AB178847	AM779786
<i>Cercopithifilaria bulboidea</i>	AB178839	AM779780
<i>Cercopithifilaria longa</i>	AB178845	AM779784

Supplementary Table 2.6: Table adapted from McNulty et al. (2012), consisting of published mitochondrial genomes of the filarial nematodes with their accession numbers, genome length, AT-rich region length, and base content (%). The *Cercopithifilaria johnstoni* draft genome is added to compare genome content against other published mitochondrial genomes.

Species	<i>B. malayi</i>	<i>D. immitis</i>	<i>O. volvulus</i>	<i>O. ochengi</i>	<i>O. flexuosa</i>	<i>W. bancrofti</i>	<i>L. loa</i>	<i>A. viteae</i>	<i>C. johnstoni</i>
Subfamily	Onchocercidae	Dirofilarinae	Onchocercidae	Onchocercidae	Onchocercidae	Onchocercidae	Dirofilarinae	Onchocercidae	Onchocercidae
Accession Number	NC_004298	NC_005305	NC_001861	KX181290	HQ214004	HQ184469	HQ186250	HQ186249	draft
Length (bp)	13,657	13,814	13,747	13,744	13,672	13,636	13,590	13,724	13, 716
length of AT-rich region (bp)	283	362	312	318	284	256	288	421	419
A%	21.6	19.3	19.3	18.9	20.3	20.5	20.8	19.6	23.7
T%	53.9	54.9	54	54.2	53.9	54.1	54.8	54	52.3
G%	16.8	19.3	19.8	20	18.6	18	17.7	19.3	16.7
C%	7.7	6.5	6.9	6.8	7.2	7.4	6.7	7.2	7.3
AT%	75.5	74.2	73.3	73.2	74.2	74.6	75.6	73.5	76

Appendix 2: Chapter Three Supplementary Material

Supplementary Table 3.1: Missing BUSCO gene IDs from the genome completeness analysis for 12 filarial nematodes including *Cercopithifilaria johnstoni*, *Acanthocheilonema viteae*, *Brugia malayi*, *Brugia pahangi*, *Brugia timori*, *Dirofilaria immitis*, *Loa loa*, *Litomosoides sigmodontis*, *Onchocerca flexuosa*, *Onchocerca ochengi*, *Onchocerca volvulus* and *Wuchereria bancrofti*.

<i>C. johnstoni</i>	<i>A. viteae</i>	<i>B. malayi</i>	<i>B. pahangi</i>	<i>B. timori</i>	<i>D. immitis</i>	<i>L. loa</i>	<i>L. sigmodontis</i>	<i>O. volvulus</i>	<i>O. ochengi</i>	<i>O. flexuosa</i>	<i>W. bancrofti</i>
EOG091H0029	EOG091H0092	EOG091H00OG	EOG091H0027	EOG091H0002	EOG091H004L	EOG091H08LW	EOG091H00DB	EOG091H01GK	EOG091H006B	EOG091H0026	EOG091H0002
EOG091H02AZ	EOG091H00JN	EOG091H01GK	EOG091H0034	EOG091H0016	EOG091H007E	EOG091H091T	EOG091H00MS	EOG091H0286	EOG091H006J	EOG091H0027	EOG091H0025
EOG091H02S6	EOG091H0131	EOG091H025R	EOG091H0037	EOG091H0025	EOG091H00OH	EOG091H0999	EOG091H00VK	EOG091H05MH	EOG091H00E0	EOG091H0029	EOG091H0029
EOG091H039S	EOG091H013G	EOG091H0286	EOG091H003H	EOG091H0026	EOG091H00OW	EOG091H0BO8	EOG091H016V	EOG091H07XH	EOG091H00EC	EOG091H0034	EOG091H003X
EOG091H03VV	EOG091H01EU	EOG091H02O4	EOG091H007E	EOG091H0027	EOG091H00YA		EOG091H01AG	EOG091H07Y2	EOG091H00JR	EOG091H003H	EOG091H004B
EOG091H03WV	EOG091H021P	EOG091H03PX	EOG091H00JR	EOG091H0029	EOG091H00YF		EOG091H01K3	EOG091H08HY	EOG091H00ME	EOG091H003N	EOG091H004P
EOG091H048H	EOG091H023L	EOG091H044G	EOG091H00N1	EOG091H0034	EOG091H0125		EOG091H02B8	EOG091H0982	EOG091H00N1	EOG091H003X	EOG091H006B
EOG091H04D3	EOG091H025R	EOG091H0464	EOG091H00OG	EOG091H003H	EOG091H014U		EOG091H02KG		EOG091H00VG	EOG091H004P	EOG091H007E
EOG091H05WA	EOG091H02AZ	EOG091H06B0	EOG091H00Q9	EOG091H003N	EOG091H01EU		EOG091H02S6		EOG091H00WC	EOG091H005M	EOG091H008D

EOG091H 06B0	EOG091H 02GU	EOG091H 07Y2	EOG091H 00SU	EOG091H 004U	EOG091H 01EY		EOG091H 02V3		EOG091H 00ZE	EOG091H 0061	EOG091H 00C4
EOG091H 06OZ	EOG091H 03BE	EOG091H 08UA	EOG091H 00ZH	EOG091H 0061	EOG091H 01JA		EOG091H 034Q		EOG091H 00ZS	EOG091H 006B	EOG091H 00EC
EOG091H 07UA	EOG091H 03FE	EOG091H 0AJN	EOG091H 0121	EOG091H 006B	EOG091H 01PY		EOG091H 039S		EOG091H 016I	EOG091H 006J	EOG091H 00ER
EOG091H 07XH	EOG091H 03SV	EOG091H 0BO8	EOG091H 01FZ	EOG091H 006J	EOG091H 0302		EOG091H 03I3		EOG091H 01CI	EOG091H 007E	EOG091H 00I6
EOG091H 08UA	EOG091H 048H		EOG091H 01IT	EOG091H 006P	EOG091H 039S		EOG091H 03UP		EOG091H 01GK	EOG091H 007U	EOG091H 00IN
EOG091H 0BO8	EOG091H 0499		EOG091H 01MN	EOG091H 007C	EOG091H 03D7		EOG091H 048H		EOG091H 01LC	EOG091H 0081	EOG091H 00IO
	EOG091H 057W		EOG091H 021P	EOG091H 007E	EOG091H 03IE		EOG091H 04L1		EOG091H 01X1	EOG091H 008D	EOG091H 00JN
	EOG091H 06B0		EOG091H 02B3	EOG091H 007U	EOG091H 03LM		EOG091H 04TX		EOG091H 023Q	EOG091H 008P	EOG091H 00JR
	EOG091H 06OZ		EOG091H 02DM	EOG091H 008D	EOG091H 040W		EOG091H 050D		EOG091H 028C	EOG091H 008Q	EOG091H 00KI
	EOG091H 074D		EOG091H 02J5	EOG091H 008U	EOG091H 048H		EOG091H 058F		EOG091H 028Y	EOG091H 0092	EOG091H 00M0
	EOG091H 07Z3		EOG091H 02NI	EOG091H 0090	EOG091H 04C4		EOG091H 05KP		EOG091H 02D7	EOG091H 00AU	EOG091H 00N1
	EOG091H 091T		EOG091H 02US	EOG091H 00C4	EOG091H 04D3		EOG091H 06B0		EOG091H 02JZ	EOG091H 00C4	EOG091H 00NH
	EOG091H 0AB9		EOG091H 03JG	EOG091H 00DB	EOG091H 04QD		EOG091H 06OZ		EOG091H 02KT	EOG091H 00CS	EOG091H 00NK
	EOG091H 0AJN		EOG091H 03Q1	EOG091H 00EC	EOG091H 05HW		EOG091H 06XM		EOG091H 02NM	EOG091H 00ER	EOG091H 00PN
	EOG091H 0BO8		EOG091H 04L1	EOG091H 00EN	EOG091H 05Q3		EOG091H 07XH		EOG091H 0395	EOG091H 00FN	EOG091H 00PT
			EOG091H 04XZ	EOG091H 00ER	EOG091H 0641		EOG091H 09QA		EOG091H 03YO	EOG091H 00G5	EOG091H 00T6
			EOG091H 04Y6	EOG091H 00FN	EOG091H 06B0		EOG091H 0A01		EOG091H 03YU	EOG091H 00HI	EOG091H 00U7

			EOG091H 050X	EOG091H 00GI	EOG091H 06OZ		EOG091H 0B5N		EOG091H 04L1	EOG091H 00HN	EOG091H 00YA
			EOG091H 05HQ	EOG091H 00HI	EOG091H 06SS		EOG091H 0BO8		EOG091H 04Q2	EOG091H 00IN	EOG091H 00ZE
			EOG091H 05HW	EOG091H 00IN	EOG091H 0717				EOG091H 04YN	EOG091H 00JR	EOG091H 00ZH
			EOG091H 05PM	EOG091H 00IO	EOG091H 072K				EOG091H 04ZK	EOG091H 00JS	EOG091H 011J
			EOG091H 06B0	EOG091H 00JN	EOG091H 074D				EOG091H 05C4	EOG091H 00K1	EOG091H 013T
			EOG091H 06E3	EOG091H 00JR	EOG091H 07N1				EOG091H 05II	EOG091H 00KI	EOG091H 016T
			EOG091H 07A3	EOG091H 00K8	EOG091H 08AH				EOG091H 05Q3	EOG091H 00L2	EOG091H 016V
			EOG091H 08H7	EOG091H 00M0	EOG091H 08LW				EOG091H 064T	EOG091H 00L8	EOG091H 017K
			EOG091H 0999	EOG091H 00MA	EOG091H 09G2				EOG091H 06GG	EOG091H 00LE	EOG091H 018G
			EOG091H 0AUJ	EOG091H 00MS	EOG091H 0AIZ				EOG091H 06NT	EOG091H 00MA	EOG091H 01IT
				EOG091H 00N1					EOG091H 0717	EOG091H 00ME	EOG091H 01IX
				EOG091H 00O1					EOG091H 072K	EOG091H 00MS	EOG091H 01KU
				EOG091H 00OG					EOG091H 075U	EOG091H 00N0	EOG091H 01LC
				EOG091H 00P3					EOG091H 077O	EOG091H 00N1	EOG091H 01MU
				EOG091H 00PT					EOG091H 0792	EOG091H 00NH	EOG091H 01OS
				EOG091H 00Q9					EOG091H 07A3	EOG091H 00O1	EOG091H 01Q0
				EOG091H 00S9					EOG091H 07DW	EOG091H 00OW	EOG091H 01S2

				EOG091H 00SU					EOG091H 07YW	EOG091H 00OX	EOG091H 01T6
				EOG091H 00T6					EOG091H 07Z3	EOG091H 00P3	EOG091H 01TQ
				EOG091H 00U7					EOG091H 086R	EOG091H 00PU	EOG091H 01WO
				EOG091H 00VG					EOG091H 08J3	EOG091H 00RF	EOG091H 0236
				EOG091H 00VK					EOG091H 0BO8	EOG091H 00SJ	EOG091H 024K
				EOG091H 00WC						EOG091H 00SU	EOG091H 026T
				EOG091H 00ZH						EOG091H 00T3	EOG091H 027A
				EOG091H 0107						EOG091H 00T7	EOG091H 0286
				EOG091H 0116						EOG091H 00TG	EOG091H 028G
				EOG091H 0125						EOG091H 00UC	EOG091H 029S
				EOG091H 012M						EOG091H 00VG	EOG091H 02AB
				EOG091H 013B						EOG091H 00VP	EOG091H 02C1
				EOG091H 013G						EOG091H 00VY	EOG091H 02FR
				EOG091H 013T						EOG091H 00WC	EOG091H 02KG
				EOG091H 014S						EOG091H 00WE	EOG091H 02N4
				EOG091H 014U						EOG091H 00WJ	EOG091H 02O4
				EOG091H 016I						EOG091H 00WM	EOG091H 02XU

				EOG091H 016T						EOG091H 00XH	EOG091H 032B
				EOG091H 016V						EOG091H 00YA	EOG091H 034Q
				EOG091H 018G						EOG091H 00YF	EOG091H 0357
				EOG091H 018I						EOG091H 00YH	EOG091H 0387
				EOG091H 0190						EOG091H 00YM	EOG091H 03A1
				EOG091H 01B8						EOG091H 00YU	EOG091H 03AV
				EOG091H 01BG						EOG091H 00ZE	EOG091H 03B5
				EOG091H 01CG						EOG091H 00ZH	EOG091H 03DA
				EOG091H 01CW						EOG091H 00ZS	EOG091H 03LM
				EOG091H 01EA						EOG091H 0107	EOG091H 03PX
				EOG091H 01EN						EOG091H 0116	EOG091H 03W9
				EOG091H 01EU						EOG091H 0121	EOG091H 03WJ
				EOG091H 01FB						EOG091H 012M	EOG091H 03WS
				EOG091H 01FZ						EOG091H 0131	EOG091H 03Y3
				EOG091H 01GK						EOG091H 013B	EOG091H 03YU
				EOG091H 01IT						EOG091H 013G	EOG091H 03ZH
				EOG091H 01IX						EOG091H 014E	EOG091H 041T

				EOG091H 01JA						EOG091H 014Q	EOG091H 044T
				EOG091H 01JV						EOG091H 014S	EOG091H 045E
				EOG091H 01LC						EOG091H 014U	EOG091H 04B8
				EOG091H 01LE						EOG091H 015E	EOG091H 04C4
				EOG091H 01MN						EOG091H 015X	EOG091H 04CB
				EOG091H 01MU						EOG091H 016F	EOG091H 04GH
				EOG091H 01N6						EOG091H 016J	EOG091H 04L1
				EOG091H 01OQ						EOG091H 019D	EOG091H 04XZ
				EOG091H 01OS						EOG091H 01AG	EOG091H 0526
				EOG091H 01PS						EOG091H 01B8	EOG091H 056U
				EOG091H 01Q0						EOG091H 01C0	EOG091H 05FT
				EOG091H 01SI						EOG091H 01CI	EOG091H 05JJ
				EOG091H 01VC						EOG091H 01CQ	EOG091H 05M3
				EOG091H 01WD						EOG091H 01DX	EOG091H 05TP
				EOG091H 01WO						EOG091H 01EA	EOG091H 05ZX
				EOG091H 01WT						EOG091H 01EK	EOG091H 0625
				EOG091H 01X3						EOG091H 01EN	EOG091H 06B0

				EOG091H 01YM						EOG091H 01EU	EOG091H 06EG
				EOG091H 01Z5						EOG091H 01FB	EOG091H 06GG
				EOG091H 020A						EOG091H 01FZ	EOG091H 06IK
				EOG091H 0219						EOG091H 01GK	EOG091H 06K6
				EOG091H 021P						EOG091H 01H5	EOG091H 06MW
				EOG091H 024K						EOG091H 01IT	EOG091H 06O1
				EOG091H 024T						EOG091H 01IX	EOG091H 06RV
				EOG091H 025I						EOG091H 01JQ	EOG091H 06W9
				EOG091H 025R						EOG091H 01KU	EOG091H 06WU
				EOG091H 025U						EOG091H 01KW	EOG091H 072K
				EOG091H 026S						EOG091H 01L2	EOG091H 073T
				EOG091H 028T						EOG091H 01MU	EOG091H 0759
				EOG091H 02AB						EOG091H 01MY	EOG091H 07DQ
				EOG091H 02AK						EOG091H 01N6	EOG091H 07K5
				EOG091H 02AZ						EOG091H 01OC	EOG091H 07RS
				EOG091H 02B3						EOG091H 01OP	EOG091H 07VA
				EOG091H 02D7						EOG091H 01OS	EOG091H 07Y2

				EOG091H 02F5						EOG091H 01PS	EOG091H 080L
				EOG091H 02FN						EOG091H 01SH	EOG091H 083D
				EOG091H 02G0						EOG091H 01SR	EOG091H 08HY
				EOG091H 02GV						EOG091H 01V3	EOG091H 08LW
				EOG091H 02HW						EOG091H 01WT	EOG091H 08RU
				EOG091H 02J5						EOG091H 01Y6	EOG091H 08XO
				EOG091H 02N2						EOG091H 01YN	EOG091H 08YC
				EOG091H 02NI						EOG091H 01Z5	EOG091H 090O
				EOG091H 02O4						EOG091H 01ZX	EOG091H 094E
				EOG091H 02QY						EOG091H 021P	EOG091H 0982
				EOG091H 02S8						EOG091H 0234	EOG091H 098B
				EOG091H 02SL						EOG091H 023L	EOG091H 09DN
				EOG091H 02TB						EOG091H 023Q	EOG091H 09EO
				EOG091H 02TJ						EOG091H 024D	EOG091H 09OH
				EOG091H 02US						EOG091H 024T	EOG091H 09S6
				EOG091H 02X0						EOG091H 025R	EOG091H 09UD
				EOG091H 02YS						EOG091H 027A	EOG091H 09YU

				EOG091H 034Q						EOG091H 027V	EOG091H 0A24
				EOG091H 034R						EOG091H 028C	EOG091H 0A7P
				EOG091H 0352						EOG091H 028T	EOG091H 0AEC
				EOG091H 0395						EOG091H 028Y	EOG091H 0B69
				EOG091H 03AL						EOG091H 02AB	EOG091H 0BO8
				EOG091H 03B5						EOG091H 02AK	
				EOG091H 03CU						EOG091H 02AZ	
				EOG091H 03D7						EOG091H 02B8	
				EOG091H 03DJ						EOG091H 02CZ	
				EOG091H 03PC						EOG091H 02D7	
				EOG091H 03PX						EOG091H 02DM	
				EOG091H 03S6						EOG091H 02FN	
				EOG091H 03TK						EOG091H 02FZ	
				EOG091H 03UR						EOG091H 02GQ	
				EOG091H 03W9						EOG091H 02GU	
				EOG091H 03WD						EOG091H 02HW	
				EOG091H 03WJ						EOG091H 02JU	

				EOG091H 03WO						EOG091H 02JZ	
				EOG091H 03WX						EOG091H 02K1	
				EOG091H 03XL						EOG091H 02KG	
				EOG091H 03Y3						EOG091H 02N2	
				EOG091H 03YO						EOG091H 02NI	
				EOG091H 040W						EOG091H 02OZ	
				EOG091H 045Z						EOG091H 02QD	
				EOG091H 0460						EOG091H 02T9	
				EOG091H 04AC						EOG091H 02US	
				EOG091H 04F1						EOG091H 02X0	
				EOG091H 04GH						EOG091H 02XP	
				EOG091H 04L1						EOG091H 02XU	
				EOG091H 04MS						EOG091H 02YS	
				EOG091H 04P2						EOG091H 0338	
				EOG091H 04PD						EOG091H 033A	
				EOG091H 04Q2						EOG091H 034Q	
				EOG091H 04RZ						EOG091H 034R	

				EOG091H 04WQ						EOG091H 0387	
				EOG091H 04XH						EOG091H 038Z	
				EOG091H 04Y6						EOG091H 0395	
				EOG091H 050D						EOG091H 03AV	
				EOG091H 051E						EOG091H 03B2	
				EOG091H 053G						EOG091H 03B5	
				EOG091H 057P						EOG091H 03BE	
				EOG091H 0596						EOG091H 03CT	
				EOG091H 059F						EOG091H 03CU	
				EOG091H 05C4						EOG091H 03D7	
				EOG091H 05FT						EOG091H 03FE	
				EOG091H 05FV						EOG091H 03FF	
				EOG091H 05I8						EOG091H 03J4	
				EOG091H 05IK						EOG091H 03JP	
				EOG091H 05JJ						EOG091H 03KF	
				EOG091H 05KP						EOG091H 03KM	
				EOG091H 05KS						EOG091H 03LO	

				EOG091H 05M3						EOG091H 03LV	
				EOG091H 05P6						EOG091H 03NW	
				EOG091H 05PJ						EOG091H 03OC	
				EOG091H 05Q3						EOG091H 03PU	
				EOG091H 05UV						EOG091H 03QK	
				EOG091H 05WB						EOG091H 03S6	
				EOG091H 05XE						EOG091H 03TW	
				EOG091H 05ZX						EOG091H 03UM	
				EOG091H 0625						EOG091H 03UR	
				EOG091H 0654						EOG091H 03VV	
				EOG091H 065E						EOG091H 03WD	
				EOG091H 0695						EOG091H 03XH	
				EOG091H 06B0						EOG091H 03XL	
				EOG091H 06GG						EOG091H 03Y3	
				EOG091H 06IK						EOG091H 03Y6	
				EOG091H 06K6						EOG091H 03YU	
				EOG091H 06MW						EOG091H 041T	

				EOG091H 06O1						EOG091H 044G	
				EOG091H 06RT						EOG091H 048H	
				EOG091H 06SD						EOG091H 0499	
				EOG091H 06W9						EOG091H 04CY	
				EOG091H 06XQ						EOG091H 04CZ	
				EOG091H 070B						EOG091H 04FI	
				EOG091H 0717						EOG091H 04L1	
				EOG091H 072K						EOG091H 04MS	
				EOG091H 074D						EOG091H 04P8	
				EOG091H 0759						EOG091H 04Q2	
				EOG091H 075U						EOG091H 04Q6	
				EOG091H 079E						EOG091H 04T9	
				EOG091H 07A3						EOG091H 04TX	
				EOG091H 07BC						EOG091H 04XH	
				EOG091H 07D4						EOG091H 04XZ	
				EOG091H 07DH						EOG091H 04Y6	
				EOG091H 07DQ						EOG091H 050X	

				EOG091H 07DW						EOG091H 054R	
				EOG091H 07EX						EOG091H 0556	
				EOG091H 07FE						EOG091H 055R	
				EOG091H 07K5						EOG091H 057H	
				EOG091H 07LU						EOG091H 057P	
				EOG091H 07RS						EOG091H 057W	
				EOG091H 07VO						EOG091H 058F	
				EOG091H 07XV						EOG091H 05CW	
				EOG091H 07XW						EOG091H 05HY	
				EOG091H 07YC						EOG091H 05I4	
				EOG091H 07Z3						EOG091H 05I8	
				EOG091H 080L						EOG091H 05II	
				EOG091H 081R						EOG091H 05KP	
				EOG091H 082Z						EOG091H 05Q3	
				EOG091H 083D						EOG091H 05Q7	
				EOG091H 0857						EOG091H 05RZ	
				EOG091H 08H7						EOG091H 05SN	

				EOG091H 08LX						EOG091H 05UG	
				EOG091H 08SY						EOG091H 05VK	
				EOG091H 08X9						EOG091H 05WA	
				EOG091H 08XO						EOG091H 05WB	
				EOG091H 091T						EOG091H 05ZX	
				EOG091H 092P						EOG091H 0641	
				EOG091H 098G						EOG091H 065E	
				EOG091H 0999						EOG091H 065N	
				EOG091H 09AA						EOG091H 0695	
				EOG091H 09D9						EOG091H 06E8	
				EOG091H 09DN						EOG091H 06EG	
				EOG091H 09G2						EOG091H 06F0	
				EOG091H 09QA						EOG091H 06GG	
				EOG091H 09S6						EOG091H 06I5	
				EOG091H 0A24						EOG091H 06IL	
				EOG091H 0A3K						EOG091H 06JZ	
				EOG091H 0A8G						EOG091H 06MW	

				EOG091H 0AEC						EOG091H 06N7	
				EOG091H 0AJN						EOG091H 06NY	
				EOG091H 0AO9						EOG091H 06RT	
				EOG091H 0B5Y						EOG091H 06RV	
				EOG091H 0BO8						EOG091H 06SD	
										EOG091H 06SS	
										EOG091H 06TA	
										EOG091H 06Y7	
										EOG091H 070S	
										EOG091H 0717	
										EOG091H 072K	
										EOG091H 0730	
										EOG091H 077O	
										EOG091H 079E	
										EOG091H 07B0	
										EOG091H 07DH	
										EOG091H 07FE	

										EOG091H 07FF	
										EOG091H 07GQ	
										EOG091H 07GY	
										EOG091H 07IQ	
										EOG091H 07LN	
										EOG091H 07N1	
										EOG091H 07PS	
										EOG091H 07UA	
										EOG091H 07VO	
										EOG091H 07XI	
										EOG091H 07Y2	
										EOG091H 07YC	
										EOG091H 07YW	
										EOG091H 07Z3	
										EOG091H 0809	
										EOG091H 083D	
										EOG091H 085T	

										EOG091H 08AH	
										EOG091H 08FP	
										EOG091H 08JL	
										EOG091H 08LX	
										EOG091H 08NA	
										EOG091H 08SZ	
										EOG091H 0905	
										EOG091H 0944	
										EOG091H 094D	
										EOG091H 0999	
										EOG091H 09AA	
										EOG091H 09CM	
										EOG091H 09GT	
										EOG091H 09QA	
										EOG091H 09VW	
										EOG091H 0A01	
										EOG091H 0A6R	

										EOG091H 0AIZ	
										EOG091H 0AO9	
										EOG091H 0ATF	
										EOG091H 0AUJ	
										EOG091H 0AZL	
										EOG091H 0BO8	

Supplementary Table 3.2: Complete RepeatModeler statistics including total repeats, number of base pairs (bp) and percentage (%). Comparison of the RepeatModeler repeat statistics of *Cercopithifilaria johnstoni* and closely related filarial nematodes. Total interspersed repeats consisting of LINEs (long interspersed nuclear elements), SINEs (short interspersed nuclear elements), DNA (DNA Transposons), LTR (long terminal repeat) and unclassified repeats. Small RNA, satellites, simple repeats and low complexity repeats are also represented in the table. The total number of repeat bases that are masked in each filarial genome are represented as “bases masked”.

Species		bases masked	SINEs	LINEs	LTR	DNA	Unclassified	Total interspersed repeats	Small RNA	Satellites	Simple repeats	Low complexity
<i>C. johnstoni</i>	total		0	686	21	208	6,490		0	56	45,684	10,273
	bp	4,925,102	0	116,370	2,658	52,432	1,736,807	1,908,267	0	7,635	2,460,891	552,231
	%	6.23	0	0.15	0	0.07	2.20	2.41	0	0.01	3.11	0.70
<i>A. viteae</i>	total		0	90	1,092	1,025	2,496		0	0	35743	10,319
	bp	3,054,604	0	7,622	337,591	142,746	456,263	944,222	0	0	1,605,806	508,053
	%	3.96	0	0.01	0.44	0.18	0.59	1.22	0	0	2.08	0.66
<i>B. malayi</i>	total		0	2,260	2,190	1,451	7,848		133	273	82,066	20,253
	bp	10,494,094	0	377,063	1,111,004	230,694	3,633,504	5,352,265	102,358	229,297	3,773,821	1,062,708
	%	11.80	0	0.43	1.26	0.26	4.12	6.07	0.12	0.26	4.28	1.20
<i>B. pahangi</i>	total		275	1,488	1,621	1,557	3,858		275	25	87,205	22,854
	bp	7,137,323	29,746	330,629	416,527	253,235	941,008	1,971,145	29,746	8,350	3,957,105	1,208,521
	%	7.88	0.03	0.37	0.46	0.28	1.04	2.18	0.03	0.01	4.37	1.33
<i>B. timori</i>	total		19	934	902	889	2,029		23	172	40,358	9,597

	bp	3,258,849	1,087	165,685	287,371	102,345	380,322	936,810	6,061	37,258	1,798,223	484,636
	%	5.02	0	0.26	0.44	0.16	0.59	1.44	0.01	0.06	2.77	0.75
<i>D. immitis</i>	total		161	1,214	1,676	786	5,173		580	140	57,238	14,076
	bp	5,384,130	18,102	170,736	510,370	91,896	1,170,680	1,961,784	69,480	49,560	2,597,281	730,439
	%	6.10	0.02	0.19	0.58	0.10	1.33	2.22	0.08	0.06	2.94	0.83
<i>L. loa</i>	total		313	3,346	3,490	2,466	9,877		515	534	69,432	14,752
	bp	13,119,135	34,584	891,633	2,464,609	897,489	3,701,868	7,990,183	142,585	272,022	3,990,601	777,463
	%	13.61	0.04	0.92	2.56	0.93	3.84	8.29	0.15	0.28	4.14	0.81
<i>L. sigmodontis</i>	total		0	172	758	294	481		0	0	29,613	6,268
	bp	1,826,171	0	16,301	103,532	56,084	111,687	287,604	0	0	1,237,223	304,394
	%	2.82	0	0.03	0.16	0.09	0.17	0.44	0	0	1.91	0.47
<i>O. flexuosa</i>	total		0	311	2,235	388	11,087		156	7	32,863	7,310
	bp	5,462,806	0	42,778	993,103	43,477	2,624,467	3,703,825	28,300	13,913	1,367,309	356,808
	%	8.06	0	0.06	1.47	0.06	3.87	5.47	0.04	0.02	2.02	0.53
<i>O. ochengi</i>	total		605	5,068	3,431	1,608	19,291		826	481	56,033	13,246
	bp	9,358,768	55,877	909,838	1,030,261	279,309	3,908,401	6,183,686	98,835	179,815	2,299,491	656,436
	%	10.21	0.06	0.99	1.12	0.30	4.26	6.75	0.11	0.20	2.51	0.72
<i>O. volvulus</i>	total		0	487	3009	863	20,693		364	66	63,138	15,242
	bp	9,890,502	0	94,663	1,242,579	166,760	4,835,858	6,339,860	77,364	90,909	2,636,212	763,968
	%	10.26	0	0.1	1.29	0.17	5.02	6.57	0.08	0.09	2.73	0.79
<i>W. bancrofti</i>	total		242	198	3,388	1321	1,983		0	38	65,719	18,907
	bp	6,286,979	58,229	75,735	774,597	174,057	434,518	1,517,136	0	74,525	3,723,278	983,501
	%	6.96	0.06	0.08	0.86	0.19	0.48	1.68	0	0.08	4.12	1.09

Appendix 3: Chapter Four Supplementary Material

Supplementary Table 4.1: List of 17/49 *Onchocerca volvulus* immunogenic relevant proteins used to identify and extract from the OrthoFinder2 analysis any possible orthologues in *Cercopithifilaria johnstoni* for further analyses. Protein obtained from Norice-Tra et al. (2017).

Immuno proteins - Norice-Tra
WBGene00248326 OVOC11517
WBGene00239986 OVOC3177
WBGene00245563 OVOC8754
WBGene00238001 OVOC1192
WBGene00244123 OVOC7314
WBGene00246034 OVOC9225
WBGene00249378 OVOC12569
WBGene00244262 OVOC7453
WBGene00246384 OVOC9575
WBGene00249437 OVOC12628
WBGene00244595 OVOC7786
WBGene00246793 OVOC9984
WBGene00249578 OVOC12769
WBGene00244720 OVOC7911
WBGene00246797 OVOC9988
WBGene00249680 OVOC12871
WBGene00237669 OVOC860

Supplementary Table 4.2: List of 31/48 *Onchocerca volvulus* serodiagnostic relevant proteins used to identify and extract from the OrthoFinder2 analysis any possible orthologues in *Cercopithifilaria johnstoni* for further analyses. Proteins obtained from McNulty et al. (2015).

Serodiagnostic - McNulty	
WBGene00249257 OVOC12448	WBGene00243136 OVOC6327
WBGene00246876 OVOC10067	WBGene00246799 OVOC9990
WBGene00249258 OVOC12449	WBGene00238022 OVOC1213
WBGene00245794 OVOC8985	WBGene00244190 OVOC7381
WBGene00246912 OVOC10103	WBGene00249209 OVOC12400
WBGene00238706 OVOC1897	WBGene00244239 OVOC7430
WBGene00246134 OVOC9325	WBGene00248296 OVOC11487
WBGene00247447 OVOC10638	WBGene00242228 OVOC5419
WBGene00239295 OVOC2486	WBGene00246557 OVOC9748
WBGene00246193 OVOC9384	WBGene00248656 OVOC11847
WBGene00247791 OVOC10982	WBGene00242632 OVOC5823
WBGene00240012 OVOC3203	WBGene00248760 OVOC11951
WBGene00246284 OVOC9475	WBGene00246561 OVOC9752
WBGene00247804 OVOC10995	
WBGene00241421 OVOC4612	
WBGene00246401 OVOC9592	
WBGene00248027 OVOC11218	
WBGene00242527 OVOC5718	

Supplementary Table 4.3: The blast results of the 30 *Cercopithifilaria johnstoni* orthologues of *Onchocerca volvulus* immunogenic proteins are described revealing their top BLAST results to the NCBI database, % identity, protein alignment length, e-value, and bit score.

Query (<i>C. johnstoni</i>)	Subject (blast NCBI)	Description (NCBI)	% identity	Alignment length	e-value	bit score
Cjn_gene4340	CDQ02499.1	BMA-UNC-87, isoform b, partial [<i>B. malayi</i>]	96.359	357	0	714
Cjn_gene7687	EJW79500.1	hypothetical protein WUBG_09591, partial [<i>W. bancrofti</i>]	56.394	477	5.35E-145	434
Cjn_gene5098	CRZ22766.1	Bm2577 [<i>B. malayi</i>]	71.429	189	1.59E-94	286
Cjn_gene7514	EJD74931.1	hypothetical protein LOAG_17826 [<i>L. loa</i>]	51.049	286	1.67E-64	221
Cjn_gene6823	CRZ22233.1	Bm8325, isoform a [<i>B. malayi</i>]	82.945	815	0	1300
Cjn_gene3855	XP_001891888.1	CAP protein [<i>B. malayi</i>]	70.78	1102	0	1454
Cjn_gene6492	EJW87928.1	3-hydroxyacyl-CoA dehydrogenase [<i>W. bancrofti</i>]	95.635	252	7.25E-176	492
Cjn_gene5271	EJW78284.1	hypothetical protein WUBG_10805 (CTLH/CRA C-terminal to LisH motif domain) [<i>W. bancrofti</i>]	94.538	238	1.12E-156	442

Cjn_gene5847	VBB26289.1	unnamed protein product (GST_N_Sigma_like) [<i>A. viteae</i>]	78.218	202	1.26E-114	334
Cjn_gene413	EJW85966.1	reticulon family protein [<i>W. bancrofti</i>]	83.898	118	3.03E-66	209
Cjn_gene8088	EJD76644.1	fructose-bisphosphate aldolase [<i>L. loa</i>]	98.072	363	0	745
Cjn_gene8269	CAA04877.1	RAL-1 protein, partial [<i>L. sigmodontis</i>]	95.266	338	0	639
Cjn_gene2996	XP_003143117.1	SH2 domain-containing protein [<i>L. loa</i>]	74.317	183	5.59E-88	267
Cjn_gene11	Q25619.1	Fatty-acid and retinol-binding protein 1 (Ov20)	77.326	172	1.52E-92	275
Cjn_gene5764	CDQ04841.1	BMA-CYN-16 [<i>B. malayi</i>]	84.483	464	0	721
Cjn_gene3138	CRZ22798.1	Bm5820, partial [<i>B. malayi</i>]	85.77	513	0	892
Cjn_gene5845	AAD16985.1	vespid allergen antigen homolog [<i>W. bancrofti</i>]	77.717	184	4.33E-105	309
Cjn_gene8368	EFO14456.2	hypothetical protein LOAG_14063 (TTR-52) [<i>L. loa</i>]	80.272	147	1.20E-79	240
Cjn_gene1728	AAC77922.1	peroxidoxin-2 [<i>O. ochengi</i>]	93.671	158	1.23E-106	312

Cjn_gene5663	EFO26115.2	filarial antigen Av33 (Ascaris pepsin inhibitor-3) [<i>L. loa</i>]	71.97	132	3.13E-52	173
Cjn_gene3697	XP_001900036.1	<i>B. malayi</i> antigen (DUF148)	48.052	154	7.70E-43	147
Cjn_gene3697	XP_001900036.1	<i>B. malayi</i> antigen (DUF148)	48.361	122	5.59E-33	121
Cjn_gene3855	NP_001254445.1	Basement membrane proteoglycan [<i>C. elegans</i>]	53.753	2398	0	2528
Cjn_gene2748	KHN78795.1	Neprilysin-2 [<i>T. canis</i>]	69.397	464	0	691
Cj_gene9844	No significant similarity found					
Cjn_gene6611	AAR06638.1	superoxide dismutase [<i>B. malayi</i>]	94.839	155	8.76E-103	299
Cjn_gene235	EFO24522.2	hypothetical protein LOAG_03960 (Chondroitin proteoglycan 4) [<i>L. loa</i>]	48.38	432	1.45E-112	347
Cjn_gene4402	EJD74824.1	hypothetical protein LOAG_17909 (Strictosidine synthase) [<i>L. loa</i>]	85.333	75	1.18E-37	136
Cjn_gene10411	CAB41740.1	secretory protein (LS110p) [<i>L. sigmodontis</i>]	78.462	65	2.81E-30	118
Cjn_gene5503	AAB03902.2	Av18 (Chromadorea ALT) [<i>A. viteae</i>]	66.942	121	2.70E-43	147

Supplementary Table 4.4: The *Cercopithifilaria johnstoni* proteins examined for the presence of the *Onchocerca volvulus* motif DGxDK from Lagatie et al. (2017). The *Cercopithifilaria johnstoni* protein secondary BLAST hit and putative function is reported with % identity, e-value and bits (bit score).

<i>C. johnstoni</i> protein	Ov Motif (DGxDK)	Secondary blast hit	Description (NCBI)	% identity	e-value	bits
Cjn_gene113	DGIDK	EJW80766.1	glycosyltransferase [<i>Wuchereria bancrofti</i>]	71.538	6.78E-57	190
Cjn_gene298	DGDDK	VDK74290.1	unnamed protein product [<i>Litomosoides sigmodontis</i>]	65	7.38E-29	119
Cjn_gene723	DGGDK	VDM12151.1	unnamed protein product [<i>Wuchereria bancrofti</i>]	59.615	1.02E-26	109
Cjn_gene896	DGWDK	XP_001893036.1	SMC family, C-terminal domain containing protein [<i>Brugia malayi</i>]	58.14	1.22E-19	92.8
Cjn_gene1838	DGSDK	No secondary hit				
Cjn_gene2051	DGSDK	VDM09492.1	unnamed protein product [<i>Wuchereria bancrofti</i>]	63	2.33E-36	136
Cjn_gene2143	DGSDK	OZC10718.1	tryptophan 2,3-dioxygenase [<i>Onchocerca flexuosa</i>]	81.818	6.8E-49	169
Cjn_gene2749	DGFDK	VDN86410.1	unnamed protein product [<i>Brugia pahangi</i>]	73.958	1.07E-41	145
Cjn_gene3213	DGKDK	VDK87698.1	unnamed protein product [<i>Litomosoides sigmodontis</i>]	98.387	6.18E-35	128
Cjn_gene3906	DGTDK	VDM11717.1	unnamed protein product [<i>Wuchereria bancrofti</i>]	82.979	2.85E-44	160
Cjn_gene3910	DGRDK	VDP15708.1	unnamed protein product [<i>Onchocerca flexuosa</i>]	95	3.71E-57	200
Cjn_gene3959	DGLDK	XP_003145750.1	hypothetical protein LOAG_10175 [<i>Loa loa</i>]	81.667	1.2E-20	93.2

Cjn_gene4253	DGEDK	VBB31589.1	unnamed protein product [<i>Acanthocheilonema viteae</i>]	71.795	2.59E-44	157
Cjn_gene5140	DGSDK	VIO86469.1	uncharacterized protein BM_BM6243 [<i>Brugia malayi</i>]	72	0.002	47
Cjn_gene5421	DGGDK	VDK86246.1	unnamed protein product [<i>Litomosoides sigmodontis</i>]	55	1.21E-16	82.4
Cjn_gene5897	DGVDK	VDM15008.1	unnamed protein product [<i>Wuchereria bancrofti</i>]	78	9.35E-47	162
Cjn_gene5916	DGTDK	XP_003139927.1	ATPase [<i>Loa loa</i>]	56	3.56E-21	97.8
Cjn_gene6634	DGLDK	VDK82384.1	unnamed protein product [<i>Onchocerca ochengi</i>]	77	3.26E-46	160
Cjn_gene6658	DGSDK	XP_003140785.1	hypothetical protein LOAG_05201 [<i>Loa loa</i>]	97	4.74E-60	205
Cjn_gene6700	DGSDK	OZC08743.1	unnamed protein product [<i>Onchocerca flexuosa</i>]	40.678	0.0000011	56.6
Cjn_gene7127	DGQDK	VDO17115.1	unnamed protein product [<i>Brugia timori</i>]	65.686	6.98E-28	112
Cjn_gene7304	DGNDK	EJW86862.1	6-phosphofructokinase [<i>Wuchereria bancrofti</i>]	65.979	1.1E-30	124
Cjn_gene7413	DGDDK	VBB25469.1	unnamed protein product [<i>Acanthocheilonema viteae</i>]	91.765	6.95E-28	115
Cjn_gene7553	DGIDK	XP_003150765.1	hypothetical protein LOAG_15226 [<i>Loa loa</i>]	95	3.08E-61	195
Cjn_gene7626	DGLDK	VBB31551.1	unnamed protein product [<i>Acanthocheilonema viteae</i>]	95	1.34E-58	204
Cjn_gene8139	DGWDK	XP_001891970.1	von Willebrand factor type C domain containing protein [<i>Brugia malayi</i>]	93	6.24E-59	195
Cjn_gene8417	DGNDK	VDK89321.1	unnamed protein product [<i>Onchocerca ochengi</i>]	78.641	1.13E-48	172
Cjn_gene9043	DGEDK	VDK83117.1	unnamed protein product [<i>Litomosoides sigmodontis</i>]	76.471	2.05E-37	133

Cjn_gene9091	DGFDK	VDK74958.1	unnamed protein product [<i>Litomosoides sigmodontis</i>]	80.328	1.56E-25	110
Cjn_gene9587	DGGDK	No secondary hit				
Cjn_gene9909	DGGDK	VDM11045.1	unnamed protein product [<i>Wuchereria bancrofti</i>]	35.664	0.004	45.4

Supplementary Table 4.5: The *Cercopithifilaria johnstoni* proteins examined for the presence of the *Onchocerca volvulus* motif PxxTQE from Lagatie et al. (2017). The *Cercopithifilaria johnstoni* protein secondary BLAST hit and putative function is reported with % identity, e-value and bits (bit score).

<i>C. johnstoni</i> protein	Ov Motif (PxxTQE)	Secondary blast hit	Description (NCBI)	% identity	e-value	bits
Cjn_gene1496	PPETQE	XP_001900927.1	F-box domain containing protein [<i>Brugia malayi</i>]	98	1.96E-64	207
Cjn_gene2474	PQTTQE	XP_001900215.1	hypothetical protein Bm1_43765 [<i>Brugia malayi</i>]	63.793	1.56E-15	79.7
Cjn_gene2824	PIDTQE	XP_003141024.1	hypothetical protein LOAG_05439 [<i>Loa loa</i>]	90	5.99E-59	187
Cjn_gene3131	PIITQE	VDM14062.1	unnamed protein product [<i>Wuchereria bancrofti</i>]	85	1.91E-55	187
Cjn_gene5166	PAVTQE	VIO86094.1	RhoGEF domain containing protein [<i>Brugia malayi</i>]	85.149	3.5E-50	180
Cjn_gene6484	PDETQE	VDK74832.1	unnamed protein product [<i>Litomosoides sigmodontis</i>]	90	7.81E-11	63.5
Cjn_gene6592	PTSTQE	VDN91657.1	unnamed protein product [<i>Brugia pahangi</i>]	94.175	5.37E-58	202
Cjn_gene6623	PQVTQE	XP_003141132.1	hypothetical protein LOAG_05547 [<i>Loa loa</i>]	96	1.83E-63	215
Cjn_gene6756	PQYTQE	XP_020304992.1	hypothetical protein LOAG_18579 [<i>Loa loa</i>]	76.531	4.54E-37	138
Cjn_gene6854	PYTTQE	VDO52301.1	unnamed protein product [<i>Onchocerca flexuosa</i>]	56.364	5.78E-10	61.2
Cjn_gene6926	PKITQE	CDQ02899.2	Bm6200, isoform b [<i>Brugia malayi</i>]	94.898	1.98E-61	200
Cjn_gene7018	PSVTQE	No secondary hit				

Cjn_gene7205	PKHTQE	XP_020307076.1	hypothetical protein, variant [<i>Loa loa</i>]	69	9.75E-33	130
Cjn_gene8203	PSSTQE	XP_020305195.1	hypothetical protein LOAG_18392 [<i>Loa loa</i>]	70	9.51E-39	147
Cjn_gene8783	PIVTQE	VDK62047.1	unnamed protein product [<i>Onchocerca ochengi</i>]	73.469	8.57E-16	82.4
Cjn_gene8792	PEMTQE	VDK89497.1	unnamed protein product [<i>Litomosoides sigmodontis</i>]	75	2.62E-49	165
Cjn_gene9173	PDSTQE	VIO95376.1	uncharacterized protein BM_BM1563 [<i>Brugia malayi</i>]	92	7.34E-61	201
Cjn_gene9345	PESTQE	VDN92441.1	unnamed protein product [<i>Brugia pahangi</i>]	96.386	8.43E-50	164
Cjn_gene9881	PVRTQE	XP_001892705.1	Papain family cysteine protease containing protein [<i>Brugia malayi</i>]	35.948	7.44E-23	98.6

Supplementary Table 4.6: The *Cercopithifilaria johnstoni* proteins examined for the presence of the *Onchocerca volvulus* motif QxSNxD from Lagatie et al. (2017). The *Cercopithifilaria johnstoni* protein secondary BLAST hit and putative function is reported with % identity, e-value and bits (bit score).

<i>C. johnstoni</i> protein	Ov Motif (QxSNxD)	Secondary blast hit	Description (NCBI)	% identity	e-value	bits
Cjn_gene236	QLSNLD	VBB29465.1	unnamed protein product [<i>Acanthocheilonema viteae</i>]	94	2.82E-59	206
Cjn_gene566	QVSNID	VDM91510.1	unnamed protein product [<i>Litomosoides sigmodontis</i>]	78.378	6.6E-53	181
Cjn_gene740	QSSNTD	XP_003136757.1	hypothetical protein LOAG_01169 [<i>Loa loa</i>]	94	2.65E-57	201
Cjn_gene1272	QTSNFD	VDO38379.1	unnamed protein product [<i>Brugia timori</i>]	88.889	3.46E-29	110
Cjn_gene1872	QQSNRD	VDN94265.1	unnamed protein product [<i>Brugia pahangi</i>]	93.684	3.78E-52	185
Cjn_gene2060	QVSNYD	XP_020306002.1	hypothetical protein LOAG_17679 [<i>Loa loa</i>]	73	1.96E-39	147
Cjn_gene2092	QCSNLD	VDN82747.1	unnamed protein product [<i>Brugia pahangi</i>]	90.909	1.3E-45	158
Cjn_gene2177	QSSNSD	VDK81681.1	unnamed protein product [<i>Onchocerca ochengi</i>]	54.455	1.23E-17	87.4
Cjn_gene2237	QSSNID	VDK61671.1	unnamed protein product [<i>Onchocerca ochengi</i>]	95.604	4.21E-53	179
Cjn_gene2285	QLSNID	VBB27065.1	unnamed protein product [<i>Acanthocheilonema viteae</i>]	56	3.4E-14	77.8
Cjn_gene2338	QDSNED	No secondary hit				

Cjn_gene2504	QRSNDD	EJW82344.1	hypothetical protein WUBG_06743 [<i>Wuchereria bancrofti</i>]	79.798	1.96E-42	147
Cjn_gene2830	QRSNLD	VDK73675.1	unnamed protein product [<i>Litomosoides sigmodontis</i>]	85.106	8.87E-48	169
Cjn_gene3336	QNSNND	VIO94178.1	Uncharacterized protein BM_BM2531 [<i>Brugia malayi</i>]	87.755	6.83E-47	171
Cjn_gene3426	QHSNED	VDK89519.1	unnamed protein product [<i>Onchocerca ochengi</i>]	82	1.96E-48	171
Cjn_gene3912	QQSNDD	XP_003148455.1	hypothetical protein LOAG_12895 [<i>Loa loa</i>]	85	2.22E-55	181
Cjn_gene4366	QSNWD	VBB32097.1	unnamed protein product [<i>Acanthocheilonema viteae</i>]	89	1.11E-49	179
Cjn_gene4382	QSSNKD	VBB26355.1	unnamed protein product [<i>Acanthocheilonema viteae</i>]	92	4.65E-54	191
Cjn_gene4529	QISNID	VDO27644.1	unnamed protein product [<i>Brugia timori</i>]	89	7.07E-58	194
Cjn_gene4783	QMSNED	VDK84344.1	unnamed protein product [<i>Litomosoides sigmodontis</i>]	97	1.19E-61	212
Cjn_gene4935	QISNED	EJW82782.1	mitochondrial chaperone BCS1 [<i>Wuchereria bancrofti</i>]	90	1.4E-46	164
Cjn_gene5157	QKSNKD	XP_020305667.1	vacuolar protein sorting-associated protein 45 [<i>Loa loa</i>]	92	3.48E-57	194
Cjn_gene5767	QASNSD	VDO23327.1	unnamed protein product [<i>Brugia timori</i>]	64.835	2.81E-31	119
Cjn_gene5823	QPSNTD	VDO13125.1	unnamed protein product [<i>Brugia timori</i>]	75.676	2.17E-28	108
Cjn_gene6256	QLSNVD	VDM08285.1	unnamed protein product [<i>Wuchereria bancrofti</i>]	75	1.72E-46	166
Cjn_gene6471	QNSNQD	VDK70153.1	unnamed protein product [<i>Litomosoides sigmodontis</i>]	78.218	2.63E-33	129
Cjn_gene6608	QYSNND	VBB31882.1	BMA-ABU-10 [<i>Brugia malayi</i>]	40.698	0.000019	52.8

Cjn_gene6761	QLSNED	CRZ26398.1	Bm4129 [<i>Brugia malayi</i>]	87.179	9.08E-14	73.6
Cjn_gene7385	QFSNDD	VDK82515.1	unnamed protein product [<i>Litomosoides sigmodontis</i>]	88	1.6E-55	191
Cjn_gene7401	QDSNVD	VDK82534.1	unnamed protein product [<i>Onchocerca ochengi</i>]	94	6.42E-56	178
Cjn_gene7670	QISNQD	VDN87187.1	unnamed protein product [<i>Brugia pahangi</i>]	51.724	0.000000964	53.5
Cjn_gene7777	QISNSD	VDK84566.1	unnamed protein product [<i>Litomosoides sigmodontis</i>]	79	1.7E-45	161
Cjn_gene7945	QLSNDD	CTP81083.1	BMA-TAG-343, isoform a [<i>Brugia malayi</i>]	48.507	4.18E-27	114
Cjn_gene8122	QRSNND	VDP18010.1	unnamed protein product [<i>Onchocerca flexuosa</i>]	82.828	3.51E-47	169
Cjn_gene8203	QISNTD	XP_001896789.1	CG18437-PA [<i>Brugia malayi</i>]	88.235	3.04E-47	170
Cjn_gene8213	QISNND	XP_020302306.1	ARCN1 protein [<i>Loa loa</i>]	91	1.5E-54	187
Cjn_gene8516	QTSNID	VDO17479.1	unnamed protein product [<i>Brugia timori</i>]	88.889	7.14E-58	187
Cjn_gene8580	QGSNHD	XP_020306733.1	CBR-IFT-81 protein [<i>Loa loa</i>]	74	7.38E-40	148
Cjn_gene8849	QRSND	VDN95123.1	unnamed protein product [<i>Brugia pahangi</i>]	67.227	2.05E-40	152
Cjn_gene8879	QSSNYD	OZC08150.1	GRIP domain protein [<i>Onchocerca flexuosa</i>]	65.714	7.17E-29	117
Cjn_gene8897	QESNDD	EJW79009.1	hypothetical protein WUBG_10081 [<i>Wuchereria bancrofti</i>]	79	5.65E-46	159
Cjn_gene9527	QNSNKD	XP_001896789.1	ecotropic viral integration site [<i>Loa loa</i>]	77.528	7.93E-33	129
Cjn_gene10102	QKSNDD	No secondary hit				

Table 4.7: The *Cercopithifilaria johnstoni* proteins examined for the presence of the *Onchocerca volvulus* epitope QQQQQQQQR from Lagatie et al. (2018). The *Cercopithifilaria johnstoni* protein secondary BLAST hit and putative function is reported with % identity, e-value and bits (bit score).

<i>C. johnstoni</i> protein	Secondary blast hit	Description (NCBI)	% identity	e-value	bits
Cjn_gene194	VDM12548.1	unnamed protein product [<i>Wuchereria bancrofti</i>]	70.909	2.82E-10	66.2
Cjn_gene2327	VDK84942.1	unnamed protein product [<i>Onchocerca ochengi</i>]	56.701	5.98E-17	83.6
Cjn_gene2766	VDN93536.1	unnamed protein product [<i>Brugia pahangi</i>]	57.843	6.06E-10	65.1
Cjn_gene2772	VDK73698.1	unnamed protein product [<i>Onchocerca ochengi</i>]	56	1.01E-17	87.8
Cjn_gene5035	No secondary hit				
Cjn_gene5350	XP_001901916.1	Tudor domain containing protein [<i>Brugia malayi</i>]	70.33	1.01E-33	133
Cjn_gene5989	VDN93709.1	unnamed protein product [<i>Brugia pahangi</i>]	70.588	1.27E-30	123
Cjn_gene6920	OZC10437.1	hypothetical protein X798_02480 [<i>Onchocerca flexuosa</i>]	63	3.5E-11	69.3
Cjn_gene7343	VDM06821.1	unnamed protein product [<i>Wuchereria bancrofti</i>]	53.061	1.87E-20	95.5
Cjn_gene7486	No secondary hit				
Cjn_gene8464	CDP93819.1	Bm9402 [<i>Brugia malayi</i>]	75	6.48E-33	122
Cjn_gene8597	No secondary hit				

Appendix 4: Chapter Five Supplementary Material

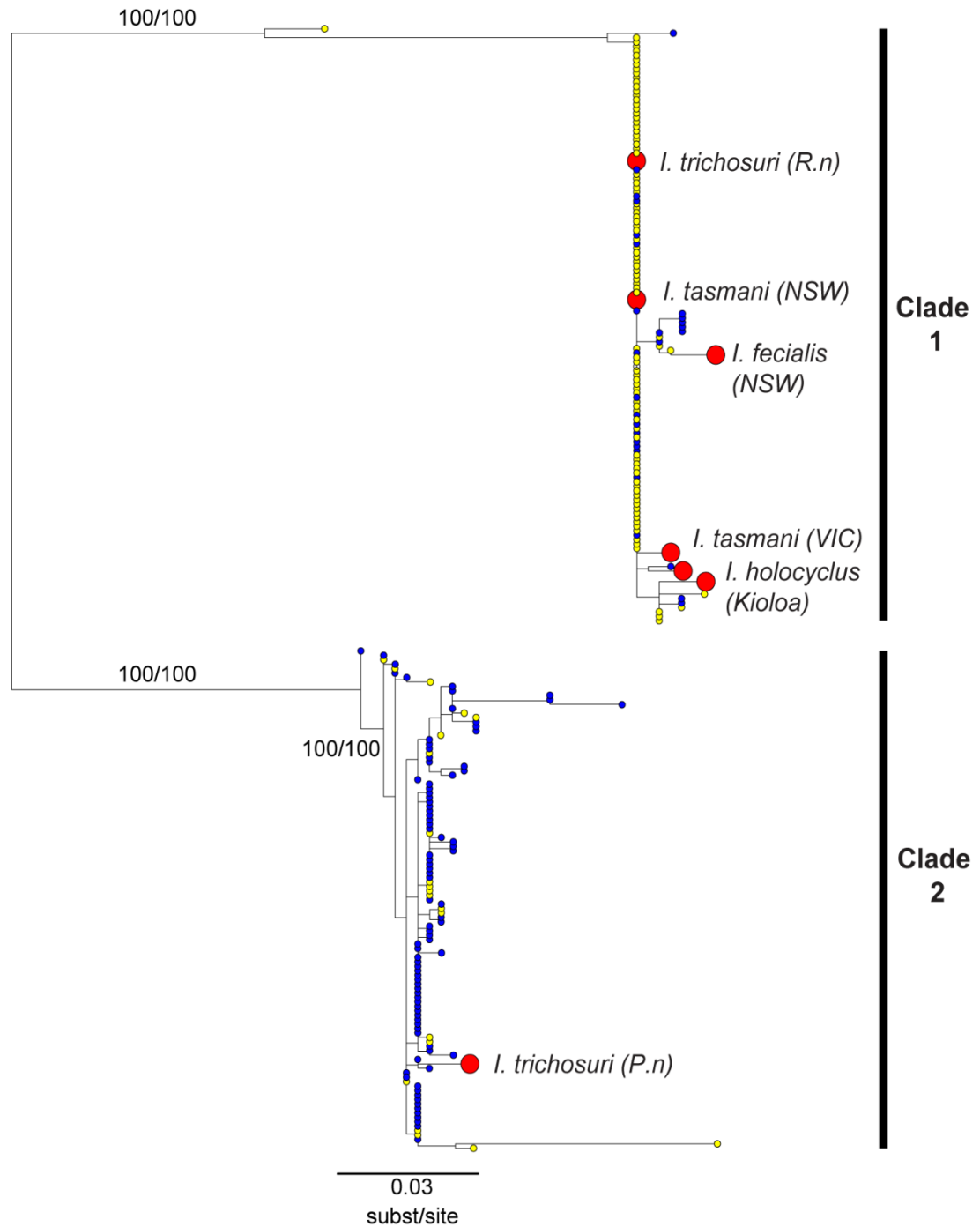


Fig 4. Maximum likelihood estimate based on the amplicon 12S of ticks collected at Kioloa and Mogo State Forest, NSW, Australia. Blue = Mogo State Forest (rats), yellow = Kioloa (flagging), red = identified voucher specimens.

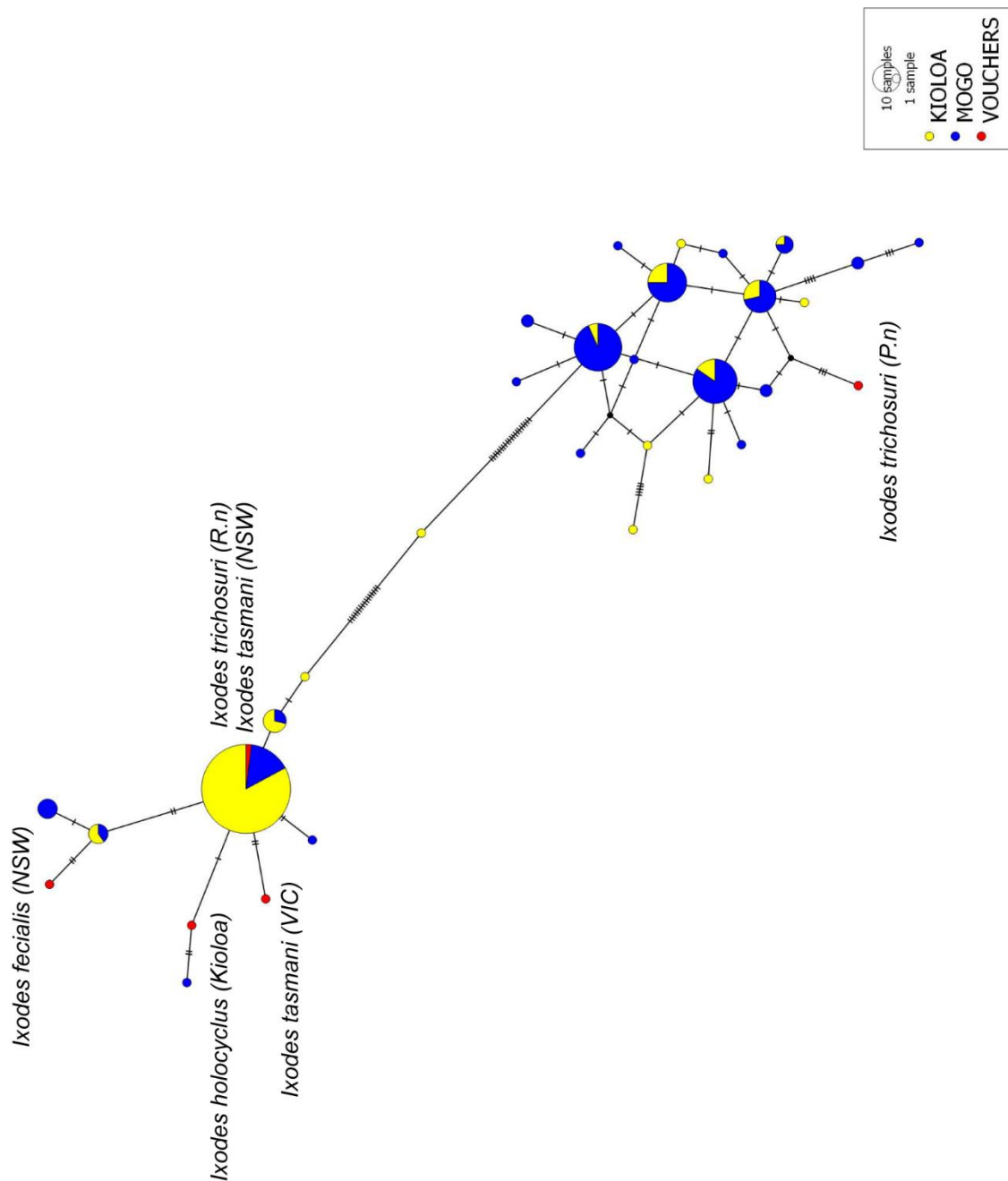


Fig. 5. TCS haplotype network based on the amplicon 12S sequenced from ticks collected from Kioloa and Mogo State Forest in NSW, Australia. Samples are coloured coded based on their collection site, Mogo State Forest (blue) or, Kioloa (yellow). Voucher specimens are coloured red.

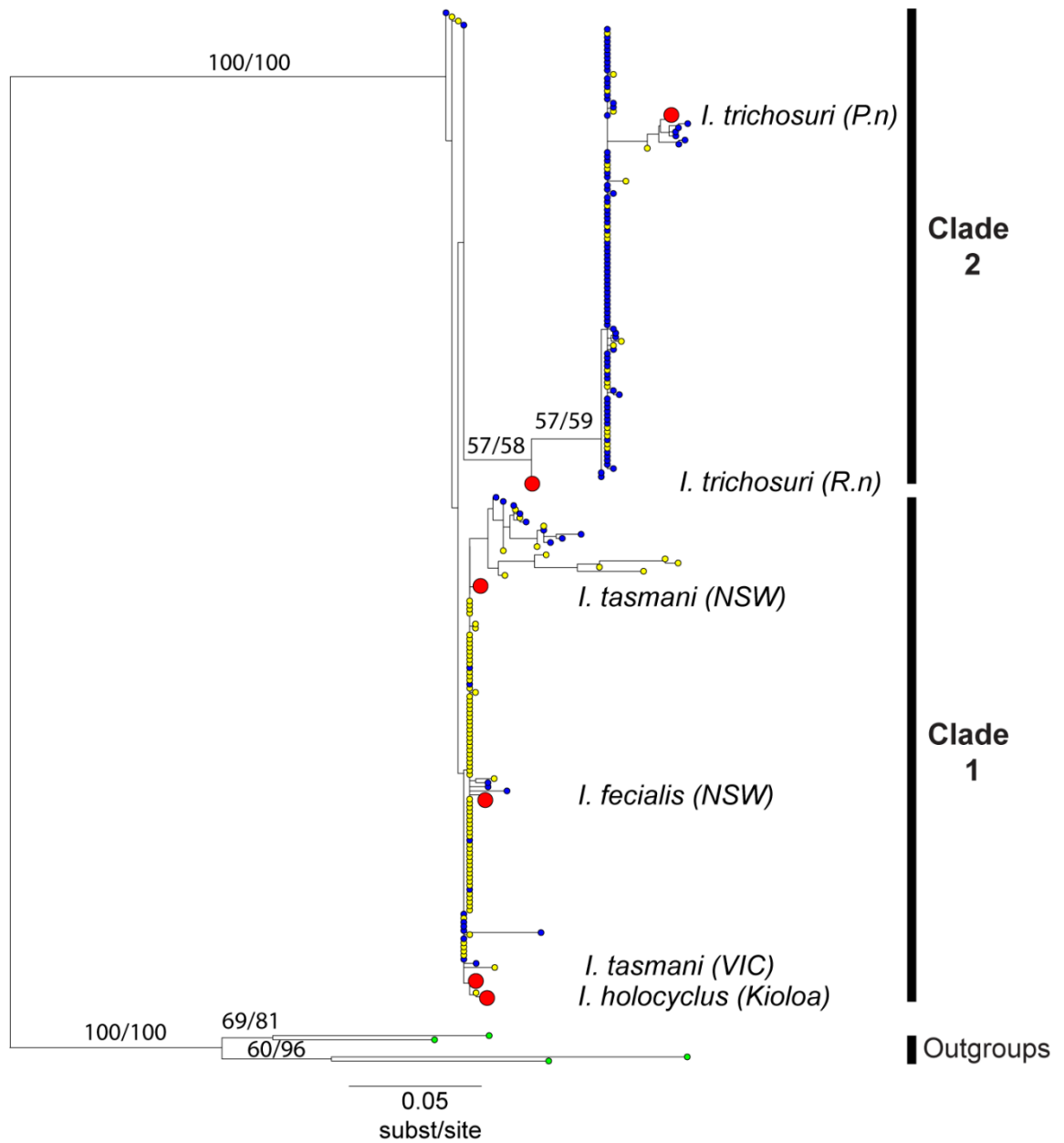


Fig. 6. Maximum likelihood estimate based on the amplicon 16S of ticks collected at Kioloa and Mogo State Forest, NSW, Australia. Blue = Mogo State Forest (rats), yellow = Kioloa (flagging), red = identified voucher specimens.

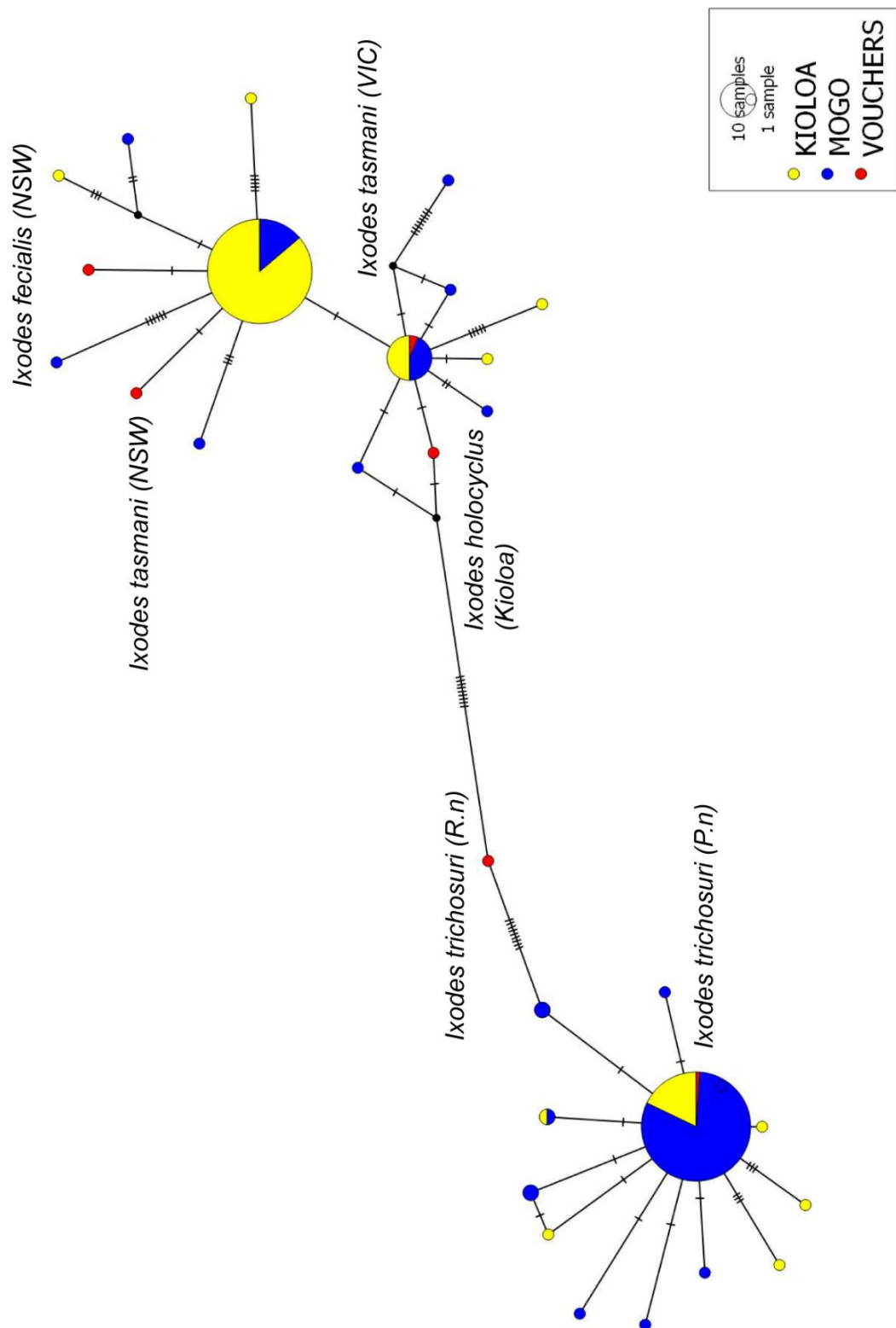


Fig. 7. TCS haplotype network based on the amplicon 16S sequenced from ticks collected from Kioloa and Mogo State Forest in NSW, Australia. Samples are coloured coded based on their collection site, Mogo State Forest (blue) or, Kioloa (yellow). Voucher specimens are coloured red.

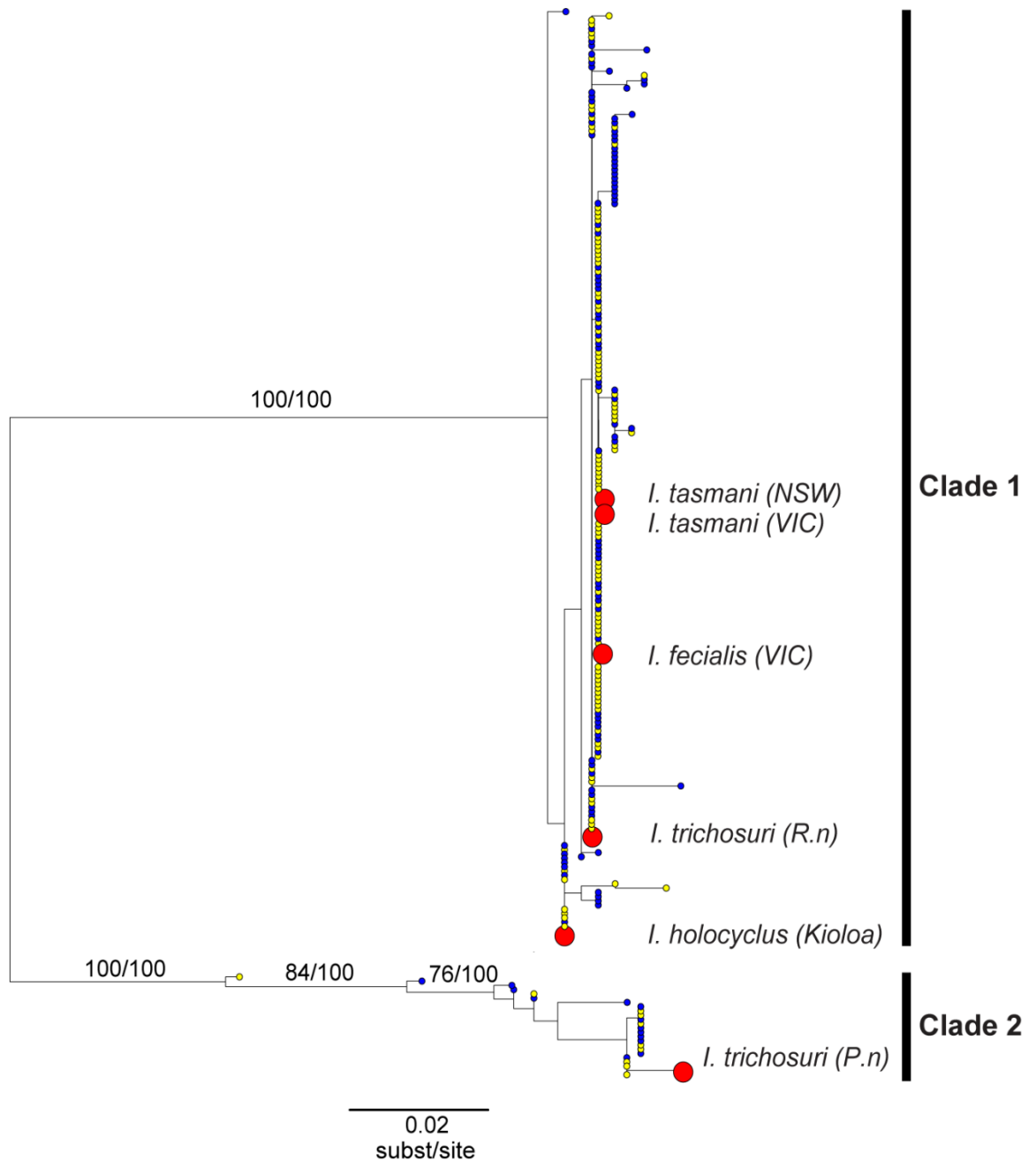


Fig. 8. Maximum likelihood estimate based on the amplicon ITS2 of ticks collected at Kioloa and Mogo State Forest, NSW, Australia. Blue = Mogo State Forest (rats), yellow = Kioloa (flagging), red = identified voucher specimens.

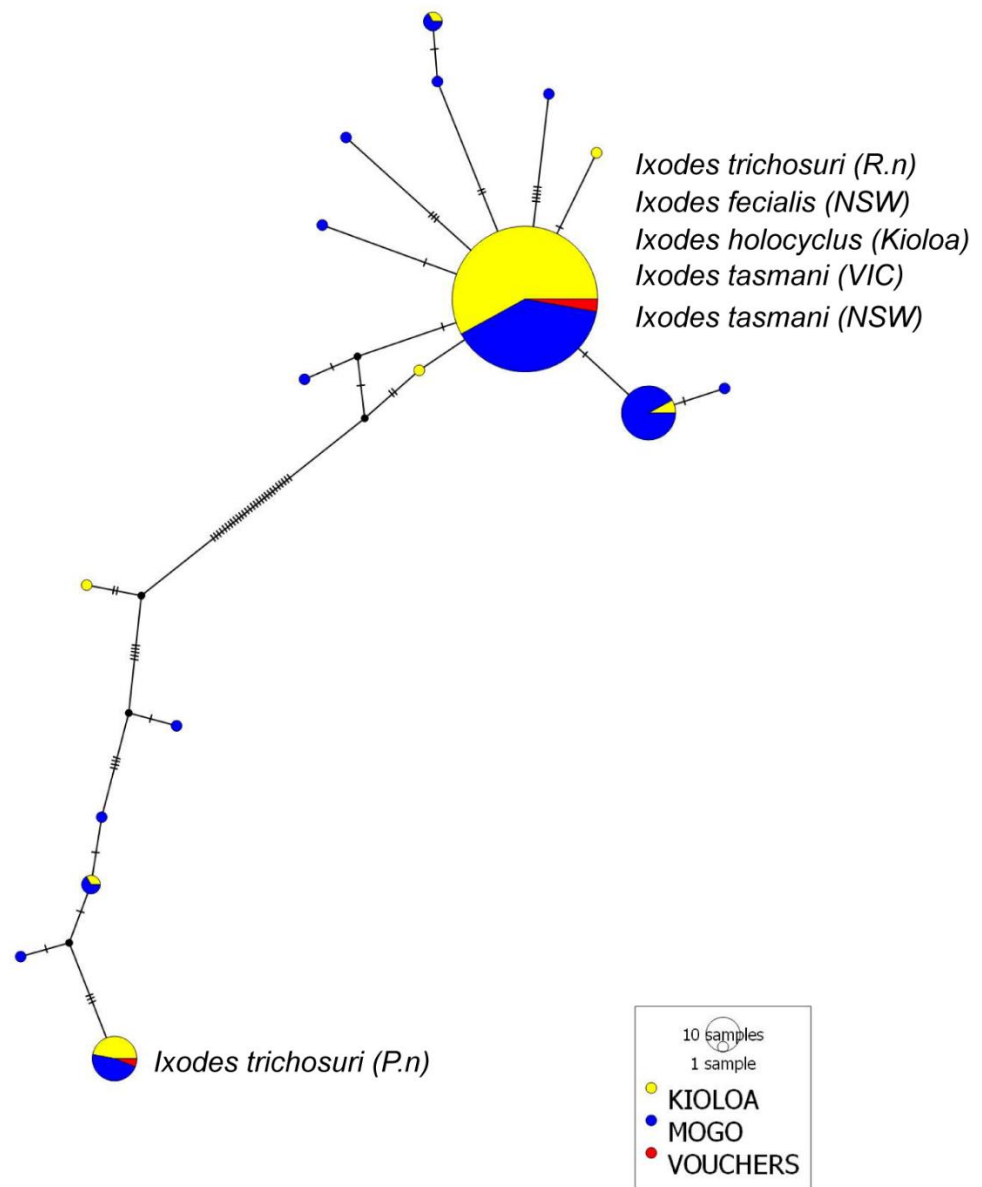
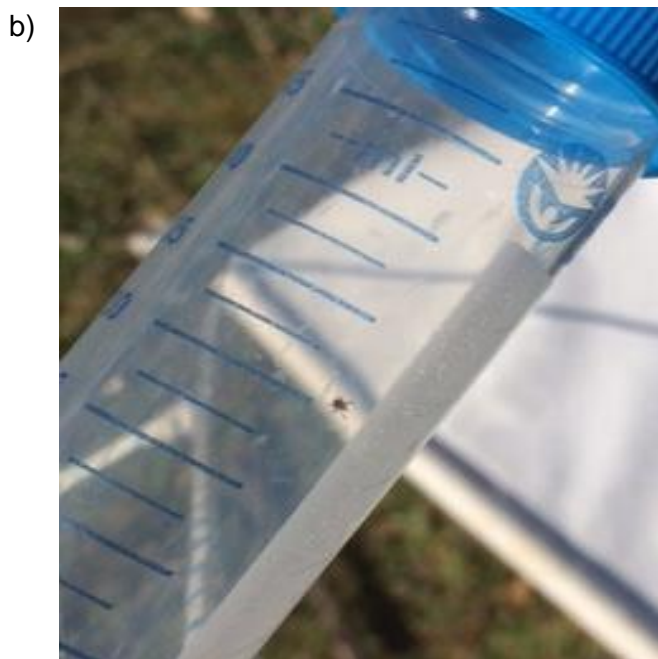


Fig. 9. TCS haplotype network based on the amplicon ITS2 sequenced from ticks collected from Kioloa and Mogo State Forest in NSW, Australia. Samples are coloured coded based on their collection site, Mogo State Forest (blue) or, Kioloa (yellow). Voucher specimens are coloured red.

Appendix 5: Chapter Six Supplementary Material



Supplementary Figure 6.1: (a) White fabric flag used for flagging in the field.
(b) Tick collected from the flag and placed in falcon tube. Photos by Kirsty McCann.



Supplementary Figure 6.2: (a) Closed tube with small hole used for bush rat tick attachment. (b) Rat housing in tub with tray used throughout the tick attachment experiments. Photos by Kirsty McCann.

Supplementary Table 6.1: Summary of tick collections from flagging field trips 2015.

Location	Sub-locations	Sampling type	Month of collection	Life stage and number of ticks		
				Larvae	Nymphs	Adults
Mogo	a-b transect	Rat collection	February	68	20	0
			April	135	3	0
		Flagging	-	0	0	0
	c-d transect	Rat collection	February	75	33	0
			April	65	12	0
		Flagging	-	0	0	0
Kioloa	Dunes	Rat collection	-	0	0	0
		Flagging	April	98	13	1
			June	22	0	0
	ANU campus	Rat collection	-	0	0	0
		Flagging	April	453	9	0
			June	60	12	1

Supplementary Table 6.2: Summary of tick collections from flagging field trips 2016.

Flagging Field Trip #1			
Start date	15.3.16	End Date	18.3.16
Site	Kioloa	Mogo	
Life stage	Nymph	Larvae	Adults
Approx. number collected	>200	>300	~10
Flagging Field Trip #2			
Start date	31.10.16	End Date	3.11.16
Site	Kioloa		Mogo
Life stage	Nymphs	Adults	Adults Paralysis ticks
Approx. number collected	>100	40	6
Flagging Field Trip #3			
Start date	27.11.16	End Date	29.11.16
Site	Kioloa		
Life stage	Adults	Nymphs	
Approx. number collected	>150	>200	

a)



b)



Supplementary Figure 6.3: (a) Identification of adult female and adult male *Ixodes holocyclus* ticks. Lighter coloured middle legs differentiate the species from other ticks. The larger tick is the female. (b) Adult male and female *Ixodes holocyclus* ticks in scintillation tube before mating. Photos by Kirsty McCann.

References

- Abraham, D., Leon, O., Leon, S., and Lustigman, S. (2001). Development of a recombinant antigen vaccine against infection with the filarial worm *Onchocerca volvulus*. *Infect. Immun.* 69, 262-270.
- Abraham, D., Leon, O., Schnyder-Candrian, S., Wang, C.C., Galioto, A.M., Kerepesi, L.A., Lee, J.J., and Lustigman, S. (2004). Immunoglobulin E and eosinophil-dependent protective immunity to larval *Onchocerca volvulus* in mice immunized with irradiated larvae. *Infect. Immun.* 72, 810-817.
- Abraham, D., Lucius, R., and Trees, A.J. (2002). Immunity to *Onchocerca spp.* in animal hosts. *Trends Parasitol.* 18, 164-171.
- Adler, P.H., Cheke, R.A., and Post, R.J. (2010). Evolution, epidemiology, and population genetics of black flies (Diptera: Simuliidae). *Infect. Genet. Evol.* 10, 846-865.
- Allen, J.E., Adjei, O., Bain, O., Hoerauf, A., Hoffmann, W.H., Makepeace, B.L., Schulz-Key, H., Tanya, V.N., Trees, A.J., Wanji, S., *et al.* (2008). Of Mice, Cattle, and Humans: The immunology and treatment of river blindness. *PLoS Negl. Trop. Dis.* 2, e217.
- Amazigo, U., Noma, M., Bump, J., Benton, B., Liese, B., Yaméogo, L., Zouré, H., and Seketeli, A. (2006). Onchocerciasis. In *Disease and mortality in Sub-Saharan Africa*, 2nd ed. (Washington DC: World Bank), pp. 215-222.
- Amazigo, U. (2008). The African Programme for Onchocerciasis Control (APOC). *Ann. Trop. Med. Parasitol.* 102.
- Anderson, J.M., Ammerman, N.C., and Norris, D.E. (2004). Molecular differentiation of metastriate tick immatures. *Vector Borne Zoonotic Dis.* 4, 334-342.

Anderson, R.C. (2001). Filarioid Nematodes. In Parasitic Diseases of Wild Mammals, pp. 342-356.

Andrews, R.H., Chilton, N.B., Beveridge, I., Spratt, D., and Mayrhofer, G. (1992). Genetic markers for the identification of three Australian tick species at various stages in their life cycles. J. Parasitol., 366-368.

Anish, R., Latha, B.R., Ramanathan, G., Sivagnanam, U.T., Sreekumar, C., and Leela, V. (2017). A novel assembly pheromone trap for tick control in dog kennels. Vet. Parasitol., 235, 57-63.

Anisimova, M., Bielawski, J.P., and Yang, Z. (2001). Accuracy and power of the likelihood ratio test in detecting adaptive molecular evolution. Mol. Biol. Evol. 18, 1585-1592.

Avise, J.C., Arnold, J., Ball, R.M., Bermingham, E., Lamb, T., Neigel, J.E., Reeb, C.A., and Saunders, N.C. (1987). Intraspecific phylogeography: the mitochondrial DNA bridge between population genetics and systematics. Annu. Rev. Ecol. Evol. Syst. 18, 489-522.

Awadzi, K., Boakye, D., Edwards, G., Opoku, N., Attah, S., Osei-Atweneboana, M., Lazdins-Helds, J., Ardrey, A., Addy, E., and Quartey, B. (2004). An investigation of persistent microfilaridermias despite multiple treatments with ivermectin, in two onchocerciasis-endemic foci in Ghana. Ann. Trop. Med. Parasitol. 98, 231-249.

Awadzi, K., Dadzie, K., Shulz-Key, H., Haddock, D., Gilles, H., and Aziz, M. (1985). The chemotherapy of onchocerciasis X. An assessment of four single dose treatment regimes of MK-933 (ivermectin) in human onchocerciasis. Ann. Trop. Med. Parasitol. 79, 63-78.

Awadzi, K., Opoku, N.O., Attah, S.K., Lazdins-Helds, J., and Kuesel, A.C. (2014). A randomized, single-ascending-dose, ivermectin-controlled, double-blind study of moxidectin in *Onchocerca volvulus* infection. PLoS Negl. Trop. Dis. 8, e2953.

- Bagai, R., and Subrahmanyam, D. (1968). Studies on the host-parasite relation in albino rats infected with *Litomosoides carinii*. *Am. J. Trop. Med. Hyg.* 17, 833-839.
- Bain, O. (2002). Evolutionary relationships among filarial nematodes. In *The Filaria World Class Parasites* (Springer, Boston, MA), pp. 21-29.
- Bain, O., Casiraghi, M., Martin, C., and Uni, S. (2008). The Nematoda Filarioidea: critical analysis linking molecular and traditional approaches. *Parasite* 15, 342-348.
- Baker, M. (2012). De novo genome assembly: what every biologist should know. *Nat. Methods* 9, 333-337.
- Bandi, C., Anderson, T.J., Genchi, C., and Blaxter, M.L. (1998). Phylogeny of *Wolbachia* in filarial nematodes. *Proc. R. Soc. Lon. Biol.* 265, 2407-2413.
- Bandi, C., Trees, A.J., and Brattig, N.W. (2001). *Wolbachia* in filarial nematodes: evolutionary aspects and implications for the pathogenesis and treatment of filarial diseases. *Vet. Parasitol.* 98, 215-238.
- Barker, S.C., and Murrell, A. (2004). Systematics and evolution of ticks with a list of valid genus and species names. *Parasitol.* 129, S15-S36.
- Barker, S.C., and Walker, A.R. (2014). Ticks of Australia. The species that infest domestic animals and humans. *Zootaxa* 3816, 1-144.
- Barker, S.C., Walker, A.R., and Campelo, D. (2014). A list of the 70 species of Australian ticks; diagnostic guides to and species accounts of *Ixodes holocyclus* (paralysis tick), *Ixodes cornuatus* (southern paralysis tick) and *Rhipicephalus australis* (Australian cattle tick); and consideration of the place of Australia in the evolution of ticks with comments on four controversial ideas. *Int. J. Parasitol.* 44, 941-953.

Barry, M.A., Murray, K.O., Hotez, P.J., and Jones, K.M. (2016). Impact of vector borne parasitic neglected tropical diseases on child health. *Arch. Dis. Child.* 101, 640.

Basáñez, M.G., Boussinesq, M., Prod'hon, J., Frontado, H., Villamizar, N.J., Medley, G.F., and Anderson, R.M. (1994). Density-dependent processes in the transmission of human onchocerciasis: intensity of microfilariae in the skin and their uptake by the simuliid host. *Parasitol.* 108, 115-127.

Basáñez, M.G., Pion, S.D., Boakes, E., Filipe, J.A., Churcher, T.S., and Boussinesq, M. (2008). Effect of single-dose ivermectin on *Onchocerca volvulus*: a systematic review and meta-analysis. *Lancet. Infect. Dis.* 8.

Basáñez, M.G., Walker, M., Turner, H.C., Coffeng, L.E., de Vlas, S.J., and Stolk, W.A. (2016). Chapter Five - River Blindness: Mathematical Models for Control and Elimination. *Adv. Parasitol.*, M.G. Basáñez, and R.M. Anderson, eds. (Academic Press), pp. 247-341.

Beati, L., and Klompen, H. (2019). Phylogeography of ticks (Acari: Ixodida). *Annu. Rev. Entomol.* 64, 379-397.

Beaver, P., Orihel, T., and Johnson, M.H. (1974). *Dipetalonema viteae* in the experimentally infected jird, *Meriones unguiculatus*. II. Microfilaremia in relation to worm burden. *J. Parasitol.*, 310-315.

Bellgard, M.I., Moolhuijzen, P.M., Guerrero, F.D., Schibeci, D., Rodriguez-Valle, M., Peterson, D.G., Dowd, S.E., Barrero, R., Hunter, A., Miller, R.J., *et al.* (2012). CattleTickBase: An integrated Internet-based bioinformatics resource for *Rhipicephalus (Boophilus) microplus*. *Int. J. Parasitol.* 42, 161-169.

Bennuru, S., Cotton, J.A., Ribeiro, J.M., Grote, A., Harsha, B., Holroyd, N., Mhashilkar, A., Molina, D.M., Randall, A.Z., and Shandling, A.D. (2016). Stage-specific transcriptome and proteome analyses of the filarial parasite *Onchocerca volvulus* and its *Wolbachia* endosymbiont. *mBio.* 7, e02028-02016.

- Bennuru, S., Lustigman, S., Abraham, D., and Nutman, T.B. (2017). Metabolite profiling of infection-associated metabolic markers of onchocerciasis. *Mol. Biochem. Parasitol.* 215, 58-69.
- Bennuru, S., Meng, Z., Ribeiro, J.M., Semnani, R.T., Ghedin, E., Chan, K., Lucas, D.A., Veenstra, T.D., and Nutman, T.B. (2011). Stage-specific proteomic expression patterns of the human filarial parasite *Brugia malayi* and its endosymbiont *Wolbachia*. *Proc. Natl. Acad. Sci.* 108, 9649-9654.
- Bennuru, S., O'Connell, E.M., Drame, P.M., and Nutman, T.B. (2018). Mining filarial genomes for diagnostic and therapeutic targets. *Trends Parasitol.* 34, 80-90.
- Bennuru, S., Oduro-Boateng, G., Osigwe, C., Del-Valle, P., Golden, A., Ogawa, G.M., Cama, V., Lustigman, S., and Nutman, T.B. (2019). Integrating multiple biomarkers to increase sensitivity for the detection of *Onchocerca volvulus* infection. *J. Infect. Dis.* 221, 1805-1815. doi:10.1093/infdis/jiz307.
- Bergsten, J. (2005). A review of long-branch attraction. *Cladistic*, 21, 163-193.
- Bernt, M., Donath, A., Jühling, F., Externbrink, F., Florentz, C., Fritzsche, G., Pütz, J., Middendorf, M., and Stadler, P.F. (2013). MITOS: Improved de novo metazoan mitochondrial genome annotation. *Mol. Phylogenet. Evol.* 69, 313-319.
- Bethony, J., Brooker, S., Albonico, M., Geiger, S.M., Loukas, A., Diemert, D., and Hotez, P.J. (2006). Soil-transmitted helminth infections: Ascariasis, Trichuriasis, and hookworm. *Lancet.* 367, 1521-1532.
- Binnington, K., and Stone, B. (1981). Developmental changes in morphology and toxin content of the salivary gland of the Australian paralysis tick *Ixodes holocyclus*. *Int. J. Parasitol.* 11, 343-351.
- Black, W., Klompen, J.S.H., and Keirans, J.E. (1997). Phylogenetic relationships among tick subfamilies (Ixodida: Ixodidae: Argasidae) based on the 18S nuclear rDNA gene. *Mol. Phylogenet. Evol.* 7, 129-144.

Blaxter, M., and Bird, D. (1997). Parasitic nematodes. In *C elegans* II, Riddle DL, Meyer BJ, et al., ed. (Cold Spring Harbor (NY): Cold Spring Harbor Laboratory Press).

Blaxter, M., De Ley, P., Garey, J., Liu, L., Scheldeman, P., Vierstraete, A., Vanfleteren, J., Mackey, L., Dorris, M., and Frisse, L. (1998). A molecular evolutionary framework for the Phylum Nematoda. *Nature*. 392, 71 - 75.

Blaxter, M., and Koutsovoulos, G. (2015). The evolution of parasitism in Nematoda. *Parasitol*. 142, S26-S39.

Blaxter, M., Kumar, S., Kaur, G., Koutsovoulos, G., and Elsworth, B. (2012). Genomics and transcriptomics across the diversity of the Nematoda. *Parasite. Immunol*. 34, 108-120.

Blees, A., Janulienė, D., Hofmann, T., Koller, N., Schmidt, C., Trowitzsch, S., Moeller, A., and Tampé, R. (2017). Structure of the human MHC-I peptide-loading complex. *Nature*. 551, 525.

Boatin, B. (2008). The Onchocerciasis Control Programme in West Africa (OCP). *Ann. Trop. Med. Parasitol*. 102.

Boatin, B.A., and Richards, F.O. (2006). Control of onchocerciasis. In *Adv. Parasitol.*, D.H. Molyneux, ed. (Academic Press), pp. 349-394.

Bockarie, M.J., Kelly-Hope, L.A., Rebollo, M., and Molyneux, D.H. (2013). Preventive chemotherapy as a strategy for elimination of neglected tropical parasitic diseases: endgame challenges. *Philos. T. R. Soc. B*. 368, 20120144.

Bolger, A.M., Lohse, M., and Usadel, B. (2014). Trimmomatic: a flexible trimmer for Illumina sequence data. *J. Bioinform*. 30, 2114-2120.

Bonnet, S., Jouglin, M., Malandrin, L., Becker, C., Agoulon, A., L'Hostis, M., and Chauvin, A. (2006). Transstadial and transovarial persistence of *Babesia*

divergens DNA in *Ixodes ricinus* ticks fed on infected blood in a new skin-feeding technique. Parasitol. 134, 197-207.

Bonnet, S., and Liu, X.Y. (2012). Laboratory artificial infection of hard ticks: a tool for the analysis of tick-borne pathogen transmission. Acarologia. 52, 453-464.

Bourguinat, C., Pion, S.D.S., Kamgno, J., Gardon, J., Gardon-Wendel, N., Duke, B.O.L., Prichard, R.K., and Boussinesq, M. (2006). Genetic polymorphism of the β -tubulin gene of *Onchocerca volvulus* in ivermectin naïve patients from Cameroon, and its relationship with fertility of the worms. Int. J. Parasitol. 132, 255-262.

Boussinesq, M. (2006). Loiasis. Ann. Trop. Med. Parasitol. 100, 715-731.

Brady, M.A., Hooper, P.J., and Ottesen, E.A. (2006). Projected benefits from integrating NTD programs in sub-Saharan Africa. Trends Parasitol. 22, 285-291.

Brattig, N.W. (2004). Pathogenesis and host responses in human onchocerciasis: impact of *Onchocerca filariae* and *Wolbachia* endobacteria. Microbes. Infect. 6.

Brossard, M., and Wikel, S. (2004). Tick immunobiology. Parasitol. 129, S161-S176.

Brown, W.M., George, M., and Wilson, A.C. (1979). Rapid evolution of animal mitochondrial DNA. Proc. Natl. Acad. Sci. 76, 1967.

Budke, C.M., Jiamin, Q., Qian, W., and Torgerson, P.R. (2005). Economic effects of echinococcosis in a disease-endemic region of the Tibetan plateau. Am. J. Trop. Med. Hyg. 73, 2-10.

Burgdorfer, W. (1984). The New Zealand white rabbit: an experimental host for infecting ticks with Lyme disease spirochetes. Yale. J. Biol. Med. 57, 609.

Burgdorfer, W., Barbour, A.G., Hayes, S.F., Benach, J.L., Grunwaldt, E., and Davis, J.P. (1982). Lyme disease-a tick-borne spirochetosis? *Science*. 216, 1317-1319.

Burnard, D., and Shao, R. (2019). Mitochondrial genome analysis reveals intraspecific variation within Australian hard tick species. *Ticks Tick-Borne Dis.* 10, 677-681.

Butler, J., and Hogsette, J. (1998). Black Flies, *Simulium spp.*(Insecta: Diptera: Simuliidae).

Campbell, W.C. (1981). An introduction to the avermectins. *NZ Vet. J.* 29, 174-178.

Capelli, G., Genchi, C., Baneth, G., Bourdeau, P., Brianti, E., Cardoso, L., Danesi, P., Fuehrer, H.-P., Giannelli, A., Ionică, A.M., et al. (2018). Recent advances on *Dirofilaria repens* in dogs and humans in Europe. *Parasite. Vector.* 11, 663.

Caporale, D.A., Rich, S.M., Spielman, A., Telford, S.R., and Kocher, T.D. (1995). Discriminating between *Ixodes* ticks by means of mitochondrial DNA sequences. *Mol. Phylogenet. Evol.* 4, 361-365.

Casiraghi, M., Anderson, T., Bandi, C., Bazzocchi, C., and Genchi, C. (2001). A phylogenetic analysis of filarial nematodes: comparison with the phylogeny of *Wolbachia endosymbionts*. *Parasitol.* 122, 93-103.

Casiraghi, M., Bain, O., Guerrero, R., Martin, C., Pocacqua, V., Gardner, S.L., Franceschi, A., and Bandi, C. (2004). Mapping the presence of *Wolbachia pipientis* on the phylogeny of filarial nematodes: evidence for symbiont loss during evolution. *Int. J. Parasitol.* 34, 191-203.

Centers for Disease Control and Prevention (2013). Progress toward elimination of onchocerciasis in the Americas-1993-2012. *MMWR Morbidity and mortality weekly report* 62, 405.

Centers for Disease Control and Prevention (2015). Onchocerciasis - Biology. April, May 21, 2013. <https://www.cdc.gov/parasites/onchocerciasis/biology.html#>

Chakravarti, B., Lass, J.H., Bardenstein, D.S., Diaconu, E., Roy, C.E., Herring, T.A., Chakravarti, D.N., and Greene, B.M. (1993). Immune-mediated *Onchocerca volvulus* sclerosing keratitis in the mouse. *Exp. Eye. Res.* 57, 21-27.

Chandy, A., Thakur, A.S., Singh, M.P., and Manigauha, A. (2011). A review of neglected tropical diseases: filariasis. *Asian. Pac. J. Trop. Med.* 4, 581-586.

Chang, S.C., Bajaj, S., and Chandy, K. (2018). ShK toxin: history, structure and therapeutic applications for autoimmune diseases. *J. Science.* 1, 1.

Cheke, R.A., and Garms, R. (2013). Indices of onchocerciasis transmission by different members of the *Simulium damnosum* complex conflict with the paradigm of forest and savanna parasite strains. *Acta. Trop.* 125, 43-52.

Chhabra, S., Chang, S.C., Nguyen, H.M., Huq, R., Tanner, M.R., Londono, L.M., Estrada, R., Dhawan, V., Chauhan, S., Upadhyay, S.K., et al. (2014). Kv1.3 channel-blocking immunomodulatory peptides from parasitic worms: implications for autoimmune diseases. *J. FASEB.* 28, 3952-3964.

Chilton, N.B. (1992). An index to assess the reproductive fitness of female ticks. *Int. J. Parasitol.* 22, 109-111.

Choi, Y.-J., Tyagi, R., McNulty, S.N., Rosa, B.A., Ozersky, P., Mafrtin, J., Hallsworth-Pepin, K., Unnasch, T.R., Norice, C.T., Nutman, T.B., et al. (2016). Genomic diversity in *Onchocerca volvulus* and its *Wolbachia* endosymbiont. *Nat. Microbiol.* 2, 16207-16207.

Choudhuri, S. (2014). Chapter 7 - Additional bioinformatic analyses involving nucleic-acid sequences. In *Bioinformatics for Beginners*, S. Choudhuri, ed. (Oxford: Academic Press), pp. 157-181.

Clifford, C.M., Sonenshine, D.E., Keirans, J.E., and Kohls, G.M. (1973).

Systematics of the subfamily Ixodinae (Acarina: Ixodidae). The subgenera of *Ixodes*. Ann. Entomol. Soc. Am. 66, 489-500.

Coffeng, L.E., Stolk, W.A., Zouré, H.G.M., Veerman, J.L., Agblewonu, K.B., Murdoch, M.E., Noma, M., Fobi, G., Richardus, J.H., Bundy, D.A.P., et al. (2013). African Programme for Onchocerciasis Control 1995–2015: Model-estimated health impact and cost. PLoS Negl. Trop. Dis. 7, e2032.

Coghlan, A. (2005). WormBook: The online review of *C. elegans* biology. WormBook.

Coghlan, A., Tyagi, R., Cotton, J.A., Holroyd, N., Rosa, B.A., Tsai, I.J., Laetsch, D.R., Beech, R.N., Day, T.A., Hallsworth-Pepin, K., et al. (2019). Comparative genomics of the major parasitic worms. Nat. Genet. 51, 163-174.

Colebunders, R., Basáñez, M.-G., Siling, K., Post, R.J., Rotsaert, A., Mmbando, B., Suykerbuyk, P., and Hopkins, A. (2018a). From river blindness control to elimination: bridge over troubled water. Infect. Dis. Poverty. 7, 21.

Colebunders, R., Hendy, A., and van Oijen, M. (2016). Nodding Syndrome in onchocerciasis endemic areas. Trends Parasitol. 32, 581-583.

Colebunders, R., Siewe, F.N., and Hotterbeekx, A. (2018b). *Onchocerciasis*-associated epilepsy, an additional reason for strengthening onchocerciasis elimination programs. Trends Parasitol. 34, 208-216.

Collins, R.C., Gonzales-Peralta, C., Castro, J., Zea-Flores, G., Cupp, M.S., and Richards, F.O. (1992). Ivermectin: reduction in prevalence and infection intensity of *Onchocerca volvulus* following biannual treatments in five Guatemalan communities. Am. J. Trop. Med. Hyg. 47.

Comandatore, F., Cordaux, R., Bandi, C., Blaxter, M., Darby, A., Makepeace, B.L., Montagna, M., and Sassera, D. (2015). Supergroup C *Wolbachia*, mutualist

symbionts of filarial nematodes, have a distinct genome structure. *Open. Biol.* 5, 150099.

Connor, D.H., Morrison, N.E., Kerdel-Vegas, F., Berkoff, H.A., Johnson, F., Tunnicliffe, R., Failing, F.C., Hale, L.N., Lindquist, K., Thornbloom, W., et al. (1970). Onchocercal dermatitis, lymphadenitis, and elephantiasis in the Ubangi territory. *Hum. Pathol.* 1, 553-579.

Conway, J.R., Lex, A., and Gehlenborg, N. (2017). UpSetR: an R package for the visualization of intersecting sets and their properties. *J. Bioinform.* 33, 2938-2940.

Cooper, P.J., Mancero, T., Espinel, M., Sandoval, C., Lovato, R., Guderian, R.H., and Nutman, T.B. (2001). Early human infection with *Onchocerca volvulus* is associated with an enhanced parasite-specific cellular immune response, *J. Infect. Dis.* 183, 1662–1668.

Cotton, J.A., Bennuru, S., Grote, A., Harsha, B., Tracey, A., Beech, R., Doyle, S.R., Dunn, M., Hotopp, J.C.D., and Holroyd, N. (2016). The genome of *Onchocerca volvulus*, agent of river blindness. *Nat. Microbiol.* 2, 16216.

Cruickshank, R.H. (2002). Molecular markers for the phylogenetics of mites and ticks. *Syst. Appl. Acarol.* 7, 3-14.

Cupp, E., Sauerbrey, M., and Richards, F. (2011). Elimination of human onchocerciasis: history of progress and current feasibility using ivermectin (Mectizan®) monotherapy. *Acta. Tropica.* 120, S100-S108.

Cupp, E.W., and Cupp, M.S. (2005). Short report: impact of ivermectin community-level treatments on elimination of adult *Onchocerca volvulus* when individuals receive multiple treatments per year. *Am. J. Trop. Med. Hyg.* 73.

Darling, A.E., Mau, B., and Perna, N.T. (2010). progressiveMauve: Multiple Genome Alignment with Gene Gain, Loss and Rearrangement. *PLoS One.* 5, e11147.

- Debrah, A.Y., Specht, S., Klarmann-Schulz, U., Batsa, L., Mand, S., Marfo-Debrekyei, Y., Fimmers, R., Dubben, B., Kwarteng, A., and Osei-Atweneboana, M. (2015). Doxycycline leads to sterility and enhanced killing of female *Onchocerca volvulus* worms in an area with persistent microfilaridermia after repeated ivermectin treatment – a randomized placebo controlled double-blind trial. Arch. Clin. Infect. Dis., civ363.
- Deng, W., Zhu, X., Skogerbø, G., Zhao, Y., Fu, Z., Wang, Y., He, H., Cai, L., Sun, H., Liu, C., et al. (2006). Organization of the *Caenorhabditis elegans* small non-coding transcriptome: genomic features, biogenesis, and expression. Genome. Res. 16, 20-29.
- Desjardins, C.A., Cerqueira, G.C., Goldberg, J.M., Hotopp, J.C.D., Haas, B.J., Zucker, J., Ribeiro, J.M., Saif, S., Levin, J.Z., and Fan, L. (2013). Genomics of *Loa loa*, a *Wolbachia*-free filarial parasite of humans. Nature. Genet. 45, 495-500.
- Diawara, L., Traore, M.O., Badji, A., Bissan, Y., Doumbia, K., and Goita, S.F. (2009). Feasibility of onchocerciasis elimination with ivermectin treatment in endemic foci in Africa: first evidence from studies in Mali and Senegal. PLoS Negl. Trop. Dis. 3.
- Dodd, S. (1921). Tick paralysis. J. Comp. Pathol. Therapeutics. 34, 309-323.
- Donnelly, J., and Peirce, M.A. (1975). Experiments on the transmission of *Babesia divergens* to cattle by the tick *Ixodes ricinus*. Int. J. Parasitol. 5, 363-367.
- Doube, B.M. (1979). Seasonal patterns of abundance and host relationships of the Australian paralysis tick, *Ixodes holocyclus* Neumann (Acarina: Ixodidae), in southeastern Queensland. Aust. J. Ecol. 4, 345-360.
- Doyle, S.R., Armoo, S., Renz, A., Taylor, M.J., Osei-Atweneboana, M.Y., and Grant, W.N. (2016). Discrimination between *Onchocerca volvulus* and *Onchocerca ochengi* filarial larvae in *Simulium damnosum* (s.l.) and their distribution throughout central Ghana using a versatile high-resolution speciation assay. Parasite. Vector. 9, 536.

Doyle, S.R., Bourguinat, C., Nana-Djeunga, H.C., Kengne-Ouafo, J.A., Pion, S.D.S., Bopda, J., Kamgno, J., Wanji, S., Che, H., Kuesel, A.C., et al. (2017). Genome-wide analysis of ivermectin response by *Onchocerca volvulus* reveals that genetic drift and soft selective sweeps contribute to loss of drug sensitivity. *PLoS Negl. Trop. Dis.* 11, e0005816.

Doyle, S.R., Illingworth, C.J.R., Laing, R., Bartley, D.J., Redman, E., Martinelli, A., Holroyd, N., Morrison, A.A., Rezanoff, A., Tracey, A., et al. (2019). Population genomic and evolutionary modelling analyses reveal a single major QTL for ivermectin drug resistance in the pathogenic nematode, *Haemonchus contortus*. *BMC. Genomics.* 20, 218.

Doyle, S.R., Tracey, A., Laing, R., Holroyd, N., Bartley, D., Bazant, W., Beasley, H., Beech, R., Britton, C., Brooks, K., et al. (2020). Extensive genomic and transcriptomic variation defines the chromosome-scale assembly of *Haemonchus contortus*, a model gastrointestinal worm. *bioRxiv.*, 2020.2002.2018.945246.

Dreyer, G., Pires, M.L., de Andrade, L.D., Lopes, E., Medeiros, Z., Tenorio, J., Coutinho, A., Noroes, J., and Figueredo-Silva, J. (1994). Tolerance of diethylcarbamazine by microfilaraemic and amicrofilaraemic individuals in an endemic area of Bancroftian filariasis, Recife, Brazil. *Trans. R. Soc. Trop. Med. Hyg.* 88, 232-236.

Duchêne, S., Archer, F.I., Vilstrup, J., Caballero, S., and Morin, P.A. (2011). Mitogenome phylogenetics: the impact of using single regions and partitioning schemes on topology, substitution rate and divergence time estimation. *PLoS One.* 6.

Duke, B. (1980). Observations on *Onchocerca volvulus* in experimentally infected chimpanzees. *Trop. Med. Parasitol.* 31, 41-54.

Duke, B.O. (1993). The population dynamics of *Onchocerca volvulus* in the human host. *Trop. Med. Parasitol.* 44.

Duke, B.O.L. (2004). Evidence for macrofilaricidal activity of ivermectin against female *Onchocerca volvulus*: further analysis of a clinical trial in the Republic of Cameroon indicating two distinct killing mechanisms. *Parasitol.* 130, 447-453.

Eberhard, M.L., Dickerson, J.W., Tsang, V.C., Walker, E.M., Ottesen, E.A., Chandrashekar, R., Weil, G.J., Trpis, M., Strobert, E., and Constantinidis, I. (1995). *Onchocerca volvulus*: Parasitological and serologic responses in experimentally infected chimpanzees and Mangabey monkeys. *Exp. Parasitol.* 80, 454-462.

Eisenbeiss, W.F., Apfel, H., and Meyer, T.F. (1991). Recovery, distribution, and development of *Acanthocheilonema viteae* third and early fourth stage larvae in adult birds. *J. Parasitol.* 77, 580-586.

Elson, L.H., Calvopina, H.M., Paredes, Y.W., Araujo, N.E., Bradley, J.E., Guderian, R.H., and Nutman, T.B. (1995). Immunity to onchocerciasis: Putative immune persons produce a Th1-like response to *Onchocerca volvulus*. *J. Infect. Dis.* 171, 652-658.

Emms, D.M., and Kelly, S. (2015). OrthoFinder: solving fundamental biases in whole genome comparisons dramatically improves orthogroup inference accuracy. *Genome. Biol.* 16, 157.

Emms, D.M., and Kelly, S. (2019). OrthoFinder: phylogenetic orthology inference for comparative genomics. *Genome. Biol.* 20.

Eng, J.K.L., and Prichard, R.K. (2005). A comparison of genetic polymorphism in populations of *Onchocerca volvulus* from untreated- and ivermectin-treated patients. *Mol. Biochem. Parasitol.* 142, 193-202.

English, A.C., Richards, S., Han, Y., Wang, M., Vee, V., Qu, J., Qin, X., Muzny, D.M., Reid, J.G., Worley, K.C., et al. (2012). Mind the Gap: Upgrading genomes with Pacific Biosciences RS long-read sequencing technology. *PLoS One.* 7, e47768.

- Falco, R.C., and Fish, D. (1991). Horizontal movement of adult *Ixodes dammini* (Acari: Ixodidae) attracted to CO₂-baited traps. J. Med. Entomol. 28, 726-729.
- Falco, R.C., and Fish, D. (1992). A comparison of methods for sampling the deer tick, *Ixodes dammini*, in a Lyme disease endemic area. Exp. Appl. Acarol. 14, 165-173.
- Feagin, J.E. (2000). Mitochondrial genome diversity in parasites. Int. J. Parasitol. 30, 371-390.
- Feasey, N., Wansbrough-Jones, M., Mabey, D.C., and Solomon, A.W. (2009). Neglected tropical diseases. Brit. Med. Bull., ldp046.
- Felsenstein, J. (2003). Inferring Phylogenies. Sinauer Associates, Sunderland, MA.
- Fenn, K., Conlon, C., Jones, M., Quail, M.A., Holroyd, N.E., Parkhill, J., and Blaxter, M. (2006). Phylogenetic Relationships of the *Wolbachia* of Nematodes and Arthropods. PLOS Pathogen, 2(10): e94.
- Ferri, E., Barbuto, M., Bain, O., Galimberti, A., Uni, S., Guerrero, R., Ferté, H., Bandi, C., Martin, C., and Casiraghi, M. (2009). Integrated taxonomy: traditional approach and DNA barcoding for the identification of filarioid worms and related parasites (Nematoda). Front. Zool. 6.
- Fischer, K., Beatty, W.L., Jiang, D., Weil, G.J., and Fischer, P.U. (2011). Tissue and stage-specific distribution of *Wolbachia* in *Brugia malayi*. PLoS Negl. Trop. Dis 5, e1174.
- Foster, J.M., Grote, A., Mattick, J., Tracey, A., Tsai, Y.-C., Chung, M., Cotton, J.A., Clark, T.A., Geber, A., Holroyd, N., et al. (2020). Sex chromosome evolution in parasitic nematodes of humans. Nat. Commun. 11, 1964.
- Foster, J.M., Zhang, Y., Kumar, S., and Carlow, C.K. (2005). Mining nematode genome data for novel drug targets. Trends Parasitol. 21, 101-104.

Fox, L.M. (2006). Ivermectin: uses and impact 20 years on. *Curr. Opin. Infect. Dis.* 19, 588-593.

Foxman, B. (2012). Chapter 5 - a primer of molecular biology. In *molecular tools and infectious disease epidemiology*, B. Foxman, ed. (San Diego: Academic Press), pp. 53-78.

Francis, H., Awadzi, K., and Ottesen, E.A. (1985). The Mazzotti reaction following treatment of onchocerciasis with diethylcarbamazine: clinical severity as a function of infection intensity. *Am. J. Trop. Med. Hyg.* 34, 529-536.

Frempong, K.K., Walker, M., Cheke, R.A., Tettevi, E.J., Gyan, E.T., Owusu, E.O., Wilson, M.D., Boakye, D.A., Taylor, M.J., and Biritwum, N.-K. (2016). Does increasing treatment frequency address sub-optimal responses to ivermectin for the control and elimination of river blindness? *Clin. Infect. Dis.*, ciw144.

Frohberger, S.J., Ajendra, J., Surendar, J., Stamminger, W., Ehrens, A., Buerfent, B.C., Gentil, K., Hoerauf, A., and Hübner, M.P. (2019). Susceptibility to *L. sigmodontis* infection is highest in animals lacking IL-4R/IL-5 compared to single knockouts of IL-4R, IL-5 or eosinophils. *Parasite. Vector.* 12, 248.

Gabaldón, T., Dessimoz, C., Huxley-Jones, J., Vilella, A.J., Sonnhammer, E.L., and Lewis, S. (2009). Joining forces in the quest for orthologs. *Genome. Biol.* 10, 403.

Gardon, J., Gardon-Wendel, N., Kamgno, J., Chippaux, J.-P., and Boussinesq, M. (1997). Serious reactions after mass treatment of onchocerciasis with ivermectin in an area endemic for *Loa loa* infection. *Lancet* 350, 18-22.

Geary, T., and Moreno, Y. (2012). Macrocyclic lactone anthelmintics: spectrum of activity and mechanism of action. *Curr. Pharm. Biotechnol.* 13, 866-872.

Gebrezgabiher, G., Mekonnen, Z., Yewhalaw, D., and Hailu, A. (2019). Reaching the last mile: main challenges relating to and recommendations to accelerate onchocerciasis elimination in Africa. *Infect. Dis. Poverty.* 8, 60.

George, P.J., Hess, J.A., Jain, S., Patton, J.B., Zhan, T., Tricoche, N., Zhan, B., Bottazzi, M.E., Hotez, P.J., Abraham, D., et al. (2019). Antibody responses against the vaccine antigens Ov-103 and Ov-RAL-2 are associated with protective immunity to *Onchocerca volvulus* infection in both mice and humans. PLoS Negl. Trop. Dis. 13, e0007730.

Gharib, W.H., and Robinson-Rechavi, M. (2013). The branch-site test of positive selection is surprisingly robust but lacks power under synonymous substitution saturation and variation in GC. Mol. Biol. Evol. 30, 1675-1686.

Ghedin, E., Wang, S., Foster, J.M., and Slatko, B.E. (2004). First sequenced genome of a parasitic nematode. Trends Parasitol. 20, 151-153.

Ghedin, E., Wang, S., Spiro, D., Caler, E., Zhao, Q., Crabtree, J., Allen, J.E., Delcher, A.L., Guiliano, D.B., and Miranda-Saavedra, D. (2007). Draft genome of the filarial nematode parasite *Brugia malayi*. Science 317, 1756-1760.

Ghosh, S., and Azhahianambi, P. (2007). Laboratory rearing of *Theileria annulata*-free *Hyalomma anatolicum anatolicum* ticks. Exp. App. Acarology. 43, 137-146.

Glover, N., Dessimoz, C., Ebersberger, I., Forslund, S.K., Gabaldón, T., Huerta-Cepas, J., Martin, M.-J., Muffato, M., Patricio, M., Pereira, C., et al. (2019). Advances and applications in the quest for orthologs. Mol. Biol. Evol. 36, 2157-2164.

Godel, C., Kumar, S., Koutsovoulos, G., Ludin, P., Nilsson, D., Comandatore, F., Wrobel, N., Thompson, M., Schmid, C.D., Goto, S., et al. (2012). The genome of the heartworm, *Dirofilaria immitis*, reveals drug and vaccine targets. FASEB J 26, 4650-4661.

Goldman, N., and Yang, Z. (1994). A codon-based model of nucleotide substitution for protein-coding DNA sequences. Mol. Biol. Evol. 11, 725-736.

- Gonsioroski, A.V., Bezerra, I.A., Utiumi, K.U., Driemeier, D., Farias, S.E., da Silva Vaz, I., and Masuda, A. (2012). Anti-tick monoclonal antibody applied by artificial capillary feeding in *Rhipicephalus (Boophilus) microplus* females. *Exp. Parasitol.* 130, 359-363.
- Grandjean, O., and Aeschlimann, A. (1972). Contribution to the study of digestion in ticks: histology and fine structure of the midgut epithelium of *Ornithodoros moubata*, Murray (Ixodoidea, Argasidae). *Acta. Tropica.* 30, 193-212.
- Grattan-Smith, P.J., Morris, J.G., Johnston, H.M., Yiannikas, C., Malik, R., Russell, R., and Ouvrier, R.A. (1997). Clinical and neurophysiological features of tick paralysis. *Brain* 120, 1975-1987.
- Graves, S.R., Jackson, C., Hussain-Yusuf, H., Vincent, G., Nguyen, C., Stenos, J., and Webster, M. (2016). *Ixodes holocyclus* tick-transmitted human pathogens in North-Eastern New South Wales, Australia. *Trop. Med. Infect. Dis.* 1, 4.
- Greene, B.M., Gbakima, A.A., Albiez, E.J., and Taylor, H.R. (1985). Humoral and cellular immune responses to *Onchocerca volvulus* infection in humans. *Rev. Infect. Dis.* 7, 789-795.
- Grencis, R.K. (2015). Immunity to helminths: resistance, regulation, and susceptibility to gastrointestinal nematodes. *Ann. Rev. Immunol.* 33, 201-225.
- Grote, A., Lustigman, S., and Ghedin, E. (2017). Lessons from the genomes and transcriptomes of filarial nematodes. *Mol. and Biochem. Parasitol.* 215, 23-29.
- Groux, H. (2003). Type 1 T-regulatory cells: their role in the control of immune responses. *Transplantation* 75, 8S-12S.
- Guglielmone, A.A., Robbins, R.G., Apanaskevich, D.A., Petney, T.N., Estrada-Peña, A., and Horak, I. (2014). The hard ticks of the world (Dordrecht Heidelberg New York London: Springer), pp. 730.

- Gulia-Nuss, M., Nuss, A.B., Meyer, J.M., Sonenshine, D.E., Roe, R.M., Waterhouse, R.M., Sattelle, D.B., de La Fuente, J., Ribeiro, J.M., and Megy, K. (2016). Genomic insights into the *Ixodes scapularis* tick vector of Lyme disease. *Nat. Commun.* 7, 10507.
- Gustavsen, K., Sodahlon, Y., and Bush, S. (2016). Cross-border collaboration for neglected tropical disease efforts—Lessons learned from onchocerciasis control and elimination in the Mano River Union (West Africa). *Globalization Health.* 12, 44.
- Gyapong, J.O., Kumaraswami, V., Biswas, G., and Ottesen, E.A. (2005). Treatment strategies underpinning the global programme to eliminate lymphatic filariasis. *Expert. Opin. Pharmaco.* 6, 179-200.
- Hafez, D., Huang, J.Y., Huynh, A.M., Valtierra, S., Rockenstein, E., Bruno, A.M., Lu, B., DesGroseillers, L., Masliah, E., and Marr, R.A. (2011). Neprilysin-2 is an important β -amyloid degrading enzyme. *Am. J. Pathol.* 178, 306-312.
- Haque, A., Chassoux, D., Ogilvie, B., and Capron, A. (1978). *Dipetalonema viteae* infection in hamsters: enhancement and suppression of microfilaraemia. *Parasitol.* 76, 77-84.
- Harnett, W., Worms, M., Kapil, A., Grainger, M., and Parkhouse, R. (1989). Origin, kinetics of circulation and fate in vivo of the major excretory–secretory product of *Acanthocheilonema viteae*. *Parasitol.* 99, 229-239.
- Hedtke, S.M., Townsend, T.M., and Hillis, D.M. (2006). Resolution of phylogenetic conflict in large data sets by increased taxon sampling. *System. Biol.* 55, 522-529.
- Hess, J.A., Zhan, B., Bonne-Année, S., Deckman, J.M., Bottazzi, M.E., Hotez, P.J., Klei, T.R., Lustigman, S., and Abraham, D. (2014). Vaccines to combat river blindness: expression, selection and formulation of vaccines against infection with *Onchocerca volvulus* in a mouse model. *Int. J. Parasitol.* 44, 637-646.

Hess, J.A., Zhan, B., Torigian, A.R., Patton, J.B., Petrovsky, N., Zhan, T., Bottazzi, M.E., Hotez, P.J., Klei, T.R., Lustigman, S., et al. (2016). The immunomodulatory role of adjuvants in vaccines formulated with the recombinant antigens Ov-103 and Ov-RAL-2 against *Onchocerca volvulus* in mice. *PLoS Negl. Trop. Dis.* 10, e0004797.

Higazi, T.B., Zarroug, I.M.A., Mohamed, H.A., ElMubark, W.A., Deran, T.C.M., Aziz, N., Katabarwa, M., Hassan, H.K., Unnasch, T.R., Mackenzie, C.D., et al. (2013). Interruption of *Onchocerca volvulus* transmission in the Abu Hamed focus, Sudan. *Am. J. Trop. Med. Hyg.* 89, 51-57.

Hirai, H., Tanaka, K., Yoshie, O., Ogawa, K., Kenmotsu, K., Takamori, Y., Ichimasa, M., Sugamura, K., Nakamura, M., Takano, S., et al. (2001). Prostaglandin D2 selectively induces chemotaxis in T helper type 2 cells, eosinophils, and basophils via seven-transmembrane receptor CRTH2. *The Journal. Exp. Med.* 193, 255-261.

Hoerauf, A. (2008). Filariasis: new drugs and new opportunities for lymphatic filariasis and onchocerciasis. *Curr. Opin. Infect. Dis.* 21, 673-681.

Hoerauf, A., Mand, S., Fischer, K., Kruppa, T., Marfo-Debrekyei, Y., Debrah, A.Y., Pfarr, K.M., Adjei, O., and Büttner, D.W. (2003). Doxycycline as a novel strategy against bancroftian filariasis—depletion of *Wolbachia* endosymbionts from *Wuchereria bancrofti* and stop of microfilaria production. *Med. Microbiol. Immunol.* 192, 211-216.

Hoerauf, A., Specht, S., Büttner, M., Pfarr, K., Mand, S., Fimmers, R., Marfo-Debrekyei, Y., Konadu, P., Debrah, A.Y., Bandi, C., et al. (2008). *Wolbachia* endobacteria depletion by doxycycline as antifilarial therapy has macrofilaricidal activity in onchocerciasis: a randomized placebo-controlled study. *Med. Microbiol. Immunol.* 197, 295-311.

Hoff, K.J. (2018). BRAKER2: User Guide.

Hoff, K.J., Lomsadze, A., Borodovsky, M., and Stanke, M. (2019). Whole-genome annotation with BRAKER. In gene prediction: methods and protocols, M. Kollmar, ed. (New York, NY: Springer New York), pp. 65-95.

Holt, C., and Yandell, M. (2011). MAKER2: an annotation pipeline and genome-database management tool for second-generation genome projects. *BMC Bioinformatics* 12, 491.

Hopkins, A. (2017). Onchocerciasis then and now: achievements, priorities and challenges. *Community Eye Health* 30, 92.

Hotez, P.J., Brindley, P.J., Bethony, J.M., King, C.H., Pearce, E.J., and Jacobson, J. (2008). Helminth infections: the great neglected tropical diseases. *Journal. Clin. Invest.* 118, 1311-1321.

Howe, K.L., Bolt, B.J., Shafie, M., Kersey, P., and Berriman, M. (2017). WormBase ParaSite – a comprehensive resource for helminth genomics. *Mol. Biochem. Parasitol.* 215, 2-10.

Hu, M., and Gasser, R.B. (2006). Mitochondrial genomes of parasitic nematodes—progress and perspectives. *Trends Parasitol.* 22, 78-84.

Hu, M., Gasser, R.B., Abs El-Osta, Y.G., and Chilton, N.B. (2003). Structure and organization of the mitochondrial genome of the canine heartworm, *Dirofilaria immitis*. *Parasitol.* 127, 37-51.

Hübner, M.P., Ehrens, A., Koschel, M., Dubben, B., Lenz, F., Frohberger, S.J., Specht, S., Quirynen, L., Lachau-Durand, S., Tekle, F., et al. (2019a). Macrofilaricidal efficacy of single and repeated oral and subcutaneous doses of flubendazole in *Litomosoides sigmodontis* infected jirds. *PLoS Negl. Trop. Dis.* 13, e0006320.

Hübner, M.P., Koschel, M., Struever, D., Nikolov, V., Frohberger, S.J., Ehrens, A., Fendler, M., Johannes, I., von Geldern, T.W., Marsh, K., et al. (2019b). In vivo

kinetics of *Wolbachia* depletion by ABBV-4083 in *L. sigmodontis* adult worms and microfilariae. PLoS Negl. Trop. Dis. 13, e0007636.

Hübner, M.P., Torrero, M.N., McCall, J.W., and Mitre, E. (2009). *Litomosoides sigmodontis*: a simple method to infect mice with L3 larvae obtained from the pleural space of recently infected jirds (*Meriones unguiculatus*). Exp. Parasitol. 123, 95-98.

Hunt, V.L., Tsai, I.J., Coghlan, A., Reid, A.J., Holroyd, N., Foth, B.J., Tracey, A., Cotton, J.A., Stanley, E.J., and Beasley, H. (2016). The genomic basis of parasitism in the *Strongyloides* clade of nematodes. Nat. Genet.

Ibeh, O., Nwoke, B., Adegoke, J., and Mafuyai, H. (2006). Cytospecies identifications of vectors of human onchocerciasis in South Eastern Nigeria. Afr. J. Biotechnol. 5, 1813-1818.

Jackson, J., Beveridge, I., Chilton, N.B., and Andrews, R.H. (2007). Distributions of the paralysis ticks *Ixodes cornuatus* and *Ixodes holocyclus* in South-Eastern Australia. Aus. Vet. J. 85, 420-424.

Jackson, J., Beveridge, I., Chilton, N.B., Andrews, R.H., and Dixon, B. (2002). Morphological comparison of the adult and larval stages of the Australian ticks *Ixodes holocyclus* Neumann, 1899 and *I. cornuatus* Roberts, 1960 (Acari: Ixodoidea). Syst. Appl. Acarol. 7, 91-108.

Jackson, J., Chilton, N.B., Beveridge, I., Morris, M., and Andrews, R.H. (1998). An electrophoretic comparison of the Australian paralysis tick, *Ixodes holocyclus* Neumann, 1899, with *I. cornuatus* Roberts, 1960 (Acari : Ixodidae). Aus. J. Zool. 46, 109-117.

Jackson, J., Chilton, N.B., Beveridge, I., Morris, M., and Andrews, R.H. (2000). Genetic variation within the ticks *Ixodes holocyclus* and *Ixodes cornuatus* from South-Eastern Australia. Int. J. Parasitol. 30, 1159-1166.

Jaleta, T.G., Rödelberger, C., Abanda, B., Eisenbarth, A., Achukwi, M.D., Renz, A., and Streit, A. (2018). Full mitochondrial and nuclear genome comparison confirms that *Onchocerca* sp. "Siisa" is *Onchocerca ochengi*. *Parasitol. Res.* 117, 1069-1077.

Johnson, E., Lustigman, S., Brotman, B., Browne, J., and Prince, A. (1991). *Onchocerca volvulus*: in vitro killing of microfilaria by neutrophils and eosinophils from experimentally infected chimpanzees. *Trop. Med. Parasitol.* 42, 351-355.

Johnson, M.H., Orihel, T., and Beaver, P. (1974). *Dipetalonema viteae* in the experimentally infected jird, *Meriones unguiculatus*. Insemination, development from egg to microfilaria, reinsemination, and longevity of mated and unmated worms. *J. Parasitol.*, 302-309.

Jones, L., Davies, C., Steele, G., and Nuttall, P. (1988). The rearing and maintenance of ixodid and argasid ticks in the laboratory. *Anim. Technol.* 39, 99-106.

Jones, P., Binns, D., Chang, H.-Y., Fraser, M., Li, W., McAnulla, C., McWilliam, H., Maslen, J., Mitchell, A., Nuka, G., et al. (2014). InterProScan 5: genome-scale protein function classification. *Bioinformatics (Oxford, England)* 30, 1236-1240.

Jongejan, F., and Uilenberg, G. (2004). The global importance of ticks. *Parasitol.* 129, S3-S14.

Kahle, D., and Wickham, H. (2013). ggmap: Spatial Visualization with ggplot2. *R. J.* 5, 144-161.

Kaire, G.H. (1966). Isolation of tick paralysis toxin from *Ixodes holocyclus*. *Toxicon.* 4, 91-97.

Kamgno, J., Pion, S.D., Chesnais, C.B., Bakalar, M.H., D'Ambrosio, M.V., Mackenzie, C.D., Nana-Djeunga, H.C., Gounoue-Kamkumo, R., Njitchouang, G.-R., Nwane, P., et al. (2017). A test-and-not-treat strategy for onchocerciasis in *Loa loa*-Endemic Areas. *N. Eng. J. Med.* 377, 2044-2052.

- Kaplan, R.M., and Vidyashankar, A.N. (2012). An inconvenient truth: global worming and anthelmintic resistance. *Vet. Parasitol.* 186, 70-78.
- Kawabata, M., Flores, G.Z., Izui, S., and Kobayakawa, T. (1984). IgM rheumatoid factors in Guatemalan onchocerciasis. *Trans. R. Soc. Trop. Med. Hyg.* 78, 356-358.
- Keddie, E.M., Higazi, T., and Unnasch, T.R. (1998). The mitochondrial genome of *Onchocerca volvulus*: Sequence, structure and phylogenetic analysis. *Mol. Biocheml. Parasitol.* 95, 111-127.
- Keiser, P.B., Reynolds, S.M., Awadzi, K., Ottesen, E.A., Taylor, M.J., and Nutman, T.B. (2002). Bacterial endosymbionts of *Onchocerca volvulus* in the pathogenesis of post treatment reactions. *J. Infect. Dis.* 185, 805-811.
- Kerepesi, L.A., Leon, O., Lustigman, S., and Abraham, D. (2005). Protective immunity to the larval stages of *Onchocerca volvulus* is dependent on Toll-like receptor 4. *Infect. Immun.* 73, 8291–8297.
- Kimura, M., and Crow, J.F. (1969). Natural selection and gene substitution. *Genet. Res.* 13, 127-141.
- Klei, T.R., and Rajan, T.V. (2002). *The Filaria*, Vol 5 (Boston, MA: Springer US, Boston, MA).
- Klompen, H., Lekveishvili, M., and Black IV, W.C. (2007). Phylogeny of parasitiform mites (Acari) based on rRNA. *Mol. Phylogene. Evol.* 43, 936-951.
- Klompen, J., Black IV, W., Keirans, J., and Oliver Jr, J. (1996). Evolution of ticks. *Annu. Rev. Entomol.* 41, 141-161.
- Klompen, J., and Oliver, J. (1993). Systematic relationships in the soft ticks (Acari: Ixodida: Argasidae). *Syst. Entomol.* 18, 313-331.

Koala, L., Nikiema, A., Post, R.J., Paré, A.B., Kafando, C.M., Drabo, F., and Traoré, S. (2017). Recrudescence of onchocerciasis in the Comoé Valley in Southwest Burkina Faso. *Acta. Tropica*. 166, 96-105.

Kocan, K.M., de la Fuente, J., and Coburn, L.A. (2015). Insights into the development of *Ixodes scapularis*: a resource for research on a medically important tick species. *Parasite. Vector*. 8, 1-6.

Kong, J.-T., Grigg, M.E., Uyetake, L., Parmley, S., and Boothroyd, J.C. (2003). Serotyping of *Toxoplasma gondii* infections in humans using synthetic peptides. *J. Infectious. Dis*. 187, 1484-1495.

Konnai, S., Saito, Y., Nishikado, H., Yamada, S., Imamura, S., Mori, A., Ito, T., Onuma, M., and Ohashi, K. (2008). Establishment of a laboratory colony of taiga tick *Ixodes persulcatus* for tick-borne pathogen transmission studies. *Jpn. J. V. Res*. 55, 85-92.

Koren, S., and Phillippy, A.M. (2015). One chromosome, one contig: complete microbial genomes from long-read sequencing and assembly. *Curr. Opin. Microbiol*. 23, 110-120.

Korf, I. (2004). Gene finding in novel genomes. *BMC Bioinformatics* 5, 59.

Kosiol, C., and Anisimova, M. (2019). Selection Acting on Genomes. In *Evolutionary Genomics: Statistical and Computational Methods*, M. Anisimova, ed. (New York, NY: Springer New York), pp. 373-397.

Krueger, A., Fischer, P., and Morales-Hojas, R. (2007). Molecular phylogeny of the filaria genus *Onchocerca* with special emphasis on Afrotropical human and bovine parasites. *Acta. Tropica*. 101, 1-14.

Krueger, A., and Hennings, I.C. (2006). Molecular phylogenetics of blackflies of the *Simulium damnosum* complex and cytophylogenetic implications. *Mol. Phylogenet. Evol*. 39, 83-90.

Krull, C., Böhme, B., Clausen, P.-H., and Nijhof, A.M. (2017). Optimization of an artificial tick feeding assay for *Dermacentor reticulatus*. *Parasite. Vector.* 10, 60.

Krzywinski, M.I., Schein, J.E., Birol, I., Connors, J., Gascoyne, R., Horsman, D., Jones, S.J., and Marra, M.A. (2009). Circos: An information aesthetic for comparative genomics. *Genome. Res.*

Kurtz, S., Phillippy, A., Delcher, A.L., Smoot, M., Shumway, M., Antonescu, C., and Salzberg, S.L. (2004). Versatile and open software for comparing large genomes. *Genome. Biol.* 5, R12.

Kuzniar, A., van Ham, R.C.H.J., Pongor, S., and Leunissen, J.A.M. (2008). The quest for orthologs: finding the corresponding gene across genomes. *Trends Genet.* 24, 539-551.

Laetsch, D., Heitlinger, E., Taraschewski, H., Nadler, S., and Blaxter, M. (2012). The phylogenetics of *Anguillicolidae* (Nematoda: *Anguilliculoidea*), swimbladder parasites of eels. *BMC. Evol. Biol.* 12, 60.

Lagatie, O., Van Dorst, B., and Stuyver, L.J. (2017). Identification of three immunodominant motifs with atypical isotype profile scattered over the *Onchocerca volvulus* proteome. *PLoS Negl. Trop. Dis.* 11, e0005330.

Lagatie, O., Verheyen, A., Van Dorst, B., Batsa Debrah, L., Debrah, A., and Stuyver, L.J. (2018). Linear epitopes in *Onchocerca volvulus* vaccine candidate proteins and excretory-secretory proteins. *Parasit. Immunol.* 40, e12587.

Lanfear, R., Calcott, B., Ho, S.Y.W., and Guindon, S. (2012). PartitionFinder: Combined selection of partitioning schemes and substitution models for phylogenetic analyses. *Mol. Biol. Evol.* 29, 1695-1701.

Larkin, M., Blackshields, G., Brown, N., Chenna, R., McGettigan, P., McWilliam, H., Valentin, F., Wallace, I., Wilm, A., and Lopez, R. (2007). Clustal W and Clustal X Version 2.0. *Bioinformatics* 23, 2947.

Le Berre, R., Garms, R., Davies, J., Walsh, J., Philippon, B., Johnson, C., Hemming, C., Lewis, D., Odiyo, P., and Crosskey, R. (1979). Displacements of *Simulium damnosum* and strategy of control against onchocerciasis. Philos. T. R. Soc. London. B, Biol. Sci. 287, 277-288.

Le, T.H., Blair, D., and McManus, D.P. (2000). Mitochondrial genomes of human helminths and their use as markers in population genetics and phylogeny. Acta Tropica. 77, 243-256.

Lefoulon, E., Bain, O., Bourret, J., Junker, K., Guerrero, R., Cañizales, I., Kuzmin, Y., Satoto, T.B.T., Cardenas-Callirgos, J.M., de Souza Lima, S., et al. (2015). Shaking the Tree: Multi-locus sequence typing usurps current Onchocercid (filarial nematode) phylogeny. PLoS Negl. Trop. Dis. 9, e0004233.

Lefoulon, E., Bain, O., Makepeace, B.L., d'Haese, C., Uni, S., Martin, C., and Gavotte, L. (2016). Breakdown of coevolution between symbiotic bacteria *Wolbachia* and their filarial hosts. Peer J. 4, e1840.

Leroy, S., Duperray, C., and Morand, S. (2003). Flow cytometry for parasite nematode genome size measurement. Molecular and Biochemical Parasitology 128, 91-93.

Lespine, A., Alvinerie, M., Vercruysse, J., Prichard, R.K., and Geldhof, P. (2008). ABC transporter modulation: a strategy to enhance the activity of macrocyclic lactone anthelmintics. Trends Parasitol. 24, 293-298.

Li, B.W., Rush, A.C., and Weil, G.J. (2014). High level expression of a glutamate-gated chloride channel gene in reproductive tissues of *Brugia malayi* may explain the sterilizing effect of ivermectin on filarial worms. Int. J. Parasitol. Drugs Drug Resist. 4, 71-76.

Li, H., and Durbin, R. (2009). Fast and accurate short read alignment with Burrows–Wheeler transform. Bioinformatics 25, 1754-1760.

Li, L., Stoeckert, C.J., and Roos, D.S. (2003). OrthoMCL: identification of ortholog groups for eukaryotic genomes. *Genome. Res.* 13, 2178-2189.

Li, R., Ren, X., Bi, Y., Ding, Q., Ho, V.W.S., and Zhao, Z. (2018). Comparative mitochondrial genomics reveals a possible role of a recent duplication of NADH dehydrogenase subunit 5 in gene regulation. *DNA. Res.* 25, 577-586.

Linard, B., Thompson, J.D., Poch, O., and Lecompte, O. (2011). OrthoInspector: comprehensive orthology analysis and visual exploration. *BMC. Bioinform.* 12, 11.

Lipner, E.M., Dembele, N., Souleymane, S., Alley, W.S., Prevots, D.R., Toe, L., Boatın, B., Weil, G.J., and Nutman, T.B. (2006). Field applicability of a rapid-format anti-Ov-16 antibody test for the assessment of onchocerciasis control measures in regions of endemicity. *J. Infect. Dis.* 194, 216-221.

Liu, D., Hunt, M., and Tsai, I.J. (2018). Inferring synteny between genome assemblies: a systematic evaluation. *BMC. Bioinform.* 19, 26.

LoGiudice, K., Ostfeld, R.S., Schmidt, K.A., and Keesing, F. (2003). The ecology of infectious disease: Effects of host diversity and community composition on Lyme disease risk. *Proc. Natl. Acad. Sci.* 100, 567-571.

Lovett, S.T. (2001). Tandem Repeats. In *Encyclopedia of Genetics*, S. Brenner, and J.H. Miller, eds. (New York: Academic Press), pp. 1932-1933.

Lucius, R., Erondı, N., Kern, A., and Donelson, J. (1988). Molecular cloning of an immunodominant antigen of *Onchocerca volvulus*. *J. Exp. Med.* 168, 1199-1204.

Lucius, R., and Textor, G. (1995). *Acanthocheilonema viteae*: rational design of the life cycle to increase production of parasite material using less experimental animals. *App. Parasitol.* 36, 22-33.

Lüder, C., Soboslay, P., Prince, A., Greene, B., Lucius, R., and Schulz-Key, H. (1993). Experimental onchocerciasis in chimpanzees: cellular responses and

antigen recognition after immunization and challenge with *Onchocerca volvulus* infective third-stage larvae. *Parasitol.* 107, 87-97.

Lustigman, S., Grote, A., and Ghedin, E. (2017). The role of 'omics' in the quest to eliminate human filariasis. *PLoS Neg. Trop. Dis.* 11, e0005464-e0005464.

Lustigman, S., James, E.R., Tawe, W., and Abraham, D. (2002). Towards a recombinant antigen vaccine against *Onchocerca volvulus*. *Trends Parasitol.* 18, 135-141.

Lv, J., Wu, S., Zhang, Y., Chen, Y., Feng, C., Yuan, X., Jia, G., Deng, J., Wang, C., Wang, Q., *et al.* (2014a). Assessment of four DNA fragments (COI, 16S rDNA, ITS2, 12S rDNA) for species identification of the Ixodida (Acari: Ixodida). *Parasite. Vector.* 7, 93-93.

Lv, J., Wu, S., Zhang, Y., Zhang, T., Feng, C., Jia, G., and Lin, X. (2014b). Development of a DNA barcoding system for the Ixodida (Acari: Ixodida). *Mitochondrial. DNA.* 25, 142-149.

MacDonald, A., Tawe, W., Leon, O., Cao, L., Liu, J., Oksov, Y., Abraham, D., and Lustigman, S. (2004). Ov-ASP-1, the *Onchocerca volvulus* homologue of the activation associated secreted protein family is immunostimulatory and can induce protective anti-larval immunity. *Parasit. Immunol.* 26, 53-62.

Mackenstedt, U., Jenkins, D., and Romig, T. (2015). The role of wildlife in the transmission of parasitic zoonoses in peri-urban and urban areas. *Int. J. Parasitol. Parasites. Wildl.* 4, 71-79.

Mackenzie, C.D., Homeida, M.M., Hopkins, A.D., and Lawrence, J.C. (2012). Elimination of onchocerciasis from Africa: possible? *Trends Parasitol.* 28, 16-22.

Mackerras, M. (1954). Two new species of *Dipetalonema* (Nematoda, Filarioidea) from Australian marsupials. *Proc. R. Soc. Queensland* 64, 51-57.

Mackerras, M. (1962). Filarial parasites (Nematoda: Filarioidea) of Australian animals. *Aus. J. Zool.* 10, 400-457.

Maddison, W., and Maddison, D. (2008). Mesquite: a modular system for evolutionary analysis. Version 2.5, build j55.

Makenga, B.J.C., Maketa, V., Bakajika, D., Ntumba, F., Mpunga, D., Murdoch, M., Hopkins, A., Noma, M., Zouré, H., and Tekle, A. (2015). Onchocerciasis control in the Democratic Republic of Congo (DRC): challenges in a post-war environment. *Trop. Med. Int. Health.* 20, 48-62.

Makepeace, B.L., and Tanya, V.N. (2016). 25 Years of the *Onchocerca ochengi* model. *Trends Parasitol.* 32, 966-978.

Mans, B.J., and Neitz, A.W. (2004). Adaptation of ticks to a blood-feeding environment: evolution from a functional perspective. *Insect. Biochem. Mol. Biol.* 34, 1-17.

Masina, S., and Broady, K. (1999). Tick paralysis: development of a vaccine. *Int. J. Parasitol.* 29, 535-541.

Mazzotti, L. (1948). Onchocerciasis in Mexico. *Proc 4th Int. Congress. Trop. Med.: Malaris.* Washington DC, 948-56

McCarthy, J.S., Wieseman, M., Tropea, J., Kaslow, D., Abraham, D., Lustigman, S., Tuan, R., Guderian, R.H., and Nutman, T.B. (2002). *Onchocerca volvulus* glycolytic enzyme fructose-1, 6-bisphosphate aldolase as a target for a protective immune response in humans. *Infect. Immun.* 70, 851-858.

McCoy, K.D., Léger, E., and Dietrich, M. (2013). Host specialization in ticks and transmission of tick-borne diseases: a review. *Front. Cell. Infect. Microbiol.* 3, 57.

McKechne, N.M., Braun, G., Connor, V., Kläger, S., Taylor, D.W., Alexander, R.A., and Gilbert, C.E. (1993). Immunologic cross-reactivity in the pathogenesis of ocular onchocerciasis. *Investig. Ophthalmol. Vis. Sci.* 34, 2888-2902.

McKechnie, N.M., Gürr, W., Yamada, H., Copland, D., and Braun, G. (2002). Antigenic Mimicry: *Onchocerca volvulus* antigen-specific T cells and ocular inflammation. *Investig. Ophthalmol. Vis. Sci.* 43, 411-418.

McLaren, D.J. (2009). The structure and development of the spermatozoon of *Dipetalonema viteae* (Nematoda: Filarioidea). *Parasitol.* 66, 447-463.

McNulty, S.N., Abubucker, S., Simon, G.M., Mitreva, M., McNulty, N.P., Fischer, K., Curtis, K.C., Brattig, N.W., Weil, G.J., and Fischer, P.U. (2012).

Transcriptomic and proteomic analyses of a *Wolbachia*-free filarial parasite provide evidence of trans-kingdom horizontal gene transfer. *PLoS One.* 7, e45777.

McNulty, S.N., Rosa, B.A., Fischer, P.U., Rumsey, J.M., Erdmann-Gilmore, P., Curtis, K.C., Specht, S., Townsend, R.R., Weil, G.J., and Mitreva, M. (2015). An integrated multiomics approach to identify candidate antigens for serodiagnosis of human onchocerciasis. *Mol. Cell. Proteomics.* 14, 3224-3233.

Mircean, M., Ionică, A. M., Mircean, V., Györke, A., Codea, A. R., Tăbăran, F. A., Taulescu, M., and Dumitrache, M. O. (2017). Clinical and pathological effects of *Dirofilaria repens* and *Dirofilaria immitis* in a dog with a natural co-infection. *Parasitol. Int.*, 66, 331-334.

Mitreva, M., Blaxter, M.L., Bird, D.M., and McCarter, J.P. (2005). Comparative genomics of nematodes. *Trends Genet.* 21, 573-581.

Mitreva, M., Jasmer, D.P., Zarlenga, D.S., Wang, Z., Abubucker, S., Martin, J., Taylor, C.M., Yin, Y., Fulton, L., and Minx, P. (2011). The draft genome of the parasitic nematode *Trichinella spiralis*. *Nat. Genet.* 43, 228-235.

Montes, C., Cuadrillero, C., and Vilella, D. (2002). Maintenance of a Laboratory Colony of *Cimex lectularius* (Hemiptera: Cimicidae) Using an Artificial Feeding Technique. *J. Med. Entomol.* 39, 675-679.

- Moreno, Y., Nabhan, J. F., Solomon, J., Mackenzie, C. D., and Geary, T. G. (2010). Ivermectin disrupts the function of the excretory-secretory apparatus in microfilariae of *Brugia malayi*. *Proc.Nat. Acad. Sci.*, 107(46), 20120-20125.
- Morris, C.P., Evans, H., Larsen, S.E., and Mitre, E. (2013). A comprehensive, model-based review of vaccine and repeat infection trials for filariasis. *Clin. Microbiol. Rev.* 26, 381-421.
- Mukhopadhyay, P., and Ghosh, D. (1988). *Litomosoides carinii* infection: pathophysiological changes in the infected albino rat. *Int. J. Parasitol.* 18, 103-107.
- Murdoch, F.A., and Spratt, D.M. (2006). Ecology of the common marsupial tick (*Ixodes tasmani* Neumann) (Acarina : Ixodidae), in eastern Australia. *Aus. J. Zool.* 53, 383-388.
- Nattestad, M., Chin, C.-S., and Schatz, M.C. (2016). Ribbon: Visualizing complex genome alignments and structural variation. *bioRxiv*, 082123.
- Nava, S., Guglielmone, A.A., and Mangold, A.J. (2009). An overview of systematics and evolution of ticks. *Front. Biosci.* 14, 2857-2877.
- Needham, G.R., and Teel, P.D. (1991). Off-host physiological ecology of ixodid ticks. *Annu. Rev. Entomol.* 36, 659-681.
- Nichio, B.T.L., Marchaukoski, J.N., and Raittz, R.T. (2017). New tools in orthology analysis: A brief review of promising perspectives. *Front. Genet.* 8.
- Njume, F.N., Ghogomu, S.M., Shey, R.A., Gaikam, L.O.T., Poelvoorde, P., Humblet, P., Kamgno, J., Robert, A., Mutesa, L., Lelubre, C., et al. (2019). Identification and characterization of the *Onchocerca volvulus* Excretory Secretory Product Ov28CRP, a putative GM2 activator protein. *PLoS Negl. Trop. Dis.* 13, e0007591.

Noma, M., Zouré, H.G., Tekle, A.H., Enyong, P.A., Nwoke, B.E., and Remme, J.H. (2014). The geographic distribution of onchocerciasis in the 20 participating countries of the African Programme for Onchocerciasis Control: priority areas for ivermectin treatment. *Parasite. Vector.* 7, 325.

Norice-Tra, C.T., Ribeiro, J., Bennuru, S., Fay, M.P., Tyagi, R., Mitreva, M., and Nutman, T.B. (2017). Insights into *Onchocerca volvulus* population biology through multilocus immunophenotyping. *J. Infect. Dis.* 216, 736-743.

Norris, D.E., Klompen, J.S.H., and Black, W.C. (1999). Comparison of the mitochondrial 12S and 16S ribosomal DNA genes in resolving phylogenetic relationships among hard ticks (Acari: Ixodidae). *Ann. Entomol. Soc. Am.* 92, 117-129.

Nurk, S., Bankevich, A., Antipov, D., Gurevich, A., Korobeynikov, A., Lapidus, A., Pribelsky, A., Pyshkin, A., Sirotkin, A., Sirotkin, Y., et al. (2013). Assembling genomes and mini-metagenomes from highly chimeric reads (Berlin, Heidelberg: Springer Berlin Heidelberg).

Nutman, T.B., Weil, G.J., Fischer, P.U., and Mitreva, M. (2016). Genomic diversity in *Onchocerca volvulus* and its *Wolbachia* endosymbiont.

Omura, S., and Crump, A. (2004). The life and times of ivermectin a success story. *Nat. Rev. Microbiol.* 2, 984-989.

Oorebeek, M., and Kleindorfer, S. (2008). Climate or host availability: what determines the seasonal abundance of ticks? *Parasitol. Res.* 103, 871.

Osawa, S., Jukes, T.H., Watanabe, K., and Muto, A. (1992). Recent evidence for evolution of the genetic code. *Microbiol. Rev.* 56, 229.

Osei-Atweneboana, M.Y., Awadzi, K., Attah, S.K., Boakye, D.A., Gyapong, J.O., and Prichard, R.K. (2011). Phenotypic evidence of emerging ivermectin resistance in *Onchocerca volvulus*. *PLoS Negl. Trop. Dis.* 5, e998.

Osei-Atweneboana, M.Y., Boakye, D.A., Awadzi, K., Gyapong, J.O., and Prichard, R.K. (2012). Genotypic analysis of β -tubulin in *Onchocerca volvulus* from communities and individuals showing poor parasitological response to ivermectin treatment. *Int. J. Parasitol.: Drugs Drug Res* 2, 20-28.

Osei-Atweneboana, M.Y., Eng, J.K., Boakye, D.A., Gyapong, J.O., and Prichard, R.K. (2007). Prevalence and intensity of *Onchocerca volvulus* infection and efficacy of ivermectin in endemic communities in Ghana: a two-phase epidemiological study. *Lancet*. 369.

Otranto, D., Brianti, E., Abramo, F., Gaglio, G., Napoli, E., Latrofa, M.S., Ramos, R.A., Dantas-Torres, F., and Bain, O. (2012). Cutaneous distribution and localization of *Cercopithifilaria* sp. microfilariae in dogs. *Vet. Parasitol.* 190, 143-150.

Otranto, D., Varcasia, A., Solinas, C., Scala, A., Brianti, E., Dantas-Torres, F., Annoscia, G., Martin, C., Mutaftchiev, Y., and Bain, O. (2013). Redescription of *Cercopithifilaria baina* Almeida and Vicente, 1984 (Spirurida, Onchocercidae) from a dog in Sardinia, Italy. *Parasite. Vector.* 6, 132.

Ottesen, E. (1984). Immunological aspects of lymphatic filariasis and onchocerciasis in man. *Trans. R. Soc. Trop. Med. Hyg.* 78, 9-18.

Ottesen, E.A. (1985). Immediate hypersensitivity responses in the immunopathogenesis of human onchocerciasis. *Rev. Infect. Dis.* 7, 796-801.

Palevich, N., Britton, C., Kamenetzky, L., Mitreva, M., de Moraes Mourão, M., Bennuru, S., Quack, T., Scholte, L.L.S., Tyagi, R., and Slatko, B.E. (2018). Tackling Hypotheticals in Helminth Genomes. *Trends Parasitol.* 34, 179-183.

Paradis, E., Jombart, T., Schliep, K., Potts, A., Winter, D., and Paradis, M.E. (2017). Package 'pegas'.

Parola, P., Paddock, C.D., Socolovschi, C., Labruna, M.B., Mediannikov, O., Kernif, T., Abdad, M.Y., Stenos, J., Bitam, I., and Fournier, P.-E. (2013). Update

on tick-borne rickettsioses around the world: a geographic approach. Clin. Microbiol. Rev. 26, 657-702.

Parra, G., Bradnam, K., and Korf, I. (2007). CEGMA: a pipeline to accurately annotate core genes in eukaryotic genomes. Bioinformatics 23, 1061-1067.

Pearlman, E., and Hall, L.R. (2000). Immune mechanisms in *Onchocerca volvulus*-mediated corneal disease (river blindness). Parasite. Immunol. 22, 625-631.

Perbandt, M., Höppner, J., Burmeister, C., Lüersen, K., Betzel, C., and Liebau, E. (2008). Structure of the extracellular glutathione s-transferase OvGST1 from the human pathogenic parasite *Onchocerca volvulus*. J. Mol. Biol. 377, 501-511.

Petralanda, I., and Piessens, W.F. (1994). Pathogenesis of onchocercal dermatitis: possible role of parasite proteases and autoantibodies to extracellular matrix proteins. Exp. Parasitol. 79, 177-186.

Piesman, J. (2002). Ecology of *Borrelia burgdorferi sensu lato* in North America. Lyme borreliosis: biology, epidemiology, and control Wallingford, Oxfordshire, UK: CAB. Int., 223-249.

Pigeault, R., Braquart-Varnier, C., Marcadé, I., Mappa, G., Mottin, E., and Sicard, M. (2014). Modulation of host immunity and reproduction by horizontally acquired *Wolbachia*. J. Insect. Parasitol. 70, 125-133.

Pilotte, N., Zaky, W.I., Abrams, B.P., Chadee, D.D., and Williams, S.A. (2016). A novel xenomonitoring technique using mosquito excreta/feces for the detection of filarial parasites and malaria. PLoS Negl. Trop. Dis. 10.

Pionnier, N.P., Sjöberg, H., Chunda, V.C., Fombad, F.F., Chounna, P.W., Njouendou, A.J., Metuge, H.M., Ndzeshang, B.L., Gandjui, N.V., Akumtoh, D.N., et al. (2019). Mouse models of *Loa loa*. Nat. Commun. 10, 1429.

Pop, M., Phillippy, A., Delcher, A.L., and Salzberg, S.L. (2004). Comparative genome assembly. Brief. Bioinformatics 5, 237-248.

- Post, R. (2005). The chromosomes of the Filariae. *Filaria J.* 4, 10-10.
- Prasad, C.S., Gupta, S., Kumar, H., and Tiwari, M. (2013). Evolutionary and functional analysis of fructose bisphosphate aldolase of plant parasitic nematodes. *Bioinformatics* 9, 1.
- Prichard, R.K., Basáñez, M.-G., Boatin, B.A., McCarthy, J.S., García, H.H., Yang, G.-J., Sripa, B., and Lustigman, S. (2012). A research agenda for helminth diseases of humans: Intervention for control and elimination. *PLoS Negl. Trop. Dis.* 6, e1549.
- Prince, A.M., Brotman, B., Johnson, E.H., Smith, A., Pascual, D., and Lustigman, S. (1992). *Onchocerca volvulus*: immunization of chimpanzees with X-irradiated third-stage (L3) larvae. *Exp. Parasitol.* 74, 239-250.
- Qamar, M. F., Maqbool, A., & Ahmad, N. (2011). Economic losses due to haemonchosis in sheep and goats. *Sci Intern*, 23(4), 321-4.
- Quinlan, A.R., and Hall, I.M. (2010). BEDTools: a flexible suite of utilities for comparing genomic features. *Bioinformatics* 26, 841-842.
- R Core Team (2017). R: A language and environment for statistical computing. <https://www.R-project.org/>
- Rambaut, A., Suchard, M., Xie, D., and Drummond, A. (2014). Tracer v1. 6. Computer program and documentation distributed by the author.
- Ramesh, A., Small, S.T., Kloos, Z.A., Kazura, J.W., Nutman, T.B., Serre, D., and Zimmerman, P.A. (2012). The complete mitochondrial genome sequence of the filarial nematode *Wuchereria bancrofti* from three geographic isolates provides evidence of complex demographic history. *Mol. Biochem. Parasitol.* 183, 32-41.
- Ramos, R.A.N., Giannelli, A., Dantas-Torres, F., Mallia, E., Passantino, G., Lia, R.P., Latrofa, M.S., Mutafovchiev, Y., and Otranto, D. (2013). *Cercopithifilaria*

rugosicauda (Spirurida, Onchocercidae) in a roe deer and ticks from Southern Italy. *Int. J. Parasitol: Parasite Wildl.* 2, 292-296.

Ramos, R.A.N., Giannelli, A., Lia, R.P., Brianti, E., Tarallo, V.D., Breitshwerdt, E.B., Dantas-Torres, F., Stanneck, D., and Otranto, D. (2014). Incidence of *Cercopithifilaria baina* in dogs and probability of co-infection with other tick-borne pathogens. *PLoS One.* 9, e88198.

Remme, J.H. (2004). Research for control: the onchocerciasis experience. *Trop. Med. Int. Health.* 9, 243-254.

Revell, L.J. (2012). phytools: an R package for phylogenetic comparative biology (and other things). *Methods. Ecol. Evol.* 3, 217-223.

Rivera, J., and Currie, D.C. (2009). Identification of Nearctic black flies using DNA barcodes (*Diptera: Simuliidae*). *Molecular Ecology Resources* 9, 224-236.

Roberts, F.H.S. (1970). Australian ticks. Published Melbourne CSIRO, 267p.

Rodrigues, M.M., and Ersching, J. (2015). Neglected Tropical Diseases, bioinformatics, and vaccines. *J. Infect. Dis.* 211, 175-177.

Rokas, A., and Carroll, S.B. (2005). More Genes or More Taxa? The Relative Contribution of Gene Number and Taxon Number to Phylogenetic Accuracy. *Mol. Biol. Evol.* 22, 1337-1344.

Rokeach, L.A., Zimmerman, P.A., and Unnasch, T.R. (1994). Epitopes of the *Onchocerca volvulus* RAL1 antigen, a member of the calreticulin family of proteins, recognized by sera from patients with onchocerciasis. *Infect. Immun.* 62, 3696-3704.

Romagnani, S. (1997). The Th1/Th2 paradigm. *Immunol. Today.* 18, 263-266.

Ronquist, F., Teslenko, M., Van Der Mark, P., Ayres, D.L., Darling, A., Höhna, S., Larget, B., Liu, L., Suchard, M.A., and Huelsenbeck, J.P. (2012). MrBayes 3.2:

efficient Bayesian phylogenetic inference and model choice across a large model space. *Syst. Biol.* 61, 539-542.

Saha, S., Bridges, S., Magbanua, Z.V., and Peterson, D.G. (2008). Empirical comparison of *ab initio* repeat finding programs. *Nucleic. Acids. Res.* 36, 2284-2294.

Sanderson, M., McMahon, M., and Steel, M. (2010). Phylogenomics with incomplete taxon coverage: the limits to inference. *BMC. Evol. Biol.* 10, 155.

Sanderson, M.J., Driskell, A.C., Ree, R.H., Eulenstein, O., and Langley, S. (2003). Obtaining Maximal Concatenated Phylogenetic Data Sets from Large Sequence Databases. *Mol. Biol. Evol.* 20, 1036-1042.

Satoguina, J., Mempel, M., Larbi, J., Badusche, M., Löliger, C., Adjei, O., Gachelin, G., Fleischer, B., and Hoerauf, A. (2002). Antigen-specific T regulatory-1 cells are associated with immunosuppression in a chronic helminth infection (onchocerciasis). *Microbes. Infect.* 4, 1291-1300.

Sauer, J., McSwain, J., Bowman, A., and Essenberg, R. (1995). Tick salivary gland physiology. *Annu. Rev. Entomol.* 40, 245-267.

Service, M. (2012). Black flies (Simuliidae). In *Medical Entomology for Students* (Cambridge: Cambridge University Press), pp. 85-97.

Selemon, M. (2018). Review on control of *Haemonchus contortus* in sheep and goat. *J Vet Med Res.* 5, 1139.

Shabalina, S.A., and Spiridonov, N.A. (2004). The mammalian transcriptome and the function of non-coding DNA sequences. *Genome. Biol.* 5, 105-105.

Shapiro, J.A., and Von Sternberg, R. (2005). Why repetitive DNA is essential to genome function. *Biol. Rev.* 80, 227-250.

- Sharma, O.P., Vadlamudi, Y., Kota, A.G., Sinha, V.K., and Kumar, M.S. (2013). Drug targets for lymphatic filariasis: a bioinformatics approach. *J. Vector. Borne. Dis.* *50*, 155.
- Shaw, M., Murrell, A., and Barker, S. (2002). Low intraspecific variation in the rRNA internal transcribed spacer 2 (ITS2) of the Australian paralysis tick, *Ixodes holocyclus*. *Parasitol. Res.* *88*, 247-252.
- Shey, R.A., Ghogomu, S.M., Njume, F.N., Gainkam, L.O.T., Poelvoorde, P., Mutesa, L., Robert, A., Humblet, P., Munyampundu, J.-P., Kamgno, J., et al. (2018). Prediction and validation of the structural features of Ov58GPCR, an immunogenic determinant of *Onchocerca volvulus*. *PLoS One.* *13*, e0202915.
- Siltberg, J., and Liberles, D. (2002). A simple covarion-based approach to analyse nucleotide substitution rates. *J. Evol. Biol.* *15*, 588-594.
- Simão, F.A., Waterhouse, R.M., Ioannidis, P., Kriventseva, E.V., and Zdobnov, E.M. (2015). BUSCO: assessing genome assembly and annotation completeness with single-copy orthologs. *Bioinformatics* *31*, 3210-3212.
- Simpson, C., and Neilson, J. (1976). The pathology associated with single and quadruple infections of hamsters with *Dipetalonema viteae*. *Trop. Med. Parasitol.* *27*, 349-354.
- Slater, G.S.C., and Birney, E. (2005). Automated generation of heuristics for biological sequence comparison. *BMC Bioinformatics* *6*, 31.
- Small, S.T., Reimer, L.J., Tisch, D.J., King, C.L., Christensen, B.M., Siba, P.M., Kazura, J.W., Serre, D., and Zimmerman, P.A. (2016). Population genomics of the filarial nematode parasite *Wuchereria bancrofti* from mosquitoes. *Mol. Ecol.* *25*, 1465-1477.
- Smit, A., Hubley, R & Green, P. (2015). RepeatMasker Open-4.0. <http://www.repeatmasker.org>

- Smythe, A.B., Holovachov, O., & Kocot, K.M. (2019). Improved phylogenomic sampling of free-living nematodes enhances resolution of higher-level nematode phylogeny. *BMC Evol. Biol.* 19, 121.
- Soares, C., Lima, C., Dolan, M., Piesman, J., Beard, C., and Zeidner, N. (2005). Capillary feeding of specific dsRNA induces silencing of the *isac* gene in nymphal *Ixodes scapularis* ticks. *Insect. Mol. Biol.* 14, 443-452.
- Soboslay, P.T., Geiger, S.M., Weiss, N., Banla, M., Lüder, C.G., Dreweck, C.M., Batchassi, E., Boatín, B.A., Stadler, A., and Schulz-Key, H. (1997). The diverse expression of immunity in humans at distinct states of *Onchocerca volvulus* infection. *Immunol.* 90, 592-599.
- Sojka, D., Franta, Z., Horn, M., Caffrey, C.R., Mareš, M., and Kopáček, P. (2013). New insights into the machinery of blood digestion by ticks. *Trends Parasitol.* 29, 276-285.
- Sojka, D., Pytelková, J., Perner, J., Horn, M., Konvičková, J., Schrenková, J., Mareš, M., and Kopáček, P. (2016). Multienzyme degradation of host serum albumin in ticks. *Ticks Tick-borne Dis.* 7, 604-613.
- Som, A. (2014). Causes, consequences and solutions of phylogenetic incongruence. *Brief. Bioinformatics* 16, 536-548.
- Song, S., Shao, R., Atwell, R., Barker, S., and Vankan, D. (2011). Phylogenetic and phylogeographic relationships in *Ixodes holocyclus* and *Ixodes cornuatus* (Acari: Ixodidae) inferred from COX1 and ITS2 sequences. *Int. J. Parasitol.* 41, 871-880.
- Specht, S., Pfarr, K.M., Arriens, S., Hübner, M.P., Klarmann-Schulz, U., Koschel, M., Sternberg, S., Martin, C., Ford, L., Taylor, M.J., *et al.* (2018). Combinations of registered drugs reduce treatment times required to deplete *Wolbachia* in the *Litomosoides sigmodontis* mouse model. *PLoS Negl. Trop. Dis.* 12, e0006116.

- Spielman, A., Wilson, M., Levine, J., and Piesman, J. (1985). Ecology of *Ixodes dammini*-borne human babesiosis and Lyme disease. *Annu. Rev. Entomol.* 30, 439-460.
- Spratt, D., and Varughese, G. (1975). A taxonomic revision of filarioid nematodes from Australian marsupials. *Aus. J. Zoology. Supplementary Series* 23, 1-99.
- Spratt, D.M., and Haycock, P. (1988). Aspects of the life history of *Cercopithifilaria johnstoni* (Nematoda: Filarioidea). In: *J. Parasitol.* 18, 1087-1092.
- Sréter, T., and Széll, Z. (2008). Onchocercosis: A newly recognized disease in dogs. *Vet. Parasitol.* 151, 1-13.
- Stamatakis, A. (2006). RAxML-VI-HPC: maximum likelihood-based phylogenetic analyses with thousands of taxa and mixed models. *Bioinformatics* 22, 2688-2690.
- Stamatakis, A. (2014). RAxML version 8: a tool for phylogenetic analysis and post-analysis of large phylogenies. *Bioinformatics* 30, 1312-1313.
- Stanke, M., Diekhans, M., Baertsch, R., and Haussler, D. (2008). Using native and syntenically mapped cDNA alignments to improve de novo gene finding. *Bioinformatics* 24, 637-644.
- Stein, L.D., Bao, Z., Blasiar, D., Blumenthal, T., Brent, M.R., Chen, N., Chinwalla, A., Clarke, L., Clee, C., Coghlan, A., et al. (2003). The genome sequence of *Caenorhabditis briggsae*: A platform for comparative genomics. *PLoS Biol.* 1, e45.
- Stingl, P., Ross, M., Gibson, D., Ribas, J., and Connor, D. (1984). A diagnostic “patch test” for onchocerciasis using topical diethylcarbamazine. *Trans. R. Soc. Trop. Med. Hygiene* 78, 254-258.
- Stolk, W.A., Walker, M., Coffeng, L.E., Basáñez, M.G., and de Vlas, S.J. (2015). Required duration of mass ivermectin treatment for onchocerciasis

elimination in Africa: a comparative modelling analysis. *Parasite. Vector.* 8, 552.
<https://doi.org/10.1186/s13071-015-1159-9>

Stoltzfus, J.D., Pilgrim, A.A., and Herbert, D.B.R. (2017). Perusal of parasitic nematode 'omics in the post-genomic era. *Mol. Biochem. Parasitol.* 215, 11-22.
Stone, B., Commins, M., and Kemp, D. (1983). Artificial feeding of the Australian paralysis tick, *Ixodes holocyclus* and collection of paralysing toxin. *Int. J. Parasitol.* 13, 447-454.

Stone, B.F., Binnington, K.C., Gauci, M., and Aylward, J.H. (1989). Tick/host interactions for *Ixodes holocyclus*: Role, effects, biosynthesis and nature of its toxic and allergenic oral secretions. *Exp. Appl. Acarol.* 7, 59-69.

Storer, E., Sheridan, A.T., Warren, L., and Wayte, J. (2003). Ticks in Australia. *Aust. J. Dermatol.* 44, 83-89.

Suh, A., Witt, C.C., Menger, J., Sadanandan, K.R., Podsiadlowski, L., Gerth, M., Weigert, A., McGuire, J.A., Mudge, J., and Edwards, S.V. (2016). Ancient horizontal transfers of retrotransposons between birds and ancestors of human pathogenic nematodes. *Nat. Commun.* 7, 11396.

Susoy, V., and Herrmann, M. (2014). Preferential host switching and codivergence shaped radiation of bark beetle symbionts, nematodes of *Micoletzky* (Nematoda: Diplogastridae). *J. Evol. Biol.* 27, 889-898.

Talavera, G., and Castresana, J. (2007). Improvement of phylogenies after removing divergent and ambiguously aligned blocks from protein sequence alignments. *Syst. Biol.* 56, 564-577.

Tallon, L.J., Liu, X., Bennuru, S., Chibucos, M.C., Godinez, A., Ott, S., Zhao, X., Sadzewicz, L., Fraser, C.M., Nutman, T.B., et al. (2014). Single molecule sequencing and genome assembly of a clinical specimen of *Loa loa*, the causative agent of loiasis. *BMC. Genomics.* 15, 788.

Tamarozzi, F., Halliday, A., Gentil, K., Hoerauf, A., Pearlman, E., and Taylor, M.J. (2011). *Onchocerciasis*: the role of *Wolbachia* bacterial endosymbionts in parasite biology, disease pathogenesis, and treatment. *Clin. Microbiol. Rev.* 24, 459-468.

Tamarozzi, F., Tendongfor, N., Enyong, P.A., Esum, M., Faragher, B., Wanji, S., and Taylor, M.J. (2012). Long term impact of large scale community-directed delivery of doxycycline for the treatment of onchocerciasis. *Parasite. Vector.* 5, 53.

Tang, J., Toe, L., Back, C., and Unnasch, T.R. (1996). Intra-specific heterogeneity of the rDNA internal transcribed spacer in the *Simulium damnosum* (Diptera: Simuliidae) complex. *Mol. Biol. Evol.* 13, 244-252.

Tarailo-Graovac, M., and Chen, N. (2009). Using RepeatMasker to identify repetitive elements in genomic sequences. *Curr. Protoc. Bioinformatics* 25, 4.10. 11-14.10. 14.

Taylor, A.E. (1960). The spermatogenesis and embryology of *Litomosoides carinii* and *Dirofilaria immitis*. *J. Helminthol* 34, 3-12.

Taylor, M.J., Hoerauf, A., and Bockarie, M. (2010). Lymphatic filariasis and onchocerciasis. *Lancet* 376, 1175-1185.

Taylor, M.J., Hoerauf, A., Townson, S., Slatko, B.E., and Ward, S.A. (2014). Anti-*Wolbachia* drug discovery and development: safe macrofilaricides for onchocerciasis and lymphatic filariasis. *Parasitol.* 141, 119-127.

Taylor, M.J., von Geldern, T.W., Ford, L., Hübner, M.P., Marsh, K., Johnston, K.L., Sjöberg, H.T., Specht, S., Pionnier, N., Tyrer, H.E., *et al.* (2019). Preclinical development of an oral anti-*Wolbachia*; macrolide drug for the treatment of lymphatic filariasis and onchocerciasis. *Sci. Transl. Med.* 11, eaau2086.

Tekle, A.H., Elhassan, E., Isiyaku, S., Amazigo, U.V., Bush, S., and Noma, M. (2012). Impact of long-term treatment of onchocerciasis with ivermectin in

Kaduna State. Nigeria: first evidence of the potential for elimination in the operational area of the African programme for onchocerciasis control. *Parasite. Vector.* 5.

Ter-Hovhannisyan, V., Lomsadze, A., Chernoff, Y.O., and Borodovsky, M. (2008). Gene prediction in novel fungal genomes using an *ab initio* algorithm with unsupervised training. *Genome. Res.* 18, 1979-1990.

The *C. elegans* Sequencing Consortium (1998). Genome Sequence of the Nematode *C. elegans*: A Platform for Investigating Biology. *Science* 282, 2012.
Thylefors, B. (2008). The Mectizan Donation Program (MDP). *Ann. Trop. Med. Parasitol.* 102.

Tomkins, J.L., Aungier, J., Hazel, W., and Gilbert, L. (2014). Towards an evolutionary understanding of questing behaviour in the tick *Ixodes ricinus*. *PLoS One* 9.

Trachana, K., Larsson, T.A., Powell, S., Chen, W.H., Doerks, T., Muller, J., and Bork, P. (2011). Orthology prediction methods: a quality assessment using curated protein families. *Bioessays* 33, 769-780.

Trees, A., Graham, S., Renz, A., Bianco, A., and Tanya, V. (2000). *Onchocerca ochengi* infections in cattle as a model for human onchocerciasis: recent developments. *Parasitol.* 120, 133-142.

Trees, A., Wahl, G., Kläger, S., and Renz, A. (1992). Age-related differences in parasitosis may indicate acquired immunity against microfilariae in cattle naturally infected with *Onchocerca ochengi*. *Parasitol.* 104, 247-252.

Trees, A.J. (1992). *Onchocerca ochengi*: Mimic, model or modulator of *O. volvulus*? *Parasitol. Today* 8, 337-339.

Troughton, D.R., and Levin, M.L. (2007). Life cycles of seven ixodid tick species (Acari: Ixodidae) under standardized laboratory conditions. *J. Medical. Entomol.* 44, 732-740.

Turaga, P. S., Tierney, T.J., Bennett, K.E., McCarthy, M.C., Simonek, S.C., Enyong, P.A., Moukate, D.W., and Lustigman, S. (2000). Immunity to onchocerciasis: cells from putatively immune individuals produce enhanced levels of interleukin-5, gamma interferon, and granulocyte-macrophage colony-stimulating factor in response to *Onchocerca volvulus* larval and male worm antigens. *Infect. Immun.*, 68, 1905–1911.

Turner, H.C., Churcher, T.S., Walker, M., Osei-Atweneboana, M.Y., Prichard, R.K., and Basáñez, M.-G. (2013). Uncertainty surrounding projections of the long-term impact of ivermectin treatment on human onchocerciasis. *PLoS Negl. Trop. Dis.* 7, e2169.

Turner, H.C., Walker, M., Attah, S.K., Opoku, N.O., Awadzi, K., Kuesel, A.C., and Basáñez, M.-G. (2015a). The potential impact of moxidectin on onchocerciasis elimination in Africa: an economic evaluation based on the Phase II clinical trial data. *Parasite. Vector.* 8, 167.

Turner, H.C., Walker, M., Churcher, T.S., Osei-Atweneboana, M.Y., Biritwum, N.K., and Hopkins, A. (2014). Reaching the London declaration on neglected tropical diseases goals for onchocerciasis: an economic evaluation of increasing the frequency of ivermectin treatment in Africa. *Clin. Infect. Dis.* 59.

Turner, H.C., Walker, M., Lustigman, S., Taylor, D.W., and Basáñez, M.-G. (2015b). Human onchocerciasis: modelling the potential long-term consequences of a vaccination programme. *PLoS Negl. Trop. Dis.* 9, e0003938.

Turner, J.D., Tendongfor, N., Esum, M., Johnston, K.L., Langley, R.S., Ford, L., Faragher, B., Specht, S., Mand, S., and Hoerauf, A. (2010). Macrofilaricidal activity after doxycycline only treatment of *Onchocerca volvulus* in an area of *Loa loa* co-endemicity: a randomized controlled trial. *PLoS Negl. Trop. Dis.* 4, e660.

Tyagi, R., Elfawal, M.A., Wildman, S.A., Helander, J., Bulman, C.A., Sakanari, J., Rosa, B.A., Brindley, P.J., Janetka, J.W., Aroian, R.V., *et al.* (2019a). Identification of small molecule enzyme inhibitors as broad-spectrum anthelmintics. *Sci. Rep.* 9, 9085.

- Tyagi, R., Rosa, B.A., and Mitreva, M. (2019b). Chapter 12 - Omics-driven knowledge-based discovery of anthelmintic targets and drugs. In *In Silico Drug Design*, K. Roy, ed. (Academic Press), pp. 329-358.
- Tyson, J.R., O'Neil, N.J., Jain, M., Olsen, H.E., Hieter, P., and Snutch, T.P. (2018). MinION-based long-read sequencing and assembly extends the *Caenorhabditis elegans* reference genome. *Genome Res.* 28, 266-274.
- Uni, S., Bain, O., Fujita, H., Matsubayashi, M., Fukuda, M., and Takaoka, H. (2013). Infective larvae of *Cercopithifilaria* spp. (Nematoda: Onchocercidae) from hard ticks (Ixodidae) recovered from the Japanese serow (Bovidae). *Parasite* 20, 1.
- Uni, S., Bain, O., Takaoka, H., Katsumi, A., Fujita, H., and Suzuki, Y. (2002). Diversification of *Cercopithifilaria* species (Nematoda: Filarioidea) in Japanese wild ruminants with description of two new species. *Parasite* 9, 293-304.
- Unnasch, T.R., Golden, A., Cama, V., and Cantey, P.T. (2018). Diagnostics for onchocerciasis in the era of elimination. *Int. Health.* 10, i20-i26.
- Unnasch, T.R., and Williams, S.A. (2000). The genomes of *Onchocerca volvulus*. *Int. J. Parasitol.* 30, 543-552.
- van Duijvendijk, G., Gort, G., Sprong, H., and Takken, W. (2017). Behavioural responses of *Ixodes ricinus* nymphs to carbon dioxide and rodent odour. *Med. Vet. Entomol.* 31, 220-223.
- Vawter, L., and Brown, W.M. (1986). Nuclear and mitochondrial DNA comparisons reveal extreme rate variation in the molecular clock. *Science* 234, 194.
- Viggers, K., and Spratt, D. (1995). The Parasites Recorded From *Trichosurus* Species (Marsupialia: Phalangeridae). *Wildlife. Res.* 22, 311-332.

- Vlaminck, J., Fischer, P.U., and Weil, G.J. (2015). Diagnostic tools for onchocerciasis elimination programs. *Trends Parasitol.* 31, 571-582.
- Vuong, P.N., Bain, O., Petit, G., and Chabaud, A. (1985). Comparative study of the cutaneous and ocular lesions of murids *Lemniscomys striatus* parasitized by *Monanema spp.* and *Artherurus africanus* parasitized by *Cercopithifilaria sp.* with those of human onchocercosis. *C. R. Acad. Sci. III.* 301, 433-437.
- Vuong, P.N., Spratt, D., Wanji, S., Aimard, L., and Bain, O. (1993). *Onchocerca*-like lesions induced by the filarioid nematode *Cercopithifilaria johnstoni*, in its natural hosts and in the laboratory rat. *Ann. Parasitol. Hum. Comp.* 68, 176-181.
- Waladde, S.M., Ochieng', S.A., and Gichuhi, P.M. (1991). Artificial-membrane feeding of the ixodid tick, *Rhipicephalus appendiculatus*, to repletion. *Exp. Appl. Acarol.* 11, 297-306.
- Walker, M., Specht, S., Churcher, T.S., Hoerauf, A., Taylor, M.J., and Basáñez, M.-G. (2015). Therapeutic efficacy and macrofilaricidal activity of doxycycline for the treatment of river blindness. *Clin. Infect. Dis.* 60, 1199-1207.
- Wall, R., and Shearer, D. (1997). Ticks (*Acarí*). In *Veterinary Entomology* (Springer Netherlands), pp. 96-140.
- Walsh, J., Davies, J., and Le Berre, R. (1979). Entomological aspects of the first five years of the Onchocerciasis Control Programme in the Volta River Basin. *Trop. Med. Parasitol.* 30, 328-344.
- Wanji, S., Kengne-Ouafo, J.A., Esum, M.E., Chounna, P.W., Adzemye, B.F., Eyong, J.E., Jato, I., Datchoua-Poutcheu, F.R., Abong, R.A., and Enyong, P. (2015). Relationship between oral declaration on adherence to ivermectin treatment and parasitological indicators of onchocerciasis in an area of persistent transmission despite a decade of mass drug administration in Cameroon. *Parasite. Vector.* 8, 667.

- Wanji, S., Tendongfor, N., Nji, T., Esum, M., Che, J.N., Nkwescheu, A., Alassa, F., Kamnang, G., Enyong, P.A., and Taylor, M.J. (2009). Community-directed delivery of doxycycline for the treatment of onchocerciasis in areas of co-endemicity with loiasis in Cameroon. *Parasite. Vector.* 2, 39.
- Ward, J., Nutman, T., Zea-Flores, G., Portocarrero, C., Lujan, A., and Ottesen, E. (1988). Onchocerciasis and immunity in humans: enhanced T cell responsiveness to parasite antigen in putatively immune individuals. *J. Infect. Dis.* 157, 536-543.
- Webster, J.P., Gower, C.M., Knowles, S.C., Molyneux, D.H., and Fenton, A. (2016). One health—an ecological and evolutionary framework for tackling Neglected Zoonotic Diseases. *Evol. Appl.* 9, 313-333.
- Wharton, D. (1947). Pathological changes in natural and experimental filariasis in the cotton rat. *J. Infect. Dis.* 307-318.
- Whittaker, C., Walker, M., Pion, S.D.S., Chesnais, C.B., Boussinesq, M., and Basáñez, M.-G. (2018). The population biology and transmission dynamics of *Loa loa*. *Trends Parasitol.* 34, 335-350.
- Whitton, C., Daub, J., Quail, M., Hall, N., Foster, J., Ware, J., Ganatra, M., Slatko, B., Barrell, B., and Blaxter, M. (2004). A genome sequence survey of the filarial nematode *Brugia malayi*: repeats, gene discovery, and comparative genomics. *Mol. Biochem. Parasitol.* 137, 215-227.
- Wickham, H. (2016). *ggplot2: Elegant graphics for data analysis* (Springer-Verlag New York).
- Wickham, H., Chang, W., Henry, L., Pedersen, T.L., Takahashi, K., Wilke, C., and Woo, K. (2016). *ggplot2: Create elegant data visualisations using the grammar of graphics*. R package version 2.
- Wiens, J.J. (1998). Does adding characters with missing data increase or decrease phylogenetic accuracy? *Syst. Biol.* 47, 625-640.

Wolstenholme, A., and Rogers, A. (2005). Glutamate-gated chloride channels and the mode of action of the avermectin/milbemycin anthelmintics. *Parasitol.* 131, S85-S95.

Wolstenholme, A.J. (2012). Glutamate-gated chloride channels. *J. Biol. Chem.* 287, 40232-40238.

Wolstenholme, A.J., Maclean, M.J., Coates, R., McCoy, C.J., and Reaves, B.J. (2016). How do the macrocyclic lactones kill filarial nematode larvae? *Invert. Neurosci.* 16, 1-9.

Wolstenholme, D.R. (1992). Animal mitochondrial DNA: structure and evolution. *Int. Rev. Cytol.* 141, 173-216.

World Health Organisation (2010). Conceptual and operational framework of onchocerciasis elimination with ivermectin treatment. African Programme for Onchocerciasis Control,
https://www.who.int/apoc/oncho_elimination_report_english.pdf.

World Health Organisation (2016). Guidelines for stopping mass drug administration and verifying elimination of human onchocerciasis: criteria and procedures.
https://apps.who.int/iris/bitstream/handle/10665/204180/9789241510011_eng.pdf?sequence=1.

World Health Organisation (2019). Elimination of human onchocerciasis: progress report, 2018-2019. *Wkly. Epidemiol. Rec. (WER)* 94, 513-524.

Xu, B., and Yang, Z. (2013) PAMLX: a graphical user interface for PAML. *Mol. Biol. Evol.* 30, 2723-2724.

Yang, Z. (1997). PAML: a program package for phylogenetic analysis by maximum likelihood. *Bioinformatics* 13, 555-556.

- Yang, Z. (2000). Phylogenetic analysis by maximum likelihood (PAML). Version 3.12. http://oldsaf.bio.caltech.edu/saf_manuals/pamlDOC.pdf
- Yang, Z. (2007). PAML 4: Phylogenetic analysis by maximum likelihood. *Mol. Biol. Evol.* 24, 1586-1591.
- Yang, Z., and Dos Reis, M. (2010). Statistical properties of the branch-site test of positive selection. *Mol. Biol. Evol.* 28, 1217-1228.
- Yatawara, L., Wickramasinghe, S., Rajapakse, R., and Agatsuma, T. (2010). The complete mitochondrial genome of *Setaria digitata* (Nematoda: Filarioidea): Mitochondrial gene content, arrangement and composition compared with other nematodes. *Mol. Biol. Parasitol.* 173, 32-38.
- Yu, G., Smith, D.K., Zhu, H., Guan, Y., and Lam, T.T.-Y. (2017). ggtree: an R package for visualization and annotation of phylogenetic trees with their covariates and other associated data. *Methods. Ecol. Evol.* 8, 28-36.
- Zerbino, D.R. (2010). Using the Velvet de novo assembler for short-read sequencing technologies. *Curr. Prot. Bioinformatics. Chapter 11*, Unit-11.15.
- Zerbino, D.R., and Birney, E. (2008). Velvet: algorithms for de novo short read assembly using de Bruijn graphs. *Genome. Res.* 18, 821-829.
- Zhang, R.L., and Zhang, B. (2014). Prospects of using DNA barcoding for species identification and evaluation of the accuracy of sequence databases for ticks (Acari: Ixodida). *Ticks Tick-Borne Dis.* 5, 352-358.
- Zouré, H., Noma, M., Tekle, A.H., Amazigo, U.V., Diggle, P.J., Giorgi, E., and Remme, J.H. (2014). The geographic distribution of onchocerciasis in the 20 participating countries of the African Programme for Onchocerciasis Control: pre-control endemicity levels and estimated number infected. *Parasite. Vector.* 7, 326.

Zoure, H.G.M., Wanji, S., Noma, M., Amazigo, U.V., Diggle, P.J., Tekle, A.H., and Remme, J.H. (2011). The geographic distribution of *Loa loa* in Africa: results of large-scale implementation of the Rapid Assessment Procedure for Loiasis (RAPLOA). PLoS Negl. Trop. Dis. 5.

Zwickl, D.J., and Hillis, D.M. (2002). Increased taxon sampling greatly reduces phylogenetic error. Syst. Biol. 51, 588-598.